

A General and Stereoselective Approach for the Construction of Azabicyclic Compounds:
Applications to the Synthesis of (+)-Amabiline and Grandisine D; Structure-based Design of
Small Molecule Inhibitors of the Menin-MLL Protein-protein Interaction

By

Timothy J. Senter

Dissertation

Submitted to the Faculty of the
Graduate School of Vanderbilt University
in partial fulfillment of the requirements

for the degree of

DOCTOR OF PHILISOPHY

in

Chemistry

May 2015

Nashville, Tennessee

Approved:

Craig W. Lindsley, Ph.D.

Gary A. Sulikowski, Ph.D.

Jeffrey N. Johnston, Ph.D.

H. Charles Manning, Ph.D.

To my fiancée Rebecca Klar

and my family:

Carolyn, Bo, Lauren, and Eric

ACKNOWLEDGMENTS

There are many people that I would like to thank for their support, guidance, and contributions towards my education. These people have played an enormous role my development as both a scientist and person, and I would like personally acknowledge them.

First I would like to thank my advisor Professor Craig Lindsley. I feel very lucky to have had the opportunity to study under such an accomplished scientist who provided guidance and unwavering support every step of the way. He allowed me to pursue my academic interests while keeping me on track, and provided a stimulating research environment full of very talented people. My education under Craig was not bound by the subject of chemistry and spilled into diverse areas such as film, music, the geography of Scotland, paintball tactics, and the necessity of extra parachutes.

I also want to thank Professor Shaun Stauffer for his mentorship and direction throughout my graduate studies. Beyond his guidance in the Menin-MLL project, he was a constant source of advice on many aspects of my graduate education and continuing career. I thank him for being a fantastic colleague and friend.

I would like to recognize my committee: Dr. Gary Sulikowski, Dr. Jeff Johnston, and Dr. Charles Manning for their time and feedback during my committee meetings. They also contributed to my development through classroom education and helpful discussion.

I would like to thank the many members of the Lindsley lab who went out of their way to help me along my way through my graduate school career. Niyi Fadeyi taught me many practical skills my first months in the lab, and served as an example of the work ethic

required to be a successful chemist. I wish him the best as he continues his career. I would also like to thank Mike Schulte, who was a great friend and colleague through my time at Vanderbilt. He was a source of great advice in scientific discussions, and along with his wife Rachel fantastic friends outside of lab. I wish them both the best as they begin new and exciting careers. I would like to thank Cody Wenthur, who was fantastic colleague and companion during our time in “the cave”. He was a great resource in pharmacology, and along with his wife Brielle were also great friends. I wish them both the best in their future endeavors. I would also like to thank other Lindsley group members Patrick Gentry, Matt O’Reilly, Pedro, Chris, Bruce, JT, Leslie, Joe, Cynthia, and Brittney for countless hours of useful discussion and making the group a fantastic place to work. I would like to acknowledge Don Stec, Matt Mulder, and Nathan Kett for their technical support and helping with analytical work in several aspects of my projects. They were both extremely helpful and always willing to take the extra time to help me tackle challenging problems.

I would like to thank my undergraduate advisor, Professor Larry French, for his support during my undergraduate research and guidance in selecting a graduate school. His willingness to extend my education to the laboratory was a catalyst in my interest to pursue graduate school. Another educator that was instrumental in my development is my high school science teacher Suzanne Riley. She was the first teacher to take my education out of the textbook and allowed me to begin asking and exploring my own questions, however misguided they may have been at the time! It is with that same love of asking questions that I continue to approach every day.

I would like to thank my parents and family for their love and support throughout my life, and especially over the last 5 years. They have always been there for me through any challenge, and I would not be where I am today without their help.

Finally, I would like to thank my Fiancée Rebecca Klar. Words can not begin to describe the enormous amount of support she has given me throughout graduate school. Our love and support for each other have allowed us to reach our goals, and I can't wait to find out what exciting things we have in store together for the future.

TABLE OF CONTENTS

	Page
DEDICATION	ii
ACKNOWLEDGMENTS	iii
LIST OF TABLES	ix
LIST OF FIGURES	x
LIST OF SCHEMES.....	xii
LIST OF ABBREVIATIONS.....	xvi
Chapter	
I. A GENERAL, STEREOSELECTIVE APPROACH TO THE CONSTRUCTION OF AZABICYCLIC RING SYSTEMS	1
1.1 Introduction.....	1
1.2 Indolizidine Ring Systems	2
1.2.1 Indolizidine Alkaloid Natural Products	2
1.2.2 Synthetic Approaches to Indolizidine Ring Systems.....	3
1.3 Pyrrolizidine Ring Systems.....	7
1.3.1 Pyrrolizidine Alkaloid Natural Products.....	7
1.3.2 Biosynthesis of Pyrrolizidine Alkaloids	9
1.3.3 Synthetic Approaches to Pyrrolizidine Ring Systems	10
1.4 Stereoselective Synthesis of Medium-sized 1- azabicyclo[<i>m.n.0</i>]alkyl Ring Systems	13
1.4.1 Previous Attempts to Access Azabicyclic Ring Systems	13
1.4.2 Chiral <i>tert</i> -Butanesulfinylimines as Chiral Directing Groups	15
1.4.3 Synthetic Approach for the Azabicyclic Ring Systems	16
1.4.4 Synthesis of Azabicyclic Ring Systems.....	17
1.4.5 Synthesis of Azabicyclic Lactam Ring Systems.....	21
1.5 Stereoselective Synthesis of Small to Large 1- azabicyclo[<i>m.n.0</i>]alkyl Ring Systems	22
1.5.1 Alternative Approach to Azabicyclic Ring Systems	22
1.5.2 Synthesis of Small to Large Azabicyclic Ring Systems.....	25
References.....	30

Experimental Methods	33
II. TOTAL SYNTHESIS OF THE ALKALOID NATURAL PRODUCTS (+)-AMABILINE AND GRANDISINE D	58
2.1 Introduction.....	58
2.1.1 Pyrrolizidine Alkaloids	59
2.1.2 Indolizidine Alkaloids.....	60
2.2 Total Synthesis of (+)-Amabiline	61
2.2.1 Introduction.....	61
2.2.2 Retrosynthetic Analysis of (+)-Amabiline.....	62
2.2.3 Synthesis of (+)-Amabiline.....	63
2.3 Total Synthesis of Grandisine D	71
2.3.1 Introduction.....	71
2.3.2 Tamura Total Synthesis of Grandisine D.....	72
2.3.3 Taylor Total Synthesis of Grandisine D	74
2.3.4 Retrosynthesis of Grandisine D	75
2.3.5 Synthesis of Grandisine D	76
2.3.6 Synthesis of Unnatural Analogue of Grandisine D.....	78
References.....	81
(+)-Amabiline Experimental Methods.....	83
Grandisine D Experimental Methods.....	97
III. GENERAL ACCESS TO CHIRAL N-ALKYL TERMINAL AZIRIDINES AND 2-SUBSTITUTED AZETIDINES VIA ORGANOCATALYSIS	116
3.1 Introduction to Aziridines	116
3.1.1 General Properties of Aziridines.....	116
3.2 Synthesis of Aziridines	118
3.2.1 Introduction.....	118
3.2.2 Aziridine Synthesis by Addition to Alkenes.....	120
3.2.3 Aziridine Synthesis by Addition to Imines	122
3.2.4 Aziridine Synthesis by Intramolecular Substitution	125
3.3 Introduction to Azetidines.....	126
3.3.1 General Properties of Azetidines	126
3.4 Synthesis of Azetidines.....	128
3.4.1 Introduction.....	128
3.4.2 Azetidine Synthesis via intramolecular cyclization	129
3.4.3 Azetidine Synthesis via Cycloaddition	131
3.5 Azetidines in Medicinal Chemistry	134

3.6 Organocatalytic Enantioselective Synthesis of Aziridines and Azetidines	135
3.6.1 Introduction.....	135
3.6.2 An Improved Synthesis of Jorgensen’s Catalyst	138
3.6.3 Studies Towards the Enantioselective Synthesis of Aziridines	140
3.6.4 Studies Towards the Enantioselective Synthesis of Azetidines.....	142
3.6.5 Synthesis of an Azetidine CaSR Antagonist.....	148
References.....	151
Experimental Methods	153
IV. DEVELOPMENT OF SMALL MOLECULE INHIBITORS OF THE MENIN- MIXED LINEAGE LEUKEMIA INTERACTION	185
4.1 Introduction.....	185
4.1.1 Protein-protein Interactions as Therapeutic Targets	185
4.1.2 Menin-MLL Interaction	186
4.1.3 Classes of Menin-MLL Inhibitors	188
4.2 Identification of Novel inhibitors of the Menin-MLL PPI	190
4.2.1 High Throughput Screen to Identify Novel Menin-MLL Inhibitors	190
4.2.2 Determination of the Minimal Pharmacophore	191
4.3 Lead Optimization of the Hydroxymethyl Piperidine Series.....	194
4.3.1 Probing the Hydrophobic Head Group Region.....	194
4.3.2 Structural Investigation of MIV-3 – menin Interactions.....	196
4.4 Structure-based design of inhibitors of the menin-MLL interaction	200
4.4.1 Optimization of Hydrophobic Head Group	200
4.4.2 Optimization of Tertiary Carbinol	204
4.4.3 Optimization of the Tail Group.....	207
4.5 Biological Characterization of Menin-MLL Inhibitors	208
4.5.1 Disruption of Fusion Protein Interaction in Cells and Expression of Downstream Targets	208
4.5.2 Proliferation and Differentiation in MLL Leukemia Cells.....	209
4.6 Optimization of DMPK properties.....	212
4.6.1 Use of Efficiency Metrics to Optimize <i>In Vitro</i> DMPK	212
4.6.2 <i>In vivo</i> Pharmacokinetics	215
4.6.3 Ancillary Pharmacology of Hydroxymethyl Piperidine Class.....	218
4.7 Conclusions.....	220
References.....	222
Experimental Methods	224
Appendix.....	251

LIST OF TABLES

Table	Page
3.1 Physical properties of 3-member ring moieties	117
3.2 cLogP, cLogD, and pK _a values of common saturated heterocycles	134
3.3 Base screen for azetidine cyclization	145
4.1 Activity of hydroxymethyl piperidine menin-MLL inhibitors	193
4.2 Potency and physical properties of cyclopentyl hydroxymethyl piperidine compounds	213
4.3 <i>In vitro</i> DMPK and <i>in vivo</i> pharmacokinetics of cyclopentyl hydroxymethyl piperidine compounds	215
4.4 Potency and <i>in vitro</i> DMPK parameters of biaryl hydroxymethyl piperidine compounds	216
4.5 <i>In vivo</i> pharmacokinetics parameters of biaryl-substituted hydroxymethyl piperidine compounds	217

LIST OF FIGURES

Figure	Page
1.1 Representative 1-azabicyclo[<i>m.n.0</i>]alkane ring systems	2
1.2 Examples of indolizidine containing natural products	3
1.3 Structure and numbering convention of pyrrolizidine alkaloids	8
1.4 Common necine bases	8
1.5 Biosynthesis of the azabicyclic core moiety of pyrrolizidine alkaloids	9
1.6 Stemaphylline and stemaphylline- <i>N</i> -oxide	13
1.7 Method for the preparation of α chiral amines	16
1.8 Mono-unsaturated 1-azabicyclo[<i>m.n.0</i>]alkane ring systems synthesized	28
2.1 Structures of pyrrolizidine alkaloids	60
2.2 Examples of indolizidine-containing natural products	61
2.3 Metabolic fate of pyrrolizidine alkaloids	62
2.4 Retrosynthetic analysis of (+)-Amabiline	63
2.5 Ellman's proposed transition state for Grignard addition into chiral <i>tert</i> -butanesulfinylimines	66
2.6 ORTEP drawing of X-ray crystallographically determined structure of 2.15	66
2.7 Coupling of 2.15 with (+)-viridifloric acid precursor 2.16	68
2.8 Structures of the indolizidine alkaloids grandisines A-G	71
2.9 Tamura's retrosynthesis of grandisine D	72
3.1 Synthetic approaches to aziridines	119
3.2 Complimentary methods of Cu-catalyzed aziridination utilizing bis(oxazoline) and di-imine ligands	121
3.3 Azetidine-based natural products and pharmaceuticals	127
3.4 Geometric configuration of azetidine	128

3.5	Enantioselective synthesis of <i>N</i> -alkyl terminal aziridines	142
3.6	Enantioselective synthesis of β -chloronitriles	146
3.7	Intramolecular cyclization for the synthesis of 2-substituted azetidines	147
4.1	Schematic of MLL wild type and MLL fusion proteins	187
4.2	X-ray co-crystal structure of MLL peptide (magenta) in complex with menin.....	188
4.3	Recently developed small molecule menin-MLL PPIs	189
4.4	Structure and activity of the most potent hit from HTS.....	191
4.5	Physical and DMPK properties of MIV-3	195
4.6	Structure and activity for MIV-3	196
4.7	Crystal structures of menin in complex with MIV-3R and MIV-3S	197
4.8	Superposition of the menin-MIV-3R and menin-MIV-3S crystal structures	198
4.9	Superposition of the crystal structures of menin-MIV-3R and the menin-MLL complexes.....	199
4.10	Inhibitory activities of MIV-3 analogues.....	202
4.11	Activities of analogues with substitution at the head group region	206
4.12	Co-immunoprecipitation experiment in HEK293 cells transfected with MLL-AF9 translocation	208
4.13	MTT cell viability assay performed for 4.29 and MIV-3R	210
4.14	Quantification of CD11b expression in MLL-AF9 transformed murine BMCs	211
4.15	Identification of major metabolites of ML399.....	218
4.16	DMPK and ancillary pharmacology profile of ML399	218
4.17	X-ray crystal structure of 4.13 in complex with menin	219

LIST OF SCHEMES

Scheme	Page
1.1 Synthesis of coniceine.....	4
1.2 Renaud synthesis of (-)-167B by intramolecular Schmidt rearrangement.....	4
1.3 Synthesis of (-)-209D via rhodium-catalyzed [2+2+2] cycloaddition.....	5
1.4 Yu Synthesis of Steviamine.....	6
1.5 RCM strategy to access indolizidine ring system 1.32	6
1.6 Shenvi Synthesis of 207A.....	7
1.7 Takahata synthesis of (-)-supinidine.....	10
1.8 Vedejs synthesis of retronecine.....	11
1.9 Tufariello synthesis of retronecine.....	11
1.10 Transannular cyclization approach to polyhydroxylated pyrrolizidines.....	12
1.11 Pearson synthesis of (+)-australine.....	12
1.12 Proposed enantioselective synthesis of 1-azabicyclo[<i>m.n.0</i>]alkane ring systems...	14
1.13 Approach to the synthesis of chiral 2-substituted pyrrolidines.....	16
1.14 Approach to synthesis of azabicyclic ring systems.....	17
1.15 Synthesis of indolizidine ring system.....	18
1.16 Synthesis of azepine ring system.....	19
1.17 Synthesis of decahydropyrrolo[1,2- <i>a</i>]azocine ring system.....	20
1.18 Synthesis of pyrrolizidine ring system.....	21
1.19 Synthesis of azabicyclic lactam ring systems.....	22
1.20 Application of γ -chloro <i>N</i> -(<i>tert</i> -butanesulfinyl)ketimines to access pyrroles and azabicyclic systems in high enantioselectivity.....	23
1.21 Approach for the synthesis of stemaphylline.....	24

1.22 Envisioned route to access diverse 1-azabicyclo[<i>m.n.0</i>]alkane cores.....	25
1.23 Stereoselective synthesis of <i>N</i> -alkyl azocines 1.129	26
1.24 RCM approaches to access the 1-azabicyclo[<i>m.n.0</i>]alkane cores.....	26
1.25 Optimal RCM conditions for the enantioselective synthesis of the unsaturated 1-azabicyclo[<i>m.n.0</i>]alkane cores 1.4.15	27
2.1 Synthesis of protected (-)-viridifloric acid.....	64
2.2 Synthesis of advanced intermediate 2.27	65
2.3 Attempted deprotection to necine base	67
2.4 Synthesis of (+)-amabiline.....	69
2.5 <i>N</i> -oxidation of amabiline to amabiline- <i>N</i> -oxide	70
2.6 Tamura's total synthesis of Grandisine D.....	73
2.7 Tamura total synthesis of grandisine D	73
2.8 Taylor synthesis of (+)-grandisine D	74
2.9 Synthesis of Grandisine B.....	75
2.10 Retrosynthesis of grandisine D	76
2.11 Synthesis of advanced intermediate 2.58	77
2.12 Synthesis of Grandisine D from advanced intermediate 2.58	78
2.13 Synthesis of advanced intermediate 2.66	79
2.14 Synthesis of unnatural analogue 2.69	80
3.1 Gabriel-Marckwald Ethylenimine Synthesis	118
3.2 Wenker Aziridine Synthesis	119
3.3 Synthesis of polyoxamic acid via Michael addition-elimination sequence	121
3.4 Mn- catalyzed aziridination of styrene	122
3.5 Jacobsen aziridination of imines	123
3.6 Chiral aziridination using sulfur ylides.....	123

3.7	Aziridination of sulfinylimines with bromoenolates via aza-Darzens reaction.....	124
3.8	Bronsted acid-catalyzed aza-Darzens en route to Mitomycin C.....	124
3.9	Synthesis of aziridines via 1,2-aminoalcohols.....	125
3.10	Organocatalytic aziridination of α,β -unsaturated aldehydes	126
3.11	Cyclization of aniline with 1,3-dichloropropane	129
3.12	Synthesis of pyrrolidines and azetidines from enantiomerically pure oxiranes	130
3.13	Mitsunobu-activated cyclization.....	130
3.14	2,4- <i>cis</i> -azetidine formation by iodocyclization of homoallylamines.....	131
3.15	Synthesis of azetidines via intramolecular amination of γ -C(sp ³)-H bonds	131
3.16	Azetidine synthesis via organocatalyzed [2+2] cycloaddition.....	132
3.17	Synthesis of <i>trans</i> -2,3,4-trisubstituted azetidines via [2+2] cycloaddition	133
3.18	Synthesis of bicyclic azetidines through [4+2] cycloaddition	133
3.19	Organocatalytic enantioselective synthesis of α -chloroaldehydes and β -fluoroamines	136
3.20	General access to chiral <i>N</i> -alkyl terminal aziridines via organocatalysis.....	136
3.21	Envisioned route to chiral <i>N</i> -alkyl terminal aziridines and 2-alkylazetidines	138
3.22	Scalable synthesis of pyrrolidine organocatalyst 3.71	139
3.23	One pot α -chlorination/reduction sequence	140
3.24	Amine displacement and intramolecular S _N 2 cyclization.....	141
3.25	Synthesis of γ -chloroamine.....	143
3.26	Cyclization of γ -chloroamine to access 2-alkylazetidines	146
3.27	Daiichi Sankyo synthesis of CaSR antagonist 2.99	148
3.28	Proposed synthesis of CaSR antagonist 3.103	149
4.1	General synthesis of hydroxymethyl piperidine compounds.....	192
4.2	Synthesis of cyclopentyl-containing hydroxymethyl piperidine compounds.....	201

4.3	Synthesis of aminomethyl piperidine 4.29	204
4.4	Synthesis of sulfonamide containing hydroxymethyl piperidine 4.31	207
4.5	Synthesis of 4.41	220

LIST OF ABBREVIATIONS

Ac	acetyl
AcOH	acetic acid
9-BBN	9-borabicyclo[3.3.1]
α	specific rotation
Ar	aryl
Bn	benzyl
Boc	<i>tert</i> -butoxycarbonyl
br	broad
Bz	benzoyl
cat	catalyst
CDCl ₃	deuterated chloroform
CH ₂ Cl ₂	dichloromethane
CHCl ₃	chloroform
CNS	central nervous system
conc	concentration
CSA	camphorsulfonic acid
CYP450	cytochrome P450
d	doublet
DABCO	1,4-diazabicyclo[2.2.2]octane
DAST	(diethylamido)sulfur trifluoride
DBU	1,8-diazabicycloundec-7-ene
DCE	1,2-dichloroethane
DCM	dichloromethane

dd	doublet of doublets
ddd	doublet of doublet of doublets
ddt	doublet of doublet of triplets
DIBALH	diisobutylaluminum hydride
Diox	dioxane
DIPEA	<i>N,N</i> -diisopropylethylamine
DMF	dimethylformamide
DMPK	drug metabolism/pharmacokinetics
DMSO	dimethylsulfoxide
dr	diastereomeric ratio
dt	doublet of triplets
ee	enantiomeric excess
ELSD	evaporative light scattering detector
eq	equivalents
ES	electrospray
Et	ethyl
Et ₂ O	diethyl ether
Et ₃ N	triethyl amine
Et ₃ SiH	triethylsilane
EtOAc	ethyl acetate
EtOH	ethanol
g	grams
GPCR	G-protein coupled receptor
Grubbs II	Grubbs second generation catalyst
h	hour(s)

H ₂ O	water
hERG	human ether-a-go-go receptor
Hex	hexanes
HMPA	hexamethylphosphoramide
HPLC	high performance liquid chromatography
HRMS	high resolution mass spectrometry
Hz	hertz
<i>i</i>	iso
IC ₅₀	half maximal inhibitory concentration
Im	imidazole
IPA	isopropyl alcohol
J	coupling constant (in Hz)
K ₂ CO ₃	pottasium carbonate
KHMDS	potassium <i>bis</i> (trimethylsilyl)amide
LCMS	liquid chromatography-mass spectrometry
LDA	lithium diisopropylamide
LHMDS	lithium <i>bis</i> (trimethylsilyl)amide
m	multiplet
M	molar
mCPBA	<i>meta</i> -chloroperoxybenzoic acid
Me	methyl
MeCN	acetonitrile
MeOD	deuterated methanol
MeOH	methanol
mg	milligram

MHz	megahertz
MIC	minimum inhibitory concentration
min	minute(s)
mL	milliliter(s)
MLL	mixed lineage leukemia
mol	mole(s)
Ms	mesyl
MS	molecular sieves
NaBH(OAc ₃)	sodium triacetoxymethylborohydride
nBuLi	<i>n</i> -butyllithium
NaOH	sodium hydroxide
NCS	<i>N</i> -chlorosuccinimide
nM	nanomolar
Pd/C	palladium on carbon
Ph	phenyl
pKa	acid dissociation constant
ppm	parts per million
PS	polymer-supported
psi	pounds per square inch
q	quartet
R	generic organic substituent
RCM	ring-closing metathesis
Rf	retention factor
rt	room temperature
rxn	reaction

s	singlet
sat	saturated
sec	seconds
sext	sextet
SFC	supercritical fluid chromatography
<i>t</i>	tert
t	triplet
TBAF	tetra- <i>n</i> -butylammonium fluoride
TBDPS	<i>tert</i> -butyldiphenylsilyl
TBS	<i>tert</i> -butyldimethylsilyl
<i>t</i> -Bu	<i>tert</i> -butyl
temp	temperature
Tf	triflate
TFA	trifluoroacetic acid
THF	tetrahydrofuran
TLC	thin-layer chromatography
TMS	trimethylsilyl
TOF	time of flight
Tol	toluene
Ts	tosyl
UV	ultraviolet
δ	chemical shifts (ppm)
Δ	heat
μ M	micromolar
μ m	micrometer

μW

microwave heating

CHAPTER I

A GENERAL, STEREOSELECTIVE APPROACH TO THE CONSTRUCTION OF AZABICYCLIC RING SYSTEMS

1.1. Introduction

Azabicyclic ring skeletons are common structural subunits found in numerous alkaloid natural products. These motifs frequently comprise the core of biologically active and pharmaceutically significant compounds (**Figure 1.1**).¹ Although 1-azabicyclo[*m.n.0*]alkane ring systems are found in a number of natural products, asymmetric approaches to access them are limited.

The first synthesis of azabicyclic ring systems dates back to the middle 19th century, when δ -coniceine was obtained from the cyclization of *N*-bromoconiine with sulfuric acid.² In general, the existing strategies for the construction of azabicyclic ring systems rely on Staudinger-aza-Wittig approaches, intramolecular cyclizations, cycloadditions ([5+2], [4+2], and [2+2+2]), ring closing metathesis (RCM) strategies, and rearrangements (nitrene and intramolecular Schmidt rearrangements).³ Enantioselective approaches to larger azabicyclic ring systems are not well explored, and most that are reported lack stereocontrol.⁴ The purpose of our research is to develop general and highly enantioselective approaches to the construction of 1-azabicyclo[*m.n.0*]alkane ring

systems and apply this methodology towards the total synthesis of alkaloid natural products. This warrants a brief introduction of indolizidine and pyrrolizidine alkaloids.

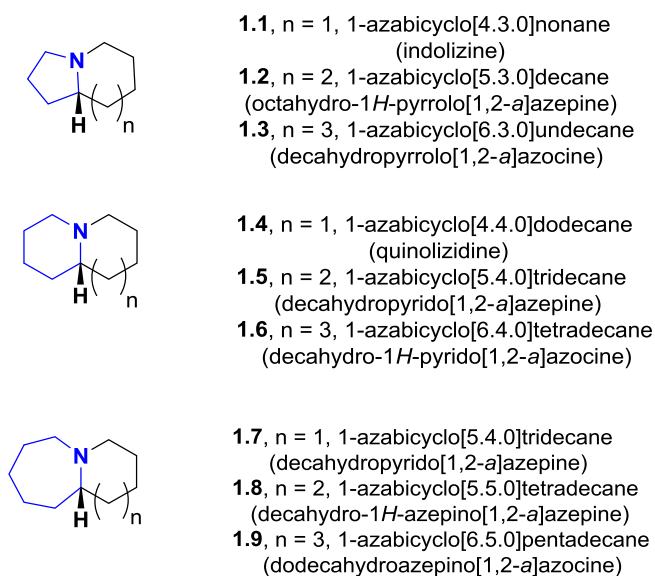


Figure 1.1. Representative 1-azabicyclo[*m.n.0*]alkane ring systems, including their alternative IUPAC nomenclature, of interest in both natural product synthesis and drug discovery.

1.2. Indolizidine Ring Systems

1.2.1. Indolizidine Alkaloid Natural Products

Indolizidine alkaloids are isolated from a multitude of natural sources, including ants, amphibians, fungi, plants, and marine species. These alkaloids possess interesting biological activities including insecticidal, antibacterial, antifungal, antiviral, and antimalarial activities. Several alkaloids of this class function as potent and subtype selective noncompetitive blockers of the nicotinic acetylcholine receptor (nAChR), which

has been implicated in neurological disease states including Alzhiemers disease, Parkinson's disease, schizophrenia, and epilepsy.⁵

Indolizidine alkaloids are defined by a conserved 1-aza-bicyclo-[4.3.0]-octane core. This moiety has been observed in many alkaloid natural products, and a variety of approaches have been developed to enable the synthesis of these compounds. Shown in **Figure 1.2** are examples of indolizidine natural products that have been the focus of total synthesis efforts.

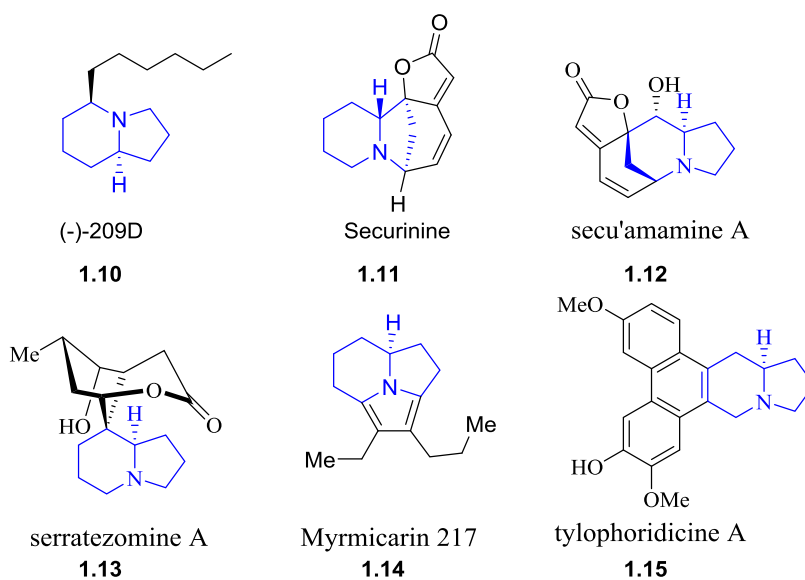


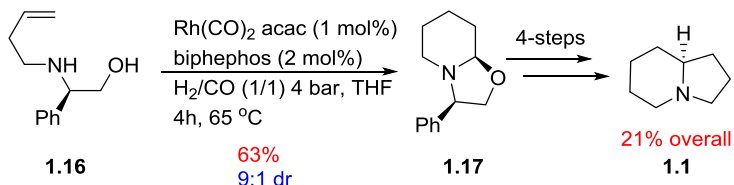
Figure 1.2. Examples of indolizidine containing natural products.

1.2.2. Synthetic Approaches to Indolizidine Ring Systems

Due to the interest in the biological properties of alkaloid natural products, there has been a great deal of focus in the synthetic community towards the asymmetric synthesis of azaheterocycles and their implementation in the total synthesis of complex

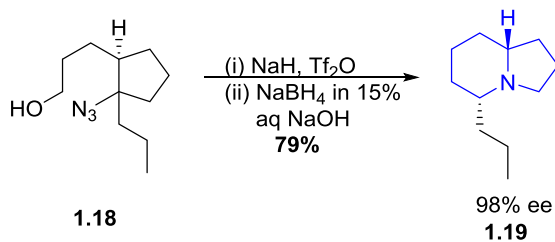
natural products. Over the past 10 years, many novel and attractive strategies for the synthesis of indolizidine natural products have been developed. However, general approaches to access these ring systems are still lacking in the literature, as most methods are designed in the context of the synthesis of specific alkaloid natural products.⁶

Recently, Mann and co-workers described a multicomponent reaction based on a cyclohydrocarbonylation (CHC) of phenylglycinol **1.16** to access **1.1** in 21% overall yield (**Scheme 1.1**).⁷ This is the most recent approach to the coniceine ring system prior to our work.



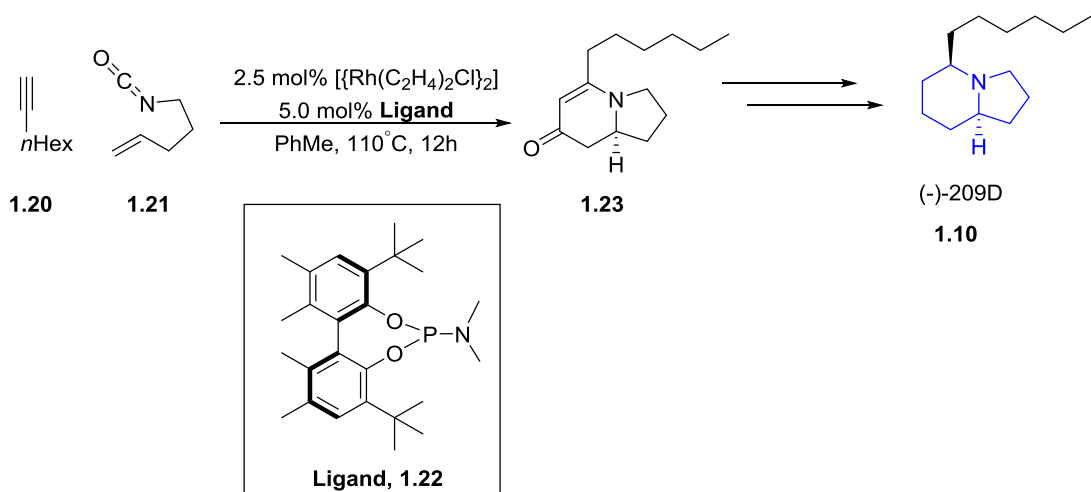
Scheme 1.1. Synthesis of coniceine

Renaud and co-workers built on previous work in the 1990s by Aube and Pearson to demonstrate the use of the intramolecular Schmidt rearrangement of primary azido alcohol **1.18** to access the indolizidine core of (-)-167B with excellent stereocontrol (**Scheme 1.2**).⁸



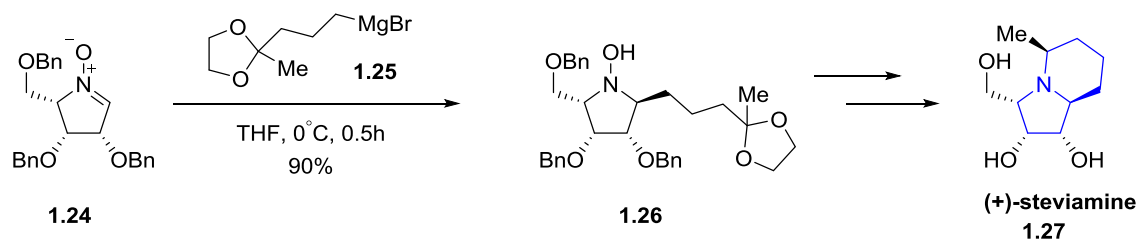
Scheme 1.2. Renaud synthesis of (-)-167B by intramolecular Schmidt rearrangement

A cycloaddition approach was utilized by Rovis and co-workers in 2006, who developed a rhodium(I)-catalyzed [2+2+2] cycloaddition between alkenyl isocyanates **1.21** and alkynes **1.20** to access indolizinones and quinolizinones.⁹ The synthetic utility of this work was subsequently demonstrated by the Rovis group in 2009 in the enantioselective synthesis of alkaloid (-)-209D (**Scheme 1.3**).¹⁰ Reduction of the α,β unsaturated carbonyl is required to access the saturated **1.10**, and the required reaction conditions limit the overall substrate scope of this approach.



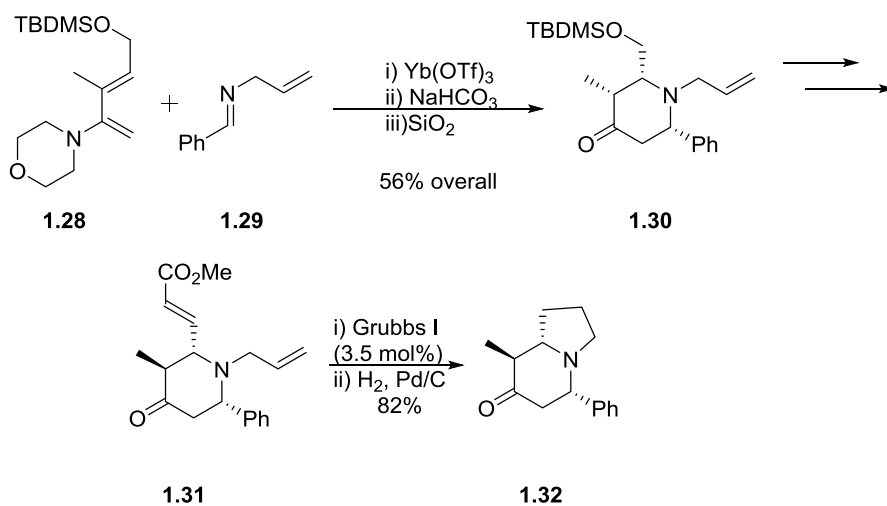
Scheme 1.3. Rovis's synthesis of (-)-209D via rhodium-catalyzed [2+2+2] cycloaddition

Yu and co-workers reported in 2010 the total synthesis of (+)-steviamine via a cyclic nitrene/reductive amination strategy, where Felkin-Anh control of the Grignard addition into the nitrene **1.1.24** is utilized to set the α -amine stereocenter, followed by reductive amination to construct the indolizidine ring system (**Scheme 1.4**).¹¹



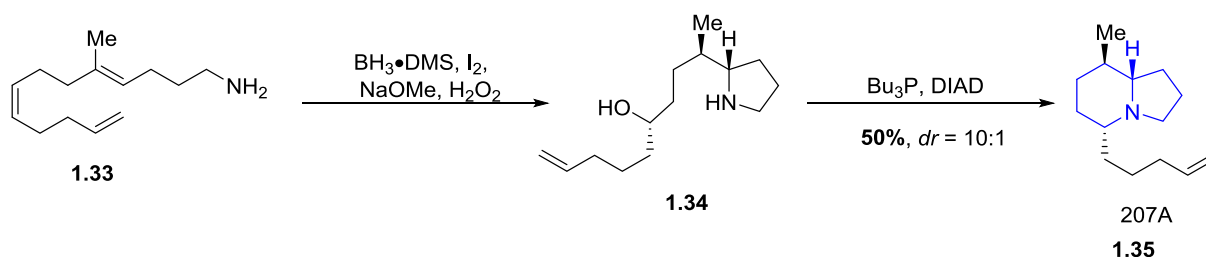
Scheme 1.4. Yu Synthesis of Steviamine

Several groups have employed ring closing metathesis in the construction of indolizidine rings of various alkaloid natural products. In 2002, Valdes and co-workers demonstrated the use of an aza-Diels Alder/RCM strategy to access 5,8-disubstituted indolizidine ring cores (**Scheme 1.5**).¹² The substitution pattern of the piperidone ring was found to exert a significant effect on the ring closing metathesis step.



Scheme 1.5. RCM strategy to access indolizidine ring system **1.32**

In 2012, Shenvi and co-workers reported a stereoselective, intramolecular, formal hydroamination of dienamines by a nitrogen-directed hydroboration (**Scheme 1.6**). This is accomplished through an alkyl shift of the boronic amide formed by treatment of **1.1.39** with borane-dimethyl sulfide and iodine, followed by Mitsunobu conditions to access the indolizidine core. This methodology was shown to access several simple indolizidine alkaloids, including 207A.¹³ The substrate scope of this approach has yet to be fully explored, and substituent pattern of the substrates have a strong effect on stereoselectivity and yield.



Scheme 1.6. Shenvi Synthesis of 207A

1.3. Pyrrolizidine Ring Systems

1.3.1 Pyrrolizidine Alkaloid Natural Products

Pyrrolizidine alkaloids (PAs) are heterocyclic compounds that are typically derived from the ester of basic alcohols known as necine bases. These alkaloids share a common 1-azabicyclo[3.3.0]octane core but differ based on oxygenation pattern and whether or not C1-C2 is saturated.¹⁴ Several natural products containing this azabicyclic core system are outlined in **Figure 1.3**.

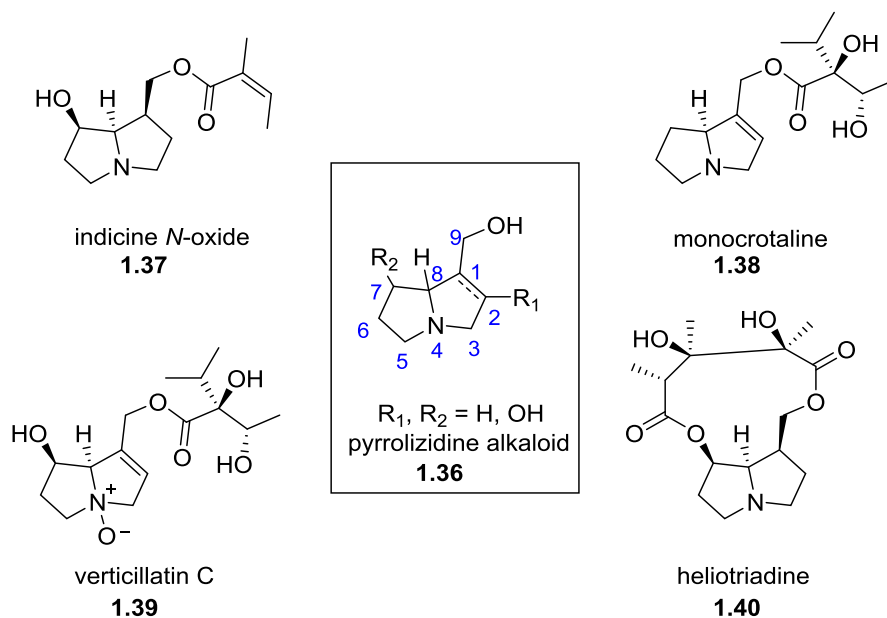


Figure 1.3. Structure and numbering convention of pyrrolizidine alkaloids, and representative examples.

While the amine bases themselves (**Figure 1.4**) are rarely isolated in nature, the corresponding mono- and diesters are more common, either as the tertiary amine or the *N*-oxide. Plants containing pyrrolizidine alkaloids are toxic to mammals, but several insect species have evolved to employ them for their own chemical defense. Interestingly, their toxicity has been attributed to metabolism of the C1-C2 unsaturated congeners leading to the generation of highly reactive alkylating reagents.¹⁵

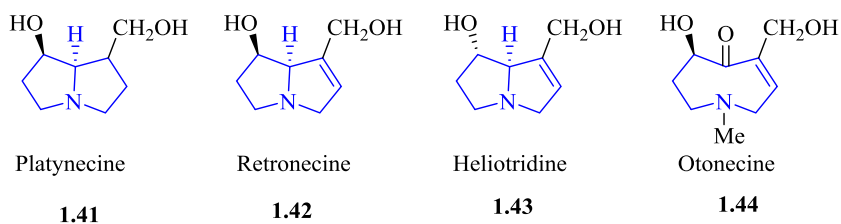


Figure 1.4. Common necine bases

1.3.2. Biosynthesis of Pyrrolizidine Alkaloids

The pyrrolizidine alkaloid class of natural products are secondary metabolites produced by the homospermidine synthase (HSS) pathway in plants, and are believed serve as a chemical defense against herbivores.¹⁶ This pathway is also representative of the biosynthesis of homologously related azabicyclic cores of other alkaloid natural products including indolizidines. The basic building blocks of pyrrolizidine alkaloids are the polyamines spermidine and putrescine. Both spermidine and putrescine are derived from arginine, and are used in the first pathway-specific step of PA biosynthesis in homospermidine formation catalyzed by HSS.¹⁷ The necine base moiety is then formed via an oxidative deamination/condensation sequence. These simple azabicyclic moieties can then be transported from the root of the plant to other organs, where additional modification results in complex alkaloid natural products.

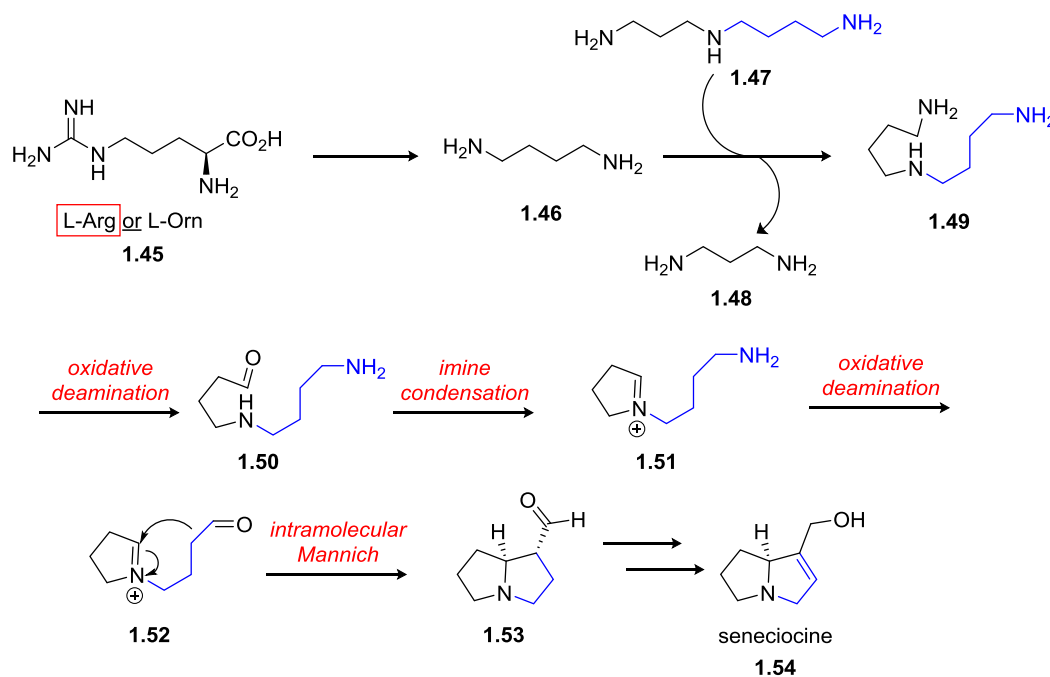
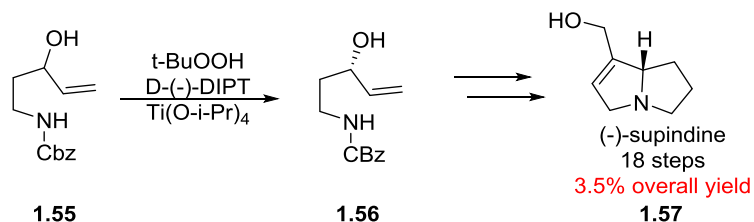


Figure 1.5. Biosynthesis of the azabicyclic core moiety of pyrrolizidine alkaloids

1.3.3. Synthetic Approaches to Pyrrolizidine Ring Systems

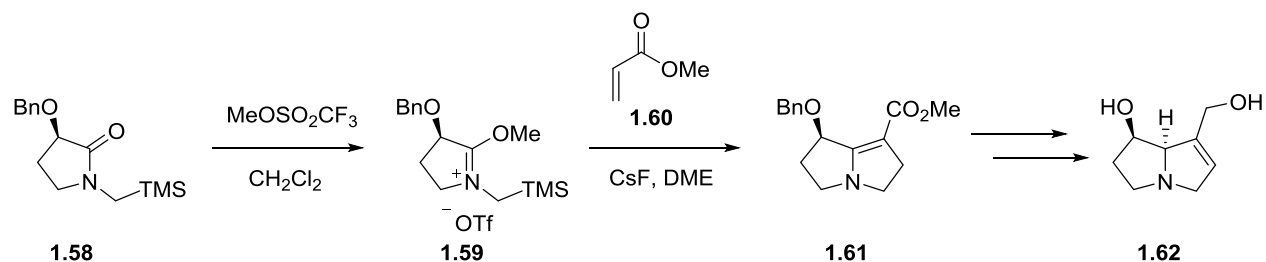
The PAs have historically proven to be synthetically challenging, which has encouraged the development of many conceptually distinct approaches towards their synthesis. Several approaches have utilized cycloaddition reactions with pyrrolidines or intramolecular substitutions to access the azabicyclic core structure. These methods are directed towards the synthesis of complex alkaloid natural products and general approaches to the pyrrolizidine ring skeleton are not well-reported in the literature.⁶

An approach to (-)-supinidine, a basic pyrrolizidine alkaloid building block, was last reported by Takahata and co-workers in 1991, where a Katsuki-Sharpless kinetic resolution of **1.55** was used to access **1.56**. The synthesis of (-)-supinidine (**1.57**) required 18 steps and was accomplished in 3.5% overall yield.¹⁸



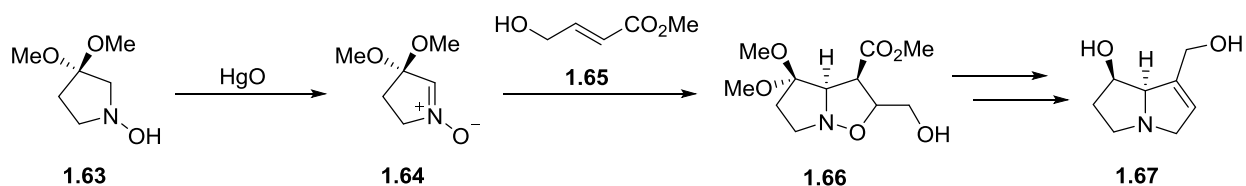
Scheme 1.7. Takahata synthesis of (-)-supinidine

In 1980, Vedejs and co-workers reported the stereoselective total synthesis of retronecine (**1.62**). This was accomplished through a 1,3 dipolar cycloaddition between azomethane ylide **1.59** and methyl acrylate for direct construction of the pyrrolizidine core **1.61** (Scheme 1.8).¹⁹



Scheme 1.8. Vedejs synthesis of retronecine

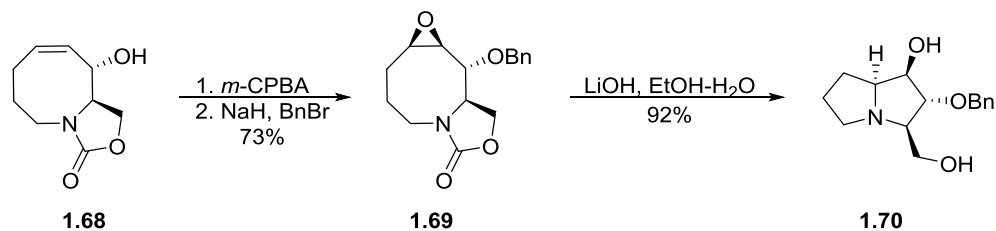
Similarly, Tufariello and co-workers in 1980 disclosed a synthesis of retronecine utilizing a nitron 1,3 dipolar cycloaddition to access the pyrrolizidine core (**Scheme 1.9**).²⁰ Oxidation of hydroxylamine **1.63** provided nitron **1.64**, which in the presence of γ -hydroxycrotonate (**1.65**) underwent cycloaddition with desired regio- and stereochemistry to provide advanced intermediate **1.66**.



Scheme 1.9. Tufariello synthesis of retronecine

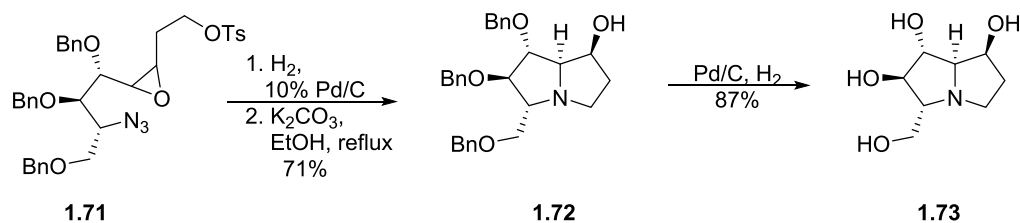
White and co-workers described in 2000 a conceptually unique approach to the synthesis of C3 alkylated hydroxylated pyrrolizidines through a ring closing metathesis / transannular cyclization method (**Scheme 1.10**). Stereoselective epoxidation of azacyclooctene **1.68** followed by transannular opening by nitrogen when treated with

lithium hydroxide produces pyrrolizidine **1.70** where the hydroxyl configurations are set unambiguously.²¹



Scheme 1.10. Transannular cyclization approach to polyhydroxylated pyrrolizidines

Pearson and co-workers reported the reductive double cyclization of azidoepoxides as an effective method to generate pyrrolizidine and indolizidine alkaloids. This was applied to the total synthesis of (+)-australine, where the reductive double-cyclization of azido epoxy tosylate **1.71** provided the pyrrolizidine **1.72**, a precursor to (+)-australine (**1.73**), in good yield (**Scheme 1.11**).²² While effective, this method suffers from poor stereoselectivity during epoxidation to access precursor **1.71**.



Scheme 1.11. Pearson synthesis of (+)-australine

A majority of these previously discussed approaches are directed towards the synthesis of alkaloid natural products with varying substitution patterns, and general approaches to the formation of these ring systems remains under-reported. Recognizing an apparent need in the literature for rapid, enantioselective approaches to these azabicyclic ring systems, we decided to study novel methods for their construction and use in the total synthesis of diverse alkaloid natural products.

1.4. Stereoselective Synthesis of Medium 1-azabicyclo[*m.n.0*]alkyl Ring Systems

1.4.1. Previous Attempts to Access Azabicyclic Ring Systems

Our efforts towards the enantioselective synthesis of azabicyclic ring systems were first born in attempts to synthesize the azepine natural product stemaphylline, a member of the *stemona* class of alkaloids (**Figure 1.6**). Stemaphylline (**1.74**) and its corresponding *N*-oxide was isolated and characterized from the root extracts of *Stemona aphylla* by Pitchaya and co-workers in 2009.²³ Plants containing these alkaloids have been historically employed in traditional medicine in their native regions, and therefore have biological properties that warrant further investigation.

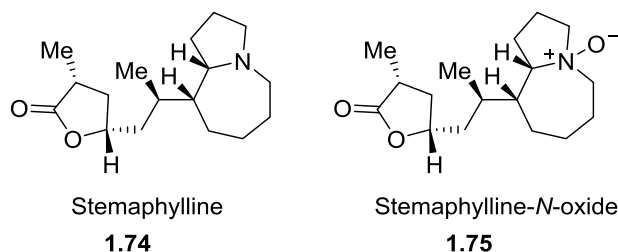
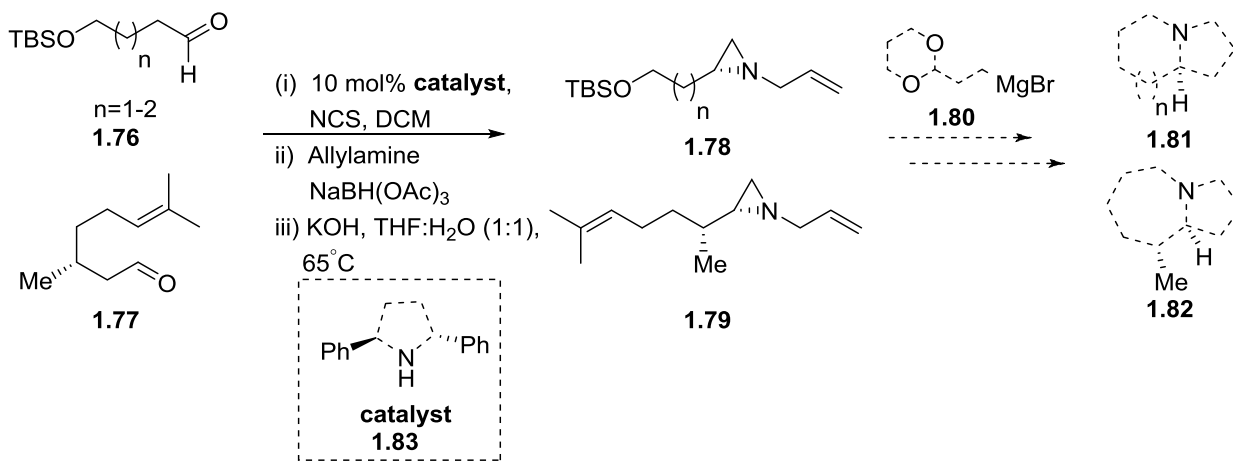


Figure 1.6. Stemaphylline and stemaphylline-*N*-oxide

Initial attempts in our lab towards the total synthesis stemaphylline utilized previous efforts for the organocatalytic enantioselective synthesis of *N*-alkyl aziridines. In this approach a Lewis acid-mediated aziridine opening/reductive elimination protocol was envisioned to install the azabicyclic skeleton of stemaphylline. Unfortunately, attempts to open the aziridine rings **1.78** and **1.79** to the corresponding amines led to complex mixtures, and efforts to optimize the reaction conditions were unsuccessful (**Scheme 1.12**). As the problems associated with the aziridine approach appeared to be difficult to overcome, a new strategy to set the α -amine stereocenter of the indolizidine core was required.



Scheme 1.12. Proposed enantioselective synthesis of 1-azabicyclo[*m.n.0*]alkane ring systems

1.4.2. Chiral *tert*-Butanesulfinylimines as Chiral Directing Groups

An established method for installation of the α -nitrogen stereocenter of chiral amines involves the formation of an *N*-substituted imine (**1.84**), followed by nucleophilic addition into the imine, and finally deprotection to the desired amine (**Figure 1.7**).¹ Many practical examples of this strategy involve placement of a chiral protecting group on the nitrogen substituent. Numerous chiral auxiliaries have been developed over the past thirty years that take advantage of nucleophilic addition into imines to set the chiral center of corresponding amines. Early studies by Franklin Davis at Temple University led to the development of *para*-toluenesulfinimines (*p*TS-imines) in their enantiomerically pure form.²⁴ Davis went on to further demonstrate that the 1,2-addition of organometallic reagents to the chiral imine could be used in asymmetric synthesis to create carbon-nitrogen stereocenters.²⁵ Building on this work, Garcia Ruano at the University of Madrid described chiral *tert*-butanesulfinimines (*t*BS-imines) in his seminal 1996 paper.²⁶ He demonstrated that enhanced diastereofacial selectivity could be achieved in the aziridination of chiral sulfinimines with sulfur ylides compared to the *p*TS-imine group. Despite the foundation laid down by Ruano, *t*BS-imines did not find wide-spread use as a chiral amine building block until the extensive studies carried out by Jonathan Ellman, who pioneered the large-scale synthesis of enantiopure *tert*-butanesulfinamide and demonstrated its versatility as a robust directing group, with an economical price, and facile installation/removal.²⁷

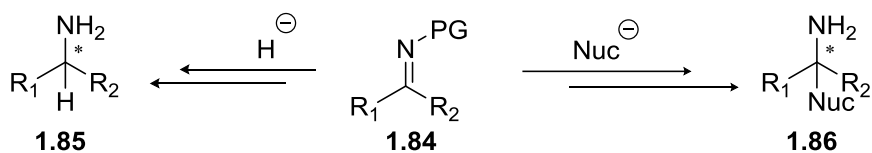
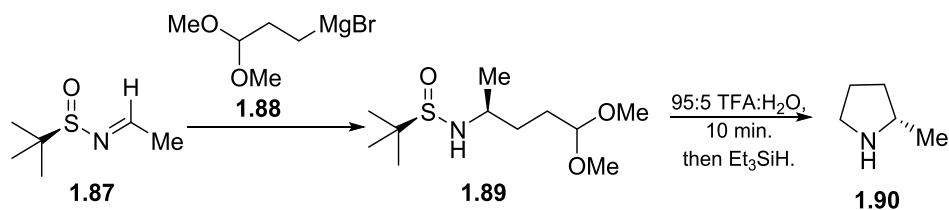


Figure 1.7. Method for the preparation of α chiral amines

1.4.3. Synthetic Approach for Azabicyclic Ring Systems

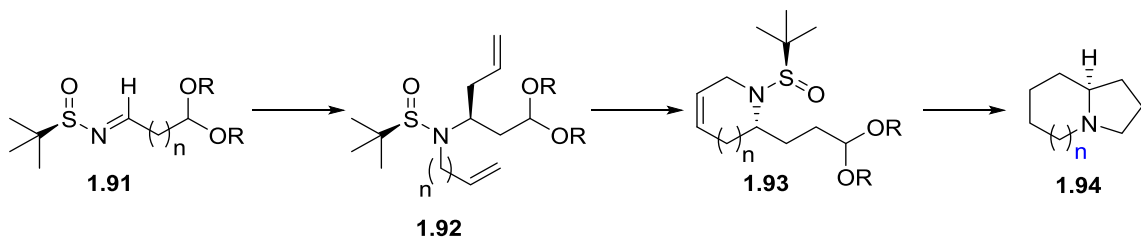
Our proposed method for the asymmetric synthesis of azabicyclic ring systems was inspired by Jonathan Ellman's enantioselective synthesis of 2-substituted pyrrolidines using *tert*-butanesulfinamide that proceeds with high yield and stereoselectivity (**Scheme 1.13**)²⁸. Addition of Grignard reagent **1.88** with a latent aldehyde moiety to a chiral aldimine provided the sulfinamide **1.89** in high yield and diastereoselectivity. A one-pot *N*-deprotection/acetal hydrolysis facilitated an intramolecular reductive amination to produce the optically active 2-substituted pyrrolidine **1.90** in high enantiomeric excess.



Scheme 1.13. Approach to the synthesis of chiral 2-substituted pyrrolidines.

We envisioned a protocol involving a diastereoselective indium-mediated allylation, *N*-alkylation to afford **1.92**, RCM to provide **1.93**, and finally a one-pot

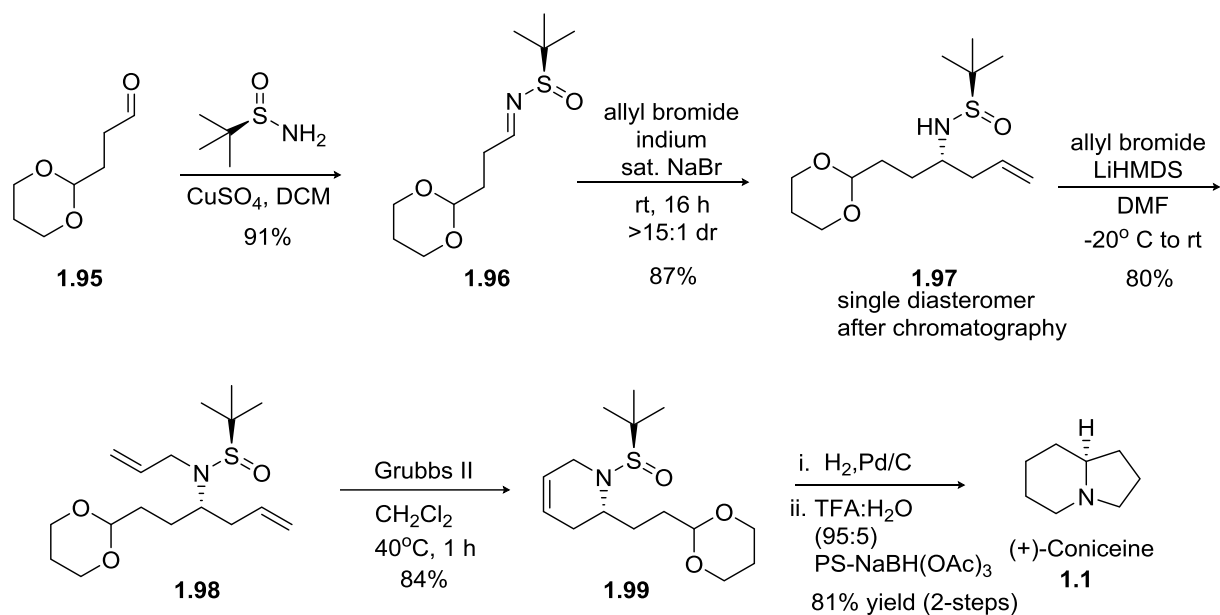
deprotection/hydrolysis/intramolecular reductive amination sequence to access azabicyclic ring skeletons **1.94** with high enantioselectivity (**Scheme 1.14**).



Scheme 1.14. Approach to synthesis of azabicyclic ring systems

1.4.4. Synthesis of Azabicyclic Ring Systems

To explore the scope and potential applications of this strategy, we began preparing pyrrolizidine, indolizidine, and azepine ring systems utilizing chiral *tert*-butanesulfinamide as a chiral directing group. Indium-mediated allylation as described by Xu and coworkers would be utilized to set the α -nitrogen stereocenter (**Scheme 1.15**).²⁹ Chiral aldimine **1.96** underwent indium-mediated allylation to afford amine **1.97** as a single diastereomer after chromatography with >15:1 diastereoselectivity. *N*-allylation followed by RCM provided **1.99** in 67% yield over the two steps. Hydrogenation to reduce the alkene, followed by a one-pot deprotection/acetal hydrolysis/reductive amination sequence provided indolizidine **1.1** as a single enantiomer in 81% yield over the two steps. This approach for (+)-coniceine, the simplest alkaloid possessing the indolizidine azabicyclic core, required only six steps and proceeded in 43% overall yield. This compared favorably to previous syntheses, with the latest having been accomplished in 21% overall yield.¹⁸

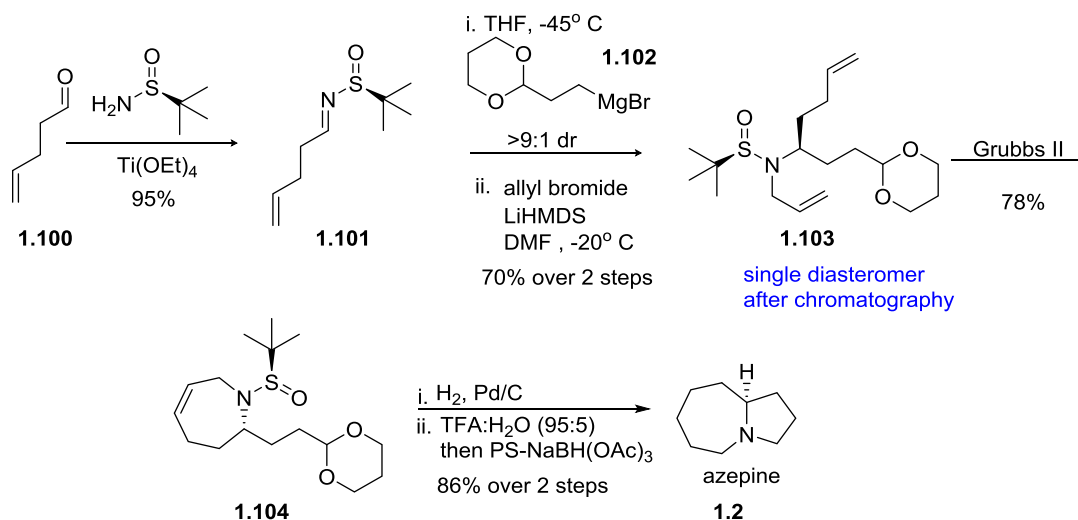


Scheme 1.15. Synthesis of indolizidine ring system

Application of this approach towards the enantioselective synthesis of pyrrolo[1,2-a]azepine **1.2** proved more challenging. In this instance we were unable to alkylate **1.97** with a number of butenyl substrates (Cl, Br, I, OMs, OTs, and OTf) and bases in a reasonable yield. Therefore, we utilized an alternative approach, where the alkene required for RCM to the 7-membered ring would be incorporated into the starting material, and the acetal would be added through Grignard addition into the imine. This circumvented the need to alkylate the *tert*-butanesulfinylamine with the butenyl substrate.

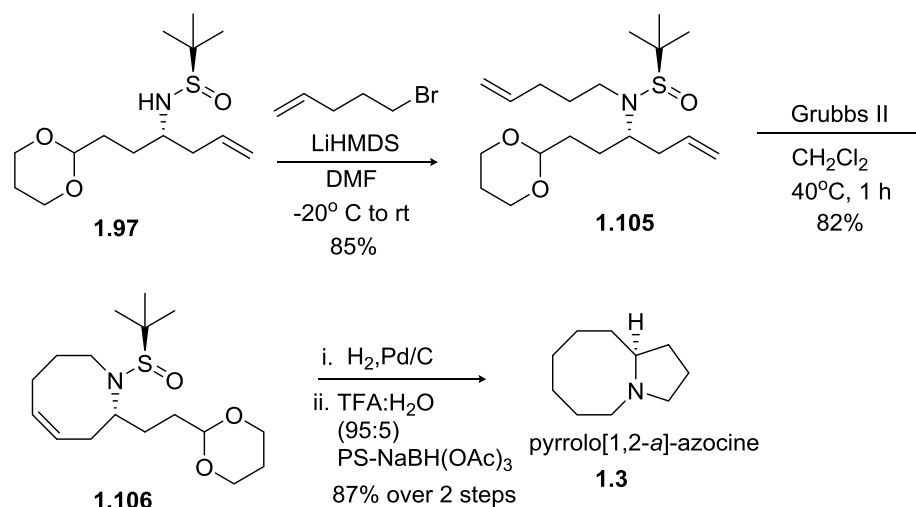
Condensation of 4-pentenal (**1.100**) with chiral *tert*-butanesulfinamine afforded the desired chiral aldimine **1.101** in 95% yield (**Scheme 1.16**). Grignard addition of **1.102** proceeded in 88% yield, which, after *N*-allylation, yielded **1.103** as a single diastereomer after chromatography, with “anti-Ellman” diastereoselectivity >9:1, as will

be later discussed.³⁰ RCM with 2nd generation Grubbs catalyst afforded **1.104** in 78% yield. Hydrogenation to reduce the alkene, followed by a one-pot deprotection/acetal hydrolysis/reductive amination sequence provided **1.2** in 86% yield over the two steps and 45% overall yield for the six step sequence.



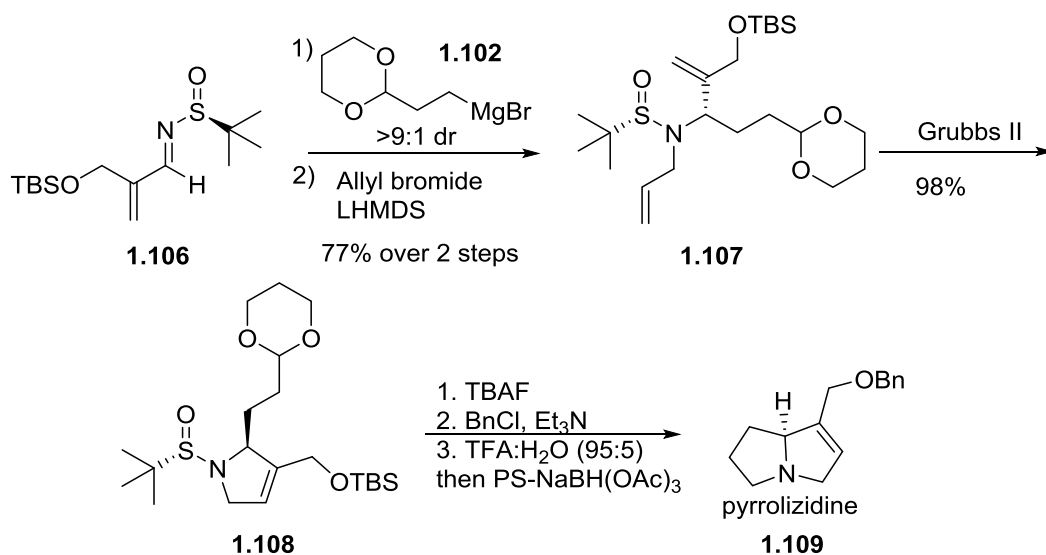
Scheme 1.16. Synthesis of azepine ring system

For the pyrrolo[1,2-*a*]azocine core **1.3**, a similar protocol was employed to that of the indolizidine core **1.1**. Alkylation of key sulfonamide **1.107** with 5-bromo-1-pentene proceeded smoothly to provide **1.105**, which then underwent RCM with Grubbs II to deliver **1.106** in 70% yield for the two steps (**Scheme 1.17**). Hydrogenation to reduce the alkene, followed by a one-pot deprotection/acetal hydrolysis/reductive amination sequence provided **1.3** in 87% yield over the two steps and 60% overall yield for the six-step sequence.



Scheme 1.17. Synthesis of decahydropyrrolo[1,2-*a*]azocine ring system

A parallel strategy was also applied to chiral aldimine **1.106** to access pyrrolizidine ring system **1.109** (Scheme 1.18). Grignard addition into aldimine **1.106**, followed by *N*-allylation facilitated **1.107** to be reached in 77% yield over two steps as a single diastereomer after chromatography. RCM then provided **1.108** in 98% yield. Alcohol deprotection, alkylation with benzyl chloride, followed by a one-pot deprotection/acetal hydrolysis/reductive amination sequence provided **1.109**. Unfortunately, further efforts to deprotect the *O*-benzyl group to the necine base were unsuccessful and led to decomposition of the starting materials. However, this strategy could potentially allow for broad derivitization at the C1 methoxy position, enabling the library synthesis of unnatural pyrrolizidine alkaloids for biological studies.

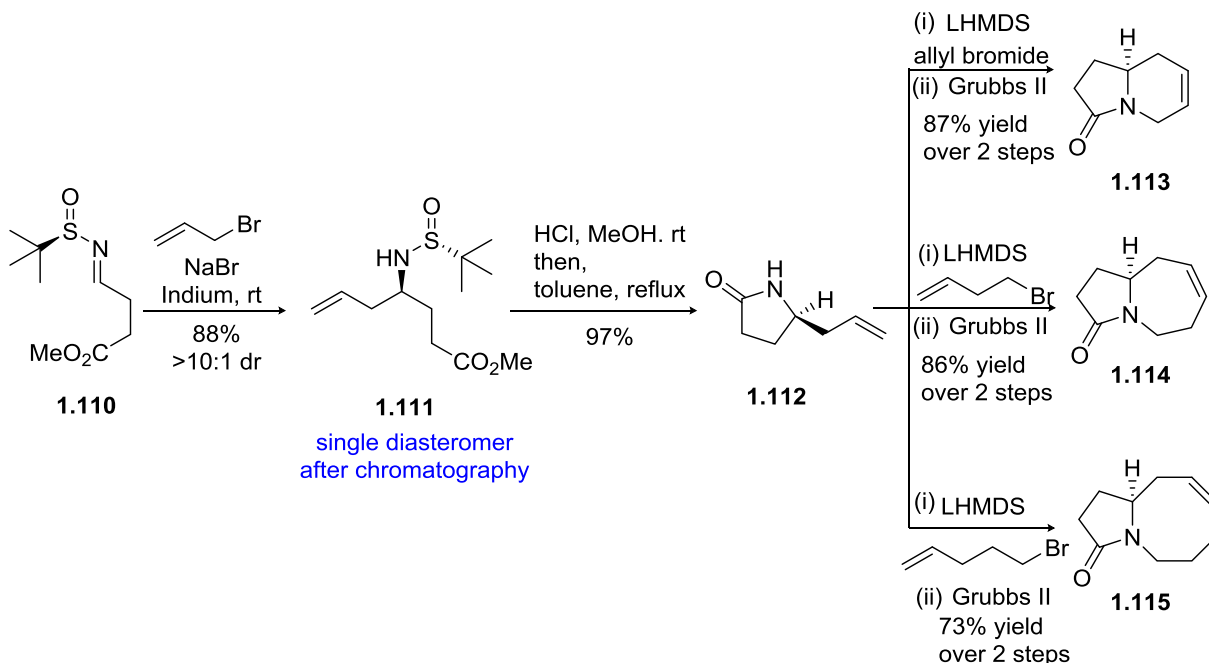


Scheme 1.18. Synthesis of pyrrolizidine ring system

1.4.5. Synthesis of Azabicyclic Lactam Ring Systems

Because many natural products possess the azabicyclic lactam ring skeletons **1.113-1.115**, we next applied our methodology to this core motif (**Scheme 1.19**).³¹ Indium-mediated allylation of chiral aldimine **1.110** proceeded in 88% yield and $>10:1$ diastereoselectivity to access **1.111**. Acid-mediated ring closure facilitated access to pyrrolidinone the key linchpin intermediate **1.112** in 97% yield. Allylation of lactam **1.112** and subsequent RCM with Grubbs II provided indolizidone **1.113** in 87% yield for the two step sequence. Similarly, alkylation of **1.112** with either butenyl bromide or pentenyl bromide, followed by RCM with Grubbs II, afforded azepinone **1.114** or azeocinone **1.115**, respectively. The azabicyclic lactam ring systems were prepared in five steps through the common linchpin intermediate **1.112**, with overall yields ranging

from 56-69%. The alkene can either be reduced or serve as a handle for further functionalization.



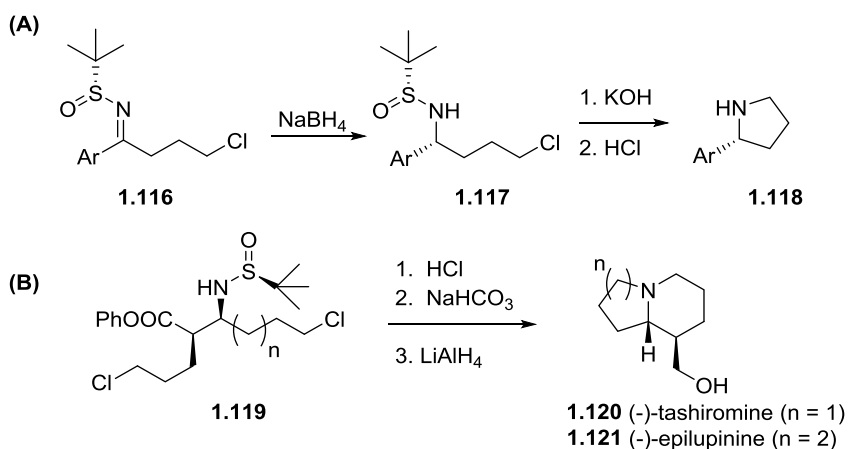
Scheme 1.19. Synthesis of azabicyclic lactam ring systems

1.5. Stereoselective Synthesis of Small to Large 1-azabicyclo[*m.n.0*]alkyl Ring Systems

1.5.1. Alternative Approach to Azabicyclic Ring Systems

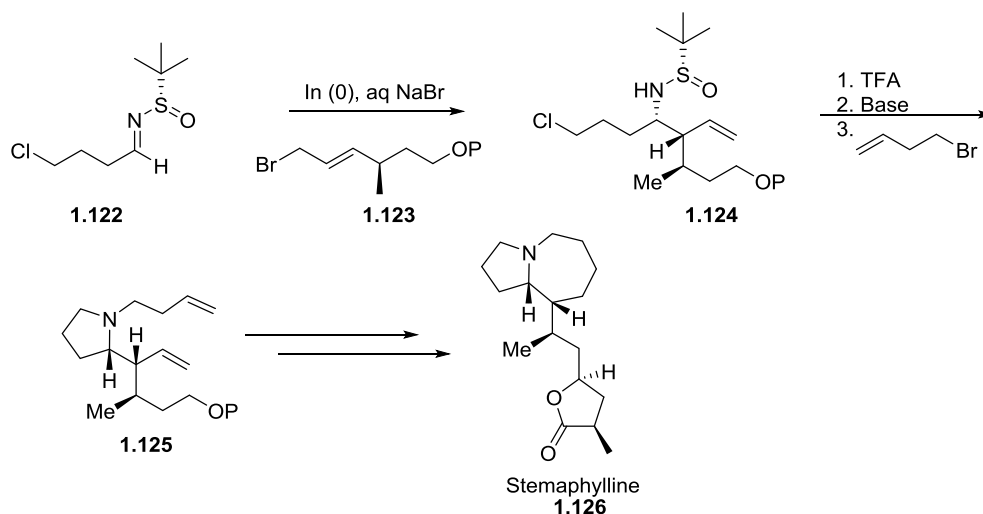
The previously described efforts towards the enantioselective synthesis of 1-azabicyclo[*m.n.0*] alkyl ring systems were a notable advance, however we believed improvements remained to be realized in order to develop a streamlined route to access small to large azabicyclic ring systems. Drawbacks of the initial methodology included the necessity for conceptually different transformations depending on the ring size required and lack of the ability for rapid access to diverse azabicyclic ring systems from a

single linchpin intermediate.³² There were also inconsistencies in alkylation to the *tert*-butanesulfinyl nitrogen which necessitated the need for a route that provided a more predictable reactivity. Given the wide commercial availability and ease of preparation of chloroalkyl alcohols, we envisioned a more modular approach than our previous methodology, which would allow for the rapid generation of diverse azabicyclic cores for applications in medicinal chemistry and diversity-oriented synthesis, as well as the total synthesis of complex natural products. De Kimpe and co-workers recently demonstrated the asymmetric synthesis of 2-arylpyrrolidines **1.118** from γ -chloro *N*-(*tert*-butanesulfinyl)ketimines **1.117** (Scheme 1.20 A), and Brown and co-workers employed a related strategy for the total synthesis of (-)-tashiromine **1.120** and (-)-epilupinine **1.121** (Scheme 1.20 B).^{33,34}



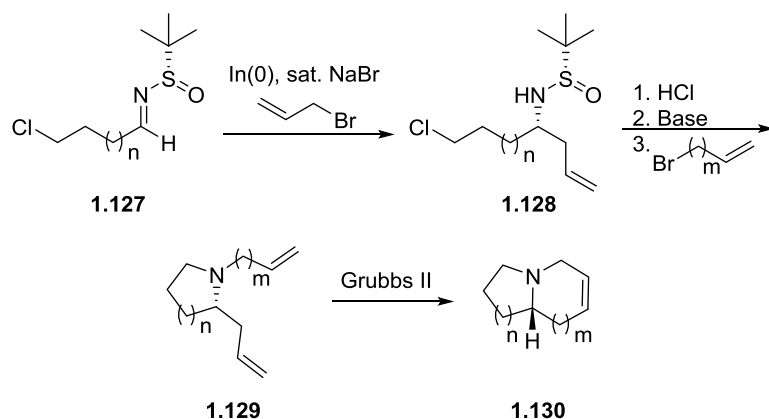
Scheme 1.20. Application of γ -chloro *N*-(*tert*-butanesulfinyl)ketimines to access pyrroles and azabicyclic systems in high enantioselectivity.

Inspired by these results, we envisioned further expanding this methodology and ultimately applying it towards the synthesis of the stemona alkaloid natural product stemaphylline. As shown in **Scheme 1.21**, the azabicyclic core would be installed through a deprotection / intramolecular cyclization / *N*-alkylation sequence, followed by ring closing metathesis.



Scheme 1.21. Approach for the synthesis of stemaphylline

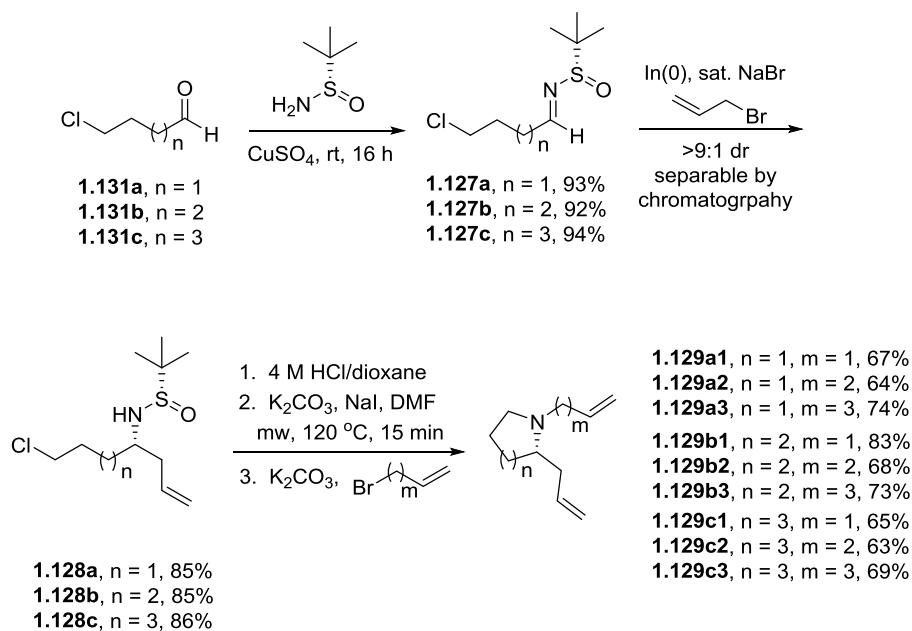
We sought to develop a protocol that would subject various chloroalkyl *N*-(*tert*-butanesulfonyl)aldimines **1.127** to an asymmetric allylation reaction to provide **1.128** in high diastereomeric ratio. Deprotection and alkylation of the pyrrolidine would afford azocines **1.129**, substrates for a ring closing metathesis reaction to provide general, enantioselective access to 1-azabicyclo[*m.n.0*]alkane cores **1.130** with an embedded olefin as a handle for further functionalization (**Scheme 1.22**).



Scheme 1.22. Envisioned route to access diverse 1-azabicyclo[*m.n.0*]alkane cores

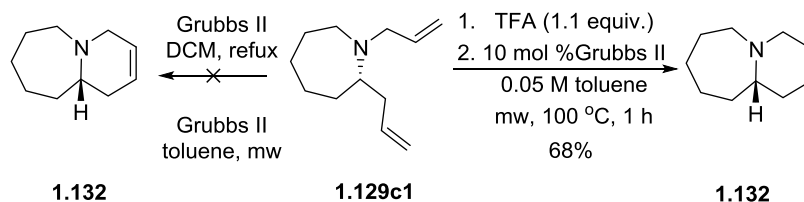
1.5.2. Synthesis of Small to Large 1-azabicyclo[*m.n.0*]alkane Ring Systems

The chloroalkyl *N*-(*tert*-butanesulfinyl)aldimines **1.127** were easily prepared in 92-94% yields by condensing the corresponding chloroaldehydes **1.131** with the Ellman (*S*)-*tert*-butanesulfinamide. A subsequent indium-mediated allylation reaction affords the anticipated (*R*)-anti-adducts **1.128** in >9:1 diastereoselectivity and up to 86% yield. After column chromatography, single diastereomers of analogs **1.128** were isolated, which were carried forward. Acid-mediated deprotection and base-induced, microwave-assisted cyclization and alkylation with the required allyl, butenyl and pentenyl bromides smoothly afforded the chiral *N*-alkyl azocines **1.129** in 63-83% yields for the three step, one-pot reaction sequence (**Scheme 1.23**). To enable the one-pot sequence, a number of bases, solvents and temperatures were evaluated; however, K_2CO_3 , NaI in DMF under microwave irradiation (120 °C, 15 min) proved to be general for our substrates, including the larger 7-azocine rings.



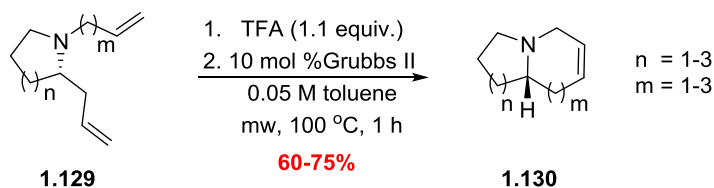
Scheme 1.23. Stereoselective synthesis of *N*-alkyl azocines **1.129**

With all of the chiral *N*-alkyl azocines **1.129** in hand, we focused on the RCM to provide the 1-azabicyclo[*m.n.0*]alkane systems **1.130**. Initial attempts following several known reaction conditions with Grubbs II failed to provide the desired unsaturated 1-azabicyclo[5.4.0]tridecane core of **1.132** (**Scheme 1.24**).



Scheme 1.24. RCM approaches to access the 1-azabicyclo[*m.n.0*]alkane cores

A survey of the literature regarding RCM methods with tertiary amines suggested that protection of the amine by *in situ* generation of ammonium salts enabled facile ring-closing.^{35,36} Thus, treatment of **1.129c1** with 1.1 equivalent of camphor sulfonic acid (CSA) in 0.05 M toluene, followed by the addition of 10 mol% of Grubbs II and microwave heating for 1 hour at 100 °C, provided the unsaturated 1-azabicyclo[5.4.0]tridecane core of **7** in 70% isolated yield. An evaluation of additional acids led to the use of trifluoroacetic acid (TFA), which was equally effective (68% yield) and allowed for simpler purification (**Scheme 1.25**).



Scheme 1.25. Optimal RCM conditions for the enantioselective synthesis of the unsaturated 1-azabicyclo[*m.n.0*]alkane cores **1.4.15**.

With a robust protocol in hand for the RCM, all of the chiral *N*-alkyl azocines **1.129** were converted, under these optimal conditions, into the desired unsaturated 1-azabicyclo[5.4.0]alkane cores **1.130** (**Figure 1.8**). Yields for the RCM reaction averaged 70% for all the substrates **1.129**, providing high yielding, stereoselective access to each of the key 1-azabicyclo[*m.n.0*]alkane systems **1.130**. Overall yields from the commercial aldehydes **1.131** ranged from 29-59%, demonstrating a general route to access these important azabicyclic ring systems.

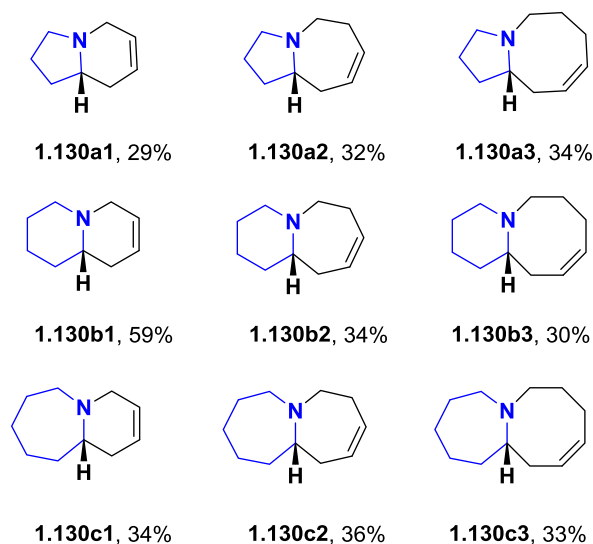


Figure 1.8. Mono-unsaturated 1-azabicyclo[*m.n.0*]alkane ring systems **1.4.15** synthesized

In summary, we have developed a novel approach for the general and enantioselective synthesis of a diverse array of small to large 1-azabicyclo[*m.n.0*]alkane ring systems with an embedded olefin handle for further functionalization. We were also able to extend this methodology to access the respective lactam congeners that are found in a host of natural products as well as pharmaceutical preparations. The stereochemistry is established via a highly diastereoselective indium-mediated allylation of an Ellman sulfinimine in greater than 9:1 *dr*, which is readily separated by column chromatography to afford a single diastereomer. This methodology allows for the rapid preparation of 1-azabicyclo[*m.n.0*]alkane ring systems that are not readily accessible through any other chemistry in excellent overall yields and, for many systems including the pyrrolo[1,2-*a*]azepine, and pyrrolo[1,2-*a*]azocine, are the only enantioselective preparations reported to date. With a strategy to stereoselectively access azabicyclic ring systems now

optimized, we next focused on the applications of this methodology to the total synthesis of alkaloid natural products.

References

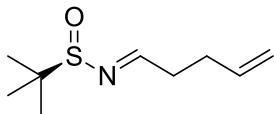
1. Ferreira, F.; Botuha, C.; Chemla, F.; Pérez-Luna, A. *Chem. Soc. Rev.* **2009**, *38*, 1162–1186.
2. Brossi, A. *The Alkaloids: Chemistry and Pharmacology, Vol. 28*; Academic Press, 1986.
3. Michael, J. P. *Nat. Prod. Rep.* **2005**, *22*, 603–626.
4. Butler, M. S.; Robertson, A. A. B.; Cooper, M. A. *Nat. Prod. Rep.* **2014**, *31*, 1612–1661.
5. Cassels, B. K.; Bermúdez, I.; Dajas, F.; Abin-Carriquiry, J. A.; Wonnacott, S. *Drug Discov. Today* **2005**, *10*, 1657–1665.
6. Bhat, C.; Tilve, S. G. *RSC Adv.* **2014**, *4*, 5405.
7. Zill, N.; Schoenfelder, A.; Girard, N.; Taddei, M.; Mann, A. *J. Org. Chem.* **2012**, *77*, 2246–2253.
8. Kapat, A.; Nyfeler, E.; Giuffredi, G. T.; Renaud, P. *J. Am. Chem. Soc.* **2009**, *131*, 17746–17747.
9. Yu, R. T.; Rovis, T. *J. Am. Chem. Soc.* **2006**, *128*, 2782–2783.
10. Yu, R. T.; Lee, E. E.; Malik, G.; Rovis, T. *Angew. Chem. Int. Ed. Engl.* **2009**, *48*, 2379–2382.
11. Hu, X.-G.; Bartholomew, B.; Nash, R. J.; Wilson, F. X.; Fleet, G. W. J.; Nakagawa, S.; Kato, A.; Jia, Y.-M.; van Well, R.; Yu, C.-Y. *Org. Lett.* **2010**, *12*, 2562–2565.
12. Barluenga, J.; Mateos, C.; Aznar, F.; Valdés, C. *Org. Lett.* **2002**, *4*, 1971–1974.
13. Pronin, S. V.; Tabor, M. G.; Jansen, D. J.; Shenvi, R. A. *J. Am. Chem. Soc.* **2012**, *134*, 2012–2015.
14. Robins, D. J. *Nat. Prod. Rep.* **1991**, *8*, 213–221.
15. White, L.; Rubiolo, P.; Bicchi, C.; Hartmann, T. *Phytochemistry* **1993**, *32*, 187–192.
16. Ober, D.; Kaltenecker, E. *Phytochemistry* **2009**, *70*, 1687–1695.

17. Dreger, M.; Stanisławska, M.; Krajewska-patan, A.; Mielcarek, S.; Mikołajczak, P. *Ł. Herba Pol.* **2009**, *55*, 127–147.
18. Zill, N.; Schoenfelder, A.; Girard, N.; Taddei, M.; Mann, A. *J. Org. Chem.* **2012**, *77*, 2246–2253.
19. Vedejs, E.; Martinez, G. R. *J. Am. Chem. Soc.* **1980**, *102*, 7993–7994.
20. Tufariello, J. J.; Lee, G. E. *J. Am. Chem. Soc.* **1980**, *102*, 373–374.
21. White, J. D.; Hrcnciar, P. *J. Org. Chem.* **2000**, *65*, 9129–9142.
22. Pearson, W. H.; Hines, J. V. *J. Org. Chem.* **2000**, *65*, 5785–5793.
23. Mungkornasawakul, P.; Chaiyong, S.; Sastraruji, T.; Jatisatienr, A.; Jatisatienr, C.; Pyne, S. G.; Ung, A. T.; Korth, J.; Lie, W. *J. Nat. Prod.* **2009**, *72*, 848–851.
24. Davis, F. A.; Friedman, A. J.; Kluger, E. W. *J. Am. Chem. Soc.* **1974**, *96*, 5000–5001.
25. Davis, F. A.; Portonovo, P. S.; Reddy, R. E.; Chiu, Y. *J. Org. Chem.* **1996**, *61*, 440–441.
26. Ruano, J. L.; Fernandez, M.; Cruz, A. A. *Tetrahedron: Asymmetry* **1996**, *7*, 3407.
27. Liu, G.; Cogan, D. a.; Ellman, J. a. *J. Am. Chem. Soc.* **1997**, *119*, 9913–9914.
28. Brinner, K. M.; Ellman, J. a. *Org. Biomol. Chem.* **2005**, *3*, 2109–2113.
29. Liu, M.; Shen, A.; Sun, X.-W.; Deng, F.; Xu, M.-H.; Lin, G.-Q. *Chem. Commun. (Camb)*. **2010**, *46*, 8460–8462.
30. *See chapter 2 “Total Synthesis of (+)-Amabiline”.*
31. Fang, F. G.; Feigelson, G. B.; Danishefsky, S. J. *Tetrahedron Lett.* **1989**, *30*, 2743.
32. Fadeyi, O. O.; Senter, T. J.; Hahn, K. N.; Lindsley, C. W. *Chemistry* **2012**, *18*, 5826–5831.
33. Tehrani, K.; D’hooghe, M.; De Kimpe, N. *Tetrahedron* **2003**, *59*, 3099.
34. Leemans, E.; Mangelinckx, S.; De Kimpe, N. *Chem. Commun. (Camb)*. **2010**, *46*, 3122–3124.
35. Merino, P.; Tejero, T.; Greco, C.; Marca, E.; Delso, I.; Gomez-SanJuan, A.; Matute, R. *Heterocycles* **2012**, *84*, 75–100.

36. Woodward, C. P.; Spiccia, N. D.; Jackson, W. R.; Robinson, A. J. *Chem. Commun. (Camb)*. **2011**, 47, 779–781.

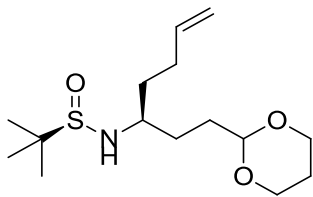
Experimental Methods

Flame-dried (under vacuum) glassware was used for all reactions. All reagents and solvents were commercial grade and purified prior to use when necessary. Thin layer chromatography (TLC) was performed on glass-backed silica gel. Visualization was accomplished with UV light, and/or the use of anisaldehyde and ceric ammonium molybdate solutions followed by charring on a hot-plate. Chromatography on silica gel was performed using Silica Gel 60 (230-400 mesh) from Sorbent Technologies. IR spectra were recorded as thin films and are reported in wavenumbers (cm^{-1}). ^1H & ^{13}C NMR spectra were recorded on Bruker DRX-400 (400 MHz) or Bruker AV-NMR (600 MHz) instrument. Chemical shifts are reported in ppm relative to residual solvent peaks as an internal standard set to δ 7.26 and δ 77.0 (CDCl_3). Mass spectra were obtained on a Micromass Q-ToF API-US mass spectrometer was used to acquire high-resolution mass spectrometry (HRMS) data. The value Δ is the error in the measurement (in ppm) given by the equation $\Delta = [(M_E - M_T) / M_T] \times 10^6$, where M_E is the experimental mass and M_T is the theoretical mass. The HRMS results were obtained with ES as the ion source and leucine enkephalin as the reference.



(R)-2-methyl-N-(pent-4-en-1-ylidene)propane-2-sulfonamide (1.101).

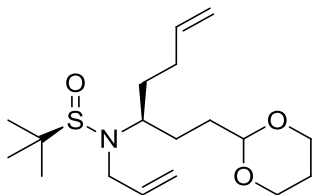
4-pentenal (11.89 mmol, 0.5 g) was dissolved in THF (40 mL) and $\text{Ti}(\text{OEt})_4$ (23.79 mmol, 2 eq.) was added followed by (*R*)-(+)-2-methyl-2-propanesulfonamide (2.0 mmol, 1.0 eq.). The mixture was stirred at rt for 5 h. The reaction is then quenched by addition of an equal volume of sat. NaHCO_3 . The resulting mixture is filtered through a pad of Celite[®] and the filter cake rinsed washed with EtOAc. The filtrate was extracted with EtOAc (3 x 40 mL), the combined organic layer was washed with water, brine and dried over magnesium sulfate. Concentration *in vacuo* gave the crude aldimine which was purified by flash chromatography (4:1 to 1:1 Hex/EtOAc) to yield the desired product 2.11 g (95%) as a colorless oil: $[\alpha]_D^{20} = +276.3$ ($c = 1.00$, CHCl_3); $^1\text{H NMR}$ (400.1 MHz, CDCl_3) δ (ppm): 8.08 (t, $J = 4.4$ Hz, 1H), 5.83 (m, 1H), 5.05 (m, 2H), 2.62 (m, 2H), 2.40 (q, $J = 6.8$, 2H); $^{13}\text{C NMR}$ (100.6 MHz, CDCl_3) δ (ppm): 168.7, 136.6, 115.7, 56.4, 35.2, 29.2, 22.2; HRMS (TOF, ES+) $\text{C}_9\text{H}_{18}\text{NOS}$ $[\text{M}+\text{H}]^+$ calc'd 188.1131, found 188.1130.



(R)-N-((S)-1-(1,3-dioxan-2-yl)hept-6-en-3-yl)-2-methylpropane-2-sulfonamide (1.133)

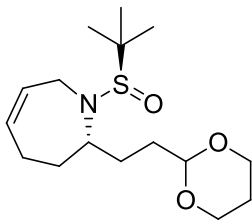
Magnesium turnings (4.99 g, 205.2 mmol) were flame dried with catalytic amount of Iodine in 500 mL reaction flask. 70 mL of THF was added, followed by dropwise addition of 2-(2-Bromoethyl)-1,3-dioxane (6.94 mL, 51.3 mmol). The reaction mixture was periodically cooled in a rt water bath to prevent refluxing. After addition of the 2-(2-bromoethyl)-1,3-dioxane solution was complete, the reaction mixture was stirred for 1 h. The solution was then transferred to a different flask and was cooled to $-78\text{ }^{\circ}\text{C}$. Upon cooling, precipitate was observed and to the solid *N-tert*-Butanesulfinyl imine **1.101** (1.63 g, 10.26 mmol) in 20 mL THF was added dropwise to the Grignard solution, the solution was stirred for overnight at $-48\text{ }^{\circ}\text{C}$ and then warmed to rt. The reaction mixture was quenched with sat NH_4Cl and extracted with EtOAc (3 x 40 mL). The organic layer was dried over sodium sulfate. Concentration *in vacuo* gave crude product as >9:1 dr, which was then purified by flash column chromatography (4:1 to 1:1 Hex/EtOAc) to yield the product in 2.74 g (88%) as a pale yellow oil: $[\alpha]_{\text{D}}^{20} = +55.1$ ($c = 1.00$, CHCl_3); $^1\text{H NMR}$ (400.1 MHz, CDCl_3) δ (ppm): 5.80 (m, 1H), 5.05 (dd, $J = 8.7, 17.2$ Hz, 1H), 4.97 (dd, $J = 8.4$ Hz, 1H), 4.51 (t, $J = 4.4$ Hz, 1H), 4.07 (dd, $J = 10.8, 5.2$ Hz, 2H), 3.75 (dt, $J = 12.4, 2.0$ Hz, 2H), 3.23 (m, 1H), 3.05 (d, $J = 6.8$ Hz, 1H), 2.15 (q, $J = 7.6$, 2H), 2.07 (m, 1H), 1.56-1.75 (m, 6H), 1.54 (m, 1H), 1.33 (d, $J = 13.6$ Hz, 1H), 1.20 (s, 9H); $^{13}\text{C NMR}$ (100.6 MHz, CDCl_3) δ (ppm): 137.9, 115.1, 101.9, 101.8, 66.8, 58.7, 56.2, 55.7, 36.9,

35.4, 31.2, 29.8, 29.7, 25.7, 25.6, 22.6; HRMS (TOF, ES+) C₁₅H₃₀NO₃S [M+H]⁺ calc'd 304.1946, found 304.1945.



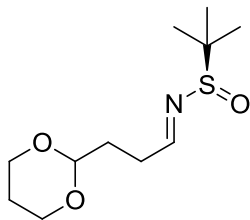
(R)-N-((S)-1-(1,3-dioxan-2-yl)hept-6-en-3-yl)-N-allyl-2-methylpropane-2-sulfonamide (1.103).

To a solution of **1.133** (303 mg, 1 mmol) in DMF (2.8 mL) at -20 °C was added 1 M LiHMDS in THF (1.76 mL, 1.76 mmol) dropwise. The mixture was stirred for 20 mins and allyl bromide (0.43 mL, 5 mmol) was added. After stirring for 2 h, the reaction was quenched with sat. NH₄Cl, extracted with EtOAc (3 x 10 mL). The organic layer was washed with water, brine and dried over Na₂SO₄. Concentration *in vacuo* gave the residue which was then purified by automated flash chromatography (4:1 Hex/EtOAc) to yield the product in 274.4 mg (80%) as a pale yellow oil: [α]_D²⁰ = -40.5 (*c* = 1.00, CHCl₃); ¹H NMR (400.1 MHz, CDCl₃) δ (ppm): 5.71-5.89 (m, 2H), 5.15 (m, 2H), 4.98 (m, 2H), 4.49 (t, *J* = 5.2 Hz, 1H), 4.08 (dd, *J* = 11.6, 4.4 Hz, 2H), 3.95 (dd, *J* = 16.4, 5.2 Hz, 1H), 3.73 (t, *J* = 12.4 Hz, 2H), 3.11 (dd, *J* = 16.4, 7.2 Hz, 2H), 2.93 (m, 1H), 2.17 (m, 1H), 2.05 (m, 2H), 1.87 (m, 1H), 1.70 (m, 1H), 1.62 (m, 4H), 1.32 (d, *J* = 13.6 Hz, 1H), 1.19 (s, 9H); ¹³C NMR (100.6 MHz, CDCl₃) δ (ppm): 137.9, 136.1, 117.4, 114.8, 101.9, 66.8, 57.8, 45.1, 33.0, 32.8, 30.7, 27.6, 25.7, 23.6; HRMS (TOF, ES+) C₁₈H₃₄NO₃S [M+H]⁺ calc'd 344.2259, found 344.2260.



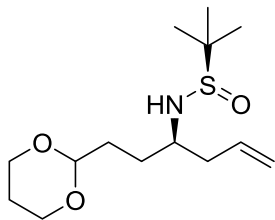
(S)-2-(2-(1,3-dioxan-2-yl)ethyl)-1-((R)-tert-butylsulfinyl)-2,3,4,7-tetrahydro-1H-azepine (1.104)

To a solution of **1.103** (195.7 mg, 0.57 mmol) in CH₂Cl₂ (60 mL) was added 2nd Gen. Grubbs (24.2 mg, 0.028 mmol). The mixture was refluxed for 1 h and concentrated. The resulting crude product was purified by automated flash chromatography (4:1 to 1:1 Hex/EtOAc) to yield the desired product 140.2 mg (78%) as yellow oil: $[\alpha]_D^{20} = +27.5$ ($c = 0.55$, CHCl₃); ¹H NMR (400.1 MHz, CDCl₃) δ (ppm): 5.71 (m, 1H), 5.62 (m, 1H), 4.54 (t, $J = 4.8$ Hz, 1H), 4.11 (dd, $J = 7.4, 4.8$ Hz, 2H), 3.64-3.88 (m, 4H), 3.52 (m, 1H), 2.28 (m, 2H), 2.05 (m, 2H), 1.86 (m, 1H), 1.58-1.73 (m, 4H), 1.33 (q, $J = 13.6$ Hz, 1H), 1.2 (s, 9H); ¹³C NMR (100.6 MHz, CDCl₃) δ (ppm): 131.1, 128.8, 102.1, 66.8, 60.8, 58.4, 42.3, 32.3, 32.2, 27.6, 25.7, 25.0, 23.5; HRMS (TOF, ES+) C₁₆H₃₀NO₃S [M+H]⁺ calc'd 316.1946, found 316.1946.



(R)-N-(3-(1,3-dioxan-2-yl)propylidene)-2-methylpropane-2-sulfinamide (1.96).

To a solution of 3-(1,3-dioxan-2-yl)propanal (2.1 g, 14.6 mmol) in CH₂Cl₂ (100 mL) was added (*R*)-2-methylpropane-2-sulfinamide (2.12 g, 17.5 mmol) and CuSO₄ (7.0 g, 43.8 mmol). The reaction mixture was stirred at rt overnight. The mixture was filtered through a through celite pad and washed with CH₂Cl₂. Concentration *in vacuo* gave the crude product which was purified by automated flash chromatography (4:1 to 1:1 Hex/EtOAc) to yield the desired product 1.91 g (91%) as yellow oil: $[\alpha]_D^{20} = -208.8$ ($c = 0.86$, CHCl₃); ¹H NMR (400.1 MHz, CDCl₃) δ (ppm): 8.11 (t, $J = 4.0$ Hz, 1H), 4.62 (t, $J = 4.8$ Hz, 1H), 4.10 (dd, $J = 6.0, 4.8$ Hz, 2H), 3.76 (m, 2H), 2.64 (sextet, $J = 4.0$ Hz, 2H), 2.07 (m, 1H), 1.93 (m, 2H), 1.32 (dm, $J = 13.8$ Hz, 1H), 1.18 (s, 9H); ¹³C NMR (100.6 MHz, CDCl₃) δ (ppm): 169.1, 101.0, 67.0, 56.7, 30.8, 30.7, 25.8, 22.5; HRMS (TOF, ES+) C₁₁H₂₂NO₃S [M+H]⁺ calc'd 248.1320, found 248.1319.

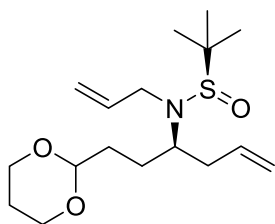


(R)-N-((R)-1-(1,3-dioxan-2-yl)hex-5-en-3-yl)-2-methylpropane-2-sulfonamide (1.97).

In-Mediated allylation were done according to procedures published by Lin and co-workers. To a reaction flask containing **1.96** (1.1 g, 4.45 mmol) and indium powder (2.05 g, 17.8 mmol) was added saturated aqueous NaBr solution (90 mL) followed by the allyl bromide (1.54 mL, 17.8 mmol). The resulting suspension stirred at rt overnight. The reaction was quenched by the addition of saturated aqueous NaHCO₃ and filtered through a pad of celite. The aqueous layer was extracted with EtOAc (3x), dried over Na₂SO₄, filtered, concentrated *in vacuo* to give the crude product as >19:1 *dr*, which was then purified by flash chromatography (1:1 Hex/EtOAc) to yield the allylation product 1.12 g (87%) as a pale yellow oil: $[\alpha]_D^{20} = -46.4$ ($c = 1.79$, CHCl₃); ¹H NMR (400.1 MHz, CDCl₃) δ (ppm): 5.77 (m, 1H), 5.16 (d, $J = 4$ Hz, 1H), 5.13 (s, 1H), 4.51 (t, $J = 4.5$ Hz, 1H), 4.08 (dd, $J = 5.0, 6.3$ Hz, 2H), 3.74 (dt, $J = 10, 2.2$ Hz, 2H), 3.30 (m, 1H), 3.23 (d, $J = 6.5$ Hz, 1H), 2.37 (m, 2H), 2.05 (m, 1H), 1.63 (m, 3H), 1.33 (br, $J = 14$ Hz, 1H), 1.19 (s, 9H); ¹³C NMR (100.6 MHz, CDCl₃) δ (ppm): 133.9, 119.0, 101.9, 66.8, 55.8, 55.0, 40.5, 31.3, 29.2, 25.7, 22.6; HRMS (TOF, ES+) C₁₄H₂₈NO₃S [M+H]⁺ calc'd 290.1790, found 290.1790.

General Procedure for *N*-alkylation:

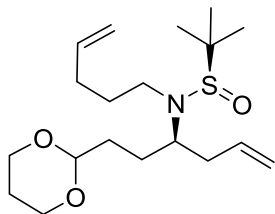
To a solution of sulfinamide **1.97** (1 equiv), in DMF at -20 °C was added LiHMDS (1 M, 1.0 equiv) and the mixture was stirred for 20 mins. Bromide (1.5 equiv.) was then added slowly to the mixture and the reaction was stirred for 3 hrs at rt. The reaction was quenched with saturated NH₄Cl solution and extracted with EtOAc (3x). The combined organic extracts were washed with water and the dried over Na₂SO₄. Filtration and concentration afforded the crude product, which was purified by flash chromatography (4:1 Hex/EtOAc).



(*R*)-*N*-((*R*)-1-(1,3-dioxan-2-yl)hex-5-en-3-yl)-*N*-allyl-2-methylpropane-2-sulfinamide (1.98).

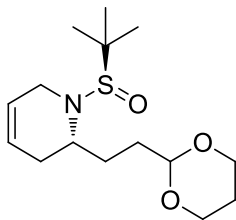
The product was prepared according to the general procedure using allyl bromide. The reaction was run on a 1 mmol scale, to afford the product as a off white gum (263.2 mg, 80%): $[\alpha]_D^{20} = +40.1$ ($c = 1.11$, CHCl₃); ¹H NMR (400.1 MHz, CDCl₃) δ (ppm): 5.82 (m, 2H), 5.03-5.21 (m, 4H), 4.49 (t, $J = 4.8$ Hz, 1H), 4.07 (dd, $J = 6.8, 4.8$ Hz, 2H), 3.94 (dd, $J = 11.6, 5.2$ Hz, 1H), 3.74 (t, $J = 12.0$ Hz, 2H), 3.20 (dd, $J = 9.6, 6.8$ Hz, 1H), 3.09 (q, $J = 6.8$ Hz, 1H), 2.24-2.41 (m, 2H), 2.34 (t, $J = 6.2$ Hz, 1H), 1.83 (m, 1H), 1.65-1.73 (m, 2H), 1.62 (m, 1H), 1.33 (d, $J = 13.6$ Hz, 1H), 1.19 (s, 9H); ¹³C NMR (100.6 MHz,

CDCl₃) δ (ppm): 136.5, 135.9, 117.4, 117.1, 102.2, 67.0, 58.2, 45.2, 39.1, 33.0, 27.6, 25.9, 23.9; HRMS (TOF, ES+) C₁₇H₃₂NO₃S [M+H]⁺ calc'd 330.2103, found 330.2104.



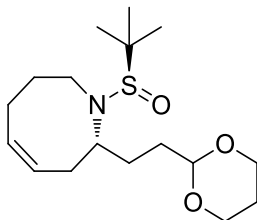
(R)-N-((R)-1-(1,3-dioxan-2-yl)hex-5-en-3-yl)-2-methyl-N-(pent-4-en-1-yl)propane-2-sulfinamide (1.105).

The product was prepared according to the general procedure using 5-bromopent-1-ene. The reaction was run on a 1 mmol scale, to afford the product as yellow oil (303.4 mg, 85 α]_D²⁰ = +39.7 (*c* = 0.91, CHCl₃); ¹H NMR (400.1 MHz, CDCl₃) δ (ppm): 5.79 (m, 2H), 5.03 (m, 4H), 4.51 (t, *J* = 4.8 Hz, 1H), 4.07 (dd, *J* = 6.8, 4.8 Hz, 2H), 3.94 (dt, *J* = 12.0, 2.4 Hz, 2H), 3.23 (m, 1H), 3.06 (q, *J* = 6.4 Hz, 1H), 2.56 (m, 1H), 2.33 (m, 2H), 2.07 (m, 3H), 1.59-1.86 (m, 6H), 1.32 (d, *J* = 13.6 Hz, 1H), 1.19 (s, 9H); ¹³C NMR (100.6 MHz, CDCl₃) δ (ppm): 137.8, 136.0, 117.1, 115.14, 102.3, 67.0, 66.9, 57.9, 42.8, 39.2, 33.1, 31.6, 29.6, 28.0, 24.0; HRMS (TOF, ES+) C₁₉H₃₆NO₃S [M+H]⁺ calc'd 358.2416, found 358.2416.



**(R)-2-(2-(1,3-dioxan-2-yl)ethyl)-1-((R)-tert-butylsulfinyl)-1,2,3,6-tetrahydropyridine
(1.99).**

To a solution of **1.98** (200 mg, 0.61 mmol) in CH₂Cl₂ (65 mL) was added 2nd Gen. Grubbs (25.9 mg, 0.030 mmol). The mixture was refluxed for 1 h and concentrated. The resulting crude product was purified by automated flash chromatography (4:1 to 1:1 Hex/EtOAc) to yield the desired product 154.2 mg (84%) as off white solid: $[\alpha]_D^{20} = +20.7$ ($c = 1.05$, CHCl₃); ¹H NMR (400.1 MHz, CDCl₃) δ (ppm): 5.69 (m, 2H), 4.53 (t, $J = 5.2$ Hz, 1H), 4.10 (dd, $J = 7.6, 4.0$ Hz, 2H), 3.85 (m, 1H), 3.76 (tt, $J = 12.0, 2.8$ Hz, 2H), 3.29-3.40 (m, 2H), 2.55 (m, 1H), 2.01-2.13 (m, 1H), 1.85-1.91 (m, 2H), 1.70-1.79 (m, 1H), 1.57-1.66 (m, 2H), 1.34 (d, $J = 13.6$ Hz, 1H), 1.16 (s, 9H); ¹³C NMR (100.6 MHz, CDCl₃) δ (ppm): 125.26, 123.57, 102.17, 67.00, 58.62, 56.90, 36.46, 32.86, 28.16, 26.88, 25.85, 23.49; HRMS (TOF, ES+) C₁₅H₂₈NO₃S [M+H]⁺ calc'd 302.1790, found 302.1788.



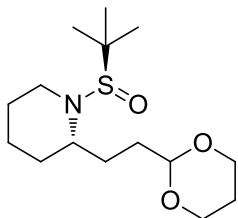
(R)-8-(2-(1,3-dioxan-2-yl)ethyl)-1-((R)-tert-butylsulfinyl)-1,2,3,4,7,8-hexahydroazocine (1.106).

To a solution of **1.105** (217.8 mg, 0.61 mmol) in CH₂Cl₂ (65 mL) was added 2nd Gen. Grubbs (25.9 mg, 0.030 mmol). The mixture was refluxed for 1 h and concentrated. The resulting crude product was purified by automated flash chromatography (4:1 to 1:1 Hex/EtOAc) to yield the desired product 178.6 mg (82%) as off white solid: $[\alpha]_D^{20} = +24.6$ ($c = 1.16$, CHCl₃); ¹H NMR (400.1 MHz, CDCl₃) δ (ppm): 5.75 (m, 2H), 4.52 (t, $J = 4.4$ Hz, 1H), 4.09 (m, 2H), 3.75 (m, 3H), 3.19 (m, 2H), 2.3-2.4 (m, 2H), 2.15-2.2 (m, 1H), 1.98-2.1 (m, 2H), 1.53-1.8 (m, 5H), 1.45 (m, 1H), 1.30 (d, $J = 13.6$ Hz, 1H), 1.18 (s, 9H); ¹³C NMR (100.6 MHz, CDCl₃) δ (ppm): 132.3, 127.6, 102.5, 67.0, 66.9, 58.2, 45.8, 32.7, 31.2, 30.9, 27.4, 25.9, 24.0, 23.9; HRMS (TOF, ES+) C₁₇H₃₂NO₃S [M+H]⁺ calc'd 330.2103, found 330.2104.

General Procedure for Alkene-Reduction:

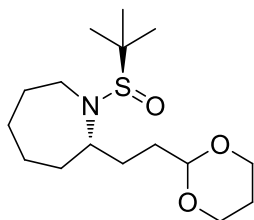
To a solution of sulfinamide (0.43 mmol) in EtOH (7 mL) was added Pd/C (45.6 mg, 0.43 mmol). The reaction mixture was purged and back filled with H₂ gas. The mixture was stirred at rt overnight. The mixture was filtered through celite pad and washed with

CH₂Cl₂. Concentration *in vacuo* gave the crude product which was used without purification.



(R)-2-(2-(1,3-dioxan-2-yl)ethyl)-1-((R)-tert-butylsulfinyl)piperidine (1.134):

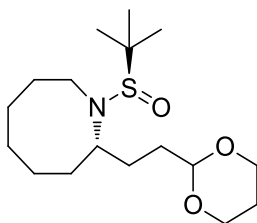
$[\alpha]_D^{20} = -3.06$ ($c = 1.00$, CHCl₃); ¹H NMR (400.1 MHz, CDCl₃) δ (ppm): 4.52 (t, $J = 5.2$ Hz, 1H), 4.09 (dd, $J = 6.4, 4.4$ Hz, 2H), 3.75 (t, $J = 11.6$ Hz, 2H), 3.19-3.26 (m, 2H), 3.04 (m, 1H), 2.02-2.12 (m, 1H), 1.77-1.92 (m, 3H), 1.46-1.72 (m, 7H), 1.34 (d, $J = 13.6$ Hz, 1H), 1.16 (s, 9H); ¹³C NMR (100.6 MHz, CDCl₃) δ (ppm): 102.3, 67.1, 59.2, 58.5, 40.7, 32.7, 29.0, 26.3, 25.9, 25.7, 23.7, 19.6; HRMS (TOF, ES+) C₁₅H₃₀NO₃S [M+H]⁺ calc'd 304.1946, found 304.1946.



(S)-2-(2-(1,3-dioxan-2-yl)ethyl)-1-((R)-tert-butylsulfinyl)azepane (1.135):

$[\alpha]_D^{20} = -1.7$ ($c = 0.33$, CHCl₃); ¹H NMR (400.1 MHz, CDCl₃) δ (ppm): 4.52 (t, $J = 5.2$ Hz, 1H), 4.10 (dd, $J = 6.8, 4.8$ Hz, 2H), 3.75 (t, $J = 12.0$ Hz, 2H), 3.48 (q, $J = 6.0$ Hz,

1H), 3.37 (m, 1H), 3.08 (m, 1H), 2.05 (m, 1H), 1.82-1.89 (m, 2H), 1.77 (m, 1H), 1.45-1.65 (m, 9H), 1.33 (d, $J = 13.6$ Hz, 1H), 1.21 (s, 9H); ^{13}C NMR (100.6 MHz, CDCl_3) δ (ppm): 101.5, 66.3, 60.8, 57.7, 42.3, 33.3, 32.1, 29.7, 27.6, 27.1, 25.3, 23.9, 23.5; HRMS (TOF, ES+) $\text{C}_{16}\text{H}_{32}\text{NO}_3\text{S}$ $[\text{M}+\text{H}]^+$ calc'd 318.2103, found 318.2101.



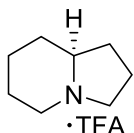
(R)-2-(2-(1,3-dioxan-2-yl)ethyl)-1-((R)-tert-butylsulfinyl)azocane (1.136):

$[\alpha]_{\text{D}}^{20} = -16.9$ ($c = 0.34$, CHCl_3); ^1H NMR (400.1 MHz, CDCl_3) δ (ppm): 4.51 (t, $J = 5.2$ Hz, 1H), 4.08 (m, 2H), 3.75 (tt, $J = 12.0, 2.4$ Hz, 2H), 3.31-3.38 (m, 2H), 3.14-3.25 (m, 2H), 2.01-2.12 (m, 1H), 1.81-1.89 (m, 2H), 1.57-1.74 (m, 8H), 1.52 (m, 1H), 1.30-1.44 (m, 3H), 1.2 (s, 9H); ^{13}C NMR (100.6 MHz, CDCl_3) δ (ppm): 102.3, 67.0, 59.7, 58.6, 43.5, 33.1, 32.8, 29.2, 28.9, 28.6, 25.9, 25.0, 24.1, 22.9; HRMS (TOF, ES+) $\text{C}_{17}\text{H}_{34}\text{NO}_3\text{S}$ $[\text{M}+\text{H}]^+$ calc'd 332.2259, found 332.2257.

General Procedure for Ring Closure.

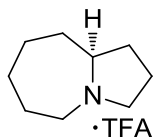
To the crude product cooled to 0 °C was added 5 ml of 95:5 TFA/ H_2O , after stirring at rt for 1 h the mixture was concentrated in vacuo to remove the TFA / H_2O solvent. The residue was dissolved in DCE and PS- $\text{NaBH}(\text{OAc})_3$ (0.5 g, 1.08 mmol) was added and

placed on a shaker overnight. The beads were filtered off and the solvent was concentrated *in vacuo* to give the crude azabicyclic product. Purification by flash chromatography gave the desired azabicyclic ring product.



(S)-octahydroindolizine (1.1).

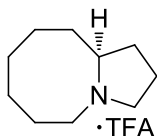
Flash chromatography (9:1:0.5 CH₂Cl₂/MeOH/NH₃) yield the product 10.1 mg (81% over 2-steps) as a yellow oil: $[\alpha]_D^{20} = +1.9$ ($c = 1.14$, EtOH); ¹H NMR (400.1 MHz, MeOD) δ (ppm): 4.44 (dt, $J = 2, 4$ Hz, 1H), 3.61, m, 1H), 3.37 (m, 1H), 3.12 (m, 1H), 2.98 (t, $J = 12.6$ Hz, 1H), 2.04 (m, 1H), 1.89-1.39 (m, 9H); ¹³C NMR (100.6 MHz, MeOD) δ (ppm): 62.2, 58.2, 45.9, 31.8, 29.8, 28.9, 23.5, 23.1; HRMS (TOF, ES+) C₈H₁₆N [M+H]⁺ calc'd 126.1277, found 126.1276.



(S)-octahydro-1H-pyrrolo[1,2-a]azepine (1.2).

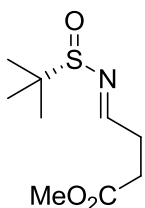
Flash chromatography (9:1:0.5 CH₂Cl₂/MeOH/NH₃) yield the product 11.9 mg (86% over 2-steps) as off white solid: $[\alpha]_D^{23} = +0.6$ ($c = +1.55$, EtOH); ¹H NMR (400.1 MHz, MeOD) δ (ppm): 4.57 (s, 1H), 3.60 (m, 2H), 3.23 (m, 1H), 3.17 (m, 1H), 2.05-1.59 (m,

12H); ^{13}C NMR (100.6 MHz, MeOD) δ (ppm): 62.21, 60.41, 46.51, 32.29, 31.83, 29.46, 27.57, 26.13, 25.74; HRMS (TOF, ES+) $\text{C}_{14}\text{H}_{18}\text{O}_4$ $[\text{M}+\text{H}]^+$ calc'd 140.1439, found 140.1439.



(S)-decahydropyrrolo[1,2-a]azocine (1.3).

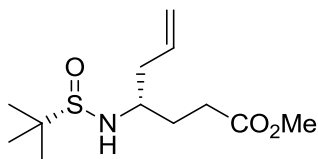
Flash chromatography (9:1:0.5 $\text{CH}_2\text{Cl}_2/\text{MeOH}/\text{NH}_3$) yield the product 13.3 mg (87% over 2-steps) as off white solid: $[\alpha]_{\text{D}}^{20} = +1.1$ ($c = 1.85$, EtOH); ^1H NMR (400.1 MHz, MeOD) δ (ppm): 3.62 (m, 2H), 3.34 (m, 1H), 3.18 (m, 2H), 1.6-2.0 (m, 14H); ^{13}C NMR (100.6 MHz, CDCl_3) δ (ppm): 60.7, 57.4, 44.2, 30.8, 28.1, 27.9, 24.6, 24.1, 24.0, 23.2; HRMS (TOF, ES+) $\text{C}_{10}\text{H}_{20}\text{N}$ $[\text{M}+\text{H}]^+$ calc'd 154.1596, found 154.1594.



(S)-methyl 4-((*tert*-butylsulfinyl)imino)butanoate (1.110).

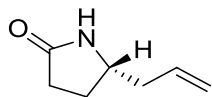
To a solution of methyl 4-oxobutanoate (10 g, 86.2 mmol) in CH_2Cl_2 (500 mL) was added (*S*)-2-methylpropane-2-sulfinamide (12.9 g, 106.2 mmol) and CuSO_4 (54.7 g, 344.0 mmol). The reaction mixture was stirred at rt overnight. The mixture was filtered

through a pad of celite and washed with CH₂Cl₂. Concentration *in vacuo* gave the crude product which was purified by automated flash chromatography (4:1 to 1:1 Hex/EtOAc) to yield the desired product 17.9 g (95%) as yellow oil: $[\alpha]_D^{20} = +178.1$ ($c = 1.67$, CHCl₃); ¹H NMR (400.1 MHz, CDCl₃) δ (ppm): 8.13 (t, $J = 2.8$ Hz, 1H), 3.68 (s, 3H), 2.82-2.94 (m, 2H), 2.70-2.82 (m, 1H), 2.59-2.67 (m, 1H), 1.17 (s, 9H); ¹³C NMR (100.6 MHz, CDCl₃) δ (ppm): 172.4, 167.3, 56.9, 51.9, 31.2, 29.2, 22.4; HRMS (TOF, ES+) C₉H₁₈NO₃S [M+H]⁺ calc'd 220.1007, found 220.1007.



(S)-methyl-4-((S)-1,1-dimethylethylsulfonamido)hept-6-enoate (1.111).

In-Mediated allylation were done according to procedures previously shown above for **1.97**. The reaction was run on a 50 mmol scale, to afford the crude product as >19:1 *dr*, which was then purified by flash chromatography (1:1 Hex/EtOAc) to yield the allylation product 11.5 g (88%) as yellow oil: $[\alpha]_D^{20} = +45.7$ ($c = 0.95$, CHCl₃); ¹H NMR (400.1 MHz, CDCl₃) δ (ppm): 5.78 (m, 1H), 5.15 (m, 2H), 3.67 (s, 3H), 3.40 (m, 1H), 3.22 (d, $J = 7.2$ Hz, 1H), 2.40 (m, 3H), 1.90 (m, 1H), 1.75 (m, 1H), 1.20 (s, 9H); ¹³C NMR (100.6 MHz, CDCl₃) δ (ppm): 173.9, 133.6, 119.6, 56.1, 55.1, 51.9, 40.1, 30.5, 30.1, 22.8; HRMS (TOF, ES+) C₁₂H₂₄NO₃S [M+H]⁺ calc'd 262.1477, found 262.1476.



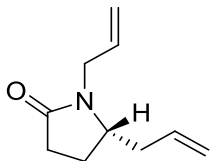
(S)-5-allylpyrrolidin-2-one (1.112).

To a solution of compound **1.111** (2.61 g, 10 mmol) in methanol (100 mL) was added 10 mL of 12 N HCl aqueous solution at room temperature. The resultant mixture was then stirred at rt for 2 h. After concentrated, the residue was dissolved in 150 mL CH₂Cl₂ and 200 mL of saturated aqueous Na₂CO₃ was added. After stirring overnight, the mixture is extracted with CH₂Cl₂; combined organic extracts were washed with water and brine and dried over Na₂SO₄. Filtration and concentration afforded the crude product, which was purified by flash chromatography (1:1 Hex/EtOAc) to yield the desired product 1.21 g (97%) as brown oil: $[\alpha]_D^{20} = +2.5$ ($c = 1.16$, CHCl₃); ¹H NMR (400.1 MHz, CDCl₃) δ (ppm); 6.43 (br s, 1H), 5.74 (m, 1H), 5.11 (d, $J = 12.7$ Hz, 2H), 3.70 (q, $J = 6.5$ Hz, 1H), 2.32 (m, 2H), 2.22 (m, 3H), 1.76 (m, 1H); ¹³C NMR (100.6 MHz, CDCl₃) δ (ppm): 173.4, 153.5, 146.9, 130.5, 125.5, 125.2, 116.6, 113.9, 111.9, 60.6, 55.7, 34.1, 28.6, 14.2; HRMS (TOF, ES+) C₇H₁₂NO [M+H]⁺ calc'd 126.0919, found 126.0921.

General Procedure for lactam N-alkylation:

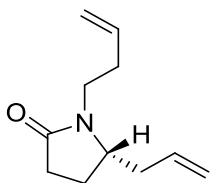
To a solution of lactam **1.112** (1 equiv), in DMF at 0 °C was added NaH (1.02 equiv) and the mixture was stirred for 10 mins and additional 10 mins at rt. At 0 °C bromide (1.5 equiv.) was then added slowly to the mixture and the reaction was warmed to rt and stirred for 2 hrs. The reaction was quenched with water and extracted with EtOAc (3x). The combined organic extract was the dried over Na₂SO₄. Filtration and concentration

afforded the crude product, which was purified by flash chromatography (1:1 Hex/EtOAc).



(S)-1,5-diallylpyrrolidin-2-one (1.137):

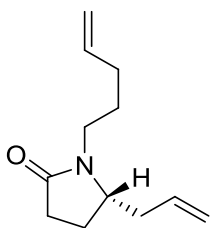
The product was prepared according to the general procedure using allyl bromide. The reaction was run on a 5 mmol scale, to afford the product as a light brown oil (800.3 mg, 97%): $[\alpha]_D^{20} = -21.4$ ($c = 0.44$, CHCl_3); $^1\text{H NMR}$ (400.1 MHz, CDCl_3) δ (ppm): 5.70 (m, 2H), 5.17 (m, 4H), 4.33 (dd, $J = 10.4, 5.2$ Hz, 1H), 3.67 (septet, $J = 4.0$ Hz, 1H), 3.55 (dd, $J = 7.2$ Hz, 1H), 2.8-2.47 (m, 3H), 2.05-2.23 (m, 2H), 1.77 (m, 1H); $^{13}\text{C NMR}$ (100.6 MHz, CDCl_3) δ (ppm): 175.03, 132.93, 132.89, 56.79, 43.25, 37.48, 30.18, 23.43; HRMS (TOF, ES+) $\text{C}_{10}\text{H}_{15}\text{NO}$ $[\text{M}+\text{H}]^+$ calc'd 166.1228, found 166.1223.



(S)-5-allyl-1-(but-3-en-1-yl)pyrrolidin-2-one (1.138):

The product was prepared according to the general procedure using 4-bromobut-1-ene. The reaction was run on a 5 mmol scale, to afford the product as colorless oil (868.2 mg,

97%): $[\alpha]_D^{20} = -26.3$ ($c = 0.73$, CHCl_3); $^1\text{H NMR}$ (400.1 MHz, CDCl_3) δ (ppm): 5.66-5.82 (m, 2H), 5.03-5.18 (m, 4H), 3.66-3.80 (m, 2H), 2.97 (m, 1H), 2.18-2.57 (m, 7H), 1.69-1.78 (m, 1H); $^{13}\text{C NMR}$ (100.6 MHz, CDCl_3) δ (ppm): 175.3, 135.3, 132.9, 118.9, 117.0, 57.0, 39.7, 37.6, 31.9, 30.3, 23.6; HRMS (TOF, ES+) $\text{C}_{11}\text{H}_{18}\text{NO}$ $[\text{M}+\text{H}]^+$ calc'd 180.1388, found 180.1387.

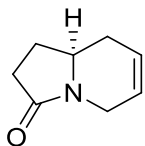


(S)-5-allyl-1-(pent-4-en-1-yl)pyrrolidin-2-one (1.139):

The product was prepared according to the general procedure using 5-bromopent-1-ene. The reaction was run on a 5 mmol scale, to afford the product as colorless oil (916.8 mg, 95%): $[\alpha]_D^{20} = -25.3$ ($c = 0.84$, CHCl_3); $^1\text{H NMR}$ (400.1 MHz, CDCl_3) δ (ppm): 5.65-5.86 (m, 2H), 4.97-5.17 (m, 4H), 3.61-3.69 (m, 2H), 2.93 (m, 1H), 2.22-2.44 (m, 3H), 2.10-2.20 (m, 1H), 2.07 (m, 3H), 1.55-1.79 (m, 3H); $^{13}\text{C NMR}$ (100.6 MHz, CDCl_3) δ (ppm): 175.2, 137.8, 132.9, 118.9, 115.3, 57.0, 40.0, 37.7, 31.3, 30.3, 26.7, 23.6; HRMS (TOF, ES+) $\text{C}_{12}\text{H}_{19}\text{NO}$ $[\text{M}+\text{H}]^+$ calc'd 194.2931, found 194.2929.

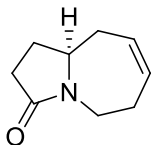
General Procedure for ring closing metathesis of *N*-alkyl lactam:

To a solution of *N*-alkyl-lactam (1 equiv), in CH₂Cl₂ was added 2nd Gen. Grubbs (0.05 equiv). The mixture was refluxed for 1 – 2 h and concentrated. The resulting crude product was purified by automated flash chromatography (1:1 Hex/EtOAc) to yield the desired product.



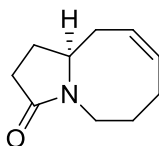
(*S*)-1,2,8,8a-tetrahydroindolizin-3(5H)-one (1.113):

The product was prepared according to the general procedure. The reaction was run on a 3 mmol scale, to afford the product as a brown oil (316.5 mg, 77%): $[\alpha]_D^{20} = -27.3$ ($c = 0.62$, CHCl₃); ¹H NMR (400.1 MHz, CDCl₃) δ (ppm): 5.78 (m, 1H), 5.69 (m, 1H), 4.24 (dd, $J = 16.0, 2.5$ Hz, 1H), 3.55 (m, 2H), 2.25-2.42 (m, 4H), 1.99 (m, 2H), 1.68 (m, 1H); ¹³C NMR (100.6 MHz, CDCl₃) δ (ppm): 174.4, 124.3, 123.6, 53.1, 40.5, 32.6, 30.1, 25.7; HRMS (TOF, ES+) C₈H₁₂NO [M+H]⁺ calc'd 138.0919, found 138.0916.



(S)-5,6,9,9a-tetrahydro-1H-pyrrolo[1,2-a]azepin-3(2H)-one (1.114).

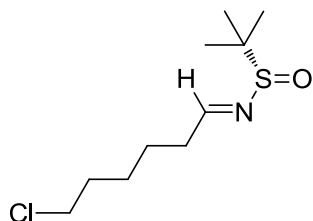
The product was prepared according to the general procedure. The reaction was run on a 3 mmol scale, to afford the product as colorless oil (339.8 mg, 75%): $[\alpha]_D^{20} = -22.3$ ($c = 0.52$, CHCl_3); $^1\text{H NMR}$ (400.1 MHz, MeOD) δ (ppm): 5.89 (m, 1H), 5.80 (m, 1H), 3.81 (m, 2H), 3.08 (dt, $J = 1.6, 8$ Hz, 1H), 2.4-2.2 (m, 7H), 1.66 (m, 1H); $^{13}\text{C NMR}$ (100.6 MHz, CDCl_3) δ (ppm): 176.89, 132.37, 129.76, 60.49, 42.61, 36.90, 31.34, 28.61, 26.48; HRMS (TOF, ES^+) $\text{C}_9\text{H}_{14}\text{NO}$ $[\text{M}+\text{H}]^+$ calc'd 152.1119, found 152.1116.



(S)-1,2,6,7,10,10a-hexahydropyrrolo[1,2-a]azocin-3(5H)-one (1.115).

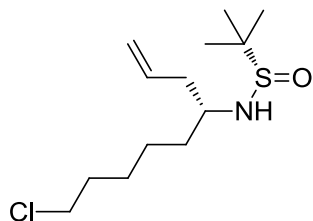
The product was prepared according to the general procedure. The reaction was run on a 3 mmol scale, to afford the product as colorless oil (252.5 mg, 51%): $[\alpha]_D^{20} = -20.8$ ($c = 0.42$, CHCl_3); $^1\text{H NMR}$ (400.1 MHz, CDCl_3) δ (ppm): 5.81 (m, 1H), 5.71 (m, 1H), 3.81 (dt, $J = 13.6, 4.0$ Hz, 1H), 3.58 (septet, $J = 4.8$ Hz, 1H), 2.74 (m, 1H), 2.34-2.45 (m, 2H), 2.21-2.32 (m, 2H), 2.11-2.20 (m, 2H), 1.97-2.10 (m, 2H), 1.64-1.76 (m, 1H), 1.48-1.52 (m, 1H); $^{13}\text{C NMR}$ (100.6 MHz, CDCl_3) δ (ppm): 175.9, 133.4, 125.8, 61.6, 42.9, 33.1,

30.5, 26.9, 24.6, 24.5; HRMS (TOF, ES+) C₁₀H₁₆NO [M+H]⁺ calc'd 166.1232, found 166.1233.



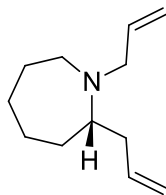
(*S,E*)-*N*-(6-chlorohexylidene)-2-methylpropane-2-sulfinamide (1.127c).

To a solution of 6-chlorohexanal (7.37 g, 54.79 mmol) in DCM (219 ml) at ambient temperature was added CuSO₄ (20.11 g, 126.02 mmol) and (*S*)-2-methylpropane-2-sulfinamide (7.64 g, 63.01 mmol) in a single batch. The reaction was stirred for 12 h, at which point the starting material was fully consumed by TLC analysis (4:1 Hex/EtOAc, *rf* = 0.35). The heterogeneous mixture was filtered through a silica pad and concentrated *in vacuo* to yield a viscous oil, which was purified by flash chromatography (4:1 Hex/EtOAc) to afford the desired product as a clear oil (12.34 g, 94%). [α]_D²⁰ = +157.9° (*c* = 1.5, MeOH). ¹H NMR (400.1 MHz, CDCl₃) δ (ppm): 8.05 (t, *J* = 4.5 Hz, 1H); 3.52 (t, *J* = 6.5 Hz, 2H); 2.53 (m, 2H); 1.79 (m, 2H); 1.66 (m, 2H); 1.51 (m, 2H); 1.18 (s, 9H). ¹³C NMR (100.6 MHz, CDCl₃) δ (ppm): 169.26, 56.64, 44.82, 35.96, 32.37, 26.56, 24.78, 22.42. HRMS (TOF, ES+) C₁₀H₂₁NOSCl [M+H]⁺ calc'd 238.1032, found 238.1034.



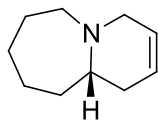
(S)-N-((R)-9-chloronon-1-en-4-yl)-2-methylpropane-2-sulfinamide (1.128c).

NaBr (380 g) was dissolved in 841 mL of deionized H₂O. To this fully dissolved saturated NaBr solution was added aldimine **1.127c** (10.00g, 42.05 mmol) and indium powder (19.31 g, 168.2 mmol). The mixture was stirred vigorously for 5 min., then allyl bromide (20.35 g, 168.2 mmol) added in a single batch. Vigorous stirring was continued for 9 h, at which point the starting material was consumed by TLC analysis (1:1 Hex/EtOAc, rf = 0.34). The mixture was quenched with NaHCO₃ and extracted x5 with EtOAc. The organic fractions were combined, washed with brine, dried over Na₂SO₄, and concentrated *in vacuo* to yield crude oil. Purification by flash chromatography (1:1 Hex/ EtOAc) afforded the desired product as a clear oil (10.10 g, 86%). $[\alpha]_D^{20} = +25.7^\circ$ (*c* = 1.5, MeOH). ¹H NMR (400.1 MHz, CDCl₃) δ (ppm): 5.77 (m, 1H); 5.15 (m, 2H); 3.52 (t, *J* = 6.5 Hz, 2H); 3.30 (sextet, *J* = 6.1 Hz, 1H); 3.21 (br d, *J* = 6.1 Hz, 1H); 2.35 (dp, *J*₁ = 6.5 Hz, *J*₂ = 10.4 Hz, 2H); 1.763 (quint., *J* = 6.5 Hz, 2H); 1.53- 1.32 (m, 5H). ¹³C NMR (100.6 MHz, CDCl₃) δ (ppm): 134.23, 119.14, 55.92, 54.83, 45.08, 40.56, 34.91, 32.60, 26.88, 24.92, 22.79. HRMS (TOF, ES+) C₁₃H₂₇NOSCl [M+H]⁺ calc'd 280.1502, found 280.1504.



(S)-1,2-diallylazepane (1.129c1).

A 4N solution of HCl / dioxanes (14.92 ml) was cooled to 0°C and slowly added to a microwave vial containing sulfinamide **1.128c** (2.0 g, 7.15 mmol). Solution was then brought to ambient temperature and stirred for an additional 45 min, and concentrated *in vacuo* to afford the deprotected amine as the HCl salt in quantitative yield. The amine was dissolved in DMF (35.9 mL), then K₂CO₃ (1.98 g, 14.34 mmol) and NaI (1.18 g, 7.89 mmol) were added in a single batch. The vial was sealed and submitted to microwave irradiation at 120°C for 15 min. LC/MS analysis showed full consumption of starting material to the cyclized secondary amine. Allyl bromide (0.954 g, 7.89 mmol) and an additional equivalent of K₂CO₃ (0.99 g, 7.15 mmol) was then added to the pale yellow solution at ambient temperature, and stirring was continued for 4 h. Mixture was dissolved in 5% LiCl solution and extracted with Et₂O (5 x 40 mL). Organic fractions were combined, washed with brine, dried over Na₂SO₄, and concentrated *in vacuo* to yield a pale yellow crude oil. Purification by flash chromatography (1:1 Hex/EtOAc) afforded the desired product as a clear oil (0.82g, 64%). $[\alpha]_D^{20} = -5.0^\circ$ ($c = 0.9$, MeOH). ¹H NMR (400.1 MHz, CDCl₃) δ (ppm): 5.82 (m, 2H); 5.19-4.93 (m, 4H); 3.22 (m, 2H); 2.85 (m, 1H); 2.70 (m, 2H); 2.26 (m, 1H); 2.06 (m, 1H); 1.75 (m, 1H); 1.66-1.38 (m, 7H). ¹³C NMR (100.6 MHz, CDCl₃) δ (ppm): 137.98, 137.51, 115.99, 115.66, 62.45, 55.71, 49.83, 39.34, 32.65, 28.88, 27.53, 25.78. HRMS (TOF, ES+) C₁₂H₂₂N [M+H]⁺ calc'd 180.1752, found 180.1751.



(S)-octahydro[1,2-a]azepine (1.130c1).

To a solution of diene 1.4.14c1 (106 mg, 0.59 mmol) in toluene (11.8 mL) was added trifluoroacetic acid (71 mg, 0.62 mmol), and Grubbs 2nd generation catalyst (49 mg, 0.06 mmol). Solution was submitted to microwave irradiation for 1 h at 100°C. The toluene was removed *in vacuo*, and the crude residue purified to afford the desired product as the TFA salt (105 mg, 68%). $[\alpha]_D^{20} = +45.2^\circ$ ($c = 1.25$, MeOH). ¹H NMR (400.1 MHz, CDCl₃) δ (ppm): 5.88 (m, 1H); 5.64 (m, 1H); 3.94 (m, 1H); 3.57 (m, 2H); 3.18-3.04 (m, 2H); 2.73 (t, 1H); 2.25 (m, 1H); 2.24-1.92 (m, 3H); 1.89-1.72 (m, 3H); 1.58 (m, 2H). ¹³C NMR (100.6 MHz, CDCl₃) δ (ppm): 126.83, 120.24, 63.64, 55.70, 54.32, 31.93, 30.59, 27.21, 26.00, 21.96. HRMS (TOF, ES+) C₁₀H₁₈N [M+H]⁺ calc'd 152.1439, found 152.1440.

CHAPTER II

TOTAL SYNTHESIS OF THE ALKALOID NATURAL PRODUCTS (+)- AMABILINE AND GRANDISINE D

2.1. Introduction

Alkaloid natural products are a large, structurally diverse group of naturally-occurring compounds originating from plants, animals, and microbes. They have a reputation as both nature's blessing and curse, responsible for the beneficial properties of natural medicines such as willow bark, and the detrimental effects of poisons such as deadly nightshade.¹ The profound biological activity found in alkaloids have led to their use as drug leads to develop treatments in various therapeutic areas such as pain relief, gastrointestinal disorders, and cardiac disorders.²⁻³ However, alkaloids are relatively underrepresented in the context of newly introduced medicines, with supply constraints of these natural products cited as a barrier to biological characterization and development of many of these compounds.⁴ Total synthesis attempts to overcome this by providing methods to access these biologically-relevant compounds in greater quantities has remained an area of interest in the organic synthesis community for decades. Our efforts towards the total synthesis of two natural products belonging to the pyrrolizidine and indolizidine alkaloid classes will be described.

2.1.1. Pyrrolizidine Alkaloids

Pyrrolizidine alkaloids (**2.1**), historically referred to as necine bases, share a common azabicyclo[3.3.0]octane core, but differ based on the oxygenation pattern and whether or not C1-C2 is saturated (**Figure 2.1**).⁵ While the amine bases themselves are rarely isolated in nature, the corresponding mono- and di-esters are more common, as either the tertiary amine or the *N*-oxide. Members of this family of alkaloids possess a wide range of biological activities including antitumor, antibacterial, anti-inflammatory, carcinogenic and hepatotoxic activity, with several members entering human clinical trials. A number of racemic routes to the pyrrolizidine alkaloid core (**2.1**) have been developed, but recent efforts have focused on asymmetric approaches. Further commentary on these approaches can be found in Chapter 1.

Plants containing pyrrolizidine alkaloids are toxic to humans and animals, however, several insect species have evolved to adapt them for their own chemical defense.⁶ Interestingly, the toxicity of these compounds has been attributed to liver metabolism of the C1-C2 unsaturated congeners leading to the generation of highly reactive alkylating agents. Our interest in the synthesis of (+)-amabiline stemmed from our success in the development of our methodology for the enantioselective synthesis of azabicyclic ring systems.

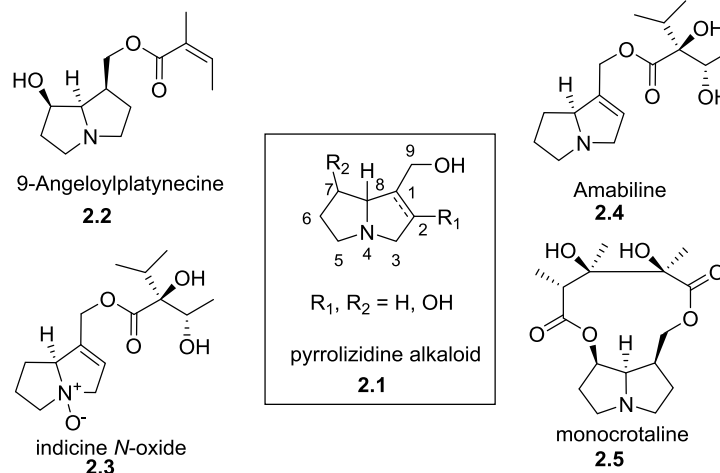


Figure 2.1. Structures of pyrrolizidine alkaloids

2.1.2. Indolizidine Alkaloids

Indolizidine alkaloids (IAs) have been isolated from a myriad of sources including ants, frog, fungi and trees. IAs have exhibited interesting biological activities including insecticidal, antibacterial, fungicidal, analgesic, and anticancer activities.⁷ Indolizidine alkaloids are defined by a 1-aza-bicyclo-[4.3.0]-octane core similar that of the pyrrolizidine alkaloids. Shown in **Figure 2.2** are several examples of indolizidine-containing natural products. This core system serves as an important scaffold in biologically active and pharmaceutically significant compounds, and the literature is rich with the total synthesis and biological evaluation of compounds containing the indolizidine skeleton.⁸

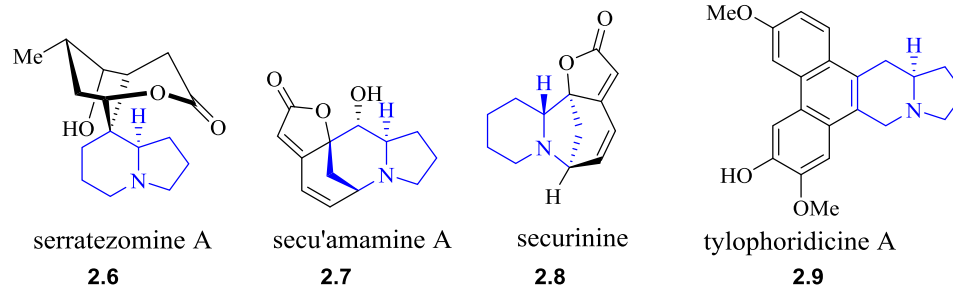


Figure 2.2. Examples of indolizidine-containing natural products.

2.2. Total Synthesis of (+)-Amabiline

2.2.1. Introduction

(+)-Amabiline is a pyrrolizidine alkaloid isolated by Smith and co-workers from the leaves of the Chinese flowering plant *Cynoglossum amabiline*.⁹ This class of alkaloids has exhibited activity at a wide range of biological targets, including subtype-specific neuronal nicotinic acetylcholine receptors and muscarinic acetylcholine receptors.¹⁰ These receptors are involved in normal central nervous system functions, such as memory and motor function, as well as pathological conditions such as Parkinson's disease, schizophrenia, and Alzheimer's disease.

There are at least three fates for the metabolism of pyrrolizidine alkaloids such as (+)-amabiline (**Figure 2.3**).^{11,12} They can be metabolized by flavin-containing monooxygenases (FMO) to the water soluble N-oxide, which leads to excretion of the compounds. Conversely, metabolism by cytochrome P450 enzymes, primarily CYP3A4, converts compounds to the dehydropyrrolizidine metabolite **2.11** that is believed to lead to toxicity in animals and humans. In the case of some insects, the presence of the

enzyme senecionine N-oxidase (SNO) will convert the compounds to the N-oxide, where they can be sequestered and used as a deterrent to other insect and animal predators. This process describes an interesting case of an animal species utilizing the defensive mechanism of a plant in the form of a compound not produced endogenously by the insect to protect itself from predators.

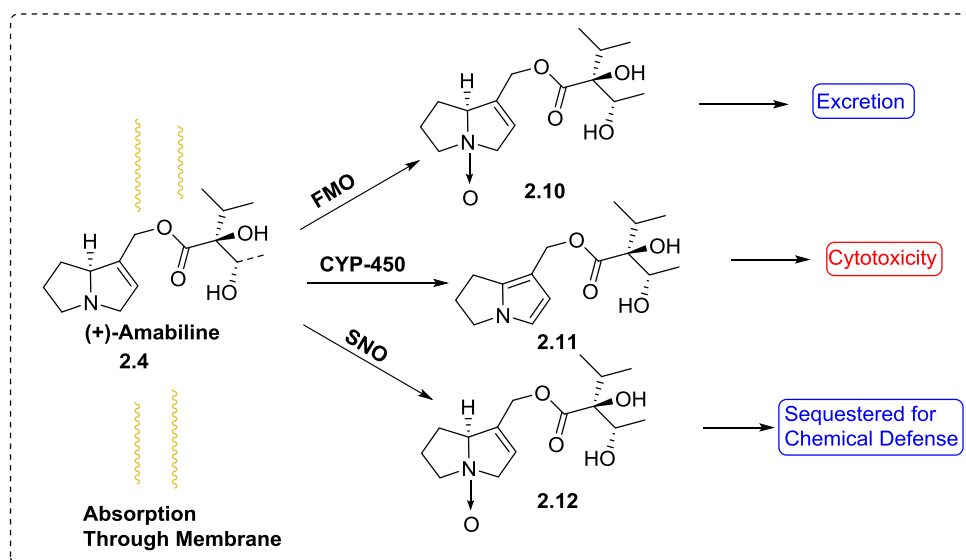


Figure 2.3. Metabolic fate of pyrrolizidine alkaloids

2.2.2. Retrosynthetic Analysis of (+)-Amabiline

Our approach for the total synthesis of (+)-amabiline was based on a retrosynthetic analysis outlined in **Figure 2.4**. Our retrosynthesis began with cleavage of the ester bond to liberate the necine base (-)-supinidine and (-)-viridifloric acid. (-)-Supinidine has been previously synthesized, but the most expedient route required was 18 steps.¹³ By employing a novel extension of our newly developed azacine methodology, the azabicyclic moiety could be accessed from **2.14**, which would be derived from the

commercial diol **2.16** and (*S*)-*tert*-butylsulfonamide **2.17**. (-)-Viridifloric acid would be prepared as prescribed by Schulz, via **2.15**, from commercial **2.18** and **2.19**.¹⁴

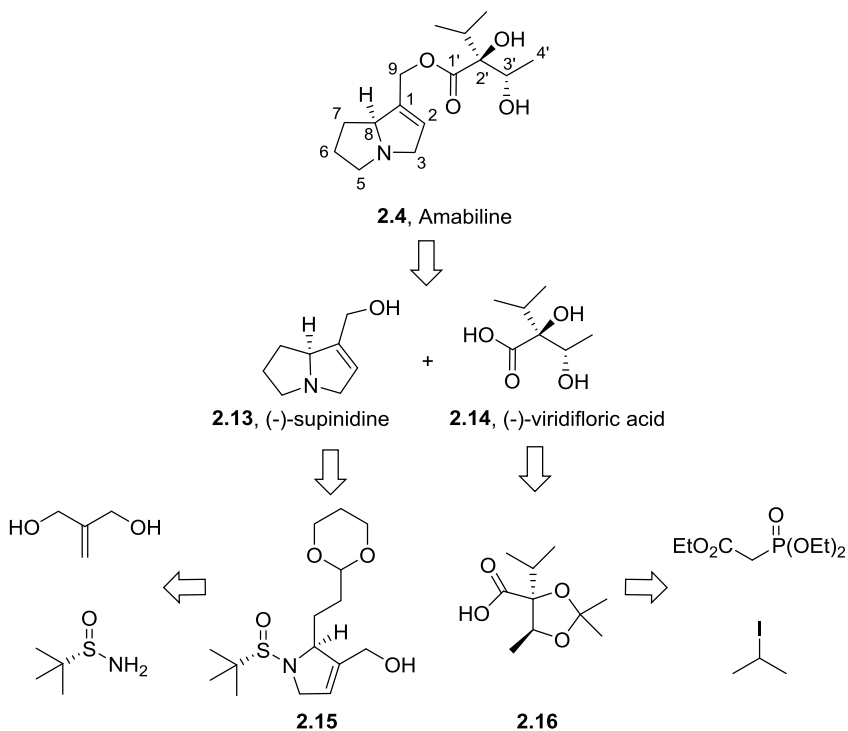
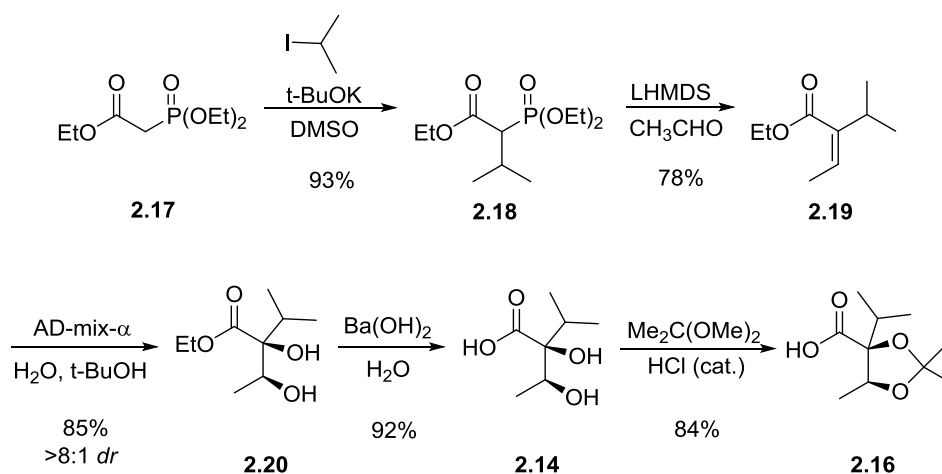


Figure 2.4. Retrosynthetic Analysis of (+)-Amabiline

2.2.3 Synthesis of (+)-Amabiline

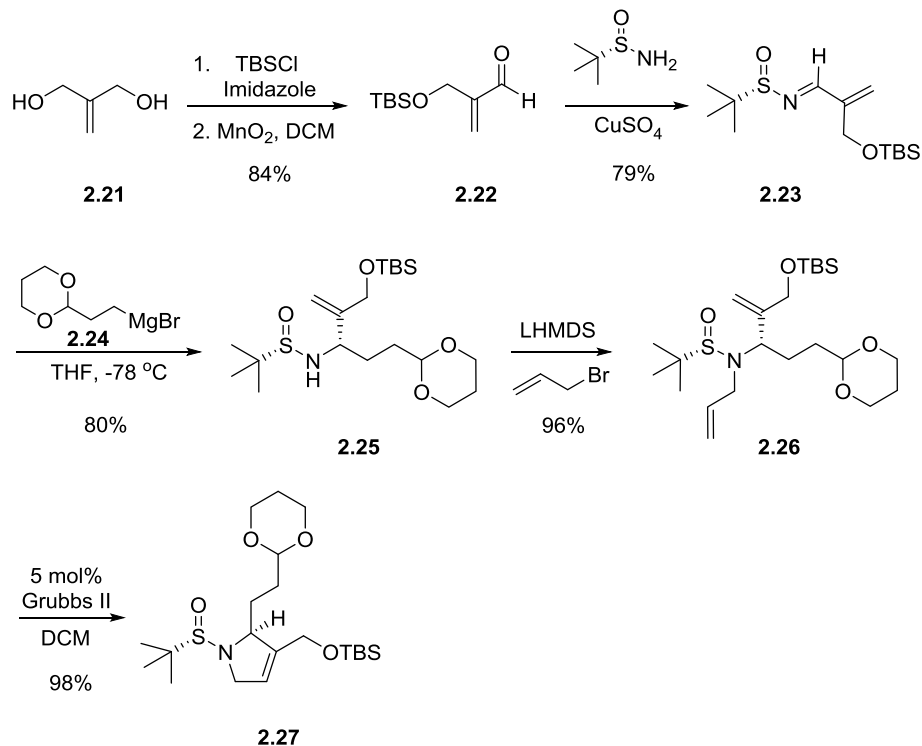
Efforts initially focused on the synthesis of **2.15** (**Scheme 2.1**). As was described in the retrosynthesis, the (-)-viridifloric acid moiety needed to be constructed in a manner that would allow for esterification with alcohol **2.14**. Alkylation of phosphonate ester **2.18** with **2.19** provided **2.20** in 93% yield. A Horner-Wadsworth-Emmons reaction with acetaldehyde provided alkene **2.21**, and although purification proved troublesome due to volatility of the low molecular weight α,β -unsaturated ester, the desired product was

obtained in 78% yield. The alkene then underwent a Sharpless dihydroxylation to afford (*S,S*)-diol **2.21** in >8:1 *dr*. Ester hydrolysis provided the (-)-viridifloric acid (**2.13**), identical in all respects to the natural acid, which was then protected as the dioxolane congener **2.15** to avoid possible complication during the subsequent esterification. Thus, the synthesis of **2.15** required five steps and proceeded in 48% overall yield.



Scheme 2.1. Synthesis of protected (-)-viridifloric acid

With **2.16** in hand, attention was now directed to the synthesis of key intermediate **2.15** (Scheme 2.2). Commercial diol **2.21** was mono-silylated, followed by MnO_2 oxidation of the allylic alcohol to deliver aldehyde **2.22** in 84% yield for the two steps. Condensation of **2.22** with (*S*)-*tert*-butyl sulfinimine gave **2.23** in 79% yield. Addition of Grignard reagent **2.24** provides **2.25** in >9:1 *dr.*, which was subsequently allylated to deliver **2.26** in 77% yield for the two steps.



Scheme 2.2. Synthesis of advanced intermediate **2.27**

The diastereoselectivity of this particular Grignard reaction is interesting as it does not follow the predicted outcome of the Ellman chelation model proposed during the seminal studies of nucleophilic additions into chiral aldimines. As shown in **Figure 2.5**, nucleophilic addition of a Grignard reagent into a chiral sulfinimine would be expected to proceed through a six-membered chelate transition state, however this rationale leads us to the opposite diastereomer than that observed in our instance, as determined by X-ray crystallography. In cases where the imine or Grignard reagent contains a heteroatom, it is possible for an intramolecular interaction to disrupt the six-member transition state. This causes the Grignard reaction to proceed through an open transition state, which is referred to as “anti-Ellman” selectivity.

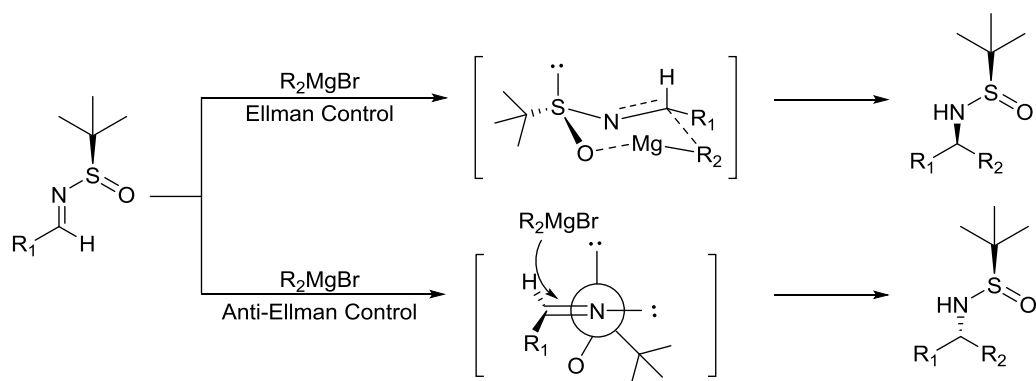


Figure 2.5. Ellman's proposed transition states for Grignard addition into chiral *tert*-butanesulfinimines

A RCM reaction of **2.26** employing Grubbs II smoothly led to pyrrolidine **2.27**, and TBAF deprotection generated the key intermediate **2.15**. Single X-ray crystallography (**Figure 2.6**) confirmed the absolute stereochemistry of **2.15** as (*S,S*).

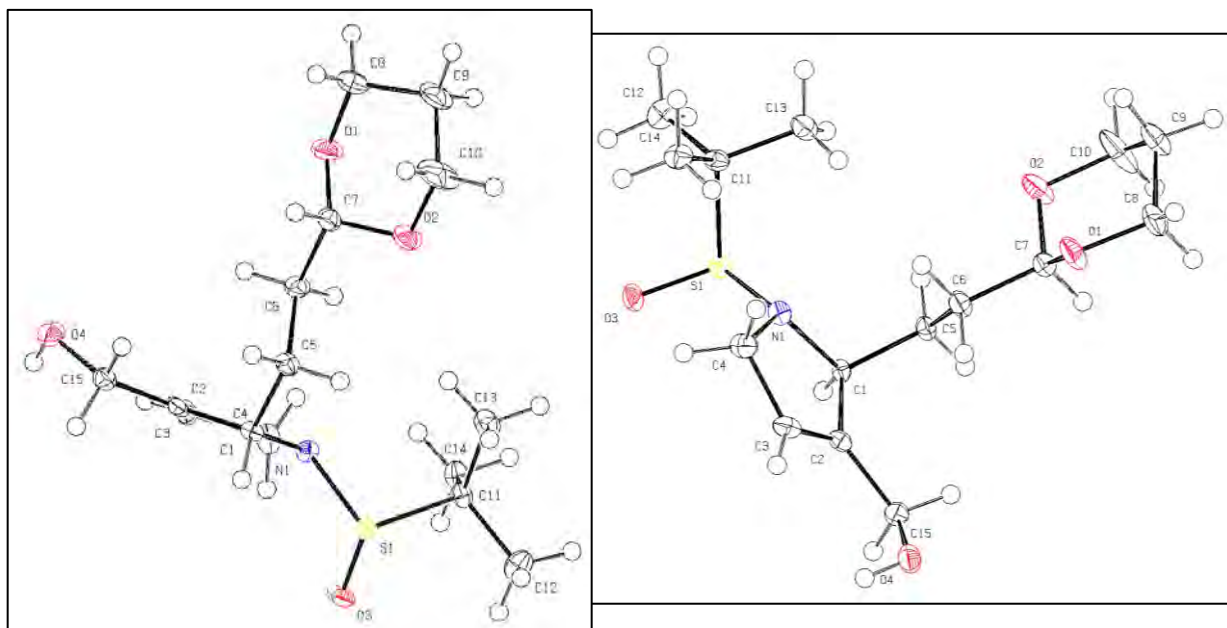
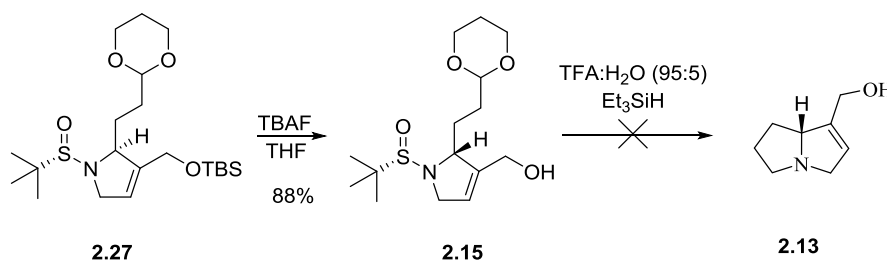


Figure 2.6. ORTEP drawing of X-ray crystallographically determined structure of **2.15**

There is speculation that the oxygen of the acetal group may disrupt the chelation of magnesium to the aldimine species, leading to an open transition state, but at this time a definitive mechanism to explain the rationale for our observed diastereoselectivity has not been proven. A similar result using this Grignard reagent was reported by Ellman and coworkers, however there was no commentary offered regarding the observed “anti-Ellman” diastereoselectivity.¹⁵

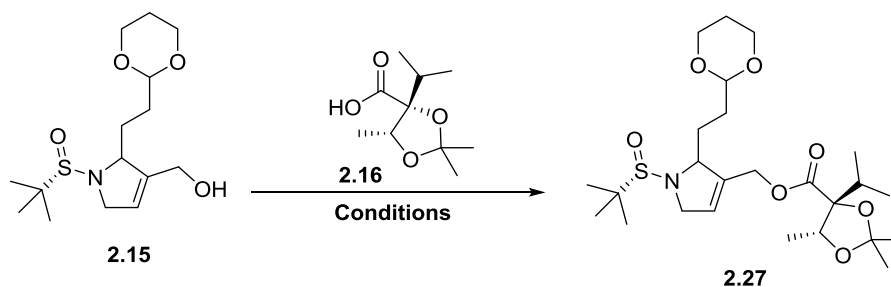
We anticipated that deprotection of the acetal and the sulfinamine of **2.15** would liberate the free aldehyde and amine, respectively, followed by an intramolecular condensation to form the imine that would then be reduced *in situ* to provide (-)-supinidine (**2.13**). However, classical Ellman conditions and a number of other variants failed to facilitate this transformation, affording complex mixtures of polar species.



Scheme 2.3. Attempted deprotection to necine base

Therefore, we elected to first couple **2.16** and **2.15**, followed by global deprotection and intramolecular reductive amination. This also proved challenging due to the sterically hindered acid **2.15**. We evaluated various coupling reagents (EDCI/DMAP, TBTU/DBU, DCC/DMAP, HATU/DIEA) and protocols, and none provided any trace of the ester product. Therefore, we decided to convert the hydroxyl

of **2.15** into a leaving group, and attempt to install the ester linkage by employing the acid as a nucleophile.¹⁶ A mesylate derivative afforded a 45% conversion to the desired ester, but **2.28**, a tosylate variant, afforded the desired ester in 82% yield (**Figure 2.7**).



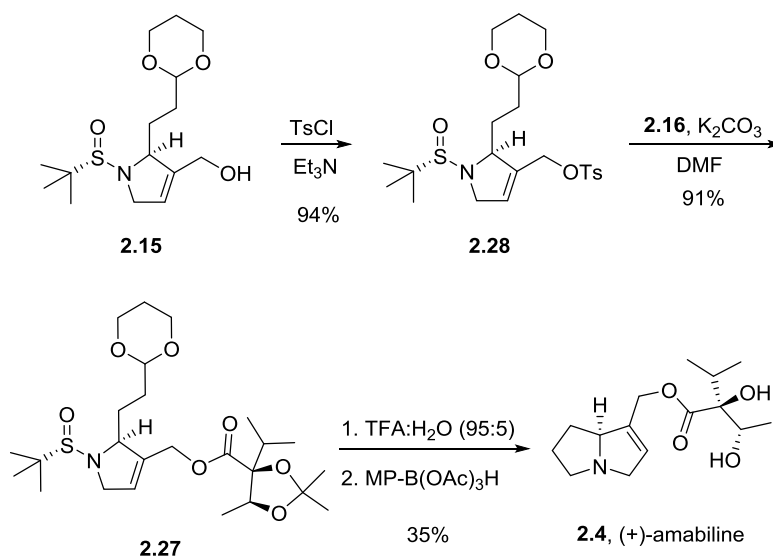
Condition	conv. (%)
PS-DCC, HOBT	0
PS-DCC/DMAP	0
DCC/DMAP	0
EDC/DMAP	0
SOCl ₂ - Pyridine, then 2.16	0
HATU, DIEA	0
TBTU, DBU	0
1. MsCl, Pyridine 2. 2.16 , Et ₃ N	45
1. PPh ₃ , I ₂ , imidazole 2. 2.16 , Et ₃ N	0*
PyClu, DIEA, II, uW	0
Ghosez Reagent, DIEA	0
1. TsCl, Pyridine 2. 2.16 , K ₂ CO ₃	82

*Iodide intermediate not isolated

Figure 2.7. Coupling of **2.15** with (+)-viridifloric acid precursor **2.16**

A final acid-mediated global deprotection of the acetal, the dioxolane, and the sulfinamide enabled the intramolecular condensation to form the imine, which was then reduced *in situ* by MP-BH(OAc)₃ to deliver (+)-amabiline (**2.4**) in 37% yield in a one-pot reaction sequence (average of 84% yield/transformation). Thus, the first total synthesis of (+)-amabiline (**2.4**) was completed in 15 synthetic steps (10 steps longest linear sequence) and in 6.2% overall yield. The synthetic (+)-amabiline was identical to the

data reported for natural **2.4**.¹⁷ Moreover, this represents a notable improvement in the synthesis of the pyrrolizidine core, as previous efforts have required up to 18 steps to deliver (-)-supinidine (**2.12**), the parent necine base, that could be used to rapidly and stereoselectively access other pyrrolizidine alkaloids and azabicyclic-ring containing compounds.

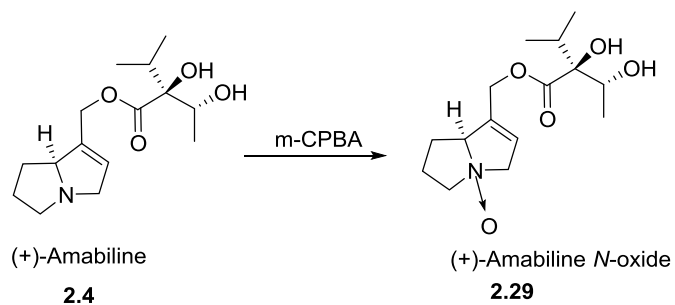


Scheme 2.4. Synthesis of (+)-amabiline

Based on the structural similarity of amabiline to other pyrrolizidine alkaloids with anticholinergic activity, we evaluated our synthetic amabiline against all five mAChR receptors (M_1 - M_5). Interestingly, amabiline possessed no activity at any of the mAChRs ($IC_{50} > 10 \mu\text{M}$).

Conversion of amabiline to the corresponding N-oxide (**2.29**) proceeded through treatment with mCPBA to facilitate *N*-oxidation. There is precedence for these conditions to demonstrate chemoselectivity for the N-oxide over the possible epoxide by-

product in closely related natural products.¹⁸ Preliminary results observed by liquid chromatography/ mass spectrometry corroborates with those reports, showing conversion to the unsaturated N-oxide, however a larger scale will be required for further studies. We plan to complete a metabolic study where treating **2.4** with human cytochrome P450 liver enzymes should show conversion to the *N*-oxide and/or dehydropyrrolizidine products, demonstrating the *in vivo* relation between the two natural products.



Scheme 2.5. *N*-oxidation of amabiline to amabiline-*N*-oxide

In summary, we have completed the first total synthesis of (+)-amabiline (**2.4**), requiring only 15 synthetic steps (10 steps longest linear sequence) in 6.2% overall yield. This highly convergent and concise synthesis will enable the preparation of unnatural, unsaturated pyrrolizidine alkaloids for additional biological evaluation.

2.3. Total Synthesis of Grandisine D

2.3.1. Introduction

Grandisines A-G are indolizidine alkaloids isolated by Carroll and co-workers from the leaves of the Australian rain forest tree *Elaeocarpus grandis* (**Figure 2.8**).¹⁹ These alkaloids display selective human δ -opioid receptor affinity. Selective activation of the δ -opioid receptor is an attractive strategy for the development of new analgesics with better side-effect profiles, making grandisines potential analgesic agents. To further investigate the interesting biology and synthetic challenge of grandisine D, we decided to pursue its total synthesis.

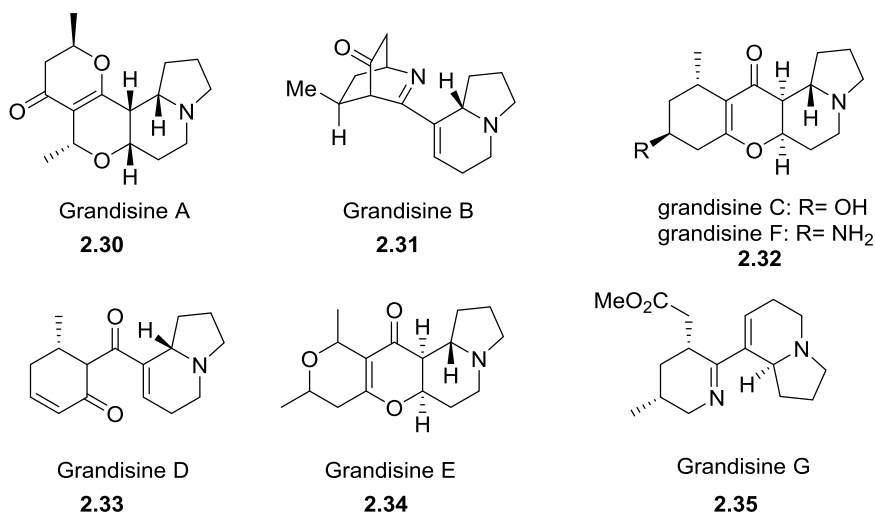


Figure 2.8. Structures of the indolizidine alkaloids grandisines A-G

2.3.2. Tamura Total Synthesis of Grandisine D

Grandisine D was previously synthesized by Tamura and co-workers in 2009.²⁰ Their synthesis featured a Bronsted-acid mediated Morita-Bayless-Hillman (MBH) ring closure and stereoselective aldol condensation with (*S*)-5-methylcyclohexenone as key steps. Deoxygenation at the C1 and C3 positions afforded grandisine D.

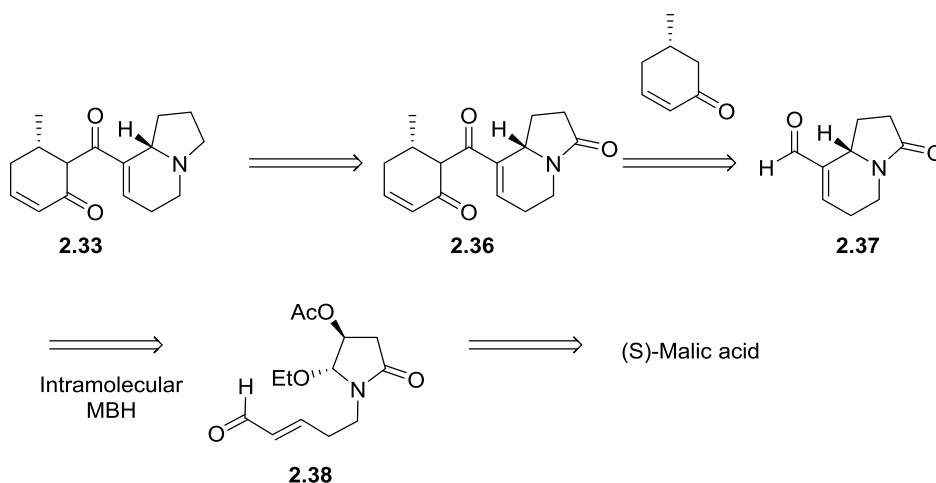
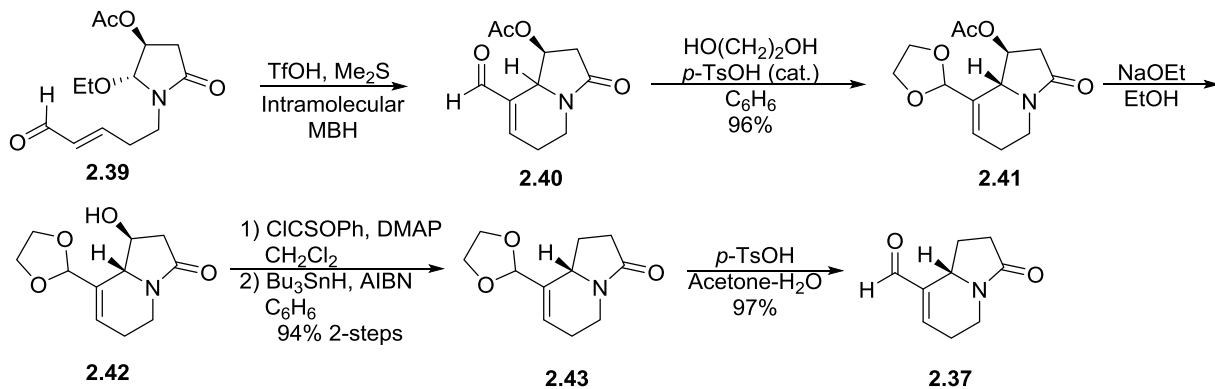


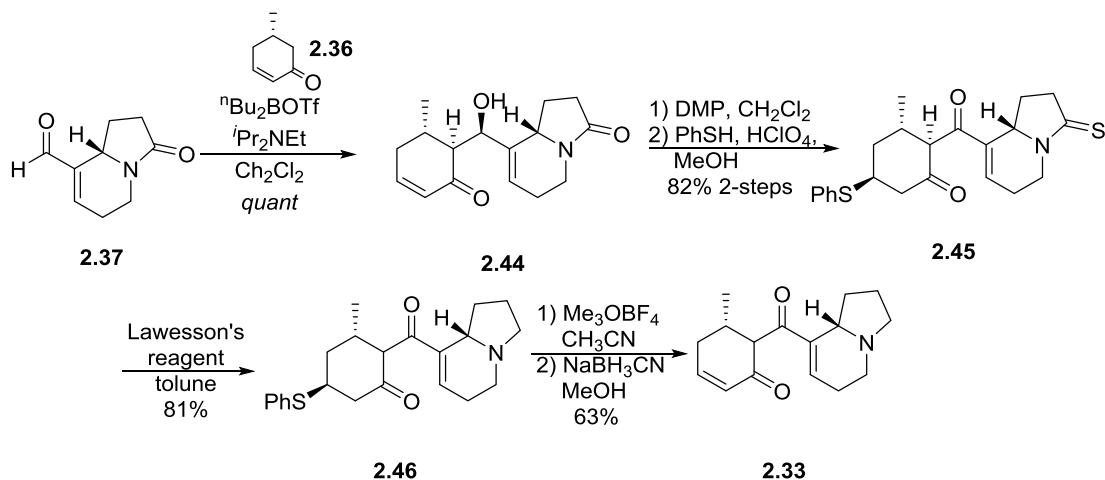
Figure 2.9. Tamura's Retrosynthesis of Grandisine D

Tamura's synthesis of Grandisine D was initiated by the synthesis of aminal **2.39** utilizing the method previously described by Lee and co-workers from (*S*)-malic acid in 6 steps. Treatment of aminal **2.39** with TfOH and Me₂S in CH₃CN effected the desired MBH ring closure in good yield and stereoselectivity (96:4). Removal of the acetoxy group of **2.42** through deacetylation followed by Barton-McCombie deoxygenation afforded lactam **2.43**.



Scheme 2.6. Tamura's total synthesis of Grandisine D

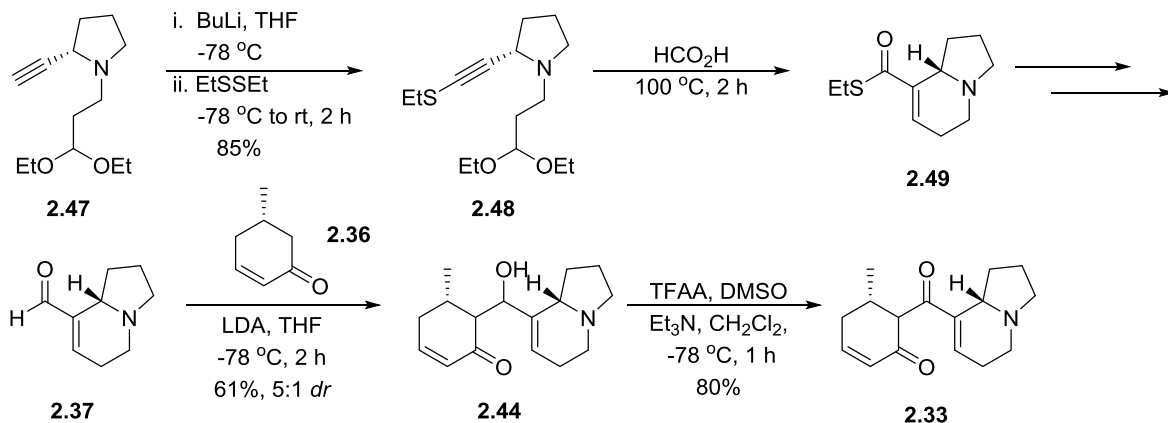
Deprotection of the acetal provided aldehyde **2.37**, which then underwent the key boron mediated aldol reaction to afford **2.44** in quantitative yield as a single diastereomer. Dess-Martin oxidation of the resulting alcohol followed by reduction of the lactam accomplished the first total synthesis of Grandisine D, requiring 26 steps.



Scheme 2.7. Tamura total synthesis of grandisine D

2.3.3. Taylor Total Synthesis of Grandisine D

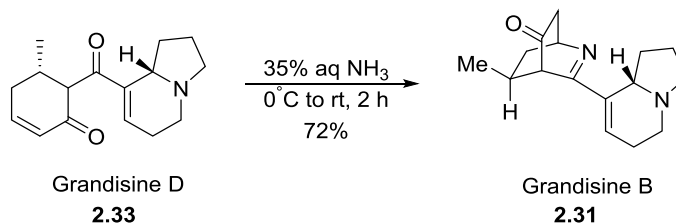
During our efforts towards the total synthesis of grandisine D, a second total synthesis of the alkaloid was reported in 2011 by Taylor and co-workers.²¹ As outlined in **Scheme 2.8**, their synthesis featured an alkyne-acetal cyclization as their key step, and was accomplished in 13 steps with 10% overall yield from the commercially available L-proline chiral starting material.



Scheme 2.8. Taylor synthesis of (+)-grandisine D

Taylor and co-workers went on to describe the synthesis of grandisine B from grandisine D in a one-pot tandem amination-amination sequence with treatment of 35% aqueous ammonia, which is interesting as the isolation procedure of the grandisine natural products also includes an extraction with aqueous ammonia. It is now believed that Grandisine B is an artifact of the isolation process and not a naturally occurring

compound. This hypothesis is further corroborated by a lack of detection of Grandisine B by (+) ESI MS in crude methanol extracts.

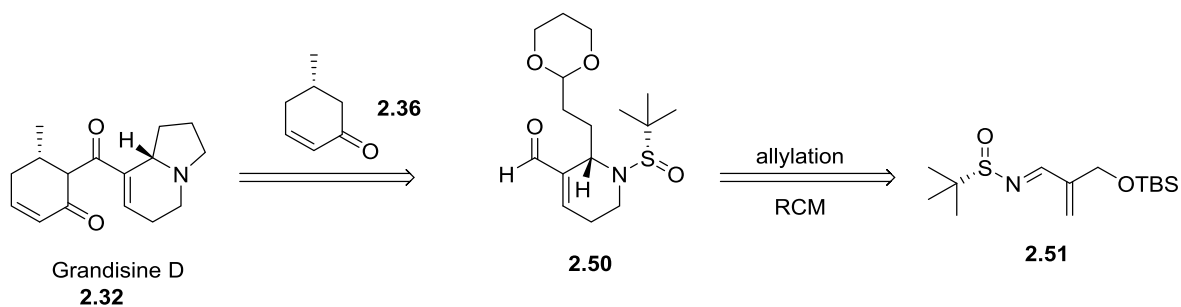


Scheme 2.9. Synthesis of Grandisine B

2.3.4. Retrosynthesis of Grandisine D.

Our interest in the total synthesis of grandisine D stemmed from our success in the application of our methodology for the enantioselective synthesis of azabicyclic ring systems and their applications towards various pyrrolizidine and stemona alkaloids.²²

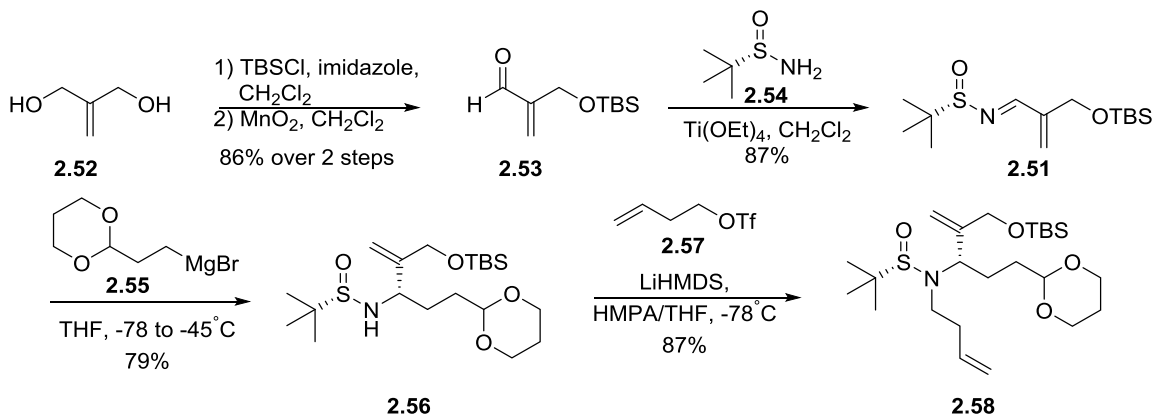
Our retrosynthesis of Grandisine D led to the same key aldol chemistry as that employed by Tamura and Taylor, but a fundamentally new approach to the indolizidine core (**Scheme 2.10**). **2.32** would be accessed by an aldol reaction between 8-formylindolizidine **1.3.22** and known (S)-5-methylcyclohexanone. 8-Formylindolizidine **2.50** would be prepared from Grignard addition and RCM of (S)-sulfinyl aldimine **2.51**.



Scheme 2.10. Retrosynthesis of grandisine D

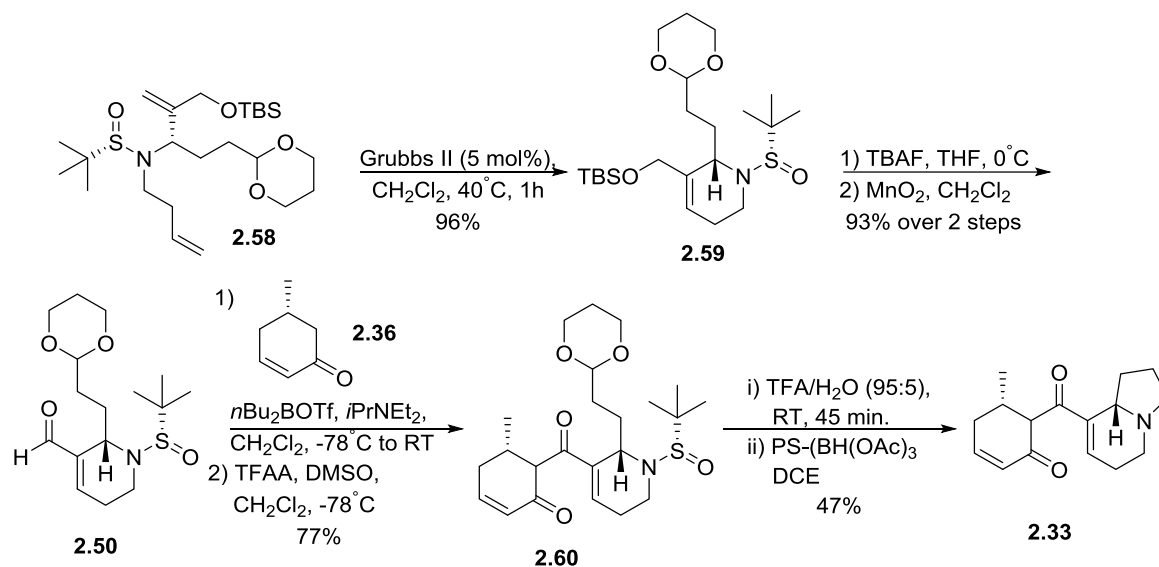
2.3.5. Synthesis of Grandisine D

Starting from commercial diol **2.52**, a mono-silylation and oxidation sequence, followed by conversion into the corresponding (S)-N-sulfinyl aldimine **2.51** under $\text{Ti}(\text{OEt})_4$ -mediated conditions proceeded in 74% yield for the three steps. Following the Ellman protocol, addition of Grignard reagent **2.55** to **2.51** afforded the desired sulfinamide **2.56** in 79% yield with >10:1 *dr*. Previous attempts towards alkylation of sulfinyl-protected amides had proven difficult; however alkylation of **2.56** with butenyl triflate and HMPA as an additive provided **2.57** as a single diastereomer after column chromatography in 87% yield (**Scheme 2.11**).



Scheme 2.11. Synthesis of advanced intermediate **2.57**

As shown in **Scheme 2.12**, a RCM reaction with Grubbs II delivered the piperidine ring in 96% yield, followed by removal of the TBS group and allylic oxidation with manganese dioxide to provide key aldehyde **2.50** in 93% yield for the two steps. Next, an aldol reaction employing boron-enolate methodology with **2.50** and enone **2.36** followed by oxidation to the ketone provided **2.60** in 77% yield. Finally, application of the one-pot deprotection/acetal hydrolysis/ reductive amination sequence afforded **2.32** in 47% yield. Our synthetic (+)-grandisine D was in agreement with the reported characterization data for the natural product, as well as the previous synthetic efforts. Thus, the total synthesis of grandisine D, employing our azabicyclic methodology, required only 11 steps from commercial starting materials in 16.4% overall yield and with excellent stereocontrol throughout. Based on previous work by Tamura and Taylor, the total synthesis of (+)-grandisine D also constitutes a formal total synthesis of (-)-grandisine B.

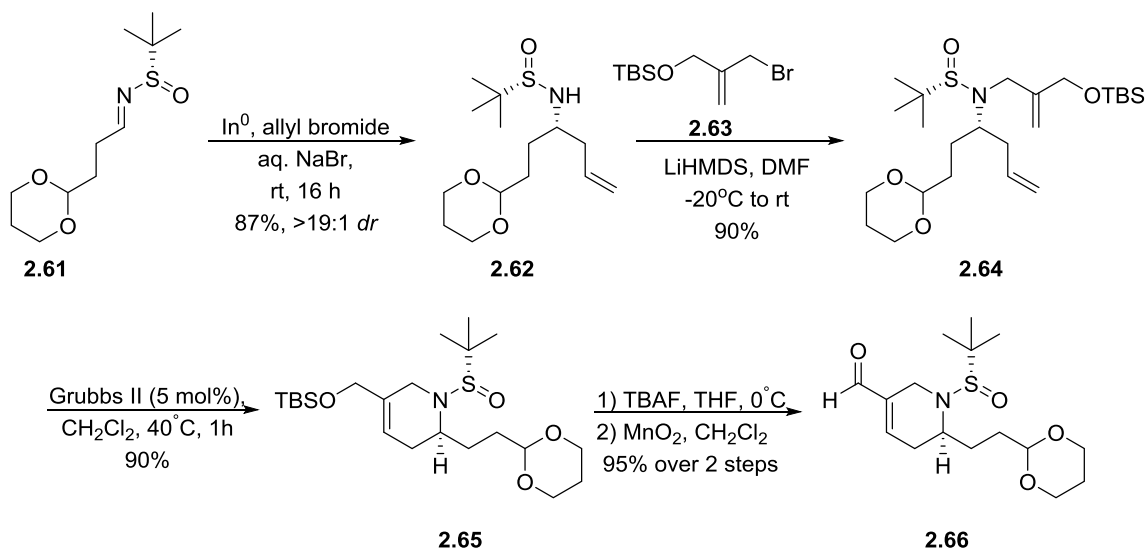


Scheme 2.12. Synthesis of Grandisine D from advanced intermediate **2.58**

2.3.6. Synthesis of Unnatural Analogue of Grandisine D

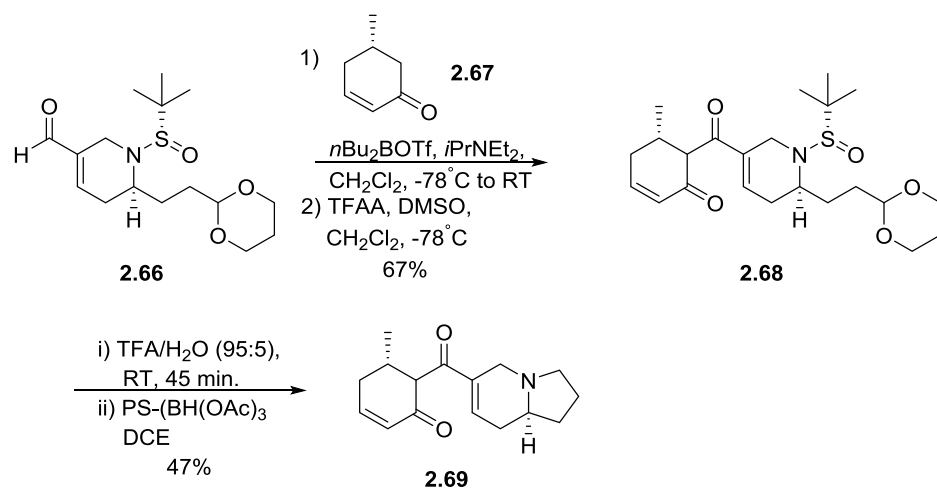
To further highlight the use of this methodology for the streamlined synthesis of diverse unnatural analogues of natural products and pharmaceutically relevant scaffolds, we applied it towards the synthesis of an unnatural analogue of (+)-grandisine D, in which the nitrogen atom was moved from 4-position to the 9-position, resulting in a fundamentally new molecular architecture. Starting with (S)-N-sulfinyl aldimine **2.61**, an indium-mediated allylation reaction afforded **2.62** in 87% yield with greater than 19:1 diastereoselectivity, and, after column chromatography, a single diastereomer. 2-methylenepropane-1,3-diol was mono-protected as a TBS ether and the remaining hydroxyl converted to the corresponding allylic bromide **2.63** in 85% yield for the two steps. Allylation of **2.62** with **2.63** provided **2.64** in 90% yield, followed by an RCM

reaction with Grubbs II afforded **2.65** in 81% yield for the two steps. Deprotection of the TBS ether and oxidation delivered key aldehyde **2.66**, in 95% yield for the two steps.



Scheme 2.13. Synthesis of advanced intermediate **2.66**

Once again, an aldol reaction employing boron-enolate methodology with **2.66** and enone **2.66**, followed by oxidation provided **2.68** in 67% yield. Finally, application of the one-pot deprotection/ acetal hydrolysis/reductive amination sequence produced the unnatural analogue of (+)-grandisine D **2.69** in 49% yield. The synthesis of **2.69** proceeded in 11 steps (the longest linear sequence was 9 steps) from commercial materials in 17.8% overall yield.



Scheme 2.14. Synthesis of unnatural analogue **2.69**

In summary, our approach towards the rapid and enantioselective synthesis of indolizidine azabicyclic systems enabled the total synthesis of (+)-grandisine D in 11 synthetic steps and 16.4% overall yield, a notable advance over the two previous syntheses, and also represents a formal total synthesis of (-)-grandisine B. This methodology allows for either enantiomer to be prepared based on the stereochemistry of the tert-butyl sulfonamide employed and the nature of the transition state in the initial allylation. The versatility of this approach was highlighted in the rapid synthesis of unnatural analogs of grandisine D, demonstrating its applicability towards the synthesis of other natural products and pharmaceutically relevant scaffolds.

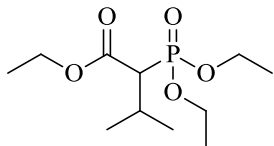
References

1. Cushnie, T. P. T.; Cushnie, B.; Lamb, A. J. *Int. J. Antimicrob. Agents* **2014**, *44*, 377–386.
2. Qiu, S.; Sun, H.; Zhang, A.-H.; Xu, H.-Y.; Yan, G.-L.; Han, Y.; Wang, X.-J. *Chin. J. Nat. Med.* **2014**, *12*, 401–406.
3. Heinrich, M.; Lee Teoh, H. *J. Ethnopharmacol.* **2004**, *92*, 147–162.
4. Amirkia, V.; Heinrich, M. *Phytochem. Lett.* **2014**.
5. Robins, D. J. *Nat. Prod. Rep.* **1991**, *8*, 213–221.
6. Hartmann, T.; Biller, A.; Witte, L.; Ernst, L.; Boppré, M. *Biochem. Syst. Ecol.* **1990**, *18*, 549–554.
7. Katavic, P. L.; Venables, D. A.; Forster, P. I.; Guymer, G.; Carroll, A. R. *Society* **2006**, 1295–1299.
8. Michael, J. P. *Nat. Prod. Rep.* **2005**, *22*, 603–626.
9. Culvenor, C.; Smith, L. *Aust. J. Chem.* **1967**, *20*, 2499.
10. Tasso, B.; Novelli, F.; Sparatore, F.; Fasoli, F.; Gotti, C. *J. Nat. Prod.* **2013**, *76*, 727–731.
11. Fu, P. P.; Xia, Q.; Lin, G.; Chou, M. W. *Drug Metab. Rev.* **2004**, *36*, 1–55.
12. Sharma, R. A.; Singh, B.; Singh, D.; Chandrawat, P. *J. Med. Plants* **2009**, *3*, 1153–1175.
13. Takahata, H.; Momose, T. *Tetrahedron* **1991**, *47*, 7635–7644.
14. Stritzke, K.; Schulz, S.; Nishida, R. *Synthesis (Stuttg.)* **2002**, 0–8.
15. Edupuganti, R.; Davis, F. A. *Org. Biomol. Chem.* **2012**, *10*, 5021–5031.
16. Castro, M. A.; del Corral, J. M. M.; García, P. A.; Rojo, M. V.; de la Iglesia-Vicente, J.; Mollinedo, F.; Cuevas, C.; San Feliciano, A. *J. Med. Chem.* **2010**, *53*, 983–993.
17. Roeder, E.; Breitmaier, E.; Birecka, H.; Frohlicht, M. *Phytochemistry* **1991**, *30*, 11–14.

18. Asibal, C. F.; Glinski, J. A.; Gelbaum, L. T.; Zalkow, L. H. *J. Nat. Prod.* **1989**, *52*, 109–118.
19. Katavic, P. L.; Venables, D. A.; Forster, P. I.; Guymer, G.; Carroll, A. R. *J. Nat. Prod.* **2006**, *69*, 1295–1299.
20. Kurasaki, H.; Okamoto, I.; Morita, N.; Tamura, O. *Org. Lett.* **2009**, *11*, 1179–1181.
21. Cuthbertson, J. D.; Godfrey, A. A.; Taylor, R. J. K. *Org. Lett.* **2011**, *13*, 3976–3979.
22. Senter, T. J.; Fadeyi, O. O.; Lindsley, C. W. **2012**, 20–22.

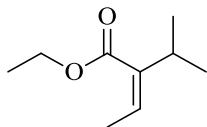
(+)-Amabiline Experimental Methods

Flame-dried (under vacuum) glassware was used for all reactions. All reagents and solvents were commercial grade and purified prior to use when necessary. Thin layer chromatography (TLC) was performed on glass-backed silica gel. Visualization was accomplished with UV light, and/or the use of anisaldehyde and ceric ammonium molybdate solutions followed by charring on a hot-plate. Chromatography on silica gel was performed using Silica Gel 60 (230-400 mesh) from Sorbent Technologies. IR spectra were recorded as thin films and are reported in wavenumbers (cm^{-1}). ^1H & ^{13}C NMR spectra were recorded on Bruker DRX-400 (400 MHz) or Bruker AV-NMR (600 MHz) instrument. Chemical shifts are reported in ppm relative to residual solvent peaks as an internal standard set to δ 7.26 and δ 77.0 (CDCl_3). Mass spectra were obtained on a Micromass Q-ToF API-US mass spectrometer was used to acquire high-resolution mass spectrometry (HRMS) data. The value Δ is the error in the measurement (in ppm) given by the equation $\Delta = [(M_E - M_T) / M_T] \times 10^6$, where M_E is the experimental mass and M_T is the theoretical mass. The HRMS results were obtained with ES as the ion source and leucine enkephalin as the reference.



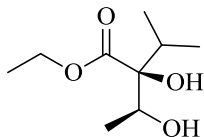
Ethyl 2-(diethoxyphosphoryl)-3-methylbutanoate (2.18)

Potassium *tert*-butoxide (6.16g, 55 mmol) was added at 0°C to a stirred solution of ethyl 2-(diethoxyphosphoryl)acetate (10 mL, 50 mmol) in 40 mL DMSO. The mixture was stirred for 30 min. until potassium *tert*-butoxide was dissolved. 2-iodopropane (5 mL, 55 mmol) was then added in a single batch. The solution was stirred for 90 min. at 60°C. After reaction complete by LCMS, the reaction was quenched with saturated NH₄Cl solution and extracted 3 times with diethyl ether. The organic layers were combined, washed once with brine, dried with MgSO₄, and concentrated *in vacuo* to yield a pale yellow oil in 12.4g (93%) sufficiently pure to carry forward. ¹H NMR (400.1 MHz, CDCl₃) δ (ppm): 4.19 (m, 6H), 2.73 (dd, J= 9, 11 Hz, 1H), 2.37 (m, 1H), 1.32 (m, 9H), 1.01 (d, J= 6.8 Hz, 3H), 0.99 (d, J= 6.8 Hz, 3H); ¹³C NMR (100.6 MHz, CDCl₃) δ (ppm): 169.23, 63.36, 63.34, 54.00, 52.68, 28.24, 21.60, 21.59, 16.24, 14.06; HRMS (TOF,ES+) C₁₁H₂₄O₅P [M+H]⁺ calc'd 267.1361, found 267.1363.



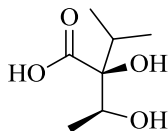
(Z)-ethyl 2-isopropylbut-2-enoate. (2.19)

A solution of (diethoxyphosphoryl)acetate 1.2.17 (6.0g, 22.56 mmol) in 70 mL anhydrous THF was cooled to -78°C under argon. To this solution was added LHMDS (26.89 mmol) and then stirred for 10 min, at which time acetaldehyde (1.39 mL, 24.81 mmol) was added in one batch. The resulting mixture was stirred at -78°C for 90 min. The reaction was quenched with saturated NH_4Cl solution and extracted 3 times with diethyl ether. The organic layers were combined, washed 1 time with brine, dried with MgSO_4 , and concentrated gently *in vacuo*. The crude product was purified by flash column chromatography (19:1 pentane/ Et_2O) to afford the product in 2.75g (78%) as a clear oil. ^1H NMR (400.1 MHz, CDCl_3) δ (ppm): 5.81 (q, $J=6.8$ Hz, 1H), 4.24 (q, $J=6.8$ Hz, 2H), 2.68 (sept 6.8 Hz, 1H), 1.88 (d, $J=7$ Hz, 3H), 1.32 (t, $J=7$ Hz, 3H), 1.06 (d, $J=6.7$ Hz, 6H); ^{13}C NMR (100.6 MHz, CDCl_3) δ (ppm): 169.32, 140.17, 129.87, 60.26, 31.67, 21.99, 15.60, 14.55; HRMS (TOF, ES^+) $\text{C}_9\text{H}_{16}\text{O}_2$ $[\text{M}+\text{Na}]^+$ calc'd 179.1048, found 179.1049.



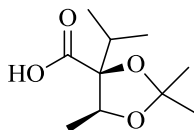
(2S,3S)-ethyl 2,3-dihydroxy-2-isopropylbutanoate (2.20).

A solution of AD-mix- α (10.43g) in a mixture of *tert*-butyl alcohol and water (75 mL, 1:1) was stirred at room temperature for 5 min. Methanesulfonamide (0.74g, 7.77 mmol) and 1.2.18 (1.2g, 7.69 mmol) were then added, and the solution was stirred at 0°C for 42 hours. Sodium sulfite (10.72g, 85.05 mmol) was added in two batches, and the mixture was stirred at room temperature for an addition 30 min. H₂O was added and the solution was extracted 4 times with ethyl acetate. The organic layers were combined and washed with 1N NaOH and brine. The organic layer was dried with MgSO₄ and the solvent was removed *in vacuo*. The crude product was purified by flash chromatography to yield the product in 1.23g (84%) as a clear oil. $[\alpha]_D^{20} = -2.9$ ($c = 10\text{mg/mL}$, MeOH); ¹H NMR (400.1 MHz, CDCl₃) δ (ppm): 4.29 (q, J= 7 Hz, 2H), 4.00 (q, J=, 6.5 Hz, 1H), 3.48 (br s, 1H), 2.17 (br s, 1H), 2.16 (sept, J= 6.8 Hz, 1H), 1.33 (t, J= 7.25 Hz, 3H), 1.22 (d, J= 6.7 Hz, 3H), 0.94 (d, J= 6.8 Hz, 3H), 0.93 (d, J= 6.8 Hz, 3H); ¹³C NMR (100.6 MHz, CDCl₃) δ (ppm): 175.05, 83.14, 70.54, 62.23, 32.49, 17.77, 17.40, 16.36, 14.44; HRMS (TOF, ES+) C₉H₁₈O₄ [M+Na]⁺ calc'd 213.1103, found 213.1102.



(2S,3S)-2,3-dihydroxy-2-isopropylbutanoic acid (2.12).

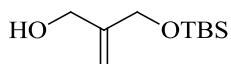
To a solution of 1.2.19 (0.5g, 2.63 mmol) in 6 mL H₂O was added Ba(OH)₂•8H₂O (0.99g, 3.156 mmol) slowly while stirring. The solution was heated to 50°C and stirred for 4 hours. Reaction was then brought to pH 2-3 with 1M HCl, at which time solution changed from cloudy white to clear, then extracted 5 times with diethyl ether. Organic layers were combined and concentrated *in vacuo*, yielding clear/white crystals in 0.40g (96%) as a white crystalline solid. $[\alpha]_D^{20} = -9.7$ (*c*= 10mg/mL, MeOH); ¹H NMR (400.1 MHz, MeOD) δ (ppm): 4.03 (q, *J*= 6.5 Hz, 1H), 2.16 (sept, *J*= 6.76 Hz, 1H), 1.25 (d, *J*= 6.5 Hz, 3H), 0.98 (d, *J*= 6.8 Hz, 3H), 0.97 (d, *J*= 6.8 Hz, 3H); ¹³C NMR (100.6 MHz, MeOD) δ (ppm); 84.06, 71.08, 33.70, 18.09, 17.88, 16.73; HRMS (TOF, ES⁺) C₇H₁₄O₄ [M+Na]⁺ calc'd 185.0790, found 185.0791.



(4S,5S)-4-isopropyl-2,2,5-trimethyl-1,3-dioxolane-4-carboxylic acid (2.14).

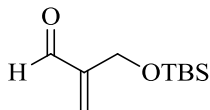
To a solution of 1.2.10 (0.265g, 1.635 mmol) in 2.615 mL dimethoxypropane was added 39.21 μ L of conc. HCl. The solution was stirred at room temperature for 2 hours until reaction was complete by TLC. Solution was concentrated *in vacuo*, and the crude product was purified by flash chromatography (1:1 Hex/EtOAc) to yield the product in

0.28 g (86%) as a white crystalline solid. $[\alpha]_D^{20} = -1.20$ ($c = 10\text{mg/mL}$, MeOH); ^1H NMR (400.1 MHz, CDCl_3) δ (ppm): 4.30 (q, $J = 6.3$ Hz, 1H), 2.05 (sept, $J = 6.86$ Hz, 1H), 1.58 (s, 3H), 1.43 (s, 3H), 1.39 (d, $J = 6.3$ Hz, 3H), 1.06 (d, $J = 6.86$ Hz, 3H), 1.03 (d, $J = 6.86$ Hz, 3H); ^{13}C NMR (100.6 MHz, CDCl_3) δ (ppm): 172.10, 109.23, 89.92, 77.09, 34.47, 27.66, 26.01, 18.09, 17.45, 16.83; HRMS (TOF, ES+) $\text{C}_{10}\text{H}_{19}\text{O}_4$ $[\text{M}+\text{H}]^+$ calc'd 203.1283, found 203.1284.



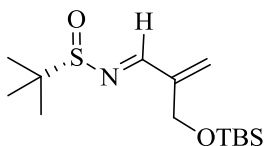
2-(((tert-butyldimethylsilyl)oxy)methyl)prop-2-en-1-ol (2.71):

To a flame-dried flask was added 350 mL dry THF, followed by addition of NaH (2.74g, 113.5 mmol). To this solution at 0°C was added 2-methylenepropane-1,3-diol (10g, 113.5 mmol) drop wise. Mixture was then brought to room temperature and stirred for 45 min. *Tert*-butyldimethylsilyl chloride (17.11g, 113.5 mmol) was added in one batch and stirring was continued for an additional 50 min. until complete by TLC. Reaction quenched with H_2O , and extracted 3 times with ethyl acetate, washed with brine, dried with anhydrous MgSO_4 , and concentrated *in vacuo*. Purification by flash chromatography (4:1 to 1:1 Hex/EtOAc) yielded the product in 20.66 g (89%) as a clear oil: ^1H NMR (400.1 MHz, CDCl_3) δ (ppm): 5.08 (d, $J = 7.4$ Hz, 2H), 4.25 (s, 2H), 4.17 (d, $J = 6$ Hz, 2H), 1.92 (t, $J = 6$ Hz, 1H), 0.92 (s, 9H), 0.09 (s, 6H); ^{13}C NMR (100.6 MHz, CDCl_3) δ (ppm): 147.35, 111.08, 65.07, 64.67, 25.78, 18.21, -5.52; HRMS (TOF, ES+) $\text{C}_{10}\text{H}_{23}\text{O}_2\text{Si}$ $[\text{M}+\text{H}]^+$ calc'd 203.1467, found 203.1466



2-(((tert-butyl dimethylsilyl)oxy)methyl)acrylaldehyde (2.22).

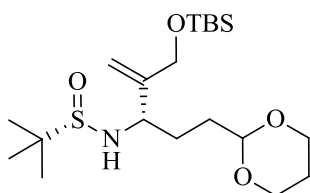
In a flame dried flask, monoprotected alcohol 1.2.13 (13.687g, 67.63 mmol) was dissolved in 200 mL DCM. While stirring, MnO₂ (29.4g, 338 mmol) was added in two batches. Mixture was then stirred for 6 hours, until reaction was determined complete by TLC. Solution was filtered through celite, concentrated *in vacuo*, and purified by flash chromatography (4:1 Hex/EtOAc) to yield product in 12.71g (89%) as a clear oil. : ¹H NMR (400.1 MHz, CDCl₃) δ (ppm): 9.62 (s, 1H), 6.52 (s, 1H) 6.11 (s, 1H), 4.40 (s, 2H), 0.92 (s, 9H), 0.09 (s, 6H); ¹³C NMR (100.6 MHz, CDCl₃) δ (ppm): 193.86, 149.74, 133.05, 59.79, 26.06, 18.52, -5.28; HRMS (TOF, ES+) C₁₀H₂₁O₂Si [M+H]⁺ calc'd 201.1311, found 203.1312.



(S,E)-N-(2-(((tert-butyl dimethylsilyl)oxy)methyl)allylidene)-2-methylpropane-2-sulfinamide (2.23).

To a solution of aldehyde 1.2.19 (9.00g, 45mmol) in 400mL DCM was added (R)-2-methylpropane-2-sulfinamide (6.54g, 54 mmol) and CuSO₄ (14.00g, 90 mmol). Solution stirred at room temperature for 16 hours. Mixture filtered through a pad of celite, with DCM as an eluent. Solution was then concentrated *in vacuo* and purified by column

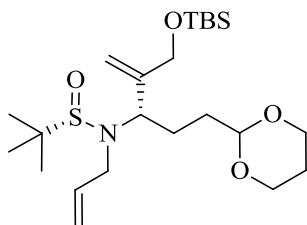
chromatography (4:1 Hex/EtOAc) to yield product in 10.75 g (79%). $[\alpha]_D^{20} = 27.276$ ($c=10$ mg/mL, MeOH); $^1\text{H NMR}$ (400.1 MHz, CDCl_3) δ (ppm): 8.26 (s, 1H), 6.13 (s, 1H), 5.82 (s, 1H), 4.48 (dt, $J=16, 7$ Hz, 2H), 1.20 (s, 9H), 0.93 (s, 9H), 0.09 (s, 6H); $^{13}\text{C NMR}$ (100.6 MHz, CDCl_3) δ (ppm): 163.32, 145.25, 127.42, 61.08, 57.62, 26.09, 22.70, 18.57, -5.23; HRMS (TOF, ES+) $\text{C}_{14}\text{H}_{30}\text{O}_2\text{SiS}$ $[\text{M}+\text{H}]^+$ calc'd 304.1767, found 304.1765.



(S)-N-((S)-2-(((tert-butyldimethylsilyl)oxy)methyl)-5-(1,3-dioxan-2-yl)pent-1-en-3-yl)-2-methylpropane-2-sulfinamide (2.25).

In a flame dried flask under Argon gas was added (2-(1,3-dioxan-2-yl)ethyl)magnesium bromide (19.8 mL, 0.5M in THF) to 30 mL THF. Mixture was then cooled to -78°C , and aldimine 1.2.20 (1.00g, 3.3 mmol) was added drop wise as a solution in 20 mL THF. Reaction was then warmed to -48°C and stirred 16 hours. Reaction was quenched with NH_4Cl and brought to room temperature. Extracted 3 times with ethyl acetate, organic layers combined and dried with Na_2SO_4 , concentrated *in vacuo* to give the crude product as >9:1 *dr* which was then purified by column chromatography (1:1 Hex/EtOAc) to afford product in 1.13 g (80%) as a clear oil: $[\alpha]_D^{20} = 1.596$ ($c=10$ mg/mL, MeOH); $^1\text{H NMR}$ (400.1 MHz, CDCl_3) δ (ppm): 5.30 (s, 1H), 5.20 (s, 1H), 5.07 (s, 1H), 4.50 (t, $J=5$ Hz, 1H), 4.22 (q, $J=13.5, 18.7$ Hz, 2H), 4.07 (dd, $J=5, 7$ Hz, 2H), 3.76 (m, 3H), 3.70 (d, $J=7$ Hz, 1H), 2.04 (m, 1H), 1.70 (m, 3H), 1.31 (br d, $J=13.6$ Hz, 1H), 1.20 (s, 9H), 0.91

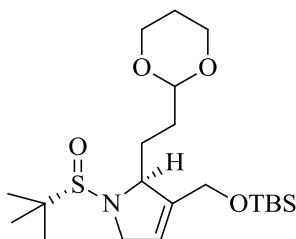
(s, 9H), 0.08 (s, 6H); ^{13}C NMR (100.6 MHz, CDCl_3) δ (ppm): 148.66, 112.74, 102.12, 67.08, 64.75, 59.33, 56.00, 31.81, 29.48, 26.14, 26.01, 22.92, 18.55, -5.20; HRMS (TOF, ES+) $\text{C}_{20}\text{H}_{42}\text{NO}_4\text{SiS}$ $[\text{M}+\text{H}]^+$ calc'd 420.2604, found 420.2603.



(S)-N-allyl-N-((S)-2-(((tert-butyldimethylsilyl)oxy)methyl)-5-(1,3-dioxan-2-yl)pent-1-en-3-yl)-2-methylpropane-2-sulfinamide (2.26).

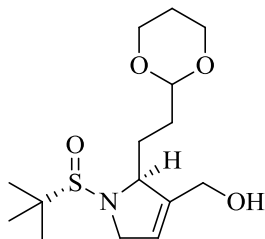
To sulfinylamine 1.2.22 (0.42 g, 1.00 mmol) in 3.0 mL DMF at -20°C was added LHMDS (1.75 mL, 1.0M in THF) drop wise. Mixture stirred at -20°C for 20 min, followed by addition of allyl bromide (0.61g, 5.0mmol) in a single batch. Reaction stirred for an additional 60 min at -20°C , at which time reaction was shown to be complete by TLC. Reaction was quenched with NH_4Cl , extracted 3 times with ethyl acetate, the organic layers combined and washed once with brine, dried with Na_2SO_4 , and concentrated *in vacuo*. Purified by column chromatography (1:1 Hex/EtOAc) to yield product in 0.46g (100%) as a pale yellow oil: $[\alpha]_{\text{D}}^{20} = -5.464$ ($c = 10\text{mg/mL}$, MeOH); ^1H NMR (400.1 MHz, CDCl_3) δ (ppm): 5.84 (m, 1H), 5.36 (s, 1H), 5.15 (m, 3H), 4.50 (t, $J = 5$ Hz, 1H), 4.08 (m, 4H), 3.91 (dd, $J = 5, 11.4$ Hz, 1H), 3.72 (t, $J = 11.6$ Hz, 2H), 3.54 (dd, $J = 4.7, 5.6$ Hz, 1H), 3.11 (dd, $J = 7.9, 8.5$ Hz, 1H), 2.01 (m, 3H), 1.63 (m, 1H), 1.51 (m, 1H), 1.33 (br d, $J = 12.9$, 1H), 1.15 (s, 9H), 0.90 (s, 9H), 0.05 (s, 6H); ^{13}C NMR (100.6

MHz, CDCl₃) δ (ppm): 145.52, 136.46, 117.93, 113.03, 102.19, 67.06, 64.98, 61.95, 57.98, 44.86, 32.76, 26.10, 24.96, 23.71, 18.48, -5.17; HRMS (TOF, ES⁺) C₂₃H₄₆NO₄SiS [M+H]⁺ calc'd 460.2917, found 460.2917.



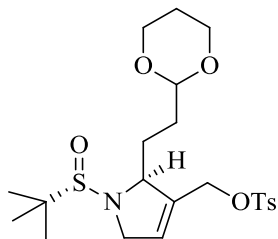
(S)-2-(2-(1,3-dioxan-2-yl)ethyl)-3-(((tert-butyldimethylsilyl)oxy)methyl)-1-((S)-tert-butylsulfinyl)-2,5-dihydro-1H-pyrrole (2.27).

In a flame-dried flask under Argon, diene 1.2.23 (0.46g, 1.0 mmol) was dissolved into 300 mL DCM. Grubbs II (0.042g, 0.05 mmol) was added to the solution in a single batch and the mixture was stirred at room temperature for 16 hours. The solution was then concentrated *in vacuo* and purified by column chromatography (1:1 Hex/EtOAc) to yield product in 0.41g (98%) as a pale yellow oil: $[\alpha]_D^{20} = 1.876$ ($c = 10\text{mg/mL}$, MeOH); ¹H NMR (400.1 MHz, CDCl₃) δ (ppm): 5.61 (s, 1H), 4.59 (br s, 1H), 4.48 (m, 2H), 4.13 (m, 2H), 4.05 (dd, $J = 5, 7$ Hz, 2H), 3.73 (t, $J = 12.4$ Hz, 2H), 3.45 (m, 1H), 2.04 (m, 1H), 1.65 (m, 3H), 1.51 (m, 1H), 1.34 (br d, $J = 13.9$ Hz, 1H), 1.21 (s, 9H), 0.90 (s, 9H), 0.05 (s, 6H); ¹³C NMR (100.6 MHz, CDCl₃) δ (ppm): 141.72, 121.90, 102.42, 71.75, 67.06, 60.08, 57.53, 47.76, 29.25, 28.52, 26.08, 24.04, 18.50, -5.26; HRMS (TOF, ES⁺) C₂₁H₄₂NO₄SiS [M+H]⁺ calc'd 432.2604, found 432.2604.



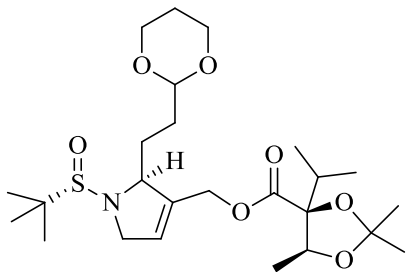
((R)-2-(2-(1,3-dioxan-2-yl)ethyl)-1-((S)-tert-butylsulfinyl)-2,5-dihydro-1H-pyrrol-3-yl)methanol (2.15).

In a flame dried flask under Argon, 1.2.24 (0.310g, 0.719 mmol) was dissolved in 14.4 mL THF. Solution was cooled to 0°C, and TBAF was slowly added. Solution was stirred at 0°C for 10 min, then warmed to room temperature, where stirring was continued 1 hour until reaction complete by TLC. Reaction was quenched by addition of H₂O and extracted 3 times with ethyl acetate. Organic layers were combined, washed 1 time with brine, dried with Na₂SO₄, and concentrated *in vacuo*. Crude product was purified by column chromatography (9:1 DCM/MeOH) to yield desired product in 0.198 g (87%) as a pale yellow crystalline solid: $[\alpha]_D^{20} = 21.11$ (*c* = 10mg/mL, MeOH); ¹H NMR (400.1 MHz, CDCl₃) δ (ppm): 5.70 (br s, 1H), 4.657 (br s, 1H), 4.51 (m, 2H), 4.12 (m, 2H), 4.06 (dd, *J* = 3, 7 Hz, 2H), 3.74 (t, *J* = 11.5 Hz, 2H), 3.50 (m, 2H), 2.04 (m, 1H), 1.70 (m, 3H), 1.52 (m, 1H), 1.33 (br d, *J* = 13.9 Hz, 1H), 1.21 (s, 9H); ¹³C NMR (100.6 MHz, CDCl₃) δ (ppm): 141.98, 123.26, 102.28, 72.02, 67.08, 59.56, 57.59, 47.81, 29.19, 28.38, 25.93, 23.99; HRMS (TOF, ES⁺) C₁₅H₂₈NO₄S [M+H]⁺ calc'd 318.1739, found 318.1737.



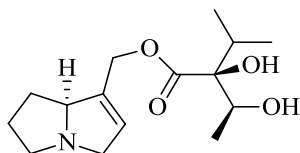
((S)-2-(2-(1,3-dioxan-2-yl)ethyl)-1-((S)-tert-butylsulfinyl)-2,5-dihydro-1H-pyrrol-3-yl)methyl 4-methylbenzenesulfonate (2.28).

In a flame dried flask under Argon, alcohol 1.2.11 (0.331g, 1.04 mmol) and Et₃N (0.212g, 2.10 mmol) were dissolved in 2.8 mL DCM and cooled to 0°C. p-Toluenesulfonyl chloride (0.191g, 1.35 mmol) was then dissolved in 2.8 mL DCM and added drop wise to reaction mixture. Stirring was continued at 0°C for 1 hour, until reaction complete by TLC. Solution was then filtered through a celite pad using DCM as the eluent, and concentrated *in vacuo*. Crude product was purified by column chromatography (4:1 DCM/Et₂O) to yield desired product in 0.42g (86%) as a pale yellow oil: $[\alpha]_D^{20} = 6.646$ ($c = 10\text{mg/mL}$, MeOH); ¹H NMR (400.1 MHz, CDCl₃) δ (ppm): 7.73 (d, $J = 8.2$ Hz, 2H), 7.36 (d, $J = 8.2$ Hz, 2H), 5.73 (s, 1H), 4.52 (m, 5H), 4.05 (dd, $J = 4.13, 7.4$ Hz, 2H), 3.72 (dt, $J = 2.4, 9.8$ Hz, 2H), 3.41 (m, 1H), 2.45 (s, 3H), 2.04 (m, 1H), 1.60 (m, 4H), 1.33 (br d, $J = 13.3$ Hz, 1H), 1.18 (s, 9H); ¹³C NMR (100.6 MHz, CDCl₃) δ (ppm): 145.25, 134.73, 132.98, 130.17, 128.17, 102.04, 71.58, 67.03, 65.78, 57.70, 47.66, 29.00, 28.04, 25.94, 23.86, 21.88; HRMS (TOF, ES⁺) C₁₅H₃₄NO₆S₂ [M+H]⁺ calc'd 472.1828, found 472.1832.



(4S,5S)-((S)-2-(2-(1,3-dioxan-2-yl)ethyl)-1-((S)-tert-butylsulfinyl)-2,5-dihydro-1H-pyrrol-3-yl)methyl 4-isopropyl-2,2,5-trimethyl-1,3-dioxolane-4-carboxylate (2.27).

In a flame dried flask under Argon, (4S,5S)-4-isopropyl-2,2,5-trimethyl-1,3-dioxolane-4-carboxylic acid (1.2.12) (0.237g, 1.175 mmol) was dissolved in 3 mL dry DMF. K_2CO_3 was added and mixture stirred at room temperature for 30 min. Tosylate 1.2.25 (0.461g, 0.979 mmol) was then added drop wise as a solution in 2 mL DMF, and mixture stirred for 90 min at room temperature, at which point reaction was complete by TLC. Solution was diluted with EtOAc, then filtered through a phase separator. Solution was washed 1 time with brine, dried with Na_2SO_4 , and concentrated *in vacuo*. Crude product was purified by column chromatography (1:1 Hex/EtOAc) to yield desired product in 0.46g (95%) as a clear oil: $[\alpha]_D^{20} = 7.4$ ($c = 10\text{mg/mL}$, MeOH); 1H NMR (400.1 MHz, $CDCl_3$) δ (ppm): 5.81 (s, 1H), 4.75 (d, $J = 14$ Hz, 1H), 4.65 (br s, 1H), 4.55 (m, 3H), 4.24 (q, $J = 6.6$ Hz, 1H), 4.05 (dd, $J = 4.7, 6.5$ Hz, 2H), 3.74 (t, $J = 12.2$ Hz, 2H), 3.47 (m, 1H), 2.15 (m, 1H), 2.04 (m, 1H), 1.70 (m, 2H), 1.60 (s, 3H), 1.51 (m, 1H), 1.40 (s, 3H), 1.33 (br d, $J = 13.3$ Hz, 1H), 1.27 (d, $J = 6.6$ Hz, 6H), 1.23 (s, 9H), 1.01 (d, $J = 6.7$ Hz, 3H), 0.98 (d, $J = 6.8$ Hz, 3H); ^{13}C NMR (100.6 MHz, $CDCl_3$) δ (ppm): 172.28, 136.41, 126.23, 109.08, 102.13, 71.93, 67.04, 60.75, 57.69, 47.78, 32.29, 29.13, 28.23, 27.18, 26.76, 25.95, 23.95, 18.98, 16.98, 16.40; HRMS (TOF, ES+) $C_{25}H_{44}NO_7S$ $[M+H]^+$ calc'd 502.2839, found 502.2836.

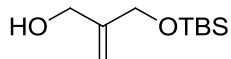


(2S,3S)-((S)-2,3,5,7a-tetrahydro-1H-pyrrolizin-7-yl)methyl-2,3-dihydroxy-2-isopropylbutanoate (2.4).

In a flame dried flask under Argon, ester 1.2.24 (0.100g, 0.20 mmol) was dissolved in 2.0 mL of 95:5 TFA/H₂O at room temperature. Solution was stirred for 90 min. at room temperature until conversion to iminium ion was observed by LC/MS. Solution was then concentrated *in vacuo*, and resulting residue was dissolved in 3mL DCE. To this solution was added MP-BH(OAc)₃ (0.5g, 2.00 mmol/g). The mixture was rotated for 16 hours, filtered and concentrated *in vacuo*. Crude product was purified by Gilson HPLC to yield product as the TFA salt. Product was converted to the free base by dissolving in DCM then adding 5 eq. PS-Carbonate, and rotating for 12 hours. Solution was filtered and concentrated *in vacuo* to yield desired product in 20 mg (37%) as a clear residue: $[\alpha]_D^{20} = 1.7$ ($c = 10\text{mg/mL}$, MeOH); ¹H NMR (400.1 MHz, CDCl₃) δ (ppm): 5.68 (s, 1H), 4.76 (br s, 1H), 4.17 (br s, 2H), 4.01 (q, J= 9.2, 12.8 Hz, 1H), 3.85 (d, J= 16 Hz, 1H), 3.38 (d, J= 16 Hz, 1H), 3.12 (pent, J= 5.16 Hz, 1H), 2.49 (m, 1H), 2.15 (m, 1H), 2.00 (m, 1H), 1.77 (m, 2H), 1.53 (m, 1H), 1.25 (d, J= 6.52 Hz, 3H), 0.93 (d, J= 6.8 Hz, 3H), 0.88 (d, J= 6.8 Hz, 3H); ¹³C NMR (100.6 MHz, CDCl₃) δ (ppm): 174.75, 137.72, 125.78, 83.48, 71.56, 70.63, 62.42, 61.90, 56.93, 32.28, 30.26, 25.97, 17.70, 17.31, 16.10; HRMS (TOF, ES+) C₁₅H₂₆NO₄ [M+H]⁺ calc'd 284.1862, found 284.1862.

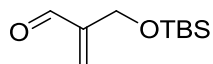
Grandisine D Experimental Methods

Flame-dried (under vacuum) glassware was used for all reactions. All reagents and solvents were commercial grade and purified prior to use when necessary. Thin layer chromatography (TLC) was performed on glass-backed silica gel. Visualization was accomplished with UV light, and/or the use of anisaldehyde and ceric ammonium molybdate solutions followed by charring on a hot-plate. Chromatography on silica gel was performed using Silica Gel 60 (230-400 mesh) from Sorbent Technologies. IR spectra were recorded as thin films and are reported in wavenumbers (cm^{-1}). ^1H & ^{13}C NMR spectra were recorded on Bruker DRX-400 (400 MHz) or Bruker AV-NMR (600 MHz) instrument. Chemical shifts are reported in ppm relative to residual solvent peaks as an internal standard set to δ 7.26 and δ 77.0 (CDCl_3). Mass spectra were obtained on a Micromass Q-ToF API-US mass spectrometer was used to acquire high-resolution mass spectrometry (HRMS) data. The value Δ is the error in the measurement (in ppm) given by the equation $\Delta = [(M_E - M_T) / M_T] \times 10^6$, where M_E is the experimental mass and M_T is the theoretical mass. The HRMS results were obtained with ES as the ion source and leucine enkephalin as the reference.



2-(((tert-butyldimethylsilyl)oxy)methyl)prop-2-en-1-ol. (2.72)

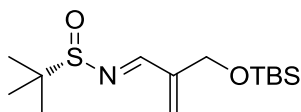
To a flame-dried flask was added 350mL dry THF, followed by addition of NaH (2.74g, 113.5 mmol). To this solution at 0°C was added 2-methylenepropane-1,3-diol (10g, 113.5 mmol) drop wise. Mixture was then brought to room temperature and stirred for 45 min. *Tert*-butyldimethylsilyl chloride (17.11g, 113.5 mmol) was added in one batch and stirring was continued for an additional 50 min. until complete by TLC. Reaction quenched with H₂O, and extracted 3 times with ethyl acetate, washed with brine, dried with anhydrous MgSO₄, and concentrated *in vacuo*. Purification by flash chromatography (4:1 to 1:1 Hex/EtOAc) yielded the product in 20.66 g (89%) as a clear oil: ¹H NMR (400.1 MHz, CDCl₃) δ (ppm): 5.08 (d, J= 7.4 Hz, 2H), 4.25 (s, 2H), 4.17 (d, J= 6 Hz, 2H), 1.92 (t, J= 6 Hz, 1H), 0.92 (s, 9H), 0.09 (s, 6H); ¹³C NMR (100.6 MHz, CDCl₃) δ (ppm): 147.35, 111.08, 65.07, 64.67, 25.78, 18.21, -5.52; HRMS (TOF, ES+) C₁₀H₂₃O₂Si [M+H]⁺ calc'd 203.1467, found 203.1466.



2-(((tert-butyldimethylsilyl)oxy)methyl)acrylaldehyde. (2.53)

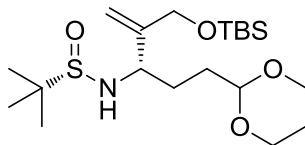
In a flame dried flask, alcohol (13.687g, 67.63 mmol) was dissolved in 200 mL DCM. While stirring, MnO₂ (29.4g, 338 mmol) was added in two batches. Mixture was then stirred for 6 hours, until reaction was determined complete by TLC. Solution was filtered through celite, concentrated *in vacuo*, and purified by flash chromatography (4:1

Hex/EtOAc) to yield product in 12.71g (89%) as clear oil. : ^1H NMR (400.1 MHz, CDCl_3) δ (ppm): 9.62 (s, 1H), 6.52 (s, 1H) 6.11 (s, 1H), 4.40 (s, 2H), 0.92 (s, 9H), 0.09 (s, 6H); ^{13}C NMR (100.6 MHz, CDCl_3) δ (ppm): 193.86, 149.74, 133.05, 59.79, 26.06, 18.52, -5.28; HRMS (TOF, ES+) $\text{C}_{10}\text{H}_{21}\text{O}_2\text{Si}$ $[\text{M}+\text{H}]^+$ calc'd 201.1311, found 201.1312.



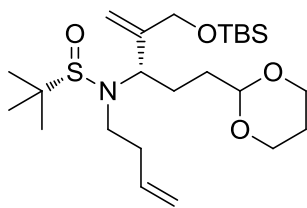
(R)-N-(2-(((tert-butyldimethylsilyl)oxy)methyl)allylidene)-2-methylpropane-2-sulfinamide (2.51)

To a solution of aldehyde (9.00g, 45 mmol) in 400 mL DCM was added (R)-2-methylpropane-2-sulfinamide (6.54g, 54 mmol) and CuSO_4 (14.00g, 90 mmol). Solution was stirred at room temperature for 16 hours. Mixture filtered through a pad of celite, with DCM as an eluent. Solution was then concentrated *in vacuo* and purified by column chromatography (4:1 Hex/EtOAc) to yield product in 10.75 g (79%). $[\alpha]_{\text{D}}^{20} = 27.276$ ($c=0.01$, MeOH); ^1H NMR (400.1 MHz, CDCl_3) δ (ppm): 8.26 (s, 1H), 6.13 (s, 1H), 5.82 (s, 1H), 4.48 (dt, $J=16, 7$ Hz, 2H), 1.20 (s, 9H), 0.93 (s, 9H), 0.09 (s, 6H); ^{13}C NMR (100.6 MHz, CDCl_3) δ (ppm): 163.32, 145.25, 127.42, 61.08, 57.62, 26.09, 22.70, 18.57, -5.23; HRMS (TOF, ES+) $\text{C}_{14}\text{H}_{30}\text{O}_2\text{SiS}$ $[\text{M}+\text{H}]^+$ calc'd 304.1767, found 304.1765.



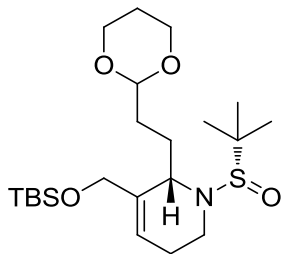
(S)-N-((S)-2-(((tert-butyldimethylsilyl)oxy)methyl)-5-(1,3-dioxan-2-yl)pent-1-en-3-yl)-2-methylpropane-2-sulfonamide. (2.56)

In a flame dried flask under Argon gas was added (2-(1,3-dioxan-2-yl)ethyl)magnesium bromide (19.8 mL, 0.5M in THF) to 30 mL THF. Mixture was then cooled to -78°C , and aldimine **1.3.23** (1.00g, 3.3 mmol) was added drop wise as a solution in 20 mL THF. Reaction was then warmed to -48°C and stirred 16 hours. Reaction was quenched with NH_4Cl and brought to room temperature. Extracted 3 times with ethyl acetate, organic layers combined and dried with Na_2SO_4 , concentrated *in vacuo*, and purified by column chromatography (1:1 Hex/EtOAc) to afford product in 1.13 g (80%) as a clear oil: $[\alpha]_{\text{D}}^{20} = 1.596$ ($c = 0.01$, MeOH); ^1H NMR (400.1 MHz, CDCl_3) δ (ppm): 5.30 (s, 1H), 5.20 (s, 1H), 5.07 (s, 1H), 4.50 (t, $J = 5$ Hz, 1H), 4.22 (q, $J = 13.5, 18.7$ Hz, 2H), 4.07 (dd, $J = 5, 7$ Hz, 2H), 3.76 (m, 3H), 3.70 (d, $J = 7$ Hz, 1H), 2.04 (m, 1H), 1.70 (m, 3H), 1.31 (br d, $J = 13.6$ Hz, 1H), 1.20 (s, 9H), 0.91 (s, 9H), 0.08 (s, 6H); ^{13}C NMR (100.6 MHz, CDCl_3) δ (ppm): 148.66, 112.74, 102.12, 67.08, 64.75, 59.33, 56.00, 31.81, 29.48, 26.14, 26.01, 22.92, 18.55, -5.20; HRMS (TOF, ES^+) $\text{C}_{20}\text{H}_{42}\text{O}_4\text{SiS}$ $[\text{M}+\text{H}]^+$ calc'd 420.2604, found 420.2603.



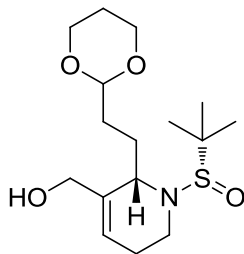
(S)-N-(but-3-en-1-yl)-N-((S)-2-(((tert-butyldimethylsilyl)oxy)methyl)-5-(1,3-dioxan-2-yl)pent-1-en-3-yl)-2-methylpropane-2-sulfonamide (2.57).

To a solution of sulfonamide **1.3.28** (100 mg, 0.24 mmol) in 3 mL THF at $-78\text{ }^{\circ}\text{C}$ was added HMPA (83 μL , 0.48 mmol) and $^n\text{BuLi}$ (94 μL , 2.5 M, 0.48 mmol). The mixture was stirred for 30 mins and a pre-cooled solution of but-3-enyl-trifluoromethanesulfonate (60 mg, 0.29 mmol) in 1 mL THF was then added slowly to the mixture. The mixture was stirred at $-78\text{ }^{\circ}\text{C}$ for 30 mins. The reaction was quenched with water and extracted with EtOAc (3x). The combined organic extracts were washed with brine and dried over Na_2SO_4 . Filtration and concentration afforded the crude product, which was purified by flash chromatography (1:1 Hex/EtOAc) to afford the product as a pale yellow oil (56 mg, 87% yield brsm): $[\alpha]_{\text{D}}^{20} = -2.53$ ($c = 1.00$, CHCl_3); $^1\text{H NMR}$ (400.1 MHz, CDCl_3) δ (ppm): 5.67-5.77 (m, 1H), 5.32 (brd, $J = 1.2$ Hz, 1H), 5.13 (s, 1H), 5.03 (dd, $J = 17.2, 1.6$ Hz, 1H), 5.02 (d, $J = 10.0$ Hz, 1H), 4.52 (t, $J = 4.8$ Hz, 1H), 4.05-4.08 (m, 4H), 3.72 (dt, $J = 12.0, 2.4$ Hz, 2H), 3.56 (dd, $J = 10.8, 4.4$ Hz, 1H), 3.29 (m, 1H), 2.58 (m, 1H), 2.38 (m, 1H), 2.25 (m, 1H), 1.95-2.23 (m, 3H), 1.67 (m, 1H), 1.50 (m, 1H), 1.32 (dm, $J = 13.8$ Hz, 1H), 1.14 (s, 9H), 0.89 (s, 9H), 0.05 (d, $J = 8.0$ Hz, 6H); $^{13}\text{C NMR}$ (100.6 MHz, CDCl_3) δ (ppm): 145.6, 135.3, 116.6, 112.9, 102.2, 67.0, 65.0, 61.7, 57.6, 42.2, 34.3, 32.8, 26.0, 25.9, 24.9, 23.7, 18.4, -5.1, -5.2; HRMS (TOF, ES+) $\text{C}_{24}\text{H}_{48}\text{NO}_4\text{SiS}$ $[\text{M}+\text{H}]^+$ calc'd 474.3073, found 474.3074.



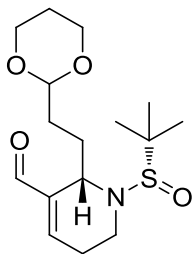
(S)-6-(2-(1,3-dioxan-2-yl)ethyl)-5-(((tert-butyldimethylsilyl)oxy)methyl)-1-((S)-tert-butylsulfinyl)-1,2,3,6-tetrahydropyridine. (2.59)

To a solution of **1.3.29** (1.2 g, 2.54 mmol) in CH₂Cl₂ (271 mL) was added 2nd Gen. Grubbs (107.7 mg, 0.127 mmol). The mixture was refluxed for 1 h and concentrated. The resulting crude product was purified by automated flash chromatography (4:1 to 1:1 Hex/EtOAc) to yield the desired product 1.005 g (89%) as yellow oil: $[\alpha]_D^{20} = +2.6$ ($c = 1.81$, CHCl₃); ¹H NMR (400.1 MHz, CDCl₃) δ (ppm): 5.75 (s, 1H), 4.49 (t, $J = 4.8$ Hz, 1 H), 4.09 (m, 4H), 3.73 (dt, $J = 12.0, 2.4$ Hz, 3H), 3.53 (dd, $J = 14.0, 6.4$ Hz, 3H), 3.12 (m, 1H), 2.45 (m, 1H), 2.05 (m, 1H), 1.87-1.79 (m, 1H), 1.78-1.69 (m, 2H), 1.66-1.58 (m, 2H), 1.32 (br d, $J = 13.2$ Hz, 1H), 1.20 (s, 9H), 0.90 (s, 9H), 0.06 (s, 6H); ¹³C NMR (100.6 MHz, CDCl₃) δ (ppm): 139.0, 122.3, 102.3, 67.0, 65.6, 58.9, 58.8, 37.8, 32.3, 27.9, 26.1, 26.0, 25.9, 25.2, 23.8, 18.5, -5.1, -5.3; HRMS (TOF, ES⁺) C₂₂H₄₄NO₄SiS [M+H]⁺ calc'd 446.2760, found 446.2762.



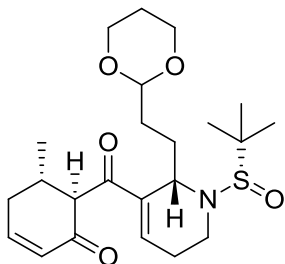
((S)-2-(2-(1,3-dioxan-2-yl)ethyl)-1-((S)-tert-butylsulfinyl)-1,2,5,6-tetrahydropyridin-3-yl)methanol. (2.72)

To a solution of silyl ether **1.3.30** (375 mg, 0.84 mmol) in THF (35 mL) under argon was added 1.0 M TBAF (1.3 mL, 1.26 mmol) dropwise at 0 °C. The mixture was warmed to rt and stirred for 2 h. The reaction was quenched with saturated NH₄Cl solution and extracted with EtOAc (3x). The combined organic extracts were washed with water and the dried over Na₂SO₄. Filtration and concentration afforded the crude product, which was purified by flash chromatography (9:1 CH₂Cl₂/MeOH) to afford the product as yellow oil (267 mg, 96%): $[\alpha]_D^{20} = +5.45$ ($c = 4.7$, CHCl₃); ¹H NMR (400.1 MHz, CDCl₃) δ (ppm): 5.82 (br s, 1H), 4.52 (t, $J = 4.8$ Hz, 1H), 4.04 (m, 4H), 3.81 (br d, $J = 7.2$ Hz, 1H), 3.74 (dt, $J = 2.4, 10$ Hz, 2H), 3.57 (q, $J = 7.2$ Hz, 1H), 3.13 (m, 1H), 2.49 (m, 1H), 2.17 (m, 2H), 1.88 (m, 2H), 1.77 (m, 2H), 1.62 (m, 1H), 1.33 (d, $J = 11$ Hz, 1H), 1.21 (s, 9H); ¹³C NMR (100.6 MHz, CDCl₃) δ (ppm): 139.81, 124.20, 102.17, 67.05, 65.46, 59.43, 58.97, 37.43, 32.33, 27.80, 25.88, 25.23, 23.87; HRMS (TOF, ES+) C₁₆H₃₀NO₄S [M+H]⁺ calc'd 332.1896, found 332.1898



(S)-2-(2-(1,3-dioxan-2-yl)ethyl)-1-((S)-tert-butylsulfinyl)-1,2,5,6-tetrahydropyridine-3-carbaldehyde (2.50).

To a solution of alcohol **1.3.40** (1.69 g, 5.11 mmol) in THF (300 mL) under argon was added MnO₂ (8.87 g, 102.1 mmol). The mixture was stirred at rt overnight. Filtration over celite and concentration afforded the pure product in 99% yield: $[\alpha]_D^{20} = +40.0$ ($c = 0.3$, CHCl₃); ¹H NMR (400.1 MHz, CDCl₃) δ (ppm): 9.34 (s, 1H), 6.91 (t, $J = 4$ Hz, 1H), 4.51 (t, $J = 4.4$ Hz, 1H), 4.05 (m, 3H), 3.70 (m, 3H), 3.23 (m, 1H), 2.84 (m, 1H), 2.17 (dt, $J = 5.2, 20$ Hz, 1H), 2.04 (m, 1H), 1.7 (m, 4H), 1.32 (br d, $J = 12.4$ Hz, 1H), 1.20 (s, 9H); ¹³C NMR (100.6 MHz, CDCl₃) δ (ppm): 192.05, 150.64, 143.48, 102.11, 67.02, 59.36, 57.12, 36.48, 32.67, 28.57, 26.76, 25.88, 23.50; HRMS (TOF, ES+) C₁₆H₂₈NO₄S [M+H]⁺ calc'd 330.1739, found 330.1741.

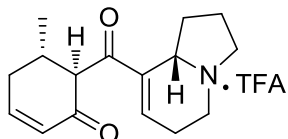


(5*S*,6*R*)-6-((*S*)-2-(2-(1,3-dioxan-2-yl)ethyl)-1-((*S*)-*tert*-butylsulfinyl)-1,2,5,6-tetrahydropyridine-3-carbonyl)-5-methylcyclohex-2-enone (2.60)

To a solution of (*S*)-5-methylcyclohex-2-enone (**1.3.7**) (43.5 mg, 0.395 mmol) in CH₂Cl₂ (2 mL) at -78 °C was added *N*-ethyl-*N*-isopropylamine (*i*Pr₂NEt) (0.103 mL, 0.592 mmol) and ⁿBu₂BOTf (0.592 mL, 0.592 mmol). The mixture was stirred at 78 °C for 1 h. Aldehyde **1.3.22** (86.6 mg, 0.263 mmol) dissolved in CH₂Cl₂ (2 mL) was added dropwise. The mixture was warm to rt and stir for 1.5 h. The reaction mixture was cooled to -78 °C and quenched with 0.1 mL each of MeOH and H₂O₂, diluted with NaHCO₃ and extracted with CH₂Cl₂ (3x). The combined organic extracts were washed with water and the dried over Na₂SO₄. Filtration and concentration afforded the crude product, which was used in the next step without purification.

To a stirred solution of DMSO (38 μL, 0.53 mmol) in CH₂Cl₂ (7 mL) at -78 °C was added drop-wise trifluoroacetic anhydride (50 μL, 0.35 mmol). After stirring at -78 °C for 30 mins, a pre-cooled solution of the crude alcohol dissolved in CH₂Cl₂ (4 mL). The reaction mixture was stirred at -78 °C for 1 h, then Et₃N (0.18 mL, 1.32 mmol) was added drop-wise. The solution was further stirred at -78 °C for a further 20 min, then warmed to rt and held for 1 h. The reaction was quenched by the addition of saturated aqueous NaHCO₃ and the aqueous layer was extracted with CH₂Cl₂ (5x), dried over Na₂SO₄,

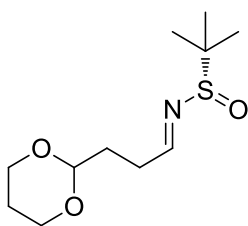
filtered, concentrated *in vacuo* to give the crude product, which was then purified by flash chromatography (1:20 MeOH/EtOAc) to yield **50** in 5:1 *dr.*, 88.4 mg (77% over 2-steps) as a pale yellow oil: $[\alpha]_D^{20} = +3.4$ ($c = 1.55$, CHCl_3); ^1H NMR (400.1 MHz, CDCl_3) δ (ppm): 6.84 (m, 1H), 6.02 (d, $J = 9.7$ Hz, 1H), 5.91 (t, $J = 3.8$ Hz, 1H), 4.52 (m, 1H), 4.21 (m, 1H), 4.07 (m, 2H), 3.73 (m, 2H), 3.61 (m, 2H), 3.20 (m, 1H), 2.66 (m, 1H), 2.53 (m, 1H), 2.40 (m, 1H), 2.34 (m, 1H), 2.10-2.09 (m, 2H), 1.87-1.73 (m, 3H), 1.61 (m, 1H), 1.33 (d, $J = 13.4$ Hz, 1H), 1.20 (s, 9H), 1.08 (d, $J = 6.88$, 3H); ^{13}C NMR (100.6 MHz, CDCl_3) δ (ppm): 200.98, 200.90, 147.6, 141.5, 128.9, 125.0, 102.2, 72.4, 67.3, 60.2, 59.2, 57.7, 36.34, 32.29, 30.95, 30.09, 27.97, 25.65, 23.53, 19.72 ; HRMS (TOF, ES+) $\text{C}_{23}\text{H}_{36}\text{NO}_5\text{S}$ $[\text{M}+\text{H}]^+$ calc'd 438.2371, found 438.2373.



Grandisine D (2.32)

1.3.31 (43.7 mg, 0.1 mmol) was dissolved in 95:5 TFA : H_2O to a final concentration of 0.1 M. After stirring for 1.5 h, the mixture was concentrated *in vacuo* and the residue was dissolved in DCE and PS- $\text{NaBH}(\text{OAc})_3$ (0.5 g, 0.5 mmol) was added and placed on a shaker for 2 h. The beads were filtered off and the solvent was concentrated *in vacuo* to give the crude product. Purification by flash chromatography (28% NH_3 -MeOH-AcOEt, 1:10:50) gave grandisine D as a pale yellow oil (12.2 mg, 47%). To a solution of the grandisine D (**41**) (9 mg, 0.034 mmol) in DCM (1 mL) at 0 °C was added dropwise TFA

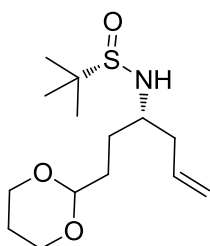
(3.6 μL , 0.051 mmol). The solution was held at 0 $^{\circ}\text{C}$ for 30 min, then warmed to rt and held for 1 h. The pale yellow solution was concentrated *in vacuo* to afford TFA salt of grandisine D (12.1 mg, Quant.) as pale yellow oil; $[\alpha]_{\text{D}}^{20} +68.8$ (c 0.09, MeOH); ^1H NMR (400.1 MHz, DMSO) δ (ppm): 10.47 (br s, 1H), 7.32 (bdd, $J = 4.0, 4.0$ Hz, 1H), 7.16 (ddd, $J = 10.0, 6.0, 2.4$ Hz, 1H), 5.94 (dd, $J = 10.0, 2.4$ Hz, 1H), 4.42 (dd, $J = 8.8, 8.8$ Hz, 1H), 4.36 (d, $J = 12.0$ Hz, 1H), 3.58-3.51 (m, 1H), 3.41-3.29 (m, 2H), 3.20-3.06 (m, 1H), 2.67-2.59 (m, 2H), 2.53-2.33 (m, 3H), 2.27-2.18 (m, 1H), 2.08-1.98 (m, 2H), 1.77-1.67 (m, 1H) 0.86 (d, $J = 6.0$ Hz, 3H); ^{13}C (100 MHz, DMSO) 198.4, 196.9, 151.9, 140.0, 137.3, 128.3, 59.1, 58.0, 52.7, 43.0, 32.7, 32.3, 28.0, 22.4, 20.4, 19.1; HRMS (TOF, ES+) $\text{C}_{16}\text{H}_{22}\text{NO}_2$ $[\text{M}+\text{H}]^+$ calc'd 260.1651, found 260.1650.



(S)-N-(3-(1,3-dioxan-2-yl)propylidene)-2-methylpropane-2-sulfinamide (2.61):

To a solution of 3-(1,3-dioxan-2-yl)propanal (10.1 g, 70.1 mmol) in CH_2Cl_2 (500 mL) was added (S)-2-methylpropane-2-sulfinamide (10.17 g, 84.1 mmol) and CuSO_4 (44.6 g, 280.4 mmol). The reaction mixture was stirred at rt overnight. The mixture was filtered through a celite pad and washed with CH_2Cl_2 . Concentration *in vacuo* gave the crude product which was purified by automated flash chromatography (4:1 to 1:1 Hex/EtOAc) to yield the desired product 15.6 g (90%) as yellow oil: $[\alpha]_{\text{D}}^{20} = +209.3$ ($c = 0.86$,

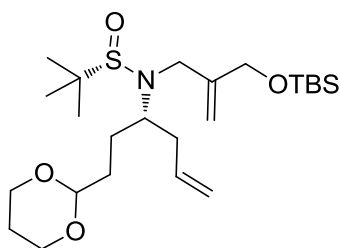
CHCl₃); ¹H NMR (400.1 MHz, CDCl₃) δ (ppm): 8.11 (t, *J* = 4.0 Hz, 1H), 4.62 (t, *J* = 4.8 Hz, 1H), 4.10 (dd, *J* = 6.0, 4.8 Hz, 2H), 3.76 (m, 2H), 2.64 (sextet, *J* = 4.0 Hz, 2H), 2.07 (m, 1H), 1.93 (m, 2H), 1.32 (dm, *J* = 13.8 Hz, 1H), 1.18 (s, 9H); ¹³C NMR (100.6 MHz, CDCl₃) δ (ppm): 169.1, 101.0, 67.0, 56.7, 30.8, 30.7, 25.8, 22.5; HRMS (TOF, ES+) C₁₁H₂₂NO₃S [M+H]⁺ calc'd 248.1320, found 248.1319.



(S)-N-((S)-1-(1,3-dioxan-2-yl)hex-5-en-3-yl)-2-methylpropane-2-sulfinamide (2.62):

Indium-mediated allylation was done according to procedures published by Lin and co-workers. To a reaction flask containing sulfinimine **1.3.32** (14.5 g, 58.7 mmol) and indium powder (27.0 g, 234.8 mmol) was added saturated aqueous NaBr solution (1174 mL, (1062.4 g of NaBr)) followed by the allyl bromide (36.8 mL, 234.8 mmol). The resulting suspension stirred at rt for 24 h. The reaction was quenched by the addition of saturated aqueous NaHCO₃ and filtered through a pad of celite. The aqueous layer was extracted with EtOAc (3x), dried over Na₂SO₄, filtered, concentrated *in vacuo* to give the crude product as >19:1 *dr*, which was then purified by flash chromatography (1:1 Hex/EtOAc) to yield the allylation product in 14.7 g (87%) as a pale yellow oil: [α]_D²⁰ = +38.9 (*c* = 1.43, CHCl₃); ¹H NMR (400.1 MHz, CDCl₃) δ (ppm): 5.77 (m, 1H), 5.16 (d, *J* = 4 Hz, 1H), 5.13 (s, 1H), 4.51 (t, *J* = 4.5 Hz, 1H), 4.08 (dd, *J* = 5, 6.3 Hz, 2H), 3.74 (dt,

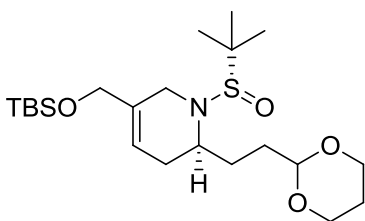
$J = 10, 2.2 \text{ Hz}, 2\text{H}), 3.30 \text{ (m, 1H)}, 3.23 \text{ (d, } J = 6.5 \text{ Hz, 1H)}, 2.37 \text{ (m, 2H)}, 2.05 \text{ (m, 1H)}, 1.63 \text{ (m, 3H)}, 1.33 \text{ (br, } J = 14 \text{ Hz, 1H)}, 1.19 \text{ (s, 9H)}$; ^{13}C NMR (100.6 MHz, CDCl_3) δ (ppm): 133.9, 119.0, 101.9, 66.8, 55.8, 55.0, 40.5, 31.3, 29.2, 25.7, 22.6; HRMS (TOF, ES+) $\text{C}_{14}\text{H}_{28}\text{NO}_3\text{S}$ $[\text{M}+\text{H}]^+$ calc'd 290.1790, found 290.1790.



(S)-N-((S)-1-(1,3-dioxan-2-yl)hex-5-en-3-yl)-N-(2-(((tert-butyl)dimethylsilyloxy)methyl)allyl)-2-methylpropane-2-sulfinamide (2.64):

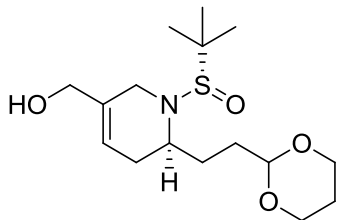
To a solution of sulfinamide **1.3.33** (1.4 g, 4.84 mmol) in 25 mL DMF at $-20\text{ }^\circ\text{C}$ was added LiHMDS (9.7 mL, 1 M in THF,) and the mixture was stirred for 20 mins at $-20\text{ }^\circ\text{C}$ and 20 mins at rt. The mixture was cooled back to $-20\text{ }^\circ\text{C}$ and **2.62** (3.83 g, 14.83 mmol) was then added slowly to the mixture and the reaction was stirred at $-20\text{ }^\circ\text{C}$ for 30 mins and rt overnight. The reaction was quenched with saturated NH_4Cl solution and extracted with EtOAc (3x). The combined organic extracts were washed with water and dried over Na_2SO_4 . Filtration and concentration afforded the crude product, which was purified by flash chromatography (4:1 to 1:1 Hex/EtOAc) to afford the product as a pale yellow oil (2.06 g, 90%): $[\alpha]_{\text{D}}^{20} = -2.3$ ($c = 0.85$, CHCl_3); ^1H NMR (400.1 MHz, CDCl_3) δ (ppm): 5.74-5.84 (m, 1H), 5.23 (s, 1H), 5.14 (s, 1H), 5.03 (m, 1H), 4.48 (t, $J = 5.2 \text{ Hz}$, 1H), 4.05 (m, 4H), 3.94 (brd, $J = 17.2 \text{ Hz}$, 1H), 3.72 (dt, $J = 12.0, 2.4 \text{ Hz}$, 2H), 3.14 (d, $J = 17.2 \text{ Hz}$,

1H), 2.96 (q, $J = 7.2$ Hz, 1H), 2.40 (dq, $J = 28.2, 6.8$ Hz, 2H), 1.89-2.09 (m, 2H), 1.61-1.80 (m, 3H), 1.32 (dm, $J = 13.8$ Hz, 1H), 1.29 (s, 9H), 1.19 (s, 9H), 0.06 (s, 6H); ^{13}C NMR (100.6 MHz, CDCl_3) δ (ppm): 145.2, 136.3, 117.2, 111.7, 102.2, 67.0, 66.9, 64.8, 62.6, 58.0, 53.6, 45.5, 39.5, 33.3, 27.3, 26.0, 25.9, 23.8, 18.5, -5.2, -5.3; HRMS (TOF, ES+) $\text{C}_{24}\text{H}_{48}\text{NO}_4\text{SiS}$ $[\text{M}+\text{H}]^+$ calc'd 474.3073, found 474.3076.



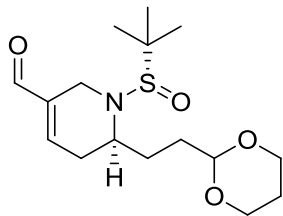
(S)-2-(2-(1,3-dioxan-2-yl)ethyl)-5-(((tert-butyldimethylsilyl)oxy)methyl)-1-((S)-tert-butylsulfinyl)-1,2,3,6-tetrahydropyridine (2.67):

To a solution of **1.3.35** (1.0 g, 2.11 mmol) in CH_2Cl_2 (260 mL) was added 2nd Gen. Grubbs (89.5 mg, 0.106 mmol). The mixture was refluxed for 1 h and concentrated. The resulting crude product was purified by automated flash chromatography (4:1 to 1:1 Hex/EtOAc) to yield the desired product 0.845 g (90%) as a yellow oil: $[\alpha]_{\text{D}}^{20} = -1.7$ ($c = 0.0181$, CHCl_3); ^1H NMR (400.1 MHz, CDCl_3) δ (ppm): 5.62 (d, $J = 4.8$ Hz, 1H), 4.51 (t, $J = 4.8$ Hz, 1 H), 4.09 (dd, $J = 4, 7.6$ Hz, 2H), 4.03 (d, $J = 4$ Hz, 1H), 3.73 (m, 3H), 3.34 (m, 2H), 2.52 (m, 1H), 2.06 (m, 1H), 1.89 (dd, $J = 6, 12.4$ Hz, 1H), 1.80 (m, 1H), 1.68 (m, 2H), 1.57 (m, 2H), 1.33 (br, d, $J = 12.4$ Hz, 1H), 1.16 (s, 9H), 0.89 (s, 9H), 0.05 (s, 6H); ^{13}C NMR (100.6 MHz, CDCl_3) δ (ppm): 135.3, 118.3, 102.3, 67.0, 65.5, 58.7, 56.8, 37.2, 32.9, 28.0, 27.0, 26.1, 25.9, 23.5, 18.5, -5.2; HRMS (TOF, ES+) $\text{C}_{22}\text{H}_{44}\text{NO}_4\text{SiS}$ $[\text{M}+\text{H}]^+$ calc'd 446.2760, found 446.2764.



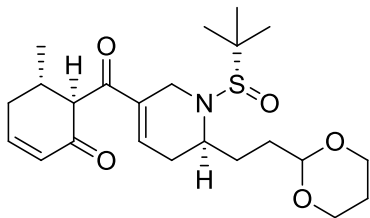
((S)-6-(2-(1,3-dioxan-2-yl)ethyl)-1-((S)-tert-butylsulfinyl)-1,2,5,6-tetrahydropyridin-3-yl)methanol (2.72)

To a solution of **1.3.36** (300 mg, 0.67 mmol) in THF (27 mL) under argon was added 1.0 M TBAF (1.01 mL, 1.01 mmol) dropwise at 0 °C. The mixture was warmed to rt and stirred for 2 h. The reaction was quenched with saturated NH₄Cl solution and extracted with EtOAc (3x). The combined organic extracts were washed with water and then dried over Na₂SO₄. Filtration and concentration afforded the crude product, which was purified by flash chromatography (9:1 CH₂Cl₂/MeOH) to afford the product as a yellow oil (210 mg, 95%): $[\alpha]_D^{20} = -116.1$ ($c = 4.7$, CHCl₃); ¹H NMR (400.1 MHz, CDCl₃) δ (ppm): 5.64 (br d, $J = 4.8$ Hz, 1H), 4.49 (t, $J = 4.8$ Hz, 1H), 4.05 (dd, $J = 11.6, 4.0$ Hz, 2H), 3.91 (m, 3H), 3.71 (tt, $J = 12.0, 3.6$, Hz, 2H), 3.33 (m, 2H), 2.96 (br s, 1H), 2.52 (br d, $J = 17.6$ Hz, 1H), 2.04 (m, 1H), 1.87 (br dd, $J = 17.6, 5.2$, Hz, 1H), 1.79-1.68 (m, 2H), 1.59-1.49 (m, 2H), 1.31 (d, $J = 12.4$ Hz, 1H), 1.14 (s, 9H); ¹³C NMR (100.6 MHz, CDCl₃) δ (ppm): 135.7, 119.8, 101.9, 66.8, 65.2, 58.6, 56.9, 36.6, 32.6, 27.7, 26.8, 25.7, 23.3; HRMS (TOF, ES+) C₁₆H₃₀NO₄S [M+H]⁺ calc'd 332.1896, found 332.1897.



(S)-6-(2-(1,3-dioxan-2-yl)ethyl)-1-((S)-tert-butylsulfinyl)-1,2,5,6-tetrahydropyridine-3-carbaldehyde (2.68)

To a solution of alcohol (150 mg, 0.45 mmol) in THF (30 mL) under argon was added MnO_2 (796 mg, 9.16 mmol). The mixture was stirred at rt overnight. Filtration over celite and concentration afforded the pure product in Quant. yield: $[\alpha]_{\text{D}}^{20} = -8.1$ ($c = 1$, MeOH); ^1H NMR (400.1 MHz, CDCl_3) δ (ppm): 9.34 (s, 1H), 6.91 (d, $J = 5.2$ Hz, 1H), 4.51 (t, $J = 4.4$ Hz, 1H), 4.12 (m, 3H), 3.72 (tt, $J = 12.0, 2.8$ Hz, 2H), 3.49 (m, 2H), 2.79 (dm, $J = 3.2$ Hz, 1H), 2.22 (ddd, $J = 19.2, 6.0, 2.0$ Hz, 1H), 2.06 (m, 1H), 1.75-1.51 (m, 4H), 1.32 (br d, $J = 12.4$ Hz, 1H), 1.18 (s, 9H); ^{13}C NMR (100.6 MHz, CDCl_3) δ (ppm): 191.9, 146.5, 138.7, 101.5, 66.7, 58.7, 56.6, 33.6, 32.3, 29.3, 26.8, 25.6, 23.2; HRMS (TOF, ES+) $\text{C}_{16}\text{H}_{28}\text{NO}_4\text{S}$ $[\text{M}+\text{H}]^+$ calc'd 330.1739, found 330.1739.

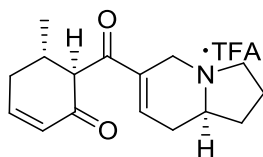


(5*S*,6*R*)-6-((*S*)-6-(2-(1,3-dioxan-2-yl)ethyl)-1-((*S*)-*tert*-butylsulfinyl)-1,2,5,6-tetrahydropyridine-3-carbonyl)-5-methylcyclohex-2-enone (2.69)

To a solution of (*S*)-5-methylcyclohex-2-enone **1.3.7** (43.5 mg, 0.395 mmol) in CH₂Cl₂ (2 mL) at -78 °C was added *N*-ethyl-*N*-isopropylpropylamine (*i*Pr₂NEt) (0.103 mL, 0.592 mmol) and ⁿBu₂BOTf (0.592 mL, 0.592 mmol). The mixture was stirred at -78 °C for 1 h. Aldehyde **1.3.37** (86.6 mg, 0.263 mmol) dissolved in CH₂Cl₂ (2 mL) was added dropwise. The mixture was warmed to rt and stirred for 1.5 h. The reaction mixture was cooled -78 °C and quenched with 0.1 mL each of MeOH and H₂O₂, diluted with NaHCO₃ and extracted with CH₂Cl₂ (3x). The combined organic extracts were washed with water and the dried over Na₂SO₄. Filtration and concentration afforded the crude product, which was used in the next step without purification.

To a stirred solution of DMSO (38 μL, 0.53 mmol) in CH₂Cl₂ (7 mL) at -78 °C was added drop-wise trifluoroacetic anhydride (50 μL, 0.35 mmol). After stirring at -78 °C for 30 mins, a pre-cooled solution of the crude alcohol was dissolved in CH₂Cl₂ (4 mL). The reaction mixture was stirred at -78 °C for 1 h, then Et₃N (0.18 mL, 1.32 mmol) was added dropwise. The solution was further stirred at -78 °C for a further 20 min, then warmed to rt and held for 1 h. The reaction was quenched by the addition of saturated aqueous NaHCO₃ and the aqueous layer was extracted with CH₂Cl₂ (5x), dried over Na₂SO₄, filtered, concentrated *in vacuo* to give the crude product, which was then

purified by flash chromatography (1:20 MeOH/EtOAc) to yield the desired product **57**, 77.0 mg (67% over 2-steps) as a pale yellow oil: $[\alpha]_D^{20} = +3.6$ ($c = 0.27$, CHCl_3); ^1H NMR (400.1 MHz, CDCl_3) δ (ppm): 6.96 (m, 1H), 6.86 (br d, $J = 5.2$ Hz, 1H), 6.02 (d, $J = 10$ Hz, 1H), 4.51 (m, 1H), 4.08 (m, 3H), 3.82 (m, 1H), 3.72 (m, 3H), 3.53 (br d, $J = 18.8$ Hz, 1H), 3.39 (m, 1H), 2.77 (m, 1H), 2.67 (m, 1H), 2.56 (m, 1H), 2.09 (m, 3H), 1.75 (m, 1H), 1.59 (m, 2H), 1.32 (br d, $J = 12.4$ Hz, 1H), 1.16 (s, 9H), 0.99 (d, $J = 6.4$ Hz, 3H); ^{13}C NMR (100.6 MHz, CDCl_3) δ (ppm): 197.73, 196.79, 149.98, 138.64, 129.34, 101.97, 67.00, 59.85, 58.91, 56.27, 34.79, 33.08, 32.90, 32.62, 29.04, 27.28, 25.88, 23.39, 22.86, 20.20; HRMS (TOF, ES+) $\text{C}_{23}\text{H}_{36}\text{NO}_5\text{S}$ $[\text{M}+\text{H}]^+$ calc'd 438.2371, found 438.2371.



(5S,6R)-6-((S)-1,2,3,5,8,8a-hexahydroindolizine-6-carbonyl)-5-methylcyclohex-2-enone (2.70):

1.3.38 (40.7 mg, 0.093 mmol) was dissolved in 95: 5 (TFA: H_2O) to a final concentration of 0.1 M. After stirring for 1.5 h, the mixture was concentrated *in vacuo*, the residue was dissolved in DCE and $\text{PS-NaBH}(\text{OAc})_3$ (0.5 g, 0.465 mmol) and was added and placed on a shaker for 2 h. The beads were filtered off and the solvent was concentrated *in vacuo* to give the crude product. Purification by flash chromatography (28% NH_3 -MeOH-AcOEt, 1:10:50) gave **1.3.39** as pale yellow oil (11.8 mg, 49%). To a solution of **1.3.39** (10 mg, 0.0386 mmol) in DCM (1 mL) at 0 °C was added dropwise

TFA (4.1 μL , 0.058 mmol). The solution was held at 0 $^{\circ}\text{C}$ for 30 min, then warmed to rt and held for 1 h. The pale yellow solution was concentrated *in vacuo* to afford TFA salt of **1.3.39** (13.7 mg, Quant.) as a pale yellow oil; $[\alpha]_{\text{D}}^{20} +2.1$ (*c* 0.05, MeOH);

^1H NMR (600.1 MHz, DMSO) δ (ppm): 10.27 (br s, 1H), 7.33 (m, 1H), 7.15 (ddd, $J = 10.2, 6.6, 2.4$ Hz, 1H), 5.96 (dd, $J = 10.2, 2.4$ Hz, 1H), 4.35 (d, $J = 12.0$ Hz, 1H), 4.30 (d, $J = 16.2$ Hz, 1H), 3.80 (m, 1H), 3.74-3.68 (m, 1H), 3.30 (br s, 1H), 3.12-3.09 (m, 1H), 2.89 (dt, $J = 19.8, 4.2$ Hz, 1H), 2.55-2.44 (m, 3H), 2.32-2.27 (m, 1H), 2.32-2.27 (m, 1H), 2.24-2.19 (m, 1H), 2.06-1.99 (m, 1H), 1.97-1.91 (m, 1H), 1.64 (q, $J = 10.2$ Hz, 1H) 0.87 (d, $J = 6.0$ Hz, 3H); $^{\delta}\text{C}$ (150.9 MHz, DMSO) 198.0, 196.8, 151.9, 140.9, 134.6, 128.4, 60.4, 59.5, 52.2, 47.8, 32.7, 32.6, 28.7, 27.6, 19.9, 19.2; HRMS (TOF, ES+) $\text{C}_{16}\text{H}_{22}\text{NO}_2$ $[\text{M}+\text{H}]^+$ calc'd 260.1651, found 260.1651.

CHAPTER III

GENERAL ACCESS TO CHIRAL N-ALKYL TERMINAL AZIRIDINES AND 2-SUBSTITUTED AZETIDINES VIA ORGANOCATALYSIS

3.1. Introduction to Aziridines

3.1.1. General properties of aziridines:

Aziridines represent an important class of nitrogen heterocycles that have been met with increasing interest in both synthetic chemistry and pharmacology over the past two decades. The synthetic utility of the aziridine group lies primarily in both its stability and ability to undergo highly regio- and stereoselective transformations. This reactivity is due to a combination of Baeyer strain of the three-membered heterocycle and electronegativity of the heteroatom, resulting in similar reactivity to that of its oxygen-containing cousin epoxides (**Table 3.1**). Diminished electronegativity of the nitrogen compared to that of oxygen, as well as the additional valency of nitrogen make aziridines less prone to ring-opening reactions. However, there is still a plentiful collection of this chemistry. In addition, aziridines can exhibit antitumor or antibiotic activity, as well as other biological properties which make them attractive synthetic targets in medicinal chemistry and the total synthesis of natural products.¹





structure	Ring Strain (calc)	cLogP (calc)	pK _a (acid)
	26.2	-0.74	7.98
	27.3	1.67	
	24.6	-0.27	
	18.9	0.33	

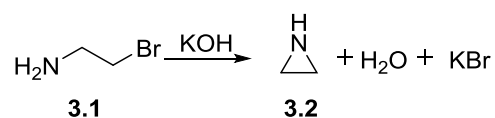
Table 3.1. Physical properties of 3-member ring moieties

As the chemistry surrounding aziridines has been developed over the last fifty years, aziridines have been classified as either activated or non-activated. This classification has been made according to whether or not nucleophilic ring-opening reactions proceed without a positive charge at the nitrogen. Activated aziridines are typically *N*-substituted with groups that stabilize the amide-like anion that results from ring-opening. This is achieved through resonance or inductive effects (sulfonyl, carbonyl, phosphoryl). Non-activated aziridines are *N*-substituted with alkyl or aryl groups, and nucleophilic ring-opening usually requires activation through Lewis acid catalysis, protonation, or quaternization of the nitrogen.

3.2. Synthesis of Aziridines:

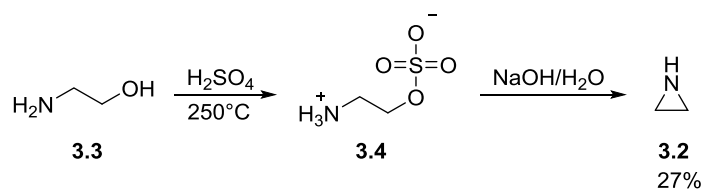
3.2.1. Introduction

While aziridines share many structural similarities with epoxides, there is a marked disparity in the range of synthetic methods available to construct aziridines. While aziridines synthesis, and especially asymmetric synthesis, has been slower to develop than epoxides, there are several strategies currently available to synthetic chemists. The first synthesis of an aziridine was reported by Gabriel in 1888.² Gabriel's synthesis of ethylenimine was accomplished by the nucleophilic ring closure of vicinal haloamines under basic conditions.



Scheme 3.1. Gabriel-Marckwald Ethylenimine Synthesis

Similarly, in 1935, an approach was developed by Wenker where vicinal aminoalcohol **3.3** was first treated with sulfuric acid to form a sulfonate salt **3.4**, which was subsequently reacted with sodium hydroxide to form the resulting aziridine (**Scheme 3.1**).³



Scheme 3.1. Wenker Aziridine Synthesis

Since these seminal publications on the synthesis of aziridines, a tremendous amount of progress has been made in approaches for the formation of aziridines that are relatively mild and stereoselective. Modern methods include addition to alkenes (nitrene transfer, addition/elimination), addition to imines (carbene and ylide methods, aza-Darzens strategies), and intramolecular nucleophilic substitution (**Figure 3.1**).⁴

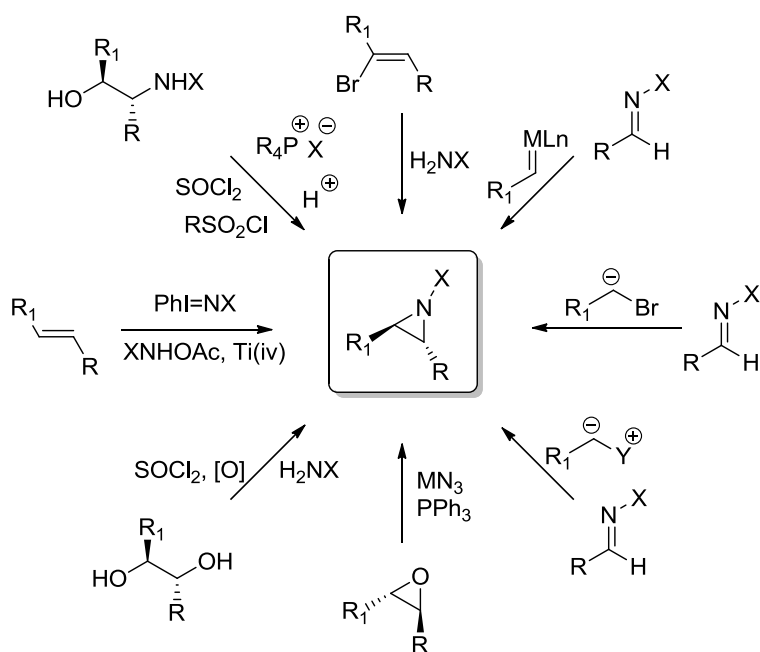


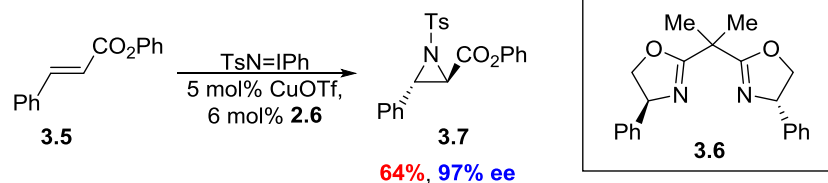
Figure 3.1. Synthetic Approaches to Aziridines

3.2.2. Aziridine Synthesis by Addition to Alkenes

A traditional approach for the direct aziridination of alkenes involves the addition of nitrenes. Nitrenes are typically generated by thermal or photochemical decomposition of azides, as well as oxidation of hydrazines. These methods require harsh reaction conditions, and, in many cases, the desired products are formed with poor stereoselectivity.¹ In the 1990s, attention was directed towards the use of metal-stabilized nitrenes in alkene aziridination, which, in the presence of chiral ligands, can provide a method for enantioselective aziridination of a wide range of alkenes.

In 1993, the Evans group developed the first copper-mediated enantioselective aziridination of *trans* olefins **3.5** with chiral bis(oxazoline) ligands **3.6** (**Figure 3.2**).⁵ The Jacobsen group concurrently optimized chiral 1,2 diimine derivatives **3.9** with copper(II) salts and found high enantioselectivities for *cis* olefins **3.8** containing at least one aromatic substituent.⁶ These two systems are complimentary in their substrate scope, however both lack good enantioselectivity for simple alkenes, and typically require up to five equivalents of alkene to achieve the reported yields.

Evans Enantioselective Aziridination of Trans Olefins:



Jacobsen Enantioselective Aziridination of Cis Olefins:

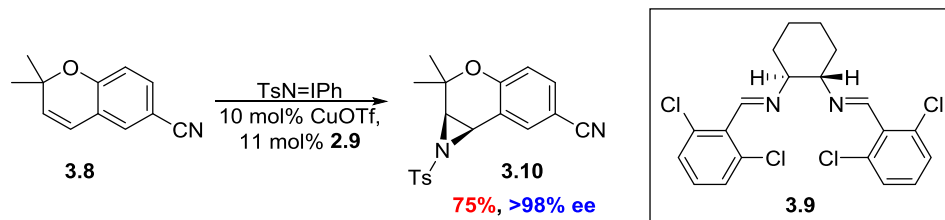
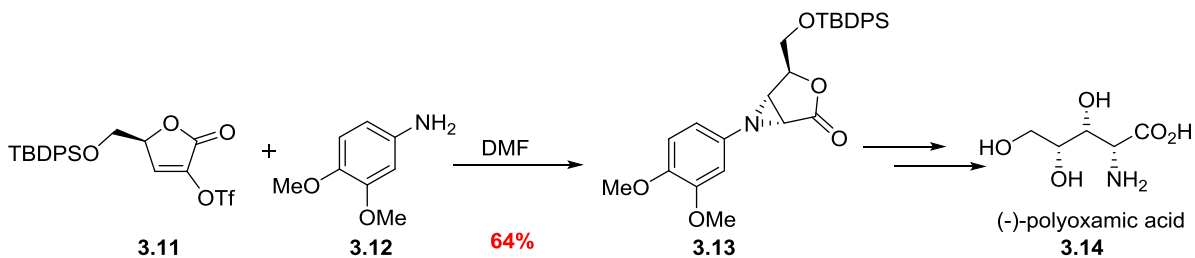


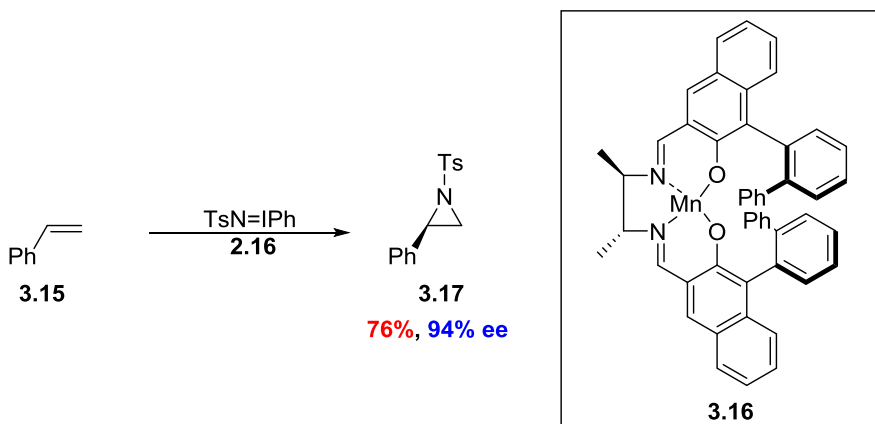
Figure 3.2. Complimentary methods of Cu-catalyzed aziridination utilizing bis(oxazoline) and di-imine ligands

Dodd and co-workers took advantage of a Michael addition-elimination sequence in their total synthesis of an unnatural enantiomer of polyoxamic acid **3.14** (Scheme 3.3).⁷ The unsaturated lactone **3.11** was reacted with 3,4-dimethoxybenzylamine (**3.12**) to afford the aziridine **3.13** as a single diastereomer.



Scheme 3.2. Synthesis of polyoxamic acid via Michael addition-elimination sequence

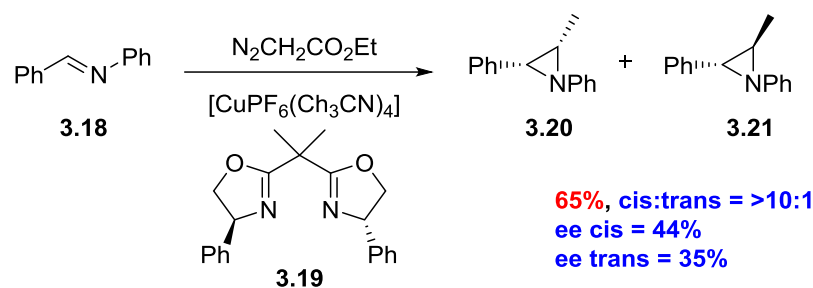
Catalytic asymmetric Mn-catalyzed aziridinations using an optimized Manganese salen complex **3.16** have been developed by Nishikori and Katsuki. The aziridination of styrene with TsN=I_{Ph} and **3.16** proceeded in high yield and enantiomeric excess (**Scheme 3.3**).^{8,9}



Scheme 3.3. Mn- catalyzed aziridination of styrene

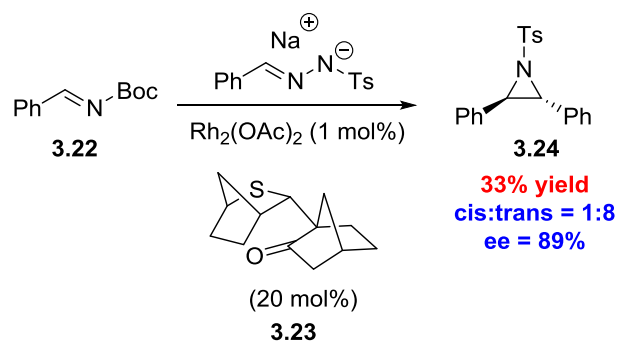
3.2.3. Aziridine Synthesis by Addition to Imines

Alternatively to the addition of nitrenes to alkenes, carbenes (or ylides) can undergo addition to imines, thus simultaneously forming one C-C bond and one C-N bond. The first enantioselective aziridination of imines was accomplished by Jacobsen and co-workers in 1995.¹⁰ This involved the addition of a metallocarbene derived from ethyl diazoacetate and copper(I)hexafluorophosphate adding to *N*-aryaldimines **3.18**.



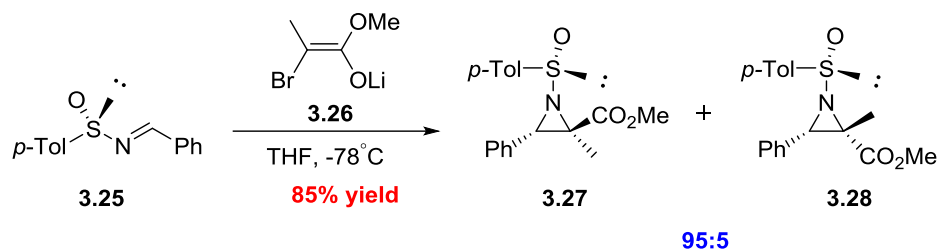
Scheme 3.4. Jacobsen azirdination of imines

An analogous strategy to the carbene methods previously described is the reaction of sulfur and iodine ylides with imines to generate the desired aziridines (**Scheme 3.6**). These ylides react with imines to give β -sulfo- or iodonium amide anions which subsequently undergo nucleophilic ring closure to provide aziridines. Aggarwal and coworkers have been very active in this area, utilizing chiral sulfides such as **3.23** to access trans disubstituted aziridines **3.24**.¹¹ This strategy avoids the need to use potentially hazardous diazoester by generating reactive chiral sulfonium intermediates from tosylhydrazones.



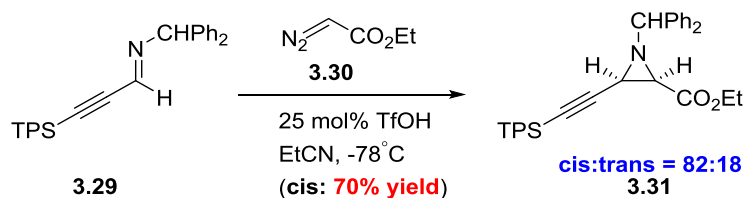
Scheme 3.5. Chiral aziridination using sulfur ylides

The aza-Darzens reaction is a well-studied and efficient aziridine-forming reaction. In 1999, Zhang and co-workers reported that S-chiral sulfinylimines **3.25** and achiral bromoenolates **3.26** undergo an asymmetric aza-Darzens reaction to form the desired un-activated aziridines **3.27** in excellent yield and stereocontrol (**Scheme 3.7**).¹²



Scheme 3.6. Aziridination of sulfinylimines with bromoenolates via aza-Darzens reaction

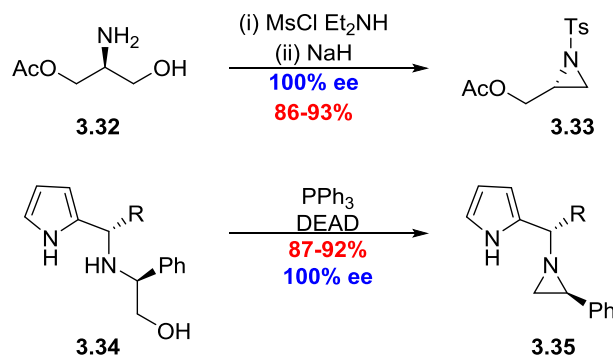
In 2004, Johnston and co-workers reported a mild protocol for the synthesis of *cis*-aziridines utilizing Bronsted acid catalysis.¹³ This approach facilitates the construction of functionally diverse *N*-alkyl aziridines such as **3.31** with excellent diastereoselectivity. This method has been applied in an approach to the aziridine-containing natural product mitomycin c, providing efficient access to the aziridine intermediate (**Scheme 3.8**).¹⁴



Scheme 3.7. Bronsted acid-catalyzed aza-Darzens en route to Mitomycin C

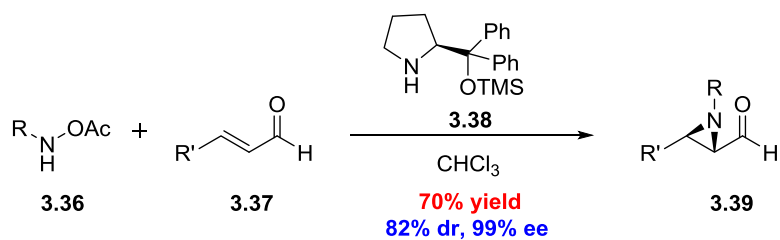
3.2.4. Aziridine Synthesis by Intramolecular Substitution

Due to extensive research on the preparation of chiral epoxides, there has been considerable interest in the multistep preparation of azetidines via chiral 1,2-azidoalcohols. Borch and co-workers demonstrated an approach to N-protected aziridines **3.33** by the intramolecular substitution of an *O*-mesylate generated from the monoacetate to access chiral aziridines (**Scheme 3.9**).¹⁵ Similarly, Savoia and coworkers reported the activation of a 1,2-aminoalcohol **3.34** under Mitsunobu conditions followed by intramolecular substitution to access substituted aziridines. Both of these methods require α -chiral amines.¹⁶



Scheme 3.8. Synthesis of aziridines via 1,2-aminoalcohols

In 2007, Cordova and co-workers reported an organocatalytic aziridination of α,β -unsaturated aldehydes with acylated hydroxycarbamates.^{17,18} Utilizing a chiral silyl-protected pyrrolidine alcohol **3.38** as an organocatalyst, 2-formylaziridines **3.39** were accessed in moderate yields with moderate to high diastereoselectivities and enantioselectivities (**Scheme 3.10**).



Scheme 3.9. Organocatalytic aziridination of α,β -unsaturated aldehydes

3.3. Introduction to Azetidines:

3.3.1. General Properties of Azetidines:

Azetidines comprise a very important class of nitrogen-containing heterocycles due to both their biological importance and increasing use in medicinal chemistry, as well as their value to synthetic chemists in the asymmetric synthesis of complex natural products. Since the discovery of penicillin by Fleming, and the subsequent structure elucidation by Dorothy Hodgkin, azetidines have received considerable attention in the biological and medical chemistry communities due to their potential value as antibiotics.¹⁹ Despite their utility, they have received relatively little attention from the chemical community compared to their higher homologous counterparts.²⁰ The problems encountered with azetidine synthesis have been posed in various ways by different natural product families, making general and versatile methods for their preparation difficult. The natural products mugineic acid, penaresidins, penicillins, and the partial nAChR agonist tebanicline contain an azetidine moiety in their core structure (**Figure 3.3**).²¹

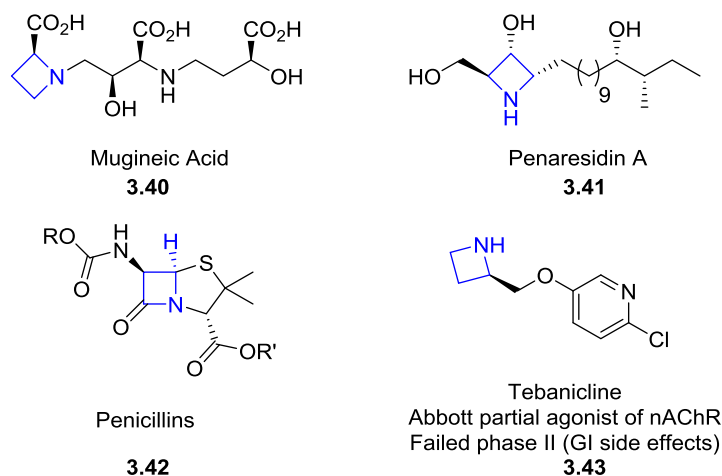


Figure 3.3. Azetidine-based natural products and pharmaceuticals

From a synthetic standpoint, the structural features of azetidine ring systems are of great importance, as they provide information on reliable ways of constructing and manipulating the strained bonds of four membered rings. The sp^3 configurations of the ring components should give a certain degree of flexibility in the orthogonally twisted σ -bonds with the deformation angle of 19.5° .²² This results in a preference for the azetidine ring to adopt a puckered conformation with a barrier of inversion that can lead to the observance of conformational isomers (**Figure 3.4**). The thermodynamic stability of the relatively flexible ring structures allows synthetic access to numerous azetidine derivatives through strategies involving cyclization and cycloaddition methodologies, and further transformations can be conducted on azetidine subunits to achieve target-directed synthesis.

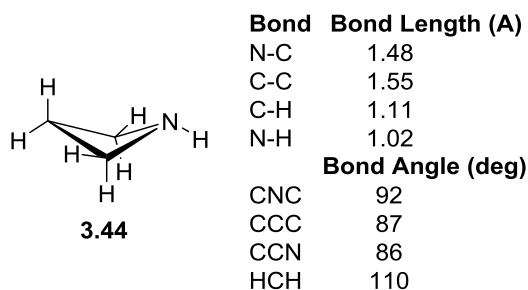


Figure 3.4. Geometric configuration of azetidine

3.4. Enantioselective Synthesis of Azetidine Rings:

3.4.1. Introduction:

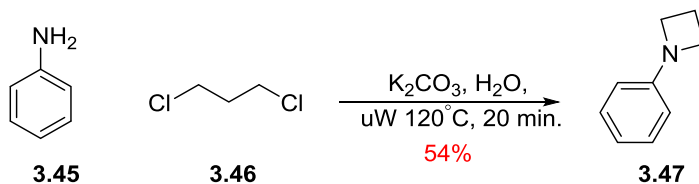
An increase in activity in the area of azetidine synthesis over the last two decades has been driven in large part by their applications in both natural product total synthesis and medicinal chemistry.²² The azetidine ring is a challenging ring systems to form due to ring strain of the desired product, making the ring closure significantly uphill in energy.²⁰ Although there are multiple reported methods for the synthesis of azetidines, few are generally applicable to form diverse arrangements of substituents, and most lack stereocontrol.²³

The general methodologies available for the preparation of azetidines can be divided into two categories: intramolecular cyclization and intermolecular [2+2] cycloaddition. The former category typically employs the nucleophilic attack of deprotonated amines onto reactive γ -carbon atoms bearing a suitable leaving group, or through carbon-carbon bond formation. The latter category consists of metal-catalyzed [2+2] cycloadditions of imines to enol ethers, similar to a Staudinger reaction.²⁴

3.4.2. Azetidine Synthesis via intramolecular cyclization

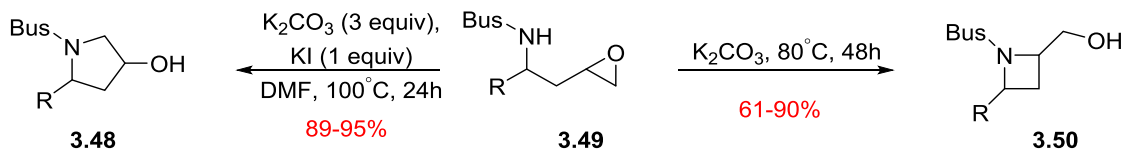
Cyclization of a pre-formed chain by nucleophilic displacement of a leaving group by a nitrogen nucleophile is the most common method to produce azetidines. Amines are the most common nitrogen nucleophile; the main drawback of this approach being competing elimination due to the strained nature of the forming azetidine ring.²³ Halogens such as chlorides and bromides are the most often encountered leaving groups in this class of cyclization, although iodines, sulfonic esters (mesylate, tosylate, triflate), epoxides, aziridines, haloniums, and diazo groups have also seen use in the literature.²⁰

In 2006, Yu and co-workers reported the cyclization of aniline with 1,3-dichloropropane (**Scheme 3.11**). The reaction was carried out in water with microwave irradiation to afford the aryl azetidine **3.47** in 54% yield.²⁵



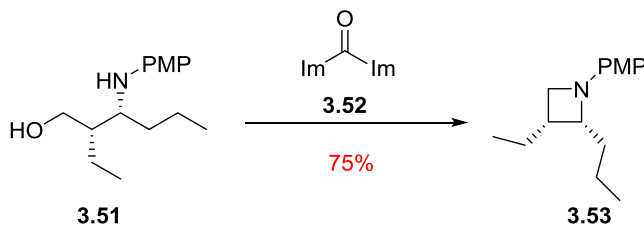
Scheme 3.10. Cyclization of aniline with 1,3-dichloropropane

In 2009, Yus and coworkers demonstrated the base-induced cyclization of enantiopure (2-aminoalkyl)oxirane **3.49**, forming 2(hydroxymethyl)azetidine **3.50** stereospecifically (**Scheme 3.12**).²⁶ By altering the reaction conditions, either the azetidine or pyrrolidine **3.48** could be accessed from a key intermediate.



Scheme 3.11. Synthesis of pyrrolidines and azetidines from enantiomerically pure oxiranes

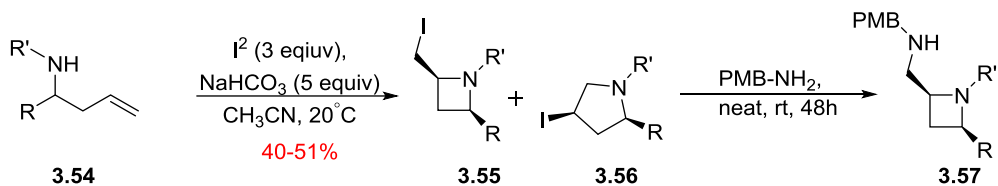
Activation of the hydroxyl group of a γ -amino alcohol through Mitsunobu conditions can also facilitate cyclization to the azetidine ring (**Scheme 3.13**). In 2004, Christmann and co-workers reported a novel cyclization of γ -amino alcohol **3.51** obtained by a stereoselective Mannich reaction, leading to the synthesis of enantiopure *cis*-2,3-disubstituted azetidine **3.53**.²⁷



Scheme 3.12. Mitsunobu-activated cyclization

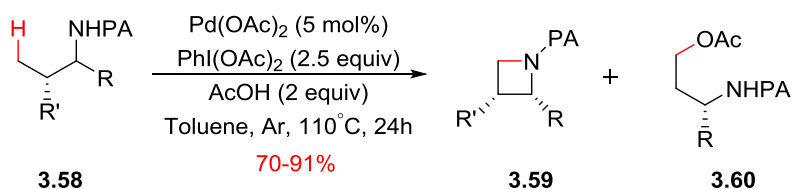
In 2010, Fossey and coworkers described an iodine-mediated cyclization of homoallyl amines **3.54** that provided access to *cis*-2,4-azetidines **3.55** through a 4-*exo*-trig cyclization (**Scheme 3.14**).²⁸ These iodoazetidines were unstable even at 4°C, and underwent ring expansion to the pyrrolidine **3.56**, retaining the *cis* configuration.

However, displacement of the iodide with a protected amine afforded the relatively stable amino azetidine **3.57** in substantially higher yield.



Scheme 3.13. 2,4-*cis*-azetidine formation by iodocyclization of homoallylamines

In 2012, Chen and coworkers reported the synthesis of azetidines **3.59** via palladium-catalyzed intramolecular amination of C-H bonds of picolinamide (PA) protected amine substrates **3.58**.²⁹ 2,3-disubstituted azetidines could be accessed in good yield. Attempts to access 2-substituted azetidines with this PA-directed C-H activation methodology suffered from the formation of an acetoxyated byproduct.



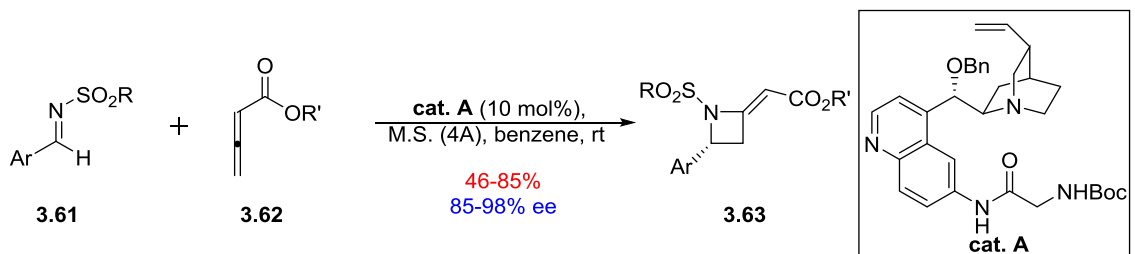
Scheme 3.14. Synthesis of azetidines via intramolecular amination of γ - $C(sp^3)$ -H bonds

3.4.3. Azetidine Synthesis via Cycloaddition

Several variations of azetidine synthesis through [2+2] cycloaddition have been recently demonstrated, allowing access to azetidines containing diverse substitution

patterns. Historically, the cycloaddition chemistry for four-membered ring systems involved the synthesis of β -lactams, from which azetidines were obtained by reduction of the amide. However throughout the last decade, there have been major advances in synthetic methodology surrounding the direct synthesis of azetidines through cycloaddition chemistry.

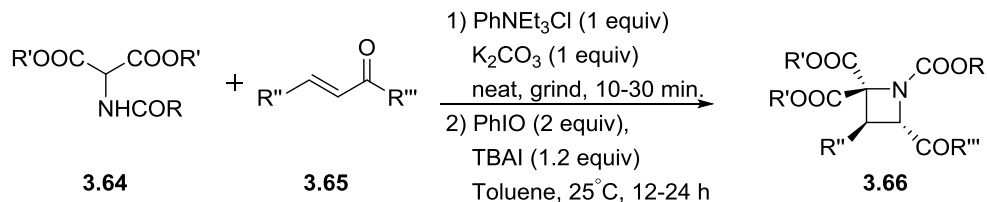
In 2003, Shi and co-workers reported an interesting DABCO-catalyzed regioselective formal [2+2] cycloaddition of N-tosylamines with allenoates during their investigation of the aza-Baylis-Hillman reaction.³⁰ This inspired Zhu and co-workers in 2011 to report the first examples of the catalytic enantioselective [2+2] cycloaddition between allenoates **3.62** and N-sulfonylimines **3.61** to give enantioenriched 2-alkylideneazetidines **3.63**.³¹ This methodology utilized a cinchona alkaloid quinidine amide as the organocatalyst.



Scheme 3.15. Azetidine synthesis via organocatalyzed [2+2] cycloaddition

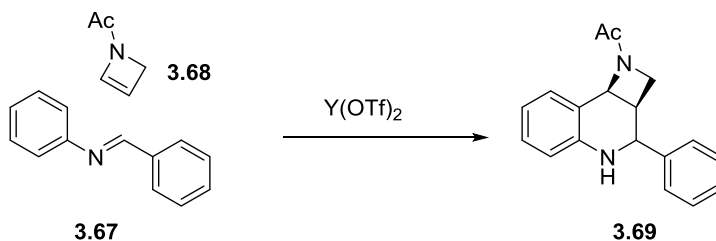
In 2010, Fan and co-workers demonstrated the stereoselective synthesis of highly functionalized azetidines from a [2+2] cycloaddition of 2-aminomalonates **3.64** with chalcones **3.65** via a grind-promoted, solvent-free Michael addition and a PhIO/Bu₄NI

mediated oxidative cyclization.³² These *trans*-2,3,4-trisubstituted azetidines **3.66** were synthesized in moderate to good yields with excellent diastereoselectivities.



Scheme 3.16. Synthesis of *trans*-2,3,4-trisubstituted azetidines via [2+2] cycloaddition

In addition, several examples of [4+2] cycloadditions utilizing the building block *N*-acetyl-2-azetine have been shown in the literature. One such example from Osbourne and coworkers in 2004 demonstrated a Lewis acid-catalyzed [4+2] cycloaddition of *N*-acetyl-2-azetine **3.68** with aromatic imines **3.67** to access bicyclic azetidine ring systems.³³



Scheme 3.17. Synthesis of bicyclic azetidines through [4+2] cycloaddition

3.5. Azetidines in Medicinal Chemistry

Saturated heterocycles present a liability to the DMPK properties of potential therapeutics due to the metabolic susceptibility of the position adjacent to or directly on the heteroatom. Both lipophilicity and charge influence metabolism, and strategies have been implemented with success to block the site of metabolism through changing the electronics of the ring and reducing hydrophobicity.³⁴ Of the saturated heterocycles containing one heteroatom, azetidines and oxetanes are the least lipophilic, and have shown in some cases to be more metabolically stable than their larger homologous counterparts.

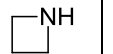
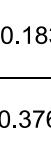
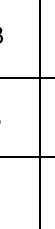
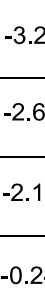
name	structure	cLogP	LogD	pK _a
azetidine		-0.183	-3.23	10.7
pyrrolidine		0.376	-2.66	11.3
piperidine		0.935	-2.10	11.2
oxetane		-0.163	-0.24	

Table 3.2. cLogP, cLogD, and pK_a values of common saturated heterocycles

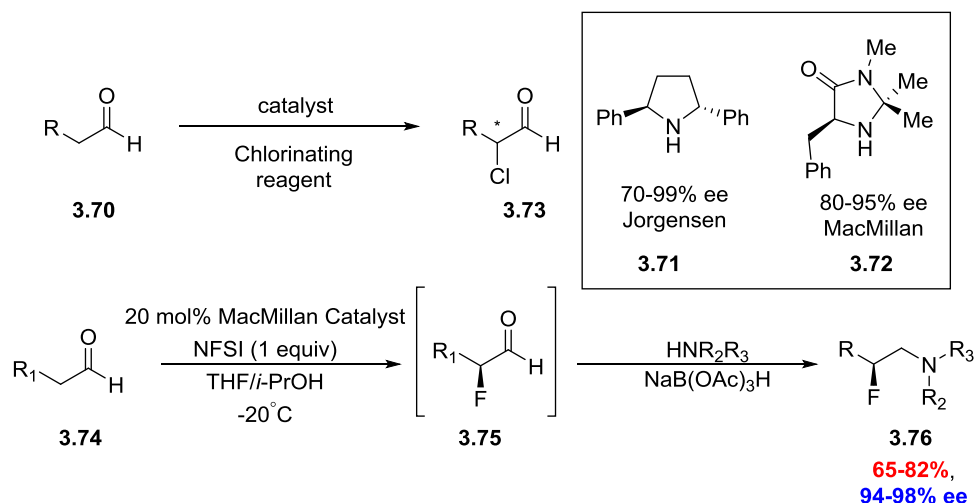
While the recent approaches to the enantioselective synthesis of azetidines have made great strides in the ability to access various types of azetidines, 2-alkyl substituted azetidines are notably scarce in literature. In a review of functional group occurrences in compounds with biological activity by Roughley and co-workers in 2011, it was noted that, although aliphatic amines comprised 43% of compounds in this data set, azetidines

made up 1.4% of this subset, and there were no occurrences of secondary azetidin-2-yl compounds.³⁵ This may demonstrate a need by the medicinal chemistry community for a general, facile, and enantioselective approach to access azetidin-2-yl compounds for the synthesis of pharmacologically active compounds.

3.6. Organocatalytic Enantioselective Synthesis of Aziridines and Azetidines

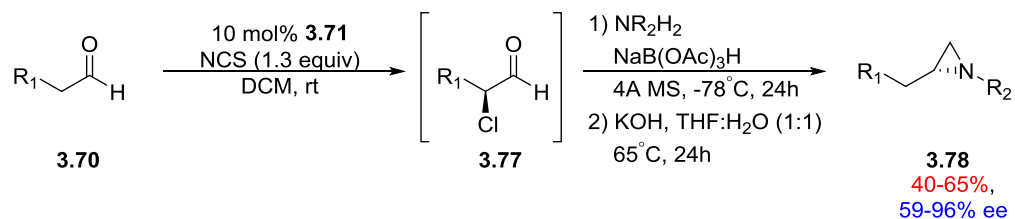
3.6.1. Introduction:

Many of the classical methods for aziridine synthesis typically incorporate an electron withdrawing group as the *N*-substituent, and the synthesis of terminal aziridines with diversity at the *N*-substituent is rare. In 2007, Kocovsky and co-workers developed an expedient protocol for the enantioselective synthesis of diaryl aziridines relying on the organocatalyzed reduction of α -chloroimines.³⁶ While this work was a notable advance, it was lacking in generality and substrate scope, as only *N*-arylaziridines could be accessed with this approach. Due to the fact that there were few synthetic methods in the literature for the enantioselective synthesis of *N*-alkylaziridines, we were motivated to develop a synthetic methodology to access *N*-alkyl terminal aziridines enantioselectively. Seminal work in this area by our lab in the organocatalytic synthesis of β - fluoroamines was inspired by the work of MacMillan and Jorgensen, reporting the enantioselective α -chlorination of aldehydes via organocatalysis (**Scheme 3.19**).



Scheme 3.18. Organocatalytic enantioselective synthesis of α -chloroaldehydes and β -fluoroamines

Based on this and previous work involving the enantioselective synthesis of β -fluoroamines, we envisioned a three-step, one-pot protocol involving the enantioselective α -chlorination of aldehydes, followed by reductive amination with a primary amine and subsequent $\text{S}_{\text{N}}2$ displacement to afford previously unattainable chiral terminal aziridines with a wide range of N-substituents (**Scheme 3.20**).

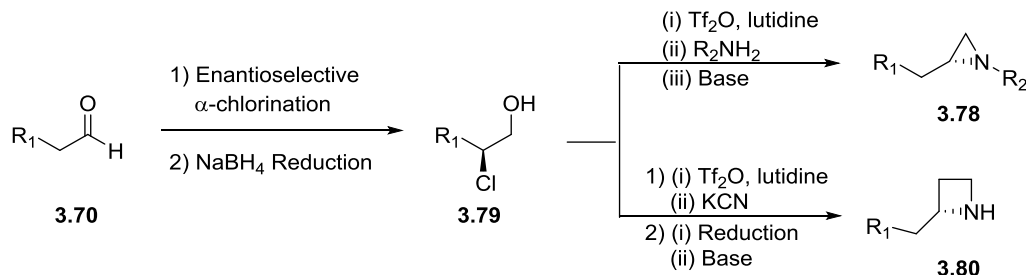


Scheme 3.19. General access to chiral *N*-alkyl terminal aziridines via organocatalysis

Initial efforts utilized the Jorgensen route to access α -chloroaldehydes, where NCS was the chlorinating agent and the optimized solvent was DCE, which made a one-pot α -chlorination / reductive elimination feasible. However, first attempts at the reductive elimination led to epimerization and loss of enantiomeric excess. It was determined that the room-temperature reductive amination was the source of epimerization and a direct correlation was found between temperature and epimerization. Reducing the temperature to -78°C resolved the epimerization problem and, with the β -chloroamine in hand, a base screen was utilized to determine optimal conditions for the aziridine ring closure. The optimal conditions were determined to be KOH in THF/H₂O (1:1). This sequence resulted in the enantioselective synthesis of *N*-alkyl terminal aziridines in 40-65% overall yield and 56-96% ee. Overall, this new approach represents the effective addition of a primary amine across an olefin to form aziridines and is a notable extension of the linchpin catalysis concept to access chiral epoxides reported by MacMillan.³⁷

While this work represents a significant improvement in the art to access aziridines, there were notable improvements to be made to this methodology. Modest enantiomeric excess was reported in some cases, presumably due to epimerization of the α -chloroaldehyde **2.77**. Furthermore, the reductive amination step is not amenable for access to larger homologous ring sizes. Given our interest in a more general, linchpin approach for the synthesis of aza-moieties and our desire to improve upon our previous methodology, we envisioned a new approach involving an *in situ* reduction of the α -chloroaldehyde to the 1,2-chloroalcohol **3.79** (**Scheme 3.21**). Intermolecular S_N2 displacement with either an amine or nitrile could afford access to β -chloro or γ -

chloroamines, respectively. Cyclization would then allow access to either the aziridine **3.78** or azetidine **3.80** from a common advanced intermediate.



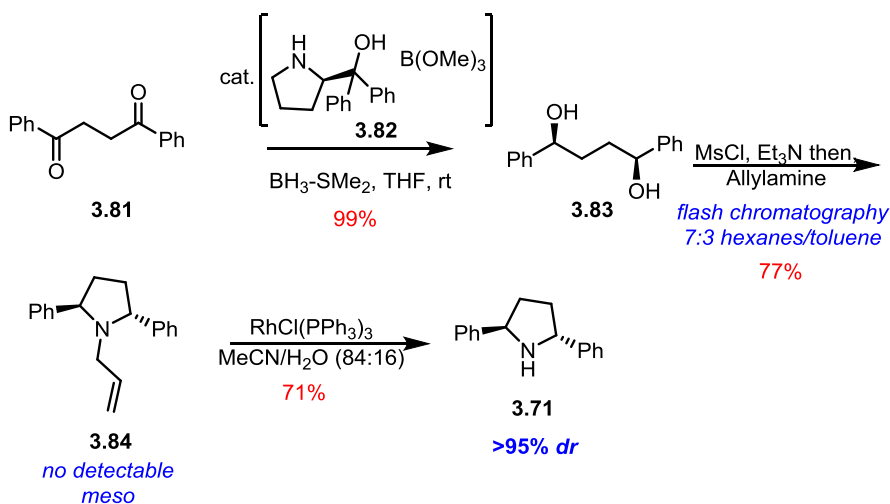
Scheme 3.20. Envisioned route to chiral *N*-alkyl terminal aziridines and 2-alkylazetidines

3.6.2. An Improved Synthesis of Jorgensen's Catalyst

Before pursuing our aziridination studies further, it was necessary to obtain the pyrrolidine organocatalyst described by the Jorgensen group for use in enantioselective α -chlorination. Unfortunately, the catalyst was no longer commercially available. We attempted to prepare the organocatalyst according to literature precedent; however, we found that for several reactions the yields were low and variable, notably including the final allyl deprotection of the pyrrolidine ring. Also importantly, the literature preparations resulted in an inseparable mixture of isomers of the final catalyst, including >18% of the *meso* isomer. We found that this caused deleterious effects in the α -chlorination reaction, affecting both the reaction rate and increasing the ratio of dichlorination vs. monochlorination. Recrystallization of the final product was achieved, successfully increasing the purity of the desired isomer to >92%. However, these conditions limited the scale and required careful regulation of temperature of the entire

apparatus (recrystallization was performed in cold room, with temperature <4 °C). Therefore, we sought to improve the synthesis to both increase the yield and reliability of the synthesis, with the goal of being able to rapidly obtain the pyrrolidine catalyst on multi-gram scale.

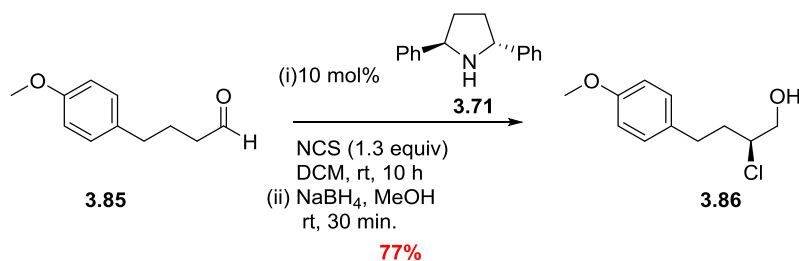
We were able to optimize the synthetic route, as outlined in **Scheme 3.22**. Notably, we found that flash column chromatography of the penultimate intermediate **3.84** with a 7:3 hexanes/toluene solvent system provided excellent separation of the desired isomer. Additionally, increasing the amount of Wilkinson's catalyst in the allyl deprotection to 10 mol% reliably improved reaction yield to 71% from <50%. These improvements allowed for the gram-scale production of catalyst **3.71** in >54% overall yield, and >97% purity.



Scheme 3.21. Scalable synthesis of pyrrolidine organocatalyst **3.71**

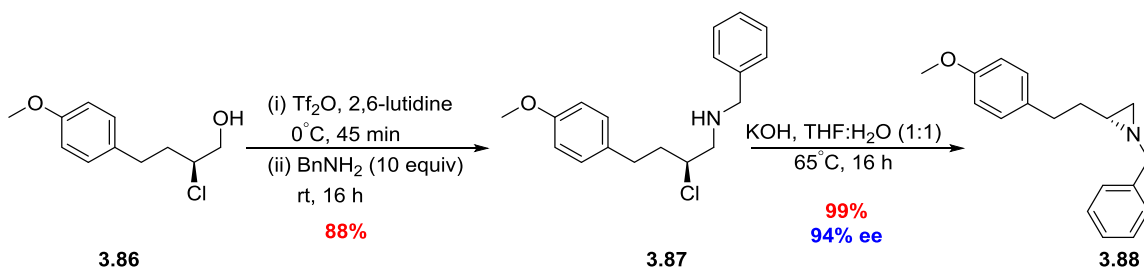
3.6.3. Studies Toward the Enantioselective Synthesis of Aziridines

With sufficient organocatalyst for α -chlorination in hand, our efforts now focused on developing a protocol for the asymmetric synthesis of *N*-alkyl terminal aziridines. Utilizing previous efforts by the Jorgensen lab, organocatalyzed α -chlorination with pyrrolidine catalyst **3.71**, followed by *in situ* reduction with NaBH₄ afforded the α -chloro alcohol **3.86** in excellent yield (Scheme 3.23).



Scheme 3.22. One pot α -chlorination/reduction sequence

The alcohol was then displaced with a primary amine, facilitated by an *in situ* triflate formation followed by S_N2 displacement to afford the secondary β -chloroamine **3.87** (Scheme 3.24). This was followed by cyclization which was achieved by heating with KOH in THF:H₂O (1:1) to cleanly afford the desired chiral *N*-alkyl terminal aziridine **3.88** in 78% overall yield from the aldehyde and 94% enantiomeric excess. Enantiomeric excess was determined by chiral SFC LCMS with a racemic sample for comparison.



Scheme 3.23. Amine displacement and intramolecular S_N2 cyclization

In order to determine the scope of this methodology, we prepared several *N*-alkyl terminal aziridines from commercially available aldehydes. As shown in **Figure 3.5**, this sequence was general and well-tolerated across various alkyl/aryl groups, as well as heteroatom-containing substrates and protecting groups. Overall yields for substrates in the two-pot sequence ranged from 50-73%, with up to 94% ee. This method compares favorably with previous routes to access aziridines described by our group.³⁸ With similar substrates, yields are improved by up to 20% while retaining similar enantioselectivity. These conditions also avoid the problem of racemization of the α -chloro aldehyde intermediate used previously for reductive amination. By effecting *in situ* reduction of this intermediate, the route described avoids the need to maintain extremely cold temperatures and avoids the potential for racemization in subsequent reaction steps.

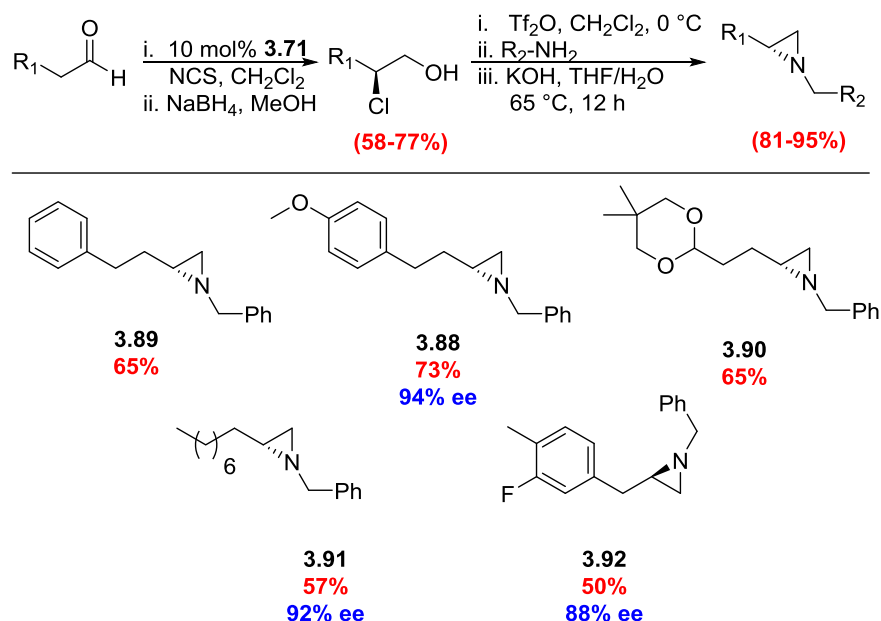


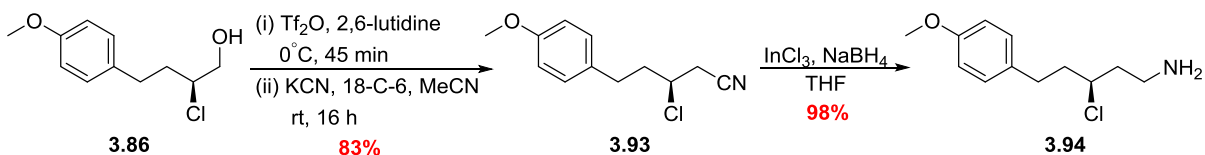
Figure 3.5. Enantioselective synthesis of *N*-alkyl terminal aziridines

3.6.4. Studies Towards the Enantioselective Synthesis of Azetidines

With an efficient method to for the enantioselective synthesis of aziridines optimized, our attention then turned to the enantioselective synthesis of secondary 2-alkylazetidines. In line with our desire to extrapolate our linchpin approach for the functionalization of aldehydes, the α -chloroalcohol **3.86** was prepared as previously described. We next sought to displace the alcohol with a nitrile group through activation of the alcohol as a triflate. Initial conditions using CH_2Cl_2 , THF, or acetonitrile as the solvent with potassium cyanide led to poor conversion at room temperature and elimination at elevated temperature. However, we found the acetonitrile with potassium cyanide and 18-crown-6 as an additive was effective in conversion to the desired nitrile after 24 hours at room temperature. Under these optimized conditions, displacement of

the *in situ* prepared triflate with potassium cyanide facilitated formation of the desired β -chloronitrile **3.93** in 83% yield. While this substrate was relatively stable at room temperature in CH_2Cl_2 solution, elevated temperatures resulted in the formation of an elimination byproduct. Similarly, the oil was highly prone to elimination, and decomposed within hours at room temperature.

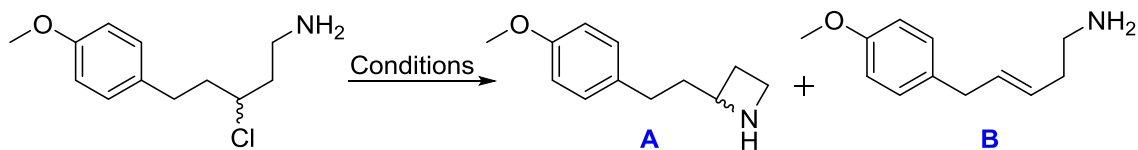
Initial attempts to subsequently reduce the nitrile with standard reducing conditions were unsuccessful, however an InCl_3 mediated reduction with NaBH_4 was sufficient to cleanly afford the γ -chloroamine **3.94** in excellent yield.



Scheme 3.25. Synthesis of γ -chloroamine

With the γ -chloroamine in hand, we focused on the cyclization conditions to afford the desired azetidine. We initially attempted the same conditions that were successful in facilitating the 3-*exo*-tet cyclization of the β -chloroamine to aziridines. However, treatment with KOH in $\text{THF}/\text{H}_2\text{O}$ led to minimal consumption of the γ -chloroamine starting material. Additionally, when other conditions were tried, we observed substantial elimination to an undesired byproduct. To find conditions that might be able to affect the 4-*exo*-tet cyclization, we performed a screen of a broad selection of organic and inorganic

bases, solvents, and temperatures. These are summarized in **Table 3.3**. Unfortunately, the competing elimination pathway remained problematic through all conditions attempted. This can be rationalized by the high energetic requirements necessary to enable ring closure to the highly strained 4-member azetidine ring. We also found that compounds that contained branched substituents, aryl groups, or heteroatoms β to the chlorine group led to nearly full conversion to the elimination product under tested conditions. However, we were able to find conditions that were able to promote cyclization favored in a 3:1 ratio with the competing elimination pathway. KOH in THF/H₂O (1:1), under high thermal conditions (170 °C) was effective in conversion to the desired azetidine **3.95**. Microwave irradiation for 1 hour at this temperature resulted in full consumption of the γ -chloroamine starting material.

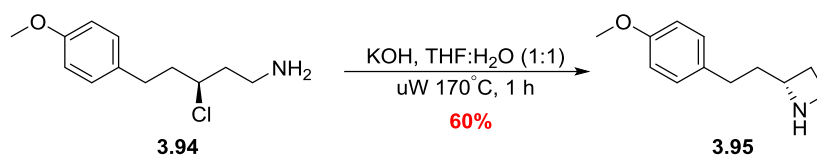


Entry	Base	Solvent	Temperature	Additive	Conversion (A:B)
1	K ₂ CO ₃	NMP	25 °C	--	0%
2	K ₂ CO ₃	NMP	120 °C ^b	--	40% (2:1)
3	K ₂ CO ₃	NMP	180 °C ^b	--	80% (2:1)
4	--	THF:H ₂ O ^a	150 °C ^b	--	75% (1.5:1)
5	NaH	DMF	25 °C	--	0%
6	NaH	DMF	65 °C	--	0%
7	NaH	DMF	25 °C	15-C-5	trace (1:2)
8	NaH	DMF	65 °C	15-C-5	<5% (0:1)
9	LHMDS	DMF	25 °C	--	60% (0:1)
10	LHMDS	DMF	25 °C	--	100% (0:1)
11	K ₂ CO ₃	DMF	25 °C	--	0%
12	K ₂ CO ₃	DMF	120 °C ^b	--	10% (2:1)
13	K ₂ CO ₃	DMF	25 °C	AgNO ₃	0%
14	K ₂ CO ₃	DMF	65 °C	AgNO ₃	0%
15	KOH	THF:H ₂ O ^a	65 °C	--	<5% (3:1)
16	KOH	THF:H ₂ O ^a	120 °C ^b	--	20% (3:1)
17	KOH	THF:H ₂ O ^a	170 °C ^b	--	100% (3:1)

*All reactions run at 0.1 mmol, 0.125M in solvent. Conversion determined by LCMS and NMR

Table 3.3. Base screen for azetidine cyclization

The optimized conditions afforded the desired azetidine **3.95** in 60% yield and 92% enantiomeric excess as determined by chiral HPLC. The overall sequence provided access to the secondary 2-alkyl azetidine in 44% overall yield from a commercially available aldehyde (**Scheme 3.26**).



Scheme 3.26. Cyclization of γ -chloroamine to access 2-alkylazetidines

In order to determine the scope of this methodology, we prepared several 2-alkyl azetidines from commercially available aldehydes. β -chloro nitriles were readily accessed from a range of β -chloro alcohols in good overall yield. Of note, these compounds were all prone to elimination as their isolated final products. Substrates with branched alkyl groups or aryl groups neighboring the chlorine were especially susceptible to elimination, as reflected in the lower yield of compounds **3.100** and **3.98**.

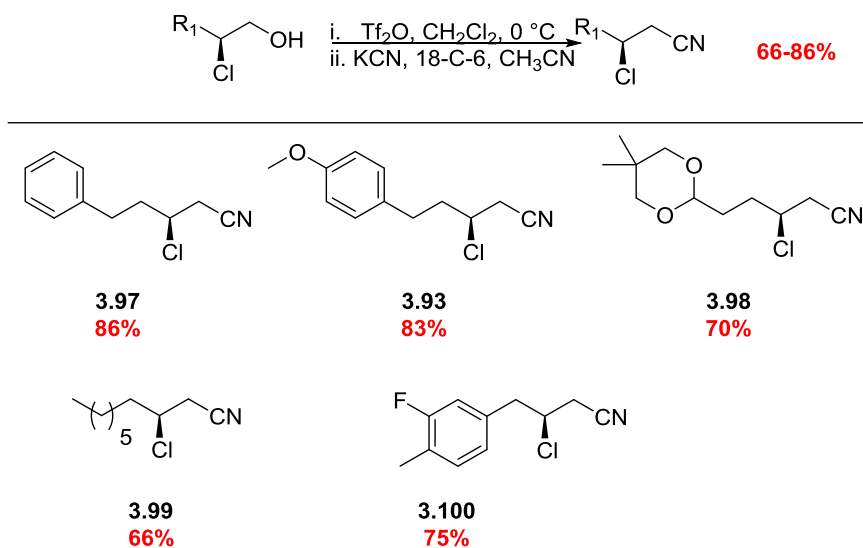


Figure 3.6. Enantioselective synthesis of β -chloronitriles

With the desired β -chloro nitriles in hand, we next subjected them to the optimized conditions for intramolecular cyclization to access the desired azetidines. Elimination was once again problematic across all substrates, owing to the high temperatures and basic conditions used. Elimination was observed across all substrates, with branched or aryl substituents increasing the ratio of elimination byproduct relative to the desired azetidine. The desired azetidines were isolated in 44-55% yield, and 84-92% ee for substrates investigated. However, the compound **3.103**, with a β -aryl substituent, led to an increase in the ratio of eliminated side product, with less than 5% of the desired azetidine product recovered.

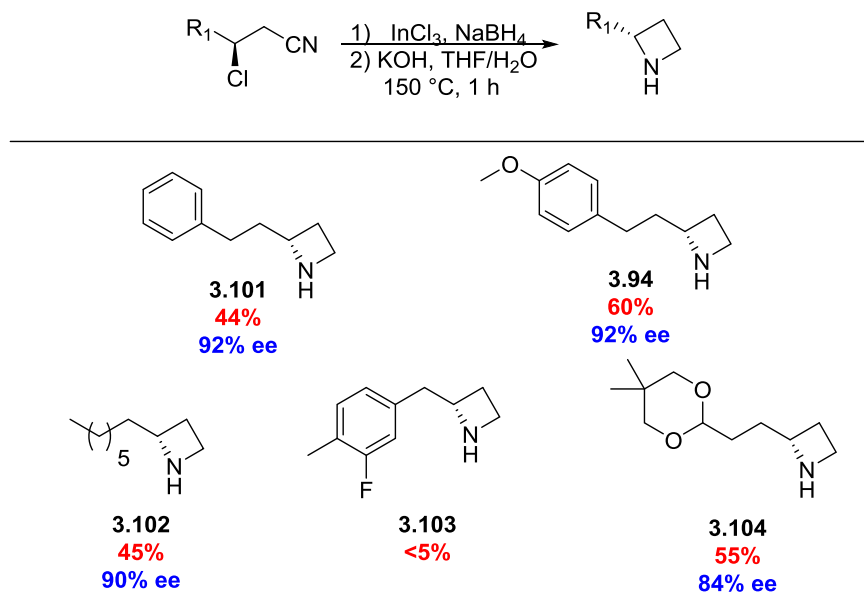
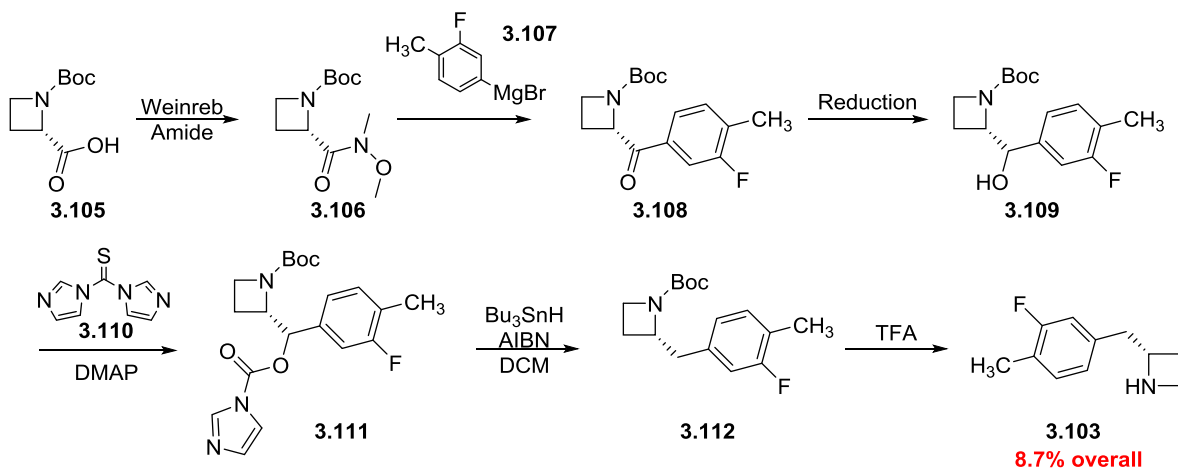


Figure 3.7. Intramolecular cyclization for the synthesis of 2-substituted azetidines.

3.6.5. Synthesis of an Azetidine CaSR Antagonist

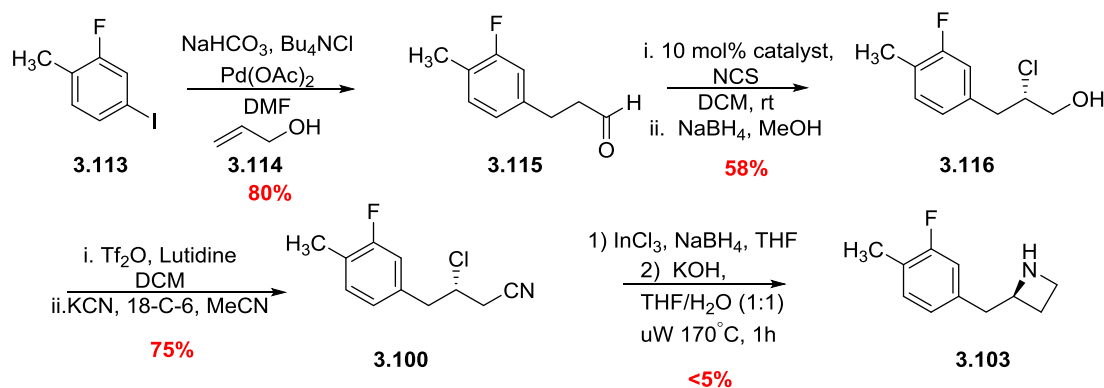
To highlight the utility of this methodology, we sought to synthesize several current biologically active compounds that contain 2-substituted azetidines. One such compound, **3.103**, is a calcium sensing receptor (CaSR) antagonist under development by Daiichi Sankyo Pharmaceuticals (**Scheme 3.27**). The current synthesis of this compound requires the use of expensive chiral starting materials and the use of toxic tin reagents to effect conversion to the desired azetidine. Furthermore, yields for this sequence were low, with an overall yield of 8.7%.



Scheme 3.27. Daiichi Sankyo synthesis of CaSR antagonist **2.99**

Our proposed synthesis of **3.103** began with a Heck reaction of commercially available **3.115** with allyl alcohol to access aldehyde **3.115**. Asymmetric α -chlorination followed by reduction provided **3.116**, which was subsequently alkylated to the β -chloronitrile **3.100**. Reduction of the nitrile followed by intramolecular ring closure

afforded the desired azetidine **3.103**. This approach requires fewer transformations, allows for greater control over stereochemistry, and avoids the use of prohibitively expensive starting materials. However, improvements are currently ongoing to optimize the yield of the final intramolecular cyclization step.



Scheme 3.28. Proposed synthesis of CaSR antagonist **3.103**

In summary, we have developed an optimized three-step procedure for the enantioselective synthesis of *N*-alkyl terminal aziridines and azetidines with alkyl substitutions at the C2 position of each heterocycle via organocatalysis. This methodology allows for the rapid preparation of the functionalized aziridines in 50-73% overall yields and 88-94% ee, and unfunctionalized azetidines in 22-32% overall yields and 84-92% ee. This new methodology addresses deficiencies in our first generation approach for the synthesis of aziridines while facilitating the synthesis of azetidines through a common advanced intermediate. Alternative methods to access azetidines that do not rely on the chiral pool is a demonstrated need in natural products synthesis and medicinal chemistry applications, and the ability to employ simple aldehydes and organocatalysts towards their synthesis allows for straightforward access to either

enantiomer. Additional refinements and applications of this methodology to the synthesis of biologically relevant small molecules are currently being investigated.

References

1. Müller, P.; Fruit, C. *Chem. Rev.* **2003**, *103*, 2905–2920.
2. Dermer, O. C.; Ham, G. E. *Ethylenimine and Other Aziridines*; Academic Press: New York, 1969.
3. Wenker, H. *J. Am. Chem. Soc.* **1935**, *57*, 2328–2328.
4. Yudin, A. K. *Aziridines and Epoxides in Organic Chemistry*; 2006.
5. Evans, D. A.; Bilodeau, M. T.; Faul, M. M. *J. Am. Chem. Soc.* **1994**, *116*, 2742–2753.
6. Li, Z.; Conser, K. R.; Jacobsen, E. N. *J. Am. Chem. Soc.* **1993**, *115*, 5326–5327.
7. Tarrade, A.; Dauban, P.; Dodd, R. H. *J. Org. Chem.* **2003**, *68*, 9521–9524.
8. Katsuki, T. *Synlett* **2003**, *2003*, 0281–0297.
9. Nishikori, H.; Katsuki, T. *Tetrahedron Lett.* **1996**, *37*, 9245–9248.
10. Hansen, K. B.; Finney, N. S.; Jacobsen, E. N. *Angew. Chemie Int. Ed. English* **1995**, *34*, 676–678.
11. Aggarwal, V. K.; Alonso, E.; Fang, G.; Ferrara, M.; Hynd, G.; Porcelloni, M. *Angew. Chem. Int. Ed. Engl.* **2001**, *40*, 1433–1436.
12. Davis, F. A.; Liu, H.; Zhou, P.; Fang, T.; Reddy, G. V.; Zhang, Y. *J. Org. Chem.* **1999**, *64*, 7559–7567.
13. Williams, A. L.; Johnston, J. N. *J. Am. Chem. Soc.* **2004**, *126*, 1612–1613.
14. Srinivasan, J. M.; Mathew, P. A.; Williams, A. L.; Huffman, J. C.; Johnston, J. N. *Chem. Commun. (Camb)*. **2011**, *47*, 3975–3977.
15. Choi, J. Y.; Borch, R. F. *Org. Lett.* **2007**, *9*, 215–218.
16. Alvaro, G.; Di Fabio, R.; Gualandi, A.; Savoia, D. *European J. Org. Chem.* **2007**, *2007*, 5573–5582.
17. Deiana, L.; Zhao, G.-L.; Lin, S.; Dziedzic, P.; Zhang, Q.; Leijonmarck, H.; Córdova, A. *Adv. Synth. Catal.* **2010**, *352*, 3201–3207.

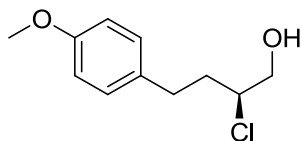
18. Vesely, J.; Ibrahem, I.; Zhao, G.-L.; Rios, R.; Córdova, A. *Angew. Chem. Int. Ed. Engl.* **2007**, *46*, 778–781.
19. Fleming, A. On the Antibacterial Action of Cultures of a *Penicillium*, with Special Reference to their Use in the Isolation of *B. influenzae*. *British journal of experimental pathology*, 1929, *10*, 226.
20. Bott, T. M.; West, F. G. *Heterocycles* **2012**, *84*, 223–264.
21. Jain, K. K. *Curr. Opin. Investig. Drugs* **2004**, *5*, 76–81.
22. Hidemi, Y.; Masaki, T.; Sengoku, T. *Heterocycles in Natural Product Synthesis*; Wiley-VCH Verlag GmbH, 2011.
23. Brandi, A.; Cicchi, S.; Cordero, F. M. *Chem. Rev.* **2008**, *108*, 3988–4035.
24. Aben, R. W. M.; Smit, R.; Scheeren, J. W. *J. Org. Chem.* **1987**, *52*, 365–370.
25. Ju, Y.; Varma, R. S. *J. Org. Chem.* **2006**, *71*, 135–141.
26. Medjahdi, M.; González-Gómez, J. C.; Foubelo, F.; Yus, M. *J. Org. Chem.* **2009**, *74*, 7859–7865.
27. Münch, A.; Wendt, B.; Christmann, M. *Synlett* **2004**, *2004*, 2751–2755.
28. Feula, A.; Male, L.; Fossey, J. S. *Org. Lett.* **2010**, *12*, 5044–5047.
29. He, G.; Zhao, Y.; Zhang, S.; Lu, C.; Chen, G. *J. Am. Chem. Soc.* **2012**, *134*, 3–6.
30. Zhao, G.-L.; Huang, J.-W.; Shi, M. *Org. Lett.* **2003**, *5*, 4737–4739.
31. Denis, J.-B.; Masson, G.; Retailleau, P.; Zhu, J. *Angew. Chem. Int. Ed. Engl.* **2011**, *50*, 5356–5360.
32. Ye, Y.; Wang, H.; Fan, R. *Org. Lett.* **2010**, *12*, 2802–2805.
33. Stevenson, P. J.; Nieuwenhuyzen, M.; Osborne, D. *Chem. Commun.* **2002**, 444–445.
34. St Jean, D. J.; Fotsch, C. *J. Med. Chem.* **2012**, *55*, 6002–6020.
35. Roughley, S. D.; Jordan, A. M. *J. Med. Chem.* **2011**, *54*, 3451–3479.
36. Malkov, A. V; Stoncius, S.; Kocovský, P. *Angew. Chem. Int. Ed. Engl.* **2007**, *46*, 3722–3724.

37. Amatore, M.; Beeson, T. D.; Brown, S. P.; MacMillan, D. W. C. *Angew. Chem. Int. Ed. Engl.* **2009**, *48*, 5121–5124.
38. Fadeyi, O. O.; Schulte, M. L.; Lindsley, C. W. *Org. Lett.* **2010**, *12*, 3276–3278.

Experimental Methods

General Methods: All NMR spectra were recorded on a Bruker 400, 500 or 600 MHz instrument. ¹H chemical shifts are reported in δ values relative to residual solvent signals in ppm. Data are reported as follows: chemical shift, integration, multiplicity (s = singlet, d = doublet, t = triplet, q = quartet, br = broad resonance, m = multiplet), coupling constant (Hz). Low resolution mass spectra were obtained on an Agilent 1200 series 6130 mass spectrometer. High resolution mass spectra were recorded on a Waters Q-TOF API-US plus Acuity system with ES as the ion source. Analytical thin layer chromatography was performed on Sorbent Technologies 250 micron silica plates. Visualization was accomplished via UV light, and/or the use of potassium permanganate solution followed by application of heat. Analytical HPLC was performed on an HP1100 with UV detection at 214 and 254 nm along with ELSD detection, LC/MS (J-Sphere80-C18, 3.0 x 50 mm, 4.1 min gradient, 7%[0.1%TFA/H₂O] : 93%[CH₃CN]). Preparative RP-HPLC purification was performed on a custom HP1100 automated purification system with collection triggered by mass detection or using a Gilson Inc. preparative UV-based system using a Phenomenex Luna C18 column (50 x 30 mm I.D., 5 μm) with an acetonitrile (unmodified)-water (0.5 mL/L NH₄OH) custom gradient. Normal-phase silica gel preparative purification was performed using an automated Combi-flash Companion from ISCO. Semi-preparative purifications were carried out via stacked

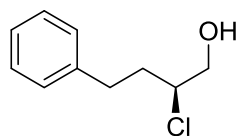
injections on a Waters Investigator SFC using a 10 x 250 mm Chiral Technologies CHIRALPAK ID column heated to 40 degrees Celsius. Analytical separations were carried out on an Agilent 1260 Infinity SFC using a 4.6 x 250 mm Chiral Technologies CHIRALPAK ID column heated to 40 degrees Celsius. Solvents for extraction, washing and chromatography were HPLC grade. All reagents were purchased from Aldrich Chemical Co. and were used without purification. All polymer-supported reagents were purchased from Argonaut Technologies and Biotage.



(S)-2-Chloro-4-(4-methoxyphenyl)butan-1-ol (3.86).

To a flame dried round bottom flask equipped with a stir bar, aldehyde **2.81** (0.25g, 1.40 mmol) was dissolved into CH₂Cl₂ (2.81 mL) at 0°C and to the stirring solution was added catalyst **3.71** (31 mg, 0.14 mmol) and then *N*-chlorosuccinimide (0.24g, 1.82 mmol). Solution was maintained at 0 °C, and stirring was continued for 12 hours, at which point starting material was consumed by ¹H NMR. Reaction was diluted with MeOH (7.0 mL) and cooled to 0°C, then NaBH₄ (0.26g, 7.02 mmol) was slowly added while stirring. The reaction was stirred for an additional 30 min. at the same temperature, then quenched with H₂O and extracted three times with EtOAc. Organic fractions were combined, washed with brine, and dried over Na₂SO₄. The organic layer was concentrated *in vacuo* and a crude oil was purified by column chromatography (4:1 Hex/EtOAc) to yield the desired product as a clear oil in 0.21g (77%). ¹H NMR (400.2 MHz, CDCl₃) δ (ppm):

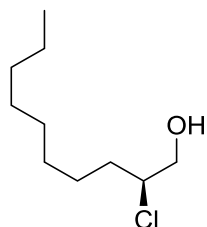
7.12 (d, $J= 8$ Hz, 2H), 6.84 (d, $J= 8$ Hz, 2H), 3.97 (m, 1H), 3.79 (s, 3H), 3.75 (m, 1H), 3.68 (dd, $J= 11.5, 6.5$ Hz, 1H), 2.84 (dt, $J= 14, 6.5$ Hz, 1H), 2.71 (dt, 14, 8 Hz, 1H), 2.01 (m, 2H); ^{13}C NMR (100.6 MHz, CDCl_3) δ (ppm): 158.2, 132.7, 129.5, 114.1, 67.2, 64.4, 55.4, 36.1, 31.5; HRMS (TOF, ES+) $\text{C}_{11}\text{H}_{15}\text{ClO}_2$ $[\text{M}+\text{H}]^+$ calc'd 275.1887, found 275.1886; Specific rotation $[\alpha]^{23}_{\text{D}} = -31.7^\circ$ ($c = 1, \text{CH}_3\text{Cl}$).



(S)-2-chloro-4-phenylbutan-1-ol (3.117).

To a flame dried round bottom flask equipped with a stir bar, 4-phenylbutanal (0.35 g, 2.36 mmol) was dissolved into CH_2Cl_2 (4.73 mL) at 0°C and to the stirring solution was added catalyst **3.71** (0.053 g, 0.024 mmol) and then *N*-chlorosuccinimide (0.410 g, 3.07 mmol). Solution was maintained at 0°C , and stirring was continued for 12 hours, at which point starting material was consumed by ^1H NMR. Reaction was diluted with MeOH (4.73 mL) and cooled to 0°C , then NaBH_4 (0.447 g, 11.82 mmol) was slowly added while stirring. The reaction was stirred for additional 30 min. at the same temperature, then quenched with H_2O and extracted three times with EtOAc. Organic fractions were combined, washed with brine, and dried over Na_2SO_4 . The organic layer was concentrated *in vacuo* and a crude oil was purified by column chromatography (4:1 Hex/EtOAc) to yield desired product as a clear oil in 0.311 g (72%). ^1H NMR (400.2 MHz, CDCl_3) δ (ppm): 7.30 (t, $J= 8.0$ Hz, 2H), 7.21 (m, 3H), 3.98 (m, 1H), 3.78 (dd, $J= 12.1, 4.0$ Hz, 1H), 3.69 (dd, $J= 12.1, 6.5$ Hz, 1H), 2.90 (quint, $J= 7.1$ Hz, 1H), 2.76

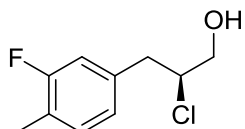
(quint, $J = 7.1$ Hz, 1H), 2.07 (m, 2H); ^{13}C NMR (100.6 MHz, CDCl_3) δ (ppm): 140.5, 128.5, 128.4, 126.2, 66.95, 64.2, 62.6, 35.7, 32.3; $[\alpha]_{\text{D}}^{23} = -26.2^\circ$ ($c = 1$, CH_3Cl).



(S)-2-chlorodecan-1-ol (3.118).

To a flame dried round bottom flask equipped with a stir bar, decanal (0.25 g, 1.60 mmol) was dissolved into CH_2Cl_2 (8.01 mL) at 0°C and to the stirring solution was added catalyst **3.71** (0.036 g, 0.16 mmol) and then *N*-chlorosuccinimide (0.278 g, 2.08 mmol). Solution was maintained at 0°C , and stirring was continued for 12 hours, at which point starting material was consumed by ^1H NMR. Reaction was diluted with MeOH (8.01 mL) and cooled to 0°C , then NaBH_4 (0.303 g, 8.01 mmol) was slowly added while stirring. The reaction was stirred for an additional 30 min. at the same temperature, then quenched with H_2O and extracted three times with EtOAc. The organic fractions were combined, washed with brine, and dried over Na_2SO_4 . The organic layer was concentrated *in vacuo* and a crude oil was purified by column chromatography (4:1 Hex/EtOAc) to yield desired product as a clear oil in 0.22 g (70%). ^1H NMR (400.2 MHz, CDCl_3) δ (ppm): 4.00 (m, 1H), 3.77 (dd, $J = 11.9, 3.5$ Hz), 3.65 (dd, $J = 11.9, 7.1$ Hz, 1H), 2.18 (br s, 1H), 1.73 (m, 2H), 1.51 (m, 1H), 1.40 (m, 1H), 1.41 (m, 1H), 1.27 (m, 10H), 0.87 (t, $J = 7.0$ Hz, 3H); ^{13}C NMR (100.6 MHz, CDCl_3) δ (ppm): 67.2, 65.5, 34.4, 31.9, 29.5, 29.3, 29.2,

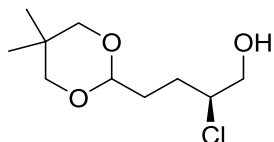
26.5, 22.8, 14.2; HRMS (TOF, ES+) Did not ionize on positive or negative ion detection mode; Specific rotation $[\alpha]_{D}^{23} = +5.9^{\circ}$ ($c = 1.1$, CH_3Cl).



(S)-2-chloro-3-(3-fluoro-4-methylphenyl)propan-1-ol (3.119).

To a flame dried round bottom flask equipped with a stir bar, 3-(3-fluoro-4-methylphenyl)propanal (0.340 g, 2.05 mmol) was dissolved into CH_2Cl_2 (5.85 mL) at 0°C and to the stirring solution was added catalyst **3.71** (0.046 g, 0.20 mmol) and then *N*-chlorosuccinimide (0.355 g, 2.66 mmol). Solution was maintained at 0°C , and stirring was continued for 12 hours, at which point starting material was consumed by ^1H NMR. The reaction was diluted with MeOH (5.85 mL) and cooled to 0°C , then NaBH_4 (0.387 g, 10.24 mmol) was slowly added while stirring. The reaction was stirred for an additional 30 min. at the same temperature, then quenched with H_2O and extracted three times with EtOAc. The organic fractions were combined, washed with brine, and dried over Na_2SO_4 . The organic layer was concentrated *in vacuo* and a crude oil was purified by column chromatography (4:1 Hex/EtOAc) to yield desired product as a clear oil in 0.234 g (58%). ^1H NMR (400.2 MHz, CDCl_3) δ (ppm): 6.97 (t, $J = 8.4$ Hz, 1H), 6.76 (s, 1H), 6.74 (d, $J = 4.0$ Hz, 1H), 4.04 (m, 1H), 3.65 (dd, $J = 12.0, 4.0$ Hz, 1H), 3.53 (dd, $J = 12.0, 6.0$ Hz, 1H), 2.95 (dd, $J = 13.7, 6.5$ Hz, 1H), 2.85 (dd, $J = 13.7, 7.5$ Hz, 1H), 2.10 (s, 3H),

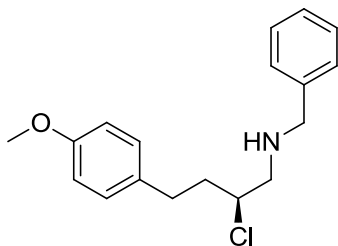
1.76 (br s, 1H); ^{13}C NMR (100.6 MHz, CDCl_3) δ (ppm): 161.2 ($J_{\text{CF}} = 247$ Hz), 136.5 ($J_{\text{CF}} = 7$ Hz), 131.4 ($J_{\text{CF}} = 6$ Hz), 124.6 ($J_{\text{CF}} = 4$ Hz), 123.4 ($J_{\text{CF}} = 18$ Hz), 115.8 ($J_{\text{CF}} = 20$ Hz), 65.7, 64.4, 39.9, 14.2 ($J_{\text{CF}} = 4$ Hz); Specific rotation $[\alpha]_{\text{D}}^{23} = -18.8^\circ$ ($c = 1$, CH_3Cl).



(S)-2-chloro-4-(5,5-dimethyl-1,3-dioxan-2-yl)butan-1-ol (3.120).

To a flame dried round bottom flask equipped with a stir bar, 4-(5,5-dimethyl-1,3-dioxan-2-yl)butanal (0.25 g, 1.34 mmol) was dissolved in CH_2Cl_2 (3.84 mL) at 0°C and to the stirring solution was added catalyst **3.71** (0.03 g, 0.13 mmol) and then *N*-chlorosuccinimide (0.233 g, 1.75 mmol). Solution was maintained at 0°C , and stirring was continued for 12 hours, at which point starting material was consumed by ^1H NMR. The reaction was diluted with MeOH (3.84 mL) and cooled to 0°C , then NaBH_4 (0.254 g, 6.72 mmol) was slowly added while stirring. The reaction was stirred for additional 30 min. at the same temperature, then quenched with H_2O and extracted three times with EtOAc. The organic fractions were combined, washed with brine, and dried over Na_2SO_4 . The organic layer was concentrated *in vacuo* and a crude oil was purified by column chromatography (4:1 Hex/EtOAc) to yield desired product as a clear oil in 0.23 g (76%). ^1H NMR (400.2 MHz, CDCl_3) δ (ppm): 4.49 (t, $J = 4.4$ Hz, 1H), 4.08 (m, 1H), 3.81 (dd, $J = 12.2, 4.0$ Hz, 1H), 3.69 (dd, $J = 11.7, 7.0$ Hz, 1H), 3.62 (d, $J = 10.8$ Hz, 2H), 3.44 (d, $J = 10.8$ Hz, 2H), 2.05 (s, 1H), 2.00-1.74 (m, 4H), 1.20 (s, 3H), 0.74 (s, 3H); ^{13}C NMR (100.6 MHz, CDCl_3) δ (ppm): 101.2, 76.6, 66.8, 64.7, 31.2, 30.1, 28.3, 22.9, 21.7;

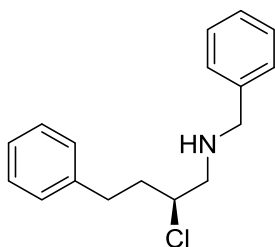
HRMS (TOF, ES+) C₁₀H₁₉ClO₃ [M+H]⁺ calc'd 222.1021, found 222.1020; Specific rotation $[\alpha]^{23}_D = -3.0^\circ$ (c = 1, CH₃Cl).



N-Benzyl-2-chloro-4-(4-methoxyphenyl)butan-1-amine (3.121).

To a flame dried round bottom flask equipped with a stir bar, alcohol **3.86** (0.30 g, 1.40 mmol) and 2,6-lutidine (0.751 g, 7.01 mmol) were dissolved in CH₂Cl₂ (7.01 mL) and cooled to 0°C. Tf₂O (1.68 mL, 1M in CH₂Cl₂, 1.68 mmol) was then added dropwise, and the solution was left to stir at 0°C for 30 minutes. At this time, the triflate solution was taken up by syringe and added dropwise to a stirring solution of benzylamine (1.52 g, 14.01 mmol) in CH₂Cl₂ (1.5 mL) at 0°C. The flask containing the triflate solution was washed 2 times with CH₂Cl₂ (1 mL) and added to the reaction. The solution was then slowly warmed to ambient temperature and stirred overnight. The reaction was quenched with NaHCO₃, diluted with CH₂Cl₂, and extracted 3 times with CH₂Cl₂. The organic layers were combined and washed with brine. The organic layer was dried over Na₂SO₄ and concentrated *in vacuo* to yield the crude product as a yellow oil. Purification by flash column chromatography (9:0.9:0.1 CH₂Cl₂/MeOH/NH₄OH) to yield the desired product as a pale yellow oil in 0.22g, (88%). Instead of flash column chromatography, crude reaction product could also be directly carried forward to the next step. ¹HNMR (400.2

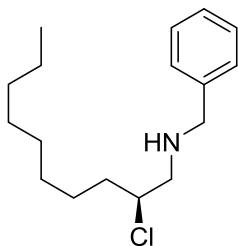
MHz, CDCl₃) δ (ppm): 7.33 (m, 4H), 7.26 (m, 1H), 7.10 (d, $J=9$ Hz, 2H), 6.83 (d, $J=9$ Hz, 2H), 4.03 (m, 1H), 3.80 (dd, 14, 13 Hz, 2H), 3.79 (s, 3H), 2.86 (dd, 6, 3 Hz, 2H), 2.80 (m, 1H), 2.01 (m, 2H); ¹³C NMR (100.6 MHz, CDCl₃) δ (ppm): 157.94, 132.82, 129.39, 129.22, 128.42, 128.15, 128.07, 127.06, 120.12, 113.86, 113.80, 62.48, 55.34, 55.21, 53.25, 37.97, 31.52, 24.41.



(S)-N-benzyl-2-chloro-4-phenylbutan-1-amine (3.122).

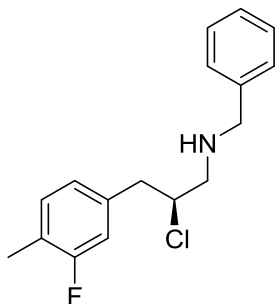
To a flame dried round bottom flask equipped with a stir bar, alcohol **3.117** (0.075 g, 0.41 mmol) and 2,6-lutidine (0.218 g, 2.04 mmol) were dissolved in CH₂Cl₂ (2.04 mL) and cooled to 0°C. Tf₂O (0.49 mL, 1M in CH₂Cl₂, 0.49 mmol) was then added dropwise, and the solution was left to stir at 0°C for 30 minutes. At this time, the triflate solution was taken up by syringe and added dropwise to a stirring solution of benzylamine (0.44 g, 4.07 mmol) in CH₂Cl₂ (0.5 mL) at 0°C. The flask containing the triflate solution was washed 2 times with CH₂Cl₂ (0.5 mL) and added to the reaction. The solution was then slowly warmed to ambient temperature and stirred overnight. The reaction was quenched with NaHCO₃, diluted with CH₂Cl₂, and extracted 3 times with CH₂Cl₂. The organic layers were combined and washed with brine. The organic layer was dried over Na₂SO₄

and concentrated *in vacuo* to yield the crude product. The crude product was isolated as a pale yellow oil quantitatively and carried forward directly to the next step.



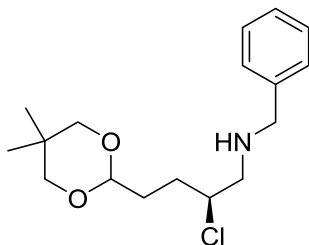
(S)-N-benzyl-2-chlorodecan-1-amine (3.123).

To a flame dried round bottom flask equipped with a stir bar, alcohol **3.118** (0.12 g, 0.60 mmol) and 2,6-lutidine (0.32 g, 2.99 mmol) were dissolved in CH_2Cl_2 (2.99 mL) and cooled to 0 °C. Tf_2O (0.72 mL, 1M in CH_2Cl_2 , 0.72 mmol) was then added dropwise, and the solution left to stir at 0°C for 30 minutes. At this time, the triflate solution was taken up by syringe and added dropwise to a stirring solution of benzylamine (0.64 g, 5.99 mmol) in CH_2Cl_2 (1.0 mL) at 0°C. The flask containing the triflate solution was washed 2 times with CH_2Cl_2 (1 mL) and added to reaction. The solution was then slowly warmed to ambient temperature and stirred overnight. The reaction was quenched with NaHCO_3 , diluted with CH_2Cl_2 , and extracted 3 times with CH_2Cl_2 . The organic layers were combined and washed with brine. The organic layer was dried over Na_2SO_4 and concentrated *in vacuo* to yield the crude product. The crude product was isolated as a pale yellow oil quantitatively and carried forward directly to the next step.



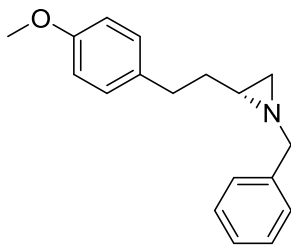
(S)-N-benzyl-2-chloro-3-(3-fluoro-4-methylphenyl)propan-1-amine (3.124).

To a flame dried round bottom flask equipped with a stir bar, alcohol **3.119** (0.20 g, 1.00 mmol) and 2,6-lutidine (0.53 g, 4.9 mmol) were dissolved in CH_2Cl_2 (4.9 mL) and cooled to 0°C . Tf_2O (1.19 mL, 1M in CH_2Cl_2 , 1.19 mmol) was then added dropwise, and the solution was left to stir at 0°C for 30 minutes. At this time, the triflate solution was taken up by syringe and added dropwise to a stirring solution of benzylamine (1.06 g, 9.90 mmol) in CH_2Cl_2 (1.5 mL) at 0°C . The flask containing the triflate solution was washed 2 times with CH_2Cl_2 (1 mL) and added to reaction. The solution was then slowly warmed to ambient temperature and stirred overnight. The reaction was quenched with NaHCO_3 , diluted with CH_2Cl_2 , and extracted 3 times with CH_2Cl_2 . The organic layers were combined and washed with brine. The organic layer was dried over Na_2SO_4 and concentrated *in vacuo* to yield the crude product. The crude product was isolated as a pale yellow oil quantitatively and carried forward directly to the next step.



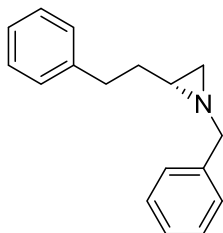
(S)-N-benzyl-2-chloro-4-(5,5-dimethyl-1,3-dioxan-2-yl)butan-1-amine (3.125).

To a flame dried round bottom flask equipped with a stir bar, alcohol **3.120** (0.10 g, 0.45 mmol) and 2,6-lutidine (0.241 g, 2.25 mmol) were dissolved in CH_2Cl_2 (2.25 mL) and cooled to 0°C . Tf_2O (0.54 mL, 1M in CH_2Cl_2 , 0.54 mmol) was then added dropwise, and the solution was left to stir at 0°C for 30 minutes. At this time, the triflate solution was taken up by syringe and added dropwise to a stirring solution of benzylamine (0.48 g, 4.50 mmol) in CH_2Cl_2 (1.00 mL) at 0°C . The flask containing the triflate solution was washed 2 times with CH_2Cl_2 (1.00 mL) and added to reaction. The solution was then slowly warmed to ambient temperature and stirred overnight. The reaction was quenched with NaHCO_3 , diluted with CH_2Cl_2 , and extracted 3 times with CH_2Cl_2 . The organic layers were combined and washed with brine. The organic layer was dried over Na_2SO_4 and concentrated *in vacuo* to yield the crude product. The crude product was isolated as a pale yellow oil quantitatively and carried forward directly to the next step.



(R)-1-Benzyl-2-(4-methoxyphenethyl)aziridine (3.88).

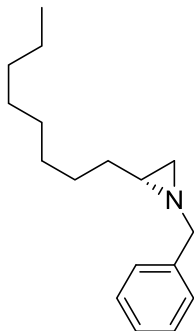
In an open microwave vial equipped with a stir bar, amine **3.121** (0.12g, 0.41 mmol) was dissolved in 1:1 THF/H₂O (2.71 mL), followed by the addition of KOH (0.15g, 2.64 mmol). The microwave vial was sealed and stirred overnight at 65 °C. The reaction mixture was allowed to cool to ambient temperature, then extracted 3 times with EtOAc. The organic layers were combined and dried over Na₂SO₄, then concentrated *in vacuo* to give the crude product as a pale yellow oil. Purification by flash column chromatography (1:1 Hex/EtOAc) afforded the desired product as a colorless oil in 0.10 g, (95%). ¹HNMR (400.2 MHz, CDCl₃) δ (ppm): 7.35 (m, 4H), 7.27 (m, 1H), 7.02 (d, *J*= 8.4 Hz, 2H), 6.80 (d, *J*= 8.4 Hz, 2H), 3.78 (s, 3H), 3.50 (d, *J*= 13.0 Hz, 1H), 3.31 (d, *J*= 13.0 Hz, 1H), 2.56 (m, 2H), 1.69 (m, 2H), 1.63 (d, *J*= 3.5 Hz, 1H), 1.48 (m, 1H), 1.39 (d, *J*= 6.6 Hz, 1H); ¹³C NMR (100.6 MHz, CDCl₃) δ (ppm): 157.9, 139.6, 134.1, 129.4, 128.5, 128.4, 127.2, 113.8, 65.1, 55.4, 39.3, 35.1, 34.2, 32.9; HRMS (TOF, ES+) C₁₈H₂₁NO [M+H]⁺ calc'd 267.1622, found 267.1622; Specific rotation [α]²³_D = +25.6° (c = 1.2, CH₃Cl).



(R)-1-benzyl-2-phenethylaziridine (3.89).

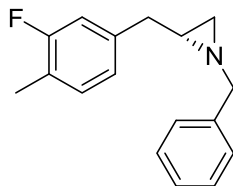
In an open microwave vial equipped with a stir bar, amine **3.122** (0.17 g, 0.62 mmol) was dissolved in 1:1 THF/H₂O (4.1 mL), followed by the addition of KOH (0.23 g, 4.04 mmol). The microwave vial was sealed and stirred overnight at 65 °C. The reaction mixture was allowed to cool to ambient temperature, then extracted 3 times with EtOAc. The organic layers were combined and dried over Na₂SO₄, then concentrated *in vacuo* to give the crude product as a pale yellow oil. Purification by flash column chromatography (1:1 Hexs/EtOAc) afforded the desired product as a colorless oil in 0.13 g, (89%).

¹H NMR (400.2 MHz, CDCl₃) δ (ppm): 7.25 (m, 4H), 7.15 (m, 3H), 7.06 (m, 1H), 7.01 (d, *J* = 7.6 Hz, 2H), 3.40 (d, *J* = 13.0 Hz, 1H), 3.20 (d, *J* = 13.0 Hz, 1H), 2.53 (m, 1H), 1.64 (m, 2H), 1.54 (d, *J* = 3.8 Hz, 1H), 1.39 (m, 1H), 1.31 (d, *J* = 6.2 Hz, 1H); ¹³C NMR (100.6 MHz, CDCl₃) δ (ppm): 142.0, 139.5, 128.5, 128.4, 128.3, 128.2, 127.2, 125.8, 65.1, 39.3, 34.8, 34.2, 33.8; HRMS (TOF, ES+) C₁₇H₁₉N [M+H]⁺ calc'd 193.0656, found 193.0656; Specific rotation [α]_D²³ = +11.0° (c = 0.9, CH₃Cl).



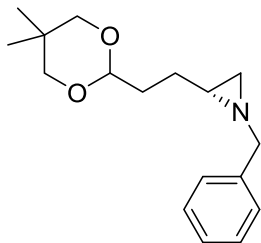
(R)-1-benzyl-2-octylaziridine (3.91).

In an open microwave vial equipped with a stir bar, amine **3.123** (0.17 g, 0.60 mmol) was dissolved in 1:1 THF/H₂O (4.0 mL), followed by the addition of KOH (0.22 g, 3.92 mmol). The microwave vial was sealed and stirred overnight at 65 °C. The reaction mixture was allowed to cool to ambient temperature, then extracted 3 times with EtOAc. The organic layers were combined and dried over Na₂SO₄, then concentrated *in vacuo* to give the crude product as a pale yellow oil. Purification by flash column chromatography (1:1 Hex/EtOAc) afforded the desired product as a colorless oil in 0.18 g, (81%). ¹H NMR (400.2 MHz, CDCl₃) δ (ppm): 7.20 (m, 5H), 3.42 (d, *J*= 12.9 Hz, 1H), 3.24 (d, *J*= 12.9 Hz, 1H), 1.53 (d, *J*= 3.7 Hz, 1H), 1.33 (m, 4H), 1.15 (m, 12H), 0.81 (t, *J*= 7.0 Hz, 3H); ¹³C NMR (100.6 MHz, CDCl₃) δ (ppm): 139.6, 128.4, 128.3, 127.1, 65.2, 39.9, 34.2, 33.2, 31.9, 29.7, 29.5, 29.4, 29.3, 27.6, 22.8, 14.2; HRMS (TOF, ES+) C₁₇H₂₇N [M+H]⁺ calc'd 245.2144, found 245.2144; Specific rotation [α]²³_D = +17.6° (c = 0.9, CH₃Cl).



(R)-1-benzyl-2-(3-fluoro-4-methylbenzyl)aziridine (3.92).

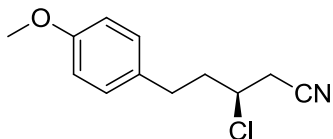
In an open microwave vial equipped with a stir bar, amine **3.124** (0.08 g, 0.29 mmol) was dissolved in 1:1 THF/H₂O (1.94 mL), followed by the addition of KOH (0.11 g, 1.89 mmol). The microwave vial was sealed and stirred overnight at 65 °C. The reaction mixture was allowed to cool to ambient temperature, then extracted 3 times with EtOAc. The organic layers were combined and dried over Na₂SO₄, then concentrated *in vacuo* to give the crude product as an oil. Purification by flash column chromatography (1:1 Hex/EtOAc) afforded the desired product as a pale yellow oil in 0.06 g, (84%). ¹H NMR (400.2 MHz, CDCl₃) δ (ppm): 7.20 (m, 5H), 6.94 (t, *J* = 8.0 Hz, 1H), 6.76 (s, 1H), 6.74 (d, *J* = 5.0 Hz, 1H), 3.34 (d, *J* = 12.1 Hz, 1H), 3.29 (d, *J* = 12.1 Hz, 1H), 2.66 (dd, *J* = 14.0, 6.6 Hz, 1H), 2.54 (dd, *J* = 14.0, 6.6 Hz, 1H), 2.15 (s, 3H), 1.65 (m, 2H), 1.39 (d, dd, *J* = 6.7 Hz, 1H); ¹³C NMR (100.6 MHz, CDCl₃) δ (ppm): 161.3 (d, *J*_{CF} = 247 Hz), 139.1 (d, *J*_{CF} = 8 Hz), 139.0, 131.1 (d, *J*_{CF} = 6 Hz), 128.2, 128.0, 126.9, 123.9 (d, *J*_{CF} = 3.6 Hz), 122.2 (d, *J*_{CF} = 20 Hz), 115.0 (d, *J*_{CF} = 22 Hz), 64.7, 40.3, 38.6, 33.7, 14.1 (d, *J*_{CF} = 4 Hz); Specific rotation [α]²³_D = -1.1° (c = 1, CH₃Cl).



(R)-1-benzyl-2-octylaziridine (3.90).

In an open microwave vial equipped with a stir bar, amine **3.125** (0.14 g, 0.45 mmol) was dissolved in 1:1 THF/H₂O (2.99 mL), followed by the addition of KOH (0.16 g, 2.92 mmol). The microwave vial was sealed and stirred overnight at 65 °C. The reaction mixture was allowed to cool to ambient temperature, then extracted 3 times with EtOAc. The organic layers were combined and dried over Na₂SO₄, then concentrated *in vacuo* to give the crude product a pale yellow oil. Purification by flash column chromatography (1:1 Hex/EtOAc) afforded the desired product as pale yellow oil in 0.11 g, (85%).

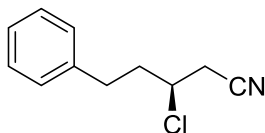
¹H NMR (400.2 MHz, CDCl₃) δ (ppm): 7.23 (m, 5H), 4.28 (t, *J* = 5.0 Hz, 1H), 3.50 (d, *J* = 10.8 Hz, 2H), 3.43 (d, *J* = 13.6 Hz, 1H), 3.27 (m, 3H), 1.61 (m, 2H), 1.55 (d, *J* = 3.4 Hz, 1H), 1.47 (m, 3H), 1.32 (d, *J* = 6.0 Hz, 1H), 1.10 (s, 3H), 0.63 (s, 3H); ¹³C NMR (100.6 MHz, CDCl₃) δ (ppm): 139.5, 128.4, 128.3, 127.0, 101.7, 77.3, 65.1, 39.5, 34.0, 32.6, 30.2, 27.6, 23.1, 21.9; HRMS (TOF, ES⁺) C₁₇H₂₅NO₂ [M+H]⁺ calc'd 275.1886, found 275.1886; Specific rotation [α]²³_D = +4.0° (c = 1, CH₃Cl).



(S)-3-Chloro-5-(4-methoxyphenyl)pentanenitrile (3.93).

To a flame dried round bottom flask equipped with a stir bar, alcohol **3.86** (0.50 g, 2.34 mmol) and 2,6-lutidine (1.25 g, 11.68 mmol) were dissolved in CH₂Cl₂ (11.68 mL) and cooled to 0°C. Tf₂O (2.80 mL, 1M in CH₂Cl₂, 2.80 mmol) was then added dropwise, and the solution was left to stir at 0°C for 30 minutes. The reaction was diluted with CH₂Cl₂ and washed with H₂O. The organic fraction was washed with brine, dried over Na₂SO₄, and concentrated *in vacuo*. The crude oil was carried forward directly to the next step.

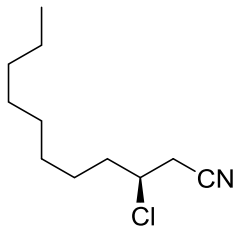
The crude triflate was dissolved in MeCN (11.68 mL), then 18-C-6 (0.12 g, 0.47 mmol) was added to the mixture and allowed to dissolve. KCN (1.52 g, 23.36 mmol) was then added, and the reaction was allowed to stir for 12 h at ambient temperature. The reaction was then quenched with NaHCO₃ and extracted three times with CH₂Cl₂. The organic fractions were combined and dried over Na₂SO₄. The organic layer was concentrated *in vacuo*, and purification by flash chromatography (4:1 Hex/EtOAc) to afford the desired product as a clear/rose colored oil in 0.43 g (83%). ¹HNMR (400.2 MHz, CDCl₃) δ (ppm): 7.11 (d, *J*= 8.5 Hz, 2H), 6.85 (d, *J*= 8.5 Hz, 2H), 3.97 (quint, *J*=6.5 Hz, 1H), 3.79 (s, 3H), 2.84 (m, 1H), 2.80 (dd, *J*= 5.6, 1Hz, 2H), 2.72 (m, 1H), 2.12 (dd, *J*= 14, 7 Hz, 2H); ¹³C NMR (100.6 MHz, CDCl₃) δ (ppm): 158.4, 131.7, 129.6, 116.2, 114.3, 55.4, 54.8, 39.3, 31.5, 27.8; HRMS (TOF, ES+) C₁₂H₁₄ClNO [M+H]⁺ calc'd 223.0762, found 223.0760; Specific rotation [α]²³_D = +10.1° (c = 0.9, CH₃Cl).



(S)-3-chloro-5-phenylpentanenitrile (3.97).

To a flame dried round bottom flask equipped with a stir bar, alcohol **3.117** (0.15, 0.82 mmol) and 2,6-lutidine (0.44 g, 4.1 mmol) were dissolved in CH_2Cl_2 (4.10 mL) and cooled to 0°C . Tf_2O (0.98 mL, 1M in CH_2Cl_2 , 0.98 mmol) was then added dropwise, and the solution was left to stir at 0°C for 30 minutes. The reaction was diluted with CH_2Cl_2 and washed with H_2O . The organic fraction was washed with brine, dried over Na_2SO_4 , and concentrated *in vacuo*. The crude oil was carried on directly to the next step.

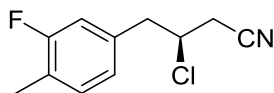
The crude triflate was dissolved in MeCN (4.10 mL), then 18-C-6 (0.04 g, 0.16 mmol) was added to the mixture and allowed to dissolve. KCN (0.53 g, 8.20 mmol) was then added, and the reaction was allowed to stir for 12 h at ambient temperature. The reaction was then quenched with NaHCO_3 and extracted three times with CH_2Cl_2 . The organic fractions were combined and dried over Na_2SO_4 . The organic layer was concentrated *in vacuo*, and purification by flash chromatography (4:1 Hex/EtOAc) afforded the desired product as a clear/rose colored oil in 0.14 g (86%). ^1H NMR (400.2 MHz, CDCl_3) δ (ppm): 7.31 (t, $J= 7.7$ Hz, 2H), 7.22 (m, 3H), 3.99 (ddt, $J= 9.7, 5.9, 5.6$ Hz, 1H), 2.92 (m, 1H), 2.81 (dd, $J= 5.9, 2.5$ Hz, 2H), 2.78 (m, 1H), 2.16 (m, 2H); ^{13}C NMR (100.6 MHz, CDCl_3) δ (ppm): 139.75, 128.84, 128.60, 128.66, 116.17, 54.80, 39.03, 32.35, 27.80; HRMS (TOF, ES+) $\text{C}_{11}\text{H}_{12}\text{ClN}$ $[\text{M}+\text{H}]^+$ calc'd 193.0656, found 193.0656; Specific rotation $[\alpha]_{\text{D}}^{23} = +2.4^\circ$ ($c = 1, \text{CH}_3\text{Cl}$).



(S)-3-chloroundecanenitrile (3.99).

To a flame dried round bottom flask equipped with a stir bar, alcohol **3.118** (0.50 g, 2.60 mmol) and 2,6-lutidine (1.39 g, 13.01 mmol) were dissolved in CH_2Cl_2 (13.01 mL) and cooled to 0°C . Tf_2O (3.12 mL, 1M in CH_2Cl_2 , 3.12 mmol) was then added dropwise, and the solution was left to stir at 0°C for 30 minutes. The reaction was diluted with CH_2Cl_2 and washed with H_2O . The organic fraction was washed with brine, dried over Na_2SO_4 , and concentrated *in vacuo*. The crude oil was carried on directly to the next step.

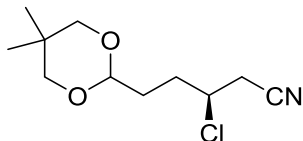
The crude triflate was dissolved in MeCN (13.01 mL), then 18-C-6 (0,137 0.52 mmol) was added to the mixture and allowed to dissolve. KCN (0.578g, 8.88 mmol) was then added, and the reaction was allowed to stir for 12 h at ambient temperature. The reaction was then quenched with NaHCO_3 and extracted three times with CH_2Cl_2 . The organic fractions were combined and dried over Na_2SO_4 . The organic layer was concentrated *in vacuo*, and purification by flash chromatography (4:1 Hex/EtOAc) afforded the desired product as a clear/rose colored oil in 0.33 g (66%). ^1H NMR (400.2 MHz, CDCl_3) δ (ppm): 4.05 (m, 1H), 2.82 (dd, $J= 6.0, 1.3$ Hz, 2H), 1.85 (m, 2H), 1.52 (m, 1H), 1.42 (m, 1H), 1.28 (m 12H), 0.87 (t, $J= 6.5$ Hz, 3H); ^{13}C NMR (100.6 MHz, CDCl_3) δ (ppm): 116.4, 55.8, 37.5, 31.9, 29.4, 29.2, 28.9, 27.7, 26.3, 22.7, 14.2; Specific rotation $[\alpha]^{23}_{\text{D}} = +0.9^\circ$ ($c = 1, \text{CH}_3\text{Cl}$).



(S)-3-chloro-4-(3-fluoro-4-methylphenyl)butanenitrile (3.100).

To a flame dried round bottom flask equipped with a stir bar, alcohol **3.119** (0.16 g, 0.81 mmol) and 2,6-lutidine (0.44g, 4.06 mmol) were dissolved in CH₂Cl₂ (4.06 mL) and cooled to 0°C. Tf₂O (0.97 mL, 1M in CH₂Cl₂, 0.97 mmol) was then added dropwise, and the solution was left to stir at 0°C for 30 minutes. The reaction was diluted with CH₂Cl₂ and washed with H₂O. The organic fraction was washed with brine, dried over Na₂SO₄, and concentrated *in vacuo*. The crude oil was carried on directly to the next step.

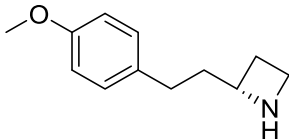
The crude triflate was dissolved in MeCN (4.06 mL), then 18-C-6 (0.04 g, 0.16 mmol) was added to the mixture and allowed to dissolve. KCN (0.53 g, 8.12 mmol) was then added, and the reaction was allowed to stir for 12 h at ambient temperature. The reaction was then quenched with NaHCO₃ and extracted three times with CH₂Cl₂. The organic fractions were combined and dried over Na₂SO₄. The organic layer was concentrated *in vacuo*, and purification by flash chromatography (4:1 Hex/EtOAc) afforded the desired product as a clear/rose colored oil in 0.15g (75%). ¹HNMR (400.2 MHz, CDCl₃) δ (ppm): 7.15 (t, *J* = 8.0 Hz, 1H), 6.90 (m, 2H), 4.23 (pent, *J* = 6.2 Hz, 1H), 3.13 (dq, *J* = 13.0, 6.8 Hz, 2H), 2.76 (dq, *J* = 17.0, 6.0 Hz, 2H), 2.26 (s, 3H); ¹³C NMR (100.6 MHz, CDCl₃) δ (ppm): 161.3 (d, *J*_{CF} = 247 Hz), 135.2 (d, *J*_{CF} = 8 Hz), 131.9 (d, *J*_{CF} = 6 Hz), 124.7 (d, *J*_{CF} = 4 Hz), 124.3 (d, *J*_{CF} = 18 Hz), 116.1, 115.8 (d, *J*_{CF} = 21 Hz), 53.4, 42.9, 26.5, 14.3 (d, *J*_{CF} = 4 Hz); HRMS (TOF, ES⁺) C₁₁H₁₁ClFN [M+H]⁺ calc'd 211.0562, found 211.0561; Specific rotation [α]_D²³ = -13.3° (c = 1, CH₃Cl).



(S)-3-chloro-5-(5,5-dimethyl-1,3-dioxan-2-yl)pentanenitrile (3.98).

To a flame dried round bottom flask equipped with a stir bar, alcohol **3.120** (0.19g, 0.89 mmol) and 2,6-lutidine (0.48g, 4.44 mmol) were dissolved in CH₂Cl₂ (4.4 mL) and cooled to 0°C. Tf₂O (0.30g, 1.07 mmol) was then added dropwise, and solution left to stir at 0°C for 30 minutes. Reaction was diluted with CH₂Cl₂ and washed with H₂O. The organic fraction was washed with brine, dried over Na₂SO₄, and concentrated *in vacuo*. The crude oil was carried on directly to the next step.

The crude triflate was dissolved in MeCN (4.4 mL), then 18-C-6 (0.05g, 0.18 mmol) was added to the mixture and allowed to dissolve. KCN (0.578g, 8.88 mmol) was then added, and the reaction was allowed to stir for 12 h at ambient temperature. The reaction was then quenched with NaHCO₃ and extracted three times with CH₂Cl₂. The organic fractions were combined and dried over Na₂SO₄. The organic layer was concentrated *in vacuo*, and purification by flash chromatography (4:1 Hex/EtOAc) afforded the desired product as a clear/rose colored oil in 0.11 g (70%). ¹HNMR (400.2 MHz, CDCl₃) δ (ppm): 4.45 (dd, *J* = 10.4, 1.6 Hz, 1H, (tt, *J* = 10.2, 3.5 Hz, 1H), 3.60 (m, 2H), 3.38 (d, *J* = 8.9 Hz, 1H), 3.20 (m, 3H), 2.54 (m, 1H), 2.07 (m, 2H), 1.71 (dt, *J* = 15.4, 5.0 Hz, 1H), 0.85 (s, 3H), 0.82 (s, 3H); ¹³C NMR (100.6 MHz, CDCl₃) δ (ppm): 117.9, 75.9, 75.7, 72.7, 68.5, 53.86, 36.7, 35.4, 28.2, 23.2, 23.1; HRMS (TOF, ES⁺) C₁₁H₁₈ClNO₂ [M+H]⁺ calc'd 231.1025, found 231.1025; Specific rotation [α]²³_D = +6.4° (c = 1.1, CH₃Cl).

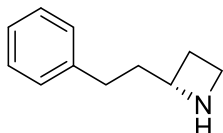


(S)-2-(4-Methoxyphenethyl)azetidine (3.94)

To a flame dried microwave vial with magnetic stir bar was added InCl_3 (0.12 g, 0.54 mmol) and NaBH_4 (0.06 g, 1.63 mmol). Anhydrous THF (1.2 mL) was added and the heterogeneous mixture was stirred under argon for 1h. **3.93** (0.12 g, 0.54 mmol) was then slowly added as a solution in THF (1.2 mL). The reaction mixture was allowed to stir at ambient temperature for 4 h. The reaction was quenched by dropwise addition (CAUTION: results in rapid generation of gas) of H_2O (1.5 mL) and the solution was heated to 75 °C for 30 min. MeOH (1.5 mL) was then slowly added, and stirring continued at 75 °C for 30 min. The reaction mixture was allowed to cool to room temperature, then filtered through a celite pad to remove solid indium byproducts. The resulting colorless solution was concentrated *in vacuo* and the residue was carried forward directly to the next step.

To an open microwave vial equipped with a stir bar, the crude residue from the previous step was dissolved in a solution of 1:1 THF/ H_2O (3.52 mL) and KOH (0.16g, 2.86 mmol) was then added. The vial was sealed and submitted to microwave irradiation at 170°C. for 1 h. The biphasic solution was extracted three times with EtOAc and washed with brine. The organic fractions were combined, dried over Na_2SO_4 , and concentrated *in vacuo*. Purification by flash column chromatography (9:0.9:0.1 $\text{CH}_2\text{Cl}_2/\text{MeOH}/\text{NH}_4\text{OH}$) afforded desired product as a light yellow oil in 40 mg (48%). $^1\text{HNMR}$ (400.2 MHz, CDCl_3) δ (ppm): 7.09 (d, J = 8.2 Hz, 2H), 6.82 (d, J = 8.2 Hz, 2H), 3.88 (quint, J = 7.6 Hz,

1H), 3.75 (s, 3H), 3.60 (q, $J= 8.3$ Hz, 1H), 2.50 (m, 2H), 2.30 (m, 1H), 2.03 (m, 1H), 1.87 (m, 2H); ^{13}C NMR (100.6 MHz, CDCl_3) δ (ppm): 159.4, 135.0, 130.3, 114.8, 59.7, 55.7, 43.6, 40.9, 31.8, 28.2; $[\alpha]_{\text{D}}^{20} = +0.8$ ($c = 1.0$, CHCl_3).

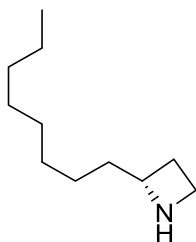


(S)-2-phenethylazetidine (3.101)

To a flame dried microwave vial with magnetic stir bar was added InCl_3 (0.09 g, 0.39 mmol) and NaBH_4 (0.04 g, 1.17 mmol). Anhydrous THF (0.86 mL) was added and the heterogeneous mixture was stirred under argon for 1h. **3.97** (0.08 g, 0.39 mmol) was then slowly added as a solution in THF (0.86 mL). The reaction mixture was allowed to stir at ambient temperature for 4 h. The reaction was quenched by dropwise addition (CAUTION: results in rapid generation of gas) of H_2O (0.86 mL) and the solution was heated to 75°C for 30 min. MeOH (1.6 mL) was then slowly added, and stirring continued at 75°C for 30 min. The reaction mixture allowed to cool to room temperature, then filtered through a celite pad to remove solid indium byproducts. The resulting colorless solution was concentrated *in vacuo* and the residue was carried forward directly to the next step.

To an open microwave vial equipped with a stir bar, the crude residue from the previous step was dissolved in a solution of 1:1 THF/ H_2O (3.13 mL) and KOH (0.14 g, 2.54 mmol) was then added. The vial was sealed and submitted to microwave irradiation at

170°C. for 1 h. The biphasic solution was extracted three times with EtOAc and washed with brine. The organic fractions were combined, dried over Na₂SO₄, and concentrated *in vacuo*. Purification by flash column chromatography (9:0.9:0.1 CH₂Cl₂/MeOH/NH₄OH) afforded the desired product as a colorless oil in 28 mg (44%).¹H NMR (400.2 MHz, CDCl₃) δ (ppm): 7.25 (t, *J* = 7.8 Hz, 2H), 7.17 (m, 3H), 3.85 (pent, *J* = 7.4 Hz, 1H), 3.57 (q, *J* = 8.3 Hz, 1H), 3.31 (m, 3H), 2.56 (m, 2H), 2.29 (m, 1H), 2.03 (m, 1H), 1.90 (m, 2H); ¹³C NMR (100.6 MHz, CDCl₃) δ (ppm): 143.1, 129.4, 126.8, 59.7, 43.6, 40.7, 32.7, 28.2; specific rotation [α]_D²⁰ = 9.6 (*c* = 1.0, CHCl₃).

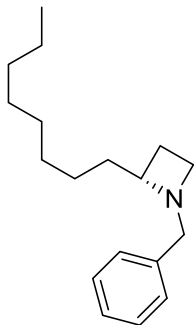


(S)-2-octylazetidine (3.102)

To a flame dried microwave vial with magnetic stir bar was added InCl₃ (0.07 g, 0.29 mmol) and NaBH₄ (0.03 g, 0.88 mmol). Anhydrous THF (0.65 mL) was added and the heterogeneous mixture was stirred under argon for 1h. **3.99** (0.06 g, 0.29 mmol) was then slowly added as a solution in THF (0.65 mL). The reaction mixture was allowed to stir at ambient temperature for 4 h. The reaction was quenched by dropwise addition (CAUTION: results in rapid generation of gas) of H₂O (0.65 mL) and the solution was heated to 75 °C for 30 min. MeOH (1.3 mL) was then slowly added, and stirring continued at 75 °C for 30 min. The reaction mixture was allowed to cool to room

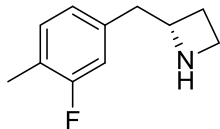
temperature, then filtered through a celite pad to remove solid indium byproducts. The resulting colorless solution was concentrated *in vacuo* and the residue was carried forward directly to the next step.

To an open microwave vial equipped with a stir bar, the crude residue from the previous step was dissolved in a solution of 1:1 THF/H₂O (2.34 mL) and KOH (0.11 g, 1.90 mmol) was then added. The vial was sealed and submitted to microwave irradiation at 170°C. for 1 h. The biphasic solution was extracted three times with EtOAc and washed with brine. The organic fractions were combined, dried over Na₂SO₄, and concentrated *in vacuo*. Purification by flash column chromatography (9:0.9:0.1 CH₂Cl₂/MeOH/NH₄OH) afforded the desired product as a light yellow oil in 22 mg (45%). ¹H NMR (400.2 MHz, CDCl₃) δ (ppm): 3.96 (pent, *J*= 7.6 Hz, 1H), 3.67 (q, *J*= 8.4 Hz, 1H), 3.40 (td, *J*= 9.0, 4.3 Hz, 1H), 3.40 (pent, *J*= 7.8 Hz, 1H), 3.33 (pent, *J*= 1.6 Hz, 1H), 2.36 (m, 1H), 2.07 (m, 1H), 1.65 (m, 1H), 1.33 (m, 12H), 0.88 (t, *J*= 6.5 Hz, 3H); ¹³C NMR (100.6 MHz, CDCl₃) δ (ppm): 59.3, 42.1, 36.8, 31.6, 29.2, 29.0, 28.9, 26.5, 24.8, 22.2, 12.9; HRMS (TOF, ES+) C₁₁H₂₃N [M+H]⁺ calc'd 169.1829, found 169.1828; specific rotation [α]_D²⁰ = +6.2 (*c* = 1.0, CHCl₃)



(S)-1-benzyl-2-octylazetidinium (3.126)

To a 0.5-2 mL microwave vial containing **3.102** (0.04 g, 0.23 mmol), benzaldehyde (0.06 g, 0.35 mmol) and acetic acid (0.124, 1.15 mmol) in CH₂Cl₂ (1.15 mL) were added, followed by MP-Cyanoborohydride (0.279 g, 0.58 mmol, 2.08 mmol/g). The vial was capped and heated to 110 °C for 7 min under microwave irradiation. After cooling, the vial was decapped and the solid phase reagent was filtered off and washed with 5 mL CH₂Cl₂. The resulting solution washed with 5 mL sat. NaHCO₃ and 5 mL H₂O. The organic phase was separated and dried over Na₂SO₄, filtered and concentrated *in vacuo*. The crude residue was purified by flash column chromatography (1:1 Hex/EtOAc) to afford the desired product as a colorless oil in 45 mg (75%). ¹H NMR (400.2 MHz, CDCl₃) δ (ppm): 7.25 (m, 5H), 3.73 (s, 2H), 3.53 (dt, *J*= 8.4, 3.0 Hz, 1H), 3.35 (m, 1H), 2.97 (q, *J*= 8.8 Hz, 1H), 2.04 (m, 1H), 1.93 (m, 1H), 1.44 (m, 2H), 1.14 (m, 12H), 0.85 (t, *J*= 7.0 Hz, 3H); ¹³C NMR (100.6 MHz, CDCl₃) δ (ppm): 135.1, 129.5, 128.8, 127.8, 67.0, 60.7, 50.4, 34.4, 31.8, 29.3, 29.3, 29.1, 25.1, 23.7, 22.6, 14.0

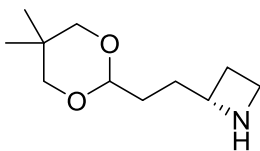


(S)-2-(3-fluoro-4-methylbenzyl)azetidine (3.103)

To a flame dried microwave vial with magnetic stir bar was added InCl_3 (0.12 g, 0.54 mmol) and NaBH_4 (0.06 g, 1.63 mmol). Anhydrous THF (1.2 mL) was added and the heterogeneous mixture was stirred under argon for 1h. **3.100** (0.12 g, 0.54 mmol) was then slowly added as a solution in THF (1.2 mL). The reaction mixture was allowed to stir at ambient temperature for 4 h. The reaction was quenched by dropwise addition (CAUTION: results in rapid generation of gas) of H_2O (1.5 mL) and the solution was heated to 75 °C for 30 min. MeOH (1.5 mL) was then slowly added, and stirring continued at 75 °C for 30 min. The reaction mixture was allowed to cool to room temperature, then filtered through a celite pad to remove solid indium byproducts. The resulting colorless solution was concentrated *in vacuo* and the residue was carried forward directly to the next step.

To an open microwave vial equipped with a stir bar, the crude residue from the previous step was dissolved in a solution of 1:1 THF/ H_2O (2.1 mL) and KOH (0.16g, 2.86 mmol) was then added. The vial was sealed and submitted to microwave irradiation at 170°C. for 1 h. The biphasic solution was extracted three times with EtOAc and washed with brine. The organic fractions were combined, dried over Na_2SO_4 , and concentrated *in vacuo*. Purification by flash column chromatography (9:0.9:0.1 CH_2Cl_2 /MeOH/ NH_4OH) afforded desired product as a light yellow oil in <5% yield. $^1\text{HNMR}$ (400.2 MHz, CDCl_3) δ (ppm): 7.23 (t, , $J= 8.0$ Hz, 1H), 7.00 (m, 2H), 4.71 (pent, , $J= 8.0$ Hz, 1H), 4.06

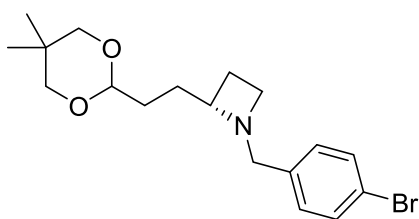
(q, , $J = 9.4$, 1H), 3.89 (m, 1H), 3.17 (dd, , $J = 7.8, 4.0$ Hz, 2H), 2.50 (m, 2H), 2.25 (s, 3H); ^{13}C NMR (100.6 MHz, CDCl_3) δ (ppm): 161.1 (d, $J_{\text{CF}} = 250$ Hz), 134.6 (d, $J_{\text{CF}} = 8$ Hz), 131.6 (d, $J_{\text{CF}} = 7$ Hz), 124.0 (d, $J_{\text{CF}} = 4$ Hz), 123.5 (d, $J_{\text{CF}} = 18$ Hz), 114.8 (d, $J_{\text{CF}} = 22$ Hz), 61.2, 42.3, 38.3, 24.4, 12.6 (d, $J_{\text{CF}} = 4$ Hz); $[\alpha]_{\text{D}}^{20} = -2.5$ ($c = 1.0$, CHCl_3); HRMS (TOF, ES+) $\text{C}_{11}\text{H}_{14}\text{FN}$ $[\text{M}+\text{H}]^+$ calc'd 179.1109, found 179.1108



(S)-2-(3-fluoro-4-methylbenzyl)azetidine (3.104)

To a flame dried microwave vial with magnetic stir bar was added InCl_3 (0.10 g, 0.43 mmol) and NaBH_4 (0.05 g, 1.30 mmol). Anhydrous THF (1.0 mL) was added and the heterogeneous mixture was stirred under argon for 1h. **3.98** (0.10 g, 0.43 mmol) was then slowly added as a solution in THF (1.0 mL). Reaction mixture was allowed to stir at ambient temperature for 4 h. The reaction was quenched by dropwise addition (CAUTION: results in rapid generation of gas) of H_2O (1.0 mL) and the solution was heated to 75 °C for 30 min. MeOH (2.0 mL) was then slowly added, and stirring continued at 75 °C for 30 min. The reaction mixture was allowed to cool to room temperature, then filtered through a celite pad to remove solid indium byproducts. The resulting colorless solution was concentrated *in vacuo* and the residue was carried forward directly to the next step.

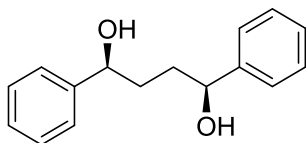
To an open microwave vial equipped with a stir bar, the crude residue from the previous step was dissolved in a solution of 1:1 THF/H₂O (3.40) and KOH (0.16 g, 2.76 mmol) was then added. The vial was sealed and submitted to microwave irradiation at 170°C. for 1 h. The biphasic solution was extracted three times with EtOAc and washed with brine. The organic fractions combined, dried over Na₂SO₄, and concentrated *in vacuo*. Purification by flash column chromatography (9:0.9:0.1 CH₂Cl₂/MeOH/NH₄OH) afforded desired product as a light yellow oil in 45 mg (55%). ¹HNMR (400.2 MHz, MeOD) δ (ppm): 3.89 (dd, *J*= 12.5, 3.6 Hz, 1H), 3.63 (m, 1H), 3.62 (d, *J*= 12.0 Hz, 1H), 3.57 (d, *J*= 12.0 Hz, 1H), 3.35 (m, 3H), 1.97 (m, 1H), 1.79 (d, *J*= 7.0 Hz, 1H), 1.50 (m, 4H), 1.35 (d, *J*= 3.4 Hz, 1H), 0.94 (s, 3H), 0.88 (s, 3H); ¹³C NMR (100.6 MHz, CDCl₃) δ (ppm): 81.8, 81.0, 79.3, 77.2, 38.1, 29.6, 29.3, 29.1, 24.1, 23.0, 22.6; [α]_D²⁰ = +1.7 (*c* = 1.0, CHCl₃); HRMS (TOF, ES+) C₁₁H₂₂NO₃S [M+H]⁺ calc'd 199.1574, found 199.1575



(S)-1-(4-bromobenzyl)-2-(2-(5,5-dimethyl-1,3-dioxan-2-yl)ethyl)azetidine (3.127)

To a flame dried vial with magnetic stir bar, **3.104** (0.04 g, 0.18 mmol) was dissolved in THF (1.76 mL). At ambient temperature was added triethylamine (0.03 g, 0.18 mmol) followed by 1-bromo-4-(bromomethyl)benzene (0.04 g, 0.18 mmol). Stirring was continued at room temperature for 12 hours, during which time the solution became opaque with white precipitant. After completion of reaction by LCMS, the reaction was

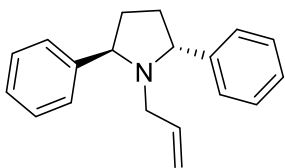
quenched with water, and extracted 3 times with EtOAc. Organic layers were combined, washed with brine, and dried over Na₂SO₄. Concentration *in vacuo* provided the crude colorless oil, which was purified by flash column chromatography (1:1 Hex/EtOAc) to provide the desired product as a clear oil in 102 mg (80%). ¹HNMR (400.2 MHz, CDCl₃) δ (ppm): 7.44 (d, *J*= 10.3 Hz, 2H), 7.21 (d, *J*= 9.4 Hz, 2H), 3.75 (dd, *J*= 12.4, 4.0 Hz, 1H), 3.57 (d, *J*= 12.0 Hz, 1H), 3.53 (d, *J*= 12.0 Hz, 1H), 3.44 (m, 3H), 3.25 (m, 5H), 1.62 (d, *J*= 12.0 Hz, 1H), 1.54 (m, 1H), 1.40 (m, 2H), 1.27 (m, 1H), 0.91 (s, 3H), 0.86 (s, 3H); ¹³C NMR (100.6 MHz, CDCl₃) δ (ppm): 138.3, 131.3, 129.8, 120.8, 81.9, 81.4, 79.8, 64.1, 53.3, 39.3, 38.6, 34.0, 29.1, 28.6, 24.1, 23.8.



(1S,4S)-1,4-diphenylbutane-1,4-diol (3.83)

To a solution of (R)-diphenyl(pyrrolidin-2-yl)methanol (638 mg, 2.52 mmol) in THF (15.7 mL, 0.16 M) was added distilled trimethylborate (0.14 mL, 25 mol %, 3.15 mmol) at ambient temperature. After 1 h, borane-dimethyl sulfide complex (2.4 mL, 25.2 mmol) was added, followed by a solution of 1,4-diphenylbutane-1,4-dione (3.00 g, 12.6 mmol) in THF (50 mL, 0.25 M) over 30 min. After 1 h, the mixture was quenched with 2M aqueous HCl (80 mL) slowly. The organic solvent was removed under reduced pressure and the resulting residue was diluted with ethyl acetate and water. The layers were separated and the aqueous layer was extracted with ethyl acetate. The combined organic layers were washed with water and brine, dried (MgSO₄), filtered, and concentrated. The

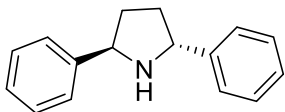
resulting oil was then purified by column chromatography 60% EtOAc/Hex to afford a colorless, viscous oil which solidified upon standing. The resulting white solid was then recrystallized in DCM/ Hexanes to afford 3.02 g (99%) as long white needles. m.p. 74.8 – 75.2 °C; ¹H NMR (400.2 MHz, CDCl₃) δ (ppm): 7.27 (m, 7H), 7.20 (m, 3H), 4.65 (m, 2H), 2.09 (br s, 2H), 1.88 (m, 2H), 1.76 (m, 2H); ¹³C NMR (100.6 MHz, CDCl₃) δ (ppm): 144.5, 128.4, 127.5, 125.7, 74.6, 35.7.



(2R,5R)-1-allyl-2,5-diphenylpyrrolidine (3.84)

To a cooled solution of (1S,4S)-1,4-diphenylbutane-1,4-diol (2.00 g, 8.26 mmol) in 68 mL DCM (0.24 M) at -20 °C, was added dry triethylamine (3.46 mL, 24.8 mmol) followed by distilled methanesulfonyl chloride (1.60 mL, 20.6 mmol) dropwise. After 1.5 hr, dry allylamine (62.0 mL, 8.26 mmol) was added and the mixture was allowed to warm to room temperature overnight. Excess allylamine was removed under reduced pressure and the crude mixture was diluted with ether and water. The layers were separated and the aqueous layer was extracted with ether and the combined organic extracts were washed with sat. NaHCO₃ and brine, dried (MgSO₄), filtered, and concentrated to give a yellow oil. The crude oil was purified by column chromatography using first a gradient system of Hex → 20% Tol/Hex until the undesired meso compound eluted, followed by 5% Et₂O/Hex to give the desired product in 1.67 g (77%, 85:15 dr) as a clear, light yellow oil. ¹H NMR (400 MHz, CDCl₃) δ (ppm): 7.50 (d, *J*= 7.2 Hz, 4H),

7.35 (t, $J=7.5$ Hz, 4H), 7.26 (m, 2H), 5.72 (m, 1H), 4.90 (m, 2H), 3.87 (t, $J=5.4$ Hz, 2H), 3.06 (d, $J=6.8$ Hz, 2H), 2.20 (m, 2H), 1.82 (m, 2H); ^{13}C NMR (100.6 MHz, CDCl_3) δ (ppm): 144.9, 133.7, 128.2, 127.4, 126.7, 117.2, 66.6, 52.6, 34.5.



(2R,5R)-2,5-diphenylpyrrolidine (3.71)

To a solution of (2R,5R)-1-allyl-2,5-diphenylpyrrolidine (910 mg, 3.45 mmol) in a solvent mixture of degassed acetonitrile and water (84:16, 5 mL) at RT was added Tris(triphenylphosphine)rhodium (I) chloride (160 mg, 0.17 mmol). The mixture was refluxed at 100 °C for 5 hr and upon completion the reaction was concentrated (to ca. 1/2 volume). The resulting residue was diluted with Et_2O and water. The layers were separated and the aqueous layer was extracted with Et_2O . The combined organic extracts were dried (MgSO_4), filtered, and concentrated. The crude oil was purified by flash chromatography (10% $\text{Et}_2\text{O}/\text{Hex}$) to afford XX g (71%) as a white solid. ^1H NMR (400 MHz, CDCl_3) δ (ppm): 7.35 (d, $J=7.2$ Hz, 4H), 7.27 (t, $J=7.5$ Hz, 4H), 7.16 (m, 2H), 4.48 (t, $J=6.8$ Hz, 2H), 2.33 (m, 2H), 1.83 (m, 2H).

CHAPTER IV

DEVELOPMENT OF SMALL MOLECULE INHIBITORS OF THE MENIN- MIXED-LINEAGE LEUKEMIA INTERACTION

4.1. Introduction

4.1.1. Protein-protein Interactions as Therapeutic Targets

Protein-protein interactions (PPIs) represent a vast class of therapeutic targets located both inside and outside the cell. PPIs play a critical role in nearly all biological processes and are dysregulated in a broad spectrum of human diseases, including cancer,¹ and small molecule modulators of PPIs are highly desired to serve as chemical tools and potential therapeutics. Despite the importance of PPIs in biology, identification of small molecule inhibitors of PPIs is considered challenging for several reasons, including large interaction areas, lack of well-defined binding pockets, and flexibility of residues on PPI interfaces.^{2,3} Discovery of cell-permeable small molecule inhibitors of PPIs provides an additional challenge due to increased molecular weight of PPI inhibitors often required to achieve high potency.⁴ This has significantly limited successful development of PPI modulators, which, twenty years ago, led to the idea that PPIs were “intractable” therapeutic targets. However, over the past 15 years, the emergence of powerful techniques such as fragment-based lead discovery (FBLD) and structure-based drug design have provided recent successes with a number of PPI inhibitors^{3,5-8}. This has

demonstrated that some PPIs are amenable to inhibition by small molecules. More importantly, advancing small molecule inhibitors of PPIs into clinical trials, such as the Bcl-2 protein family inhibitor ABT-263 (Navitoclax)⁹ and the MDM2 inhibitor RG7112¹⁰, provides an important proof-of-principle that small molecule inhibitors of PPIs may serve as novel therapeutic agents and justifies the efforts in developing novel PPIs inhibitors.

4.1.2. Menin-MLL interaction

The protein-protein interaction between menin and Mixed Lineage Leukemia (MLL) plays a critical role in acute leukemias with translocations of the *MLL* gene.¹¹ Fusion of *MLL* with one out of over 60 partner genes results in expression of chimeric MLL fusion proteins, which enhances proliferation of hematopoietic cells and blocks hematopoietic differentiation, ultimately leading to acute leukemias.¹² The MLL leukemias represent a heterogeneous group of acute myeloid leukemias (AML) and acute lymphoblastic leukemias (ALL), accounting for about 5-10% of acute leukemias in adults¹³ and ~70% of acute leukemias in infants.¹⁴ Patients with leukemias harboring MLL translocations have a very poor prognosis with existing therapies (20% event-free survival at 3 years), and novel targeted therapies are urgently needed to treat these leukemias.^{12,15}

The MLL fusion proteins preserve the N-terminal MLL fragment of approximately 1400 amino acids fused with the fusion partner.¹⁵⁻¹⁸ Importantly, the N-terminal fragment of MLL, retained in all MLL fusion proteins, is involved in the interactions with the scaffold protein menin, which is a highly specific binding partner.^{11,19,20} This interaction plays a critical role in the MLL-fusion protein-mediated leukemogenic

transformations.^{11,21} MLL fusion proteins are required for regulation of target gene expression, including *HOXA9* and *MEIS1* genes, both of which are essential for leukemogenic activity of MLL fusions.¹¹ Therefore, menin represents a critical oncogenic cofactor of MLL fusion proteins in acute leukemias, and disruption of the protein-protein interaction between menin and MLL with small molecules represents a possible therapeutic strategy to develop new targeted drugs for mixed-lineage leukemia patients.

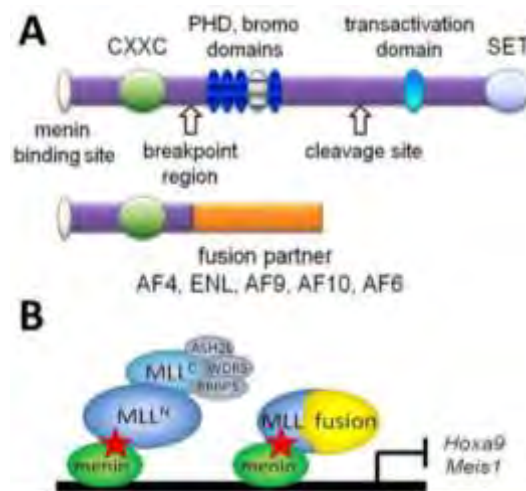


Figure 4.1. **A.** Schematic of MLL wild type (top) and MLL fusion proteins (bottom). **B.** Role of menin in recruitment of MLL wild type and MLL fusion to the *Hoxa9* promoter. Inhibition of the menin-MLL interaction by small molecules (red stars) should down-regulate expression of *Hoxa9* and *Meis1*.

Menin interacts with two MLL fragments located within the N-terminal region, with MBM1 (menin-binding motif 1 corresponding to MLL₄₋₁₅) representing the high affinity menin binding motif.¹⁹ The group of Jolanta Grembecka at the University of Michigan previously reported a high resolution crystal structure of the menin-MBM1 complex, which demonstrated that MLL binds to a large central cavity on menin.^{22,23}

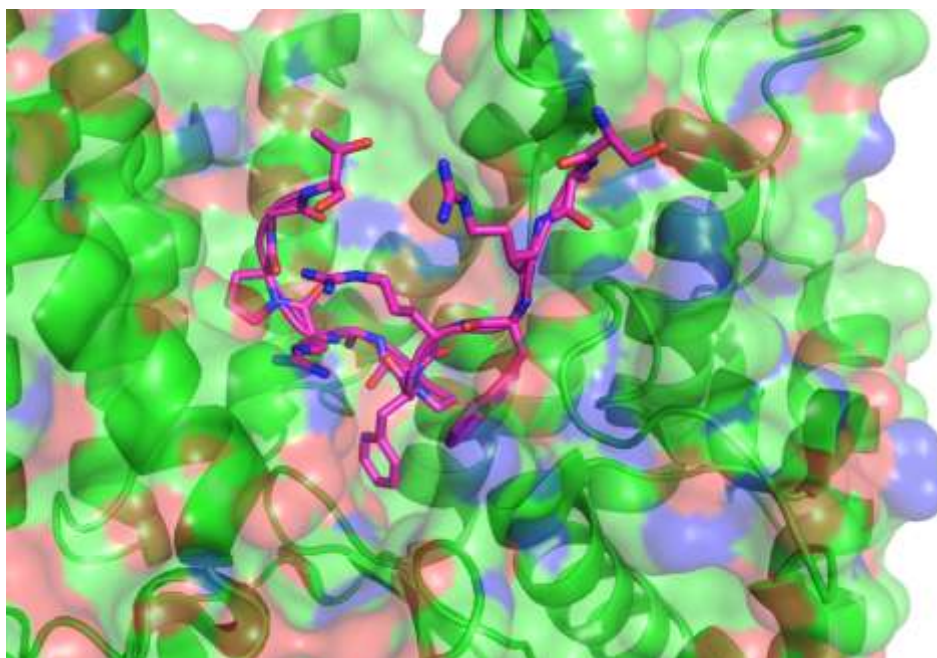


Figure 4.2. X-ray co-crystal structure of MLL peptide (magenta) in complex with menin (PDB 4GQ6)

4.1.3. Classes of Menin-MLL Inhibitors

To date, several inhibitors of the menin-MLL interaction have been developed. These include peptidomimetics such as MCP-1 and multiple classes of small molecule inhibitors including the thienopyrimidines and hydroxymethylpiperidines (**Figure 4.3**). However, no systemically available menin-MLL inhibitor tool compounds have been described. Historically, PPI inhibitors have higher molecular weights and increased lipophilicity compared to typical orally available drugs.²² Two commonly employed metrics to compare or assess the drug-like properties of compounds include ligand efficiency ($LE = \Delta G/HA$), and lipophilic ligand efficiency ($LLE = pIC_{50} - \log P$). The LE of published PPI compounds (0.24) have been lower than desired for systemically

available drugs (>0.3), and the LLE is typically below the desired value of >5.²² Although these metrics are not definitively predictive of systemic availability, the limitations highlight the unique challenges presented in the development of PPI inhibitors.

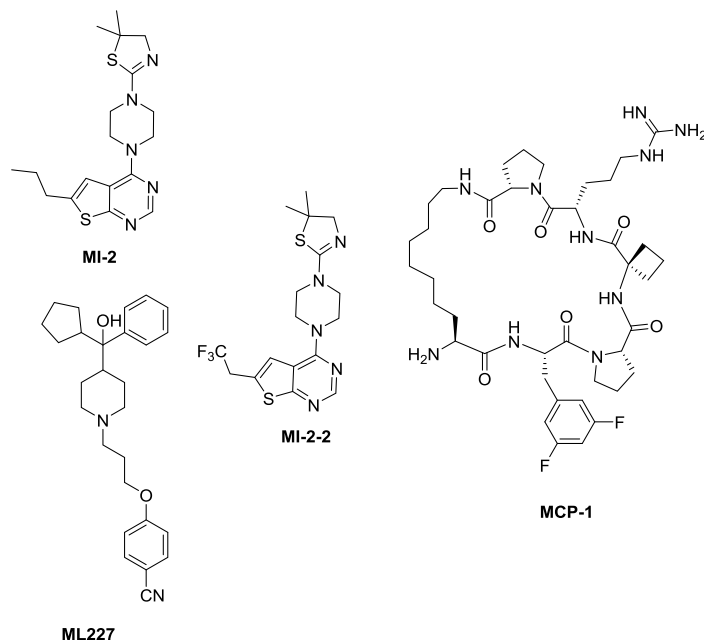


Figure 4.3. Recently developed small molecule menin-MLL PPIs

The lack of systemically available compounds, together with the pressing need to develop menin-MLL inhibitors suitable for *in vivo* studies in animal models of MLL leukemia, emphasizes a clear demand for identification of novel menin-MLL inhibitors with distinct chemical scaffolds suitable for optimization of potency and physicochemical properties. The development of potent small molecule inhibitors of the menin-MLL interaction with reduced off-target ancillary pharmacology and improved metabolic stability could allow for systemic administration to animals. This would greatly help

facilitate studies into the biological consequences of inhibiting the menin-MLL interaction and its impact on leukemia development.

4.2. Identification of Novel Inhibitors of the Menin-MLL PPI

4.2.1. High Throughput Screen to Identify Novel Menin-MLL Inhibitors

To identify new inhibitors of the menin-MLL interaction, we performed a high throughput screen of ~288,000 small molecules at the NIH MLPCN (Molecular Libraries Probe Centers Network, <https://mli.nih.gov/mli>) using a fluorescence polarization (FP) assay with a fluorescein-labeled MLL-derived peptide, MBM1.¹⁹ A stepwise procedure, including FP assay for primary screening, followed by HTRF (Homogenous Time Resolved Fluorescence) assay for secondary screening and NMR STD (Saturation Transfer Difference) experiments to validate direct binding of compounds to menin, was applied to identify menin-MLL inhibitors. The most potent compound identified in the screen was **4.1**, belonging to the hydroxymethylpiperidine class, which exhibited a half maximal inhibitory concentration (IC₅₀) value of 12.8 μM for inhibition of the menin-MLL interaction (**Figure 4.4a**). We validated direct binding of **4.1** to menin using STD NMR experiments, resulting in a strong STD effect (**Figure 4.4b**). Importantly, addition of the MLL peptide strongly decreased the STD effect observed for **4.1**, demonstrating that **4.1** and MLL compete for binding to menin. These results confirm reversible and specific binding of **4.1** hydroxymethylpiperidine compound to menin.

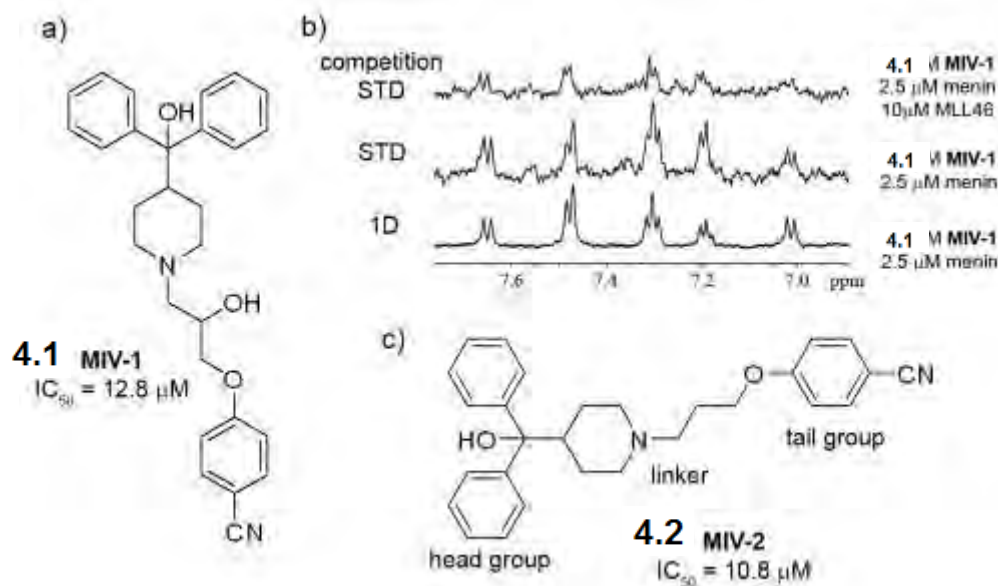
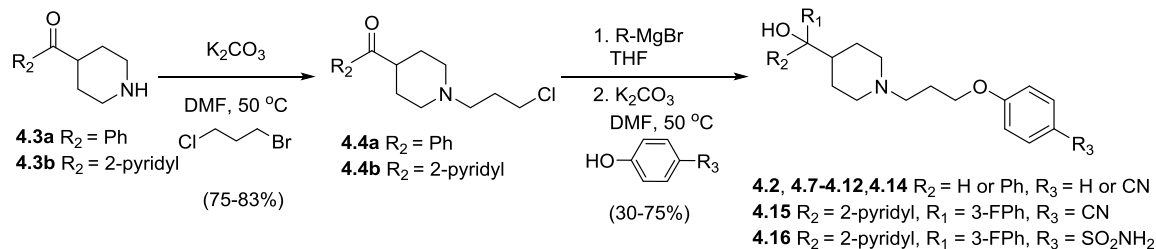


Figure 4.4. (a) Structure and activity of the most potent hit from HTS, **4.1**. (b) NMR STD experiments demonstrating binding of **4.1** to menin and competition with MLL (competition STD). (c) Structure and activity for **4.2**

4.2.2. Determination of the Minimal Pharmacophore

After identifying **4.1** as a novel menin-MLL inhibitor, we performed synthetic efforts to identify a minimal pharmacophore within **4.1** required for efficient inhibition of the menin-MLL interaction. The HTS hit **4.1**, **4.5**, and **4.6**, were readily prepared starting from either diphenyl(piperidin-4-yl)methanol or 4-benzhydrylpiperidine using a one-pot two-step procedure.²⁴ Our initial strategy, involving pre-installation of the nitrile tail group prior to Grignard addition led to final products contaminated with trace amounts of an inseparable side-product presumed to result from Grignard addition to the nitrile ($R_3 = CN$). To circumvent this issue, we performed a selective alkylation of piperidines **4.3a-b** using 1-bromo-3-chloropropane to afford chloride intermediates **4.4a-b** in good yield (Scheme 4.1).



Scheme 4.1. General synthesis of hydroxymethyl piperidine compounds.

Addition of Grignard reagents to **4.4a-b** provided the crude carbinol chlorides in high conversion. Subsequent alkylation using the appropriate phenol reagent led to final target compounds. We found that removal of the hydroxyl group from **4.1** in the linker region, resulting in compound **4.2**, slightly increased the activity (IC₅₀ = 10.8 μM). Thus, to facilitate synthesis and reduce the number of resulting stereoisomers, we eliminated the central hydroxyl group from subsequent analogs. In contrast, removal of the hydroxyl group from the quaternary carbon in the head group region resulted in **4.5** with decreased inhibitory activity by more than 20-fold, emphasizing the importance of this group in binding to menin (Table 4.1). Similarly, the binding affinity was markedly decreased by removing the nitrile within the tail group region, which resulted in **4.6** with an IC₅₀ > 250 μM. Based on this data, we concluded that **4.2** represents the minimal pharmacophore for the hydroxymethylpiperidine class of menin-MLL inhibitors.

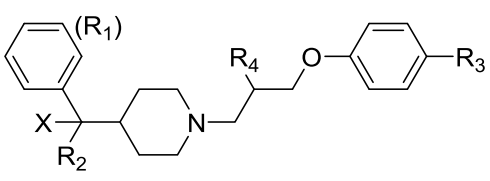
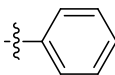
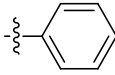
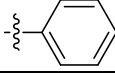
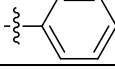
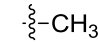
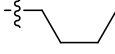
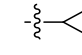
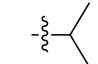
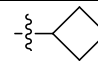
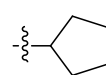
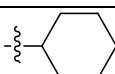
					
Compound	R ₂	-X	R ₃	R ₄	IC ₅₀ (μM)
4.1		-OH	-CN		12.8 ± 1.6
4.2		-OH	-CN		10.8 ± 0.2
4.5		-H	-CN	-H	205 ± 63
4.6		-OH	-H	-H	>250
4.7	-H	-OH	-CN	-H	234 ± 22
4.8		-OH	-CN	-H	295 ± 50
4.9		-OH	-CN	-H	15.3 ± 3.8
4.10		-OH	-CN	-H	11.2 ± 3.9
4.11		-OH	-CN	-H	4.1 ± 0.6
4.12		-OH	-CN	-H	4.0 ± 1.4
4.13 (MIV-3)		-OH	-CN	-H	0.39 ± 0.04
4.14		-OH	-CN	-H	1.7 ± 0.6

Table 4.1. Activity of hydroxymethyl piperidine menin-MLL inhibitors

4.3. Lead Optimization of the Hydroxymethyl Piperidine Class

4.3.1. Probing the Hydrophobic Head Group Region

Compound **4.2** was used as a lead for medicinal chemistry optimization to improve potency of hydroxymethylpiperidine class. First, we explored replacement of one of the phenyl rings at the head group region of **4.2** with different hydrophobic groups (**Table 4.1**). Interestingly, we found a pronounced structure-activity relationship (SAR) for modifications at this site. The inhibitory activity of **4.7**, with a hydrogen replacing the phenyl group, was weak ($IC_{50} = 234 \mu\text{M}$), and the potency did not improve upon addition of a methyl group at this position (**4.8**). Introducing more bulky hydrophobic substituents resulted in increased inhibition of the menin-MLL interaction. For example, *n*-butyl (**4.9**) or cyclopropyl (**4.11**) substituents yielded about a 20-fold increase in activity versus **4.8** (**Table 4.1**). Furthermore, analogues with *iso*-propyl (**4.11**) and cyclobutyl (**4.12**) groups had further improved IC_{50} values ($IC_{50} = 4.1 \mu\text{M}$ and $4.0 \mu\text{M}$, respectively). Finally, cyclopentyl was identified as the most optimal saturated carbocycle at this position, resulting in compound **4.13 (MIV-3)**,²⁴ with an IC_{50} of 390 nM measured for the racemic mixture. Further increase in ring size decreased activity, as cyclohexyl analogue **4.14** was about four-fold less active than **MIV-3**. Based on this data, we concluded that cyclopentyl was the preferred hydrophobic group at the R2 position. **MIV-3** was declared as a first generation MLPCN probe for the menin-MLL interaction, and was given the designation **ML227**. In light of the promising *in vitro* activity of **MIV-3**, it was characterized for tier 1 drug metabolism and pharmacokinetic (DMPK) properties, and screened in a Eurofins radioligand binding panel of over 60 G protein-coupled receptors, ion channels, and transporters at a concentration of $10 \mu\text{M}$. These studies revealed that

MIV-3 possessed several limitations, precluding its use in animal models of mixed-lineage leukemia. These included a high predicted hepatic clearance at near the rate of hepatic blood flow, and a low fraction unbound value from plasma proteins of approximately 1% (PPB $f_u = 0.004, 0.013$). Additionally, **MIV-3** was a low micromolar inhibitor of multiple CYP450 isoforms, as well as possessed significant off-target activity, most notably, binding to the human ether-a-go-go (hERG) potassium channel.

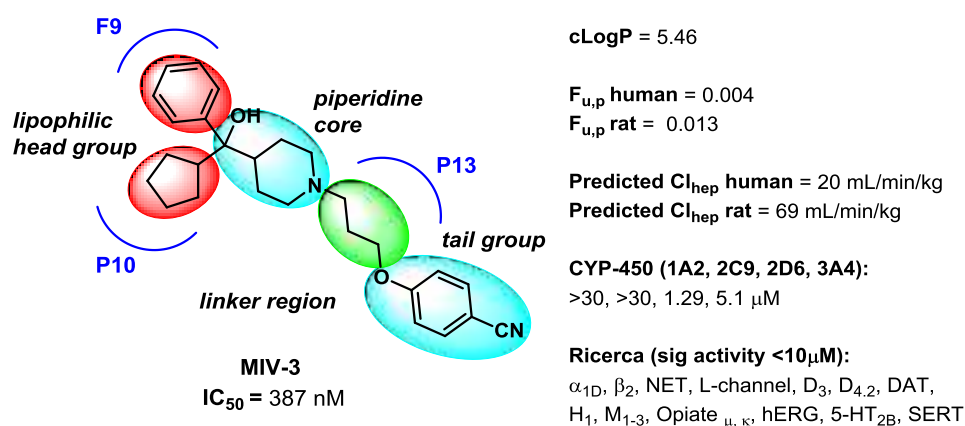


Figure 4.5. Physical and DMPK properties of **MIV-3**.

MIV-3 represents a racemic mixture, and to assess the activity of individual enantiomers, the racemic mixture was separated by chiral SFC. Interestingly, the R enantiomer, **MIV-3R**, was only about 2-fold more potent than the S enantiomer (**MIV-3S**) as assessed by the FP assay ($IC_{50} = 270 \text{ nM}$ and 529 nM for **MIV-3R** and **S**, respectively). The dissociation constants (K_d) for binding of both enantiomers of **MIV-3** to menin using Isothermal Titration Calorimetry (ITC) were determined, and it was found that they both bind to menin with nanomolar affinities ($K_d = 285 \text{ nM}$ and 952 nM for R and S isomers, respectively), consistent with the IC_{50} values (**Figure 4.6**). Overall,

development of **MIV-3R** represents a more than 40-fold improvement in activity compared to the parent compound **4.1**. Interestingly, there was a relatively small difference observed in inhibition of the menin-MLL interaction by both enantiomers of **MIV-3**.

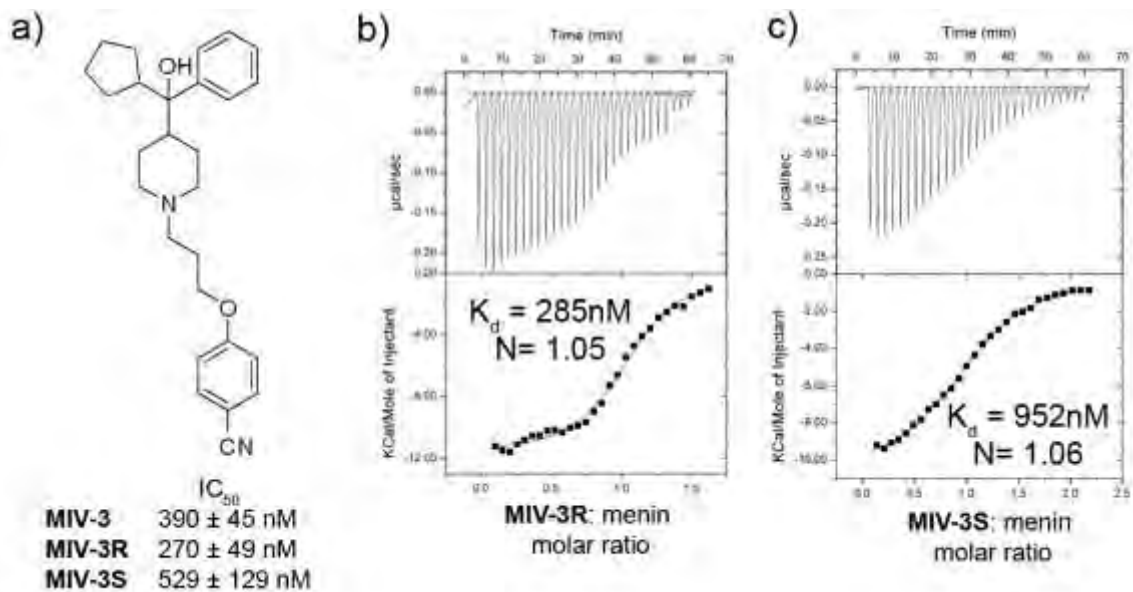


Figure 4.6. (a) Structure and activity for **MIV-3** and two individual enantiomers (b, c) ITC experiments demonstrating direct and specific binding of both enantiomers of **MIV-3** to menin. N corresponds to the stoichiometry of ligand binding to menin

4.3.2. Structural Investigation of **MIV-3** -menin Interaction

In order to establish the molecular basis for the binding of **MIV-3** to menin and understand the similar binding affinity between the two enantiomers, the crystal structures of menin in complex with both enantiomers of **MIV-3** were determined (Figure 4.7).

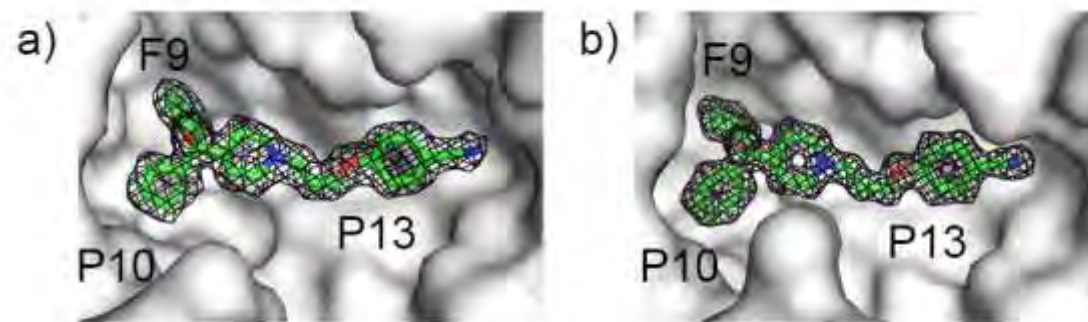


Figure 4.7. Crystal structures of menin in complex with **MIV-3R** (a) and **MIV-3S** (b) with 2Fo-Fc electron density maps for ligands contoured at the 1σ level. Menin is shown in surface representation and location of F9, P10 and P13 pockets is labeled.

It was discovered that both enantiomers bind in similar conformations to the MLL binding site on menin, and occupy three hydrophobic pockets: F9, P10 and P13 (**Figure 4.8**). There is close overlap of the binding modes of both enantiomers of **MIV-3**, with the only difference being an alternate positioning of the head group substituents between the F9 and P10 hydrophobic pockets on menin.

The menin-**MIV-3** interactions are predominately mediated by the hydrophobic contacts, with only one direct hydrogen bond formed between the nitrile group of both enantiomers of **MIV-3** and the indole nitrogen of Trp341 on menin (**Figure 4.8**). An additional water-mediated hydrogen bond involves a hydroxyl at the head group region of **MIV-3** and the Asp180 side chain on menin.

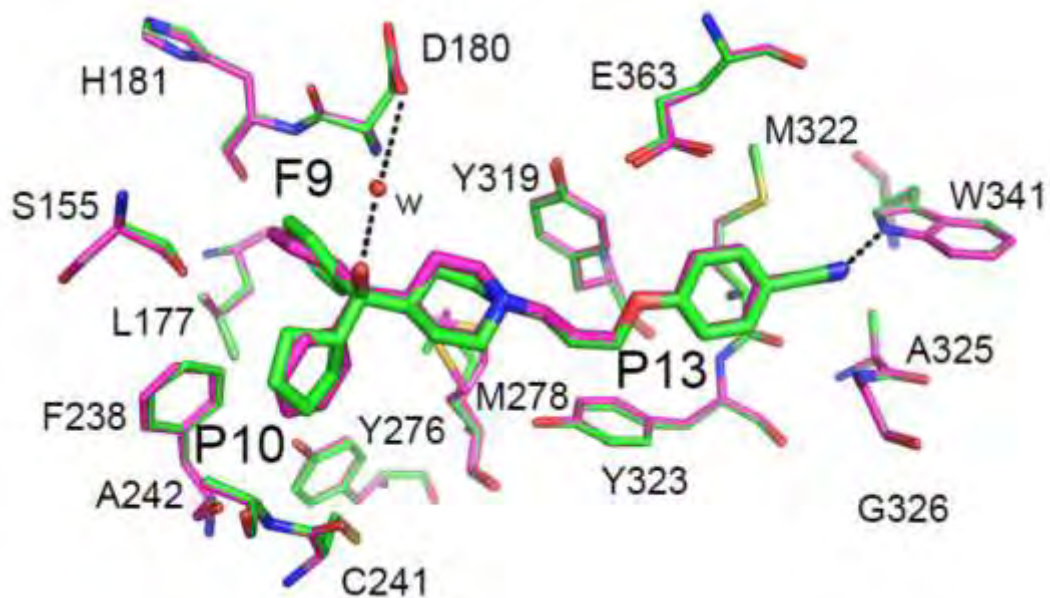


Figure 4.8. Superposition of the menin-**MIV-3R** and menin-**MIV-3S** crystal structures showing binding mode of ligands and key protein residues in the binding site.

The importance of the hydrogen bonds involving the head group hydroxyl and tail group nitrile is reflected by a more than 20-fold decrease in the activity of the analogues deficient in the corresponding functional groups, such as compounds **4.5** and **4.6** (Table **4.1**). Of note, binding of **MIV-3** to menin does not induce conformational changes of the protein.

In the co-crystal structure with the more potent enantiomer, **MIV-3R**, the phenyl ring occupies the F9 pocket on menin formed by the side chains of hydrophobic residues Leu177, Phe238, Ser155, Met278 and backbone of Asp180 and His181 (Figure 4.8). The cyclopentyl ring occupies to the P10 pocket and interacts with the side chains of Ala242, Cys241, Tyr276, Phe238 and Ser155. In case of the **MIV-3S** enantiomer, the positions of the cyclopentyl and phenyl rings are swapped between these two pockets on menin. The piperidine ring and tail groups in both enantiomers of **MIV-3** bind to menin in the same

manner, extending towards the P13 pocket and Trp341. The alkoxy portion of the linker fits into the P13 pocket formed by Tyr319 and Tyr323, while the benzonitrile moiety extends beyond the P13 pocket, where it approaches Met322 and Glu363 side chains to form a hydrogen bond with the side chain of Trp341. The interaction of the benzonitrile moiety is of particular interest as this region of the binding site is not occupied by the MLL peptide or the previously identified thienopyrimidine class of menin-MLL inhibitors (**Figure 4.9**).

The novel interaction identified for the new hydroxymethylpiperidine class offered the possibility to introduce additional contacts with menin to further improve affinity through rationally designed modifications, and this structural information explains the SAR data for this class of menin-MLL inhibitors (**Table 4.1**).

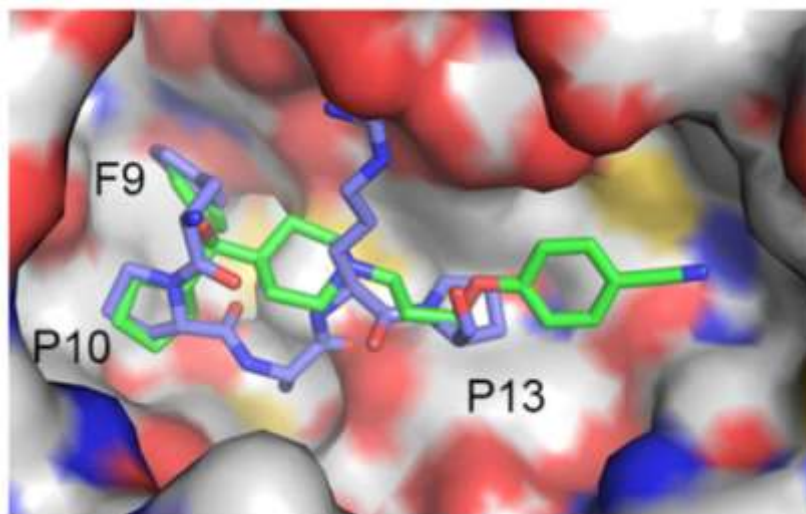


Figure 4.9. Superposition of the crystal structures of menin-**MIV-3R** (green carbons) and the menin-**MLL** (blue carbons, PDB code 4GQ6) complexes.

In our previous studies, we found that three hydrophobic residues in the MLL-derived peptide MBM1, namely Phe9, Pro10 and Pro13, have the most critical contributions for binding to menin and their mutation to alanine residues reduce binding affinity by 30-

1000 fold.^{19,22} Superposition of the MLL MBM1 peptide and both enantiomers of **MIV-3** bound to menin demonstrates a close overlap of these small molecule inhibitors with the critical residues of MLL required for potent binding to menin (**Figure 4.9**). Specifically, the phenyl ring in the head group of the more potent enantiomer, **MIV-3R**, overlaps with the phenyl side chain of Phe9 in MLL, while the cyclopentyl ring in **MIV-3R** adopts a similar position and conformation as the Pro10 side chain in MLL. This closely mimics the critical MLL interactions with menin. Furthermore, the alkoxy portion of the linker in **MIV-3R** mimics the interactions of MLL Pro13 with menin, while the benzonitrile moiety extends beyond the P13 pocket towards a previously unexplored region of the binding site. Overall, the potent activity of **MIV-3R** results from mimicking key interactions of MLL with menin in F9, P10 and P13 pockets, as well as additional contacts beyond the P13 pocket, which provides further opportunity for optimization of these compounds.

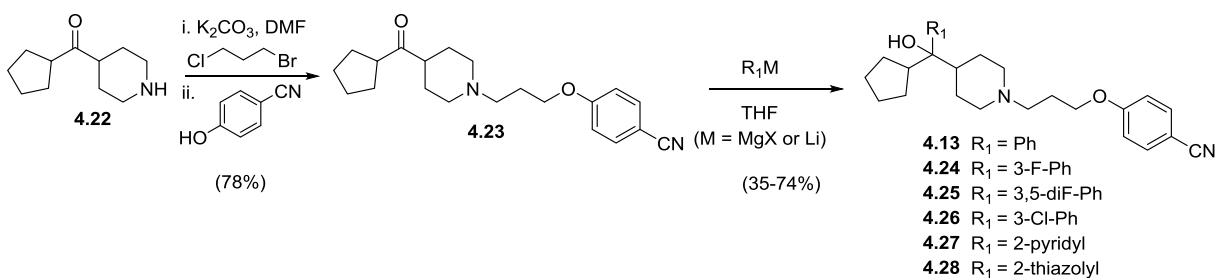
4.4. Structure-based design of nanomolar inhibitors of the menin-MLL interaction

4.4.1. Optimization of Hydrophobic Head Group

The crystal structure of menin in complex with both enantiomers of **MIV-3** was used for rational design of new analogues to further improve potency and physicochemical properties of this class of compounds. Four regions in **MIV-3** were explored for modifications to rationally design new compounds based upon structural data, as described in **Figure 4.5**.

Synthesis of cyclopentyl hydroxymethyl piperidines, **MIV-3** and **4.17-4.21**, is outlined in **Scheme 4.2**. In order to circumvent low yields due to competing reduction of

the sterically hindered ketones by alkyl Grignard reagents²⁵ we employed a strategy involving introduction of the saturated cycloalkyl followed by a second aryl or alkyl group. Thus, initial introduction of the cycloalkyl was accomplished using a known two-step procedure starting from *N*-benzylpiperidine-4-carbonitrile to give a key starting aminoketone **4.23**.²⁶



Scheme 4.2. Synthesis of cyclopentyl-containing hydroxymethyl piperidine compounds.

Subsequent one-pot double alkylation using **4.22** and 1-bromo-3-chloropropane afforded piperidine **4.23** in 78% yield. Grignard or stabilized aryl lithium additions afforded final target compounds **4.13**, **4.24-4.27** in moderate to good yield. Over-addition of these aryl Grignard and lithium reagents to the nitrile was not evident for substrate **4.23** and all final compounds displayed excellent purity (>98 %).

First, we explored additional optimization of R1 substituents that bind to the F9 pocket on menin (**Figure 4.10a**). As demonstrated above, the phenyl ring in **MIV-3R** closely mimics the interactions of MLL Phe9 with menin, and therefore it was used to design further modifications. In the crystal structure of menin in complex with the **MI-2-2** thienopyrimidine inhibitor we found a favorable C-F---C=O dipolar interaction between a fluorine atom in **MI-2-2** and the backbone of His181.²² Based on the menin-**MIV-3R**

co-crystal structure, we anticipated that introducing a fluorine into position 3 of the phenyl ring should result in similar contacts and improved activity.

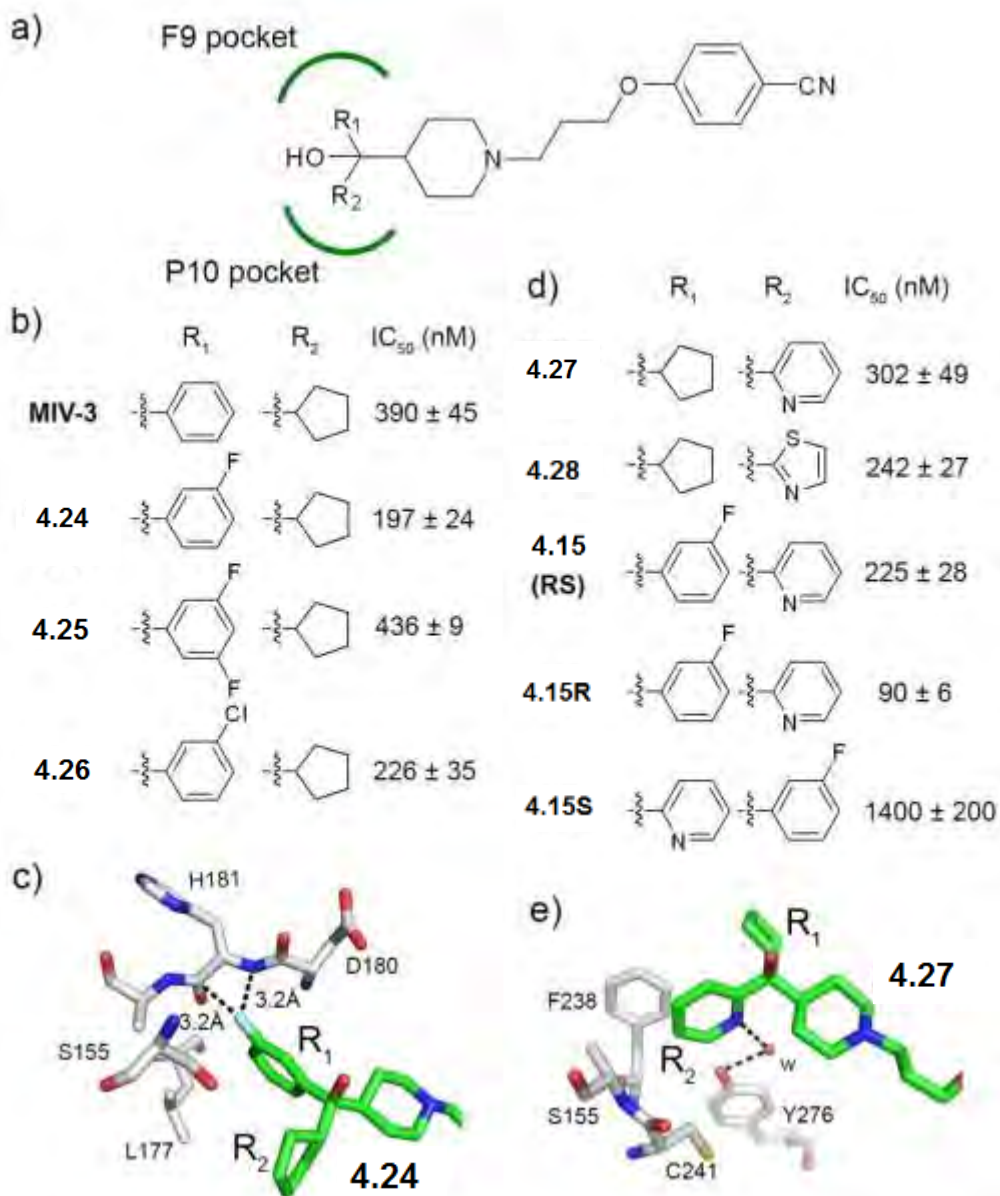


Figure 4.10. (a) General structure of the hydroxymethylpiperidine class. (b) Inhibitory activities of MIV-3 analogues. (c) Crystal structure of menin in complex with **4.24**. (d) Structures and activities for analogues with modifications introduced simultaneously at R₁ and R₂. (e) Crystal structure of menin in complex with **4.27**.

Introduction of a 3-fluoro to give compound **4.24** resulted in a 2-fold improvement in potency versus **MIV-3** (**Figure 4.10b**). The binding mode of **4.24** to menin was confirmed by solving the crystal structure of the complex (**Figure 4.10c**) which confirmed the presence of a dipolar interaction between the fluorine atom in **4.24** and the backbone amide of His181 on menin. Introducing a chloro substituent at the same position (**4.26**) or incorporation of an additional fluorine to the phenyl ring (**4.25**) resulted in a weaker inhibitory activity (**Figure 4.10b**). As a result of the structure guided-design, we found that the 3-fluoro substituted phenyl represents the preferred substituent identified to interact with the F9 pocket on menin.

We next performed optimization of the R2 substituent that interacts with the P10 pocket. In the complex of menin with **MIV-3R**, this pocket is occupied by the cyclopentyl ring, which is not optimal for further derivitization and contributes significantly to the lipophilic character and oxidative metabolism of the molecule. The analysis of the apo structure of menin and the complex with **MIV-3** revealed the presence of a water molecule, which forms a hydrogen bond with Tyr 276, located in proximity to the ortho position of the phenyl ring in **MIV-3**. Therefore, we introduced a nitrogen atom via replacement of phenyl with a pyridine or thiazole ring to engage in favorable interactions with this structural water molecule.

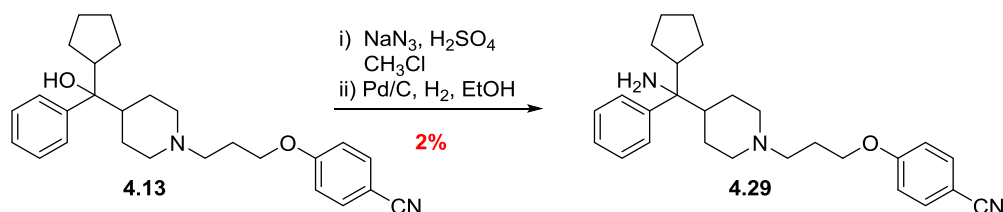
These efforts resulted in **4.27** and **4.28**, both of which showed improved potency and increased polarity versus **MIV-3**. The existence of a water-mediated hydrogen bond between **4.27** and Tyr276 was confirmed by solving the crystal structure of the complex (**Figure 4.10**). Testing separated enantiomers of **4.27**, showed a ~4-fold greater inhibitory activity for the S enantiomer ($IC_{50} = 195$ nM). The optimal substituents identified to

interact with F9 and P10 pockets were then combined, and we synthesized the hybrid 3-fluorophenyl-2-pyridyl congener **4.15**, with ~3-fold improved IC_{50} value ($IC_{50} = 90$ nM for **R** enantiomer of **4.15**) (Figure 4.10d). Importantly, introduction of a heterocyclic instead of phenyl ring to occupy the P10 pocket substantially increased polarity, decreasing the cLogP by a full order of magnitude.

4.4.2. Optimization of Tertiary Carbinol

The crystal structure of **MIV-3** enantiomers with menin revealed that the solvent exposed hydroxyl group in the head group region is involved in a water-mediated hydrogen bond with Asp180 (Figure 4.11b). Based on structural data, it was anticipated that introducing a positively charged group, such as an amino moiety, would result in additional favorable electrostatic interactions with adjacent Asp180 and other acidic residues located in this region of the binding site (e.g. Asp153, Glu 359).

Preparation of tertiary carbinamine compound **4.29** was accomplished via solvolysis of carbinol **4.13** in the presence of sodium azide in chloroform and sulfuric acid (Scheme 4.3).



Scheme 4.3. Synthesis of aminomethyl piperidine **4.29**.

The crude azide was reduced using palladium on carbon with atmospheric hydrogen in EtOH to afford amine **4.29**. Despite efforts to screen for alternative conditions to improve solvolysis and formation of the azide intermediate, facile formation of a major elimination side product leading to the olefin elimination byproduct remained problematic. Resolution of racemic **4.29** was accomplished using chiral SFC to afford single enantiomers **4.29S** and **4.29R** for which the stereochemical configuration was subsequently inferred on the basis of the absolute configuration observed in the electron density map of the X-ray structure of the respective menin complex with **4.29**.

Compound **4.29** showed an almost 6-fold increase in inhibition of the menin-MLL interaction ($IC_{50} = 67\text{nM}$ for racemic mixture) versus **MIV-3** (**Figure 4.11**). The binding mode of **4.29** was not affected by incorporating the amino group, as validated by the crystal structure of menin in complex with **4.29R** enantiomer.

4.29R represents the most potent inhibitor of the menin-MLL interaction reported for this class ($IC_{50} = 56\text{ nM}$), which binds to menin with a $K_d = 85\text{ nM}$. These results demonstrate the importance of considering long range electrostatic interactions in designing protein ligands to achieve efficient binding.

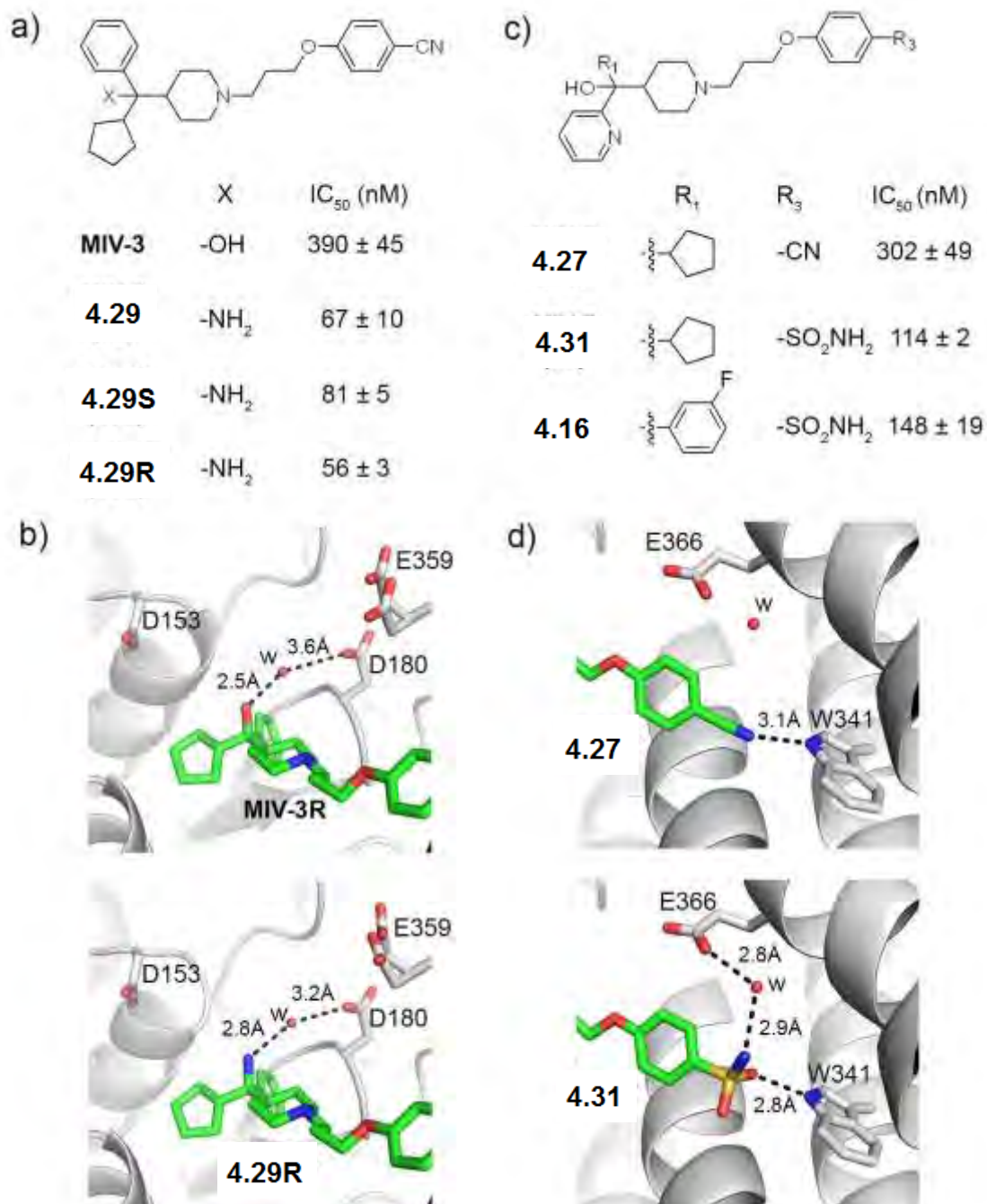
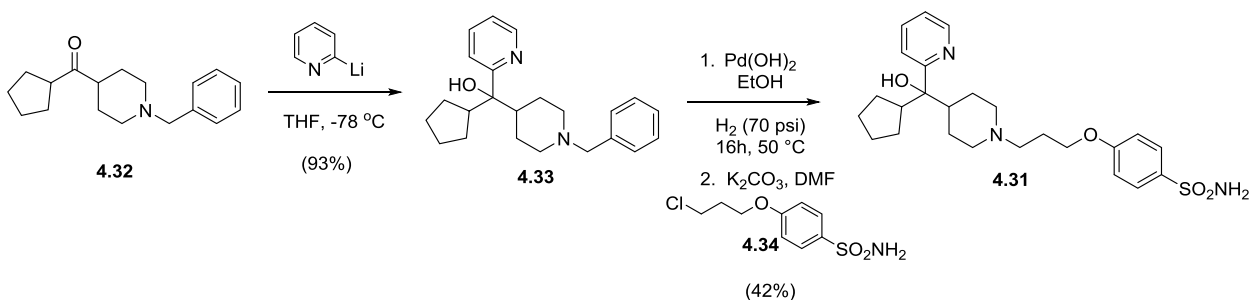


Figure 4.11. (a) Structures and activities of analogues with substitution at the head group region. (b) Comparison of the crystal structures of menin in complex with **4.29R** (bottom) and **MIV-3R** (top) (c) Structures and activities of analogues with substitution of nitrile at the tail group region. (d) Comparison of the crystal structures of menin in complex with **4.31** (bottom) and **4.27** (top).

4.4.3. Optimization of the Tail Group

The crystal structure of menin with **4.27** was utilized to guide replacement of the nitrile, with the goal of further improving polarity while retaining the hydrogen bond with Trp341 (**Figure 4.11d**). Based on the menin-**4.27** structure, we screened several polar substituents at the 4-position of the aryl tail group. Compounds such as the sulfonamide analogue **4.31** were prepared according to **Scheme 4.4**.

Preparation of **4.31** began with 2-pyridyl lithium addition to the benzyl protected ketone **4.32** to provide **4.33** in excellent yield (**Scheme 4.4**). Hydrogenolysis of the *N*-benzyl of **4.33** using Pearlman's catalyst overnight in ethanol with heating, followed by alkylation of the crude deprotected piperidine using chloride **4.34**, afforded target sulfonamide **4.31**.



Scheme 4.4. Synthesis of sulfonamide containing hydroxymethyl piperidine **4.31**.

The sulfonamide analogue **4.31** showed ~3-fold improved inhibitory activity (IC₅₀ = 114nM) versus the corresponding nitrile analogue **4.29**, while **4.16** demonstrated a modest ~1.5-fold improvement in IC₅₀ versus the corresponding nitrile derivative **4.15** (**Figure 4.11d**). The binding mode of **4.31** to menin was validated by crystallographic studies, confirming the existence of the hydrogen bonds with the side chain of Trp341

and also the presence of an additional water-mediated hydrogen bond with Glu366, resulting in increased potency. This suggests that the sulfonamide is a viable replacement for the nitrile in this class of menin-MLL inhibitors, which allows for significant increase in polarity relative to the nitrile analogues.

4.5. Biological Characterization of Menin-MLL Inhibitors

4.5.1. Disruption of Fusion Protein Interaction in Cells and Expression of Downstream Targets

To assess the mechanism of action of this new class of menin-MLL inhibitors, they were evaluated for their effect on blocking the activity of MLL fusion proteins in leukemia cells. For these studies the most potent inhibitor developed, **4.29**, and the corresponding hydroxyl analogue, **MIV-3R**, were selected. A co-immunoprecipitation (co-IP) experiment was performed in HEK-293 cells transfected with Flag-MLL-AF9 which showed that low micromolar concentrations of both **4.29** and **MIV-3R** effectively disrupt the menin-MLL-AF9 interaction (**Figure 4.12a**).

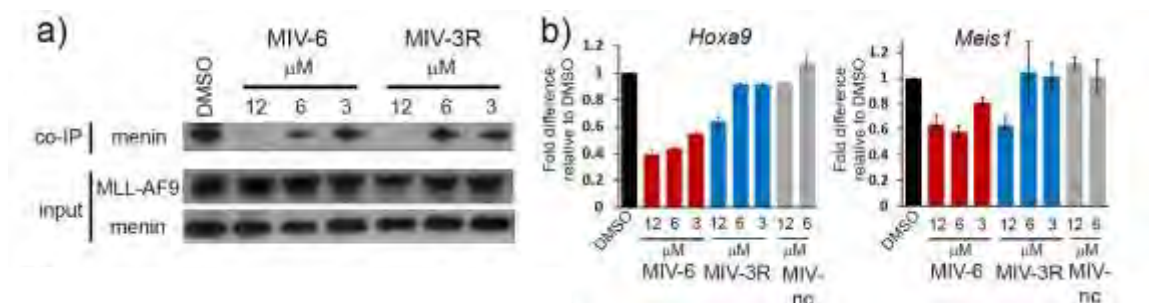


Figure 4.12. (a) Co-immunoprecipitation experiment in HEK293 cells transfected with MLL-AF9. (b) Quantitative real-time PCR performed in MLL-AF9-transformed murine bone marrow cells after 6 days of treatment with compounds.

Importantly, the expression levels of menin and MLL-AF9 were not affected upon treatment. This data demonstrates that both **4.29** and **MIV-3R** can reach the target protein and effectively disrupt the menin-MLL fusion protein interaction in human cells.

The menin-MLL fusion protein interaction is required for the maintenance of high expression level of *HOXA9* and *MEIS1* in MLL leukemia cells and for leukemic transformation by MLL fusions.¹¹ To assess whether **4.29** and **MIV-3R** affect the expression level of *HOXA9* and *MEIS1*, real time quantitative PCR (qRT-PCR) experiments were performed in MLL-AF9 transformed murine bone marrow cells (BMC). Treatment with both **4.29** and **MIV-3R** resulted in a dose-dependent reduction in the expression level of *Hoxa9* and *Meis1* as compared to the DMSO control, with a 50% decrease in *Hoxa9* levels upon treatment with 3 μ M **4.29** (**Figure 4.12b**). The effects on expression level of target genes correlates well with the *in vitro* inhibition observed for these compounds as **4.29** showed about 4-fold more pronounced effect on *Hoxa9* expression. Importantly, the negative control compound, **4.7**, which is a weak menin-MLL inhibitor (IC₅₀ = 234 μ M), did not show any effect on *Hoxa9* and *Meis1* expression. These results demonstrate that **4.29** and **MIV-3R** inhibit the menin-MLL fusion protein interaction in cells which results in a decrease in MLL-fusion protein-dependent gene expression. This suggests on-target effects for these compounds and validates their mechanism of action.

4.5.2. Proliferation and Differentiation in MLL Leukemia Cells

Disruption of the menin-MLL fusion protein interaction is expected to result in growth arrest and differentiation of MLL leukemia cells.^{11,27} Therefore, the activity of

4.29 and **MIV-3R** were tested in murine BMCs transformed with either MLL-AF9 or Hoxa9/Meis1 (HM-2), with the later serving as a negative control.

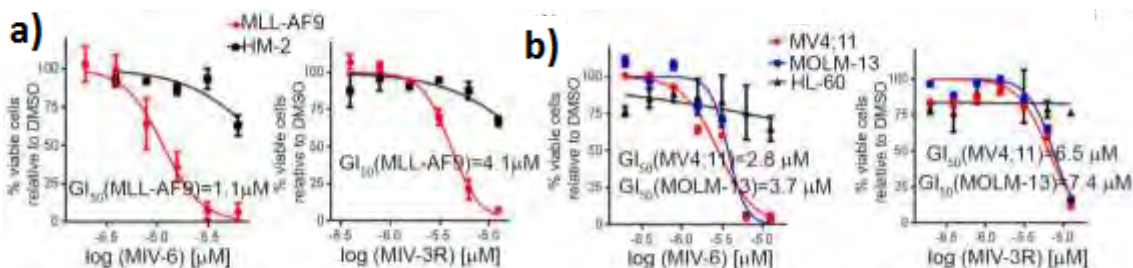


Figure 4.13. (a) Titration curves from MTT cell viability assay performed for **4.29** and **MIV-3R** after 7 days of treatment of MLL-AF9 and Hoxa9/Meis1 (HM-2) transformed murine BMCs. (b) Titration curves from MTT cell viability assay performed for **4.29** and **MIV-3R** after 7 days of treatment of human MLL leukemia cell lines (MV4;11 and MOLM-13) and control cell line HL-60 (non-MLL leukemia cell line)

A strong and dose-dependent inhibition of cell proliferation was observed for both compounds in MLL-AF9 transformed BMCs (**Figure 4.13a**), with $GI_{50} = 1.1 \mu\text{M}$ for **4.29**, which showed a 4-fold more pronounced effect than **MIV-3R** ($GI_{50} = 4.5 \mu\text{M}$), consistent with its higher *in vitro* activity. In contrast, these two compounds have a limited effect on proliferation of Hoxa9/Meis1 transformed BMCs, demonstrating selectivity towards MLL fusion-transformed cells. Similar effects were observed in human MLL leukemia cell lines. Treatment of MV4;11 and MOLM13 cells harboring MLL-AF4, MLL-AF9 fusion proteins, respectively, with **4.29** and **MIV-3R** resulted in dose-dependent inhibition of cell proliferation, with a more pronounced effect observed for **4.29** (**Figure 4.13b**). Marginal effects on cell proliferation were observed upon treatment of HL-60 promyelocytic leukemia cells, which served as a negative control cell line.

Finally, the effect of hydroxy- and aminomethylpiperidine compounds on differentiation of MLL fusion protein-dependent cells was assessed. The MLL-AF9 BMCs undergo differentiation upon treatment with **4.29** and **MIV-3R**, as assessed by flow cytometry analysis of CD11b expression, which serves as a differentiation marker of myeloid cells.

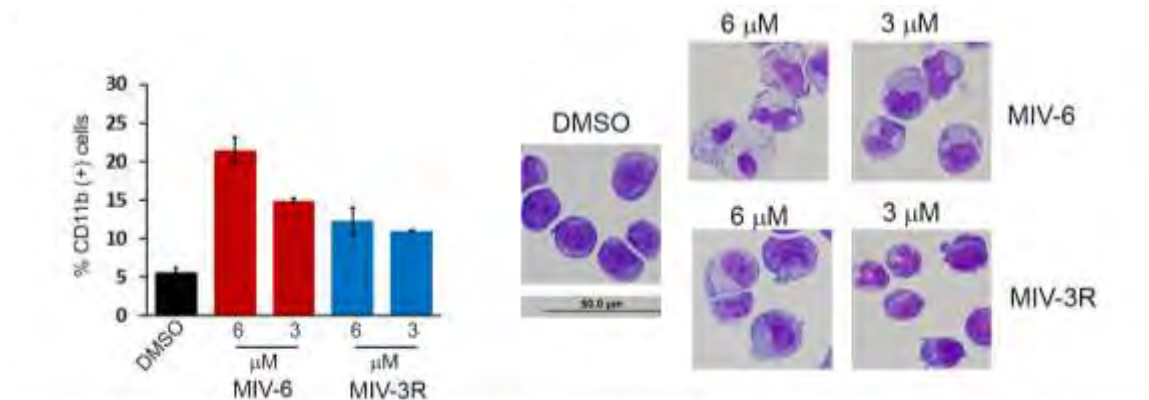


Figure 4.14. Quantification of CD11b expression in MLL-AF9 transformed murine BMCs treated for 6 days with **4.29** and **MIV-3R** as detected by flow cytometry (left). Wright-Giemsa-stained cytopins for MLL-AF9 transformed murine BMCs after 7 days of treatment (right).

Treatment with more potent **4.29** induces an increase in CD11b expression (**Figure 4.14**). In addition, Wright-Giemsa staining of MLL-AF9 BMCs treated with low micromolar concentrations of **4.29** and **MIV-3R** revealed significant changes in morphology of these cells, such as decreased nuclei to cytoplasm ratio, multi-lobed nuclei and highly vacuolated cytoplasm. This demonstrates myeloid differentiation upon treatment with both inhibitors (**Figure 4.14**). Treatment with higher concentration of **4.29** (6 μM) resulted in terminal differentiation. These provide further evidence to confirm the on-target effects and specific mechanism of action for the hydroxy- and aminomethylpiperidine inhibitors on the menin-MLL interaction.

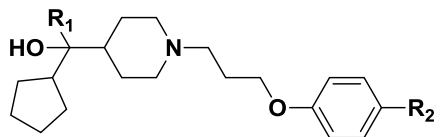
4.6. Optimization of DMPK properties for Hydroxymethyl Piperidine Series

4.6.1. Use of Efficiency Metrics to Optimize *In Vitro* DMPK

As previously discussed, first generation menin-MLL inhibitors such as **MIV-3** were useful *in vitro* tool compounds, but possessed several limitations precluding its use in animal models of mixed lineage leukemia. These included low potency, undesired ancillary activity, poor metabolic stability, and high *in vivo* clearance in rat. Efforts to address these DMPK liabilities paralleled a lead optimization campaign focused on the development of low-nanomolar tool compounds for in-depth *in vitro* studies discussed in previous sections.

Co-crystal structures of **MIV-3** in complex with menin were used to perform optimization with a systematic structure-based design approach (**Figure 4.8**). As shown in **Figure 4.5**, the lead structure **MIV-3** possessed four regions that were targeted for optimization of potency and DMPK properties: 1) a lipophilic head group containing a tertiary carbinol, 2) a basic piperidine core, 3) an acyclic propyl linker, and 4) a benzonitrile tail group.

Initial efforts were focused on strategies to reduce cLogP and utilized efficiency metrics including ligand efficiency (LE) and lipophilicity-dependent ligand efficiency (LELP) to address high metabolic clearance and low systemic exposure, an issue identified with **MIV-3**. The three pendent rings of the lipophilic head group and tail group were identified as liabilities to oxidative metabolism by CYP450 enzymes. Analogs prepared were consistent with previous efforts for the hydroxymethylpiperidine series.



Entry	R ₁	R ₂	IC ₅₀	cLogP	LE/LELP
4.13			390	5.46	0.29/17.9
MIV-3			242	3.80	0.30/11.2
4.28			302	3.90	0.29/13.8
4.31			114	2.78	0.28/9.9
4.35			1100	5.37	0.25/21.74
4.25			437	5.74	0.26/21.77
4.26			226	6.16	0.28/21.69
4.24			197	5.59	0.29/19.53
4.36			28000	4.60	0.20/22.90

Table 4.2. Potency and physical properties of cyclopentyl hydroxymethyl piperidine compounds.

We introduced heterocycles and substituted phenyl rings to the lipophilic head group (Table 4.2). Of note, compounds 4.27, 4.28, and 4.31 featured replacement of the phenyl ring with either a pyridine or thiazole. This substitution led to an increase in

potency while improving the cLogP by a full log unit. This was reflected in LELP, with compound **4.28** showing an improvement to 11.2. As demonstrated in **Table 4.2**, LELP proved to be a responsive indicator for driving improvements in both potency and lipophilicity, and was used to rank order compounds for *in vitro* DMPK studies. Subsequent efforts focused on retaining the cyclopentyl group while overall polarity was addressed at the tail group. Structural analysis of **MIV-3** in complex with menin revealed that the nitrile of the tail group engaged in a hydrogen bond interaction with Trp341, and this information was used to investigate additional polar substituents that contained a hydrogen bond acceptor.

The sulfonamide group was identified as a suitable replacement in terms of potency while decreasing the cLogP by over a full log unit. Compound **4.31** displayed favorable LELP (9.9), within the target range for an *in vivo* candidate.

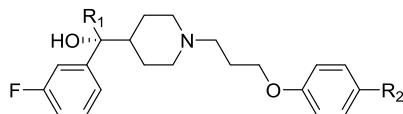
Table 4.3 describes tier 1 DMPK studies for the cyclopentyl compounds. **MIV-3** was predicted to be rapidly cleared near the rate of blood flow in both human and rat liver microsomes, with a fraction unbound from plasma proteins of approximately 1% (PPB f_u (h, r) = 0.004, 0.013). Substitution of the phenyl group with the thiazole **4.28** led to a 2-fold decrease in intrinsic clearance. Similar improvements were observed by substitution with a pyridyl group. Replacement of the nitrile of the tail group with a sulfonamide in **4.31** further attenuated intrinsic clearance relative to **MIV-3** (CL_{int} (h, r) = 16.2, 271) while displaying a significantly higher PPB f_u (h, r, 0.291, 0.342).

Entry	CL _{int} (h, r)	CL _{hep} (h, r)	PPB fu (h, r, m)	CL _p	t _{1/2} (h)	V _{ss}
4.13	124	18	0.004			
	918	65	nd 0.013			
4.28	77.4	16.5	0.117			
	558	62.2	nd 0.192			
4.31	16.2	9.13	0.291	293	0.2	4.3
	271	55.6	nd 0.342			

Table 4.3. *In vitro* DMPK and *in vivo* pharmacokinetics of cyclopentyl hydroxymethylpiperidine compounds.

4.6.2. *In vivo* Pharmacokinetics of Hydroxymethyl Piperidine Compounds

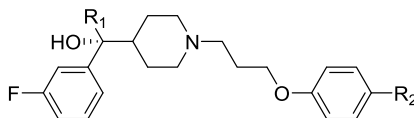
When optimized analogue **4.31** was submitted for *in vivo* pharmacokinetic studies, it was still rapidly cleared with a half life of <0.2 h (**Table 4.3**). Identification of the metabolites suggested that oxidation of the cyclopentyl ring by CYP450 enzymes was a major metabolic liability. Earlier SAR studies suggested that similar sized aryl or heterocyclic rings could serve as suitable replacements for the cyclopentyl group while improving stability to oxidative metabolism. Of the compounds tested, the 3-fluorophenyl was identified as the optimal substituent to maintain potency while ameliorating CYP450 oxidation. We synthesized hybrid compounds containing heteroaryl/aryl substituents at the lipophilic head group and tail group as shown in **Table 4.4**. These compounds lowered the ClogP of the series from above 5 to below 2.5, while improving LELP to below 10, and potency to below 100 nM, our desired endpoints for evaluation in *in vivo* studies. Improvements in these metrics reflected well in *in vitro* tier 1 DMPK studies, for the first time providing compounds with predicted hepatic clearance of less than half the rate of blood-flow in both human and rodent models



Entry	R ₁	R ₂	IC ₅₀	cLogP	LE/LELP	CL _{int} (h, r)	CL _{hep} (h, r)	PPB fu (h, r, m)
4.37			460	3.62	0.27/13.4	69.4 273	16.1 55.7	0.04 nd 0.108
4.15 (R)			90	3.57	0.30/12.2	nd nd	10 39	0.049 0.013 nd
4.38			246	3.00	0.29/11.6	21 17	10.5 13.6	0.267 nd 0.178
4.16			148	2.36	0.28/9.1	20 506	14.8 52.2	0.170 0.322 0.166

Table 4.4. Potency and *in vitro* DMPK parameters of biaryl hydroxymethyl piperidine compounds.

We advanced a selection of these compounds to *in vivo* cassette studies of pharmacokinetic properties as shown in **Table 4.5**. Importantly, replacement of the cyclopentyl group, an identified liability in metabolic identification studies, significantly improved half-life *in vivo*. Of particular interest was **4.15R**, which had a half-life of 10 hours in rat and 5.5 hours in mouse. This compound was designated as **ML399**, the second generation probe for *in vivo* evaluation in animal models of mixed-lineage leukemia.



Entry	R ₁	R ₂	IC ₅₀	CL _p	t _{1/2} (h)	V _{ss}
4.37			460	32	2.8	7.2
4.15 (R)			90	12	10.1	7.4
4.38			246	26	1.4	4.4
4.16			148	32	2.5	4.6

Table 4.5. *In vivo* pharmacokinetics parameters of biaryl hydroxymethyl piperidine compounds.

In order to determine the relevant metabolic pathways of **ML399**, metabolite identification experiments were performed using rat hepatic S9 fraction (**Figure 4.15**). This analysis revealed that the pyridyl group, used to replace the cyclopentyl ring, did not undergo oxidative metabolism. The major metabolite identified in rat S9 was *N*-dealkylation at the piperidine core (**M₁**), followed by oxidation of the 3-fluorophenyl substituent (**M₂**).

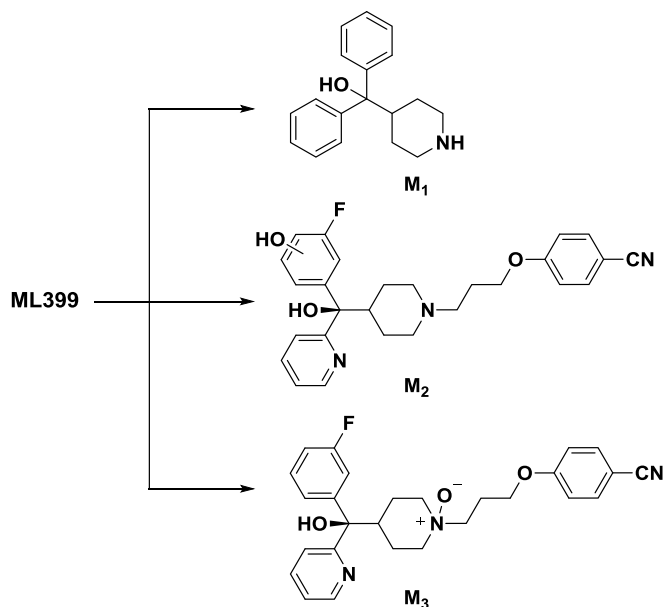


Figure 4.15. Identification of major metabolites of ML399.

4.6.3. Ancillary Pharmacology of Hydroxymethyl Piperidine Class

ML399 was screened in a Eurofins radioligand binding panel of over 60 G protein-coupled receptors, ion channels, and transporters at a concentration of 10 μM . Several significant activities at ancillary targets were identified with ML399. Of note was binding activity at the hERG potassium channel, a known target for this class of terfenidine-type scaffolds. This was also observed for the sulfonamide analog of ML399. Relevant activities are summarized in **Figure 4.16**.

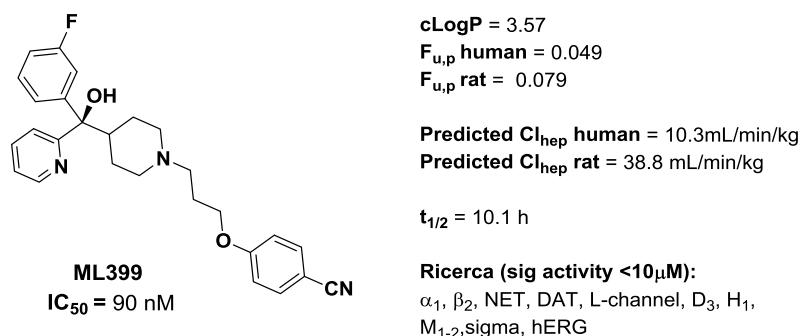


Figure 4.16. DMPK and ancillary pharmacology profile of ML399.

Several strategies to address hERG binding are ongoing, including attenuation of basicity of the tertiary amine and adding further polarity to the scaffold. Structural studies of **4.13** in complex with menin revealed that the propyl linker region occupied a relatively unhindered area of the binding pocket, and could possibly tolerate further derivitization with electron withdrawing and polar groups. Given the precedence for utilizing β -hydroxyl or $-\text{fluoro}$ functionalizations to attenuate basicity of piperidine scaffolds, we focused on implementing these features in the propyl linker region.

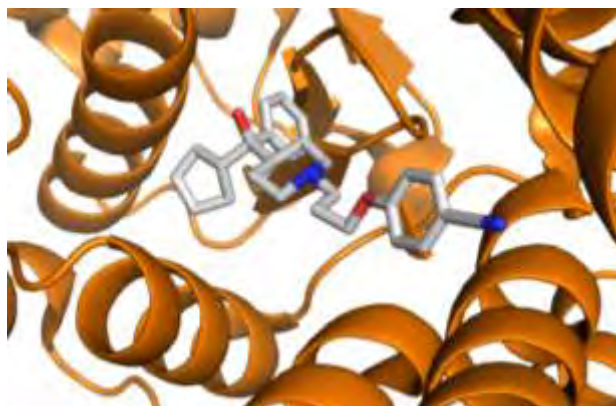
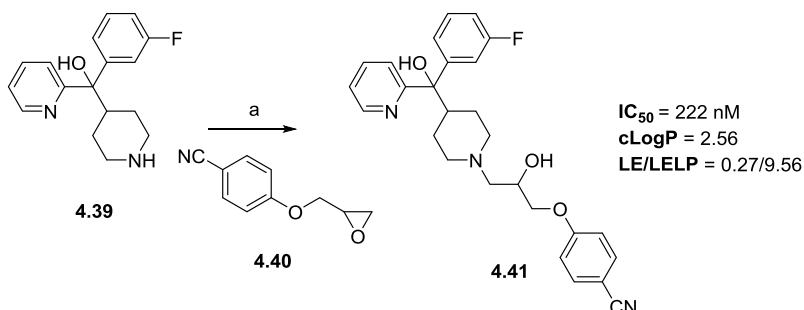


Figure 4.17. X-ray crystal structure of **4.13** in complex with menin.

The hydroxyl-substituted compound **4.41** was synthesized according to **Scheme 4.5**. The piperidine accessed in **Scheme 4.1** affected epoxide ring opening in 56% yield to provide the desired compound. The secondary alcohol provides an attractive handle for further derivitization of the propyl linker region, however attempts towards deoxofluorination to provide the fluorinated analogue have proven challenging due to the

β -heteroatom effects of the propyl chain. Substitution with polar groups such as the hydroxyl were well-tolerated, with the racemic **4.41** retaining potency of the related biaryl congeners. This suggests that further functionalization of the propyl linker region could be exploited to address ancillary activities.



Scheme 4.5. Synthesis of **4.41**. Reagents and conditions: (a) Acetonitrile, 22, K_2CO_3 , $30^\circ C$, 4h, 67%

4.7. Conclusions

Menin is a critical oncogenic cofactor of MLL fusion proteins, and the protein-protein interaction between menin and MLL fusion proteins represents a validated and attractive therapeutic target in acute leukemias with translocations of *MLL* gene.^{11,20,28}

The development of a novel class of the menin-MLL inhibitors, the hydroxy- and aminomethylpiperidine compounds, were identified by a high throughput screen at the NIH MLPCN. Medicinal chemistry optimization of the HTS hit led to a significant improvement in inhibitory activity, resulting in development of **ML227**.

The availability of co-crystal structures of menin with **ML227** enabled the rational design of modifications to improve both the binding affinity as well as to optimize their physicochemical properties. The resulting compound **4.29** represents the

most potent menin-MLL inhibitor developed in these series, providing ~230-fold improvement in the activity versus the initial HTS hit **4.1**. Importantly, despite a relatively low molecular weight ($M_w = 416$ Da), **4.29** inhibits the menin-MLL interaction with an affinity similar to the four-fold larger 12-amino acid MLL-derived peptide. Consequently, the ligand efficiency (LE) index²⁹ for this compound is relatively high (LE = 0.31 for **4.29**) as compared to 0.24 average value reported for PPI inhibitors.⁵

Biological studies demonstrated that this novel class of menin-MLL inhibitors has promising on-target biological activity, and represent an attractive chemical scaffold for further optimization as they closely mimic all critical interactions of MLL with menin.²²

A parallel effort incorporating analysis of physical properties and metrics, as well as rational design informed by metabolic identification studies were used to develop inhibitors of the menin-MLL interaction with improved potency and stability *in vivo*. This will allow for the evaluation of the hydroxymethylpiperidine class of compounds in animal models of mixed lineage leukemia.

References

1. Kar, G.; Gursoy, A.; Keskin, O. *PLoS Comput. Biol.* **2009**, *5*, e1000601.
2. Fry, D. C. *Biopolymers* **2006**, *84*, 535.
3. Buchwald, P. *IUBMB life* **2010**, *62*, 724.
4. Azzarito, V.; Long, K.; Murphy, N. S.; Wilson, A. J. *Nat. Chem.* **2013**, *5*, 161.
5. Wells, J. A.; McClendon, C. L. *Nature* **2007**, *450*, 1001.
6. Morelli, X.; Bourgeas, R.; Roche, P. *Current opinion in chemical biology* **2011**, *15*, 475.
7. Arkin, M. R.; Whitty, A. *Current opinion in chemical biology* **2009**, *13*, 284.
8. Smith, M. C.; Gestwicki, J. E. *Expert reviews in molecular medicine* **2012**, *14*, e16.
9. Tse, C.; Shoemaker, A. R.; Adickes, J.; Anderson, M. G.; Chen, J.; Jin, S.; Johnson, E. F.; Marsh, K. C.; Mitten, M. J.; Nimmer, P.; Roberts, L.; Tahir, S. K.; Xiao, Y.; Yang, X.; Zhang, H.; Fesik, S.; Rosenberg, S. H.; Elmore, S. W. *Cancer Res.* **2008**, *68*, 3421.
10. Ray-Coquard, I.; Blay, J. Y.; Italiano, A.; Le Cesne, A.; Penel, N.; Zhi, J.; Heil, F.; Rueger, R.; Graves, B.; Ding, M.; Geho, D.; Middleton, S. A.; Vassilev, L. T.; Nichols, G. L.; Bui, B. N. *Lancet Oncol.* **2012**, *13*, 1133.
11. Yokoyama, A.; Somerville, T. C.; Smith, K. S.; Rozenblatt-Rosen, O.; Meyerson, M.; Cleary, M. L. *Cell.* **2005**, *123*, 207.
12. Slany, R. K. *Hematol. Oncol.* **2005**, *23*, 1.
13. Marschalek, R. *Br. J. Haematol.* **2011**, *152*, 141.
14. Tomizawa, D.; Koh, K.; Sato, T.; Kinukawa, N.; Morimoto, A.; Isoyama, K.; Kosaka, Y.; Oda, T.; Oda, M.; Hayashi, Y.; Eguchi, M.; Horibe, K.; Nakahata, T.; Mizutani, S.; Ishii, E. *Leukemia* **2007**, *21*, 2258.
15. Popovic, R.; Zeleznik-Le, N. J. *J. Cell Biochem.* **2005**, *95*, 234.

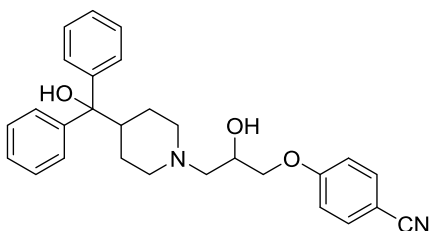
16. Hess, J. L. *Trends Mol. Med.* **2004**, *10*, 500.
17. Krivtsov, A. V.; Armstrong, S. A. *Nat. Rev. Cancer.* **2007**, *7*, 823.
18. Slany, R. K. *Haematologica* **2009**, *94*, 984.
19. Grembecka, J.; Belcher, A. M.; Hartley, T.; Cierpicki, T. *J. Biol. Chem.* **2010**, *285*, 40690.
20. Caslini, C.; Yang, Z.; El-Osta, M.; Milne, T. A.; Slany, R. K.; Hess, J. L. *Cancer Res.* **2007**, *67*, 7275.
21. Yokoyama, A.; Cleary, M. L. *Cancer Cell.* **2008**, *14*, 36.
22. Shi, A.; Murai, M. J.; He, S.; Lund, G.; Hartley, T.; Purohit, T.; Reddy, G.; Chruszcz, M.; Grembecka, J.; Cierpicki, T. *Blood* **2012**, *120*, 4461.
23. Murai, M. J.; Chruszcz, M.; Reddy, G.; Grembecka, J.; Cierpicki, T. *J. Biol. Chem.* **2011**, *286*, 31742.
24. Manka, J.; Daniels, R. N.; Dawson, E.; Daniels, J. S.; Southall, N.; Jadhav, A.; Zheng, W.; Austin, C.; Grembecka, J.; Cierpicki, T.; Lindsley, C. W.; Stauffer, S. R. In *Probe Reports from the NIH Molecular Libraries Program* Bethesda (MD), 2013.
25. Cowan, D. O.; Mosher, H. S. *J Org Chem* **1962**, *27*, 1.
26. Honkanen, E.; Pippuri, A.; Kairisalo, P.; Nore, P.; Karppanen, H.; Paakkari, I. *Journal of medicinal chemistry* **1983**, *26*, 1433.
27. Grembecka, J.; He, S.; Shi, A.; Purohit, T.; Muntean, A. G.; Sorenson, R. J.; Showalter, H. D.; Murai, M. J.; Belcher, A. M.; Hartley, T.; Hess, J. L.; Cierpicki, T. *Nat. Chem. Biol.* **2012**, *8*, 277.
28. Chen, Y. X.; Yan, J.; Keeshan, K.; Tubbs, A. T.; Wang, H.; Silva, A.; Brown, E. J.; Hess, J. L.; Pear, W. S.; Hua, X. *Proc. Natl. Acad. Sci. U S A.* **2006**, *103*, 1018.
29. Hopkins, A. L.; Groom, C. R.; Alex, A. *Drug discovery today* **2004**, *9*, 430.
30. A detailed description of the HTS screen is provided at PubChem Bioassay, AID: 1766:
<http://pubchem.ncbi.nlm.nih.gov/assay/assay.cgi?aid=1766>).

Experimental Methods

General Methods: All NMR spectra were recorded on a Bruker 400, 500 or 600 MHz instrument. ¹H chemical shifts are reported in δ values relative to residual solvent signals in ppm. Data are reported as follows: chemical shift, integration, multiplicity (s = singlet, d = doublet, t = triplet, q = quartet, br = broad resonance, m = multiplet), coupling constant (Hz). Low resolution mass spectra were obtained on an Agilent 1200 series 6130 mass spectrometer. High resolution mass spectra were recorded on a Waters Q-TOF API-US plus Acuity system with ES as the ion source. Analytical thin layer chromatography was performed on Sorbent Technologies 250 micron silica plates. Visualization was accomplished via UV light, and/or the use of potassium permanganate solution followed by application of heat. Analytical HPLC was performed on an HP1100 with UV detection at 214 and 254 nm along with ELSD detection, LC/MS (J-Sphere80-C18, 3.0 x 50 mm, 4.1 min gradient, 7% [0.1% TFA/H₂O] : 93% [CH₃CN]). Preparative RP-HPLC purification was performed on a custom HP1100 automated purification system with collection triggered by mass detection or using a Gilson Inc. preparative UV-based system using a Phenomenex Luna C18 column (50 x 30 mm I.D., 5 μ m) with an acetonitrile (unmodified)-water (0.5 mL/L NH₄OH) custom gradient. Normal-phase silica gel preparative purification was performed using an automated Combi-flash Companion from ISCO. Semi-preparative purifications were carried out via stacked injections on a Waters Investigator SFC using a 10 x 250 mm Chiral Technologies CHIRALPAK ID column heated to 40 degrees Celsius. Analytical separations were carried out on an Agilent 1260 Infinity SFC using a 4.6 x 250 mm Chiral Technologies CHIRALPAK ID column heated to 40 degrees Celsius. Solvents for extraction, washing

and chromatography were HPLC grade. All reagents were purchased from Aldrich Chemical Co. and were used without purification. All polymer-supported reagents were purchased from Argonaut Technologies and Biotage.

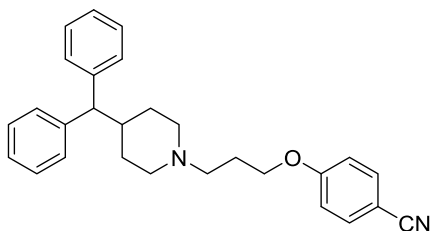
2. Procedures and Products



4-(2-hydroxy-3-(4-(hydroxydiphenylmethyl)piperidin-1-yl)propoxy)benzonitrile (4.1)

In a round bottom flask equipped with a stir bar, diphenyl(piperidin-4-yl)methanol (500 mg, 1.77 mmol) was dissolved in DMF (3.54 mL). Potassium carbonate (294 mg, 2.12 mmol) was added in a single batch followed by epibromohydrin (291 mg, 2.12 mmol). The reaction mixture was warmed to 50 °C and stirred for 6 h. 4-hydroxybenzonitrile (264 mg, 2.21 mmol) was then added in a single batch, and stirring was continued at 50 °C for 18 h. The reaction was quenched with H₂O and extracted with EtOAc. The combined organic layers were washed with brine, and dried over Na₂SO₄. Concentration *in vacuo* afforded the crude product as an oil, which was purified by flash chromatography (9:1 CH₂Cl₂/MeOH) to provide the desired product as a clear amorphous solid in 509 mg (65%). ¹H NMR (400 MHz, CDCl₃) δ (ppm): 7.56 (2H, d, *J* = 9 Hz), 7.47 (4H, d, *J* = 7.6 Hz), 7.30 (4H, t, *J* = 8 Hz), 7.19 (2H, t, *J* = 7.5 Hz), 6.96 (2H, d, *J* = 9 Hz), 4.07 (1H, m), 3.99 (2H, m), 3.05 (1H, d, *J* = 11 Hz), 2.89 (1H, d, *J* = 11

Hz), 2.49 (3H, m), 2.33 (2H, m), 2.05 (1H, dt, $J = 11.5, 3$ Hz), 1.53 (3H, m); ^{13}C NMR (100.6 MHz, CDCl_3) δ (ppm): 162.1, 145.9, 134.1, 128.4, 126.8, 125.8, 119.3, 115.5, 104.4, 79.6, 70.7, 65.3, 60.5, 56.0, 52.9, 44.0, 26.7, 26.4; HRMS (ES+, M+H) calc'd for $\text{C}_{28}\text{H}_{31}\text{N}_2\text{O}_3$: 443.2335, found: 443.2334

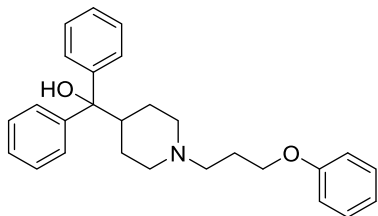


4-(3-(4-benzhydrylpiperidin-1-yl)propoxy)benzonitrile (4.5)

In a round bottom flask equipped with a stir bar, 4-benzhydrylpiperidine (2.1 g, 8.46 mmol) was combined with K_2CO_3 (6.9 g, 50 mmol) in DMF (40 mL), followed by 1-bromo-3-chloropropane (1.6 g, 10 mmol). The reaction progress was monitored by LC-MS, and upon full consumption of starting material, 4-cyanophenol (1.3 g, 11 mmol) was added and the reaction allowed to stir overnight. The mixture was poured onto water and extracted with EtOAc, washed with brine and dried over Na_2SO_4 . The volatiles were removed under reduced pressure and the crude mixture purified on silica gel (9:1 $\text{CH}_2\text{Cl}_2/\text{MeOH}$) to afford 2.7 g (78%) of 4-(3-(4-benzoylpiperidin-1-yl)propoxy)benzonitrile: ^1H NMR (400 MHz, CDCl_3) δ (ppm): 7.57 (2H, d, $J = 8.7$ Hz), 7.29 (8H, m), 7.12 (2H, m), 6.94 (2H, m), 4.05 (2H, t, $J = 6.5$ Hz), 3.52 (1H, d, $J = 10.9$ Hz), 2.90 (2H, d, $J = 11.7$ Hz), 2.50 (2H, t, $J = 7.2$ Hz), 2.14 (1H, m), 1.97 (4H, m), 1.59 (2H, d, $J = 13$ Hz), 1.26 (2H, m); ^{13}C NMR (100.6 MHz, CDCl_3) δ (ppm): 162.5, 143.9,

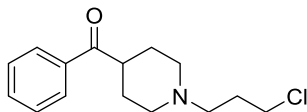
134.1, 128.6, 128.2, 126.3, 119.4, 115.3, 103.9, 66.9, 59.0, 55.4, 54.2, 39.7, 31.5, 26.8;

HRMS (ES+, M+H) calc'd for C₂₈H₃₀N₂O: 411.2436, found: 411.2434



(1-(3-phenoxypropyl)piperidin-4-yl)diphenylmethanol (4.6)

In a round bottom flask equipped with a stir bar, diphenyl(piperidin-4-yl)methanol (300 mg, 1.06 mmol) was dissolved in DMF (3.0 mL). Potassium carbonate (295 mg, 2.13 mmol) was added in a single batch followed by 1-bromo-3-chloropropane (184 mg, 1.17 mmol). The mixture was stirred for 6 h, at which point starting material was consumed by TLC observation. Phenol (190 mg, 1.60 mmol) was added to the stirring mixture, and the mixture was warmed to 50 °C and stirred for 18 h. The reaction mixture was quenched with H₂O, and extracted with EtOAc. Combined organic layers were washed with brine and dried over Na₂SO₄. Concentration *in vacuo* afforded the crude product, which was purified by flash chromatography (9:1 CH₂Cl₂/MeOH) to provide the desired product in 399 mg (88%) as a white powder. ¹H NMR (400 MHz, CDCl₃) δ (ppm): 7.51 (4H, d, *J* = 7.5 Hz), 7.31 (6H, m), 7.21 (2H, t, *J* = 7.5 Hz), 6.95 (1H, t, *J* = 7.5 Hz), 6.90 (2H, d, *J* = 8.2 Hz), 4.02 (2H, t, *J* = 6 Hz), 3.09 (2H, d, *J* = 11.5 Hz), 2.61 (2H, t, *J* = 7.4 Hz), 2.50 (1H, m), 2.16-2.00 (4H, m), 1.61 (4H, m); ¹³C NMR (100.6 MHz, CDCl₃) δ (ppm): 159.0, 146.1, 129.6, 128.4, 126.7, 120.8, 114.6, 79.6, 66.2, 55.5, 54.2, 44.1, 26.8, 26.2; HRMS (ES+, M+H) calc'd for C₂₇H₃₂NO₂: 402.2433, found: 402.2433



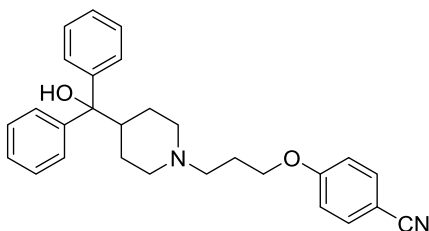
(1-(3-chloropropyl)piperidin-4-yl)(phenyl)methanone (4.4a)

To a solution of phenyl(piperidin-4-yl)methanone (500 mg, 2.64 mmol) in dry DMF (8.8 mL) was added potassium carbonate (803 mg, 5.81 mmol) followed by 1-bromo-3-chloropropane (500 mg, 3.17 mmol). Mixture was warmed to 50 °C and stirred for 4 h. The reaction was quenched with H₂O and extracted three times with EtOAc. The organic layers were combined and washed with sat. aqueous NaCl, then dried over Na₂SO₄ and filtered. Concentration *in vacuo* provided the crude product which was purified by flash chromatography (9:1 CH₂Cl₂/MeOH) to yield the desired product in 533 mg (75%) as a white powder. ¹H NMR (400 MHz, CDCl₃) δ (ppm): 7.92 (2H, d, *J* = 7.7 Hz), 7.54 (1H, t, *J* = 7.7 Hz), 7.45 (2H, t, *J* = 7.7 Hz), 3.59 (2H, t, *J* = 6.1 Hz), 3.23 (1H, m), 2.96 (2H, m), 2.49 (2H, t, *J* = 7.2 Hz), 2.11 (2H, td, *J* = 11.2, 3.5 Hz), 1.95 (2H, quintet, *J* = 6.6 Hz), 1.84 (4H, m); ¹³C NMR (100.6 MHz, CDCl₃) δ (ppm): 202.6, 136.0, 132.8, 128.6, 127.8, 55.5, 53.3, 43.6, 43.2, 30.0, 28.7; HRMS (ES⁺, M+H) calc'd for C₁₅H₂₁NOCl: 266.1312, found: 266.1312

General Procedure A:

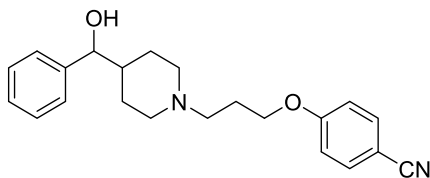
A solution of (1-(3-chloropropyl)piperidin-4-yl)(phenyl)methanone (100 mg, 0.35 mmol.) in THF (1.4 mL) was cooled to 0 °C. To this was added organomagnesium halide (2 equiv.) dropwise with stirring. The solution was then slowly warmed to ambient temperature, and stirring continued for 2 h, at which point starting material was consumed by TLC analysis. The reaction was quenched with saturated NH₄Cl and

extracted with EtOAc. The organic layers were combined and dried over Na₂SO₄. Solution was then transferred to a round-bottom flask, concentrated *in vacuo* to remove solvent, and then dissolved in DMF (1.0 mL). K₂CO₃ (98 mg) was added, followed by 4-hydroxybenzotrile (63 mg, 0.53 mmol). Mixture was warmed to 50 °C and stirred for 6 h. The reaction mixture was quenched with H₂O and extracted with EtOAc. The organic layers were combined and washed with sat. aqueous NaCl and dried over Na₂SO₄. Concentration *in vacuo* provided the crude product, which was purified by flash chromatography (9:1 CH₂Cl₂/MeOH) to provide the desired products.



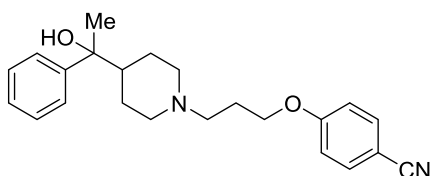
4-(3-(4-(hydroxydiphenylmethyl)piperidin-1-yl)propoxy)benzonitrile (4.2)

Phenylmagnesium bromide (3.0 M in Et₂O) was used as described in general procedure A to provide the desired product in 99 mg (66%): ¹H NMR (400 MHz, CDCl₃) δ (ppm): 7.55 (2H, d, *J* = 8.7 Hz), 7.48 (4H, d, *J* = 7.7 Hz), 7.30 (4H, t, *J* = 7.7 Hz), 7.18 (2H, t, *J* = 7.7 Hz), 6.92 (2H, d, *J* = 8.7 Hz), 4.03 (2H, t, *J* = 6.2 Hz), 2.98 (2H, d, *J* = 11.8 Hz), 2.47 (3H, m), 2.30 (1H, br s), 1.98 (4H, m), 1.51 (4H, m); ¹³C NMR (100.6 MHz, CDCl₃) δ (ppm): 162.4, 146.05, 134.1, 128.4, 126.7, 125.9, 119.4, 115.3, 103.8, 79.6, 66.8, 55.1, 54.3, 44.2, 26.7, 26.5; HRMS (ES⁺, M+H) calc'd for C₂₈H₃₁N₂O₂: 427.2386, found: 427.2390



4-(3-(4-(hydroxy(phenyl)methyl)piperidin-1-yl)propoxy)benzonitrile (4.7)

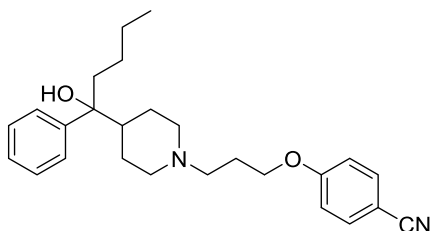
Cyclohexylmagnesium bromide (18% in THF) was used as described in general procedure A to provide the desired product in 36 mg (30%): ^1H NMR (400 MHz, CDCl_3) δ (ppm): 7.55 (2H, d, $J = 8$ Hz), 7.32 (5H, m), 6.92 (2H, d, $J = 8$ Hz), 4.38 (1H, d, $J = 8$ Hz), 4.03 (2H, t, $J = 6$ Hz), 3.02 (1H, d, $J = 11$ Hz), 2.89 (2H, d, $J = 11$ Hz), 1.96 (7H, m), 1.63 (1H, m), 1.46 (1H, m), 1.29 (2H, m); ^{13}C NMR (100.6 MHz, CDCl_3) δ (ppm): 162.3, 143.3, 134.1, 128.5, 127.8, 126.7, 119.4, 115.3, 103.9, 78.9, 66.8, 55.3, 53.8, 53.7, 43.2, 28.5, 28.4, 26.6; HRMS (ES+, M+H) calc'd for $\text{C}_{22}\text{H}_{27}\text{N}_2\text{O}_2$: 351.2073, found: 351.2074



4-(3-(4-(1-hydroxy-1-phenylethyl)piperidin-1-yl)propoxy)benzonitrile (4.8)

Methylmagnesium Bromide (3.0 M in Et_2O) was used as described in general procedure A to provide the desired product in 73 mg (58%): ^1H NMR (400 MHz, CDCl_3) δ (ppm): 7.55 (2H, d, $J = 8.5$ Hz), 7.40 (2H, d, $J = 7.8$ Hz), 7.33 (2H, t, $J = 7.5$ Hz), 7.24 (1H, t, $J = 7.4$ Hz), 6.92 (2H, d, $J = 9$ Hz), 4.02 (2H, t, $J = 6.4$ Hz), 2.97 (2H, t, $J = 12$ Hz), 2.47 (2H, t, $J = 7.4$ Hz), 1.97 (2H, m), 1.88 (2H, m), 1.63 (2H, m), 1.56 (3H, s), 1.51 (1H, m), 1.41 (2H, m); ^{13}C NMR (100.6 MHz, CDCl_3) δ (ppm): 162.4, 147.4, 134.0, 128.1, 126.8,

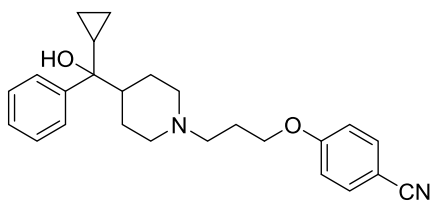
125.4, 119.4, 115.3, 103.9, 76.1, 66.9, 55.2, 54.3, 47.4, 26.7, 26.7, 26.6, 26.6; HRMS (ES+, M+H) calc'd for C₂₃H₂₉N₂O₂: 365.2229, found: 365.2228



4-(3-(4-(1-hydroxy-1-phenylpentyl)piperidin-1-yl)propoxy)benzonitrile (4.9)

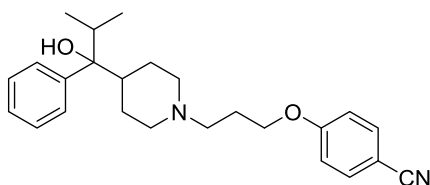
n-Butylmagnesium chloride (2.0 M in THF) was used as described in general procedure

A to provide the desired product in 64 mg (45%): ¹H NMR (400 MHz, CDCl₃) δ (ppm): 7.54 (2H, d, *J* = 8 Hz), 7.33 (4H, m), 7.21 (1H, m), 6.91 (2H, d, *J* = 9.1 Hz), 4.02 (2H, t, *J* = 6.4 Hz), 3.01 (1H, d, *J* = 11.2 Hz), 2.90 (1H, d, *J* = 11.2), 2.45 (2H, t, *J* = 7.2 Hz), 1.95 (3H, m), 1.82 (4H, m), 1.62 (1H, m), 1.39 (3H, m), 1.25 (3H, m), 0.92 (1H, m), 0.82 (3H, t, *J* = 7.2 Hz); ¹³C NMR (100.6 MHz, CDCl₃) δ (ppm): 162.5, 145.1, 134.1, 128.0, 126.4, 125.9, 119.4, 115.3, 103.9, 78.4, 66.9, 55.2, 54.3, 46.9, 39.0, 26.7, 26.5, 26.1, 25.7, 23.3, 14.1; HRMS (ES+, M+H) calc'd for C₂₆H₃₅N₂O₂: 407.2699, found: 407.2701



4-(3-(4-(cyclopropyl(hydroxy)(phenyl)methyl)piperidin-1-yl)propoxy)benzonitrile (4.10)

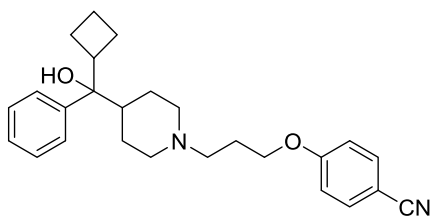
Cyclopropylmagnesium bromide (0.5 M in THF) was used as described in general procedure A to provide the desired product in 74 mg (56%): ^1H NMR (400 MHz, CDCl_3) δ (ppm): 7.55 (2H, d, $J = 9$ Hz), 7.45 (2H, d, $J = 8$ Hz), 7.33 (2H, t, $J = 7.5$ Hz), 7.23 (1H, t, $J = 7.2$ Hz), 6.92 (2H, d, $J = 9$ Hz), 4.03 (2H, t, $J = 6.2$ Hz), 3.01 (1H, d, $J = 11$ Hz), 2.95 (1H, d, $J = 11$ Hz), 2.48 (2H, t, $J = 7.2$ Hz), 1.94 (4H, m), 1.79 (2H, m), 1.49 (3H, m), 1.35 (1H, m), 0.60 (1H, m), 0.53 (1H, m), 0.32 (1H, m), 0.09 (1H, m); ^{13}C NMR (100.6 MHz, CDCl_3) δ (ppm): 162.4, 146.8, 134.1, 128.1, 134.1, 128.0, 126.7, 125.7, 119.4, 115.3, 103.9, 75.9, 66.9, 55.2, 54.4, 54.3, 48.0, 26.8, 26.7, 26.6, 18.2, 2.7, -0.1; HRMS (ES+, M+H) calc'd for $\text{C}_{25}\text{H}_{31}\text{N}_2\text{O}_2$: 391.2386, found: 391.2383



4-(3-(4-(1-hydroxy-2-methyl-1-phenylpropyl)piperidin-1-yl)propoxy)benzonitrile (4.11)

Isopropylmagnesium chloride (2.0 M in THF) was used as described in general procedure A to provide the desired product in 56 mg (41 %): ^1H NMR (400 MHz, CDCl_3) δ (ppm): 7.54 (2H, d, $J = 9$ Hz), 7.32 (4H, m), 7.21 (1H, t, $J = 7$ Hz), 6.90 (2H, d, $J = 9$ Hz), 4.00

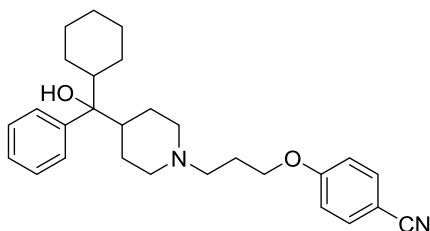
(2H, t, $J = 6$ Hz), 3.00 (1H, d, $J = 11.5$ Hz), 2.97 (1H, d, $J = 11.5$ Hz), 2.50 (2H, t, $J = 7$ Hz), 2.32 (1H, sept, $J = 7$ Hz), 2.05-1.84 (6H, m), 1.45 (1H, m), 1.25 (3H, m), 0.87 (3H, d, $J = 7$ Hz), 0.76 (3H, d, $J = 7$ Hz); ^{13}C NMR (125.8 MHz, CDCl_3) δ (ppm): 162.4, 142.8, 134.1, 127.7, 126.6, 126.5, 119.4, 115.3, 103.9, 80.3, 66.8, 55.2, 54.3, 54.2, 42.9, 33.3, 26.5, 25.9, 17.4, 16.4; HRMS (ES+, M+H) calc'd for $\text{C}_{25}\text{H}_{33}\text{N}_2\text{O}_2$: 393.2542, found: 393.2542



4-(3-(4-(cyclobutyl(hydroxy)(phenyl)methyl)piperidin-1-yl)propoxy)benzonitrile (4.12)

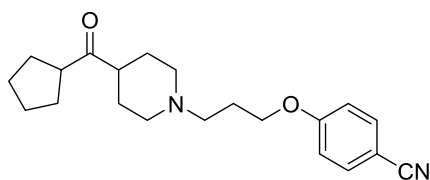
Cyclobutylmagnesium Bromide (0.2 M in THF) was prepared by dissolving cyclobutyl bromide (150 mg, 1.1 mmol) in THF (5.0 mL), followed by addition of magnesium (25 mg, 1.1 mmol) and a catalytic amount of iodine. The mixture was stirred for 2 h at ambient temperature, and was used as described in general procedure A to provide the desired product in 85 mg (60 %): ^1H NMR (400 MHz, CDCl_3) δ (ppm): 7.54 (2H, d, $J = 8$ Hz), 7.34 (2H, d, $J = 7.5$ Hz), 7.30 (2H, t, $J = 7.5$ Hz), 7.20 (1H, t, $J = 7$ Hz), 6.90 (2H, d, $J = 9$ Hz), 4.00 (2H, t, $J = 6$ Hz), 3.14 (1H, pent, $J = 9$ Hz), 2.97 (1H, d, $J = 11$ Hz), 2.89 (1H, d, $J = 11$ Hz), 2.44 (2H, t, $J = 7.5$ Hz), 2.14 (1H, pent, $J = 9$ Hz), 1.94 (4H, m), 1.80 (4H, m), 1.59 (4H, m), 1.41 (1H, m), 1.28 (2H, m); ^{13}C NMR (100.6 MHz, CDCl_3) δ (ppm): 162.4, 143.8, 134.1, 127.9, 126.6, 126.3, 119.2, 115.3, 103.9, 73.3, 68.8, 55.2,

54.3, 54.2, 45.5, 42.6, 26.9, 26.6, 26.4, 23.4, 23.1, 17.6; HRMS (ES+, M+H) calc'd for C₂₆H₃₃N₂O₂: 405.2542, found: 405.2539



4-(3-(4-(cyclohexyl(hydroxy)(phenyl)methyl)piperidin-1-yl)propoxy)benzonitrile (4.14)

Cyclohexylmagnesium bromide (18% in THF) was used as described in general procedure A to provide the desired product in 59 mg (39%): ¹H NMR (400 MHz, CDCl₃) δ (ppm): 7.54 (2H, d, *J* = 9 Hz), 7.31 (4H, m), 7.22 (1H, t, *J* = 7.5 Hz), 6.90 (2H, d, *J* = 9 Hz), 4.01 (2H, t, *J* = 6.5 Hz), 3.00 (1H, d, *J* = 11 Hz), 2.94 (1H, d, *J* = 11 Hz), 2.46 (2H, t, *J* = 7 Hz), 2.00-1.60 (12H, m), 1.50 (1H, d, *J* = 12 Hz), 1.29 (5H, m), 0.97 (2H, m), 0.77 (1H, m); ¹³C NMR (100.6 MHz, CDCl₃) δ (ppm): 162.4, 143.2, 134.1, 127.7, 126.5, 126.4, 119.4, 115.5, 103.9, 80.2, 68.9, 55.3, 54.4, 54.3, 44.2, 42.4, 27.5, 26.9, 26.8, 26.7, 26.6, 26.5, 26.4, 25.9; HRMS (ES+, M+H) calc'd for C₂₈H₃₇N₂O₂: 433.2855, found: 433.2854



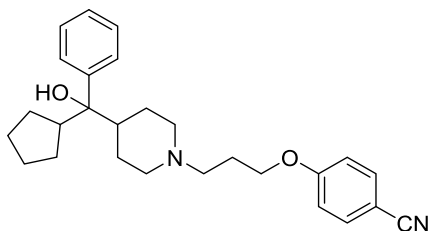
4-(3-(4-(cyclopentanecarbonyl)piperidin-1-yl)propoxy)benzonitrile (4.23)

Cyclopentyl(piperidin-4-yl)methanone (2.70 g, 10.0 mmol) was combined with K₂CO₃ (6.9 g, 50.0 mmol) in DMF (40.0 mL), followed by 1-bromo-3-chloropropane (1.55 g,

10.0 mmol). The reaction progress was monitored by LC-MS and upon completion of the reaction 4-cyanophenol (1.3 g, 11.0 mmol) was added and the reaction allowed to stir overnight. The mixture was poured onto water and extracted with EtOAc, washed with brine and dried over Na₂SO₄. The volatiles were removed under reduced pressure and the crude mixture purified on silica gel (9:1 CH₂Cl₂/MeOH) to provide the desired product in 2.71 g (78%) as a light yellow oil: ¹H NMR (600 MHz, CDCl₃) δ (ppm): 7.56 (2H, d, *J* = 9.0 Hz), 6.93 (2H, d, *J* = 9.0 Hz), 4.05 (2H, t, *J* = 6.5 Hz), 3.00 (1H, quintet, *J* = 7.7 Hz), 2.94 (2H, m), 2.49 (2H, t, *J* = 7.1 Hz), 2.42 (1H, m), 1.99 (4H, m), 1.79 (4H, m), 1.68 (6H, m), 1.56 (2H, m); ¹³C NMR (150.9 MHz, CDCl₃) δ (ppm): 215.7, 162.5, 134.1, 119.4, 115.3, 103.9, 66.8, 55.1, 53.4, 49.4, 48.2, 29.5, 28.1, 26.7, 26.2; HRMS (ES+, M+H) calc'd for C₂₁H₂₉N₂O₂: 341.2229, found: 341.2228

General procedure B:

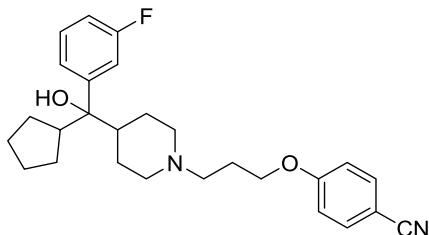
4-(3-(4-(cyclopentanecarbonyl)piperidin-1-yl)propoxy)benzotrile (30 mg, 0.09 mmol) was dissolved in THF (0.7 mL). Organometallic (2 equiv.) was added dropwise to the solution with stirring. Reaction was then warmed to 50 °C, and stirring was continued for 2 h. Reaction was quenched with sat. aqueous NH₄Cl, and extracted with EtOAc. The combined organic fractions were washed with saturated NaCl and dried over Na₂SO₄. Concentration *in vacuo* provided the crude product, which was purified by flash column chromatography (9:1 CH₂Cl₂/MeOH) to provide the desired products in 35 – 74% yield.



**4-(3-(4-(cyclopentyl(hydroxy)(phenyl)methyl)piperidin-1-yl)propoxy)benzonitrile
(4.13, MIV-3)**

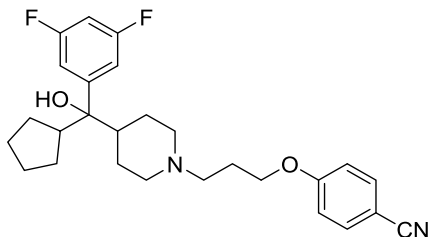
Phenylmagnesium bromide (1.0 M in THF) was used as described in general procedure B to provide the desired product in 46 mg (74%): Chiral Separation: Semi-preparative purifications were carried out via stacked injections on a Waters Investigator SFC using a 10 x 250 mm Chiral Technologies CHIRALPAK IA column heated to 40 °C. The eluent was 55% EtOH(0.1% DEA) in CO₂ at a flow rate of 15 mL/minute. Backpressure was maintained at 100 bar. The *first* eluting peak (**11S**), retention time = 0.95 min. was inferred as the *S* stereoisomer based upon the absolute configuration observed in the electron density map of the X-ray structure of the **MIV-3S**-Menin complex. The *second* eluting peak (**11R**), retention time = 2.3 min. was inferred as the *R* stereoisomer based upon the absolute configuration observed in the electron density map of the X-ray structure of the **MIV-3R**-Menin complex. ¹H NMR (400 MHz, CDCl₃) δ (ppm): 7.54 (2H, d, *J* = 9 Hz), 7.37 (2H, d, *J* = 8 Hz), 7.30 (2H, t, *J* = 8 Hz), 7.22 (1H, t, *J* = 7 Hz), 6.88 (2H, d, *J* = 9 Hz), 4.07 (2H, t, *J* = 6 Hz), 3.21 (2H, m), 2.67 (3H, m), 2.19 (2H, m), 2.05 (2H, m), 1.95 (1H, m), 1.82 (1H, m), 1.72 (1H, m), 1.64 (1H, m), 1.59-1.40 (7H, m), 1.25 (1H, m), 1.07 (1H, m); ¹³C NMR (100.6 MHz, CDCl₃) δ (ppm): 162.4, 143.9, 134.0, 127.7, 126.5, 126.4, 119.4, 115.3, 103.8, 79.6, 68.9, 55.2, 54.5, 54.4, 45.8, 45.3, 27.5,

27.3, 26.7, 26.4, 26.1, 26.0, 25.6; HRMS (ES+, M+H) calc'd for C₂₇H₃₅N₂O₂: 419.2699, found: 419.2698



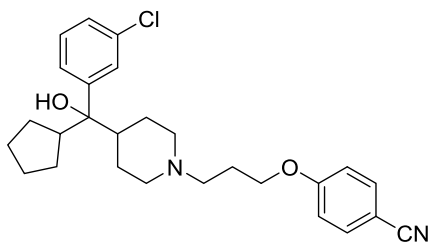
4-(3-(4-(cyclopentyl(3-fluorophenyl)(hydroxy)methyl)piperidin-1-yl)propoxy)benzonitrile (4.24)

3-Fluorophenylmagnesium bromide (1.0 M in THF) was used as described in general procedure B to provide the desired product in 22 mg (57%): ¹H NMR (400 MHz, CDCl₃) δ (ppm): 7.55 (2H, d, *J* = 9 Hz), 7.26 (1H, m), 7.13 (2H, m), 6.90 (3H, m), 4.02 (2H, t, *J* = 6 Hz), 3.06 (2H, m), 2.66 (1H, quintet, *J* = 8.5 Hz), 2.55 (2H, m), 2.03 (3H, m), 1.93 (1H, d, *J* = 13 Hz), 1.71 (4H, m), 1.57 (1H, m), 1.47 (6H, m), 1.10 (2H, m); ¹³C NMR (100.6 MHz, CDCl₃) δ (ppm): 162.8 (d, *J*_{CF} = 247 Hz), 162.3, 146.8 (d, *J*_{CF} = 6 Hz), 134.1, 129.1 (d, *J*_{CF} = 8 Hz), 122.3 (d, *J*_{CF} = 3 Hz), 119.4, 115.3, 114.1 (d, *J*_{CF} = 24 Hz), 113.4 (d, *J*_{CF} = 21 Hz), 103.9, 79.4, 66.7, 55.1, 54.2, 54.1, 46.0, 45.2, 27.4, 26.8, 26.3, 26.1, 26.0, 25.9, 25.5; HRMS (ES+, M+H) calc'd for C₂₇H₃₄N₂O₂F: 437.2604, found: 437.2604



4-(3-(4-(cyclopentyl(3,5-difluorophenyl)(hydroxy)methyl)piperidin-1-yl)propoxy)benzotrile (4.25)

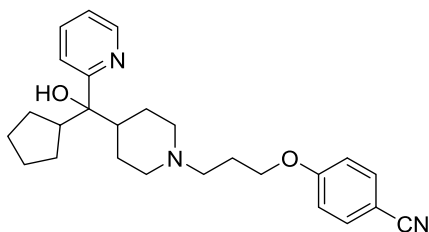
3,5-Difluorophenylmagnesium bromide (0.5 M in THF) was used as described in general procedure B to provide the desired product in 15 mg (36%): ^1H NMR (400 MHz, CDCl_3) δ (ppm): 7.55 (2H, d, $J = 9$ Hz), 6.91 (4H, t, $J = 8$ Hz), 6.66 (1H, tt, $J = 9.0, 2.2$ Hz), 4.00 (2H, t, $J = 6.3$ Hz), 2.99 (2H, d, $J = 11$ Hz), 2.60 (1H, quintet, $J = 9$ Hz), 2.47 (2H, t, $J = 7$ Hz), 1.93 (5H, m), 1.75 (1H, m), 1.68-1.32 (10H, m), 1.05 (2H, m); ^{13}C NMR (100.6 MHz, CDCl_3) δ (ppm): 162.83 (dd, $J_{\text{CF}} = 247, 12$ Hz), 162.3, 148.6 (t, $J_{\text{CF}} = 8$ Hz), 134.1, 119.4, 115.3, 109.8 (d, $J_{\text{CF}} = 24$ Hz), 104.0, 102.0 (t, $J_{\text{CF}} = 24$ Hz), 79.5, 77.3, 66.7, 55.2, 54.2, 54.1, 46.1, 45.4, 27.3, 26.9, 26.4, 26.2, 25.9, 25.5; HRMS (ES+, M+H) calc'd for $\text{C}_{27}\text{H}_{33}\text{N}_2\text{O}_2\text{F}_2$: 455.2510, found: 455.2513



4-(3-(4-((3-chlorophenyl)(cyclopentyl)(hydroxy)methyl)piperidin-1-yl)propoxy)benzotrile (4.26)

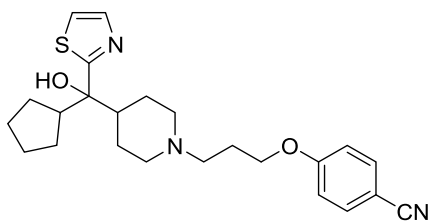
3-Chlorophenylmagnesium bromide (0.5 M in THF) was used as described in general procedure B to provide the desired product in 24 mg (60%): ^1H NMR (400 MHz,

CDCl₃) δ (ppm): 7.56 (2H, d, $J = 8.7$ Hz), 7.42 (1H, s), 7.26 (2H, t, $J = 7.6$ Hz), 7.22 (1H, m), 6.92 (2H, d, $J = 8.7$ Hz), 4.02 (2H, t, $J = 6.3$ Hz), 2.97 (2H, d, $J = 11$ Hz), 2.70 (1H, quintet, $J = 9$ Hz), 2.47 (2H, t, $J = 7$ Hz), 1.95 (5H, m), 1.76 (1H, m), 1.71-1.41 (9H, m), 1.29 (1H, m), 1.04 (2H, m); ¹³C NMR (100.6 MHz, CDCl₃) δ (ppm): 162.4, 146.2, 134.1, 133.9, 128.9, 127.0, 126.8, 125.0, 119.4, 115.3, 103.9, 79.5, 66.8, 55.2, 54.3, 54.2, 45.9, 45.3, 27.5, 27.1, 26.5, 26.3, 26.1, 26.0, 25.6; HRMS (ES+, M+H) calc'd for C₂₇H₃₄N₂O₂Cl: 453.2309, found: 453.2305



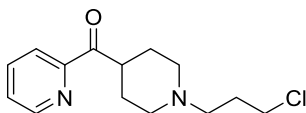
4-(3-(4-(cyclopentyl(hydroxy)(pyridin-2-yl)methyl)piperidin-1-yl)propoxy)benzotrile (4.27)

2-Pyridylmagnesium bromide (0.25 M) was used as described in general procedure B to provide the desired product in 13 mg (35%). ¹H NMR (400 MHz, CDCl₃) δ (ppm): 8.52 (1H, d, $J = 5$ Hz), 7.70 (2H, t, $J = 8$ Hz), 7.57 (2H, d, $J = 8$ Hz), 7.31 (1H, d, $J = 8$ Hz), 7.21 (1H, dd, $J = 8, 5$ Hz), 6.92 (2H, d, $J = 8$ Hz), 5.72 (1H, br s), 4.03 (2H, t, $J = 6$ Hz), 3.03 (1H, m), 2.56 (3H, m), 2.09-1.75 (7H, m), 1.65 (2H, m), 1.49 (4H, m), 1.15 (2H, m), 0.76 (1H, m); ¹³C NMR (125.8 MHz, CDCl₃) δ (ppm): 162.2, 161.5, 147.0, 136.6, 134.1, 122.2, 121.1, 119.3, 115.3, 104.1, 78.1, 66.6, 55.1, 54.3, 54.2, 45.8, 45.4, 29.8, 27.1, 26.5, 26.1, 25.7; HRMS (ES+, M+H) calc'd for C₂₆H₃₄N₃O₂: 420.2651, found: 420.2650



4-(3-(4-(cyclopentyl(hydroxy)(thiazol-2-yl)methyl)piperidin-1-yl)propoxy)benzonitrile (4.28)

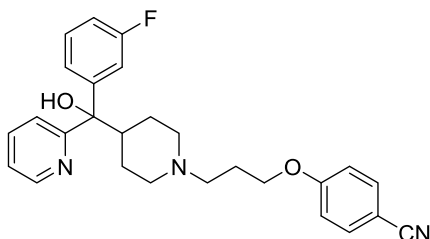
Thiazol-2-yllithium (0.15 M in THF) was prepared by dissolving 2-bromothiazole (72.2 mg, 0.44 mmol) in THF and cooling to $-78\text{ }^{\circ}\text{C}$. *n*-Butyllithium (0.18 mL, 2.5 M in hexanes) was slowly added, and then stirred for 20 min. at $-78\text{ }^{\circ}\text{C}$. The solution was then used as described in general procedure B to provide the desired product in 47 mg (75%): ^1H NMR (400 MHz, CDCl_3) δ (ppm): 7.70 (1H, d, $J = 3.2$ Hz), 7.54 (2H, d, $J = 8.7$ Hz), 7.28 (1H, d, $J = 3.2$ Hz), 6.91 (2H, d, $J = 8.7$ Hz), 4.02 (2H, t, $J = 6$ Hz), 3.40 (1H, br s), 3.03 (2H, d, $J = 11.2$ Hz), 2.55 (3H, m), 2.05-1.85 (6H, m), 1.75 (2H, m), 1.47 (8H, m), 1.21 (1H, m); ^{13}C NMR (100.6 MHz, CDCl_3) δ (ppm): 175.7, 162.3, 114.6, 134.1, 141.6, 134.1, 119.4, 119.2, 115.3, 103.9, 80.9, 66.8, 55.1, 54.1, 47.5, 45.1, 26.7, 26.4, 26.3, 26.0, 25.8, 25.5; HRMS (ES⁺, M+H) calc'd for $\text{C}_{24}\text{H}_{32}\text{N}_3\text{O}_2\text{S}$: 426.2215, found: 426.2212



(1-(3-chloropropyl)piperidin-4-yl)(pyridin-2-yl)methanone (4.4b)

To a solution of piperidin-4-yl(pyridin-2-yl)methanone (791 mg, 2.72 mmol) in dry DMF (9.1 mL) was added potassium carbonate (1.13 g, 8.16 mmol) followed by 1-bromo-3-chloropropane (514 mg, 3.26 mmol). Mixture was warmed to $50\text{ }^{\circ}\text{C}$ and stirred for 4 h.

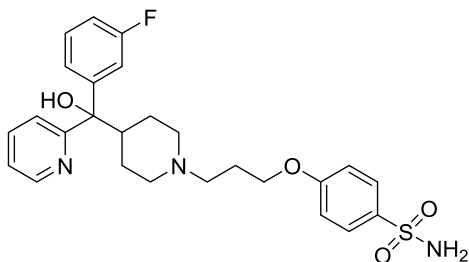
The reaction was quenched with H₂O and extracted three times with EtOAc. The organic layers were combined and washed with sat. aqueous NaCl, then dried over Na₂SO₄ and filtered. Concentration *in vacuo* provided the crude product which was purified by flash chromatography (9:1 CH₂Cl₂/MeOH) to yield the desired product in 790 mg (83%) as a light yellow oil: ¹H NMR (400MHz,CDCl₃) δ (ppm): 8.66 (1H, d, *J* = 4.4 Hz), 8.01 (1H, d, *J* = 8.3 Hz), 7.82 (1H, t, *J* = 7.8 Hz), 7.44 (1H, m), 3.83 (1H, m), 3.59 (2H, t, *J* = 6.5 Hz), 2.95 (2H, d, *J* = 11.2 Hz), 2.50 (2H, t, *J* = 7.2 Hz), 2.16 (2H, m), 1.94 (4H, m), 1.77 (2H, m); ¹³C NMR (100.6 MHz, CDCl₃) δ (ppm): 203.7, 152.7, 148.8, 136.9, 126.9, 122.4, 55.7, 53.2, 43.3, 42.2, 30.0, 28.1; HRMS (ES+, M+H) calc'd for C₁₄H₂₀N₂OCl: 267.1264, found: 267.1263



4-(3-(4-((3-fluorophenyl)(hydroxy)(pyridin-2-yl)methyl)piperidin-1-yl)propoxy)benzonitrile (4.15)

A solution of (1-(3-chloropropyl)piperidin-4-yl)(pyridin-2-yl)methanone (100 mg, 0.35 mmol.) in THF (1.41 mL) was cooled to 0 °C. To this was added 3-Fluorophenylmagnesium bromide (1.0 M in THF) dropwise with stirring. The solution was then slowly warmed to ambient temperature, and stirring continued for 2 h, at which point starting material was consumed by TLC analysis. The reaction was quenched with sat. aqueous NH₄Cl and extracted with EtOAc. The organic layers were combined and

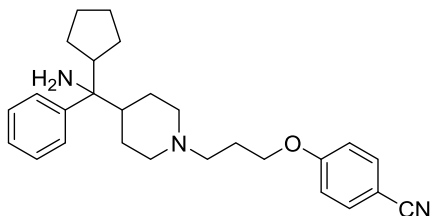
dried over Na₂SO₄. Solution was then transferred to a round-bottom flask, concentrated *in vacuo* to remove solvent, and then dissolved in DMF (1.0 mL). K₂CO₃ (76 mg, 0.55 mmol) was added, followed by 4-hydroxybenzotrile (131 mg, 1.10 mmol). Mixture was warmed to 50 °C and stirred for 6 h. The reaction mixture was quenched with H₂O and extracted with EtOAc. The organic layers were combined and washed with sat. aqueous NaCl and dried over Na₂SO₄. Concentration *in vacuo* provided the crude product, which was purified by reverse-phase HPLC chromatography to provide the desired product as an off-white powder in 106 mg (65%). Chiral Separation: Semi-preparative purifications were carried out via stacked injections on a Waters Investigator SFC using a 10 x 250 mm Chiral Technologies CHIRALPAK ID column heated to 40 °C. The eluent was 50% IPA (0.1% DEA) in CO₂ at a flow rate of 15 mL/minute. Backpressure was maintained at 100 bar. The *first* eluting peak (**18R**), retention time = 3.09 min.. The *second* eluting peak (**18S**), retention time = 3.79 min. ¹H NMR (500 MHz, CDCl₃) δ (ppm): 8.85 (1H, d, *J* = 6 Hz), 8.43 (1H, d, *J* = 7.4 Hz), 8.37 (1H, t, *J* = 7.4 Hz), 7.79 (1H, t, *J* = 6.6 Hz), 7.59 (4H, m), 7.37 (1H, dd, *J* = 16, 8 Hz), 6.96 (3H, m), 4.33 (1H, br s), 4.01 (2H, t, *J* = 6 Hz), 3.59 (3H, m), 3.25 (2H, m), 3.07 (1H, m), 2.58 (1H, m), 2.44 (3H, m), 1.72 (1H, d, *J* = 14 Hz), 1.59 (1H, d, *J* = 14 Hz); ¹³C NMR (125.8 MHz, CDCl₃) δ (ppm): 162.8 (d, *J*_{CF} = 247 Hz), 162.2, 161.9, 148.4 (d, *J*_{CF} = 6.2 Hz), 147.4, 137.4, 134.1, 129.8 (d, *J*_{CF} = 8.1 Hz), 122.4, 121.5, 120.4, 119.4, 115.3, 113.9, 113.7, 113.5, 113.3, 104.0, 78.6, 66.7, 54.9, 54.0, 26.5, 25.6, 25.3; HRMS (ES+, M+H) calc'd for C₂₇H₂₉N₃O₂F: 446.2244, found: 446.2248



4-(3-(4-((3-fluorophenyl)(hydroxy)(pyridin-2-yl)methyl)piperidin-1-yl)propoxy)benzenesulfonamide (4.16)

A solution of (1-(3-chloropropyl)piperidin-4-yl)(pyridin-2-yl)methanone (100 mg, 0.35 mmol.) in THF (1.41 mL) was cooled to 0 °C. To this was added 3-fluorophenylmagnesium bromide (1.0 M in THF) dropwise with stirring. The solution was then slowly warmed to ambient temperature, and stirring continued for 2 h, at which point starting material was consumed by TLC analysis. The reaction was quenched with saturated NH₄Cl and extracted with EtOAc. The organic layers were combined and dried over Na₂SO₄. Solution was then transferred to a round-bottom flask, concentrated *in vacuo* to remove solvent, and then dissolved in DMF (1.0 mL). K₂CO₃ (76 mg, 0.55 mmol) was added, followed by 4-hydroxybenzenesulfonamide (190 mg, 1.10 mmol). Mixture was warmed to 50 °C and stirred for 6 h. The reaction mixture was quenched with H₂O and extracted with EtOAc. The organic layers were combined and washed with sat. aqueous NaCl and dried over Na₂SO₄. Concentration *in vacuo* provided the crude product, which was purified by reverse-phase HPLC chromatography to provide the desired product as an off-white powder in 136 mg (74%): ¹H NMR (400 MHz, CDCl₃) δ (ppm): 8.47 (1H, d, *J* = 4.9 Hz), 7.82 (2H, d, *J* = 8.9 Hz), 7.67 (1H, td, *J* = 10, 7 Hz), 7.44 (1H, d, *J* = 8 Hz), 7.36 (2H, m), 7.26 (1H, m), 7.16 (1H, m), 6.93 (2H, d, *J* = 9 Hz), 6.87 (1H, m), 6.05 (1H, br s), 5.10 (1H, br s), 4.02 (2H, t, *J* = 6 Hz), 2.92 (2H, m), 2.46 (2H, t, *J* = 7 Hz), 2.36 (1H, t, *J* = 11 Hz), 1.94 (4H, m), 1.62 (2H, m), 1.45 (1H, d, *J*

= 13 Hz), 0.97 (1H, d, $J = 13$ Hz); ^{13}C NMR (100.6 MHz, CDCl_3) δ (ppm): 163.1 (d, $J_{\text{CF}} = 242$ Hz), 162.5, 162.1, 148.4 (d, $J_{\text{CF}} = 7$ Hz), 147.3, 137.4, 133.8, 129.8 (d, $J_{\text{CF}} = 8$ Hz), 128.6, 122.3, 121.5, 120.4, 114.8, 113.7 (d, $J_{\text{CF}} = 21$ Hz), 113.4 (d, $J_{\text{CF}} = 22$ Hz), 78.6, 66.9, 55.0, 54.1, 54.0, 44.7, 26.7, 26.0, 25.8; HRMS (ES+, M+H) calc'd for $\text{C}_{26}\text{H}_{31}\text{N}_3\text{O}_4\text{SF}$: 500.2019, found: 500.2020

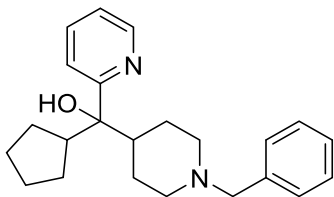


4-(3-(4-(cyclopentyl(hydroxy)(phenyl)methyl)piperidin-1-yl)propoxy)benzotrile (4.29)

A CHCl_3 (4.78 mL, 0.25 M) solution of 4-(3-(4-(cyclopentyl(hydroxy)(phenyl)methyl)piperidin-1-yl)propoxy)benzotrile (1.0 g, 2.39 mmol) and sodium azide (1.16 g, 17.9 mmol) was cooled to 0 °C. To the solution, H_2SO_4 was added dropwise (0.28 mL, 9.3 mmol). The mixture was allowed to warm to rt over 4h with stirring, then cooled to 0 °C and treated with NH_4OH until pH was basic. The biphasic solution was extracted with CH_2Cl_2 (3x) and the organic layers combined and dried over MgSO_4 . Concentration under reduced pressure and concentration *in vacuo* afforded a crude oil which was purified by flash column chromatography (9:1 $\text{CH}_2\text{Cl}_2/\text{MeOH}$) to afford a colorless oil comprising an inseparable mixture of the desired azide and an elimination byproduct in 30 mg that was carried on to the next step.

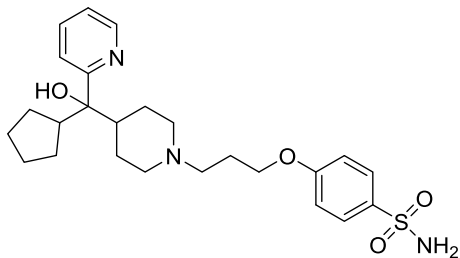
4-(3-(4-(Azido(cyclopentyl)(phenyl)methyl)piperidin-1-yl)propoxy)benzotrile (30 mg, 0.07 mmol) was dissolved in degassed EtOH (0.5 mL) and Pd/C (2.7 mg) added in one

portion. Reaction was placed under a balloon of H₂ gas and allowed to stir for 4 h at ambient temperature. The reaction was filtered over Celite and rinsed with MeOH. The filtrate was concentrated to afford an oil. RP-HPLC preparative purification afforded the desired product as a TFA salt. The mixture was treated with a StratoSpheres SPE MP-carbonate resin cartridge to give title compound as a free base in 20 mg (2%). Chiral Separation: Semi-preparative purifications were carried out via stacked injections on a Waters Investigator SFC using a 10 x 250 mm Chiral Technologies CHIRALPAK ID column heated to 40 °C. The eluent was 50% MeOH(0.1% DEA) in CO₂ at a flow rate of 15 mL/minute. Backpressure was maintained at 100 bar. The *first* eluting peak (**19S**), retention time = 3.97 min. was inferred as the *S* stereoisomer based upon the absolute configuration observed in the electron density map of the X-ray structure of the **4.29 R-Menin** complex. The *second* eluting peak (**19R**), retention time = 5.38 min. was inferred as the *R* stereoisomer based upon the absolute configuration observed in the electron density map of the X-ray structure of the **4.29 R-Menin** complex. ¹H NMR (600 MHz, CDCl₃) δ 7.54 (2H, d, *J* = 6.0 Hz), 7.43 (2H, d, *J* = 7.2 Hz), 7.31 (2H, t, *J*=7.2 Hz), 7.22 (1H, t, *J* = 7.2 Hz), 6.91 (2H, d, *J* = 6.0 Hz), 4.02 (2H, t, *J* = 8.4 Hz), 3.05-2.96 (2H, m), 2.62 (1H, m), 2.47 (2H, br s), 1.96-1.89 (4H, m), 1.73 (1H, m), 1.62-1.40 (9H, m), 1.29-1.24 (2H, m), 1.13-1.05 (2H, m); ¹³C NMR (150.9 MHz, CDCl₃) δ (ppm): 162.4, 144.5, 134.1, 127.6, 127.5, 126.1, 119.42, 115.3, 103.9, 66.9, 61.3, 55.2, 54.7, 54.6, 46.4, 45.6, 27.6, 27.1, 26.7, 26.6, 26.5, 25.9, 25.6; HRMS (ES+, M+H) calc'd for C₂₈H₃₀N₂O₂: 418.858, found: 418.2857



(1-benzylpiperidin-4-yl)(cyclopentyl)(pyridin-2-yl)methanol (4.33)

2-Bromopyridine (873 mg, 5.54 mmol), was dissolved in THF (30 mL), and cooled to -78 °C. To this solution was added *n*-butyllithium (2.2 mL, 2.5 M in hexanes, 5.53 mmol) dropwise with stirring. Stirring was continued for 20 min. (1-Benzylpiperidin-4-yl)(cyclopentyl)methanone (500 mg, 1.84 mmol) dissolved in THF (2.0 mL), was added dropwise to stirring solution of pyridin-2-yllithium at -78 °C. The mixture was stirred for 20 min. and then slowly warmed to room temperature. Reaction was stirred for 2 h, then quenched with sat. aqueous NH₄Cl. The mixture was extracted with EtOAc, and the organic layers combined and washed with sat. aqueous NaCl and dried over Na₂SO₄. Concentration *in vacuo* provided the crude product, which was purified by flash column chromatography (9:1 CH₂Cl₂/MeOH) to provide the desired product as a white solid in 599 mg (93%): ¹H NMR (400 MHz, CDCl₃) δ (ppm): 8.51 (1H, d, *J* = 4.7 Hz), 7.66 (1H, t, *J* = 8.1 Hz), 7.30-7.17 (7H, m), 5.66 (1H, br s), 3.45 (2H, d, *J* = 2.0 Hz), 2.90 (2H, m), 2.62 (1H, quintet, *J* = 8.5 Hz), 1.97-1.61 (8H, m), 1.47 (4H, m), 1.14 (2H, m), 0.69 (1H, m); ¹³C NMR (125.8 MHz, CDCl₃) δ (ppm): 162.1, 146.9, 138.5, 136.3, 129.3, 128.2, 127.0, 121.9, 121.2, 78.3, 63.5, 54.5, 54.3, 46.0, 45.8, 27.9, 27.1, 26.6, 26.5, 26.2, 25.7; HRMS (ES⁺, M+H) calc'd for C₂₃H₃₁N₂O: 351.2436, found: 351.2433

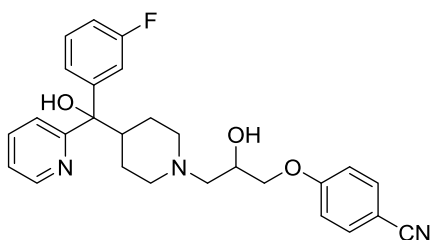


4-(3-(4-(cyclopentyl(hydroxy)(pyridin-2-yl)methyl)piperidin-1-yl)propoxy)benzenesulfonamide (4.31)

In a Parr vessel, (1-benzylpiperidin-4-yl)(cyclopentyl)(pyridin-2-yl)methanol (500 mg, 1.84 mmol) was dissolved in EtOH (10 mL). The solution was degassed by bubbling Argon through the solution for 10 min. Pd(OH)₂ was then added and the vessel was quickly inserted into the Parr Shaker apparatus. The system was purged with H₂ three times, and H₂ pressure was then set to 70 psi. The vessel was heated to 50 °C, and shaken for 12-24 h. When the reaction progress was complete by LCMS, the mixture was filtered through a celite pad and washed with EtOH. The filtrate was concentrated *in vacuo* to yield the crude product, which was carried forward to the next step.

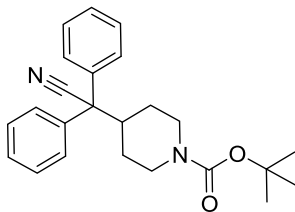
Cyclopentyl(piperidin-4-yl)(pyridin-2-yl)methanol (30 mg, 0.12 mmol) was dissolved in DMF (1.0 mL). 4-(3-chloropropoxy)benzenesulfonamide (29 mg, 0.12 mmol) and K₂CO₃ (32 mg, 0.23 mmol) were added and reaction was warmed to 50 °C. Stirring was continued overnight. The reaction mixture was quenched with aqueous NH₄Cl. The mixture was extracted with EtOAc, and the organic layers combined and washed with sat. aqueous NaCl and dried over Na₂SO₄. Concentration *in vacuo* provided the crude product, which was purified by RP-HPLC to provide the desired product as a white solid in 23 mg (42%): ¹H NMR (500 MHz, CDCl₃) δ (ppm): 8.45 (1H, d, *J* = 4.7 Hz), 7.80 (2H, d, *J* = 8.4 Hz), 7.65 (1H, t, *J* = 7.8 Hz), 7.27 (1H, d, *J* = 7.8 Hz), 7.17 (1H, t, *J* = 6.1 Hz), 6.90 (2H, d, *J* = 7.8 Hz), 5.66 (1H, br s), 5.06 (2H, br s), 3.98 (2H, t, *J* = 6.4 Hz),

2.98 (1H, d, $J = 10.2$ Hz), 2.91 (1H, d, $J = 10.2$ Hz), 2.58 (1H, m), 2.44 (2H, m), 1.96-1.69 (8H, m), 1.60-1.42 (6H, m), 1.12 (2H, m), 0.69 (1H, m); ^{13}C NMR (125.8 MHz, CDCl_3) δ (ppm): 162.4, 161.8, 147.0, 136.5, 133.8, 128.6, 122.0, 121.2, 114.8, 78.3, 66.9, 55.2, 54.5, 54.4, 45.8, 45.7, 27.6, 27.1, 26.6, 26.5, 26.4, 26.1, 25.7; HRMS (ES+, M+H) calc'd for $\text{C}_{25}\text{H}_{36}\text{N}_3\text{O}_4\text{S}$: 474.2427, found: 474.2430



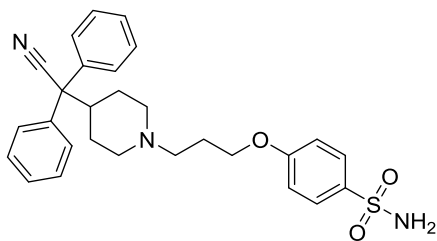
4-(3-(4-((3-fluorophenyl)(hydroxy)(pyridin-2-yl)methyl)piperidin-1-yl)-2-hydroxypropoxy)benzonitrile (4.41)

In a round bottom flask with stir bar, amine **4.39** (0.47 g, 1.22 mmol), was dissolved in MeCN (6.08 mL) To the stirring solution was added K_2CO_3 (0.252 g, 1.82 mmol) in a single batch. After 5 minutes stirring, epoxide **4.40** (0.426 g, 2.43 mmol) was added at room temperature. The mixture was then heated to 40 °C and stirring continued 2h. The reaction mixture was then filtered and eluted with EtOAc, and the filtrate was concentrated *in vacuo* to give a white solid, which was purified by flash column chromatography (1:1 Hex/EtOAc) to provide the desired product as a white powder in 300 mg (54%).



tert-butyl 4-(cyanodiphenylmethyl)piperidine-1-carboxylate (4.42)

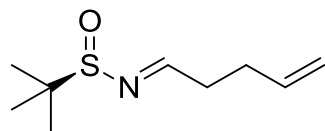
tert-butyl 4-bromopiperidine-1-carboxylate (1.00 g, 3.78 mmol) and 2,2-diphenylacetonitrile (1.23 g, 6.34 mmol) was dissolved in THF (10.6 mL), and t-BuOK (0.71 g, 6.34 mmol) was carefully added. Reaction was stirred at ambient temperature overnight and monitored by LCMS. After completion, the reaction was quenched with H₂O and extracted three times with EtOAc. The organic layers were washed with brine, dried over Na₂SO₄, and concentrated *in vacuo*. The crude oil was purified by flash column chromatography (4:1 Hex/EtOAc) to provide product as white gummy powder in 1.11 g (75%)



4-(3-(4-(cyanodiphenylmethyl)piperidin-1-yl)propoxy)benzenesulfonamide (4.43)

In a round bottom flask with stir bar, **4.42** (0.30 g, 0.80 mmol) was dissolved in 4M HCl/Dioxanes (3.98 mL, 15.94 mmol) at ambient temperature. The clear solution was stirred for 3h until reaction was complete by LCMS analysis. The solution was concentrated *in vacuo* to provide the deprotected amine as the HCl salt in quantitative yield. This product was used directly in the following step.

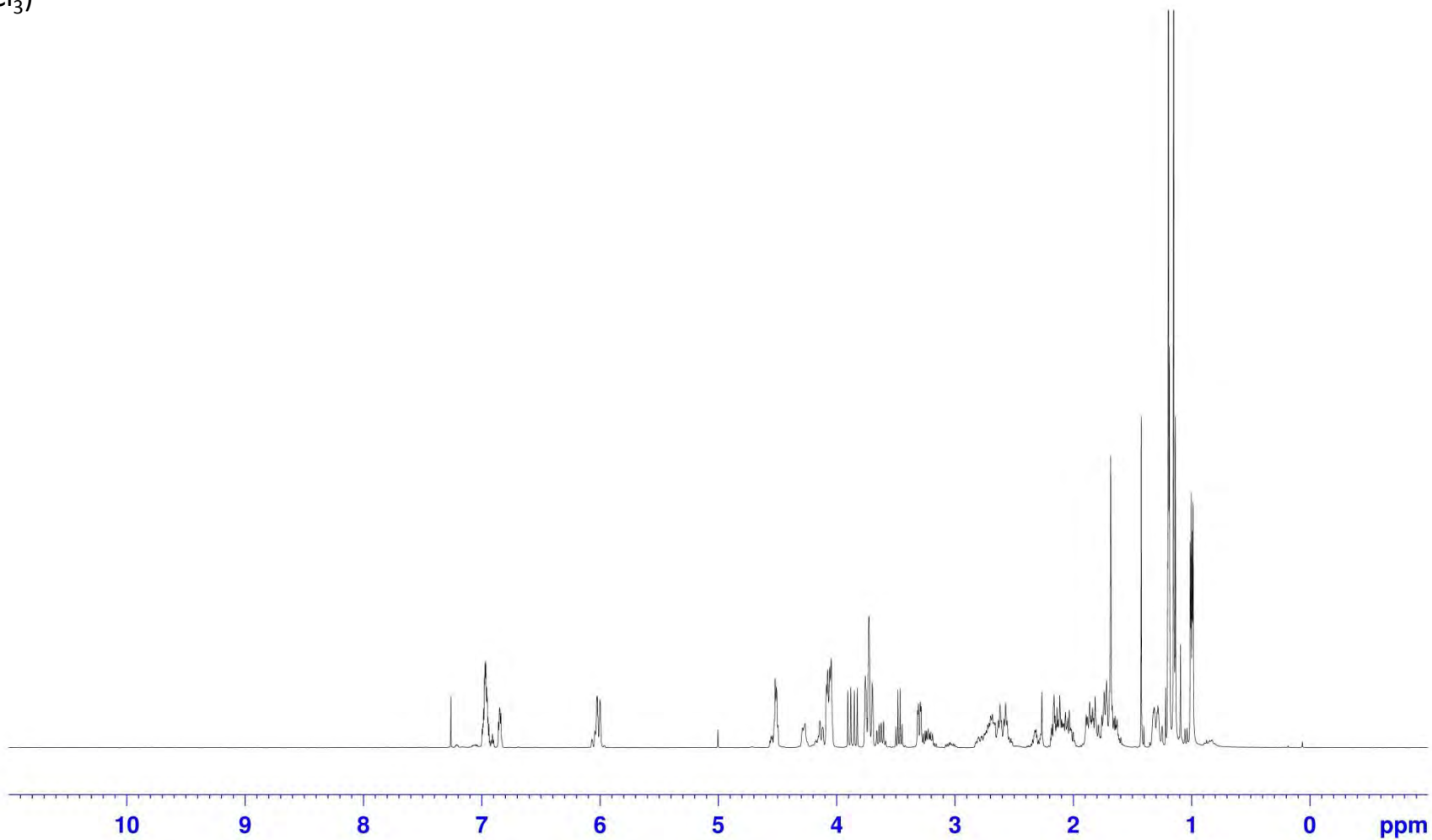
The deprotected piperidine was dissolved in DMF (4.00 mL) in a round bottom flask with stir bar. To this was added K_2CO_3 followed by 1-bromo-3-chloropropane. Reaction was heated to 40 °C and stirring continued for 4h until progress complete by LCMS analysis. At this time 4-hydroxybenzenesulfonamide was added and stirring continued at 40 °C for 16h. The mixture was then cooled to ambient temperature and filtered to remove solid K_2CO_3 and precipitants. Crude reaction mixture was purified by reverse-phase HPLC chromatography (5-95% MeCN in 5% NH_4OH/H_2O) to provide the desired product as a white crystalline solid in 0.31 g (80%).

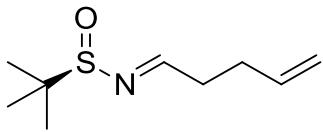


1.101

^1H NMR spectrum (400 MHz,
 CDCl_3)

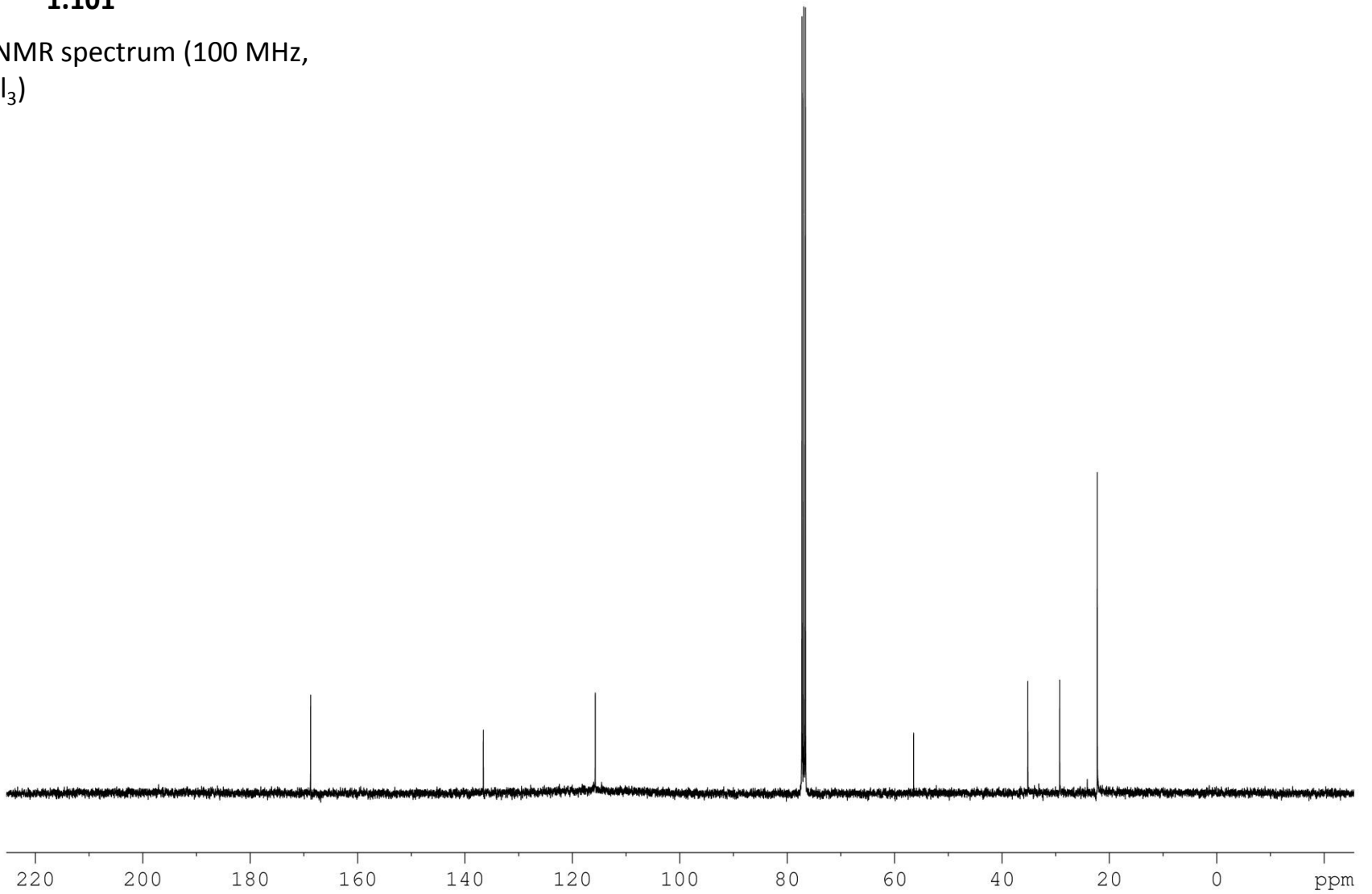
Appendix

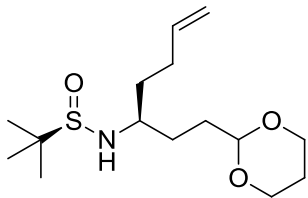




1.101

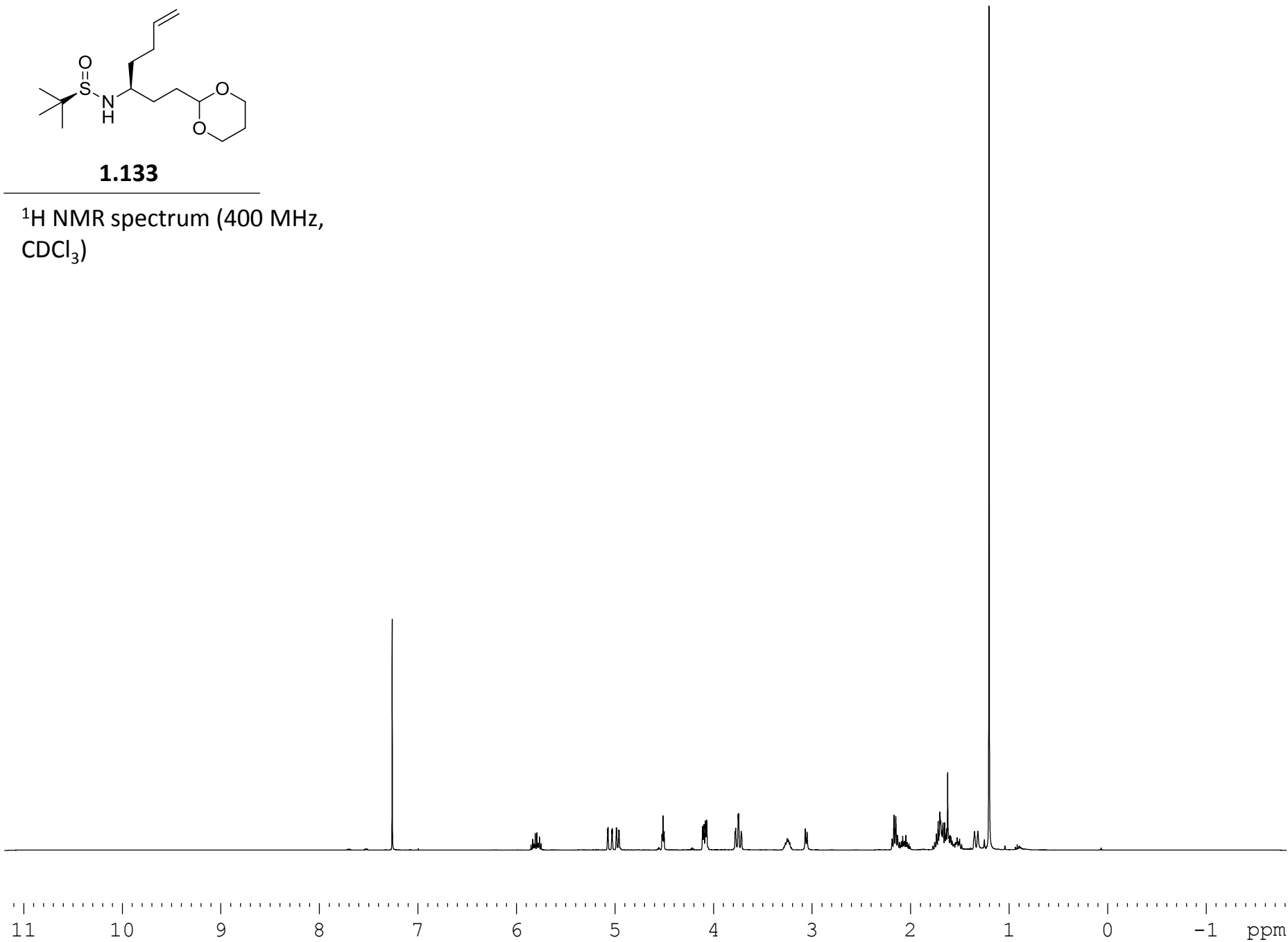
^{13}C NMR spectrum (100 MHz,
 CDCl_3)

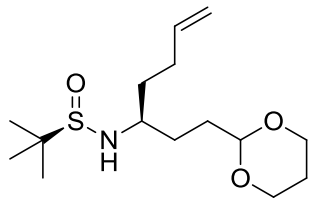




1.133

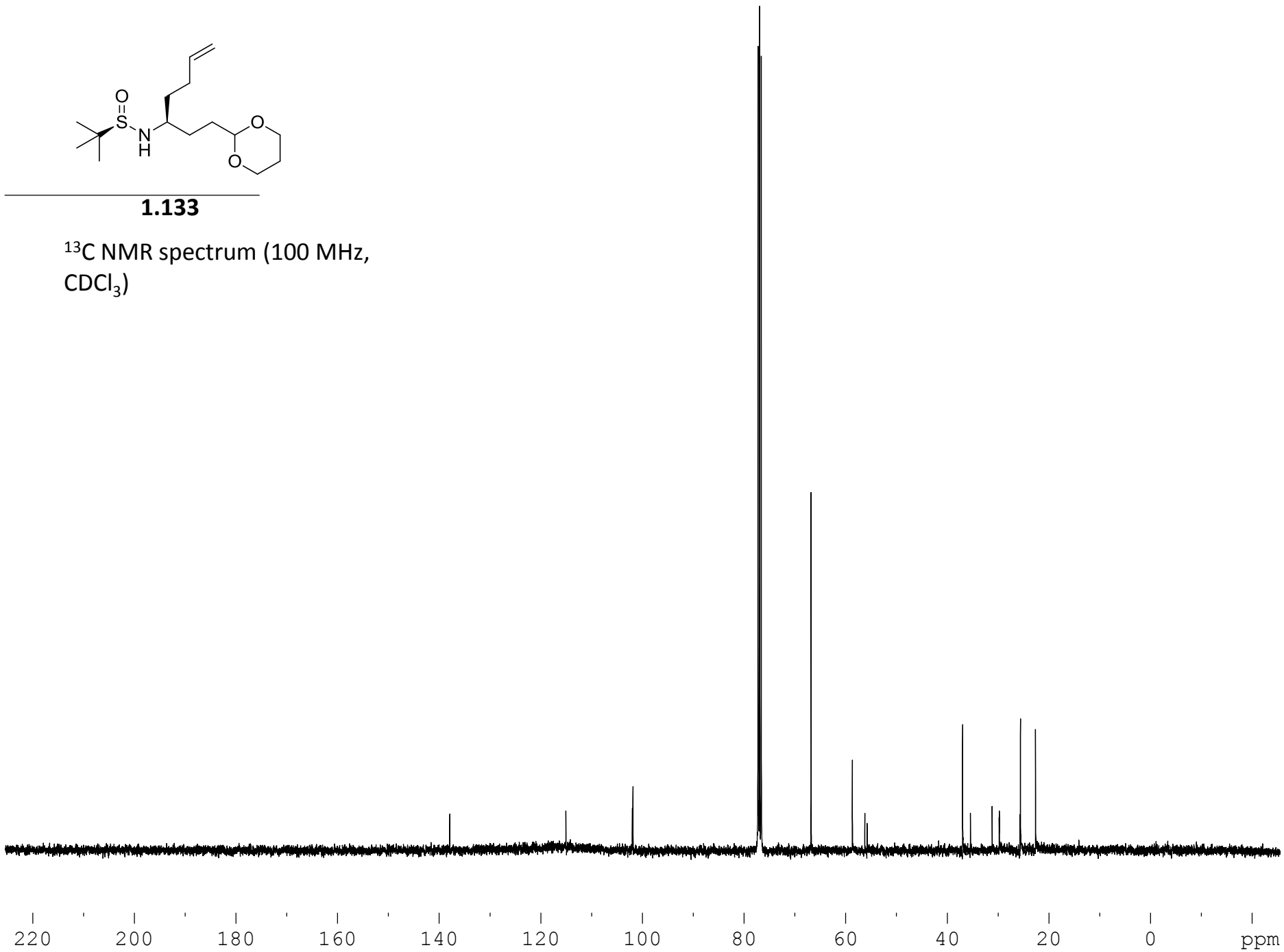
^1H NMR spectrum (400 MHz,
 CDCl_3)

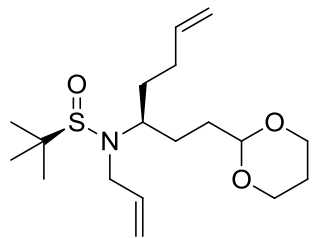




1.133

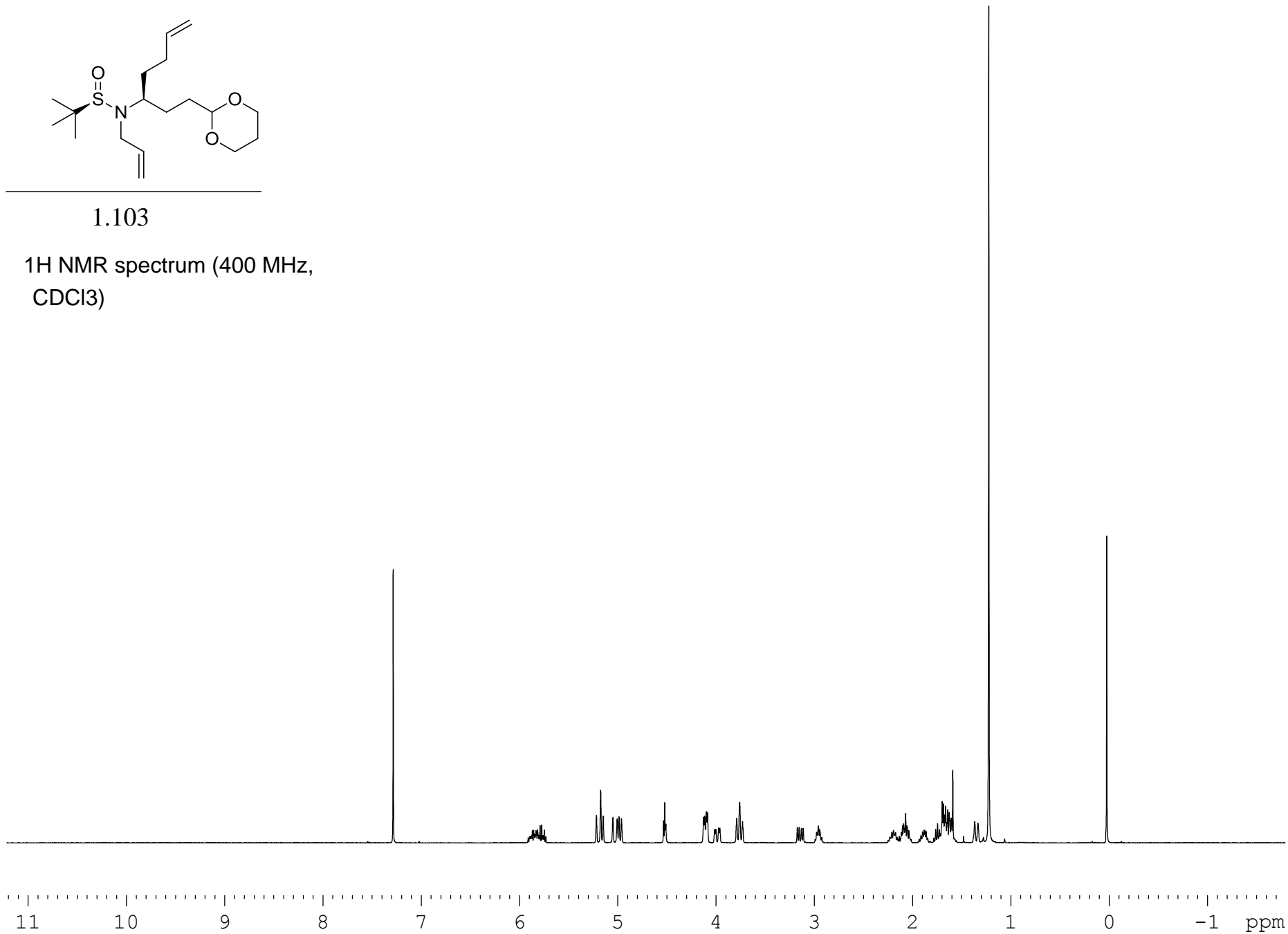
^{13}C NMR spectrum (100 MHz,
 CDCl_3)

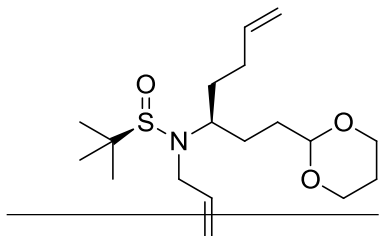




1.103

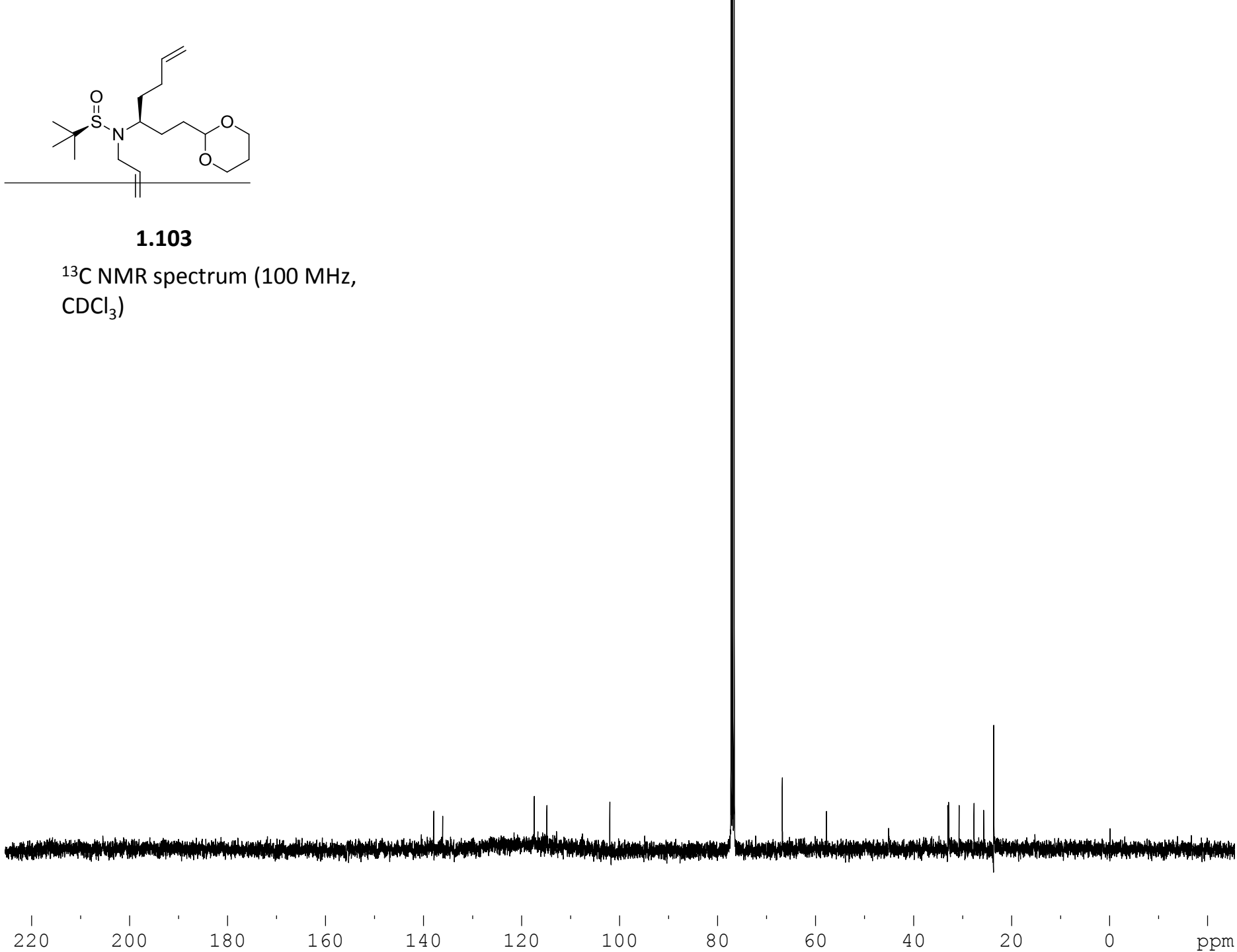
¹H NMR spectrum (400 MHz,
CDCl₃)

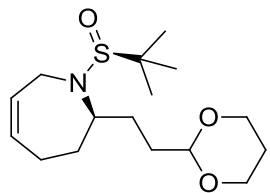




1.103

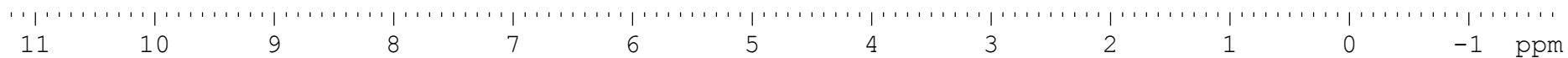
^{13}C NMR spectrum (100 MHz,
 CDCl_3)

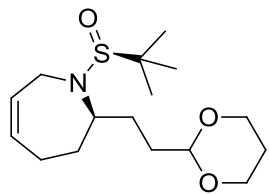




1.104

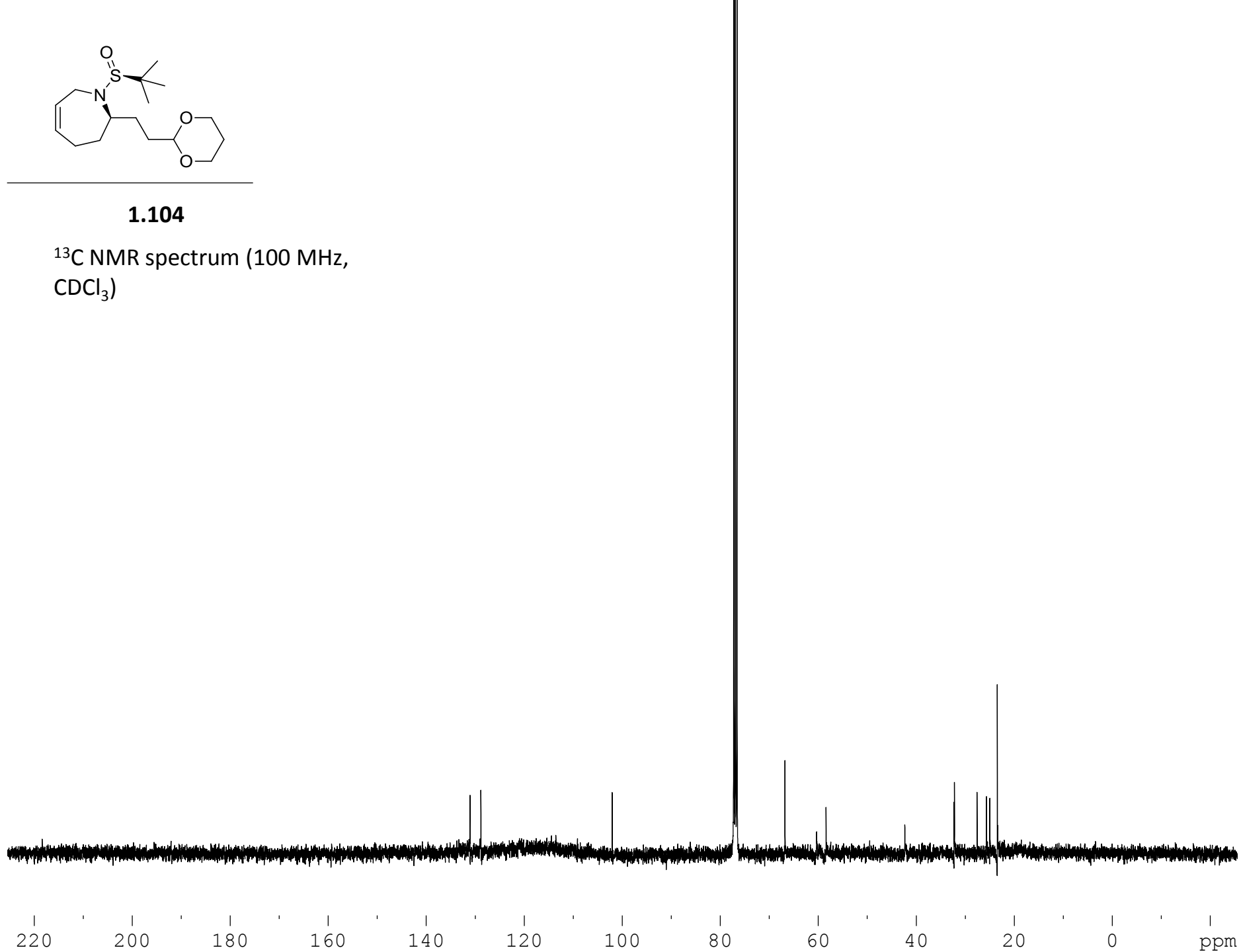
^1H NMR spectrum (400 MHz,
 CDCl_3)

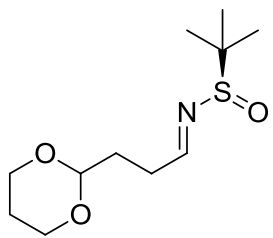




1.104

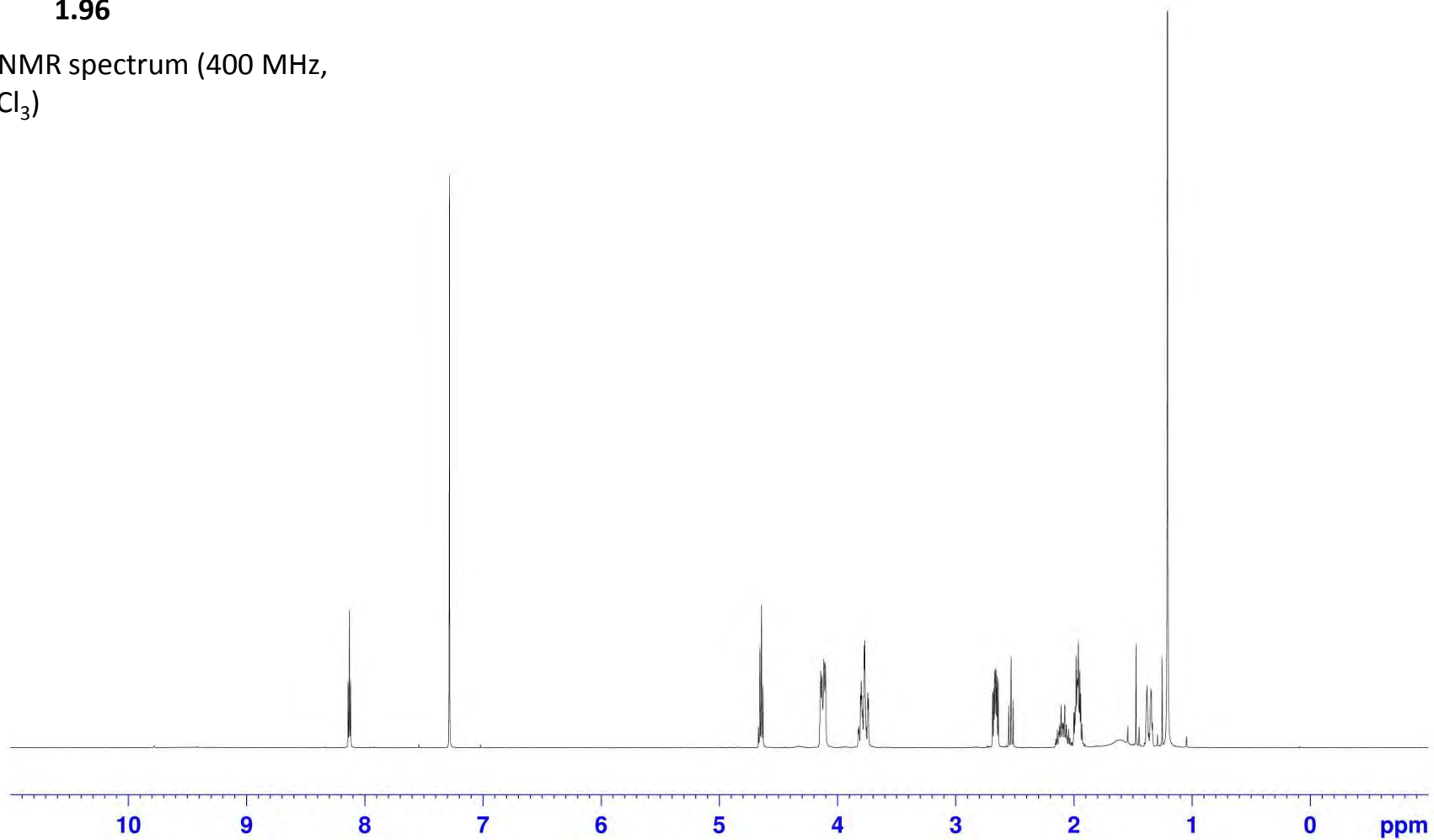
^{13}C NMR spectrum (100 MHz,
 CDCl_3)

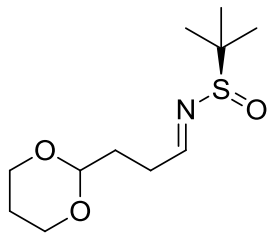




1.96

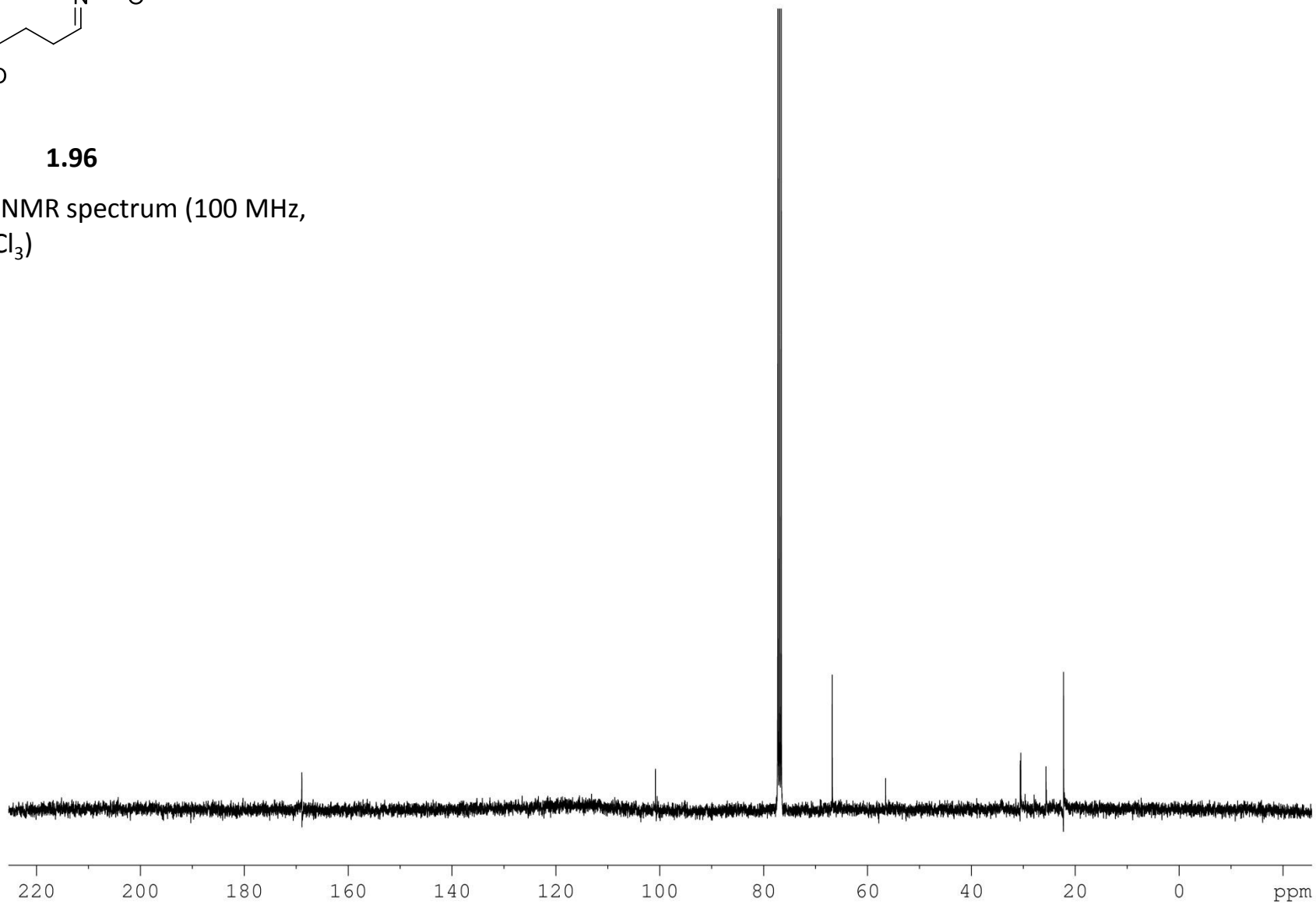
^1H NMR spectrum (400 MHz,
 CDCl_3)

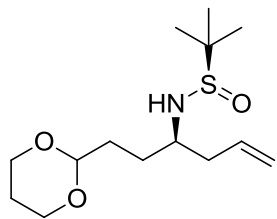




1.96

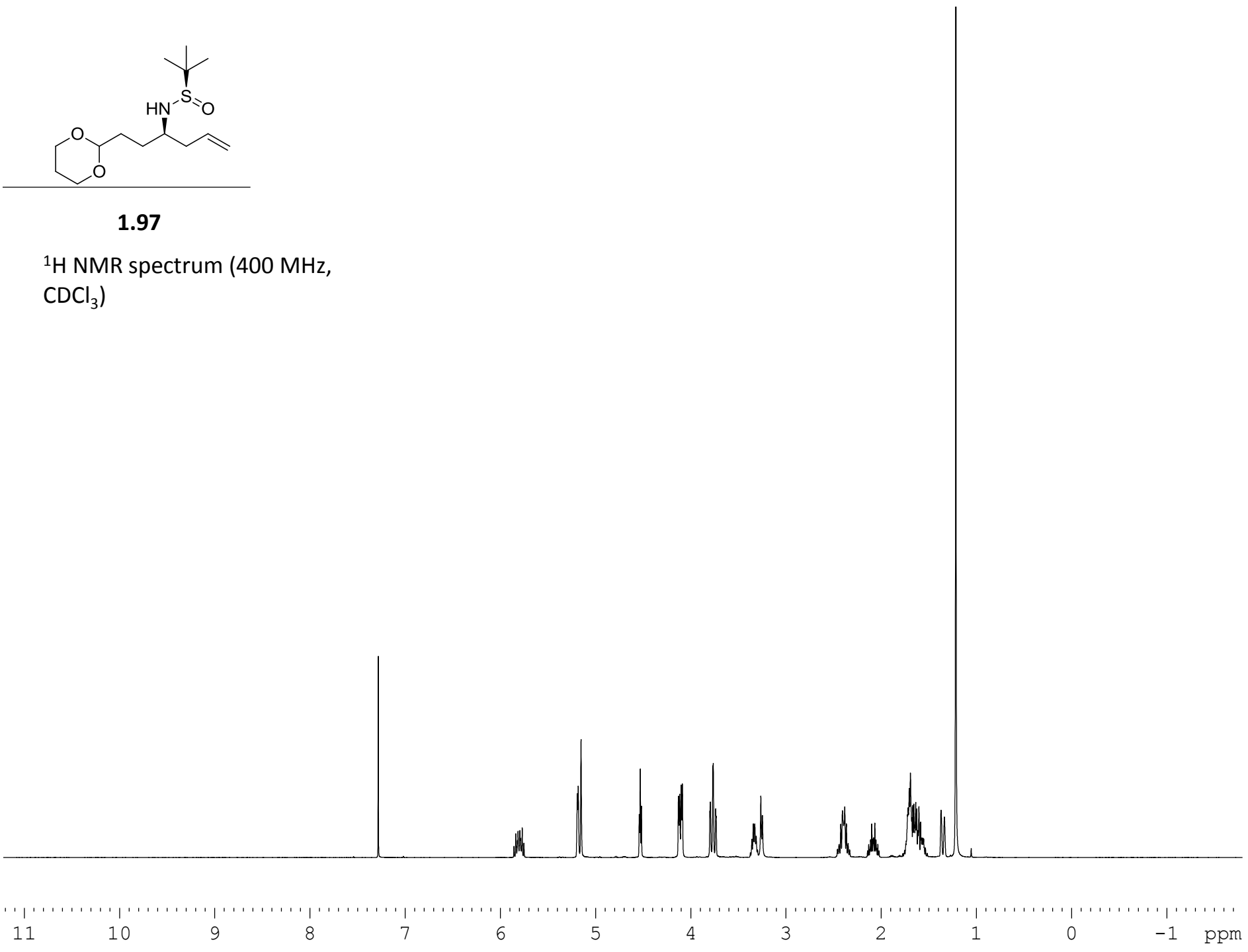
^{13}C NMR spectrum (100 MHz,
 CDCl_3)

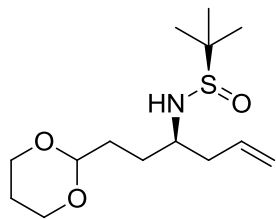




1.97

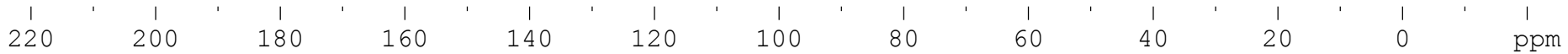
^1H NMR spectrum (400 MHz,
 CDCl_3)

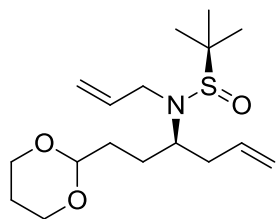




1.97

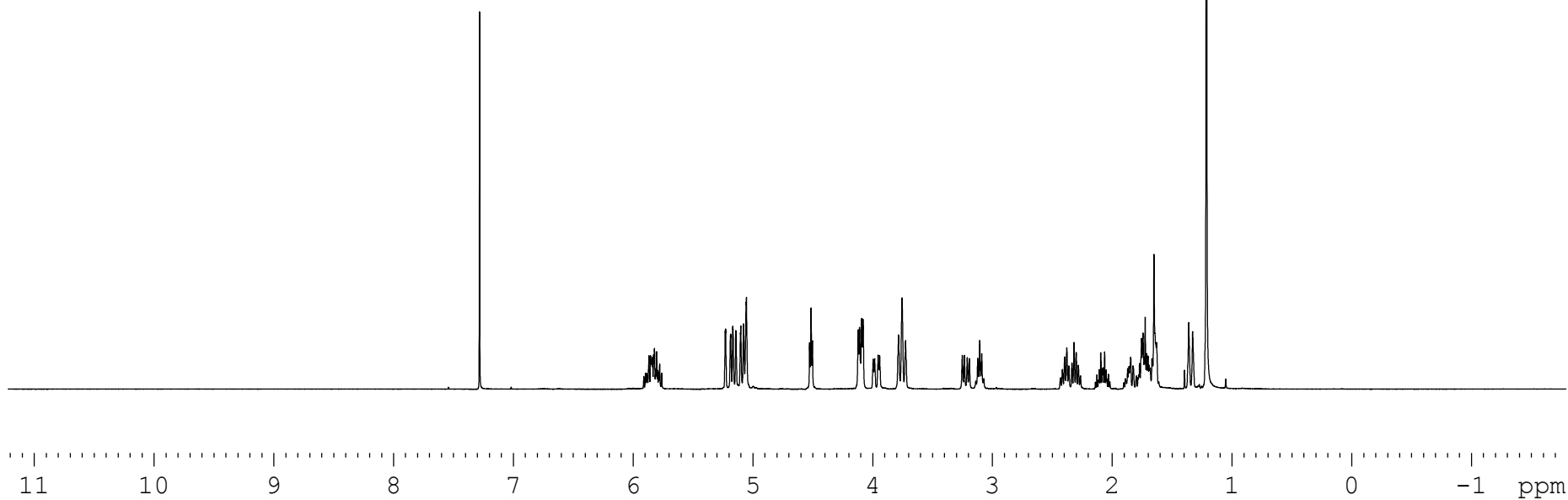
^{13}C NMR spectrum (100 MHz,
 CDCl_3)

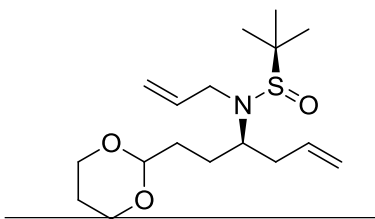




1.98

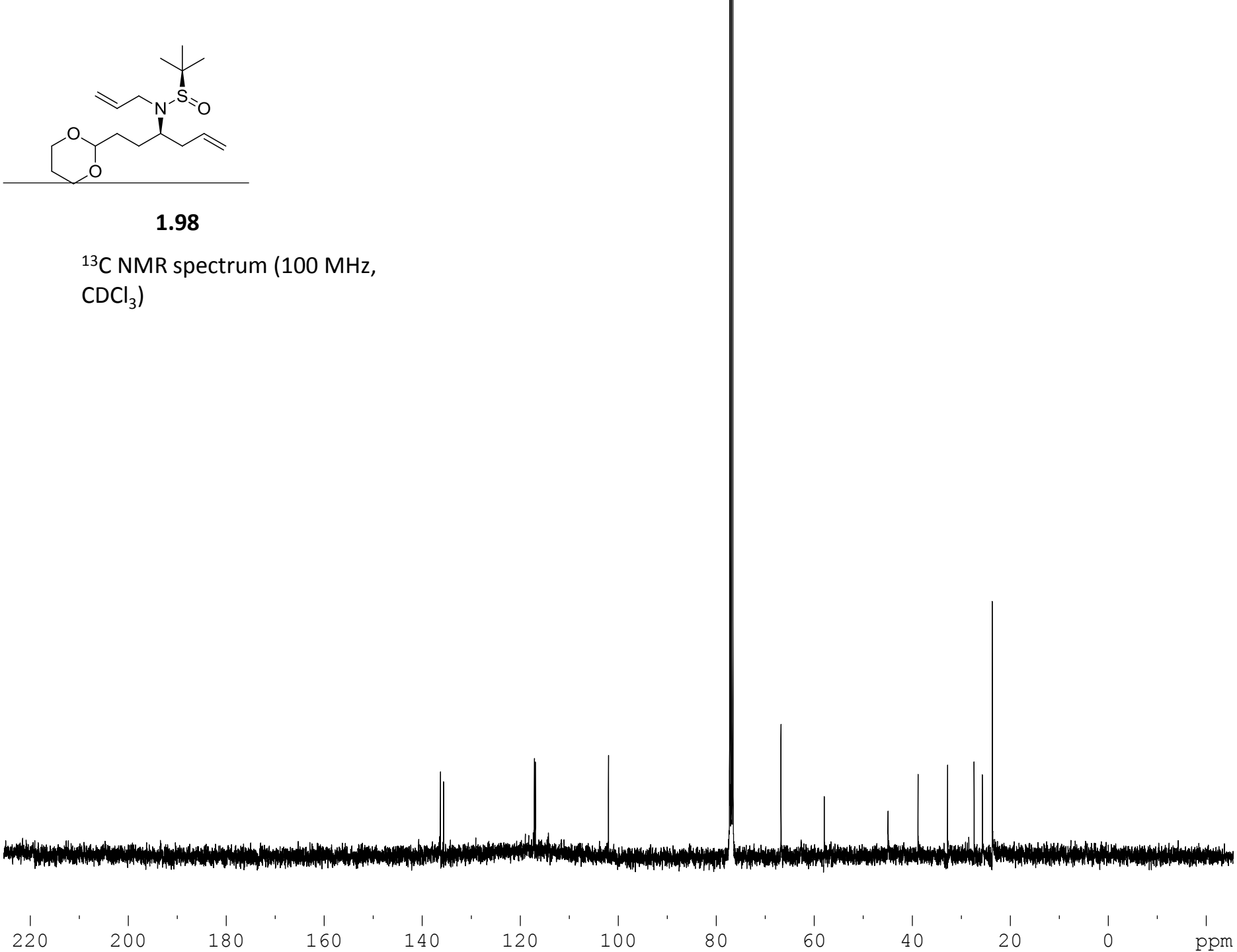
^1H NMR spectrum (400 MHz,
 CDCl_3)

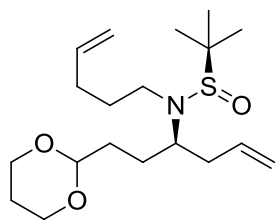




1.98

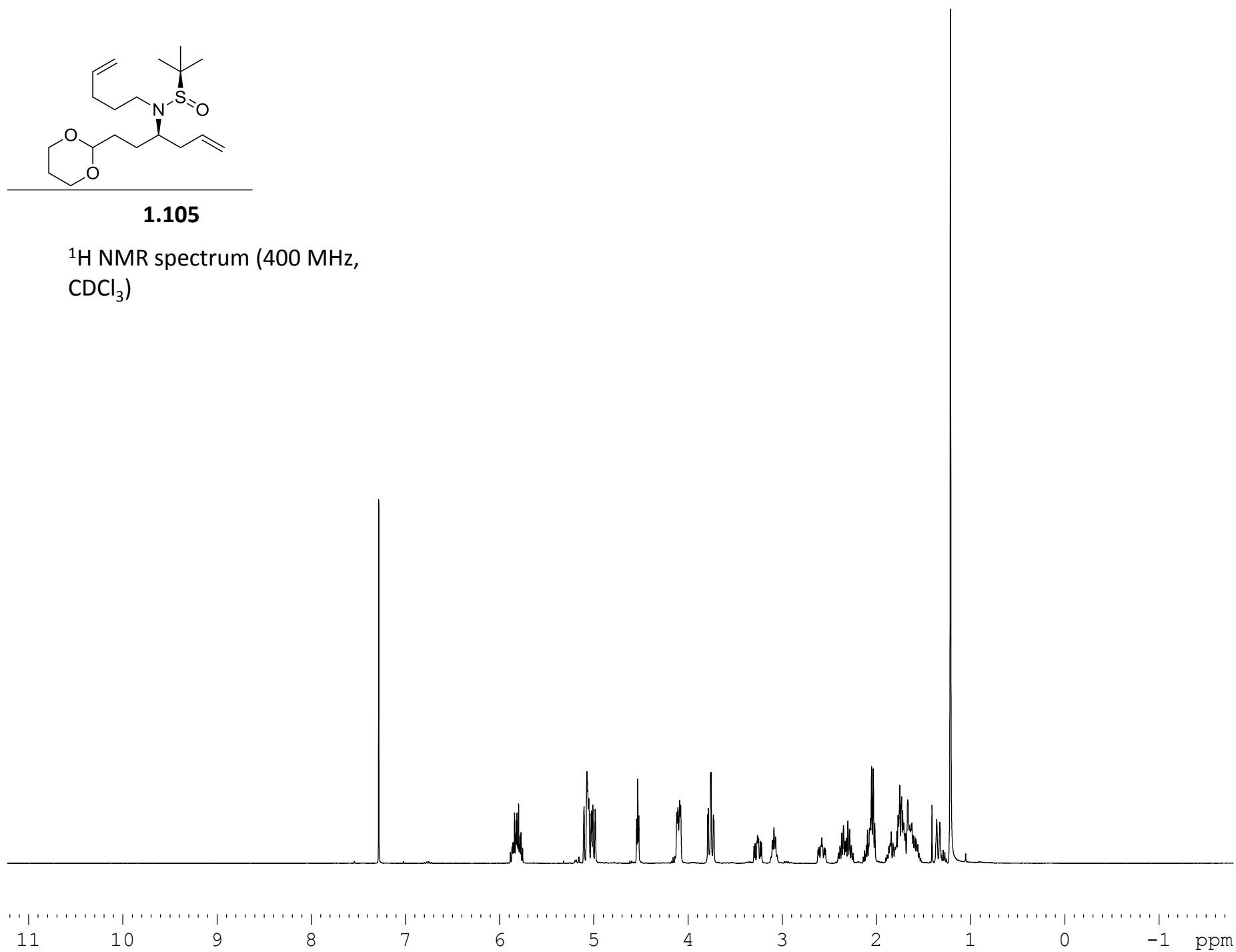
^{13}C NMR spectrum (100 MHz,
 CDCl_3)

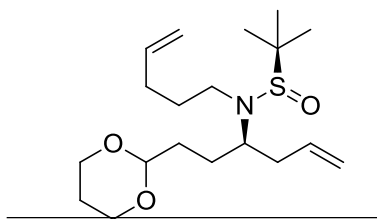




1.105

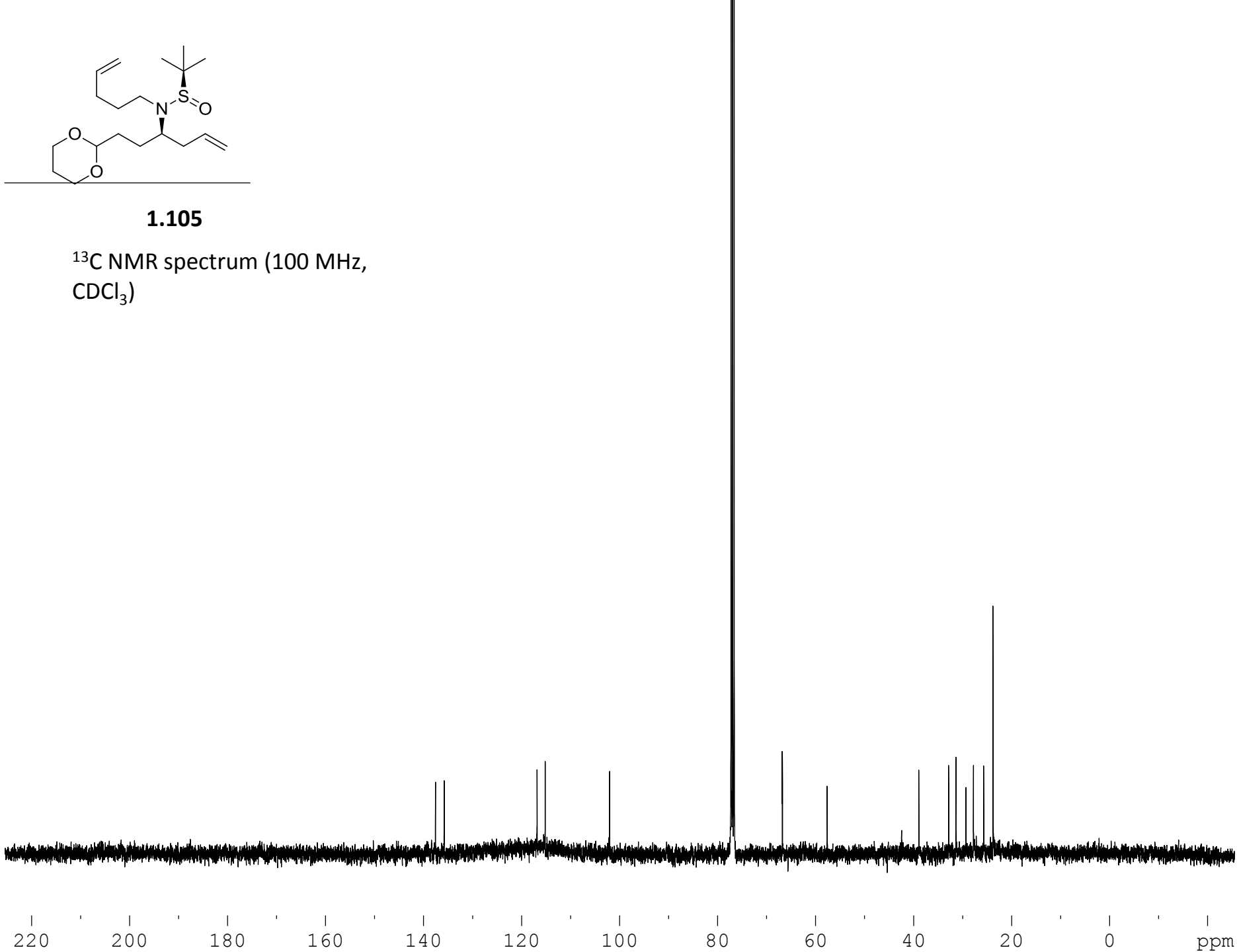
^1H NMR spectrum (400 MHz,
 CDCl_3)

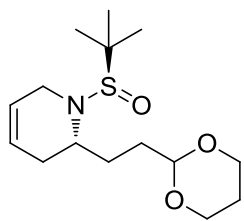




1.105

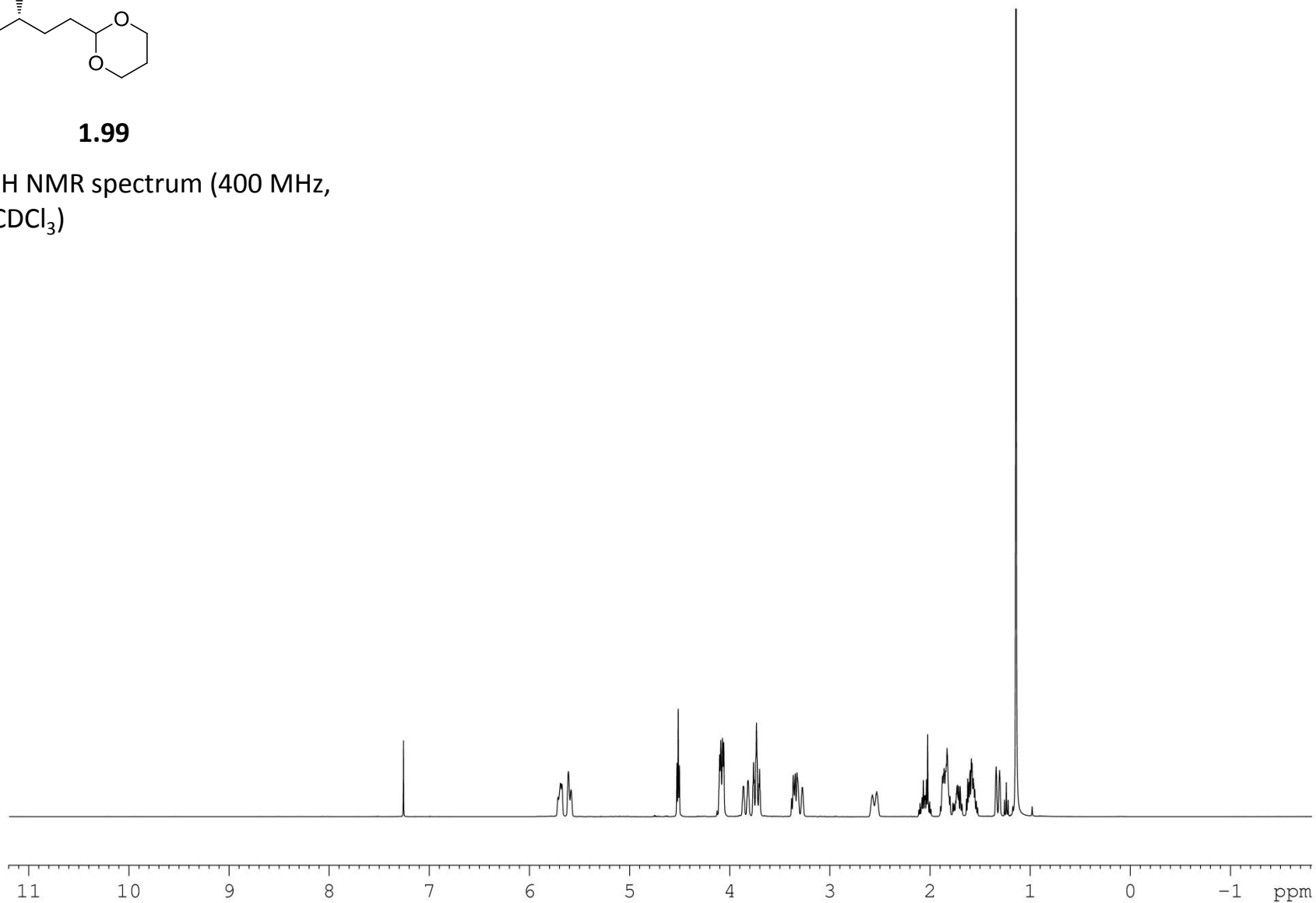
¹³C NMR spectrum (100 MHz,
CDCl₃)

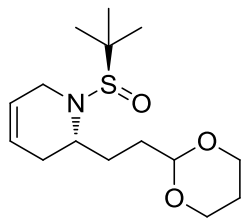




1.99

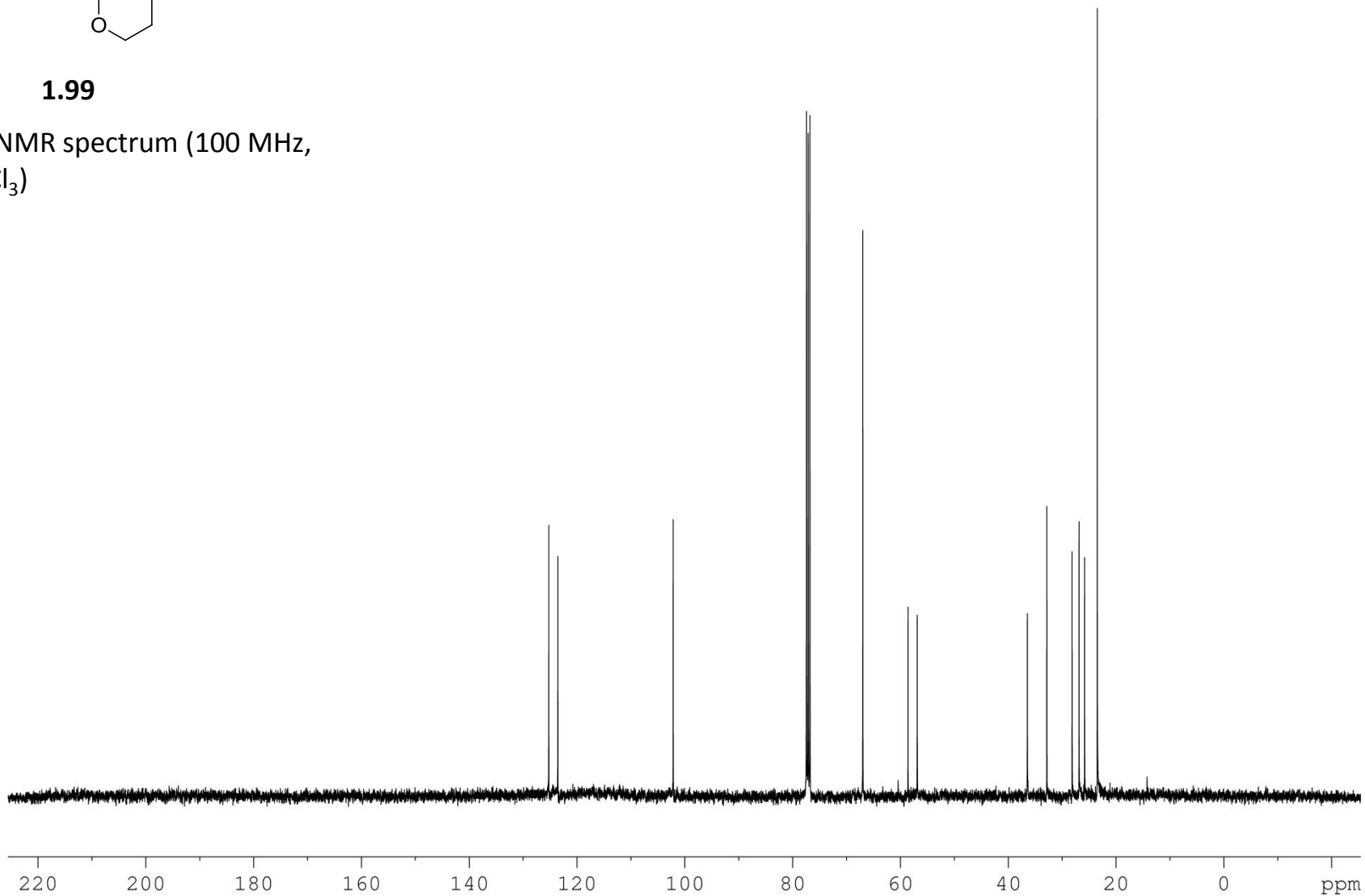
^1H NMR spectrum (400 MHz,
 CDCl_3)

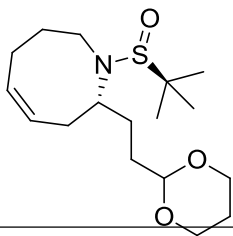




1.99

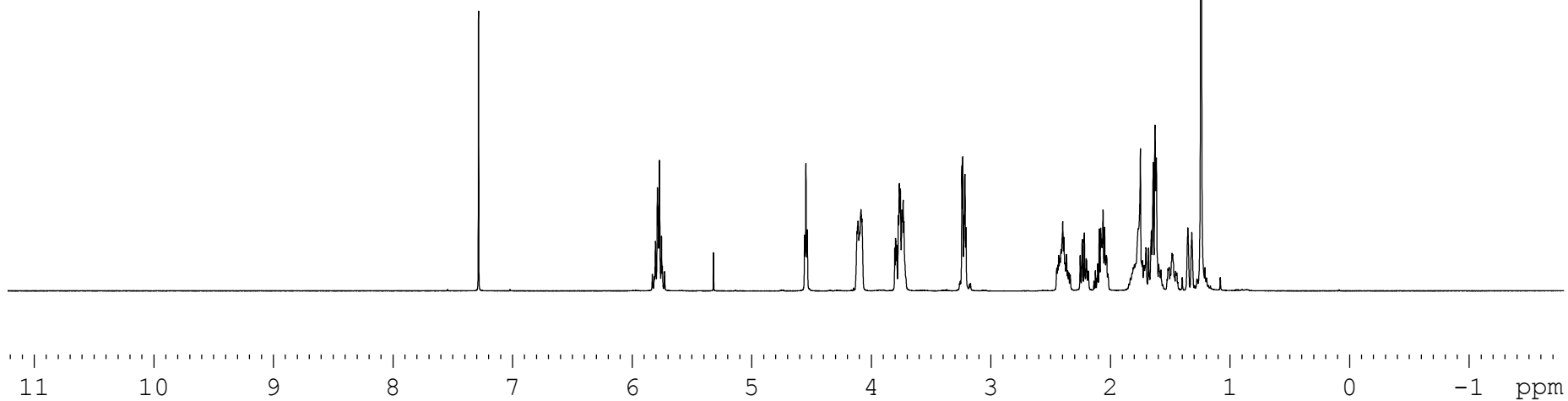
^{13}C NMR spectrum (100 MHz,
 CDCl_3)

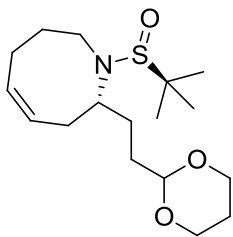




1.106

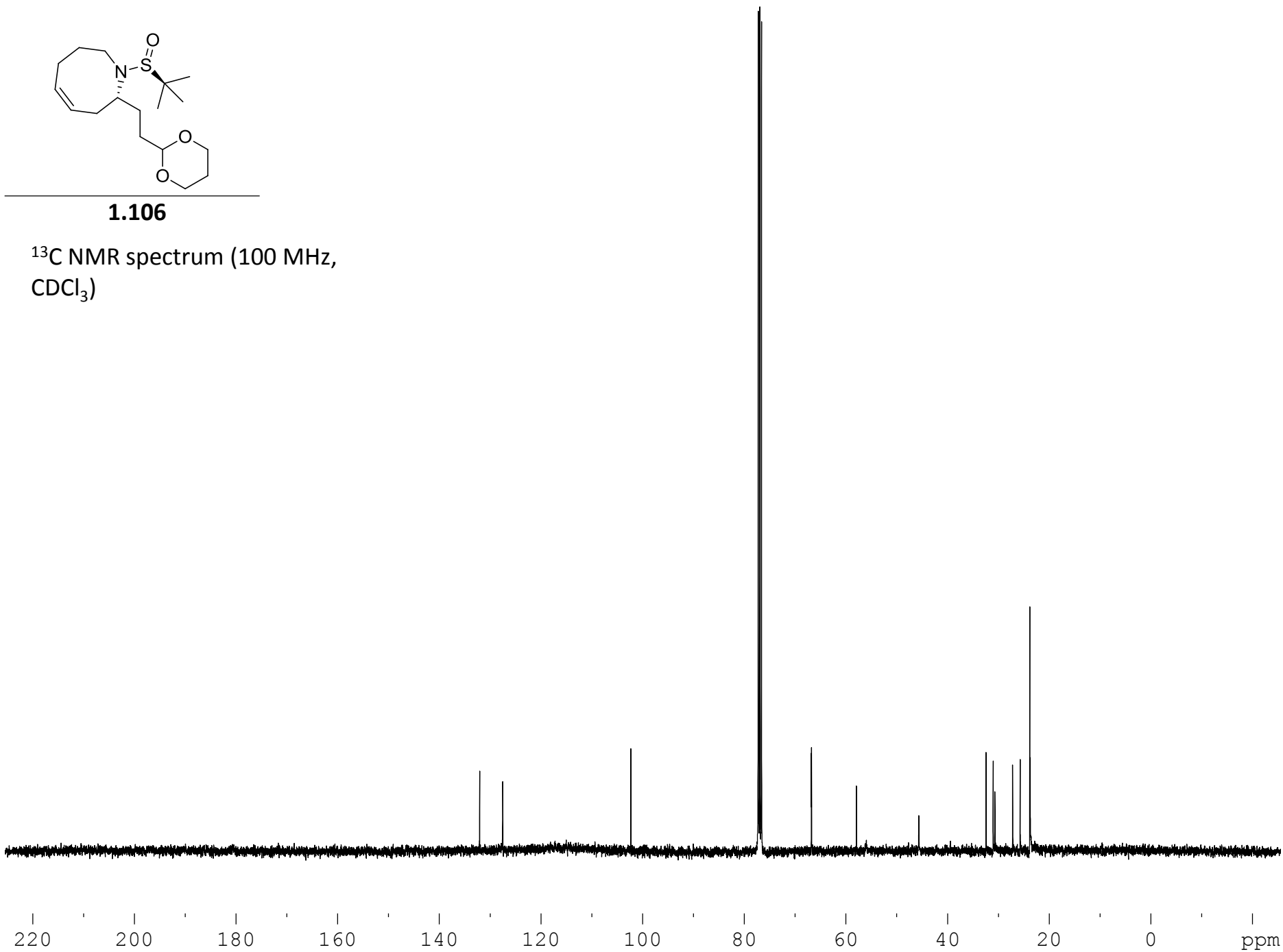
^1H NMR spectrum (400 MHz,
 CDCl_3)

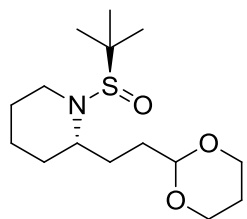




1.106

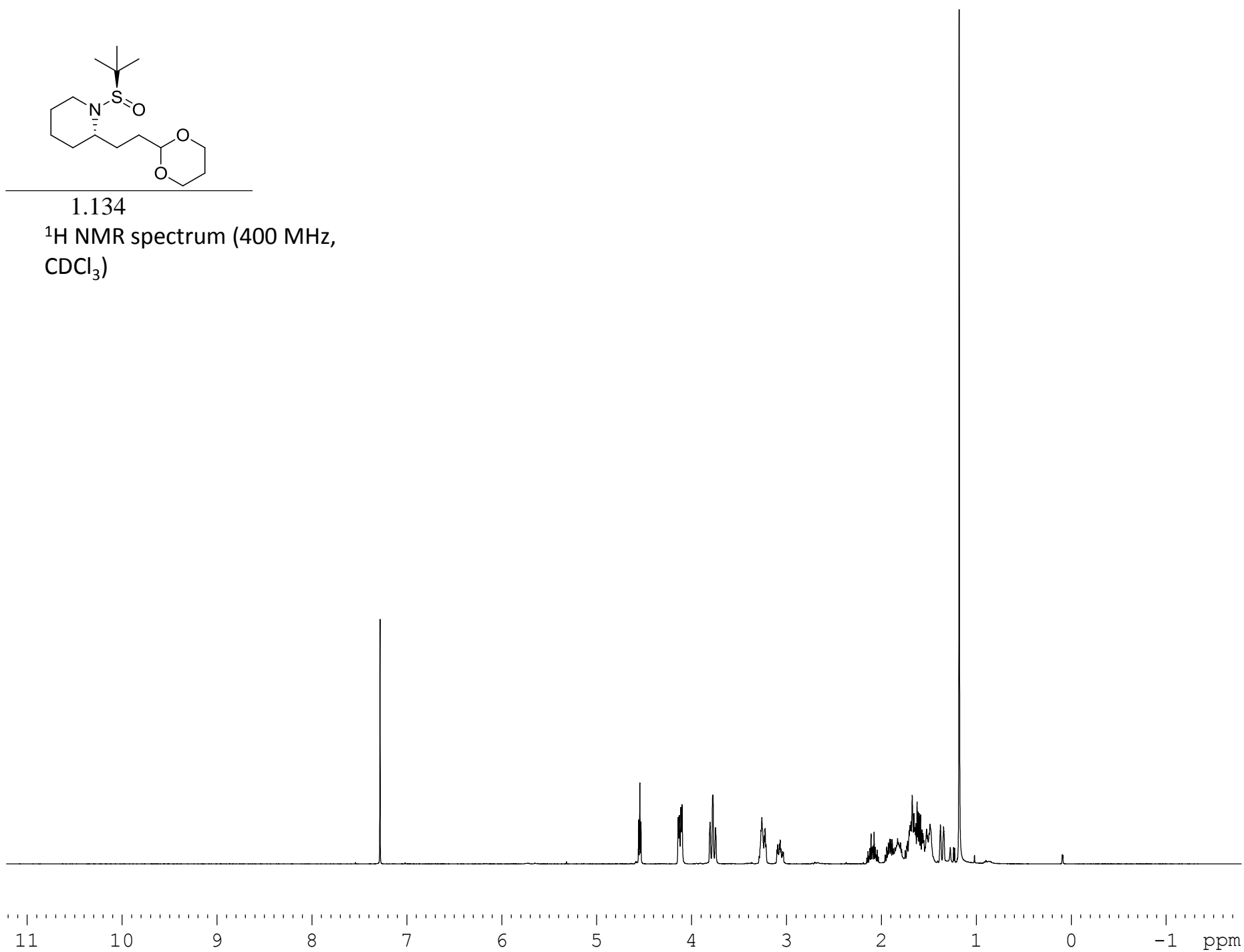
^{13}C NMR spectrum (100 MHz,
 CDCl_3)

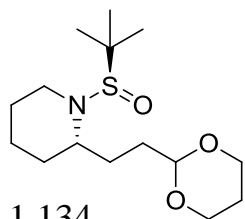




1.134

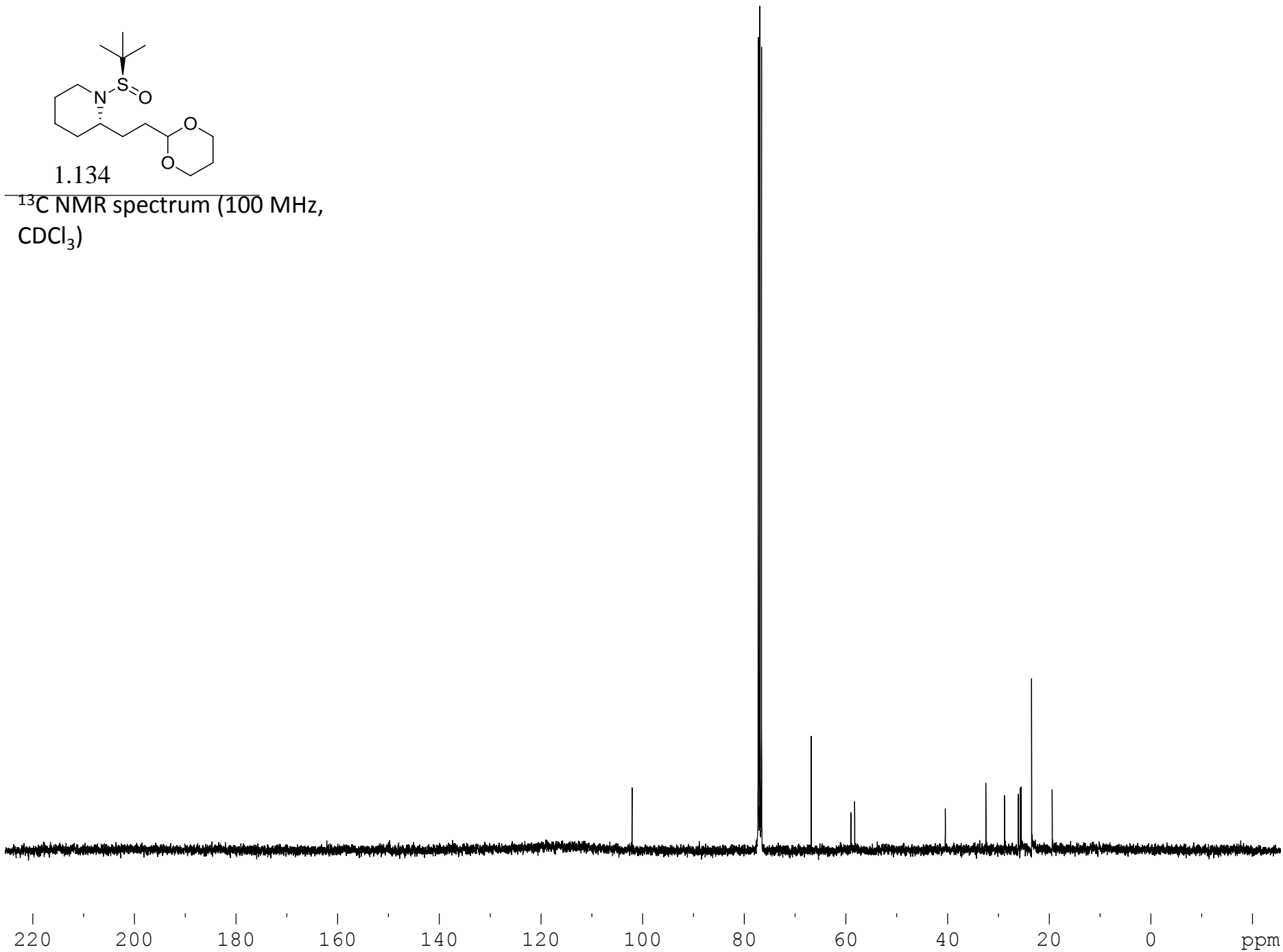
^1H NMR spectrum (400 MHz,
 CDCl_3)

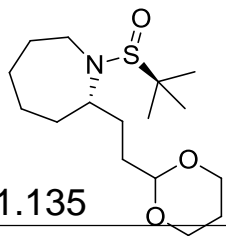




1.134

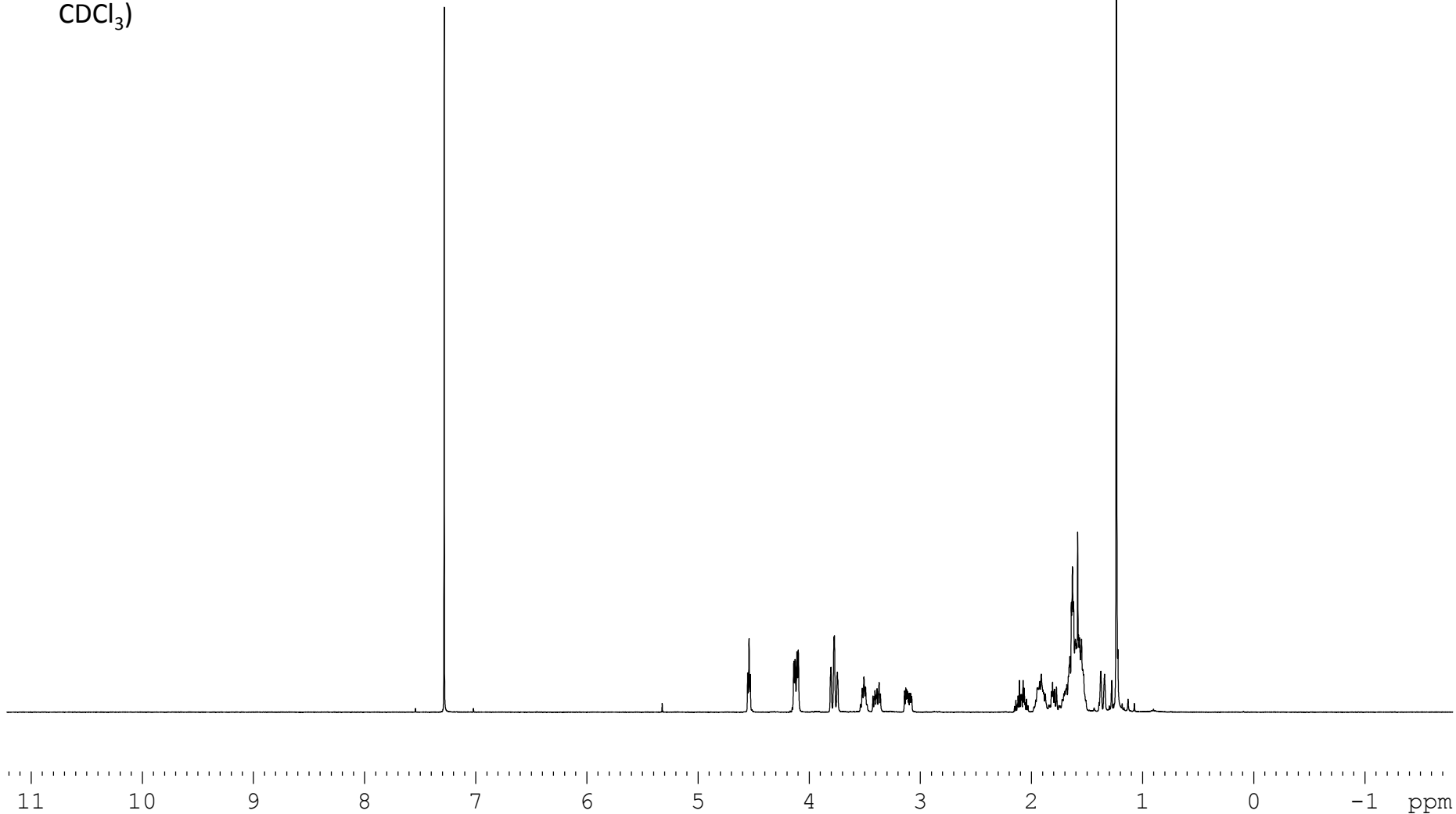
^{13}C NMR spectrum (100 MHz, CDCl_3)

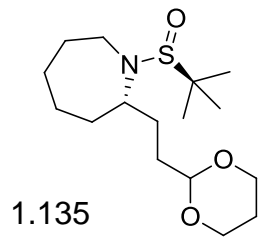




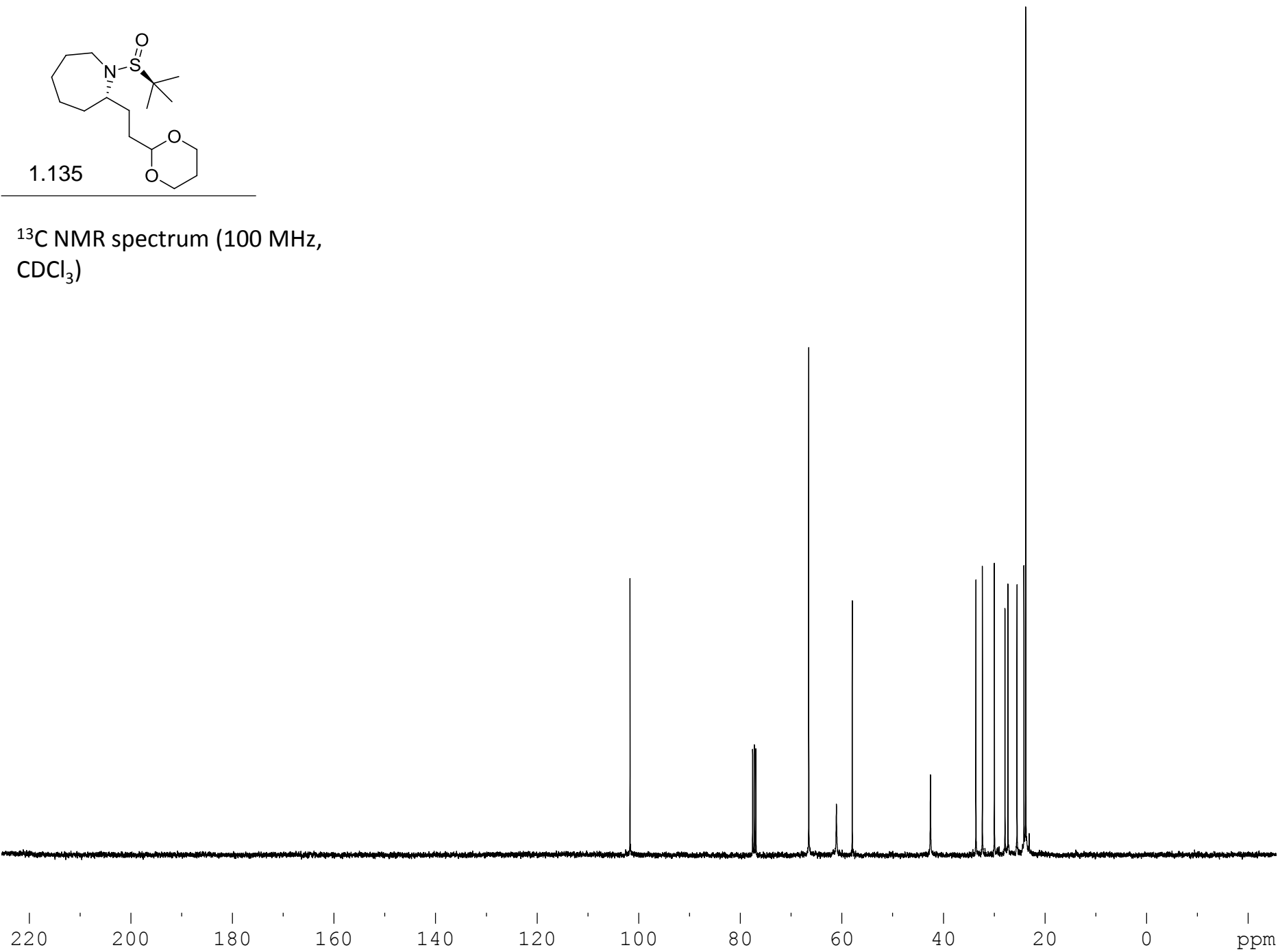
1.135

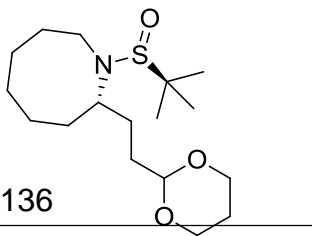
^1H NMR spectrum (400 MHz, CDCl_3)





^{13}C NMR spectrum (100 MHz,
 CDCl_3)

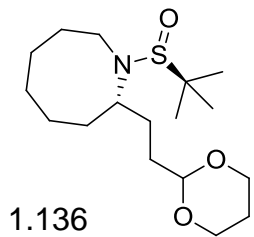




1.136

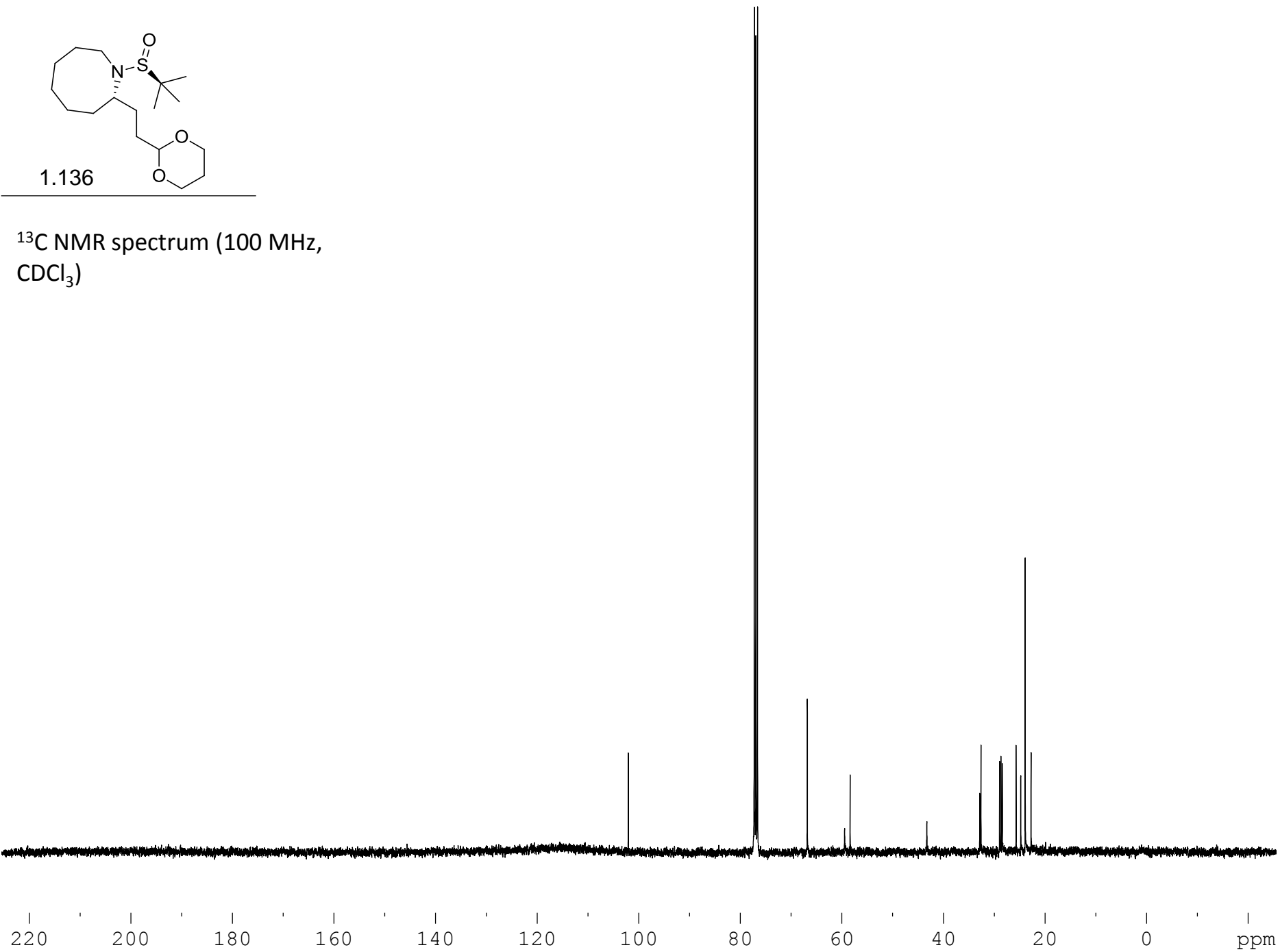
^1H NMR spectrum (400 MHz, CDCl_3)

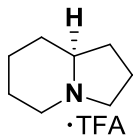




1.136

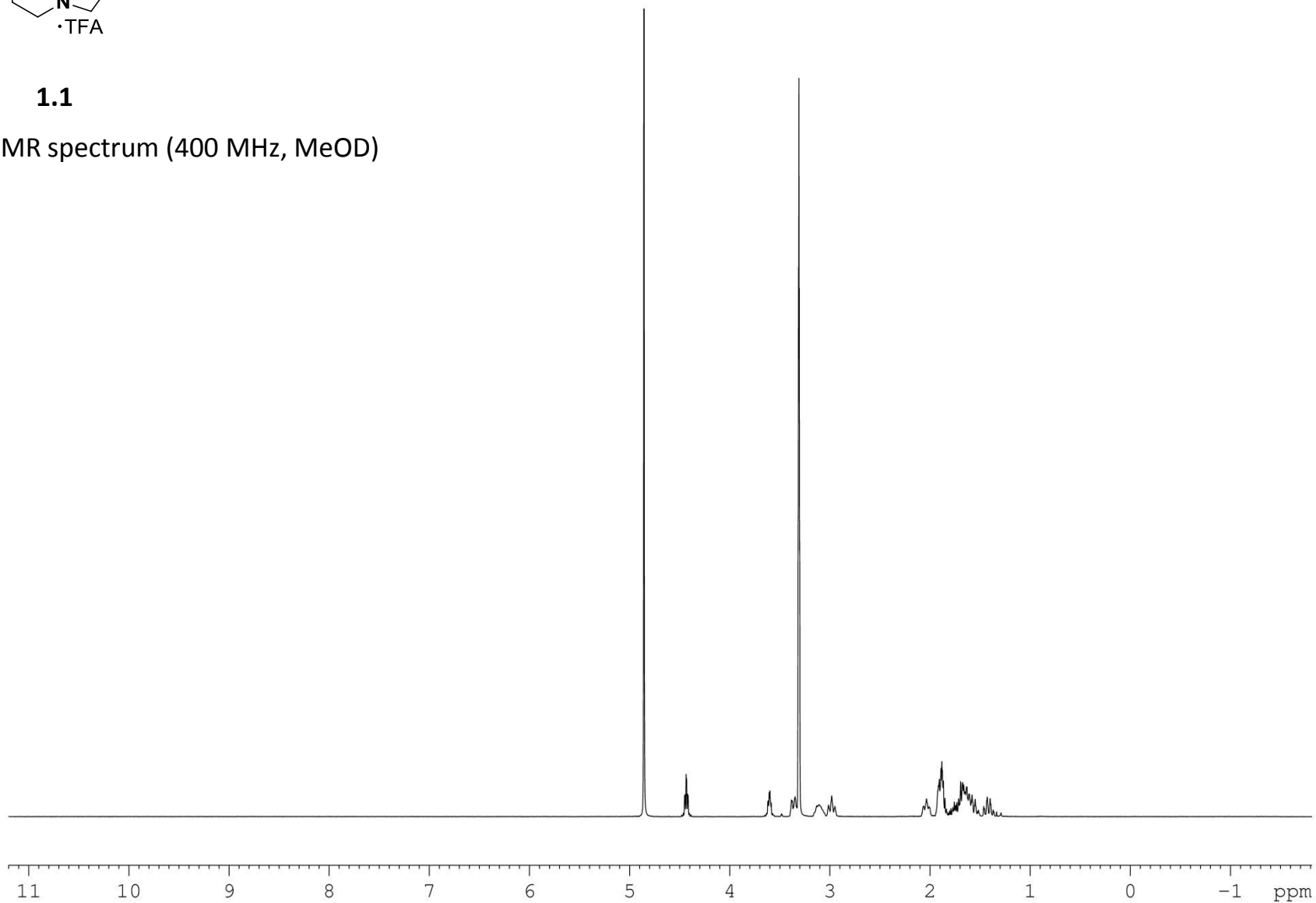
^{13}C NMR spectrum (100 MHz, CDCl_3)

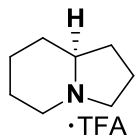




1.1

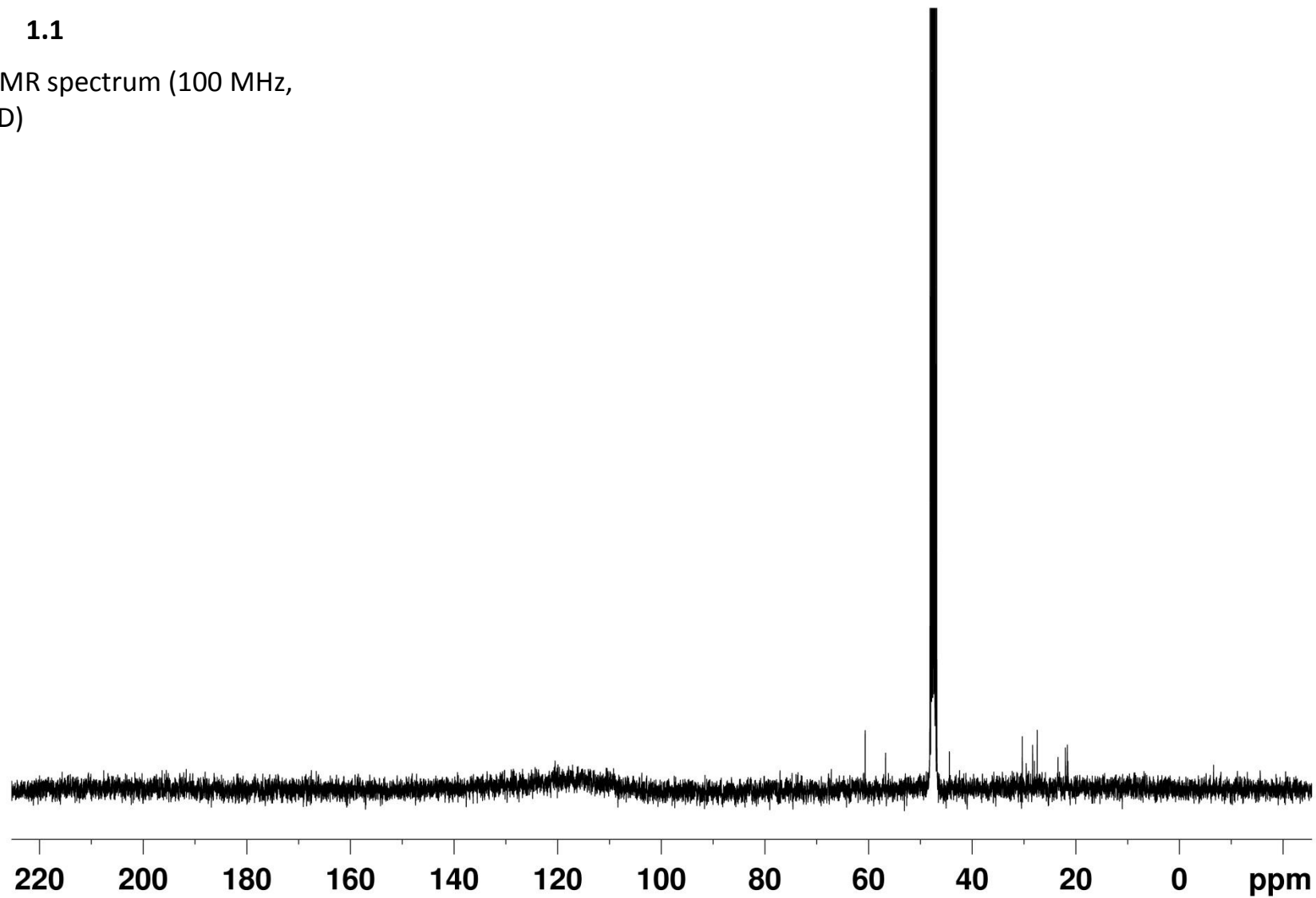
^1H NMR spectrum (400 MHz, MeOD)

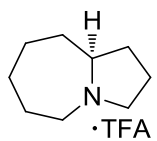




1.1

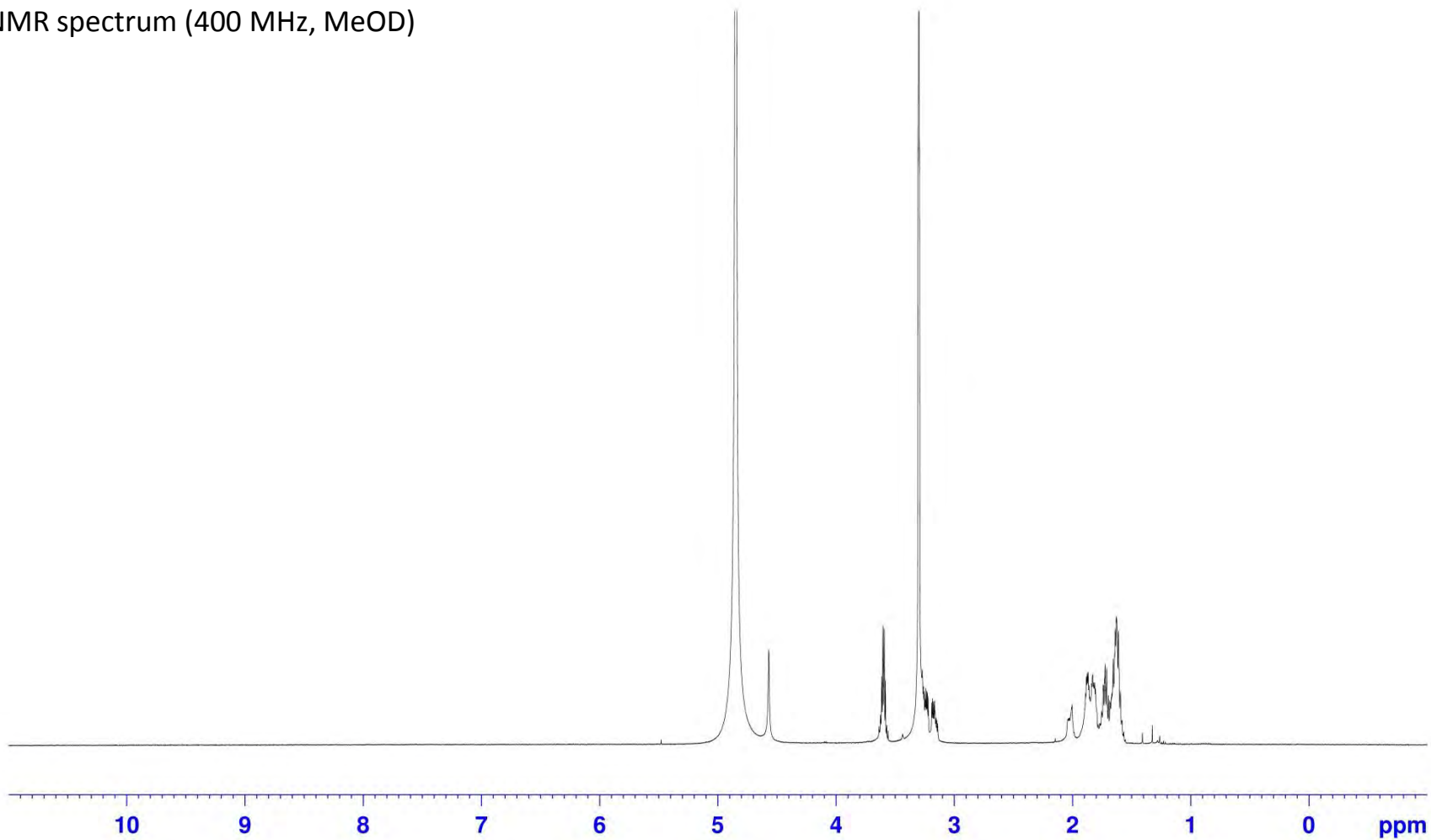
^{13}C NMR spectrum (100 MHz,
MeOD)

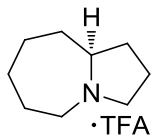




1.2

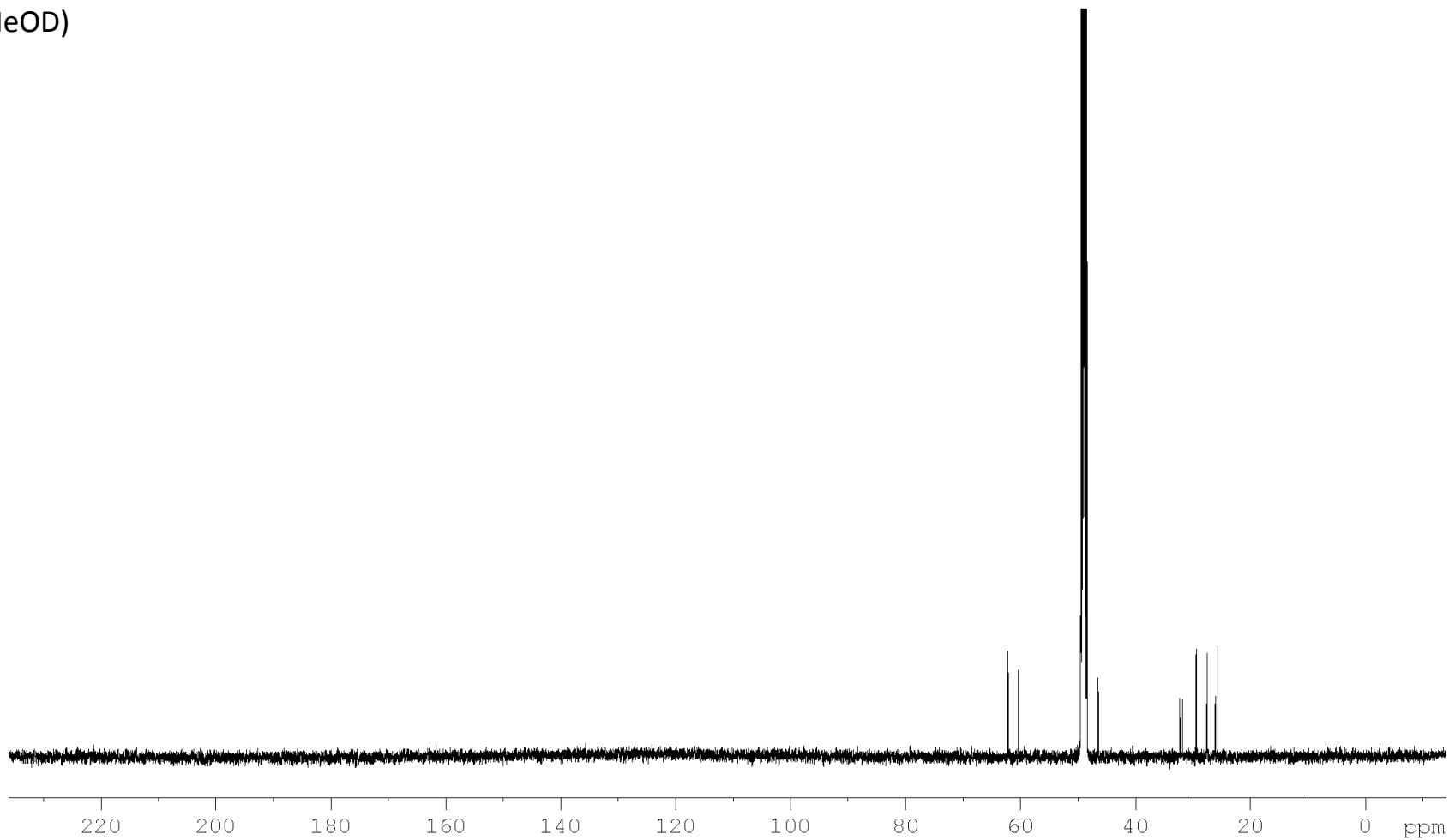
¹H NMR spectrum (400 MHz, MeOD)

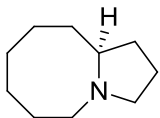




1.2

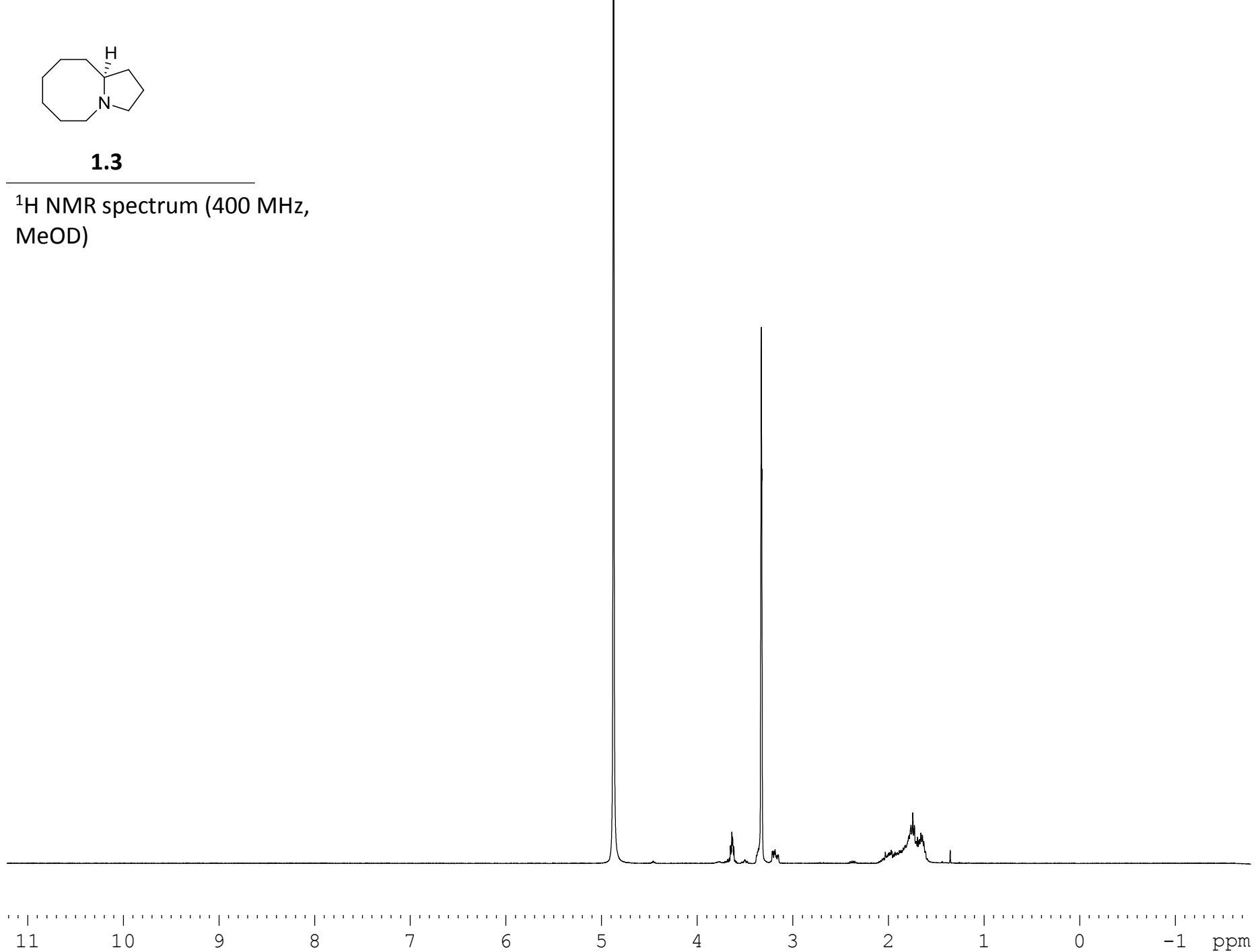
¹³C NMR spectrum (100 MHz,
MeOD)

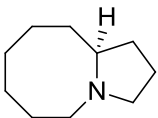




1.3

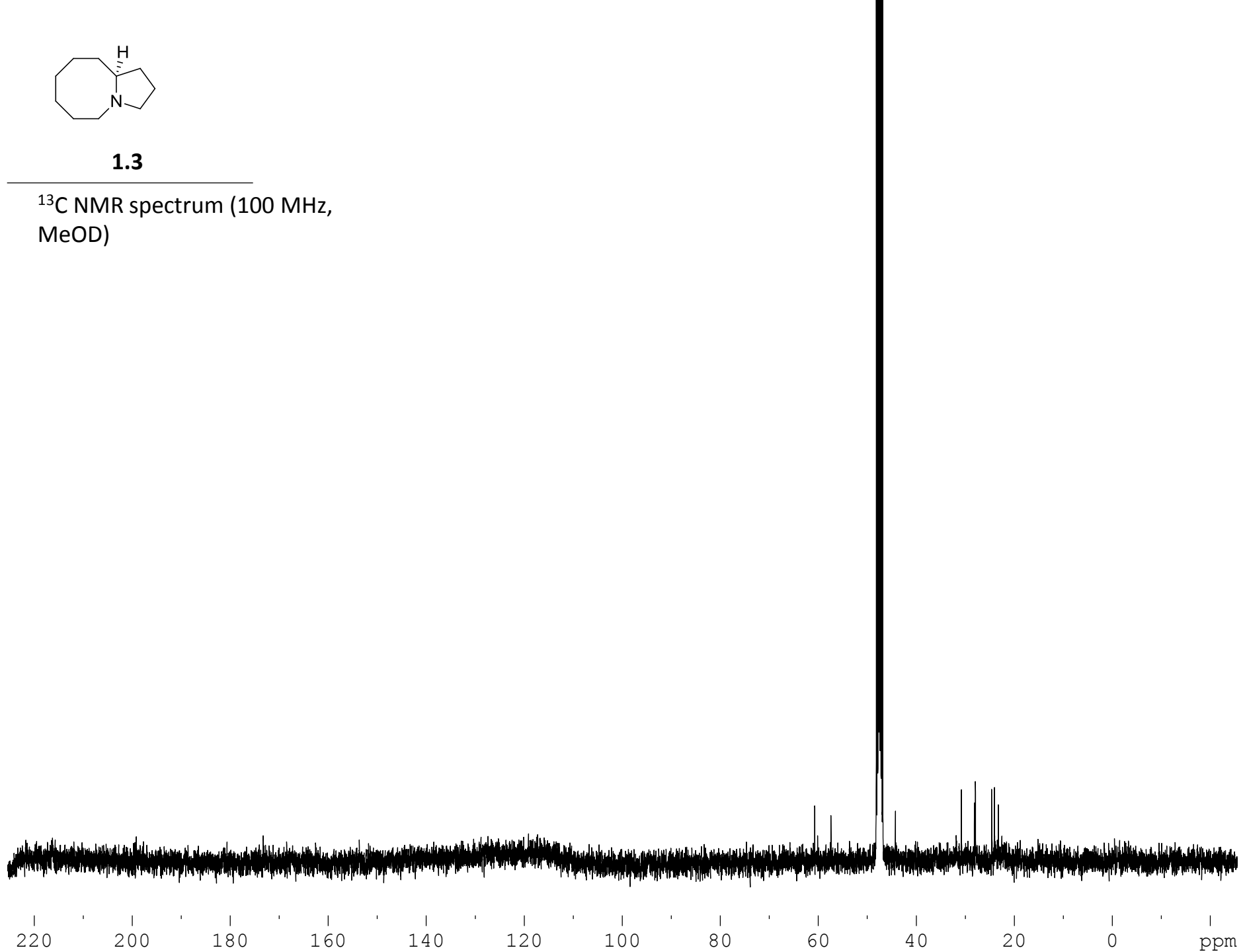
¹H NMR spectrum (400 MHz,
MeOD)

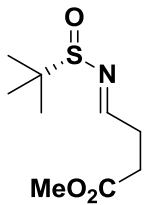




1.3

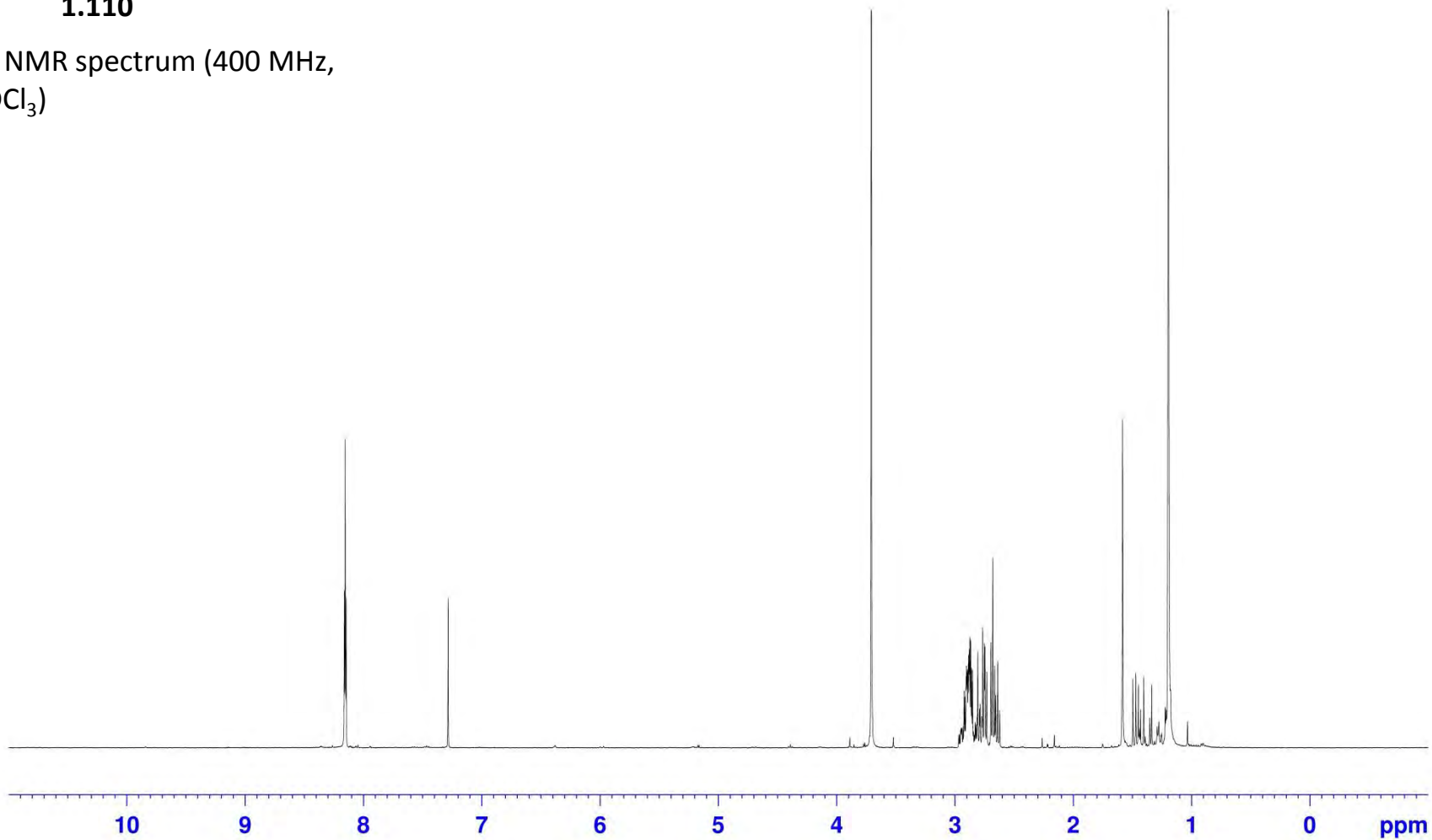
^{13}C NMR spectrum (100 MHz,
MeOD)

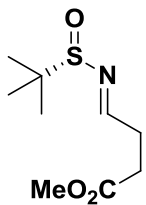




1.110

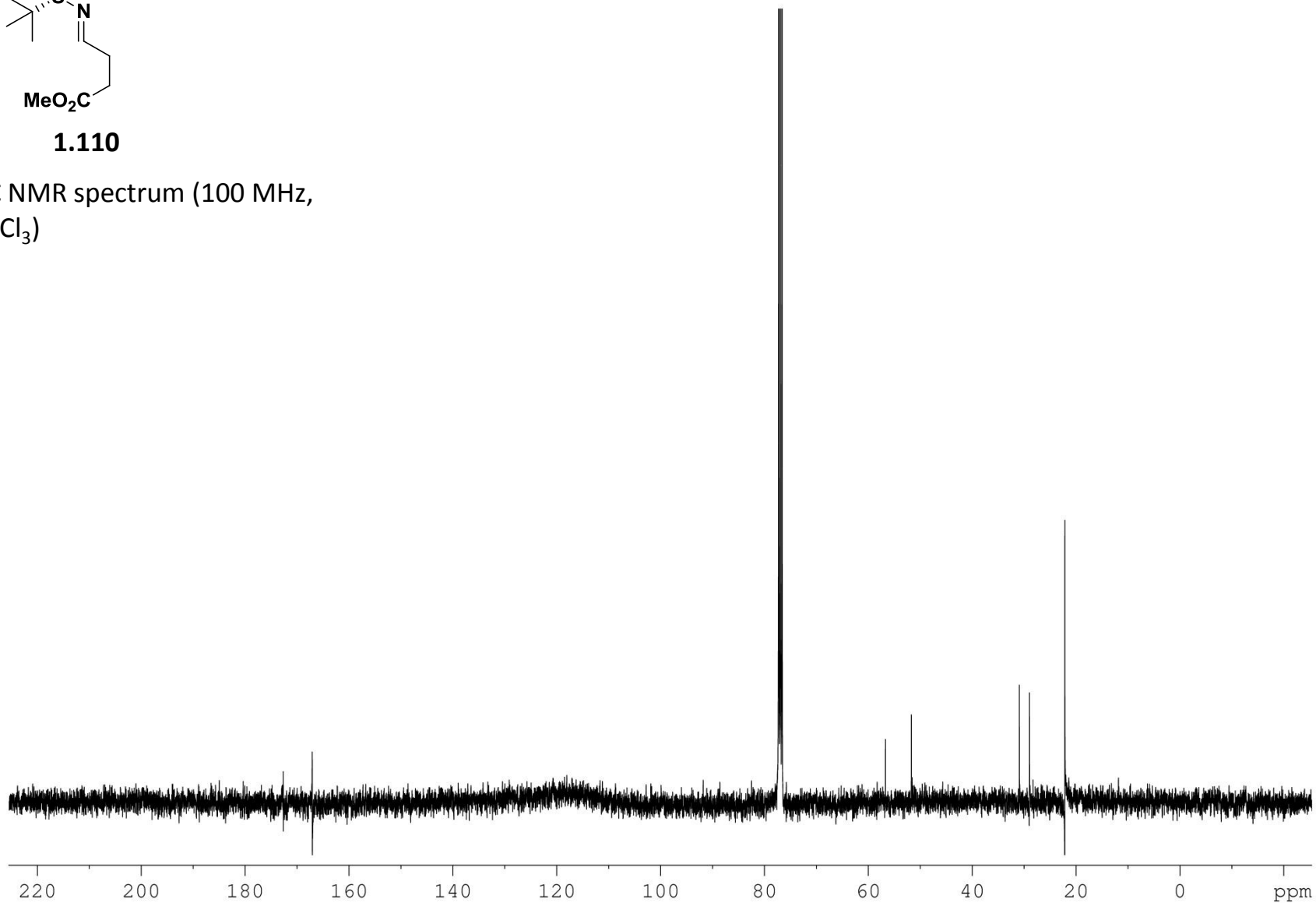
^1H NMR spectrum (400 MHz,
 CDCl_3)

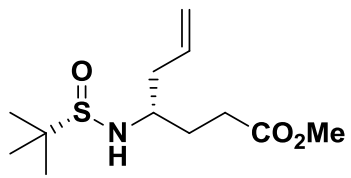




1.110

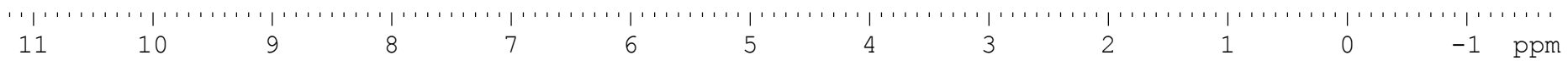
^{13}C NMR spectrum (100 MHz,
 CDCl_3)

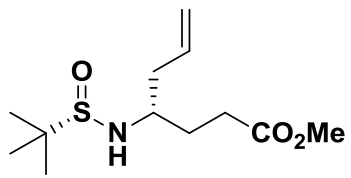




1.111

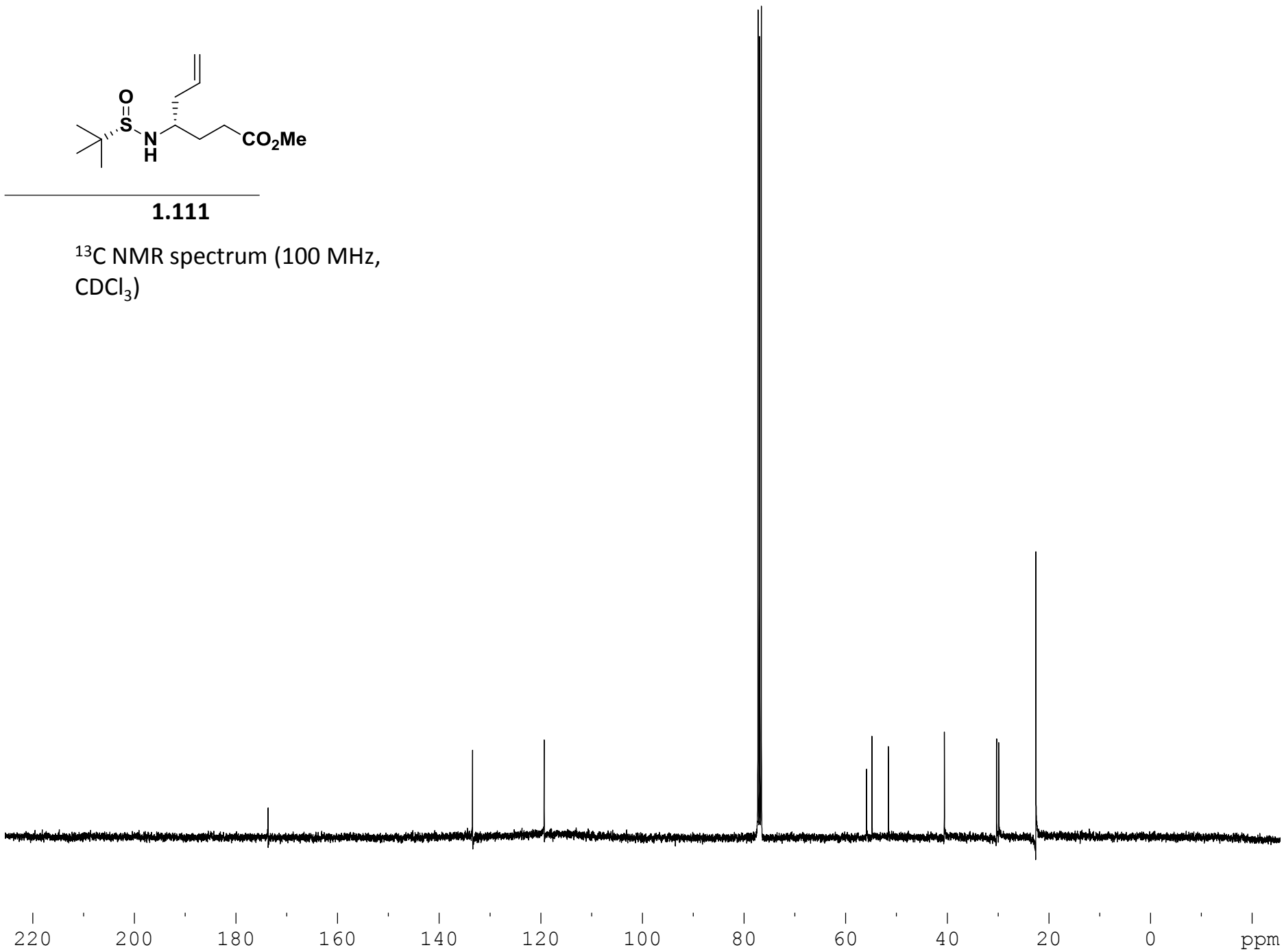
¹H NMR spectrum (400 MHz,
CDCl₃)

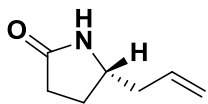




1.111

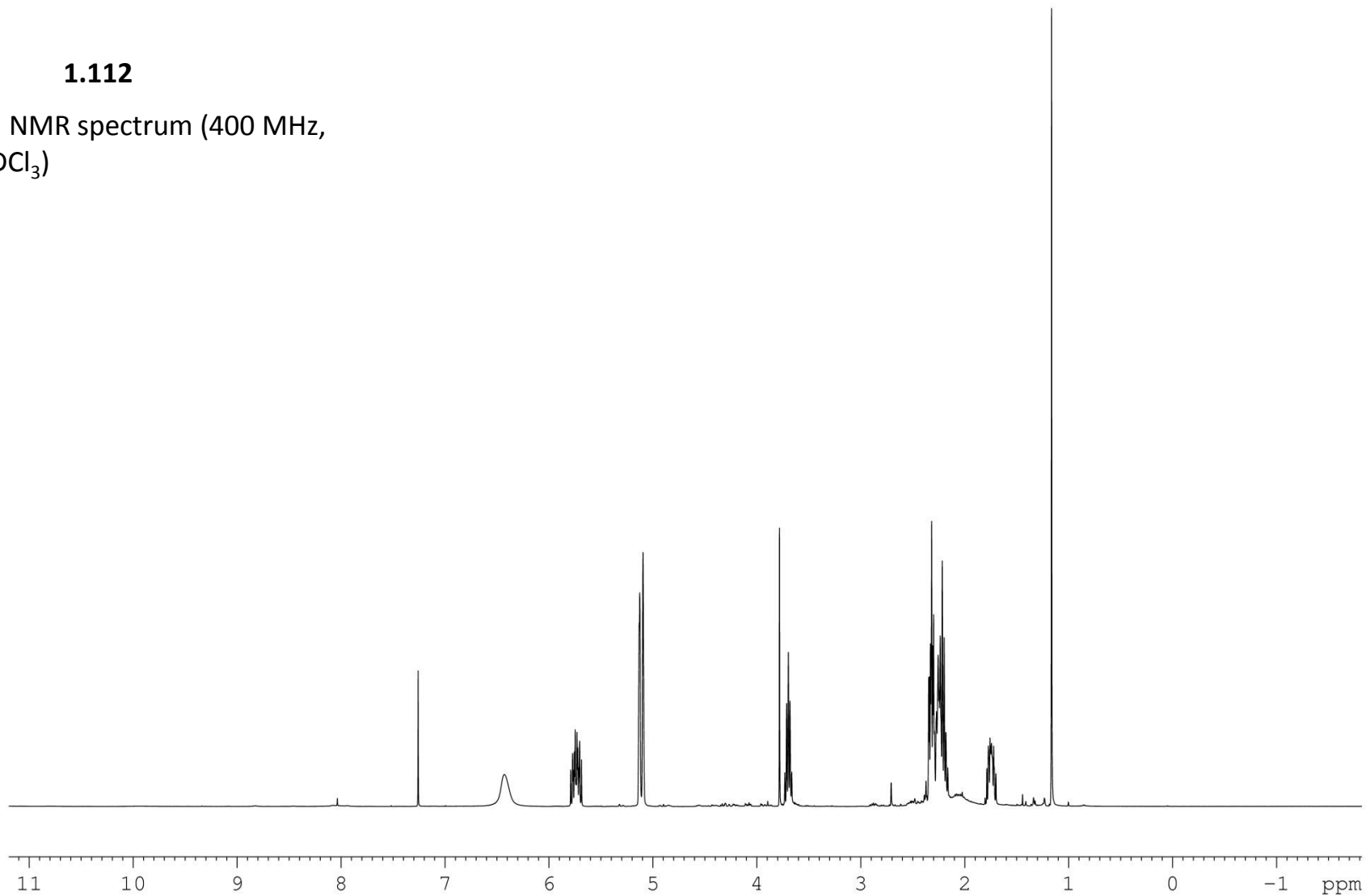
¹³C NMR spectrum (100 MHz,
CDCl₃)

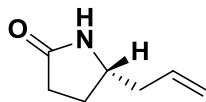




1.112

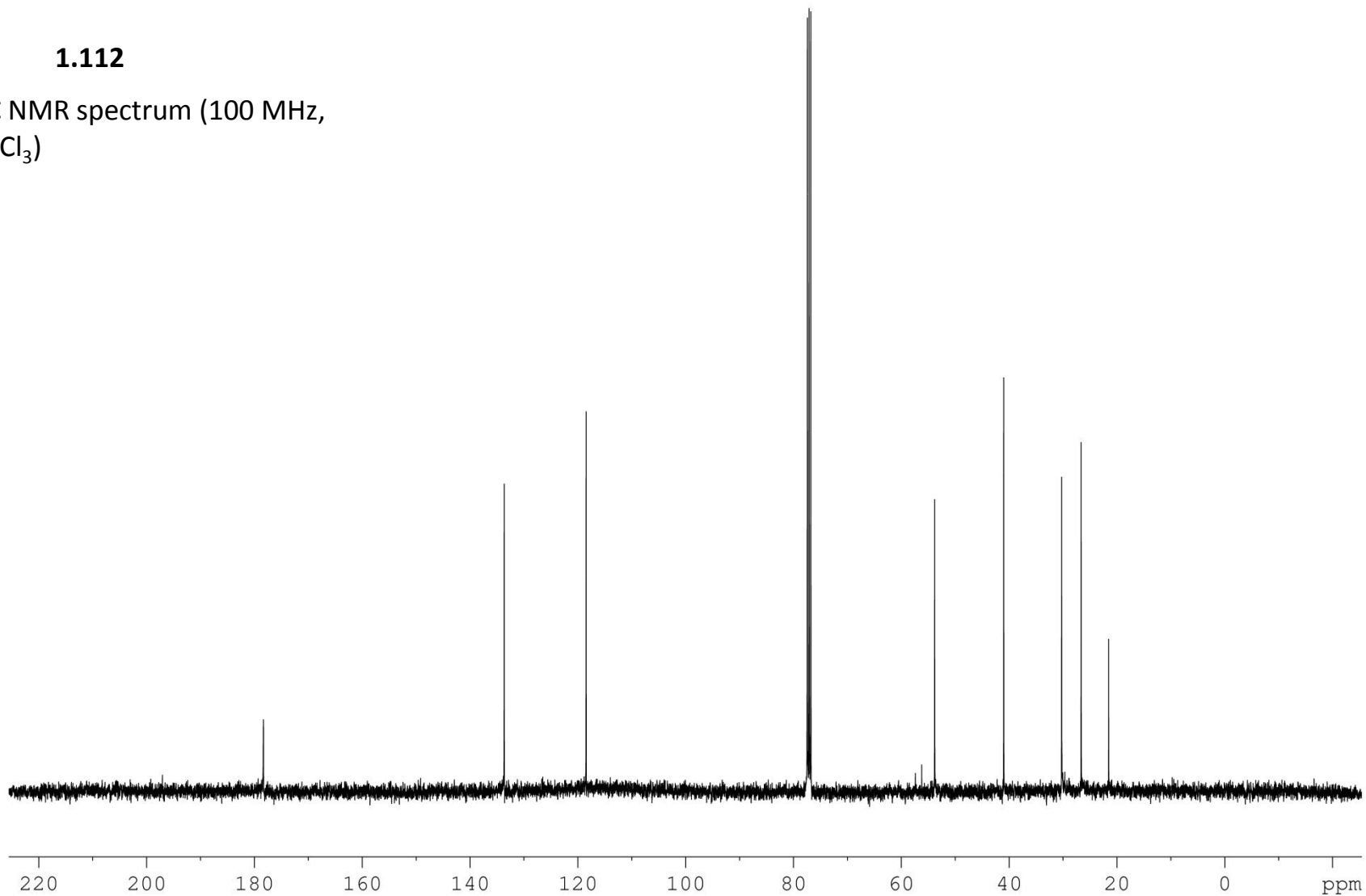
^1H NMR spectrum (400 MHz,
 CDCl_3)

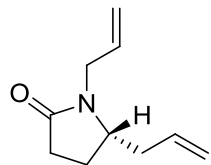




1.112

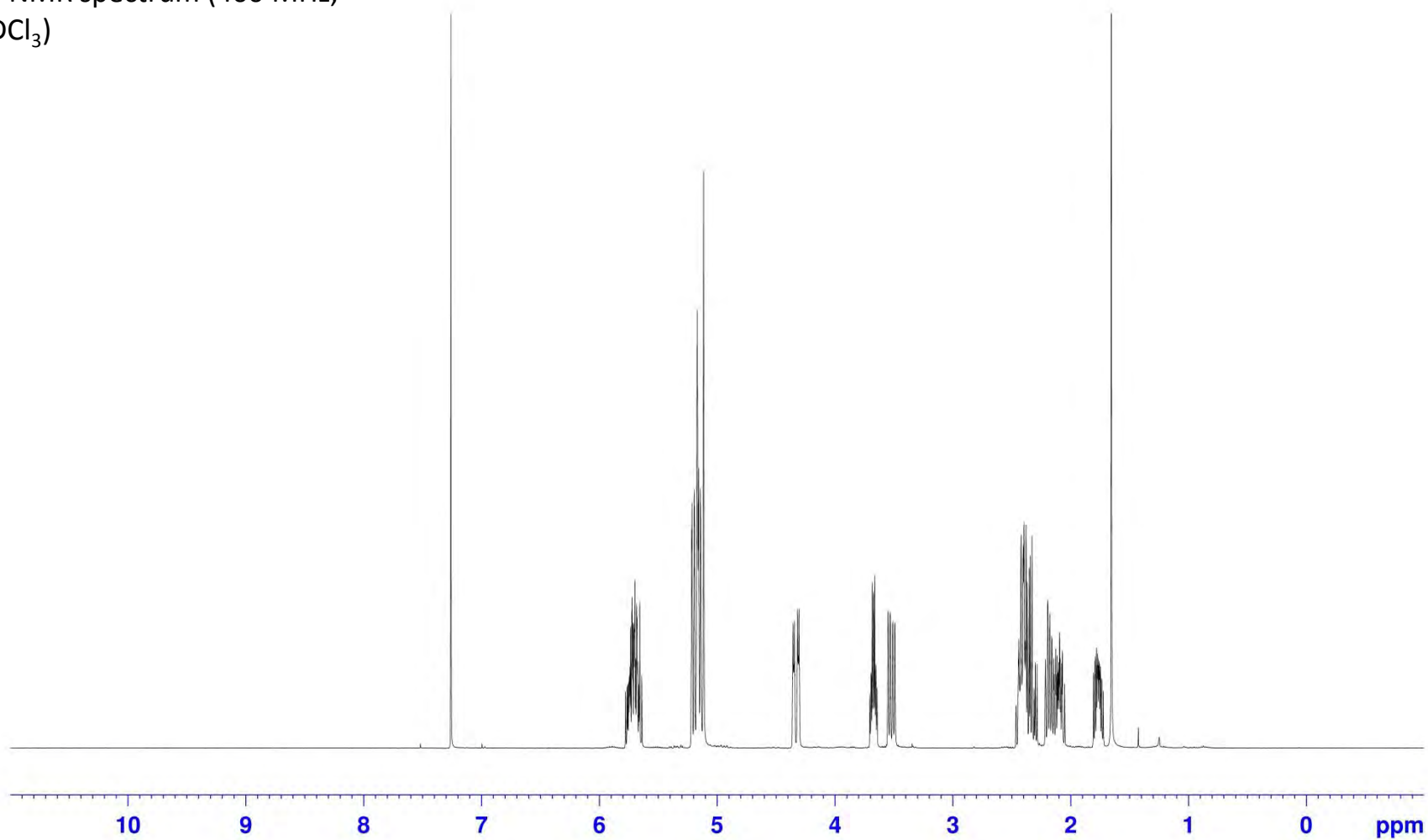
^{13}C NMR spectrum (100 MHz,
 CDCl_3)

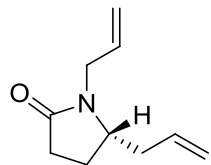




1.137

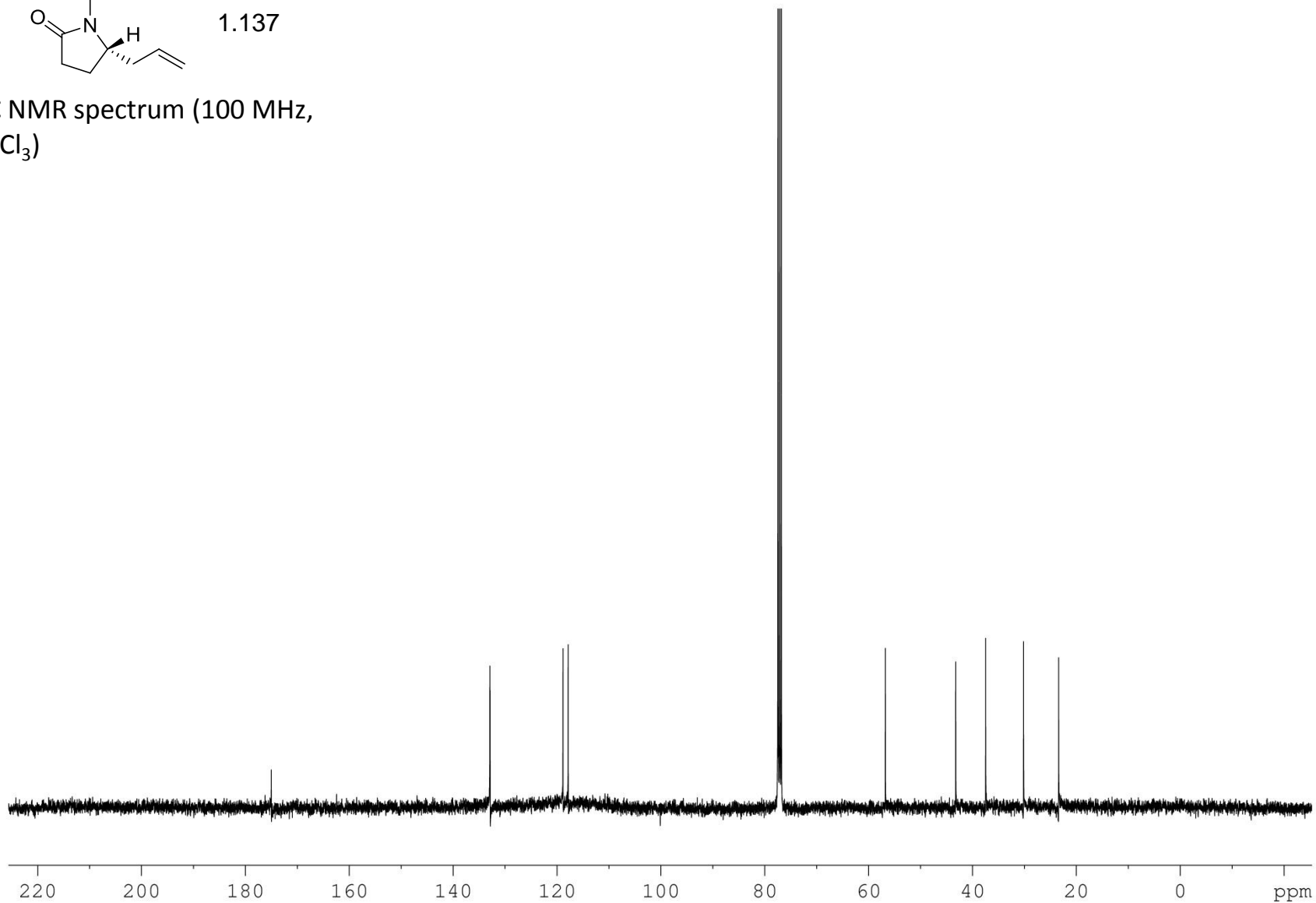
^1H NMR spectrum (400 MHz, CDCl_3)

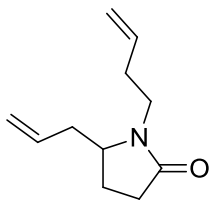




1.137

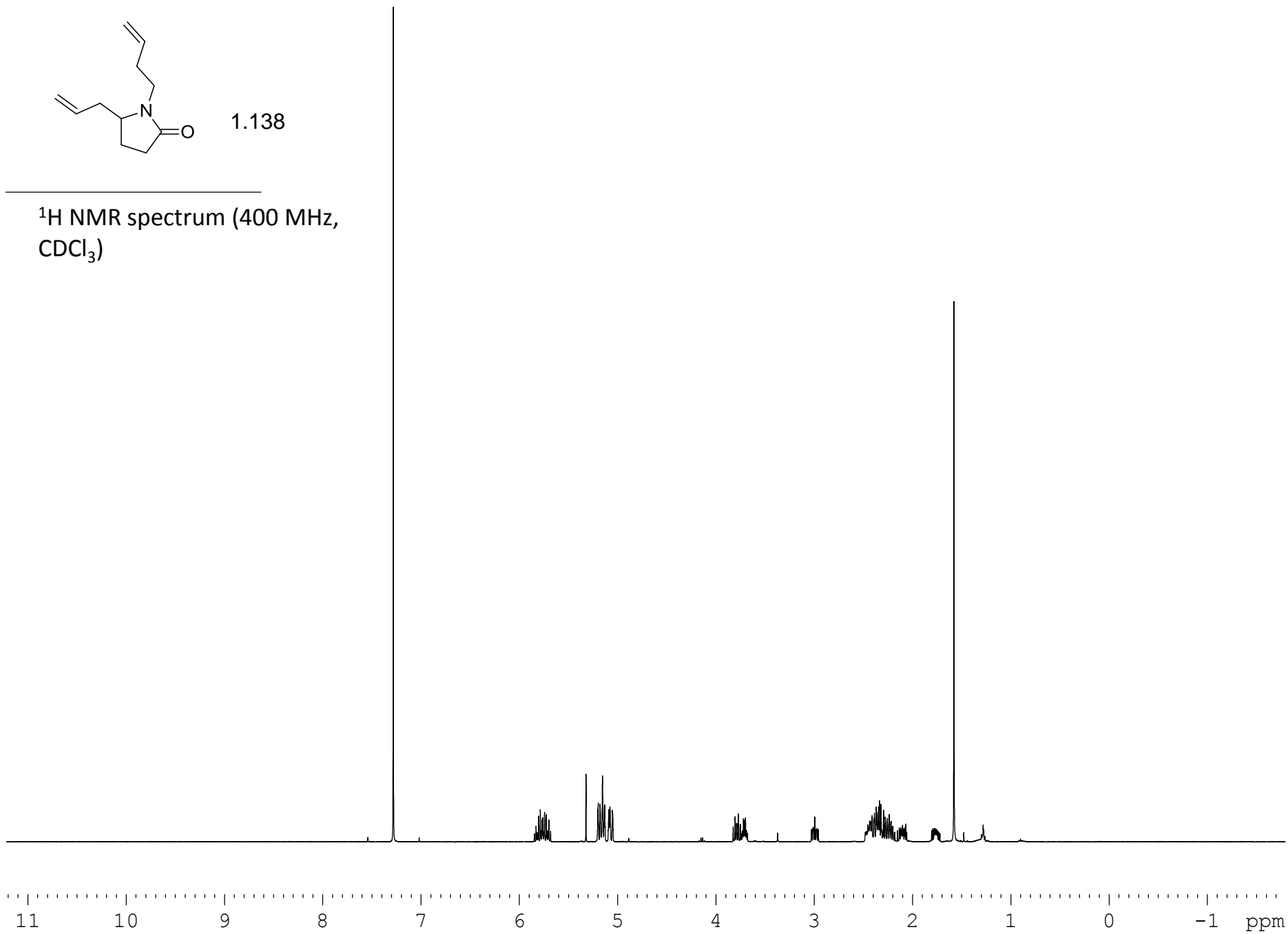
^{13}C NMR spectrum (100 MHz,
 CDCl_3)

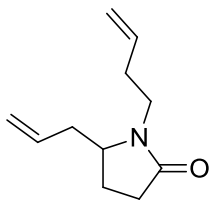




1.138

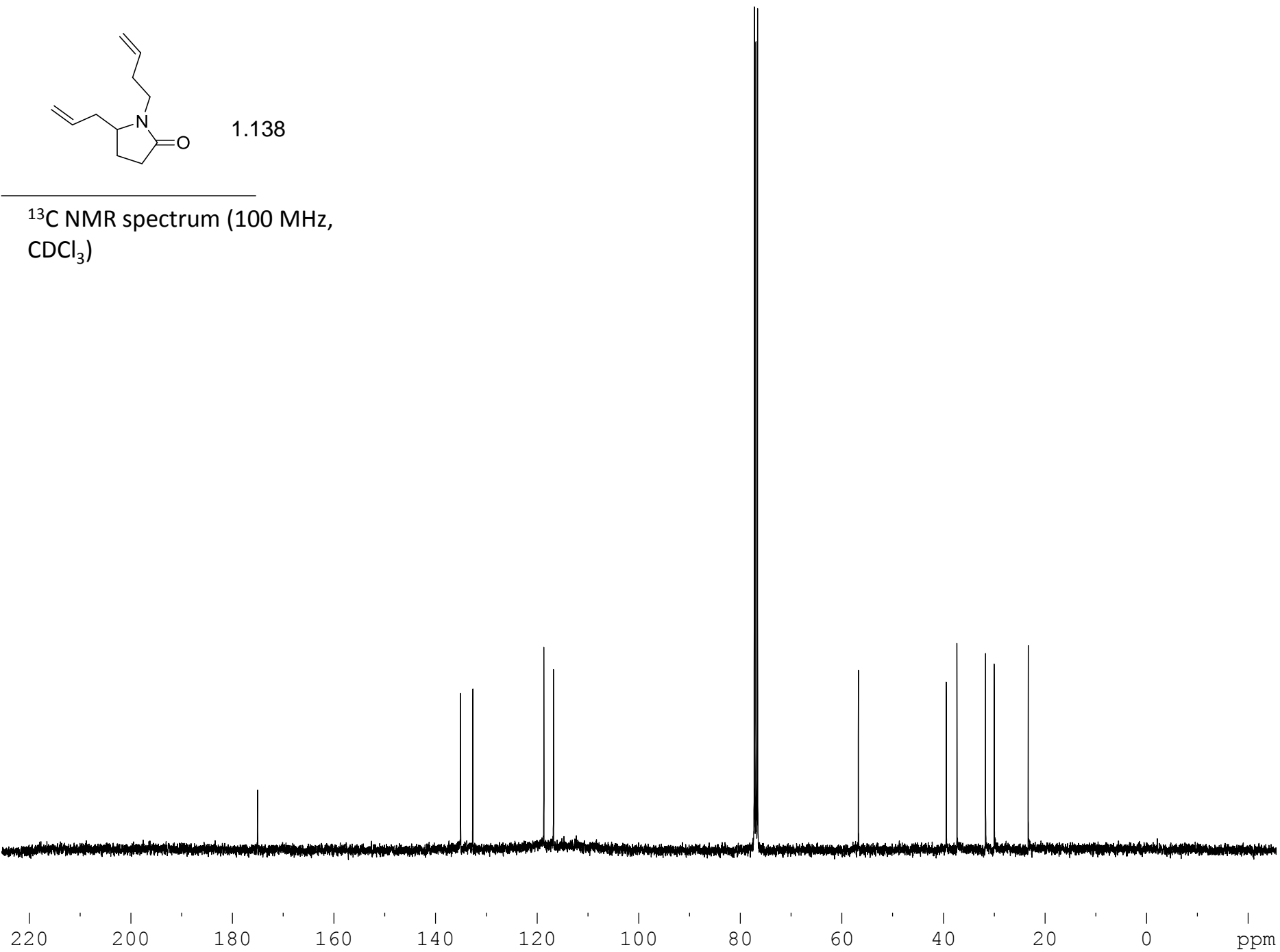
¹H NMR spectrum (400 MHz,
CDCl₃)

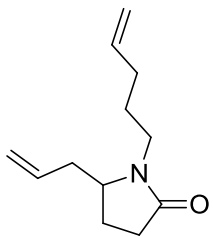




1.138

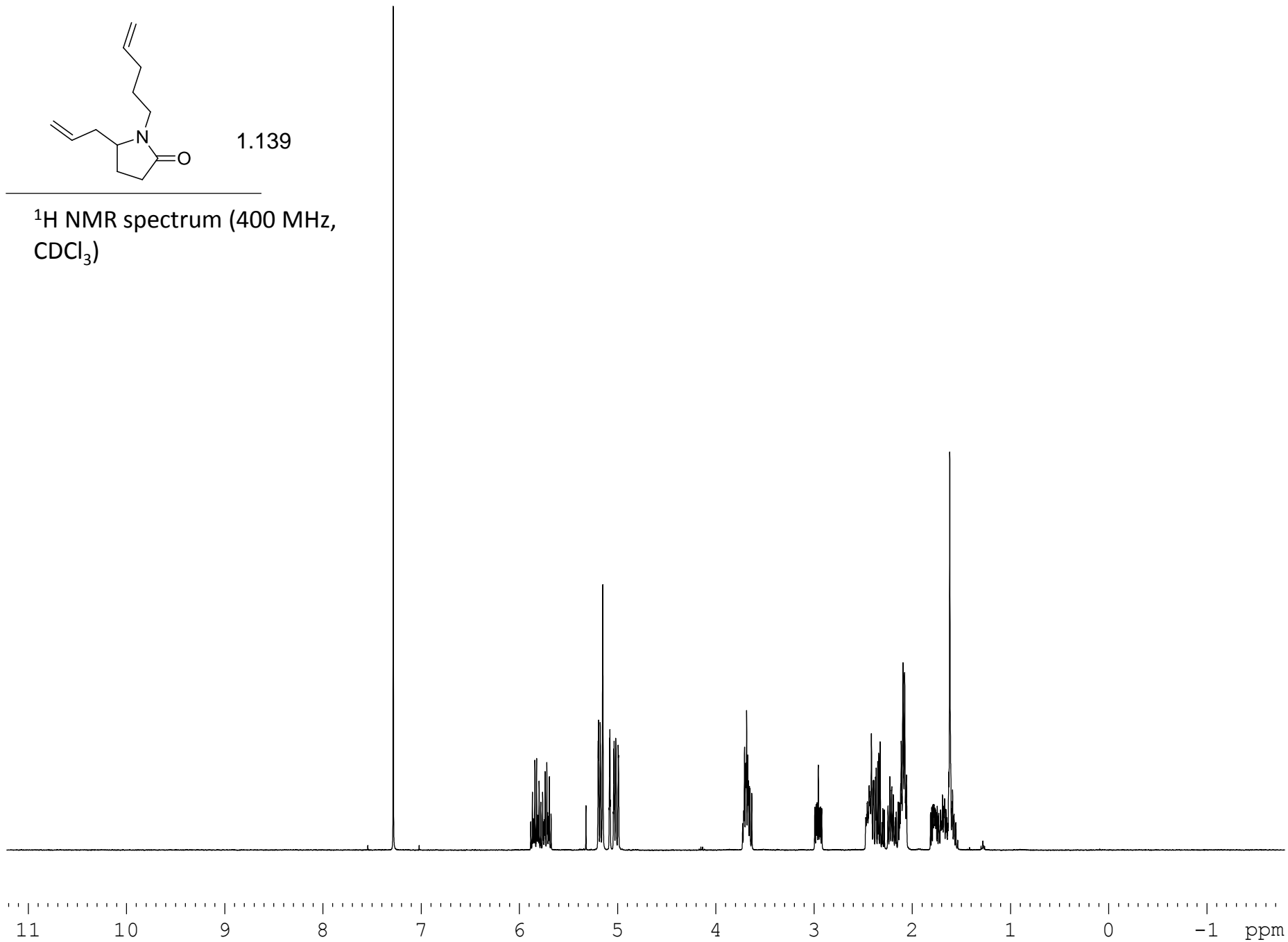
^{13}C NMR spectrum (100 MHz,
 CDCl_3)

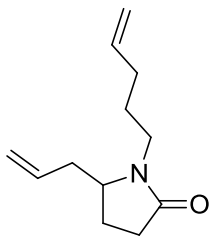




1.139

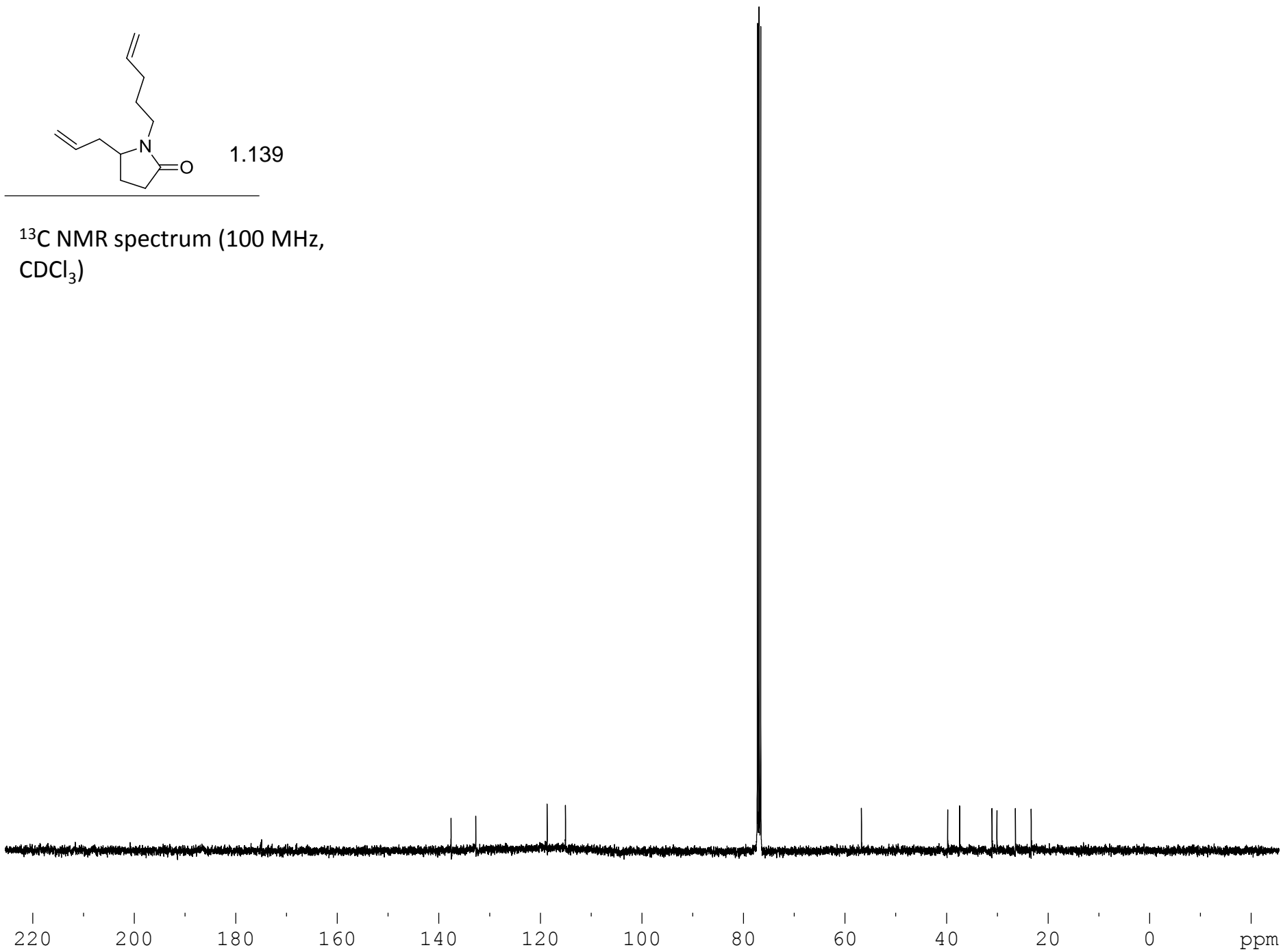
^1H NMR spectrum (400 MHz,
 CDCl_3)

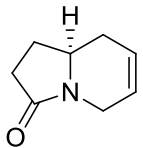




1.139

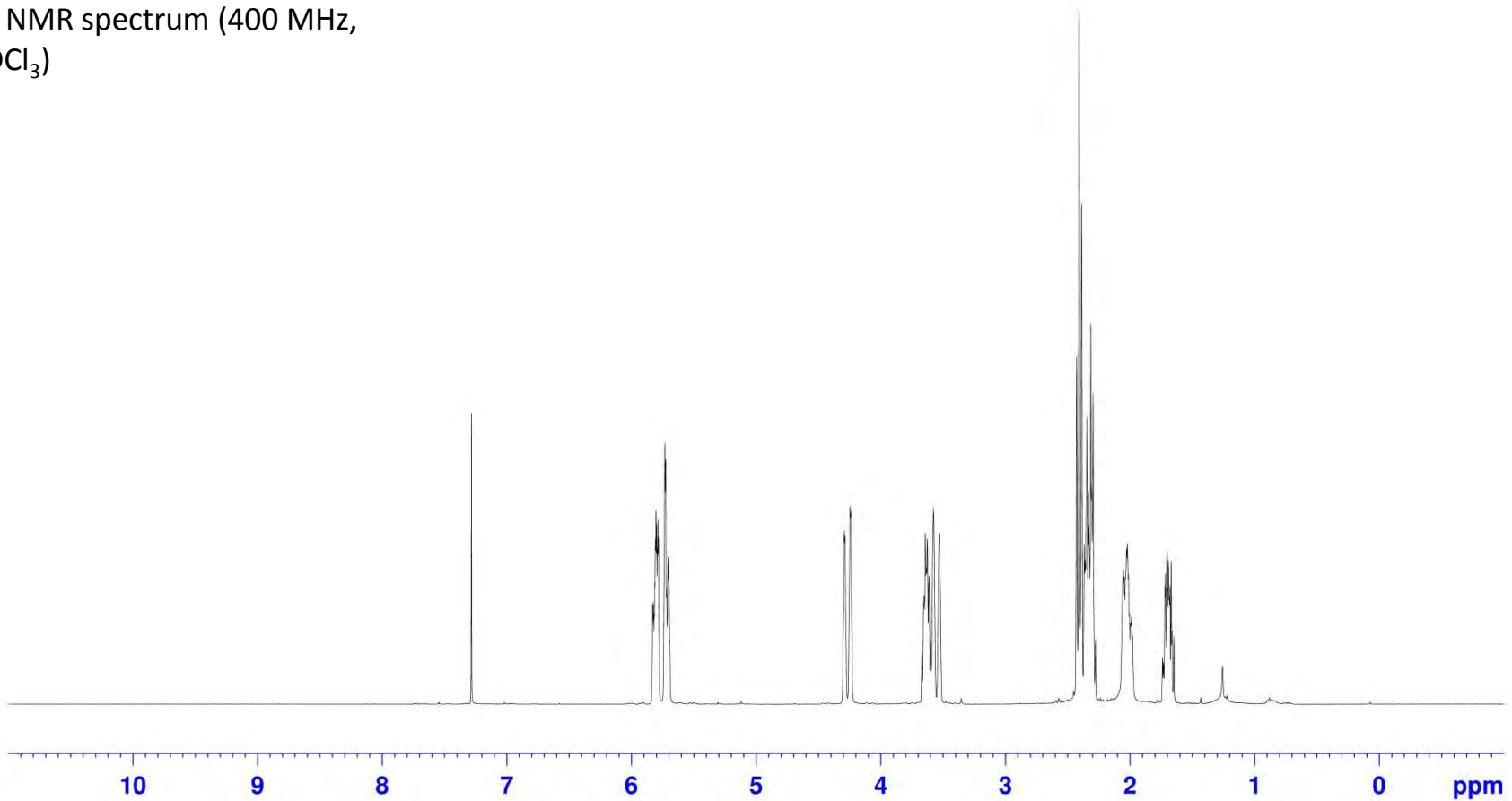
^{13}C NMR spectrum (100 MHz,
 CDCl_3)

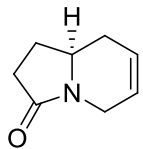




1.113

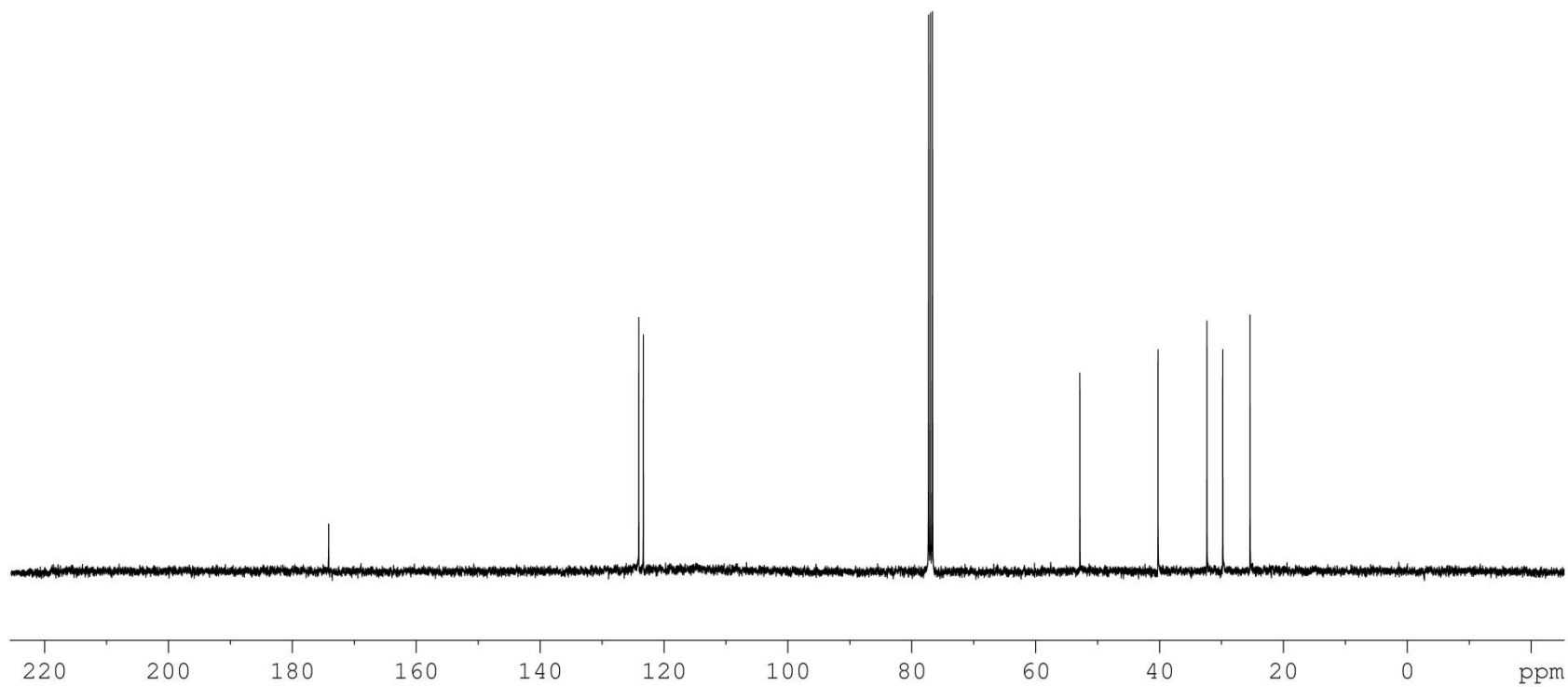
^1H NMR spectrum (400 MHz,
 CDCl_3)

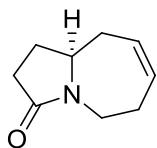




1.113

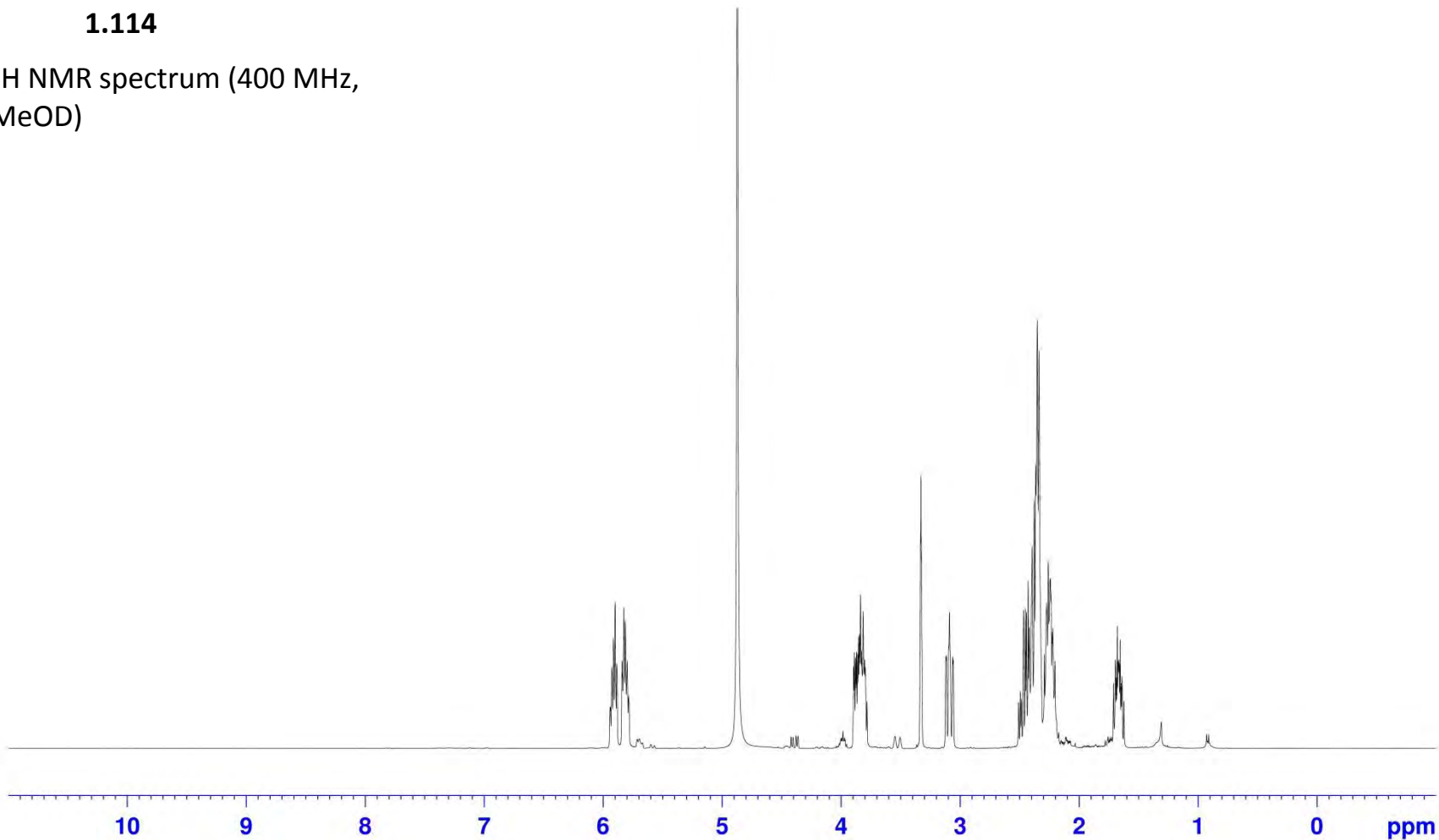
^{13}C NMR spectrum (100 MHz,
 CDCl_3)

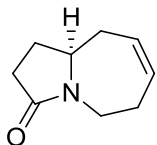




1.114

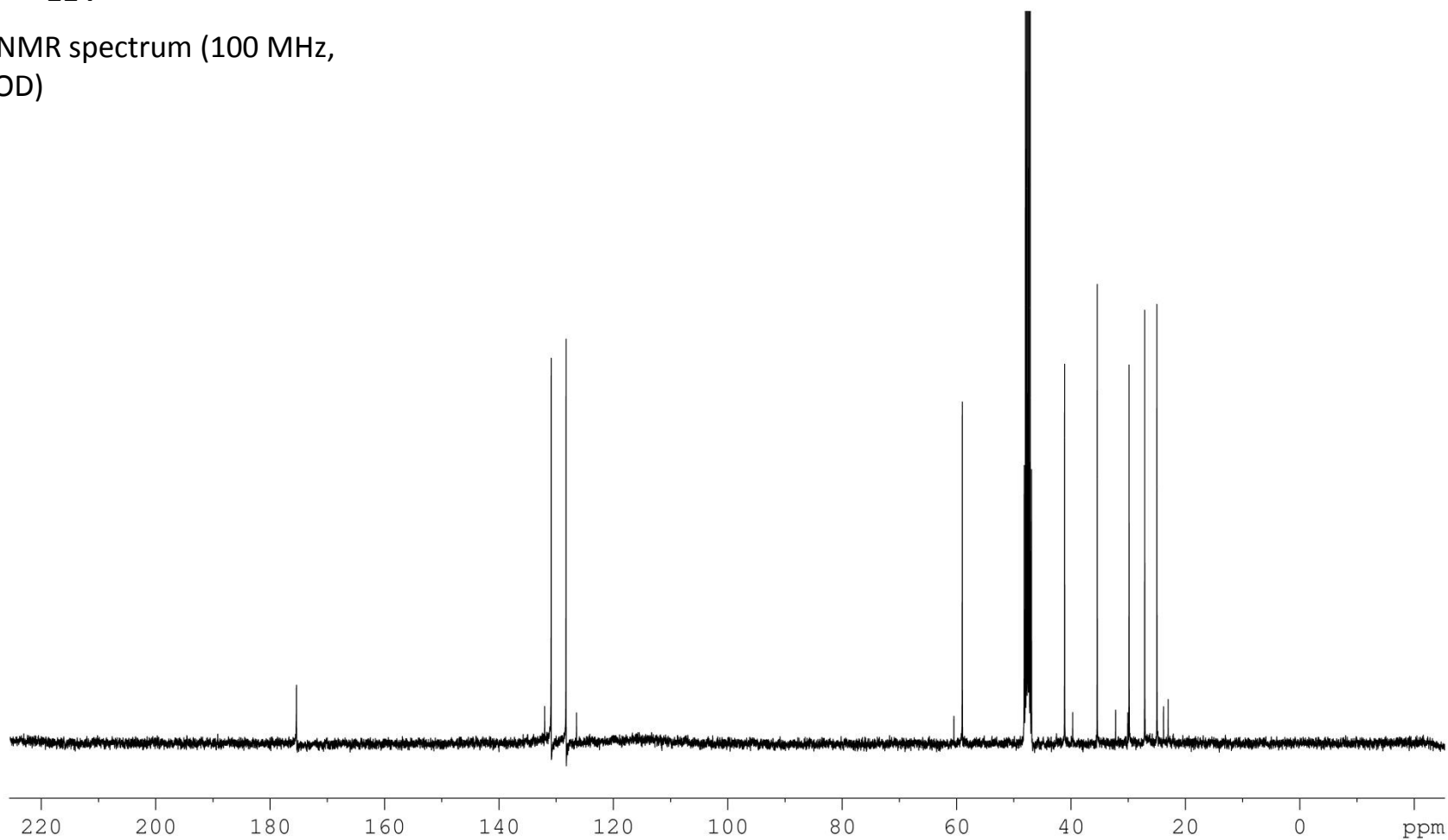
¹H NMR spectrum (400 MHz,
MeOD)

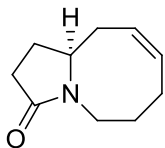




114

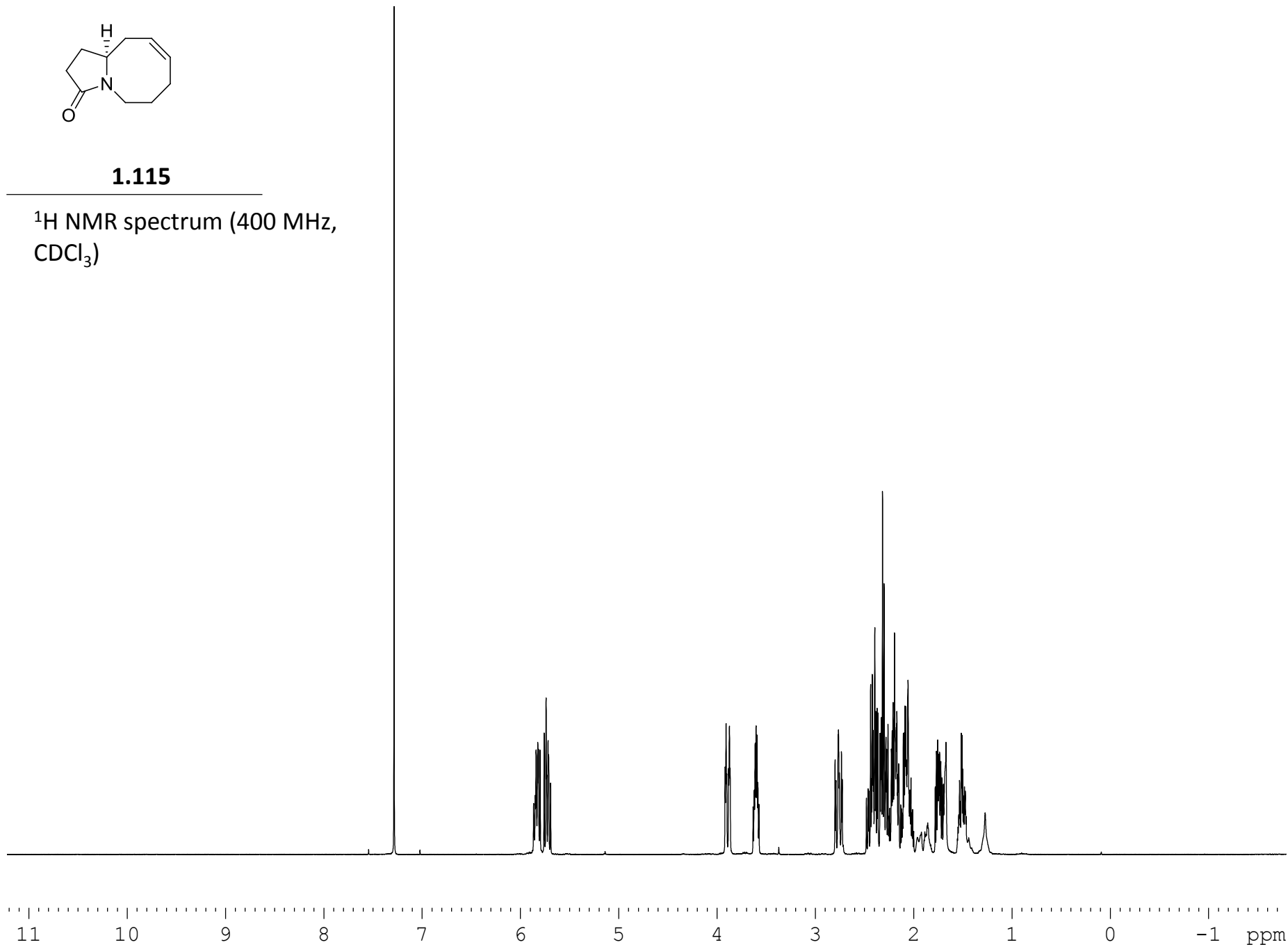
^{13}C NMR spectrum (100 MHz,
MeOD)

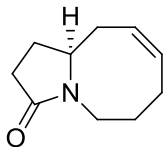




1.115

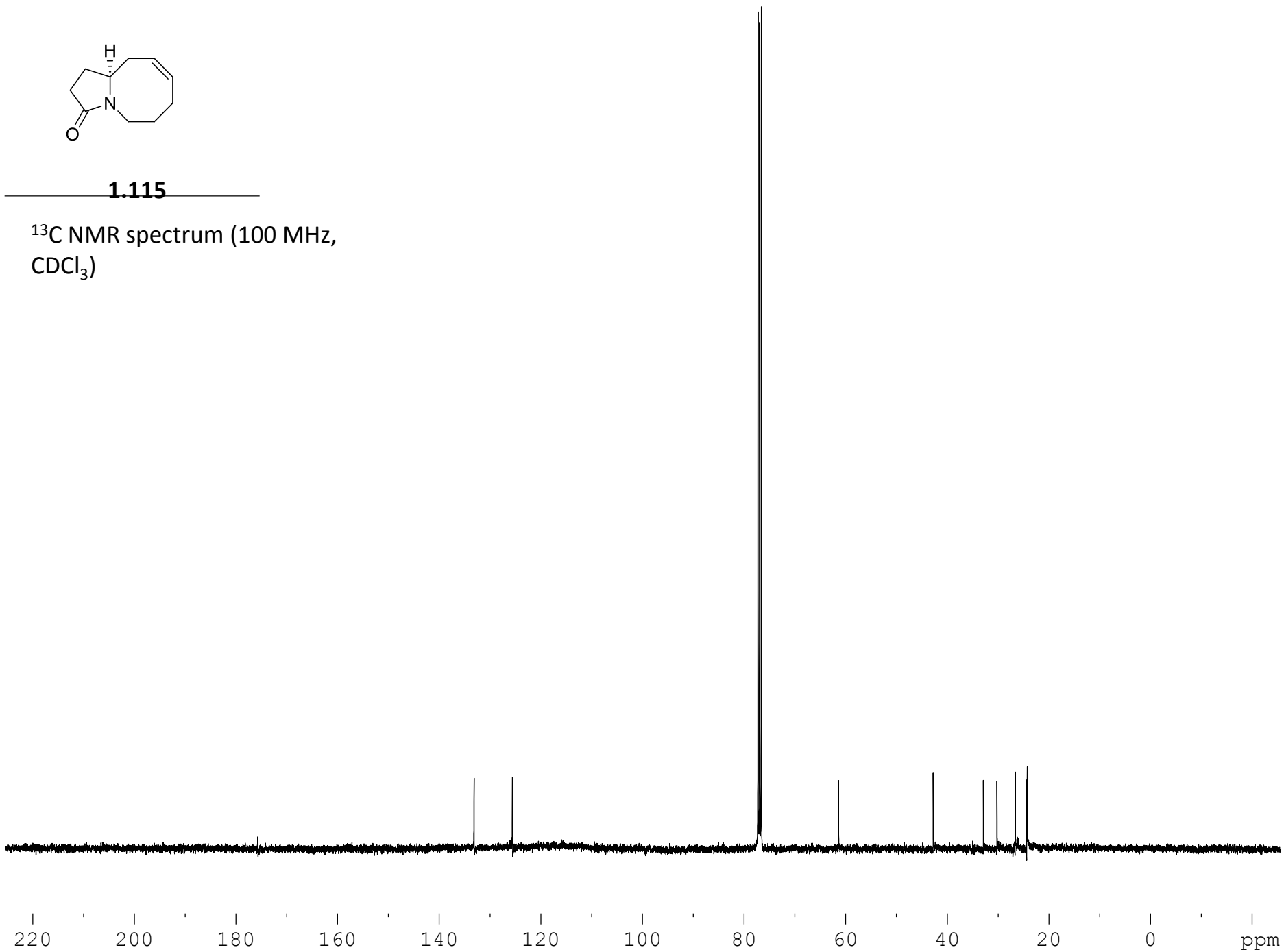
^1H NMR spectrum (400 MHz,
 CDCl_3)

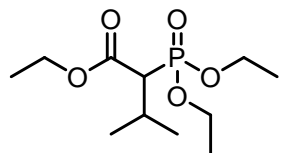




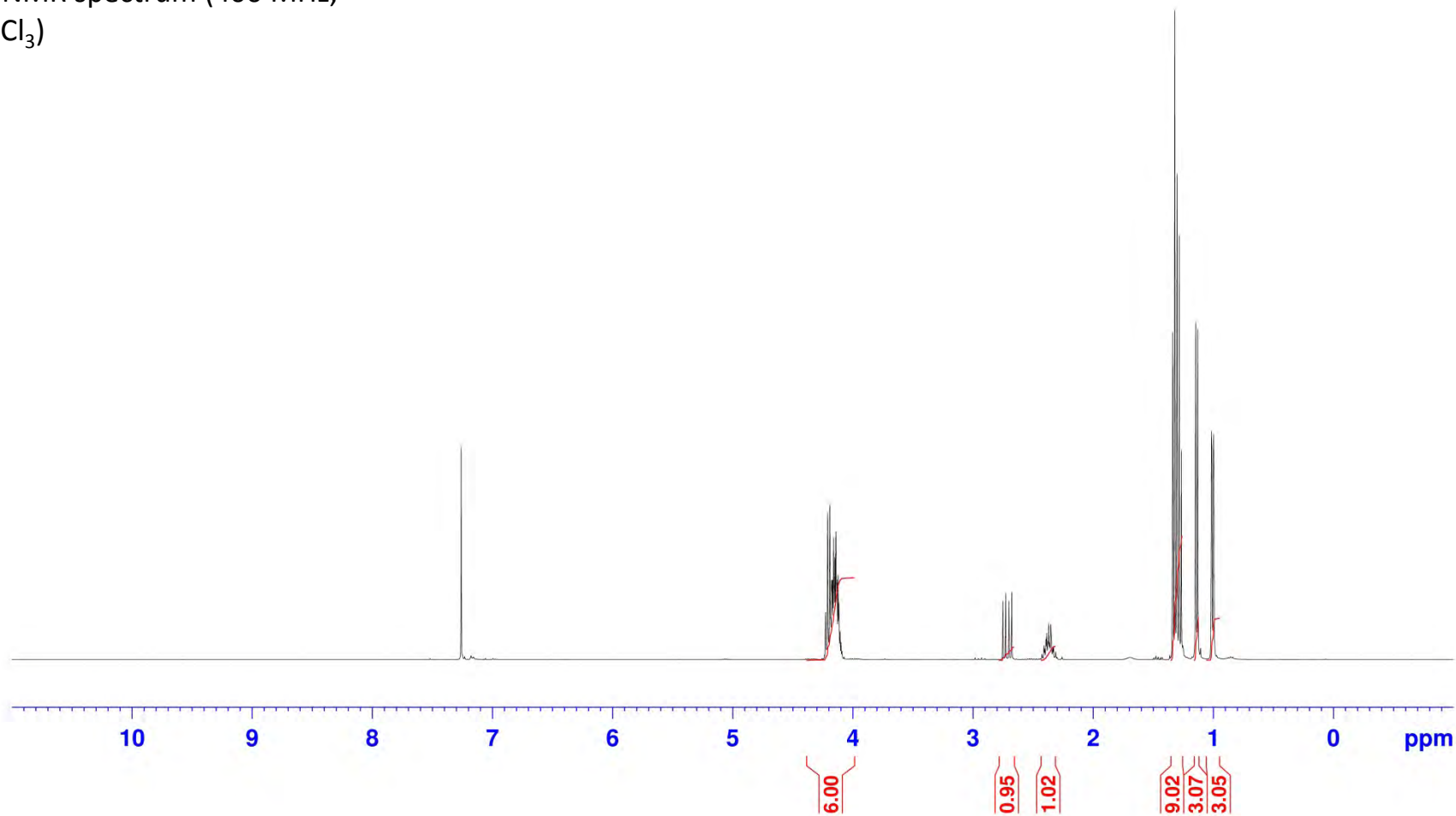
1.115

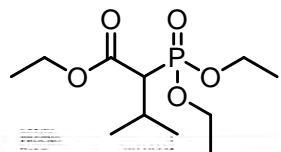
^{13}C NMR spectrum (100 MHz,
 CDCl_3)



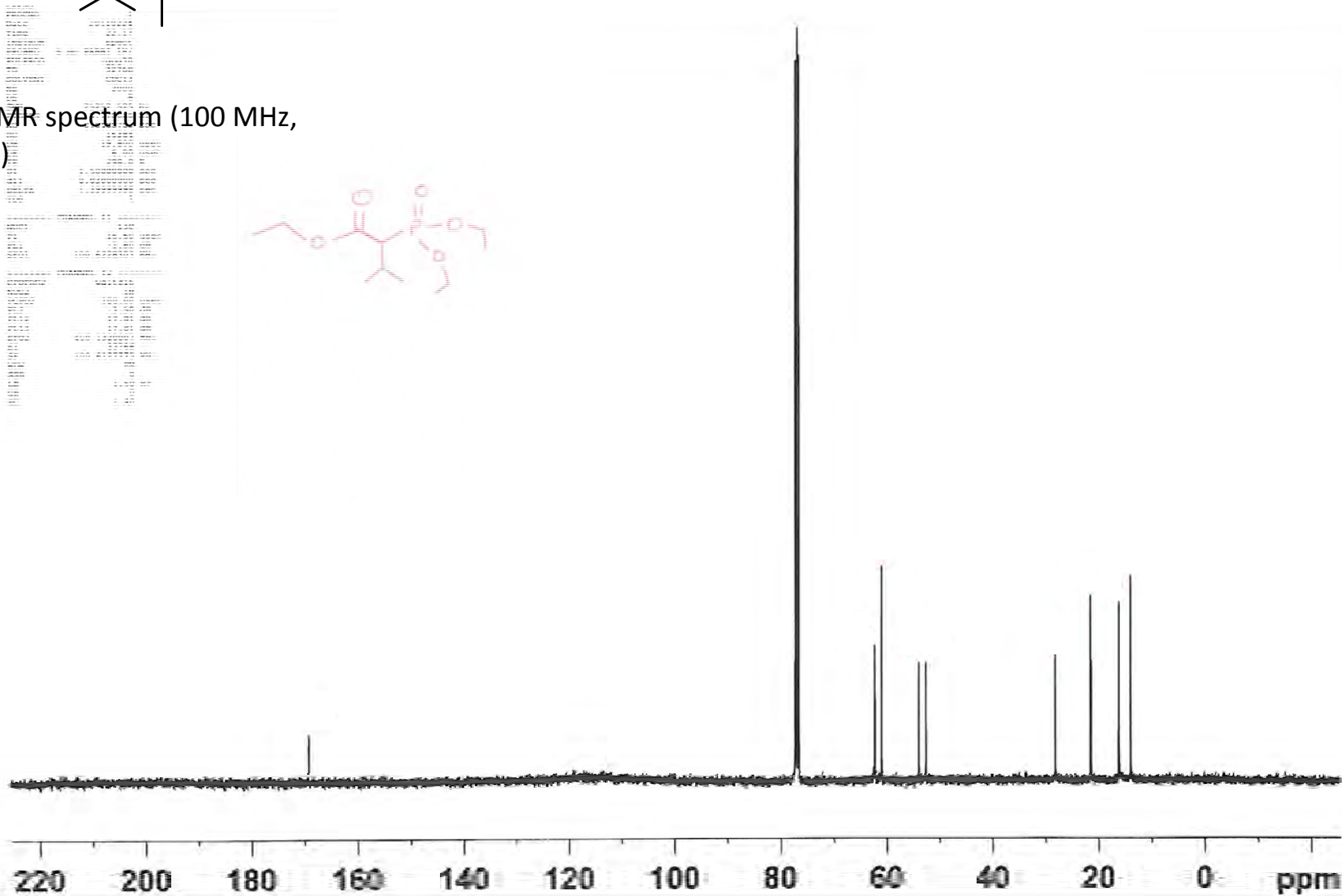


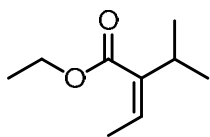
^1H NMR spectrum (400 MHz, CDCl_3)



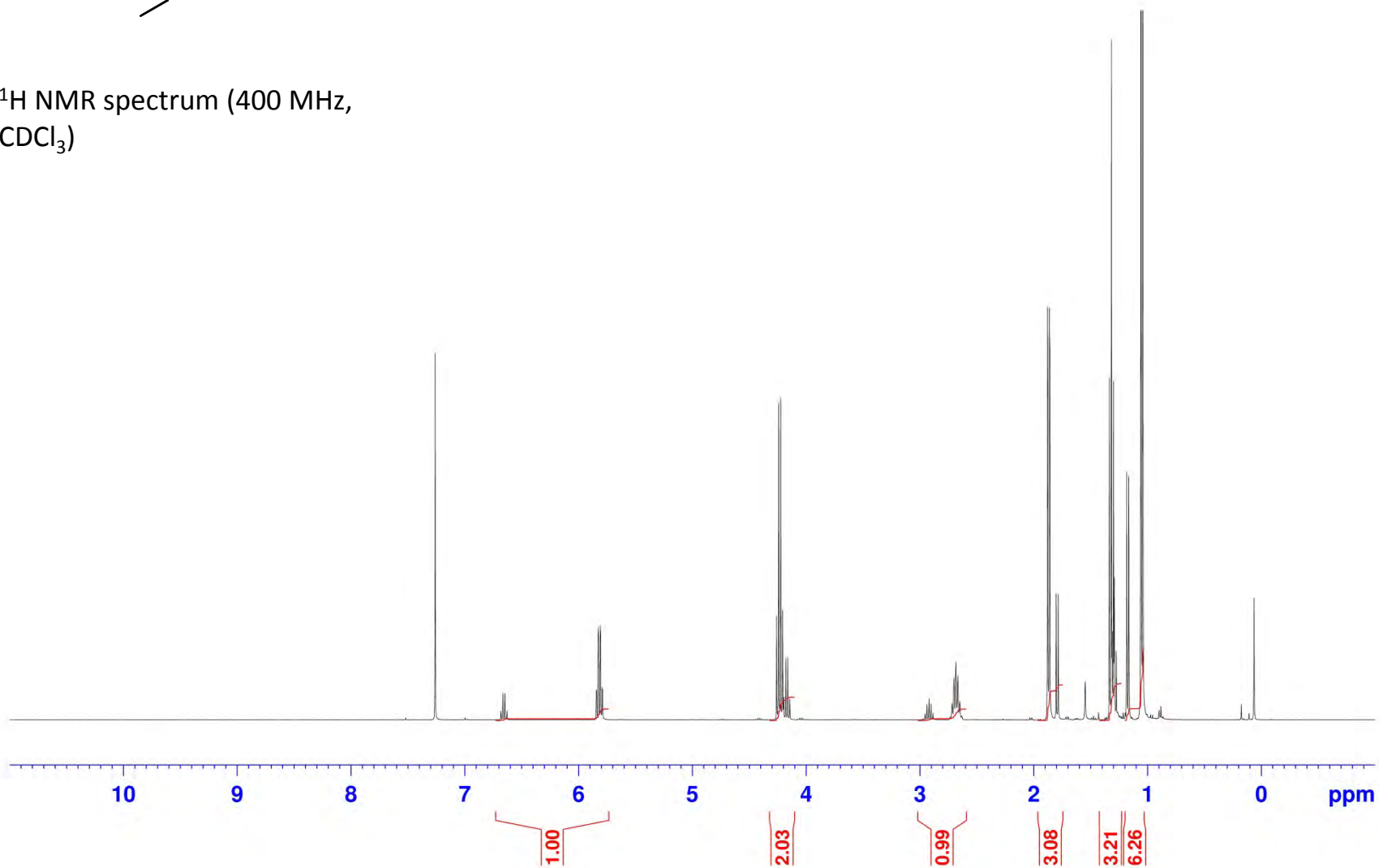


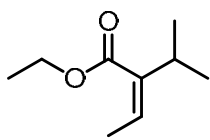
^{13}C NMR spectrum (100 MHz, CDCl_3)





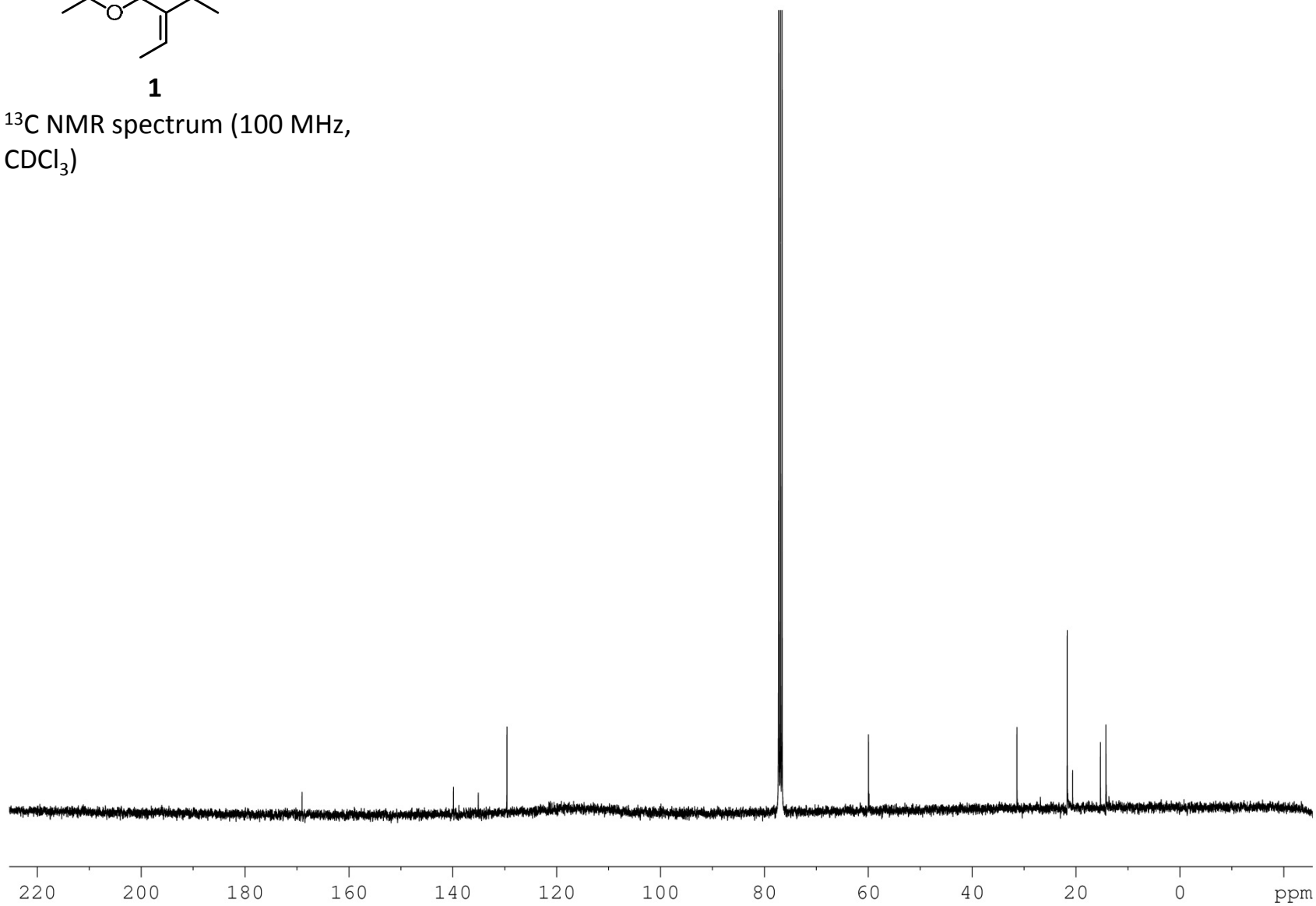
^1H NMR spectrum (400 MHz,
 CDCl_3)

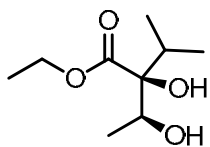




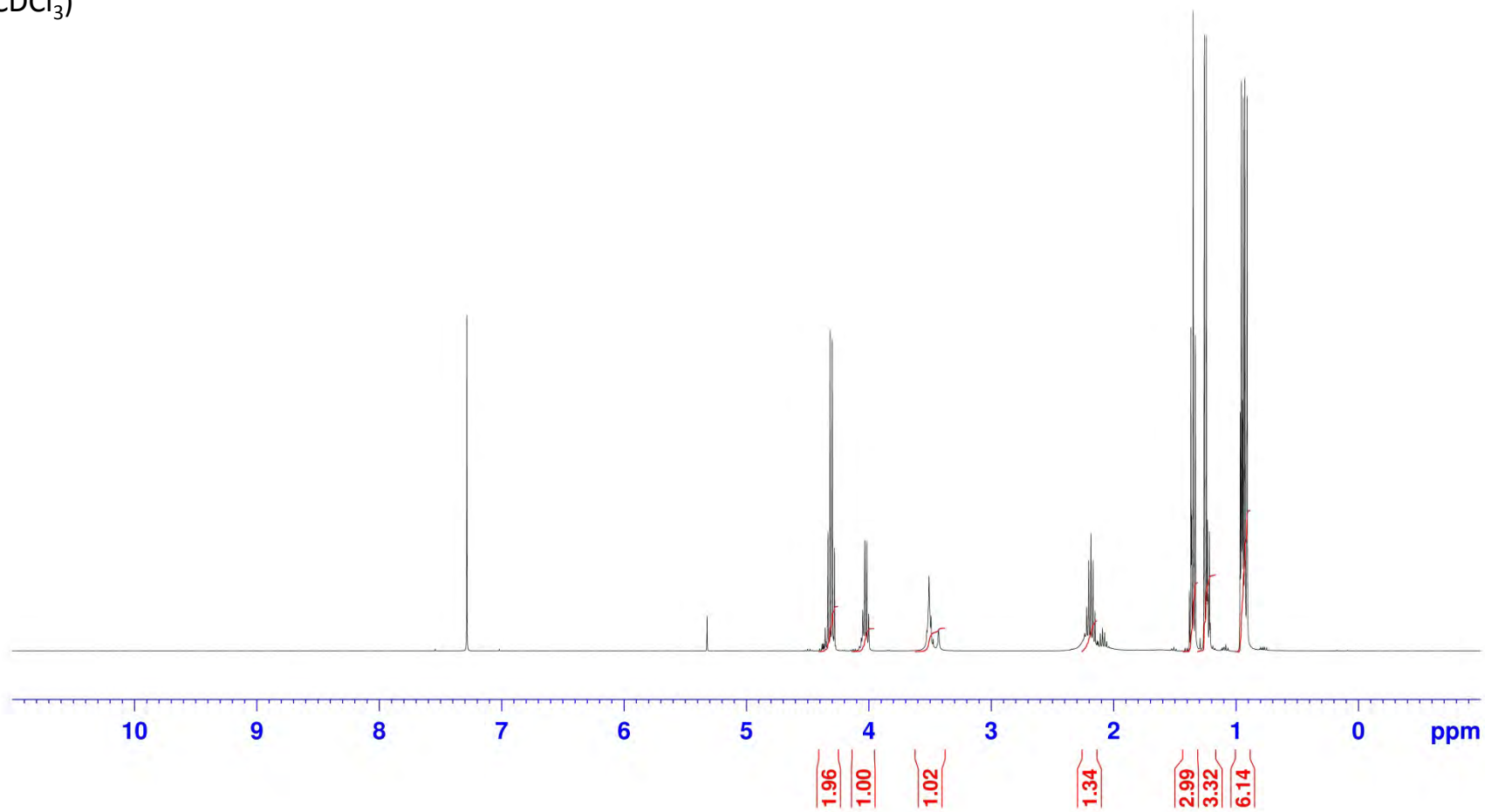
1

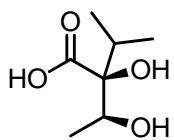
^{13}C NMR spectrum (100 MHz,
 CDCl_3)



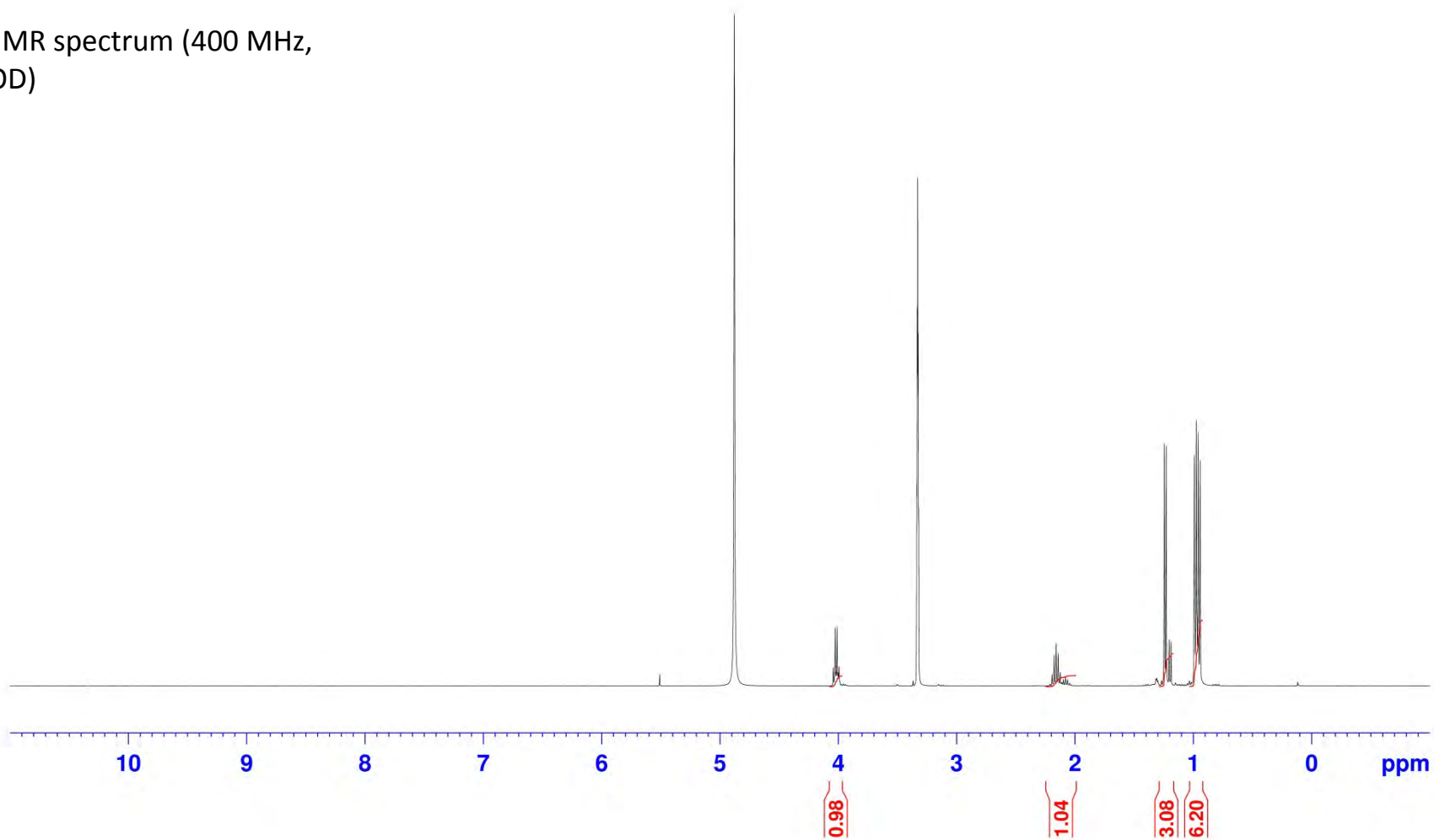


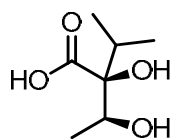
^1H NMR spectrum (400 MHz,
 CDCl_3)



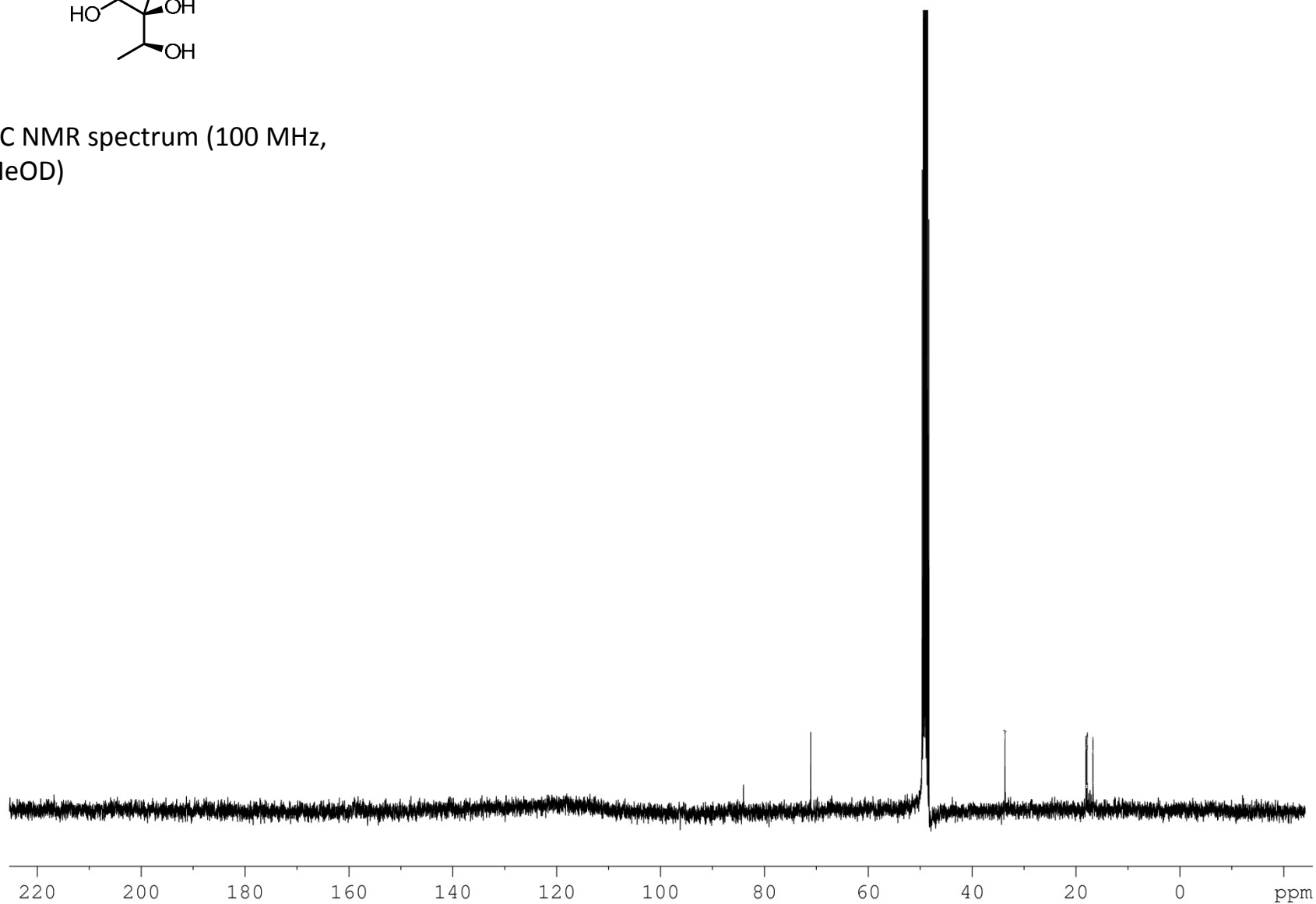


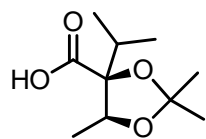
^1H NMR spectrum (400 MHz,
MeOD)



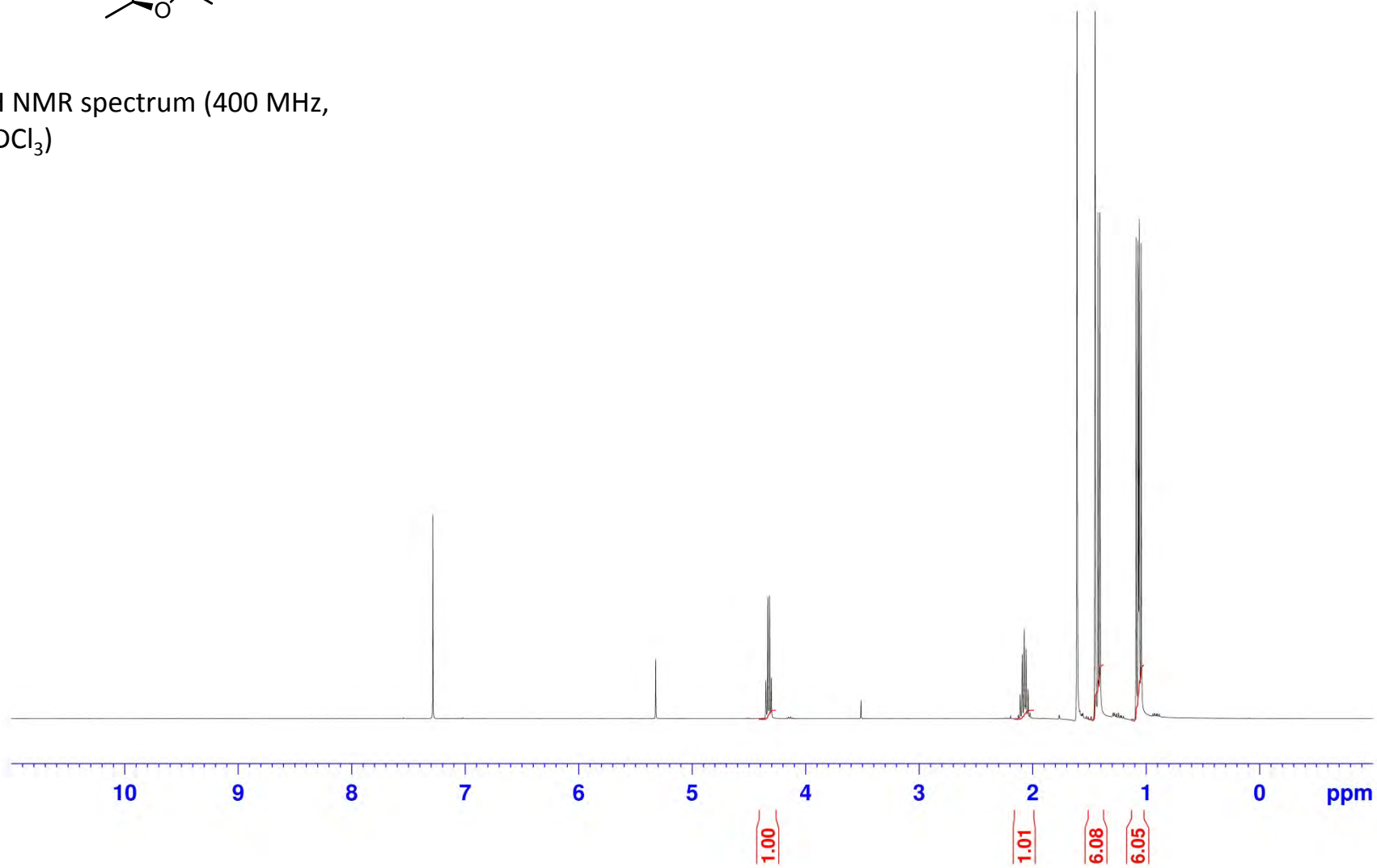


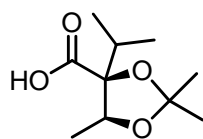
^{13}C NMR spectrum (100 MHz,
MeOD)



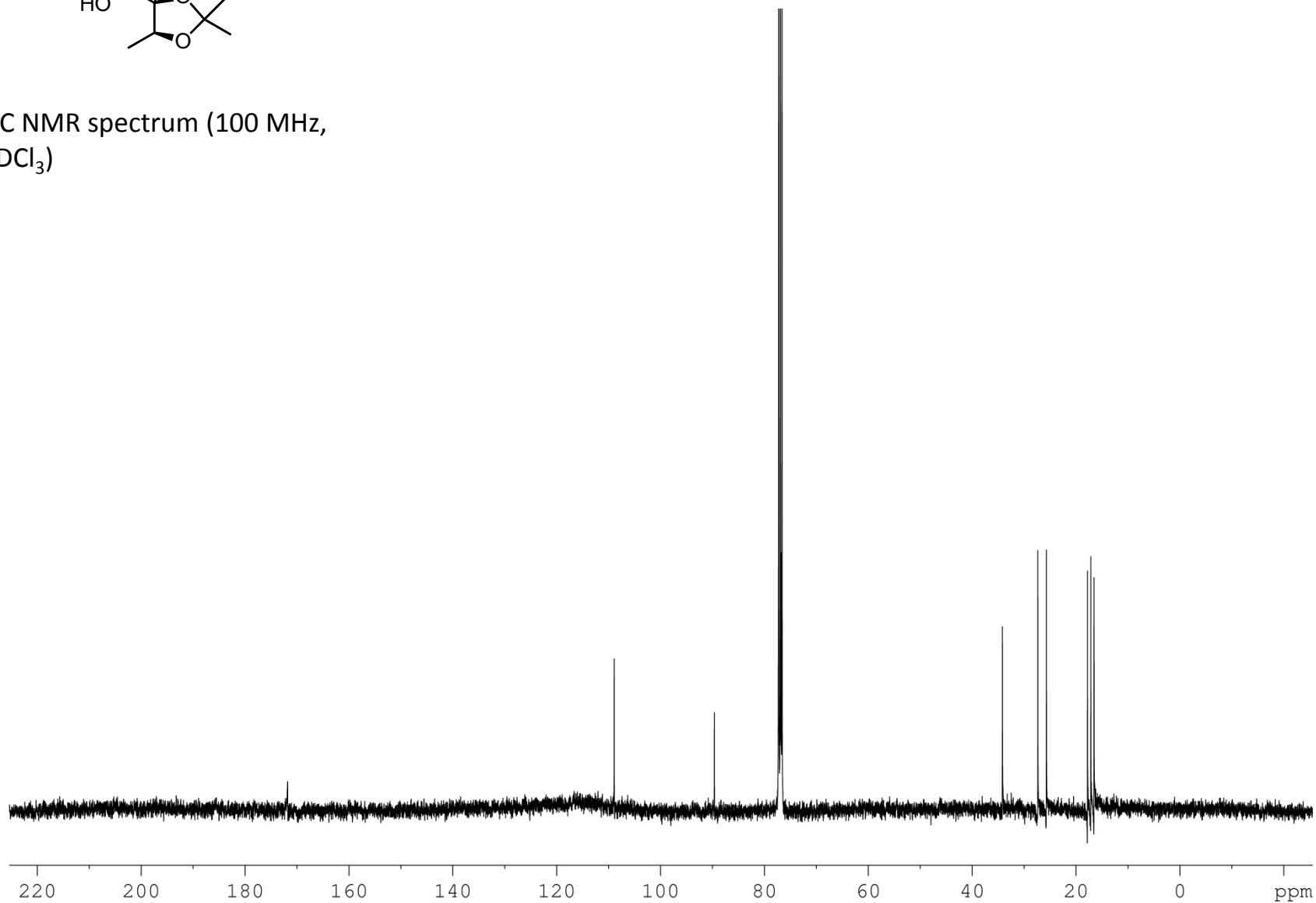


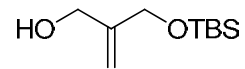
^1H NMR spectrum (400 MHz, CDCl_3)



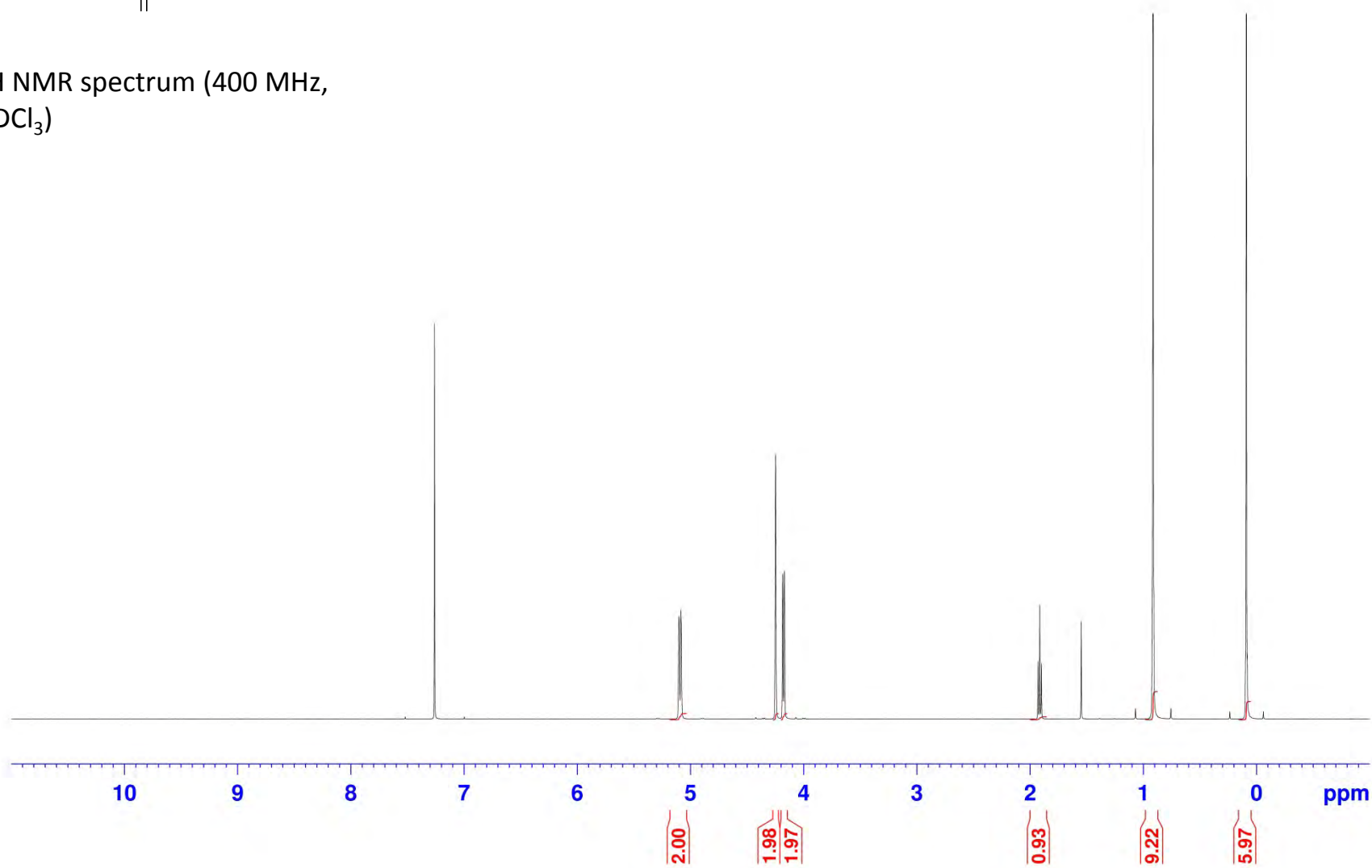


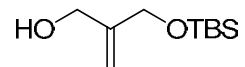
^{13}C NMR spectrum (100 MHz, CDCl_3)



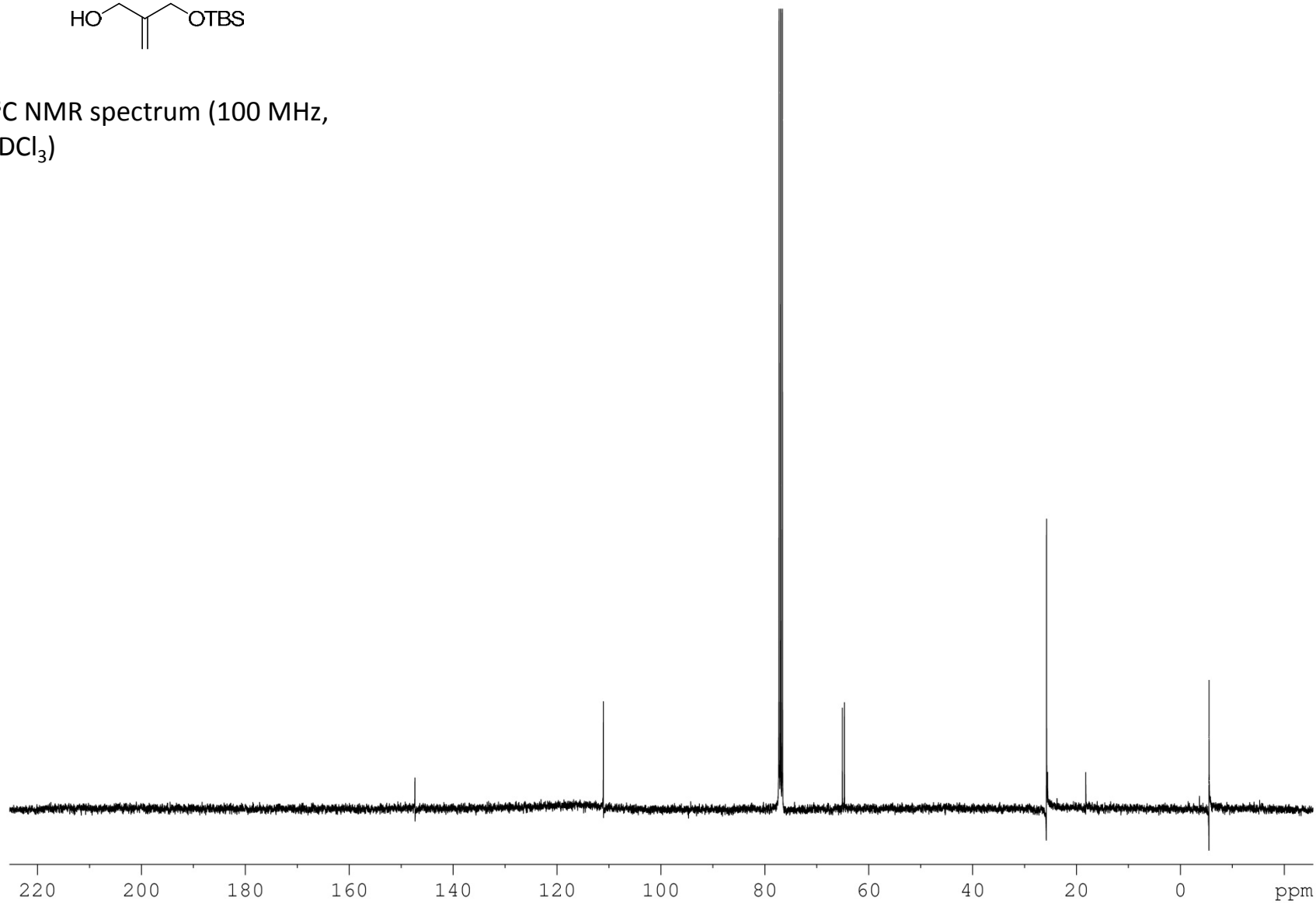


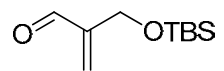
^1H NMR spectrum (400 MHz,
 CDCl_3)



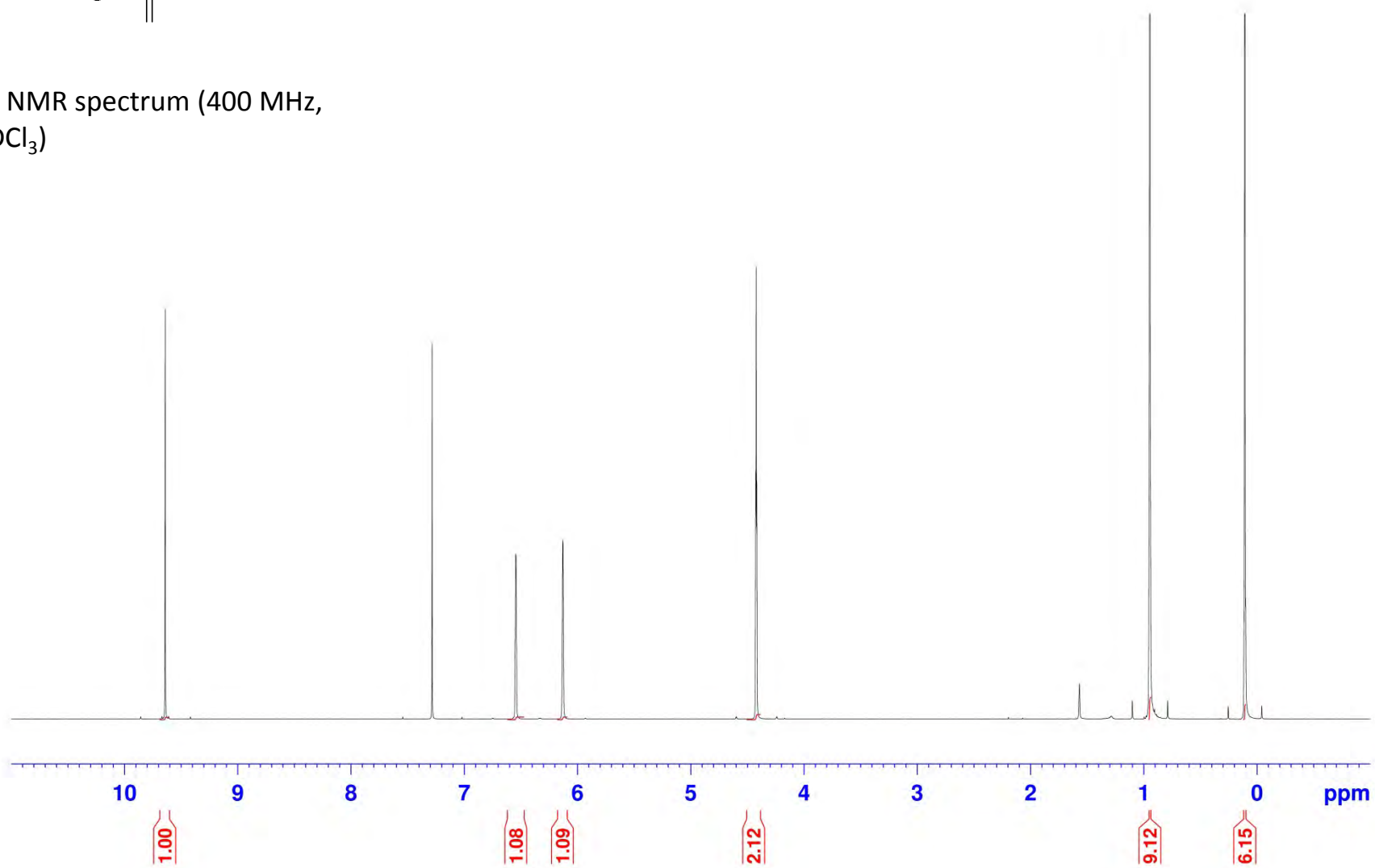


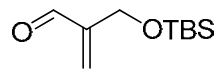
^{13}C NMR spectrum (100 MHz,
 CDCl_3)



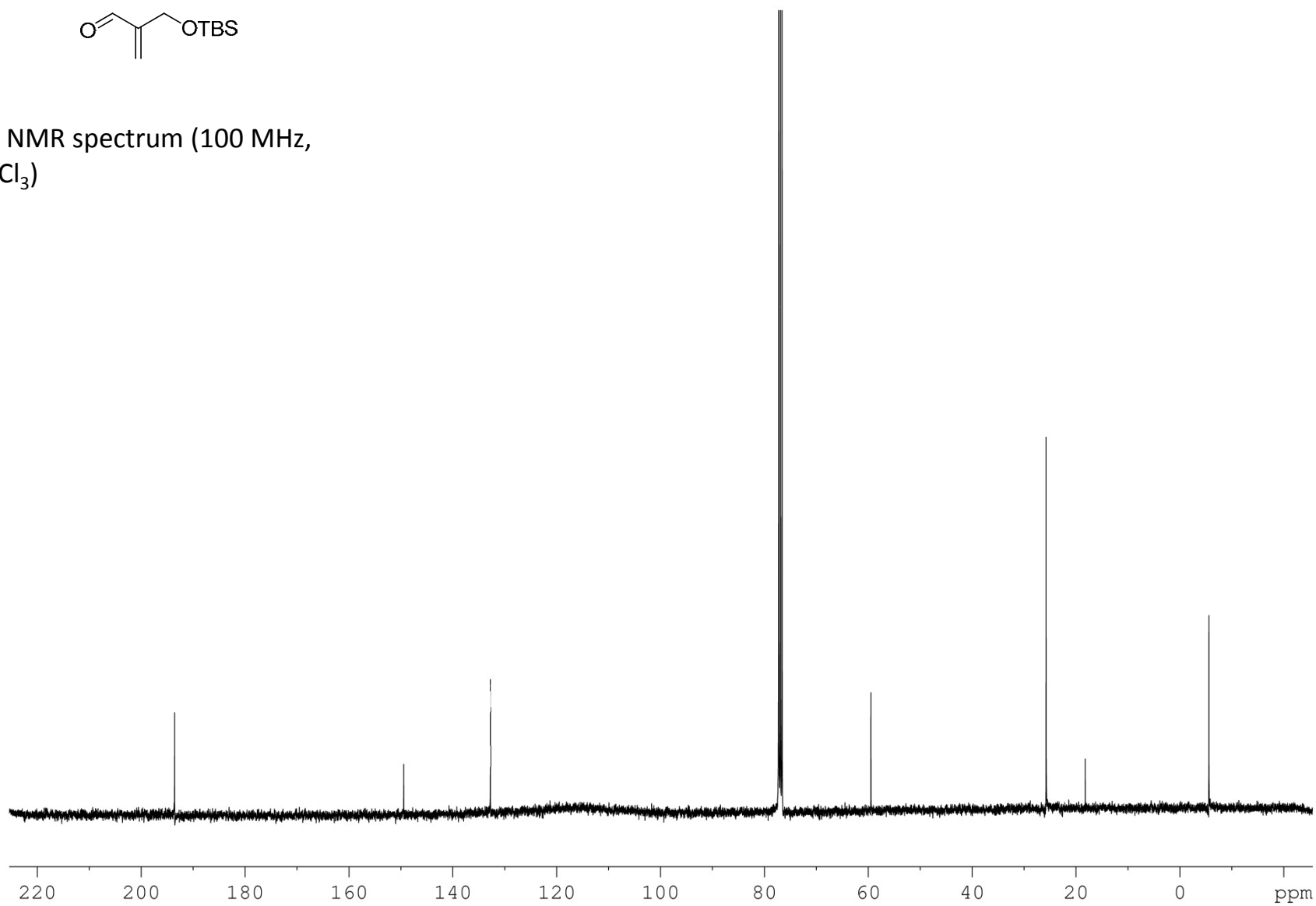


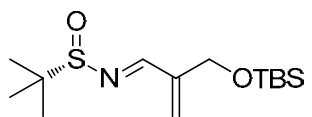
^1H NMR spectrum (400 MHz,
 CDCl_3)



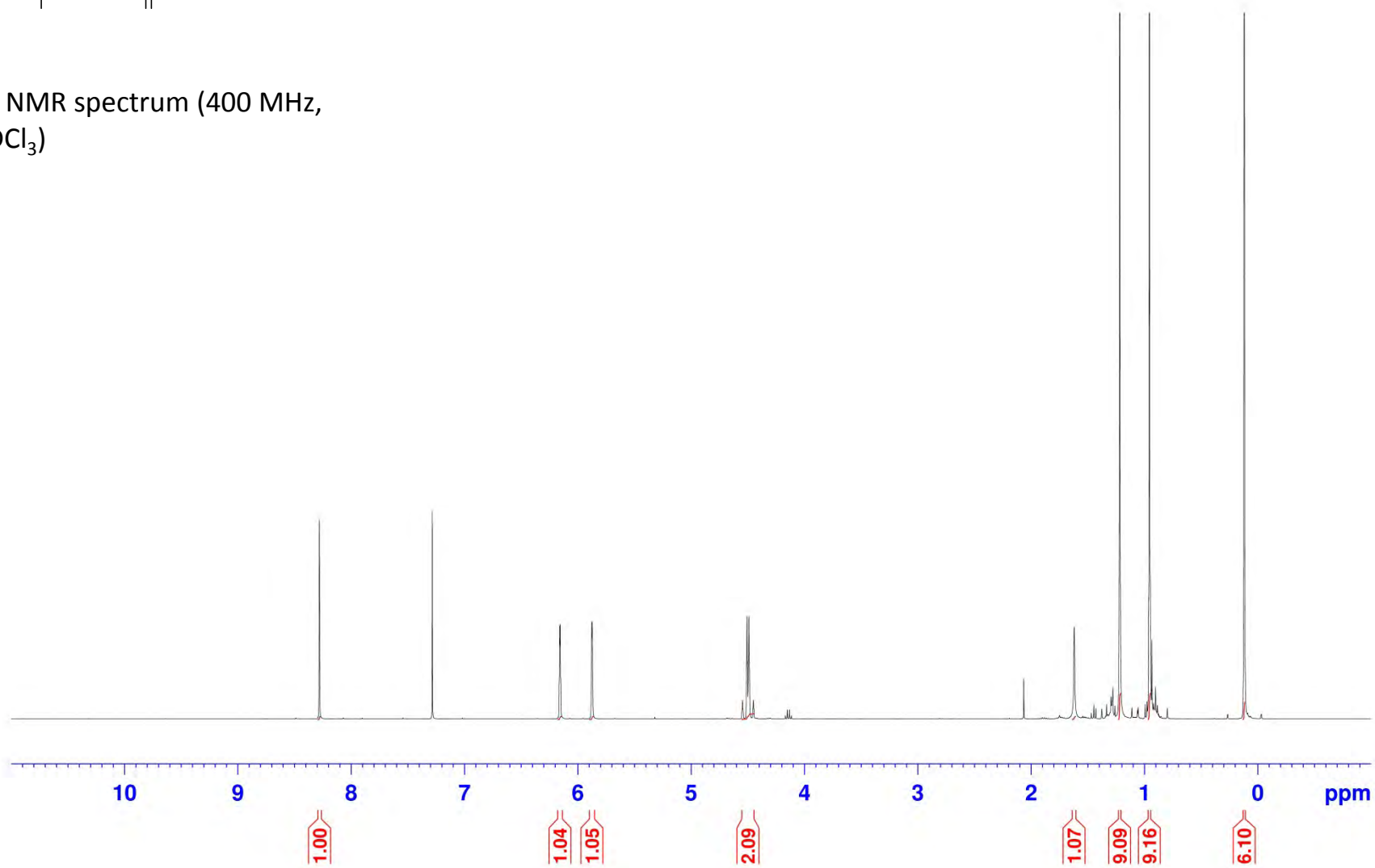


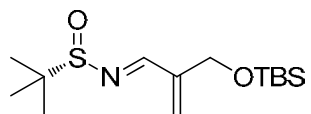
^{13}C NMR spectrum (100 MHz,
 CDCl_3)



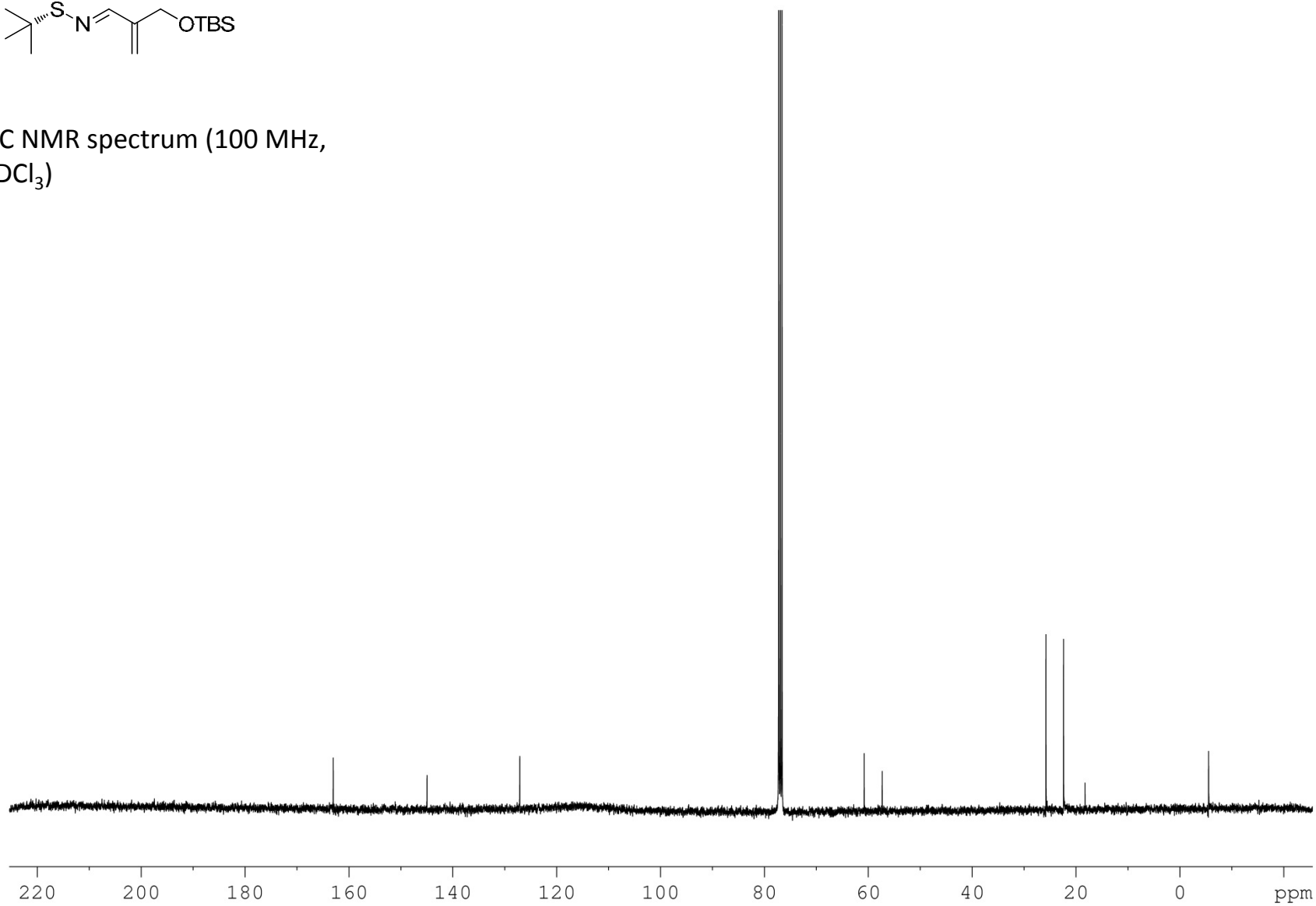


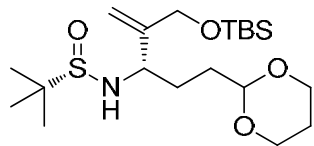
^1H NMR spectrum (400 MHz, CDCl_3)



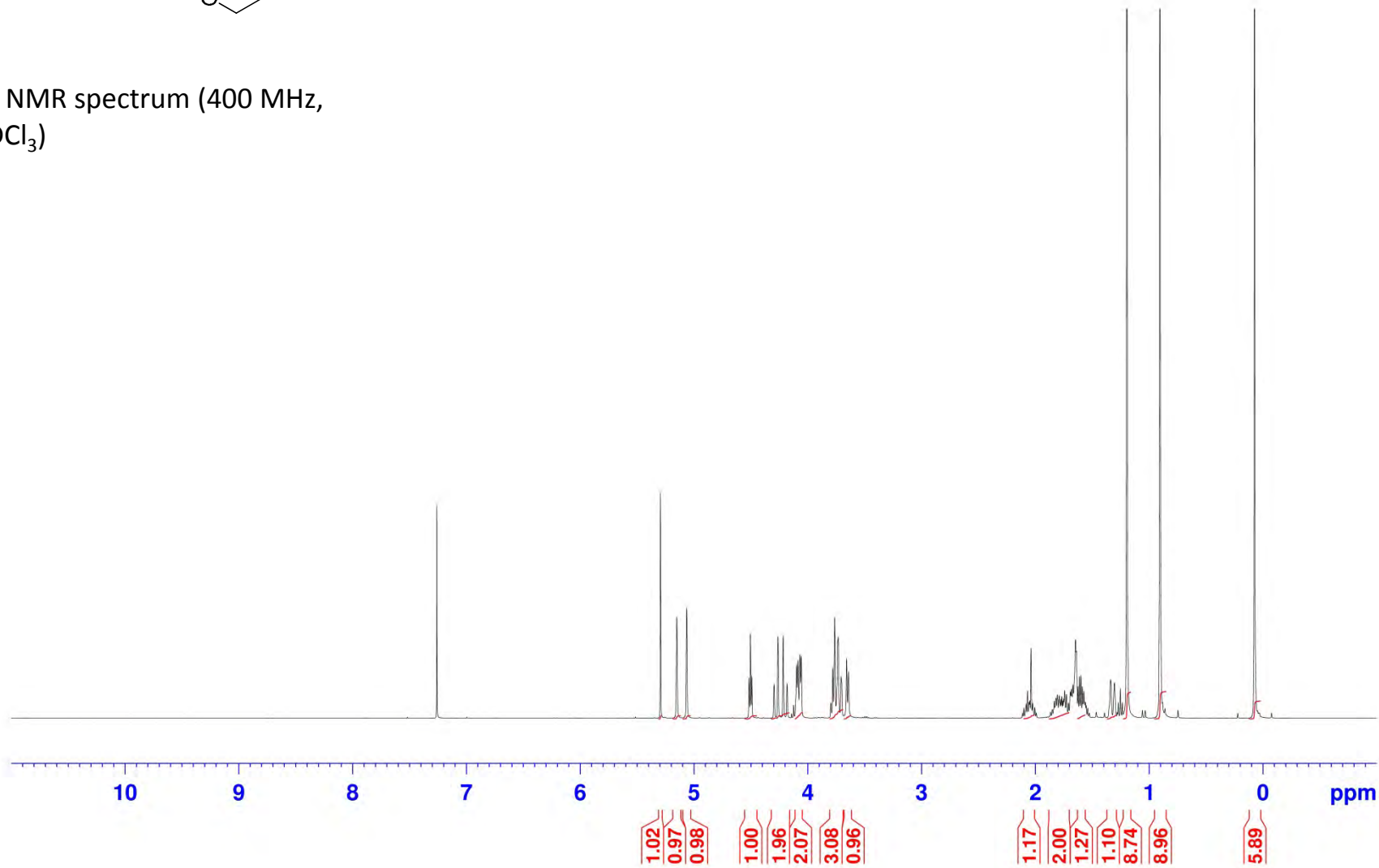


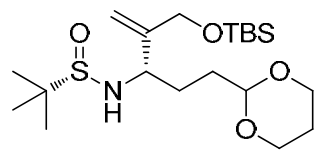
^{13}C NMR spectrum (100 MHz,
 CDCl_3)





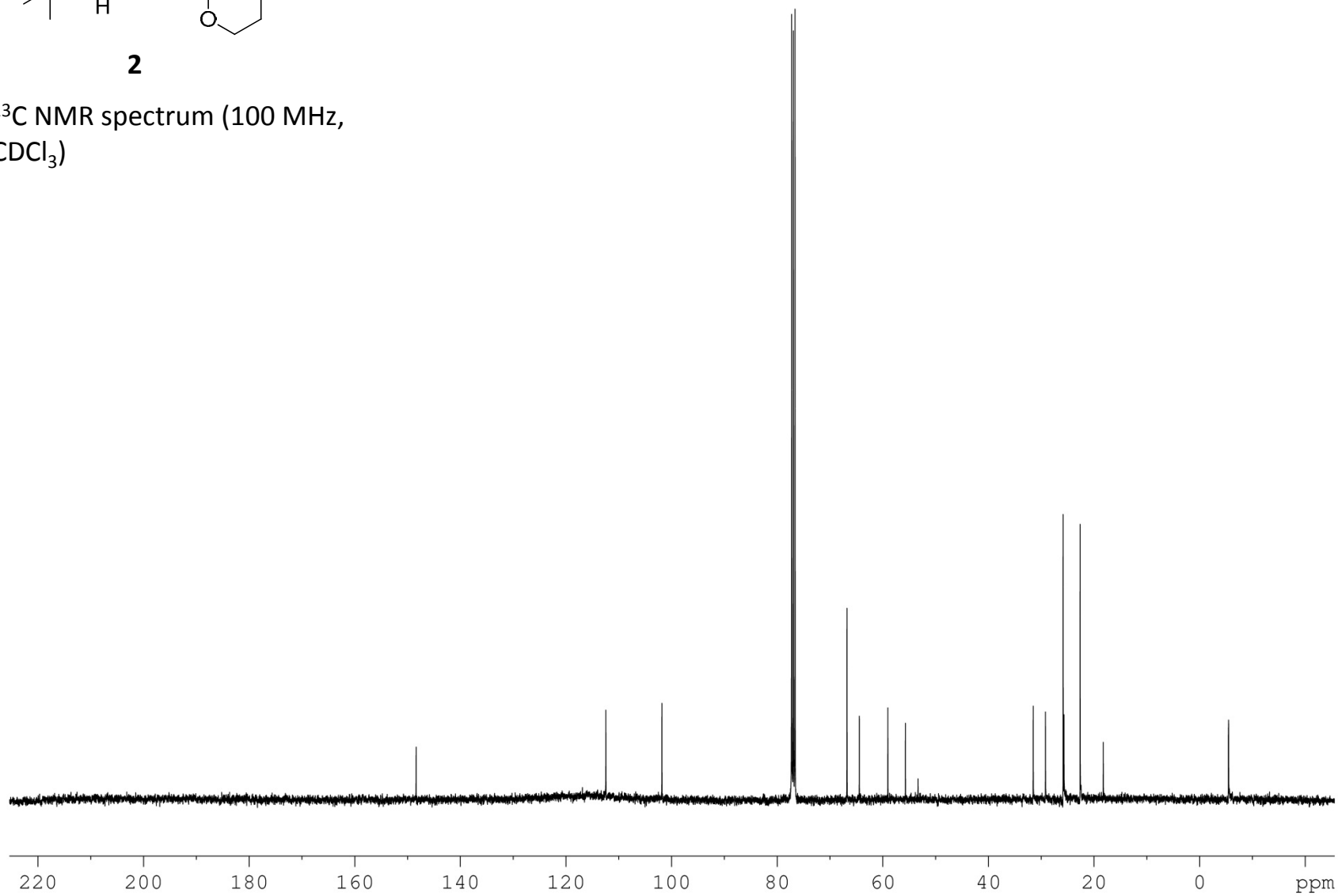
^1H NMR spectrum (400 MHz, CDCl_3)

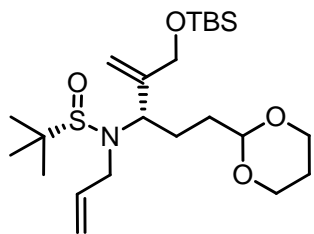




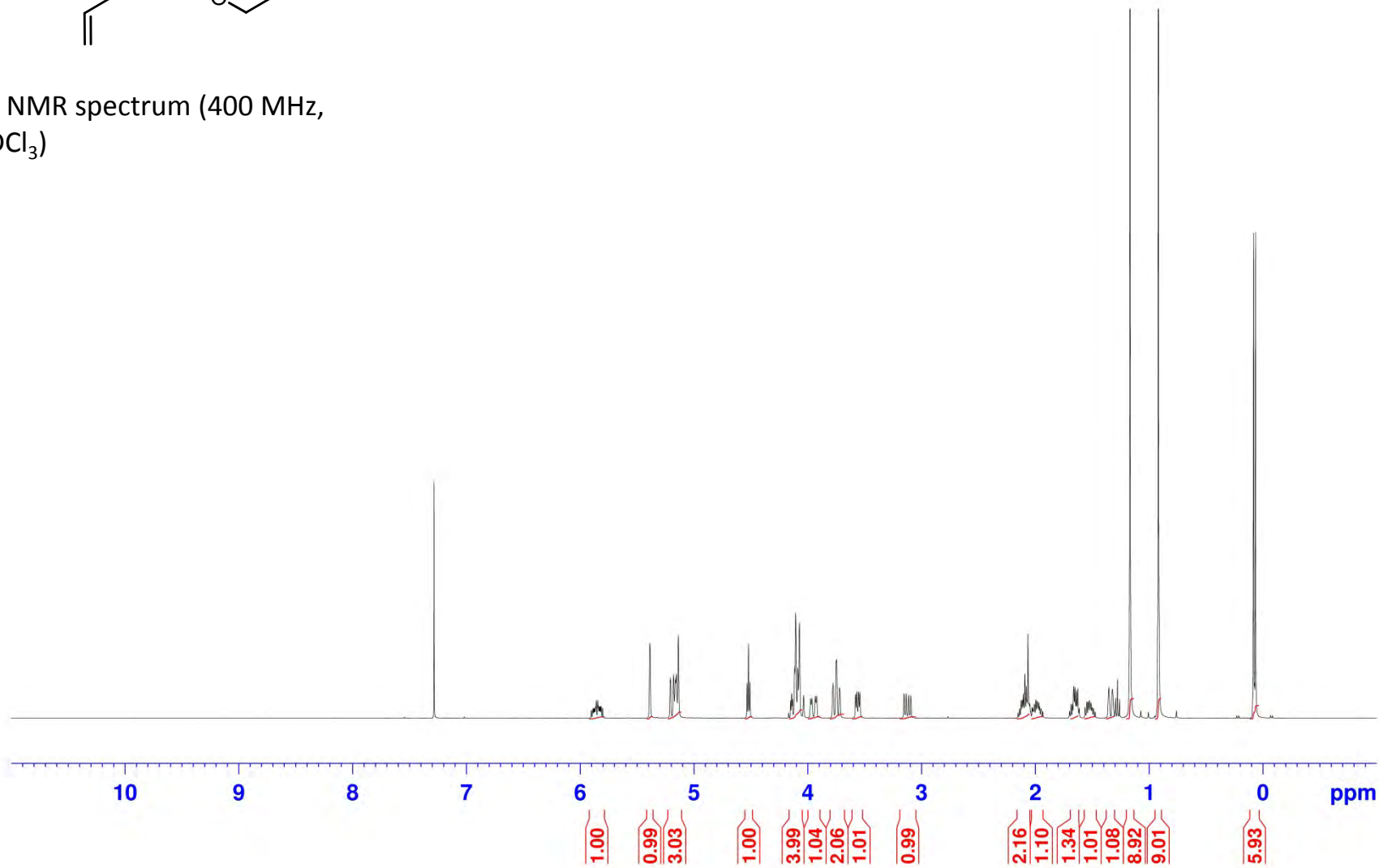
2

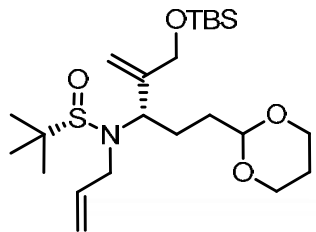
^{13}C NMR spectrum (100 MHz,
 CDCl_3)



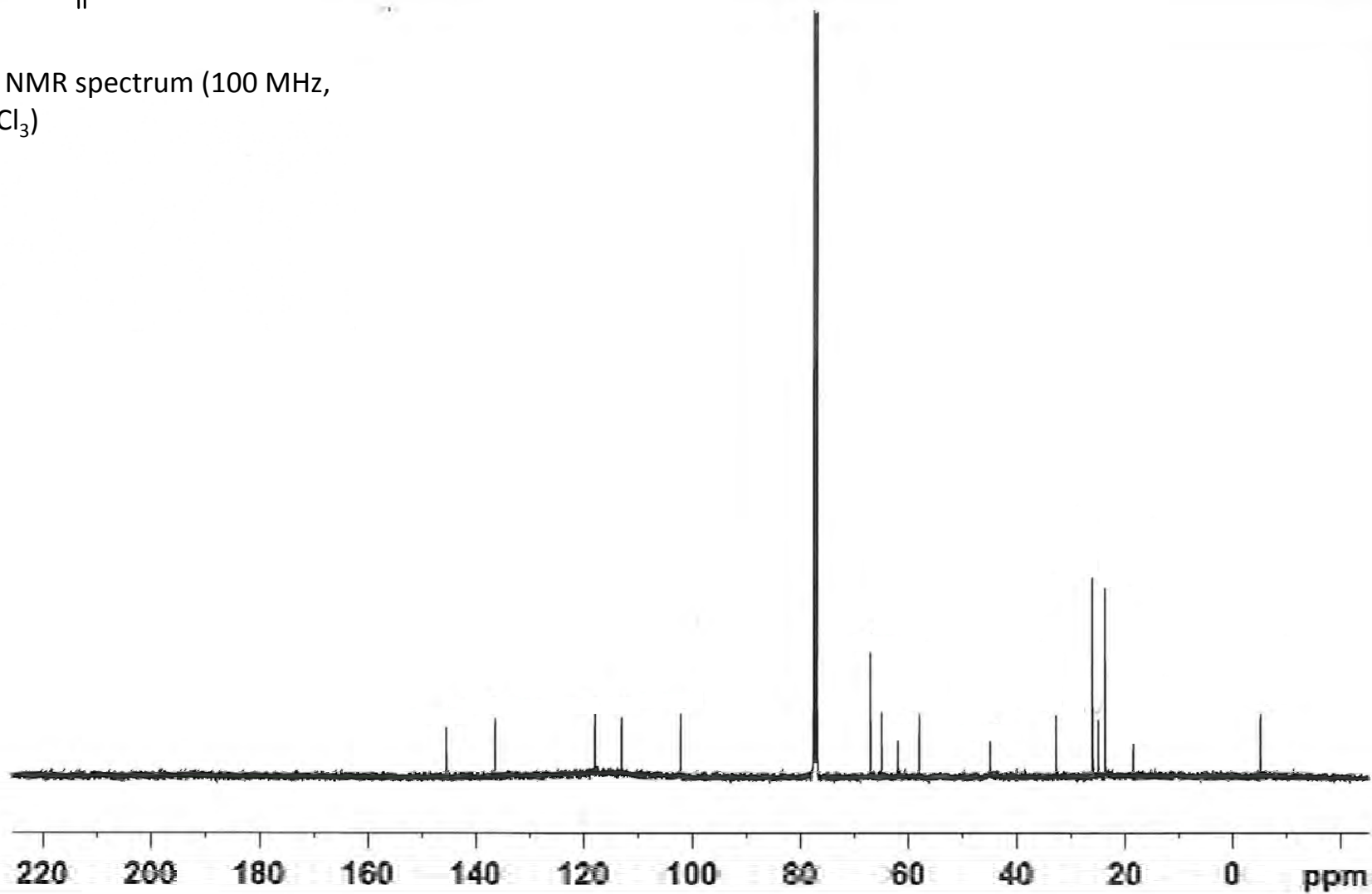


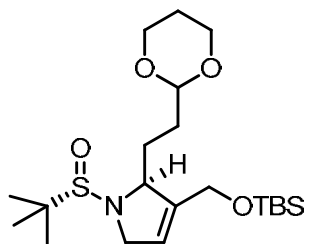
^1H NMR spectrum (400 MHz, CDCl_3)



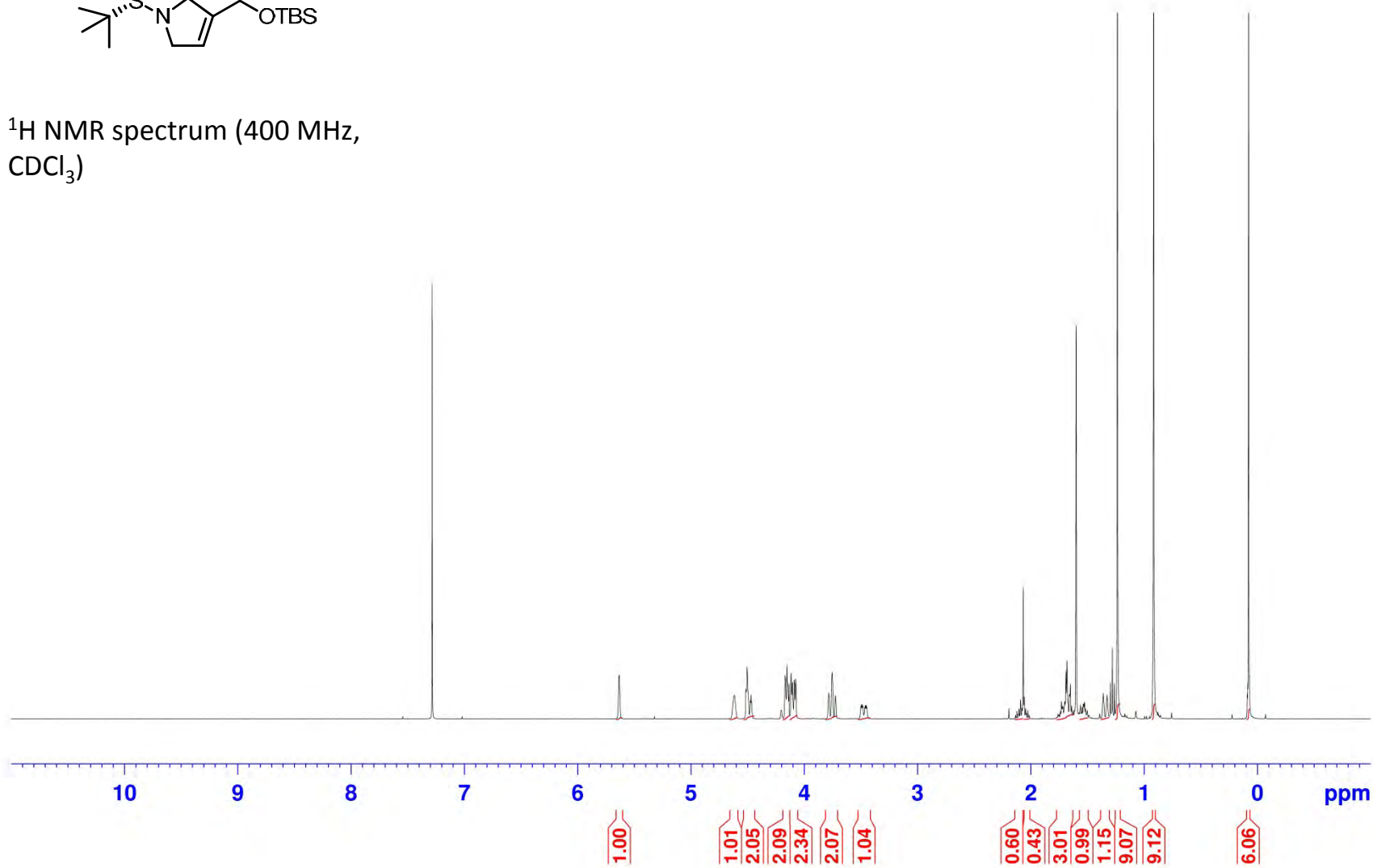


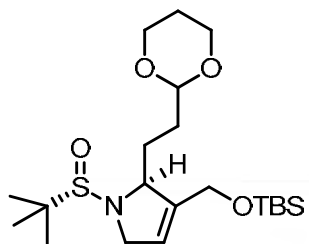
^{13}C NMR spectrum (100 MHz, CDCl_3)



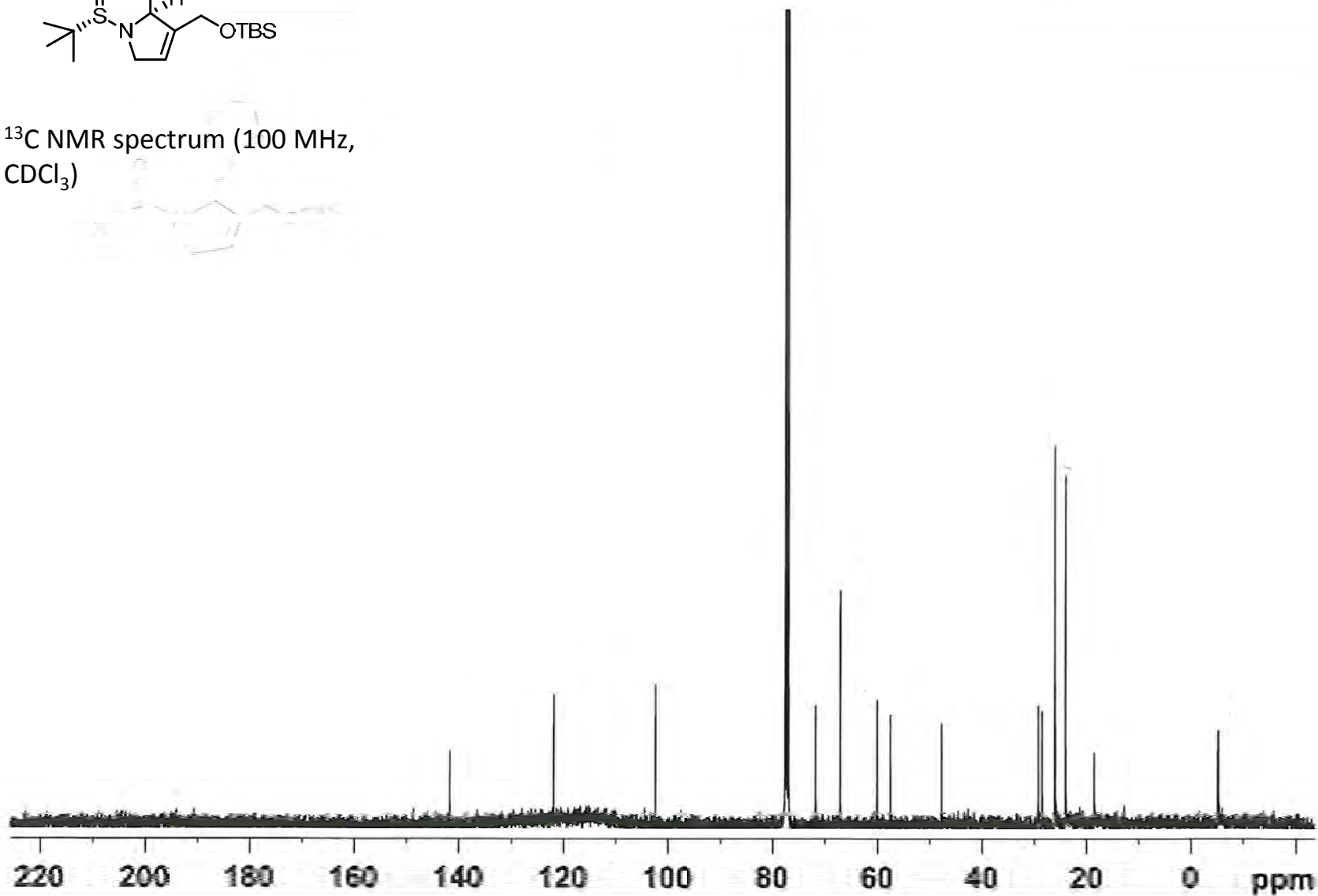


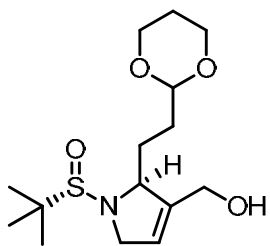
^1H NMR spectrum (400 MHz, CDCl_3)



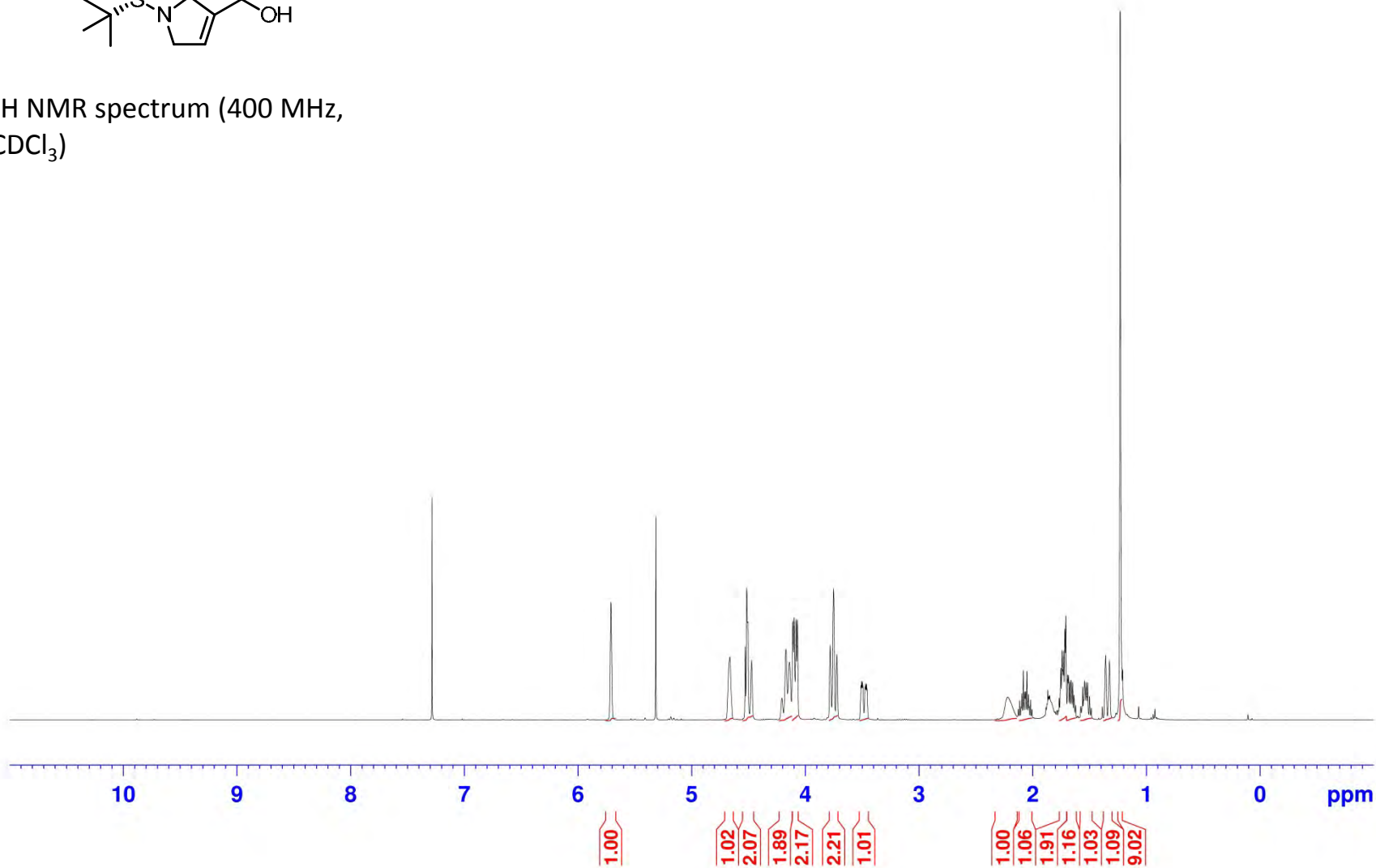


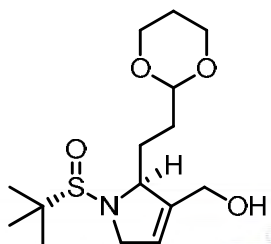
¹³C NMR spectrum (100 MHz, CDCl₃)



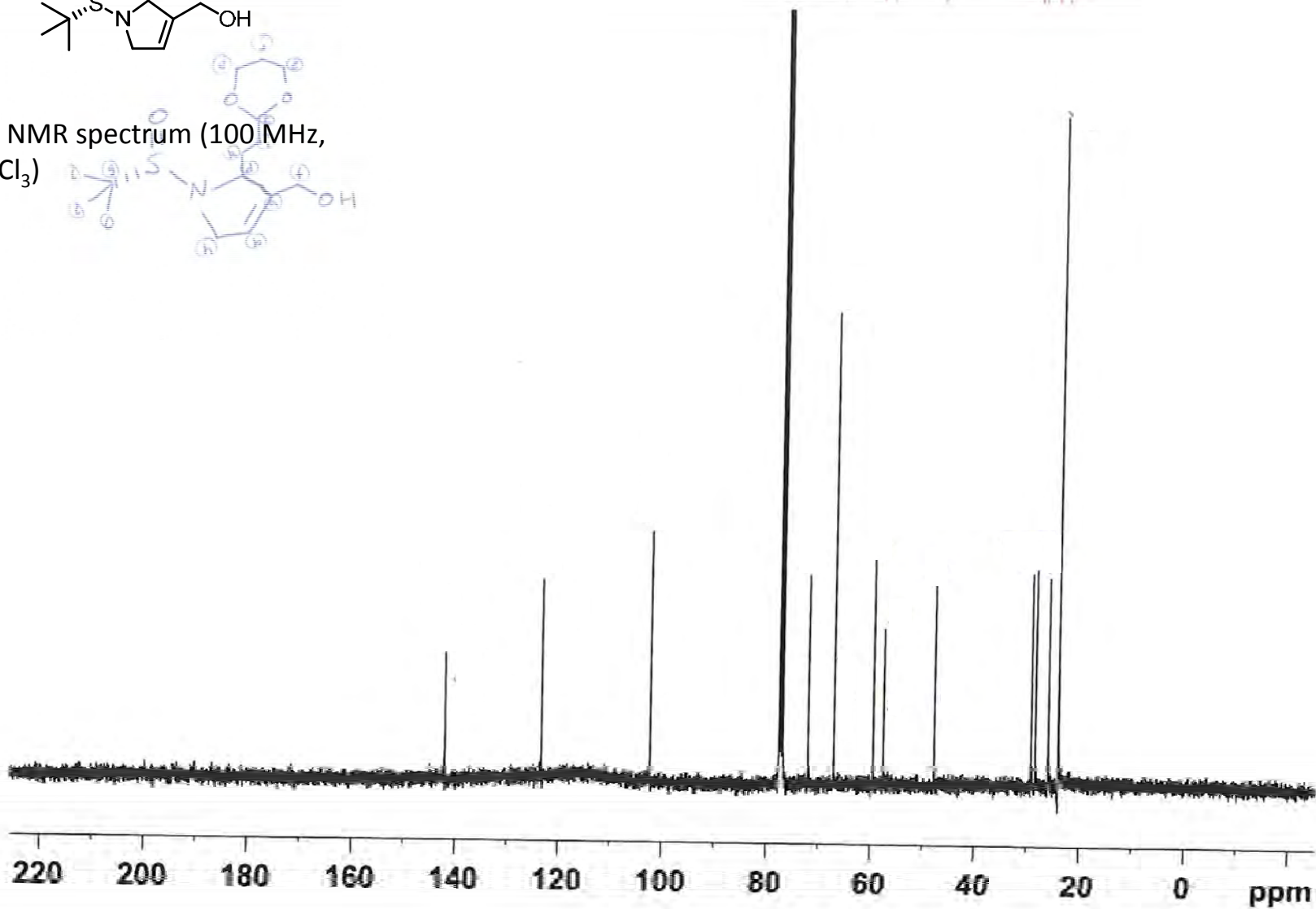
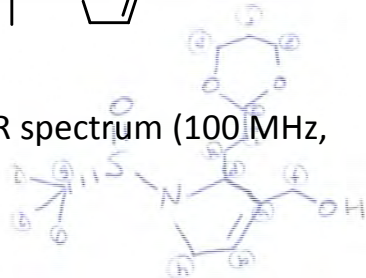


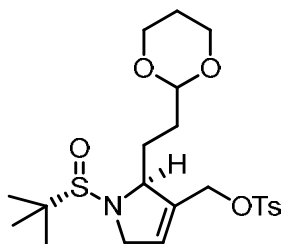
^1H NMR spectrum (400 MHz, CDCl_3)



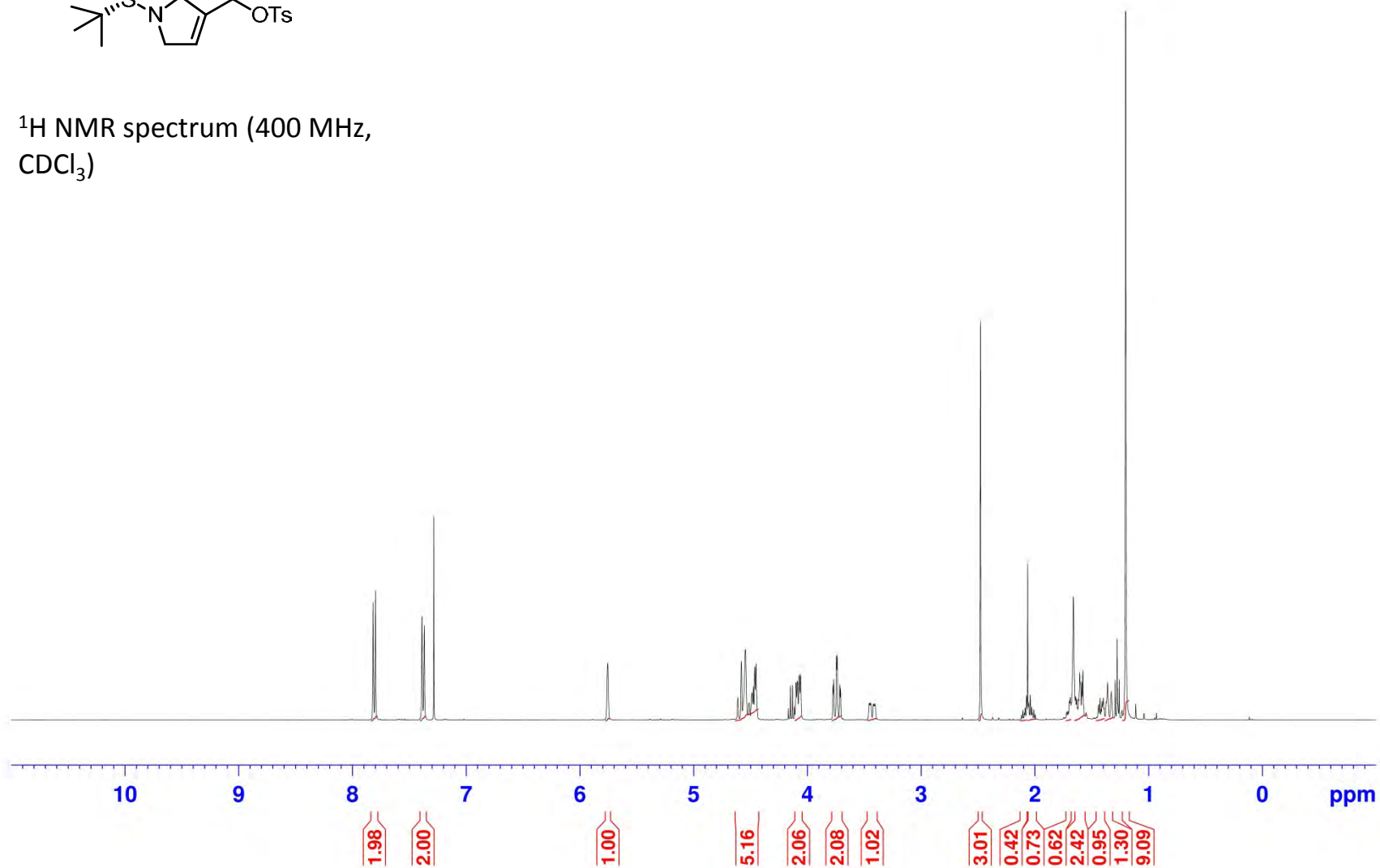


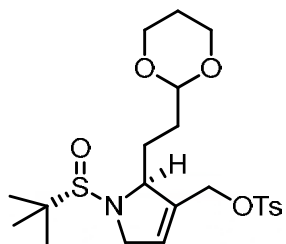
^{13}C NMR spectrum (100 MHz, CDCl_3)



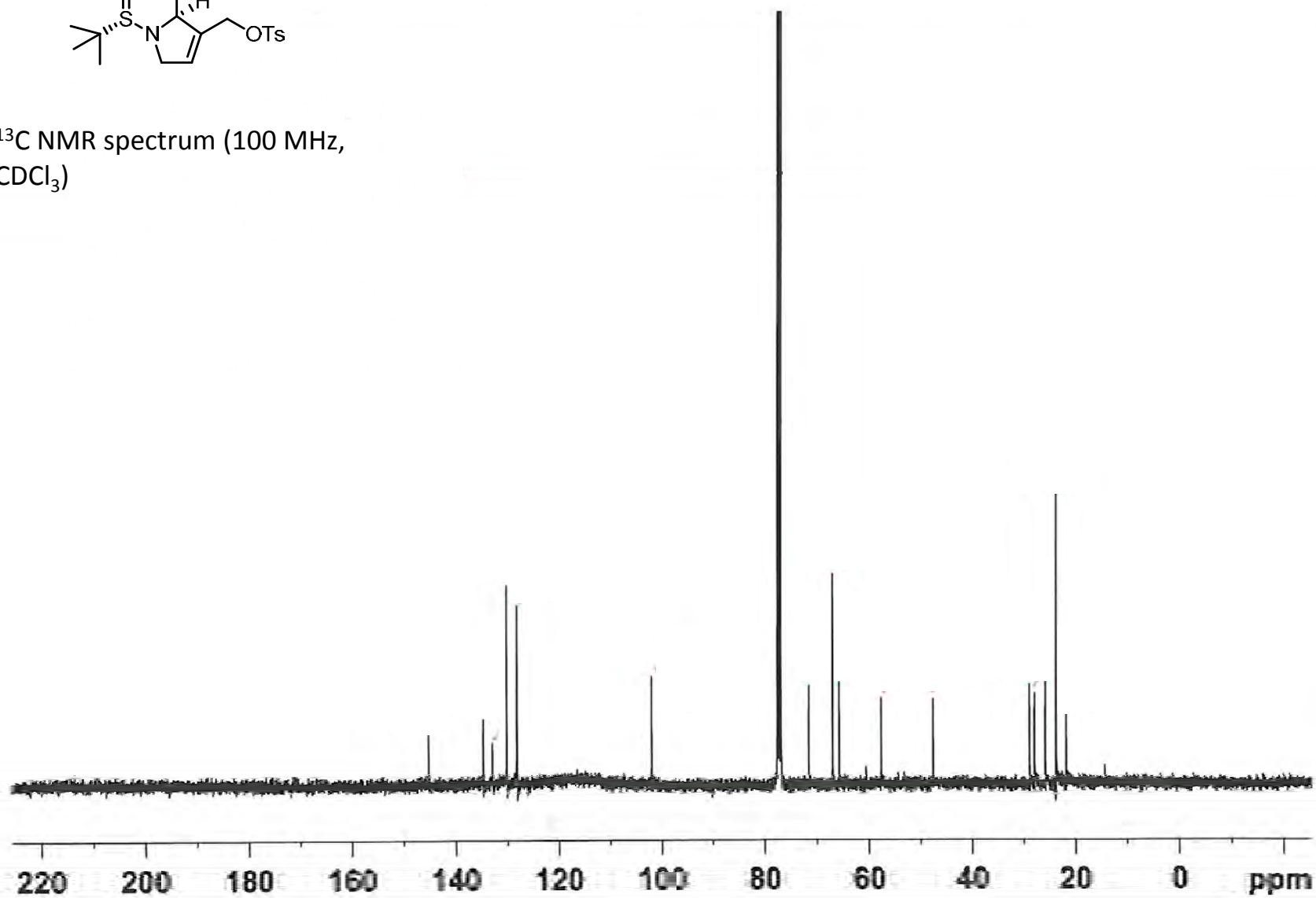


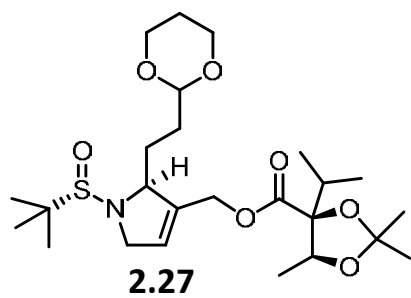
^1H NMR spectrum (400 MHz, CDCl_3)



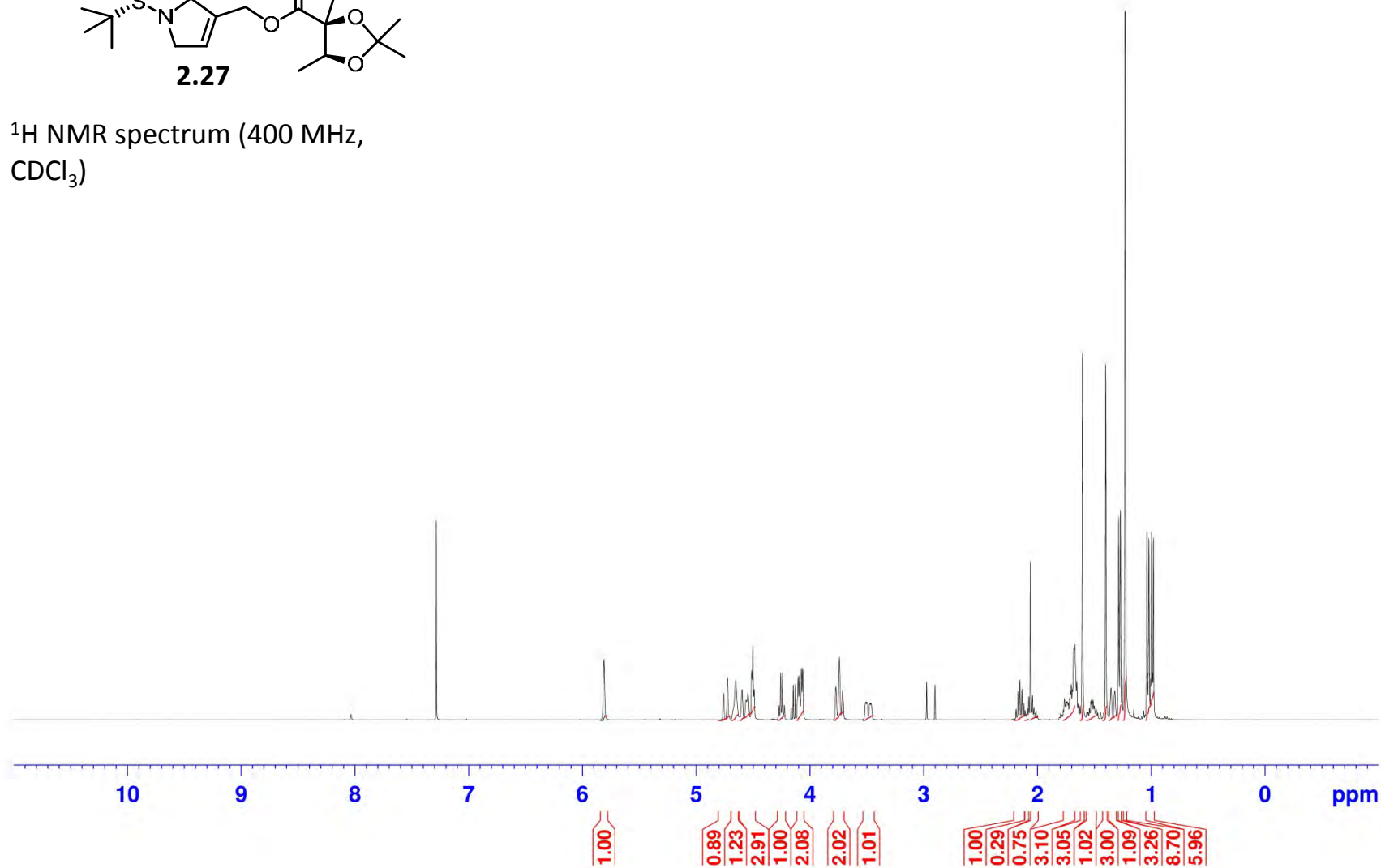


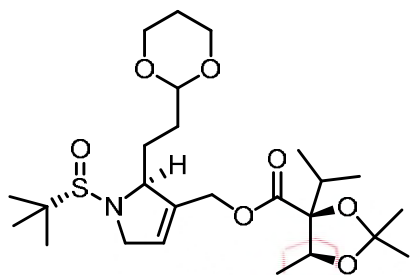
^{13}C NMR spectrum (100 MHz, CDCl_3)





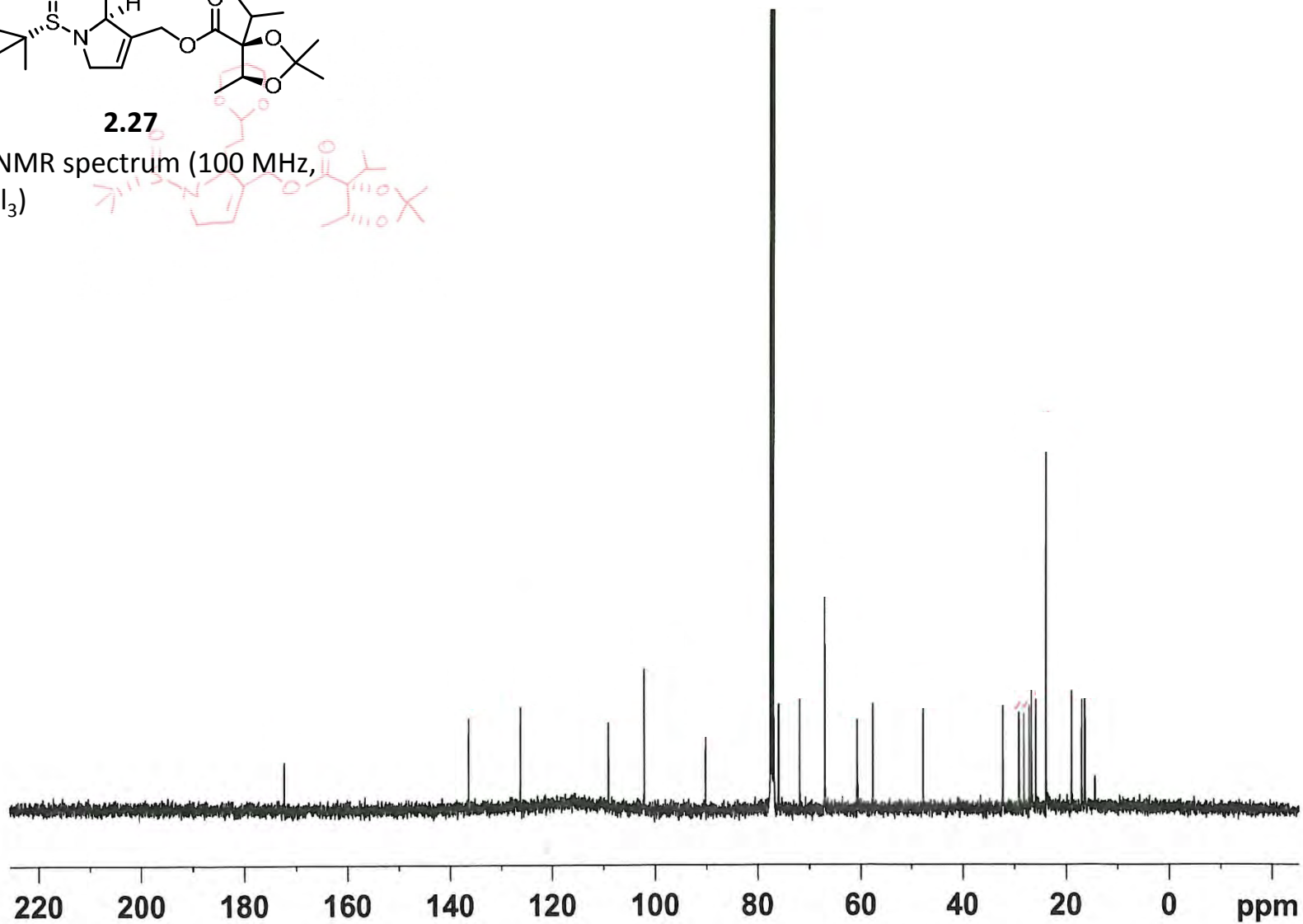
^1H NMR spectrum (400 MHz, CDCl_3)

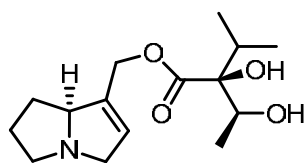




2.27

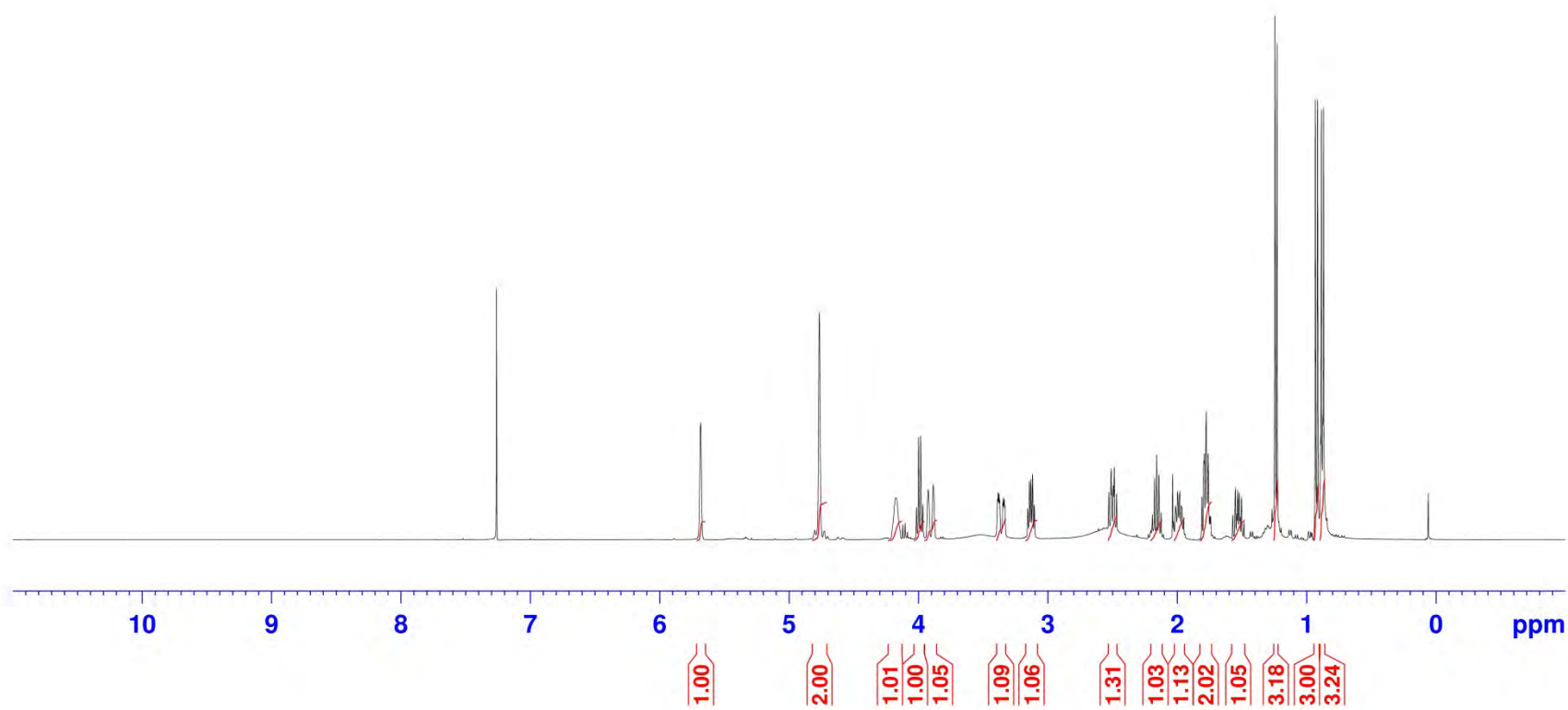
^{13}C NMR spectrum (100 MHz, CDCl_3)

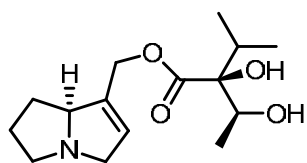




2.4

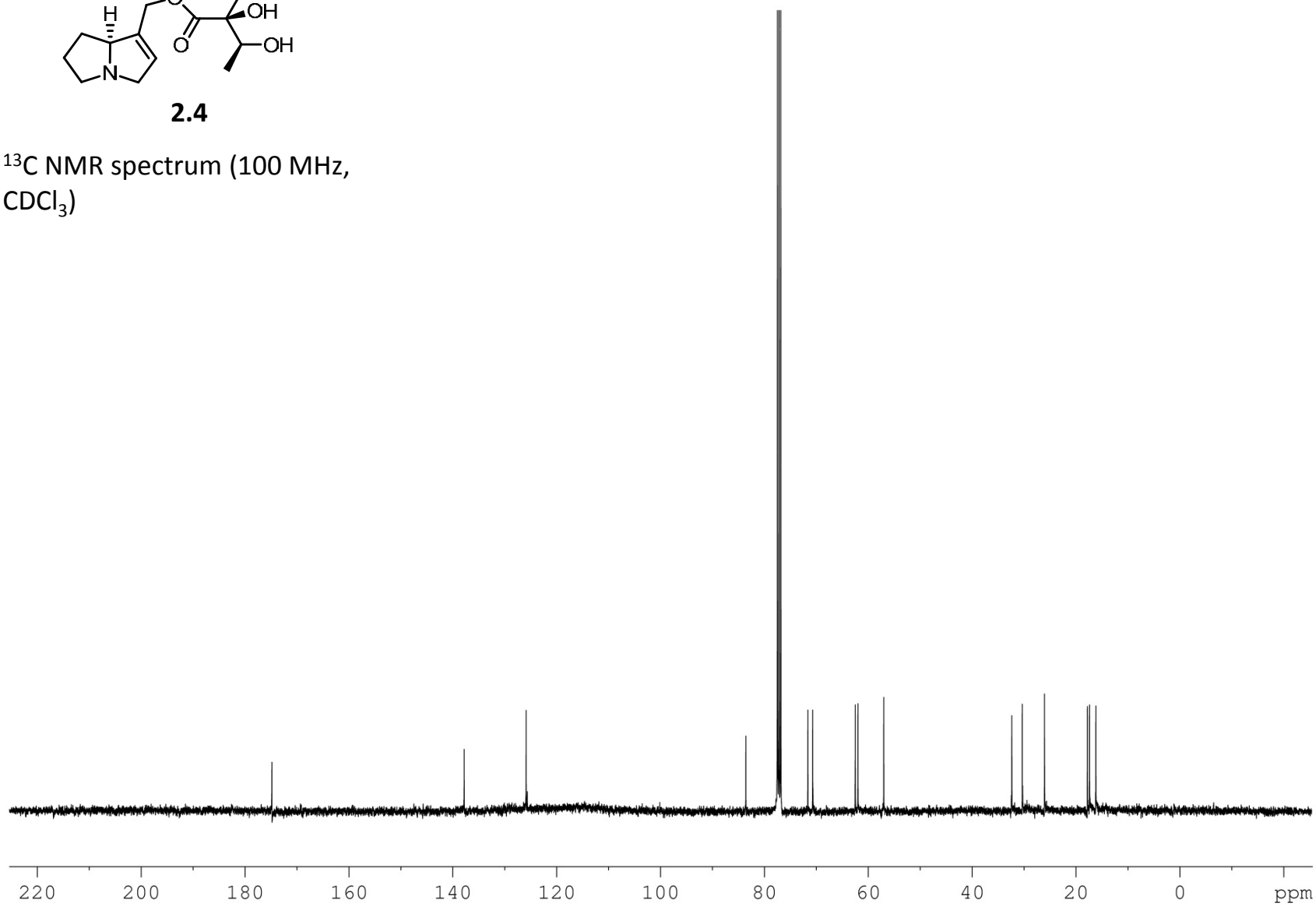
¹H NMR spectrum (400 MHz,
CDCl₃)

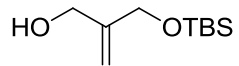




2.4

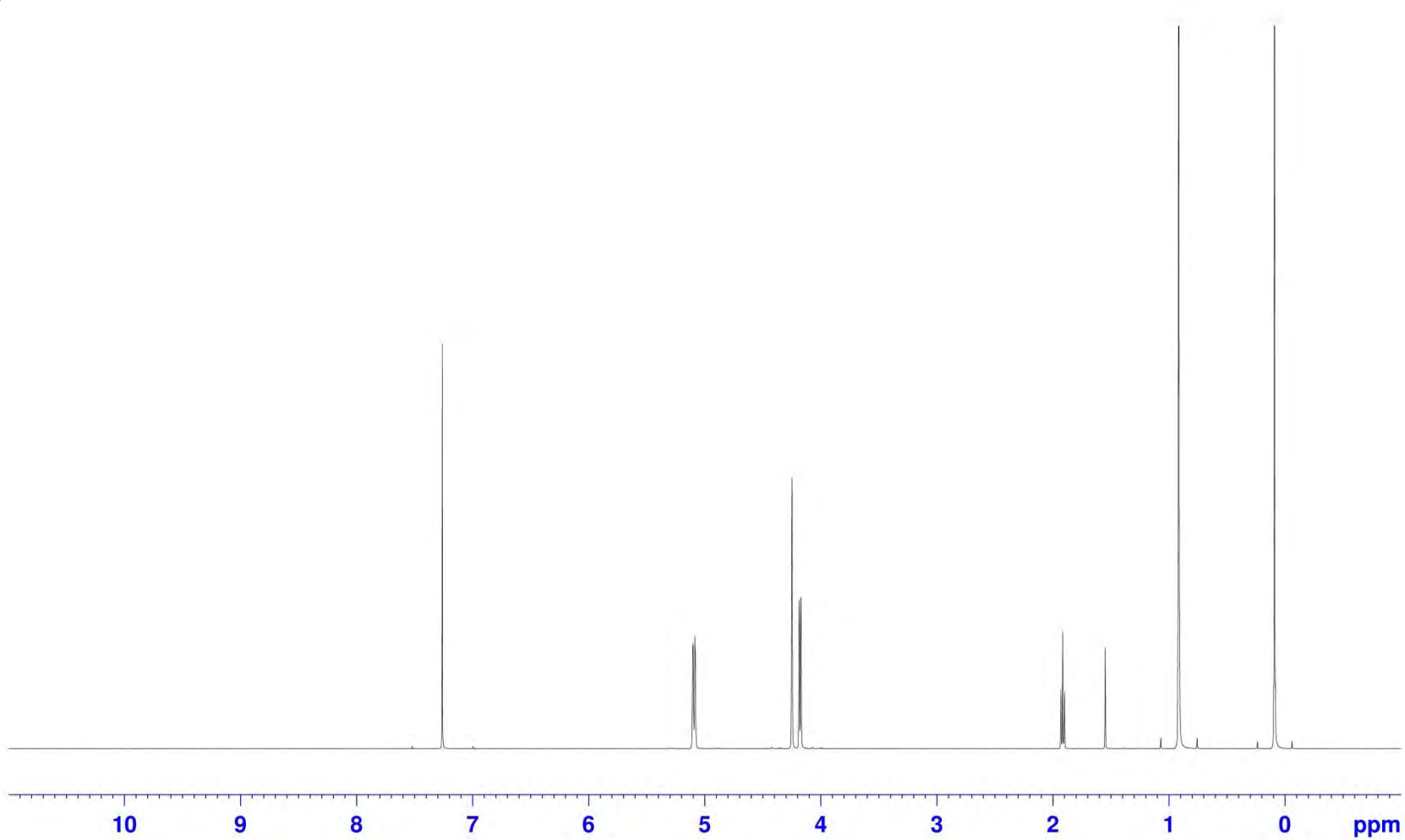
^{13}C NMR spectrum (100 MHz,
 CDCl_3)

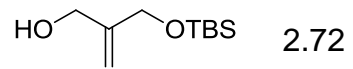




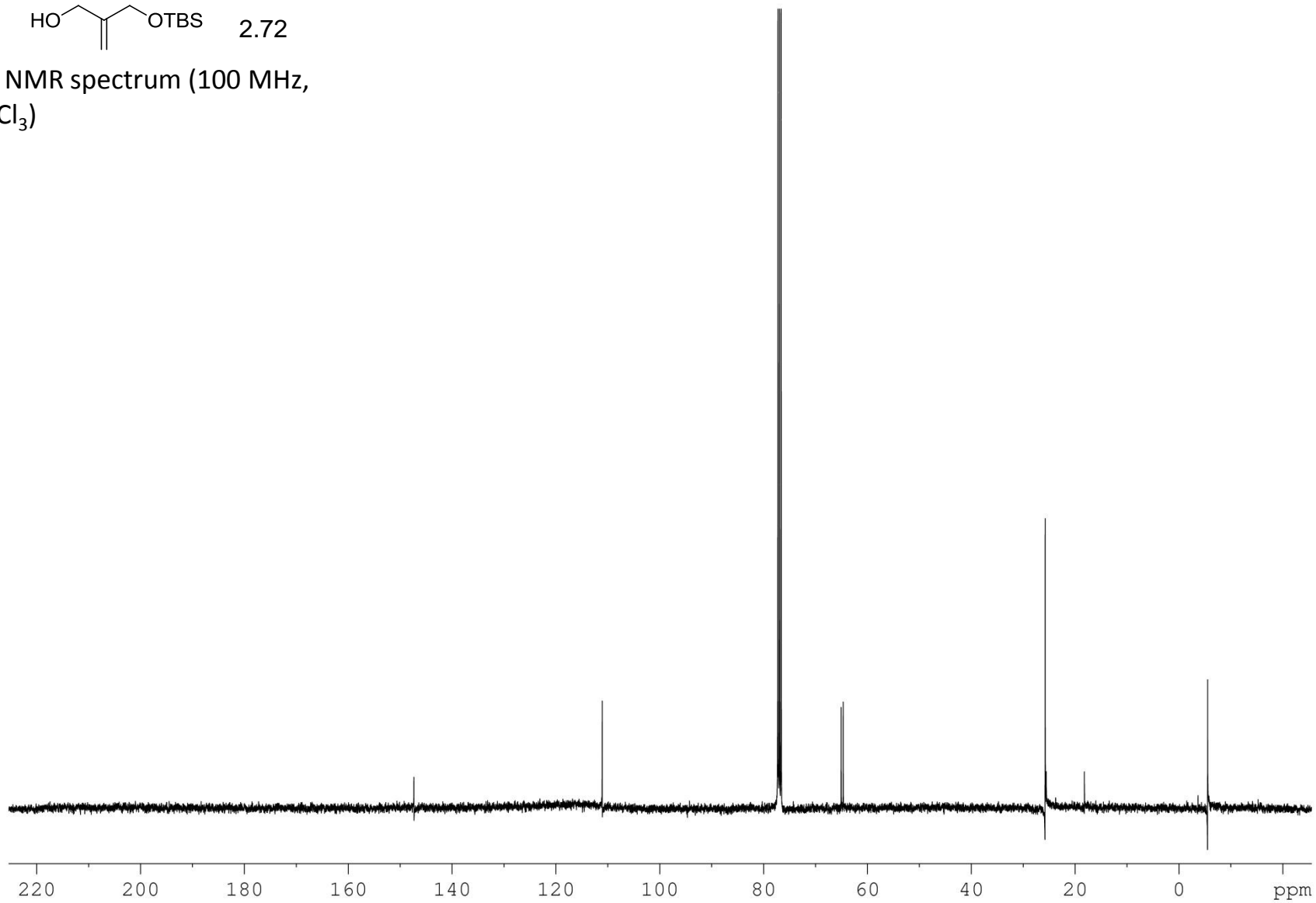
2.72

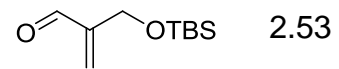
^1H NMR spectrum (400 MHz,
 CDCl_3)



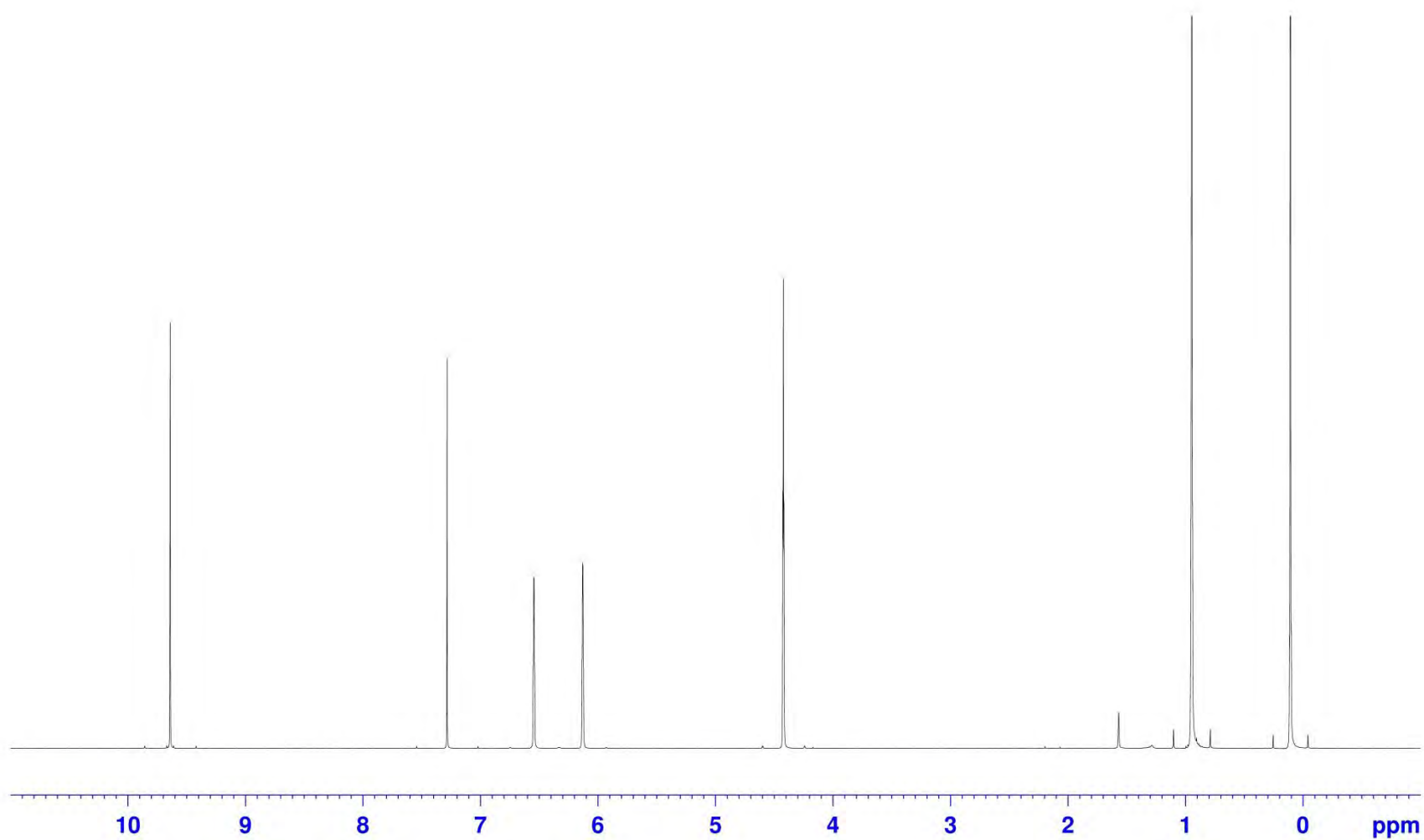


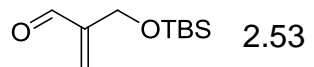
^{13}C NMR spectrum (100 MHz,
 CDCl_3)



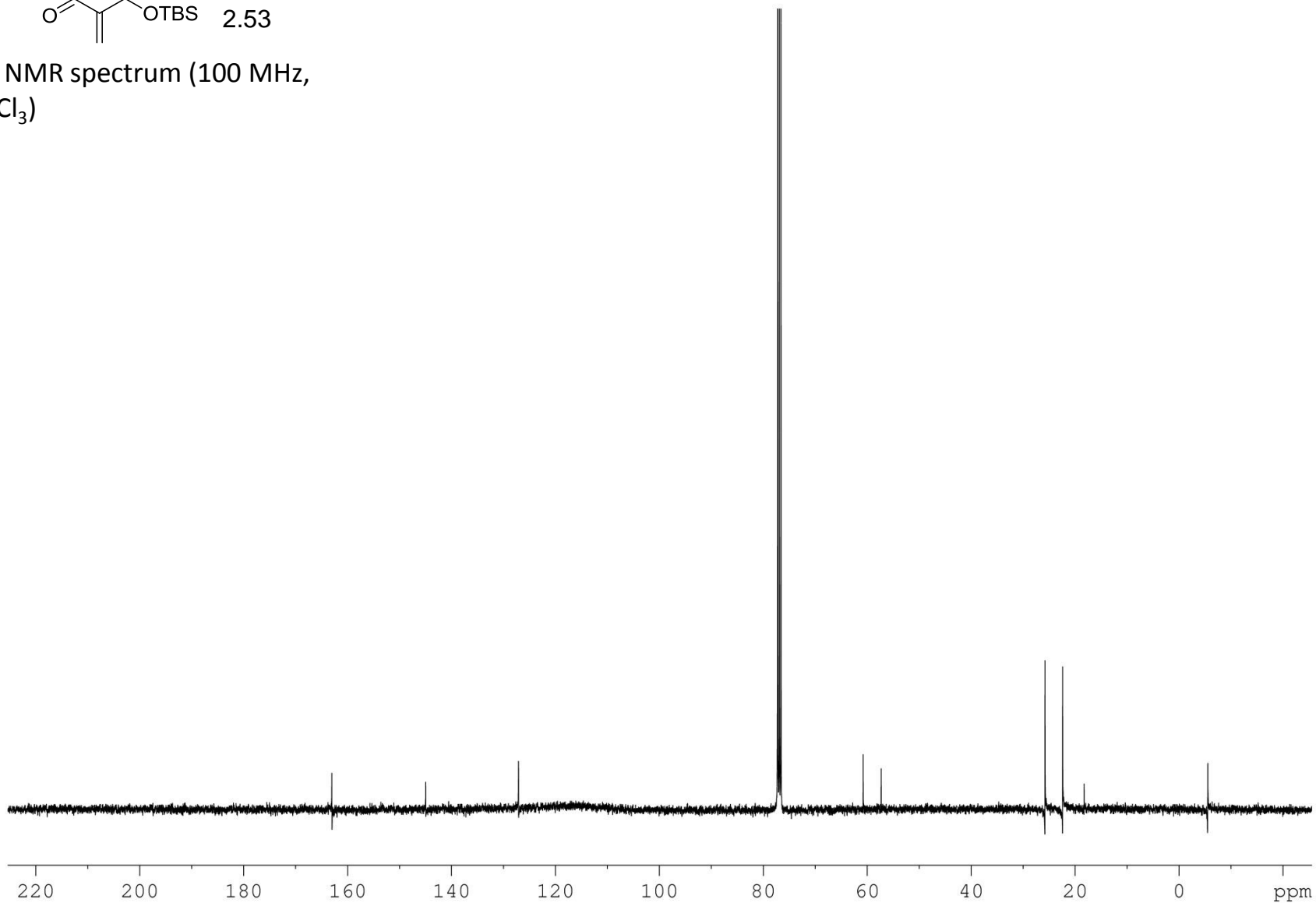


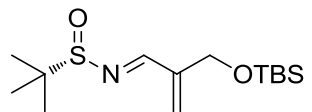
^1H NMR spectrum (400 MHz, CDCl_3)





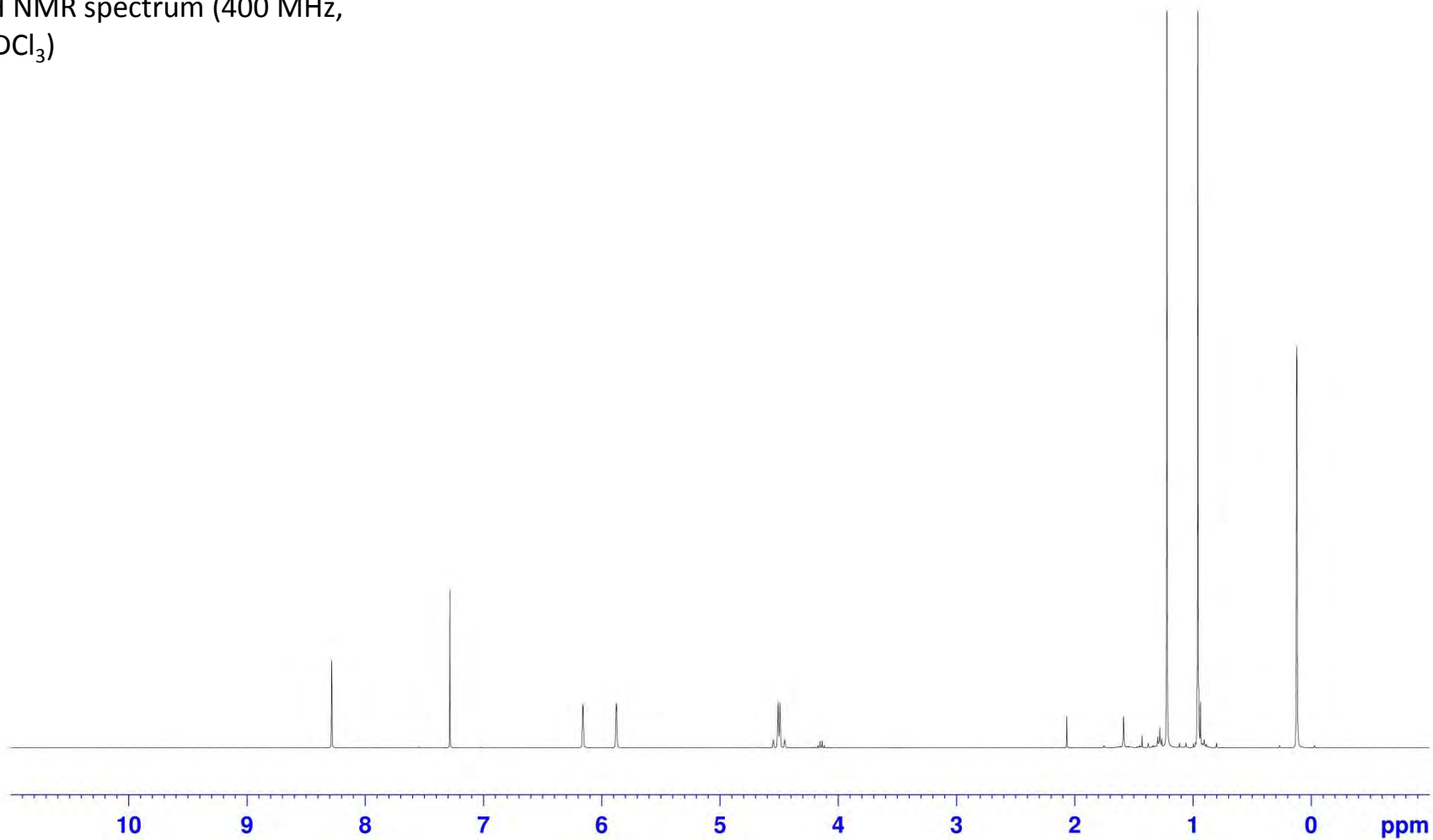
^{13}C NMR spectrum (100 MHz,
 CDCl_3)

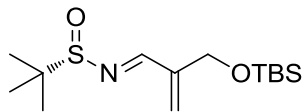




2.51

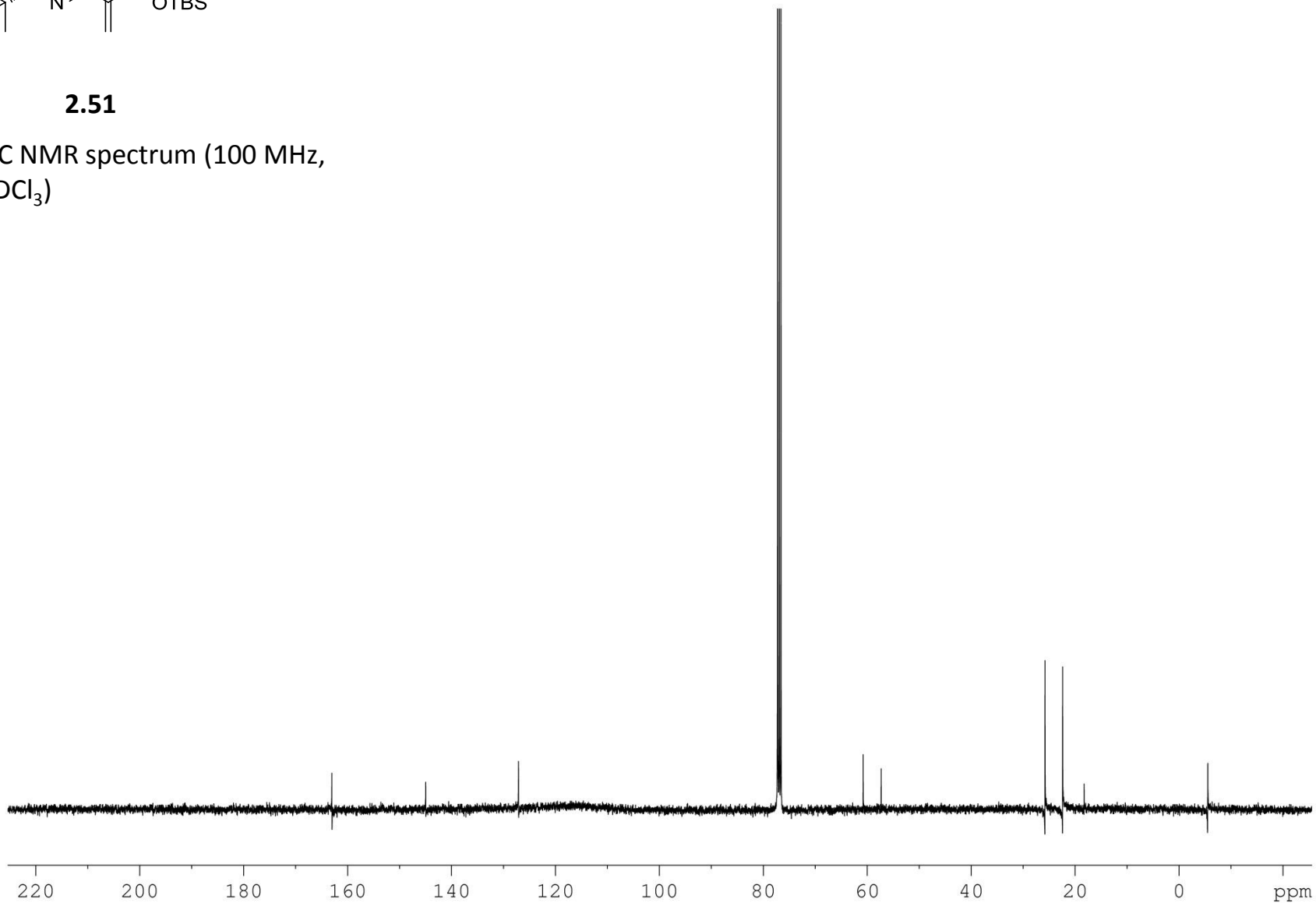
¹H NMR spectrum (400 MHz,
CDCl₃)

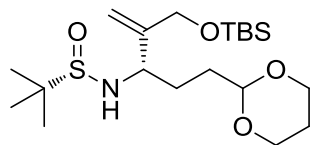




2.51

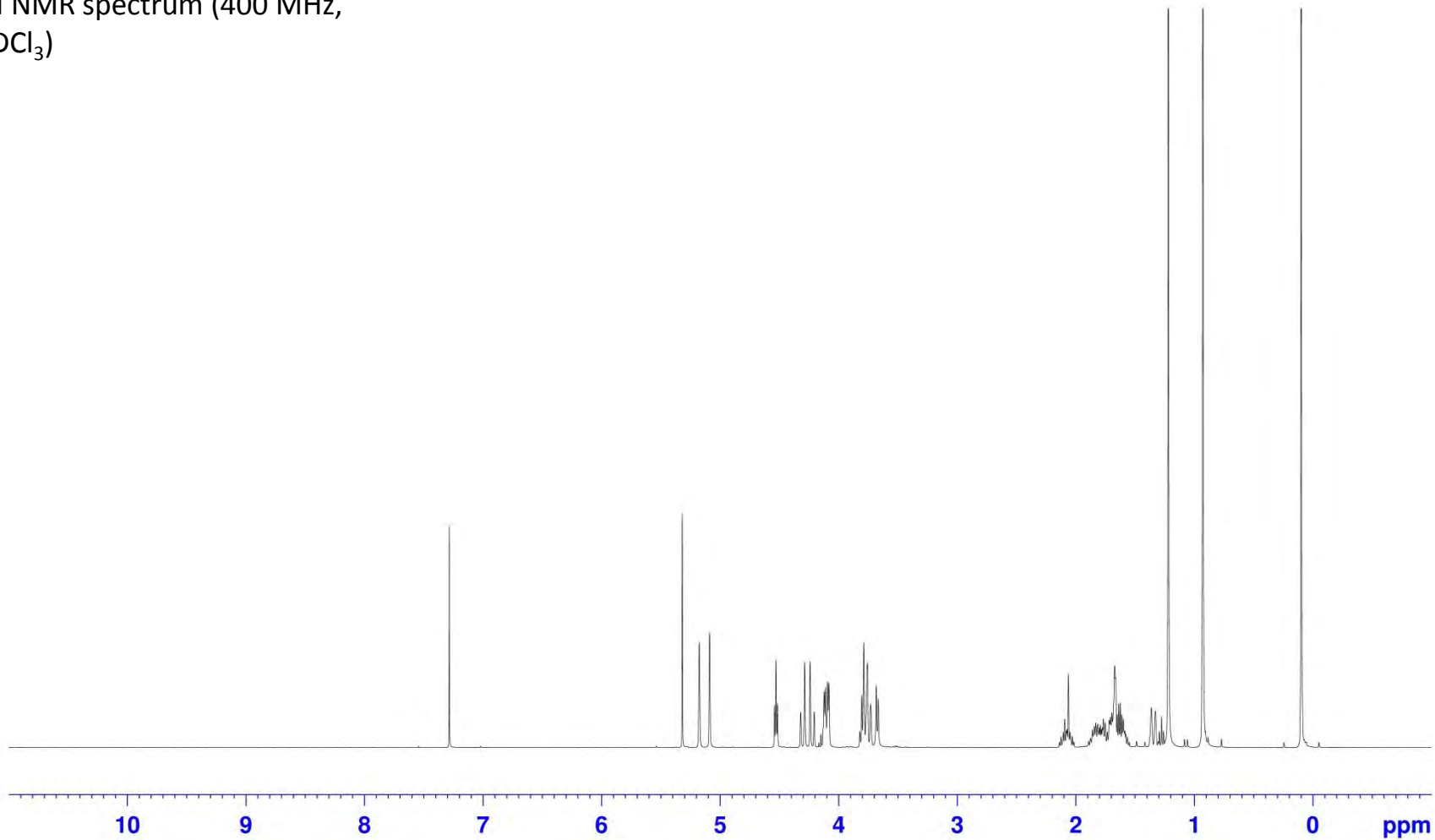
^{13}C NMR spectrum (100 MHz,
 CDCl_3)

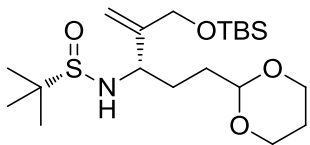




2.56

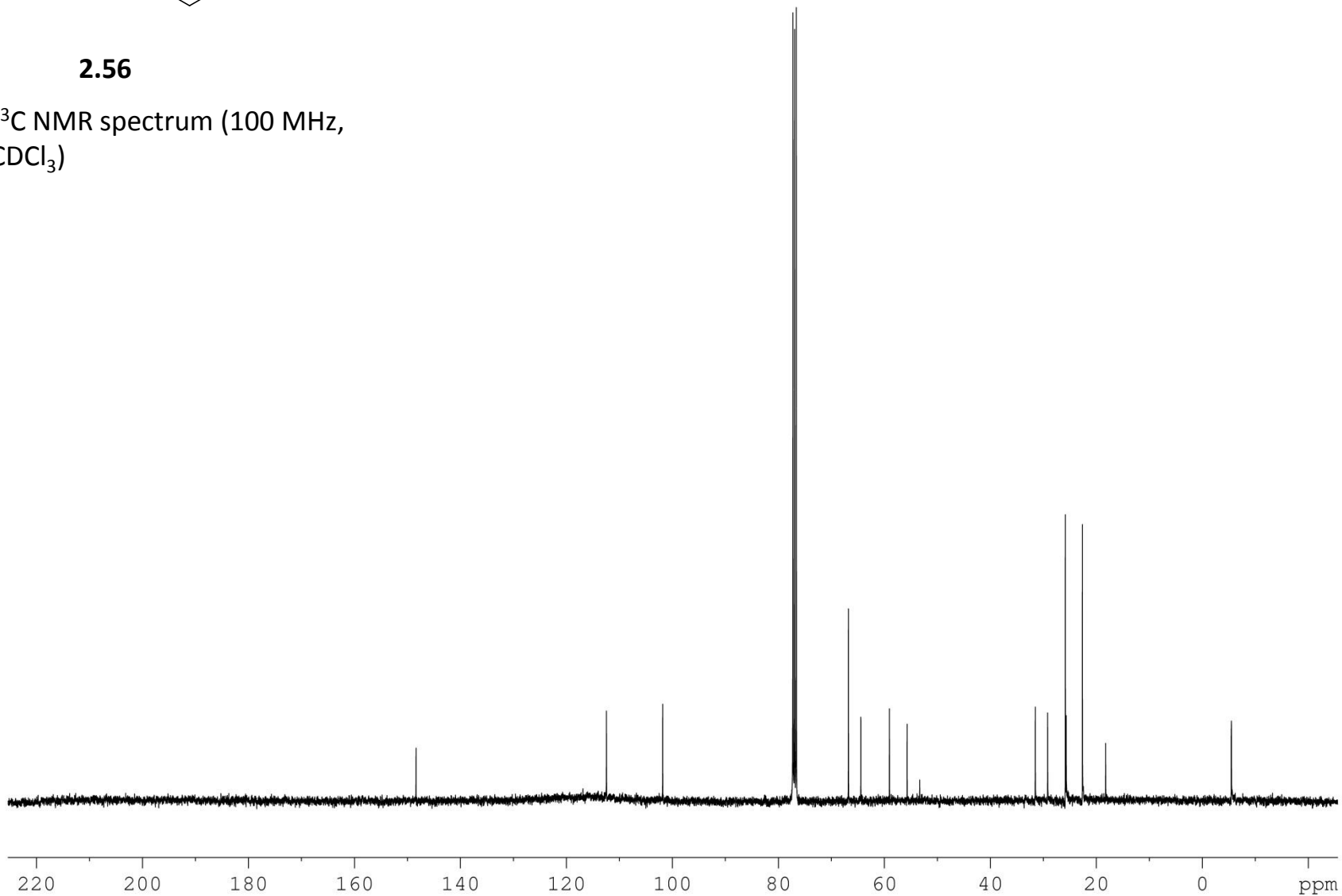
^1H NMR spectrum (400 MHz,
 CDCl_3)

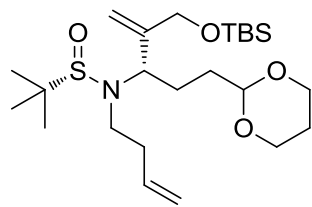




2.56

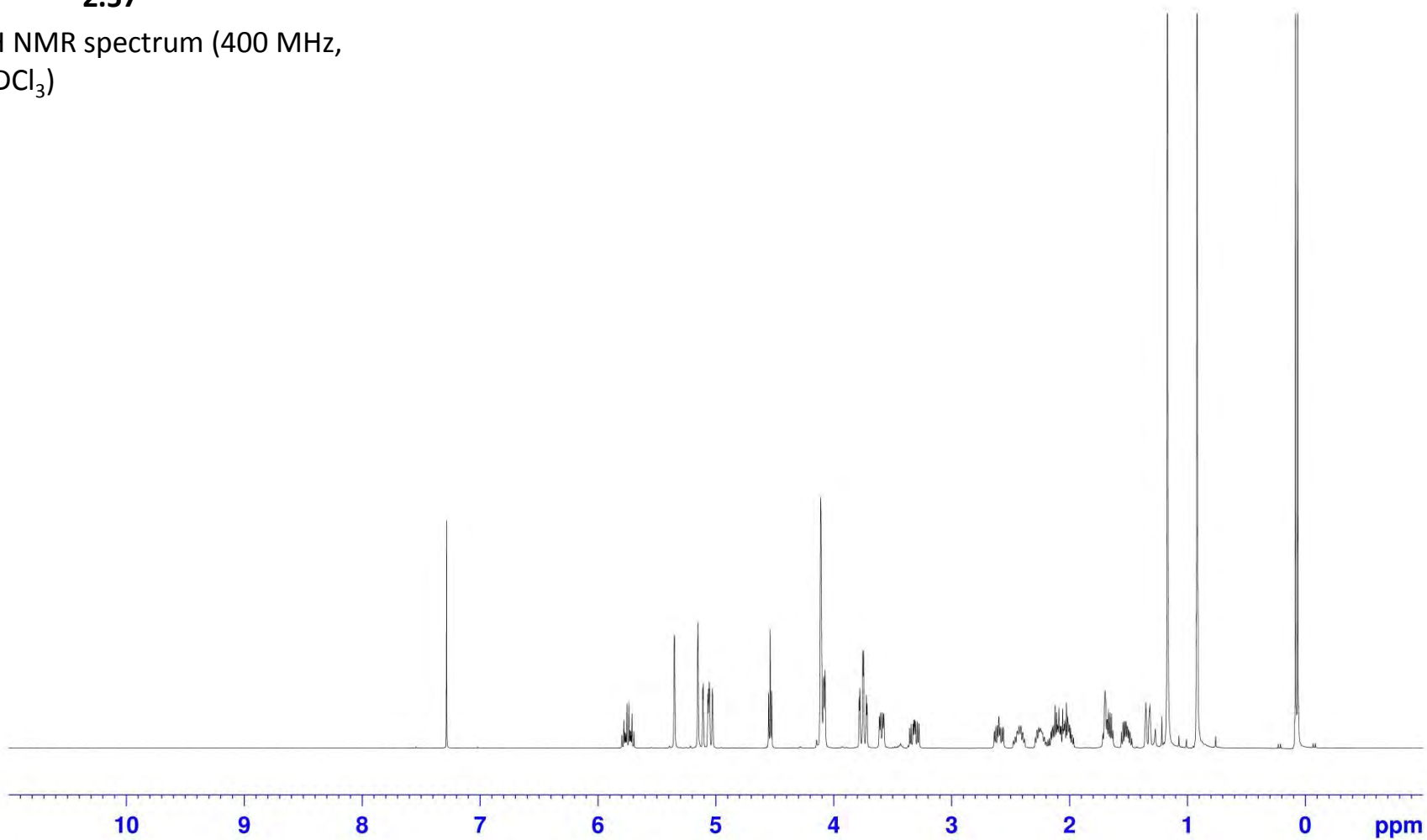
^{13}C NMR spectrum (100 MHz,
 CDCl_3)

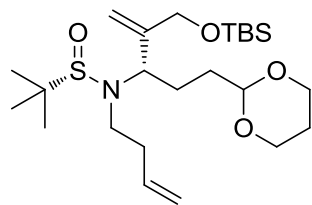




2.57

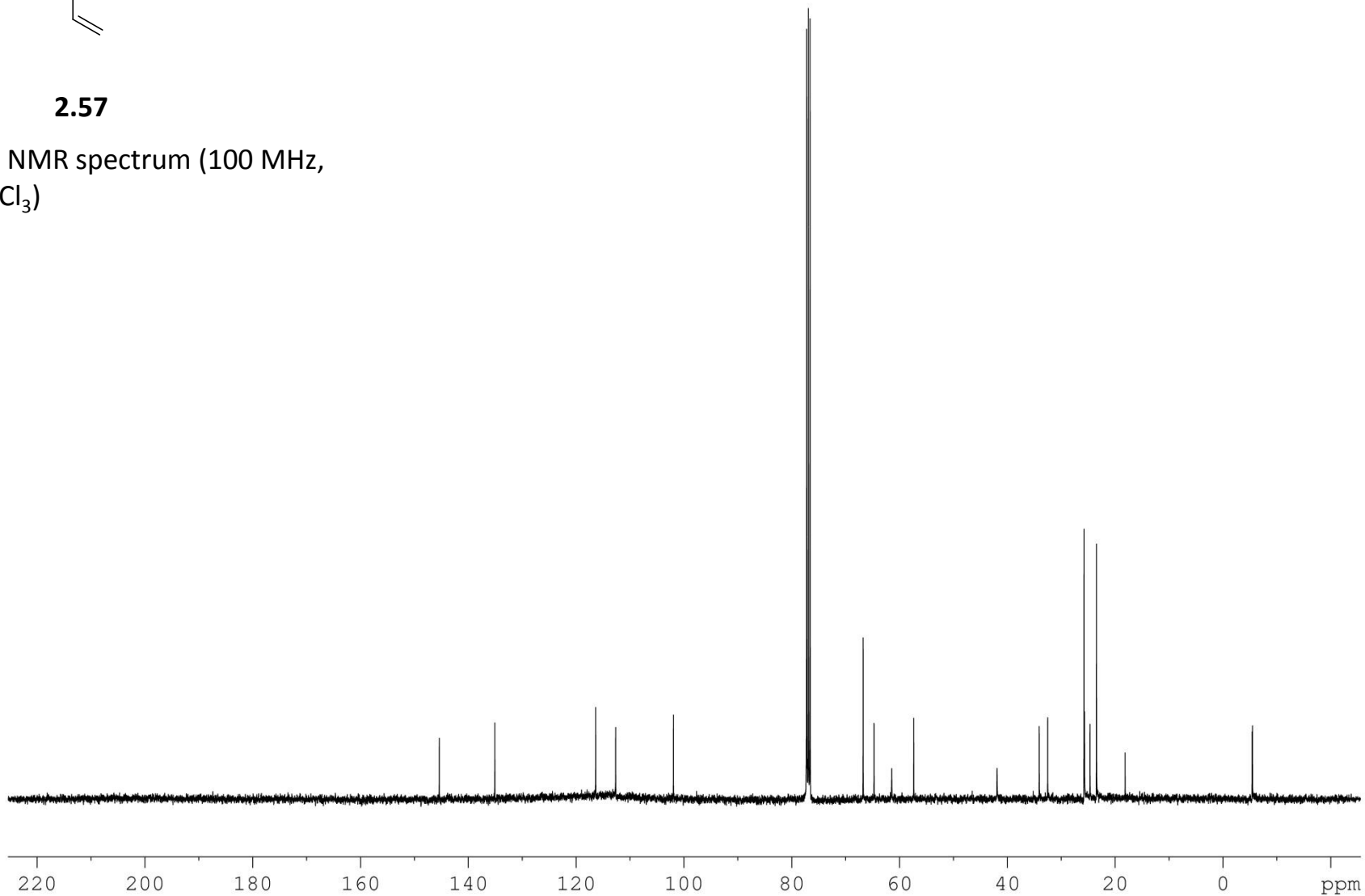
^1H NMR spectrum (400 MHz,
 CDCl_3)

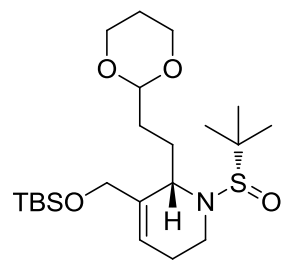




2.57

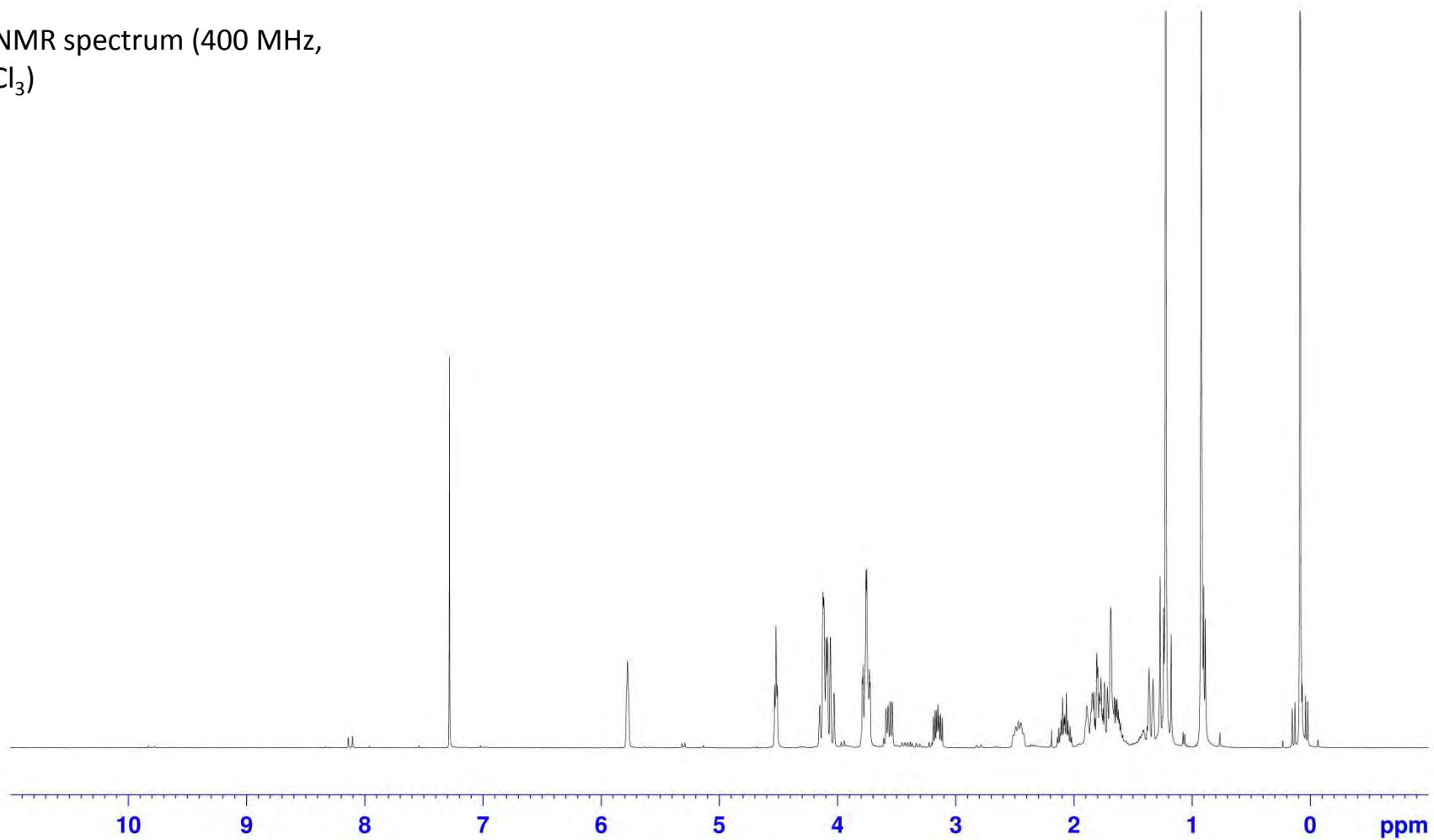
^{13}C NMR spectrum (100 MHz,
 CDCl_3)

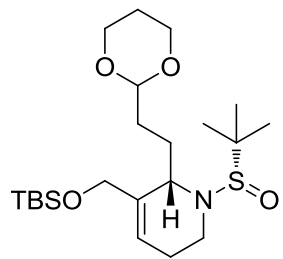




2.59

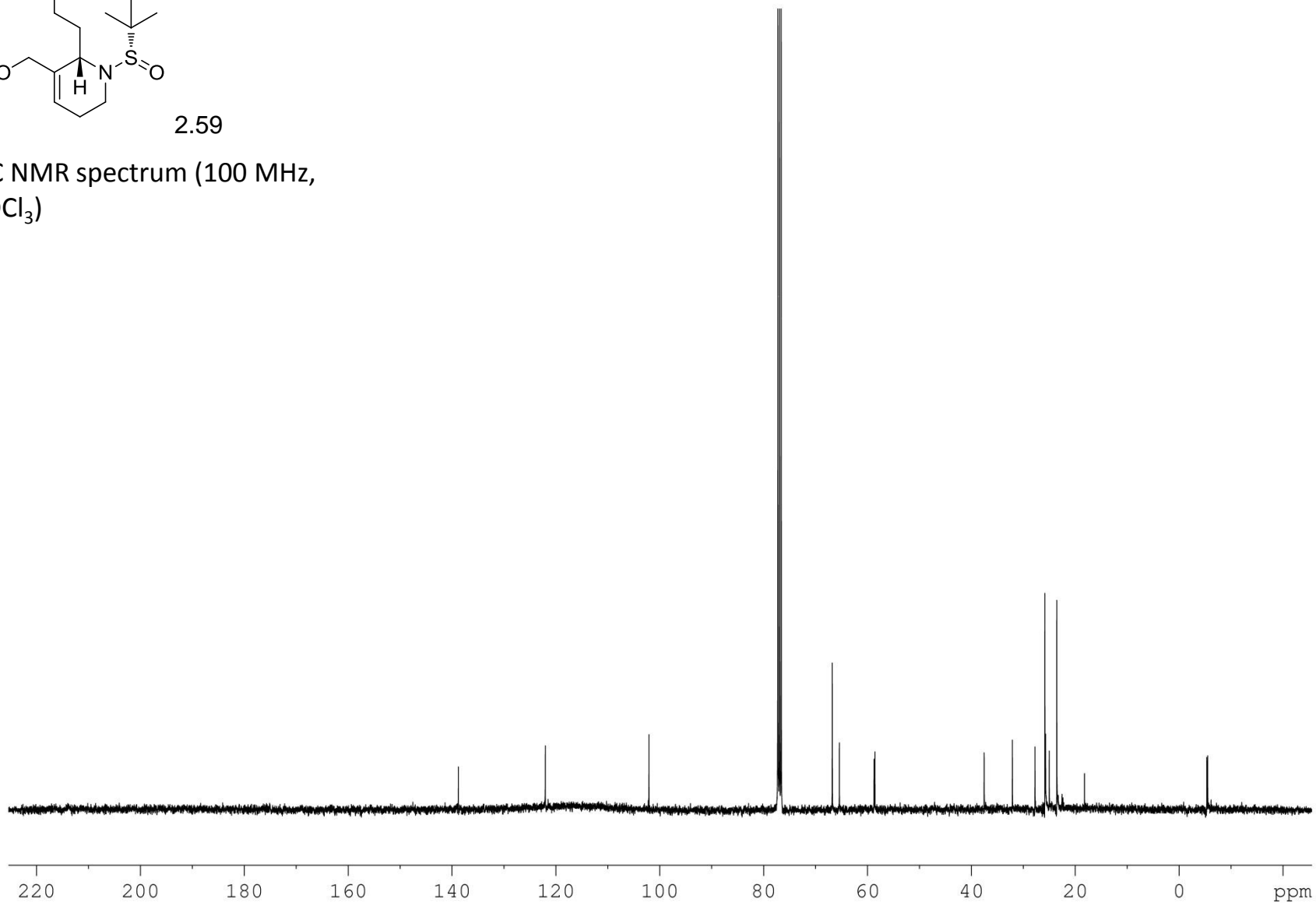
^1H NMR spectrum (400 MHz, CDCl_3)

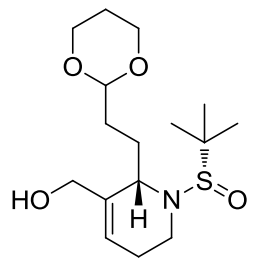




2.59

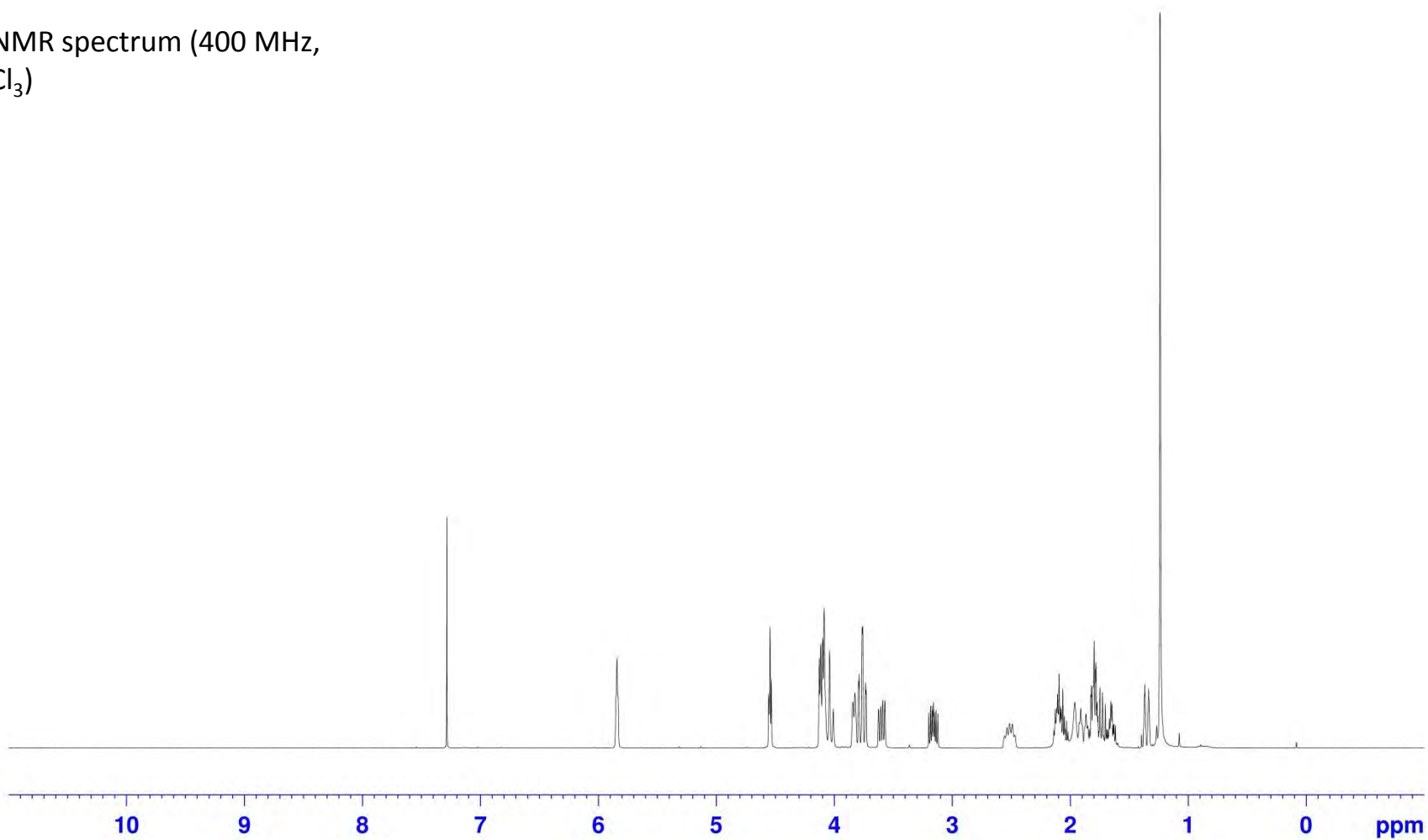
¹³C NMR spectrum (100 MHz, CDCl₃)

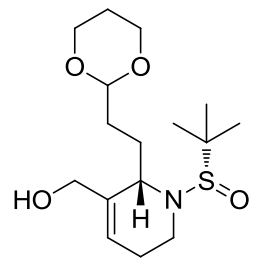




2.72

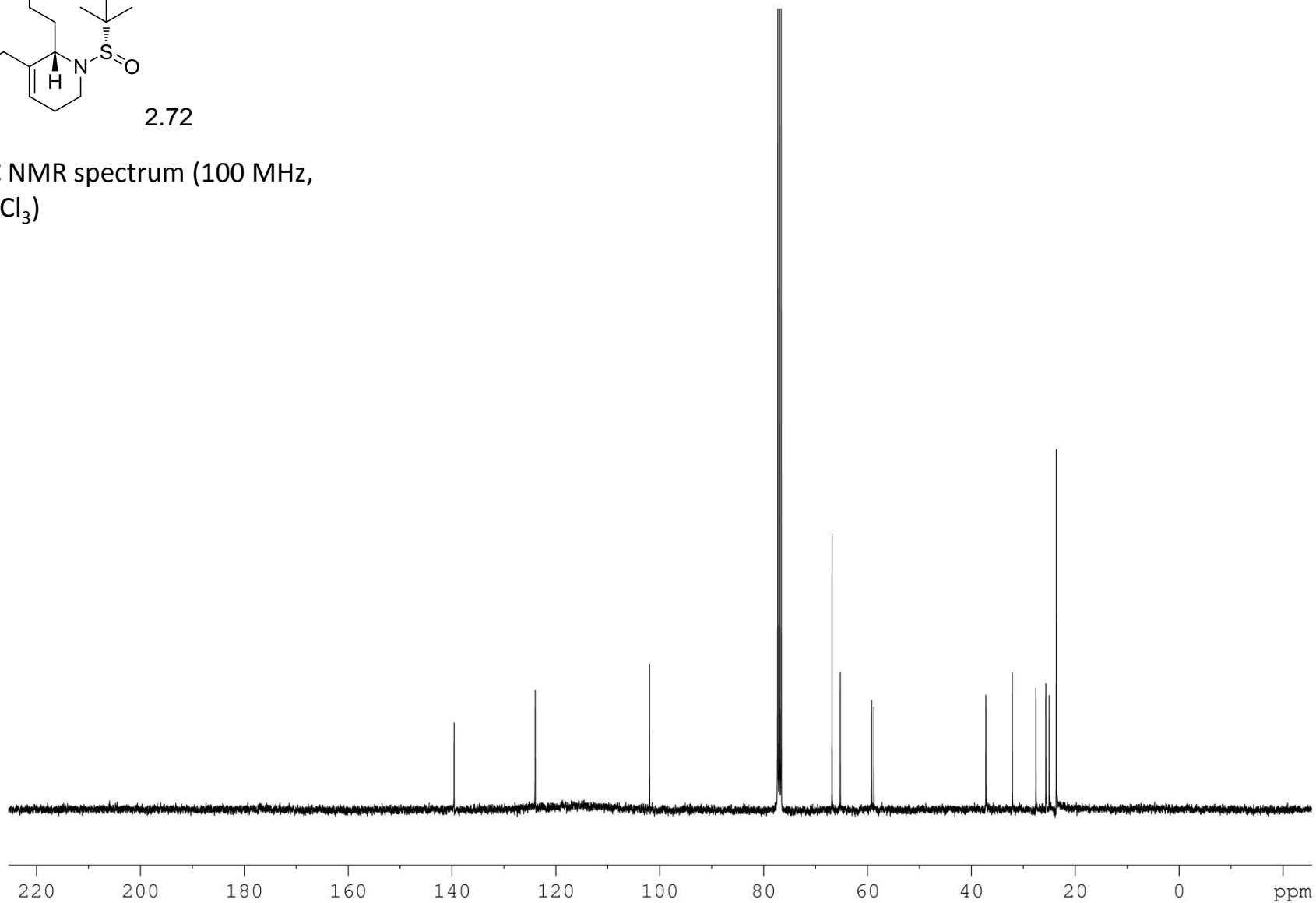
¹H NMR spectrum (400 MHz, CDCl₃)

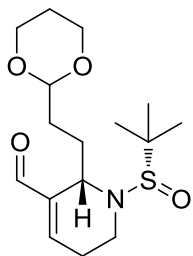




2.72

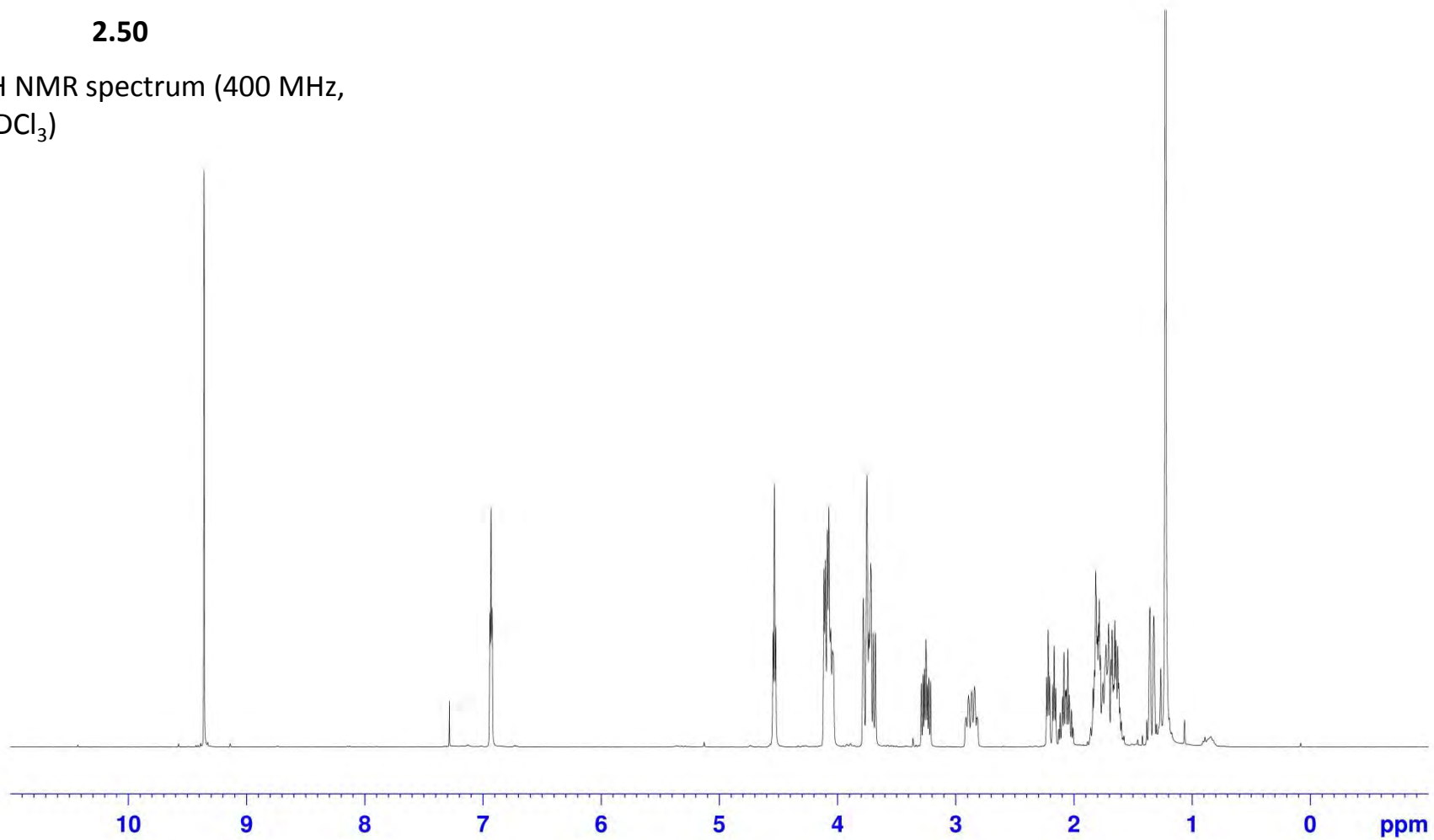
¹³C NMR spectrum (100 MHz, CDCl₃)

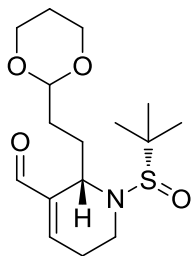




2.50

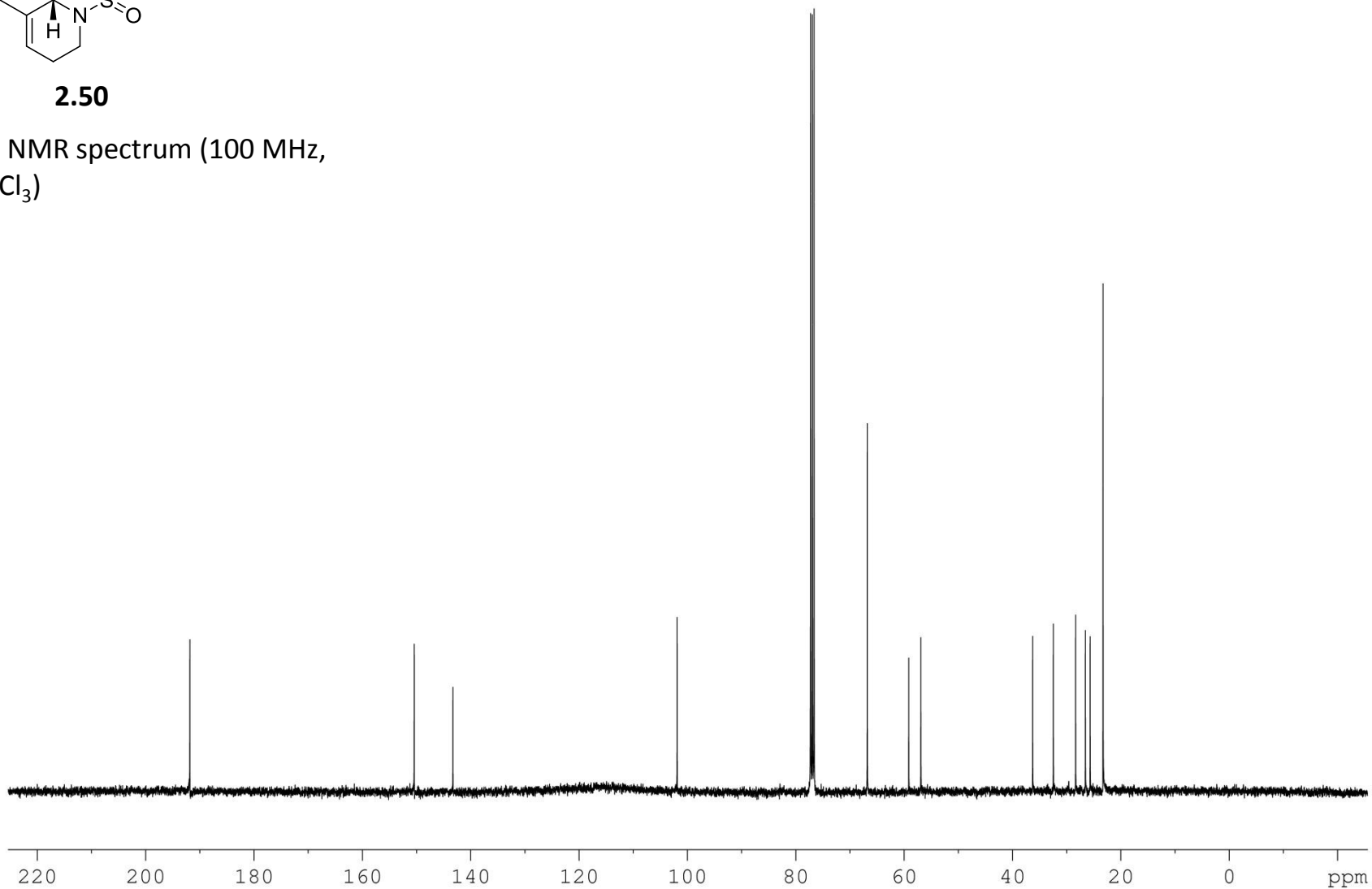
^1H NMR spectrum (400 MHz,
 CDCl_3)

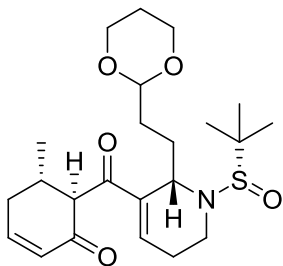




2.50

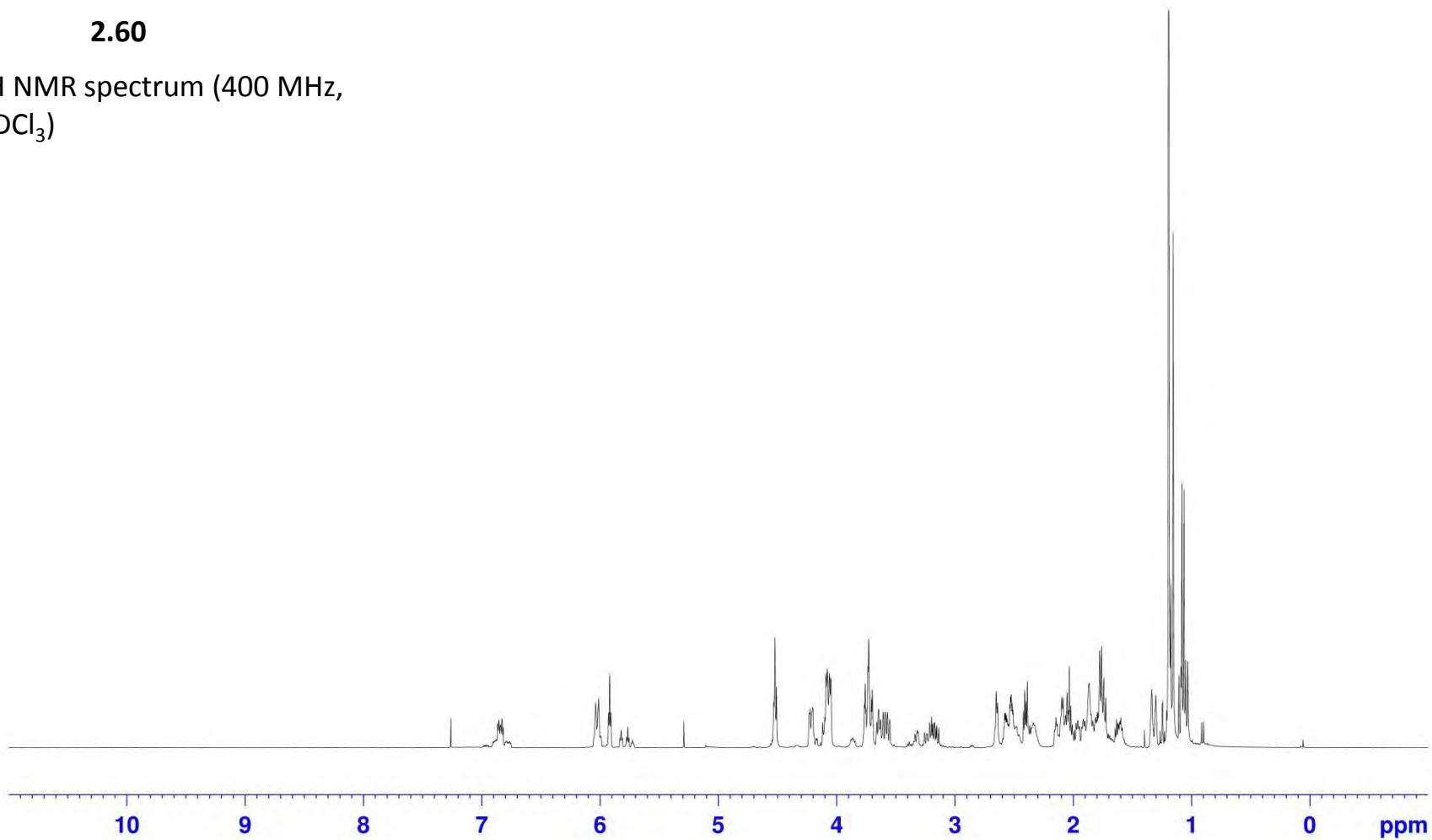
^{13}C NMR spectrum (100 MHz,
 CDCl_3)

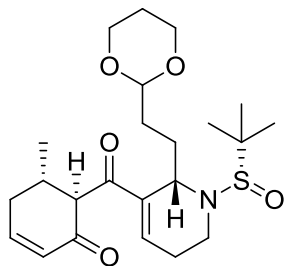




2.60

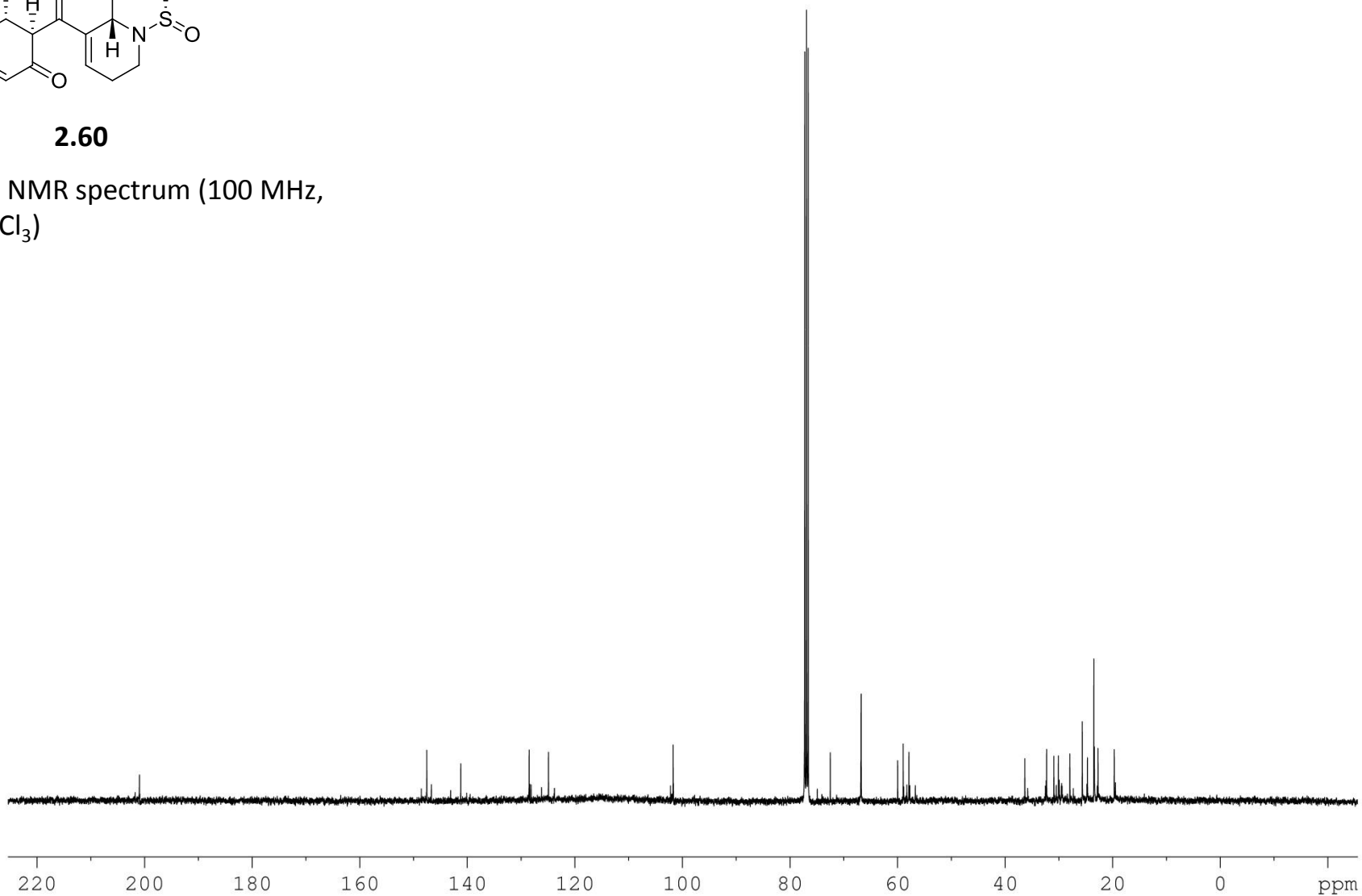
^1H NMR spectrum (400 MHz,
 CDCl_3)

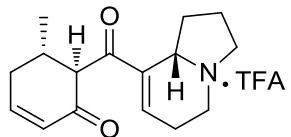




2.60

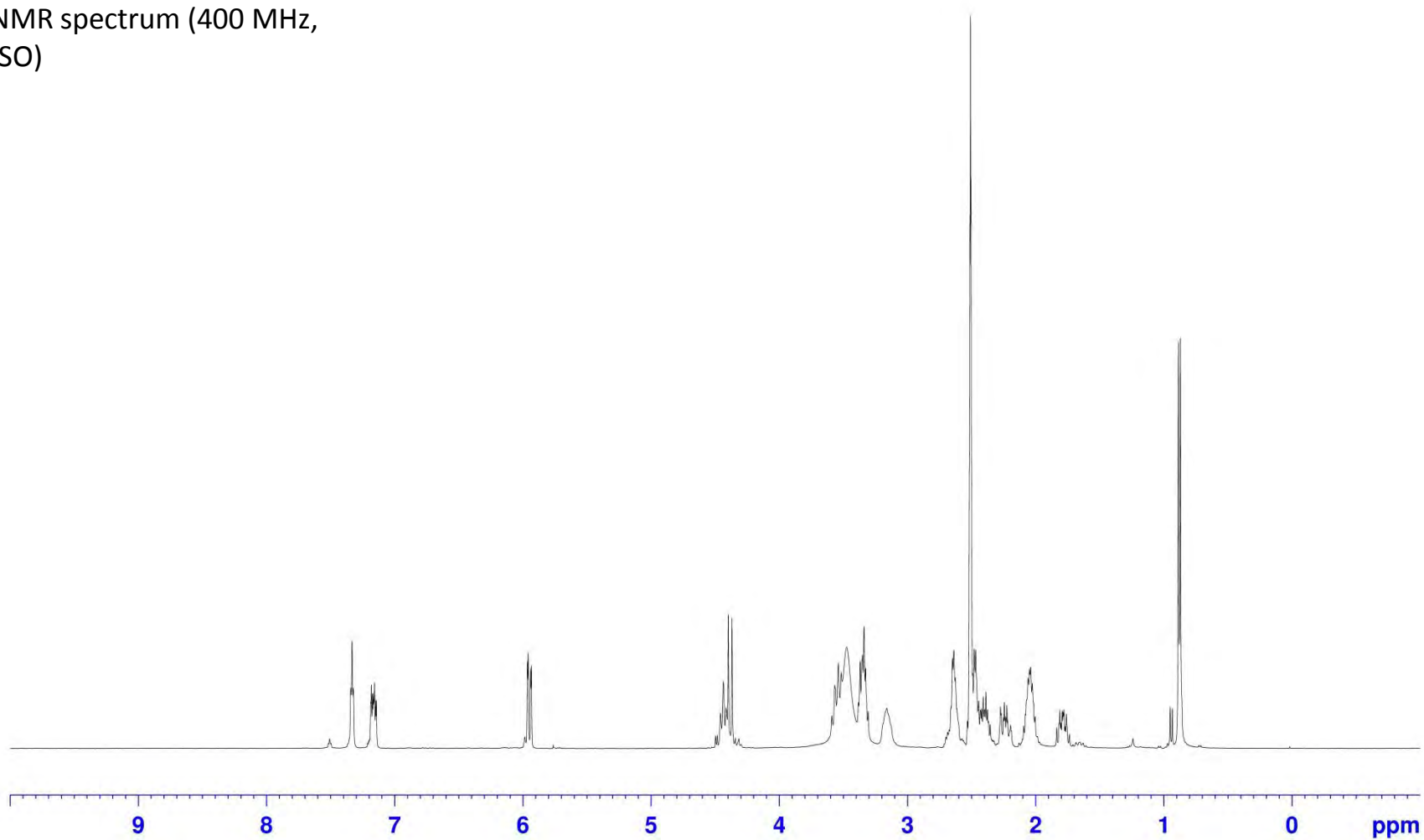
^{13}C NMR spectrum (100 MHz,
 CDCl_3)

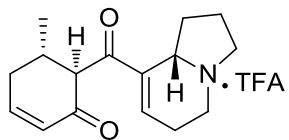




2.32

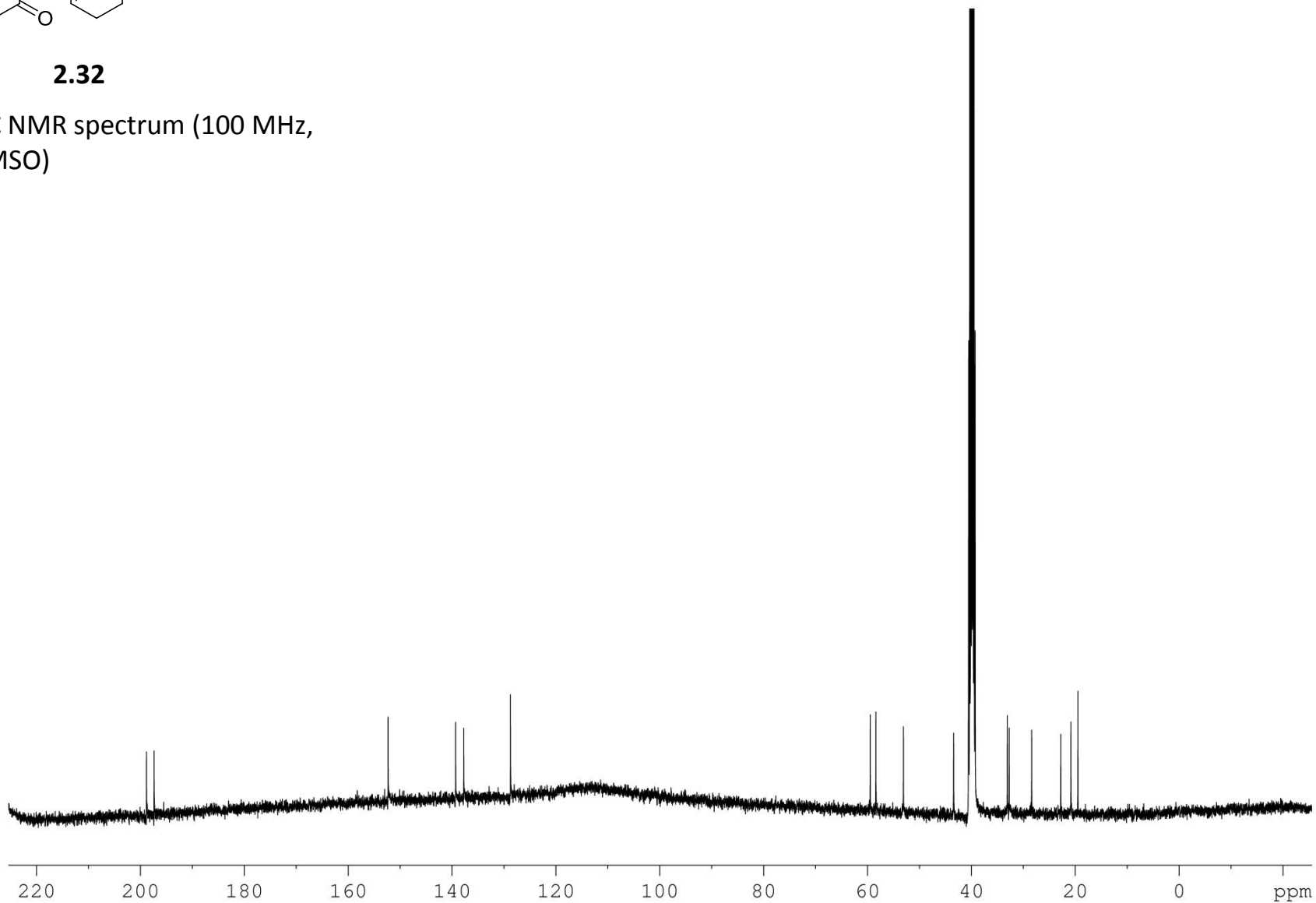
^1H NMR spectrum (400 MHz, DMSO)

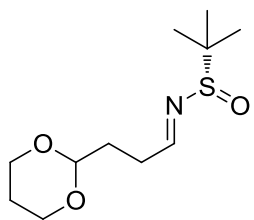




2.32

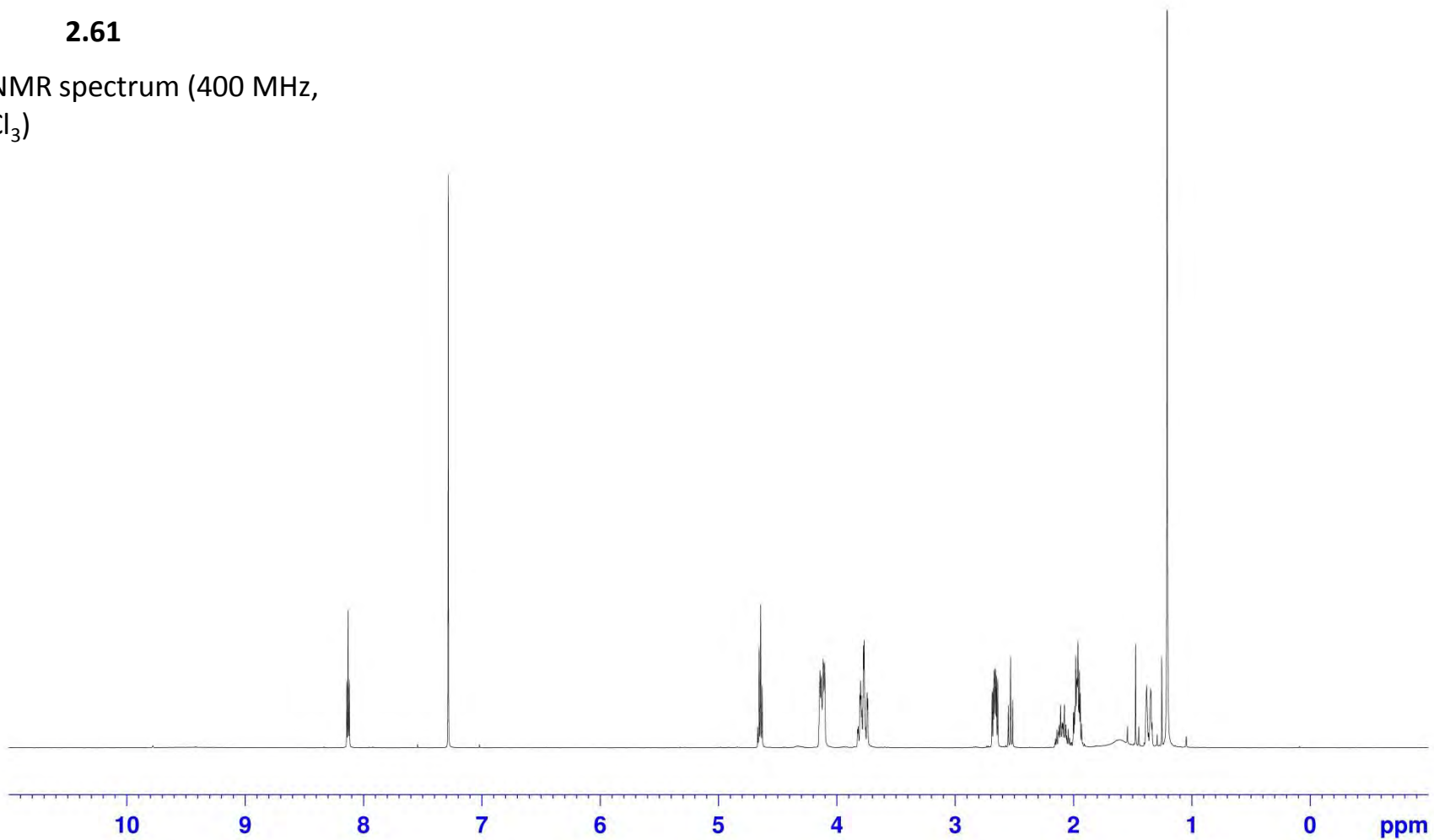
^{13}C NMR spectrum (100 MHz,
DMSO)

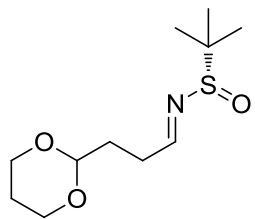




2.61

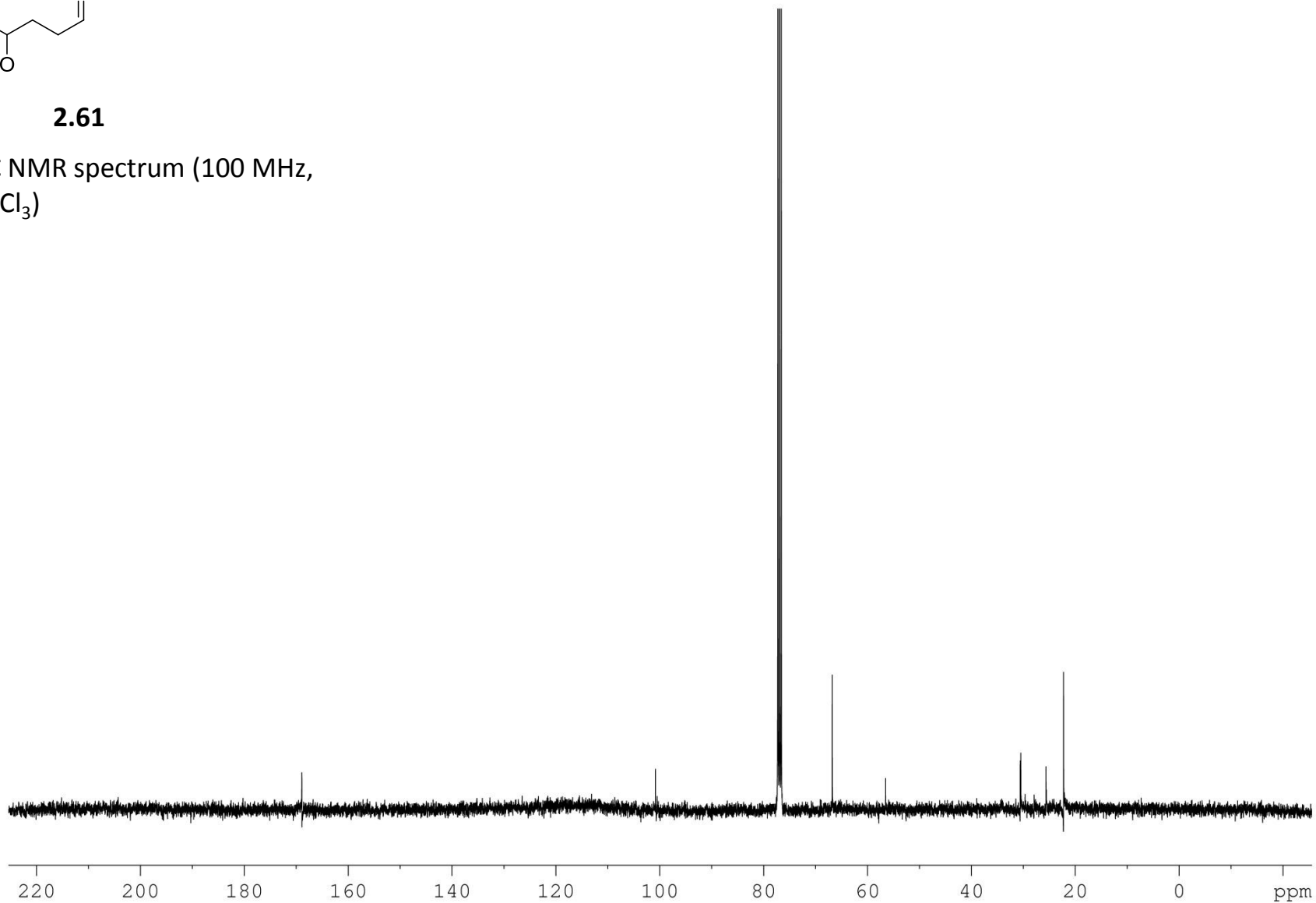
^1H NMR spectrum (400 MHz,
 CDCl_3)

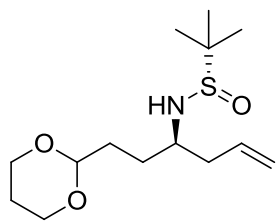




2.61

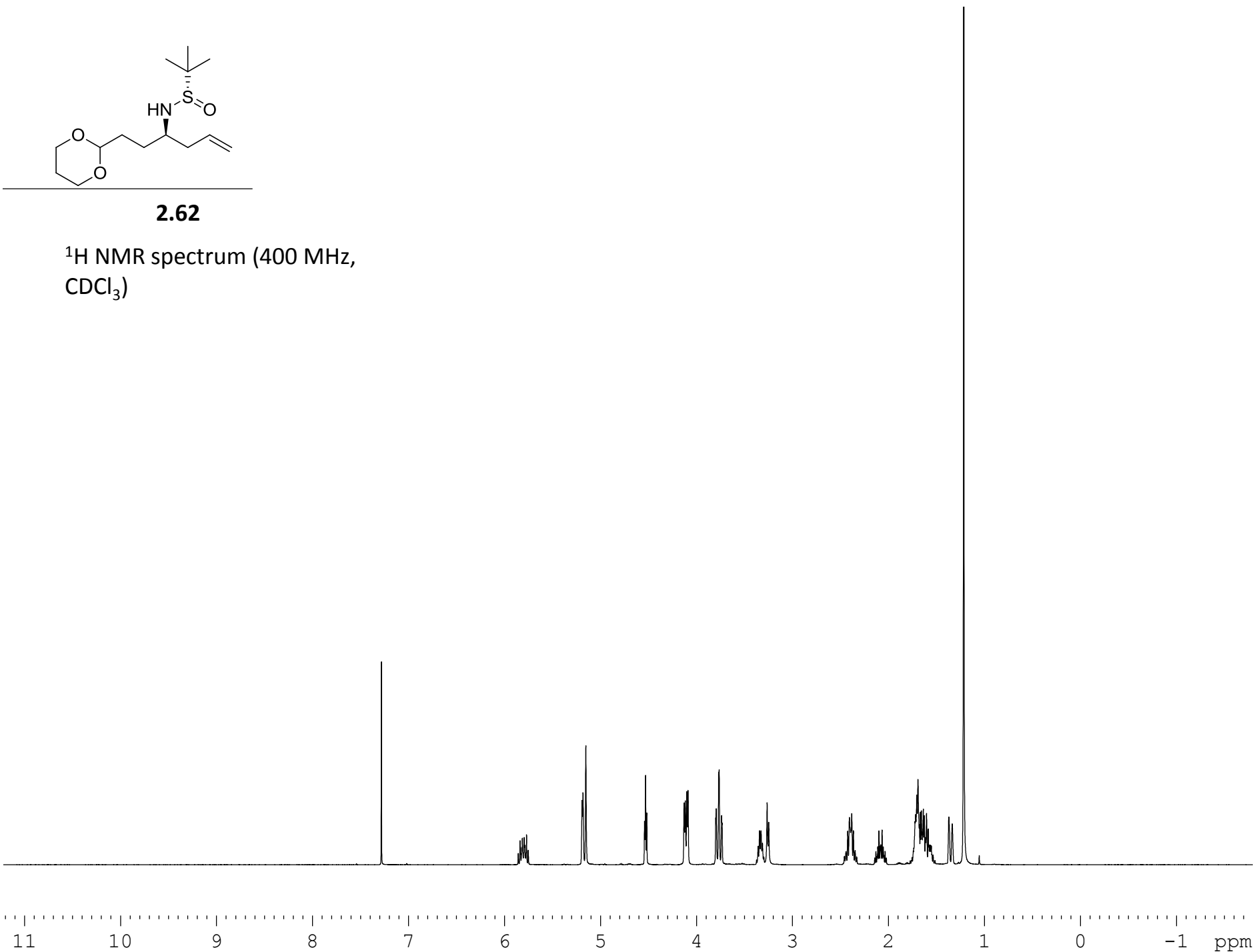
^{13}C NMR spectrum (100 MHz,
 CDCl_3)

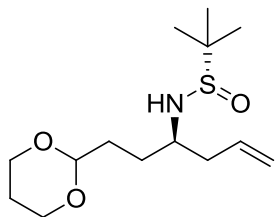




2.62

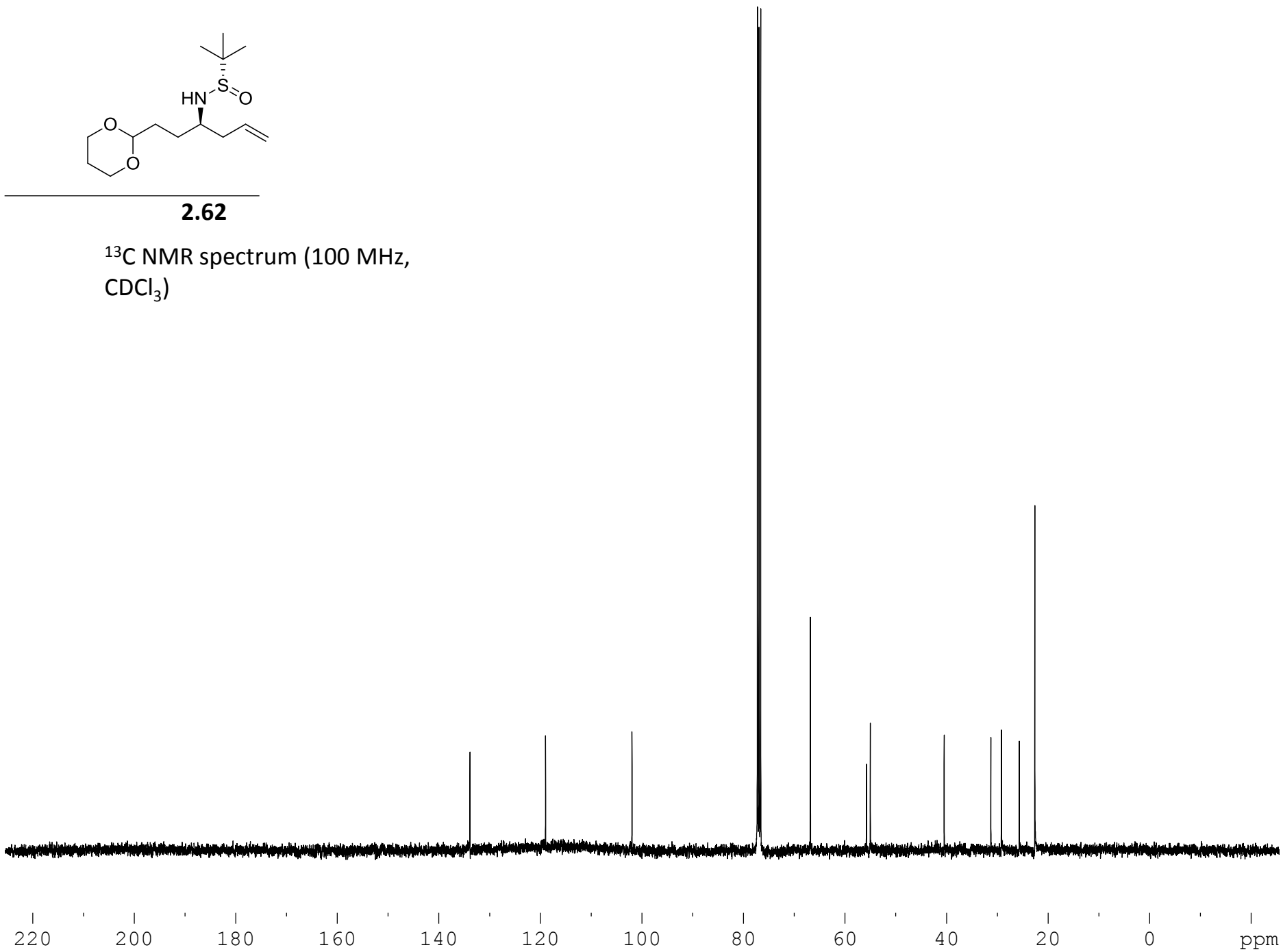
^1H NMR spectrum (400 MHz,
 CDCl_3)

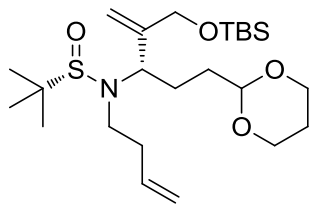




2.62

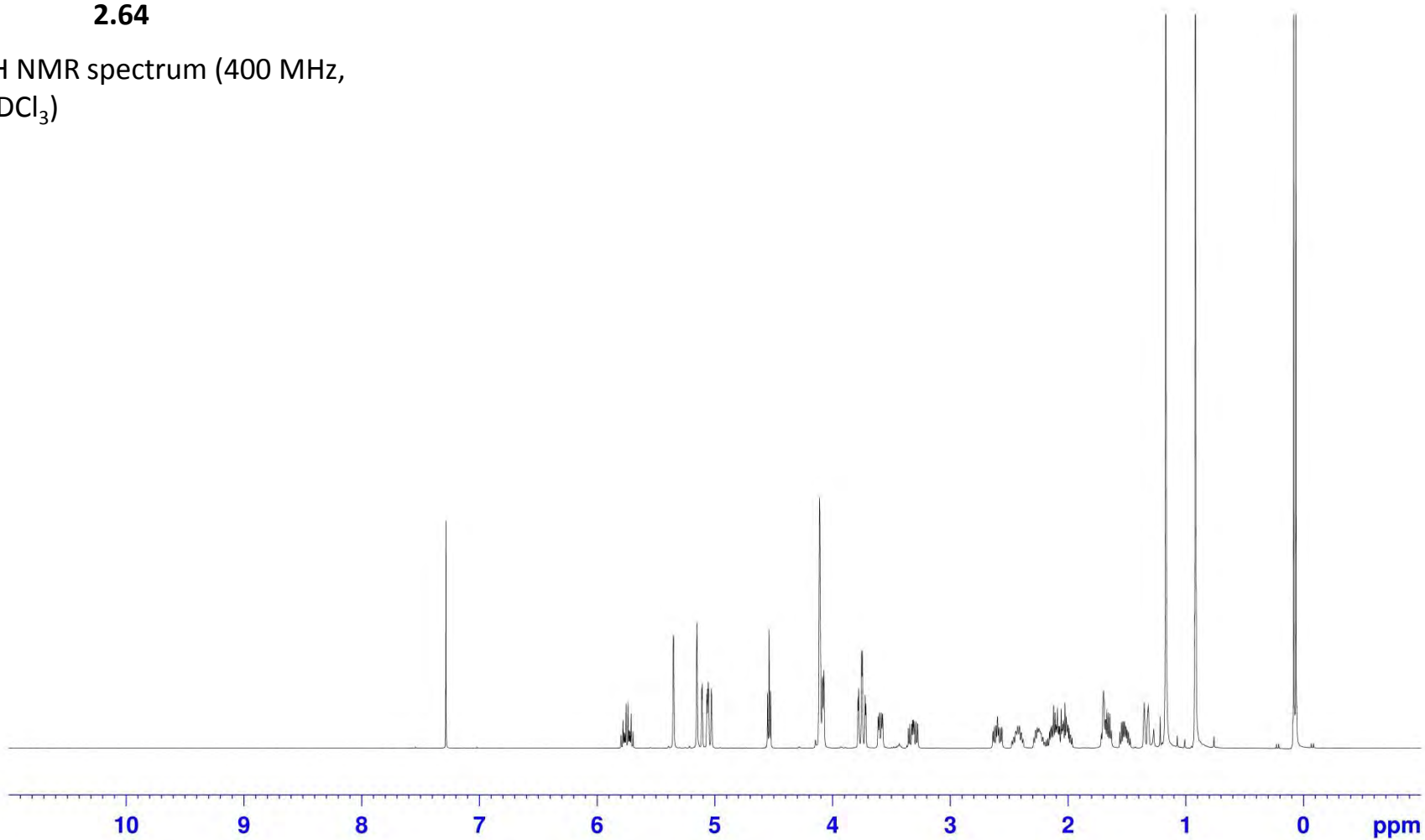
^{13}C NMR spectrum (100 MHz,
 CDCl_3)

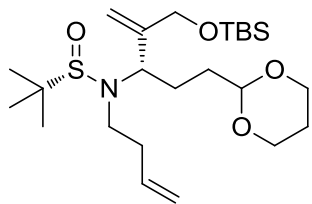




2.64

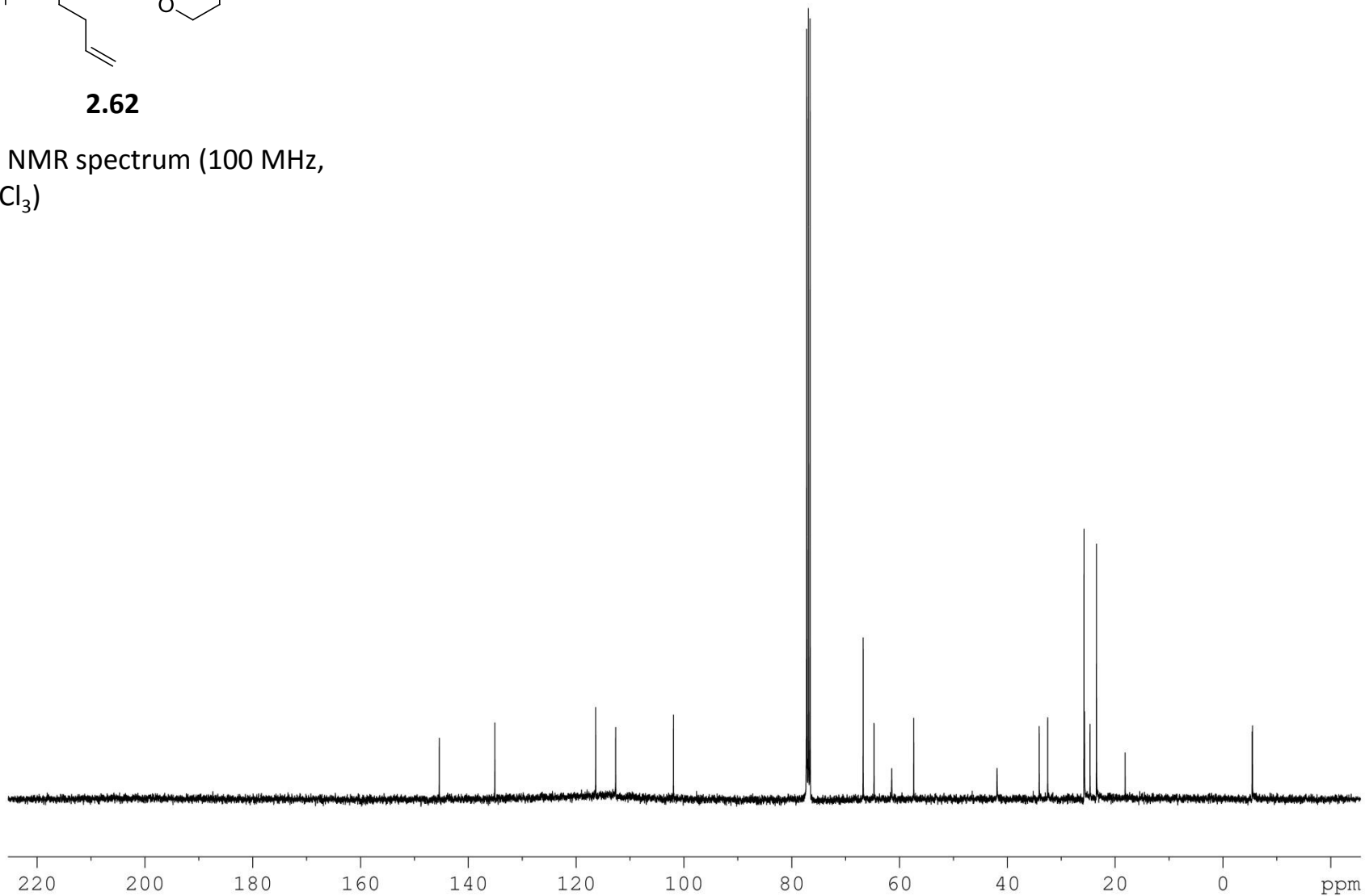
^1H NMR spectrum (400 MHz, CDCl_3)

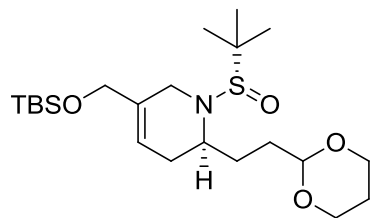




2.62

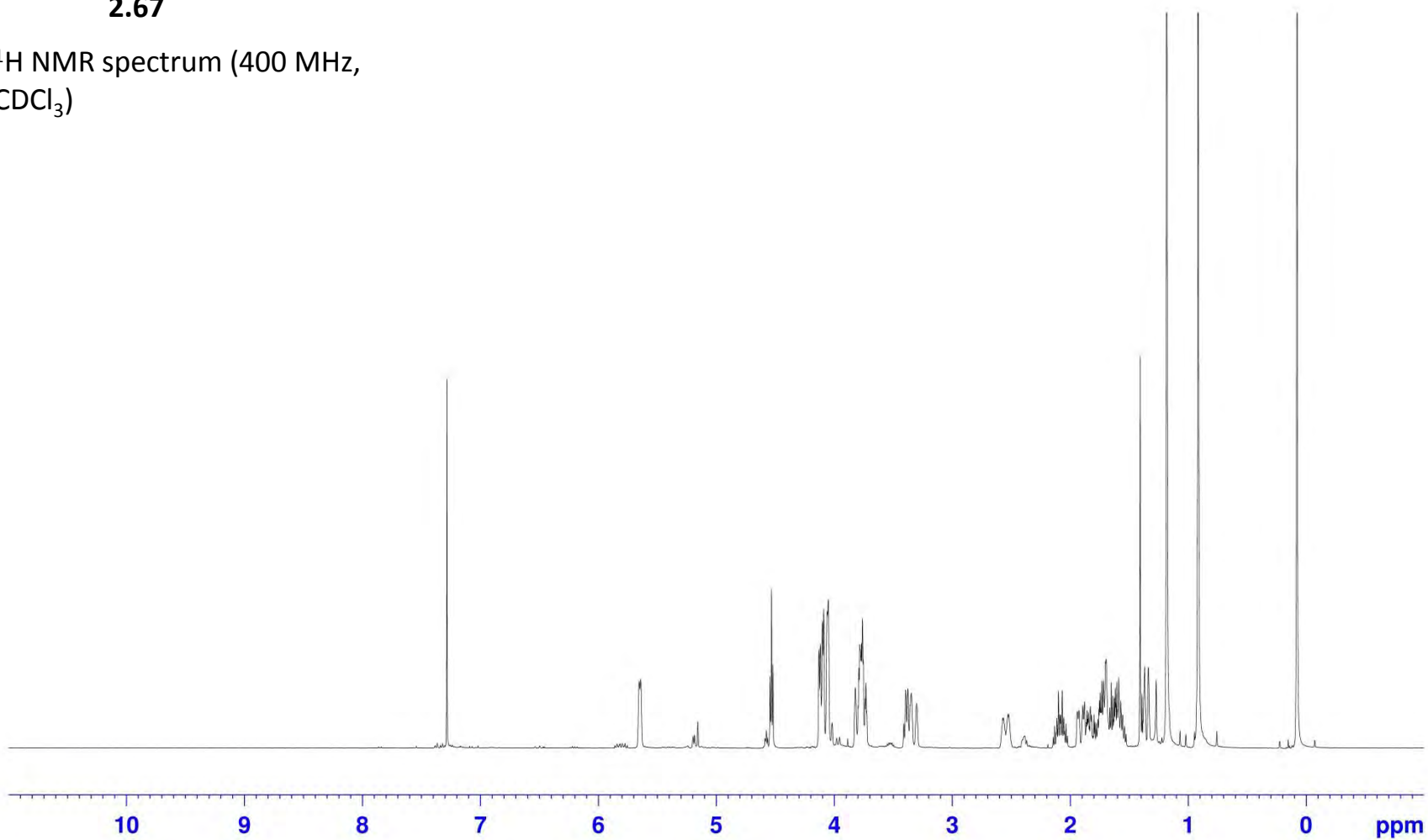
^{13}C NMR spectrum (100 MHz,
 CDCl_3)

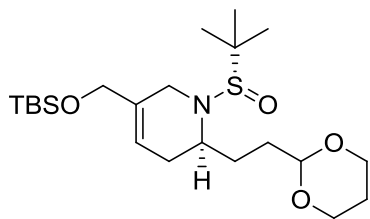




2.67

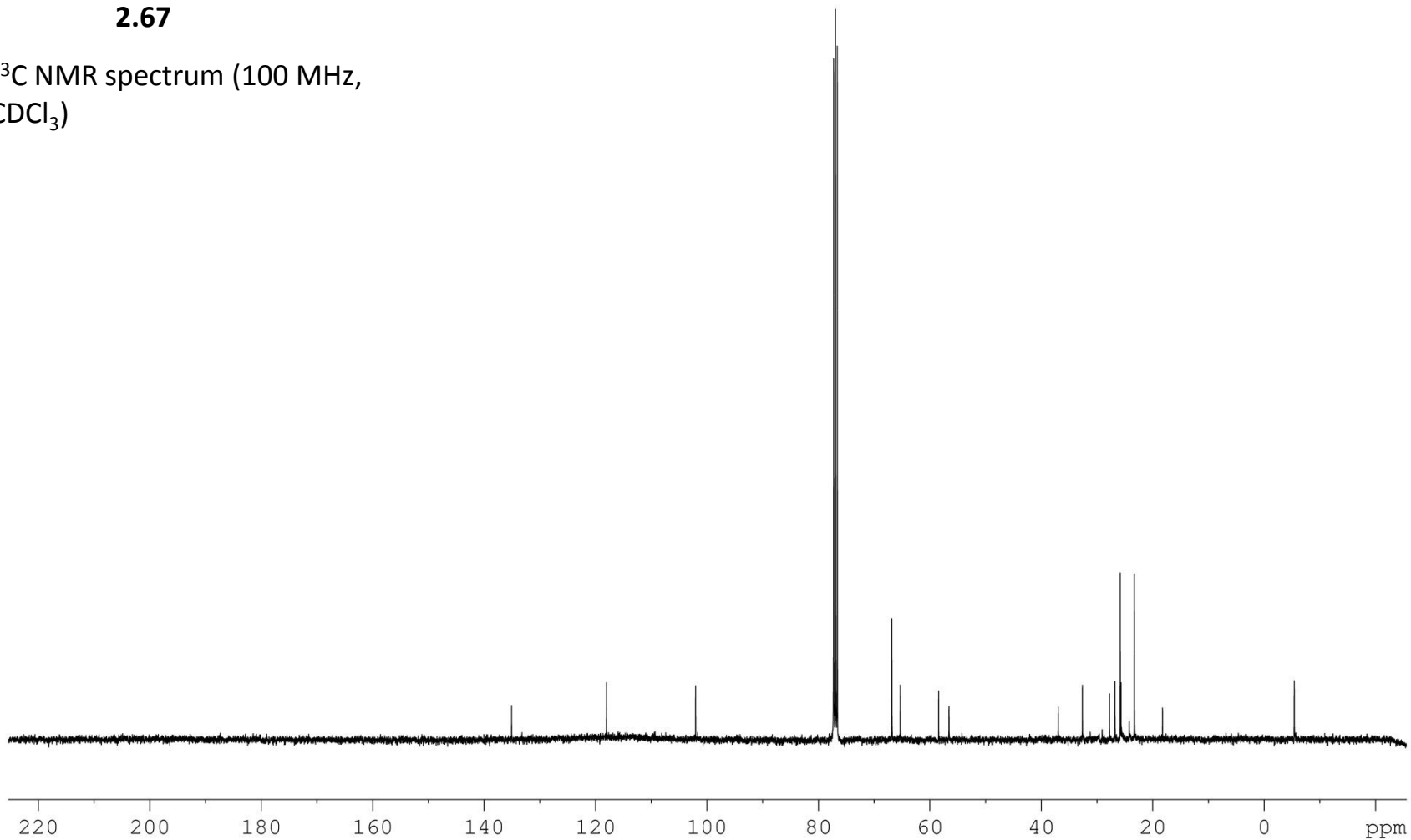
^1H NMR spectrum (400 MHz, CDCl_3)

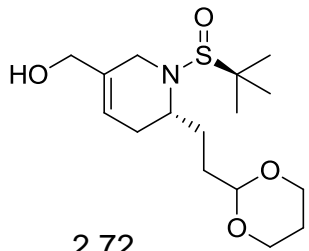




2.67

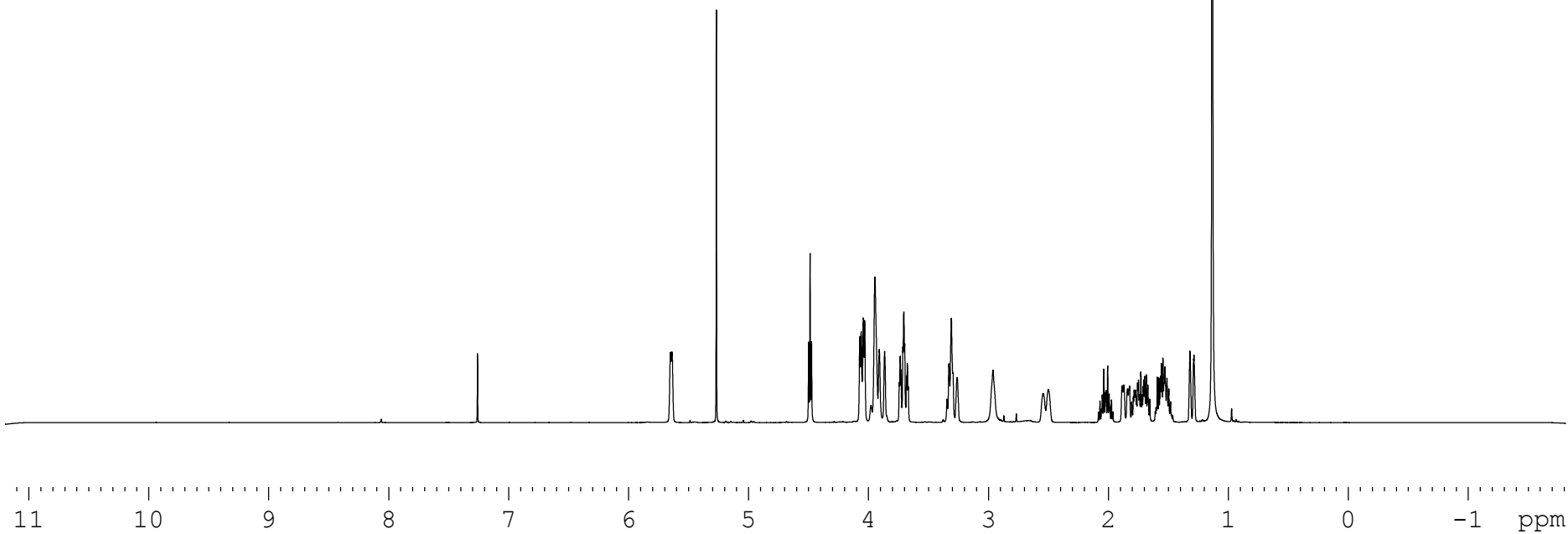
^{13}C NMR spectrum (100 MHz,
 CDCl_3)

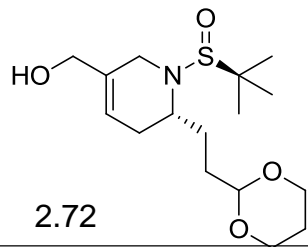




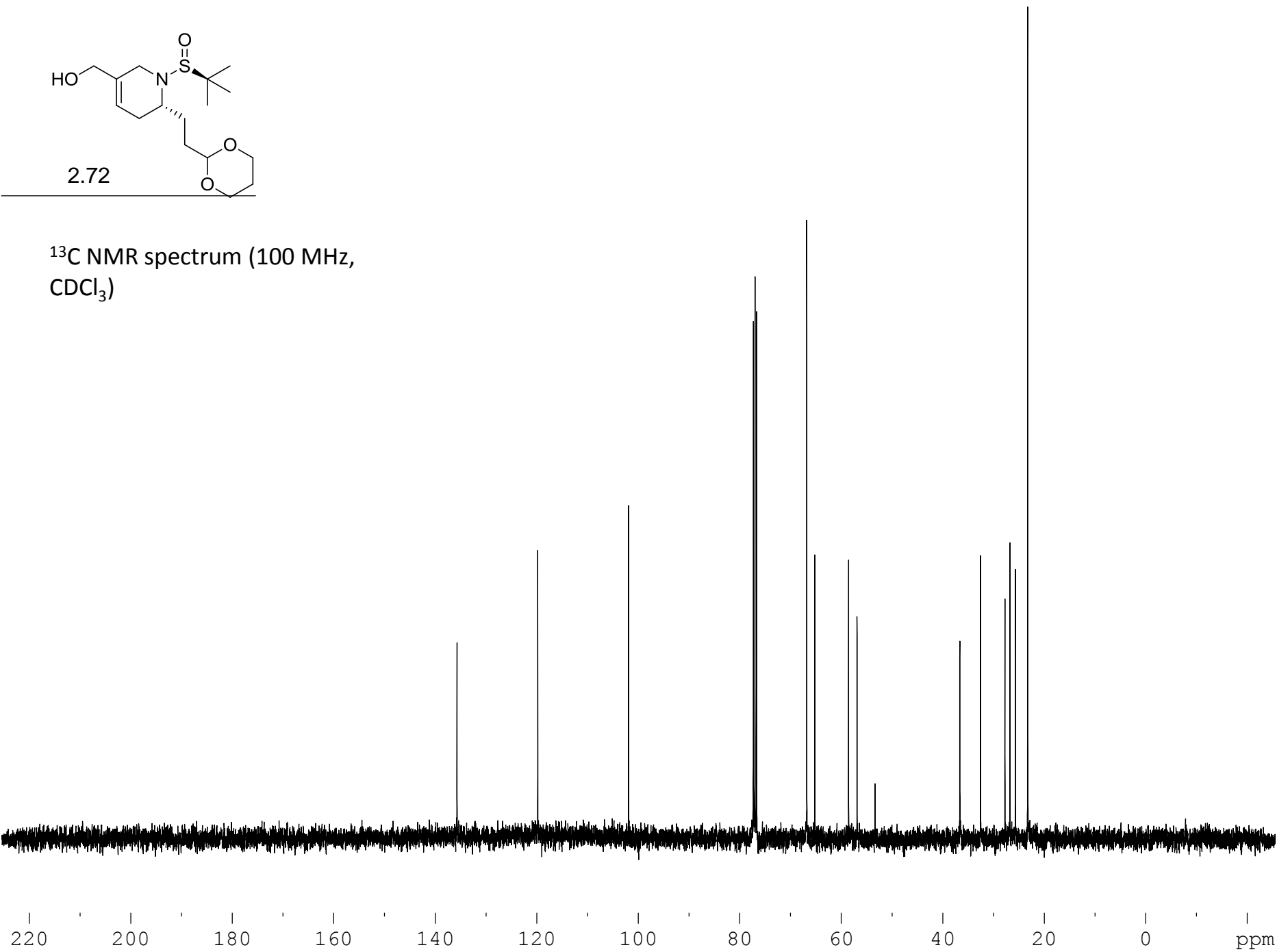
2.72

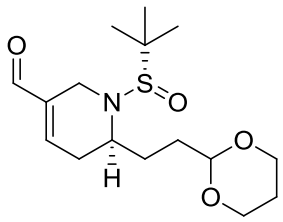
^1H NMR spectrum (400 MHz, CDCl_3)





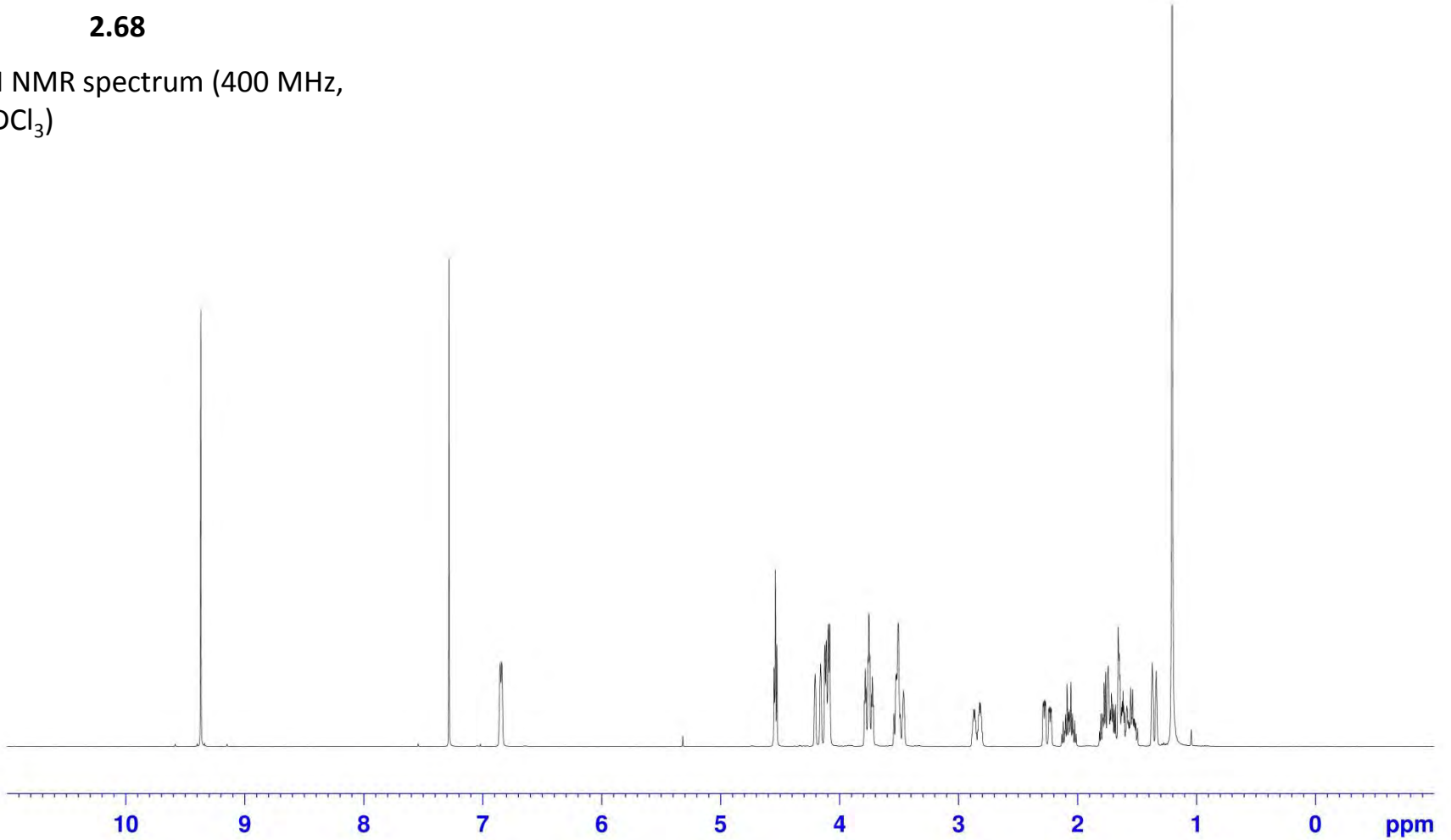
^{13}C NMR spectrum (100 MHz,
 CDCl_3)

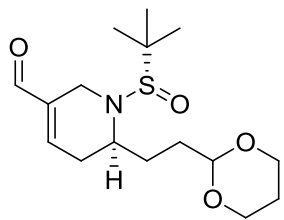




2.68

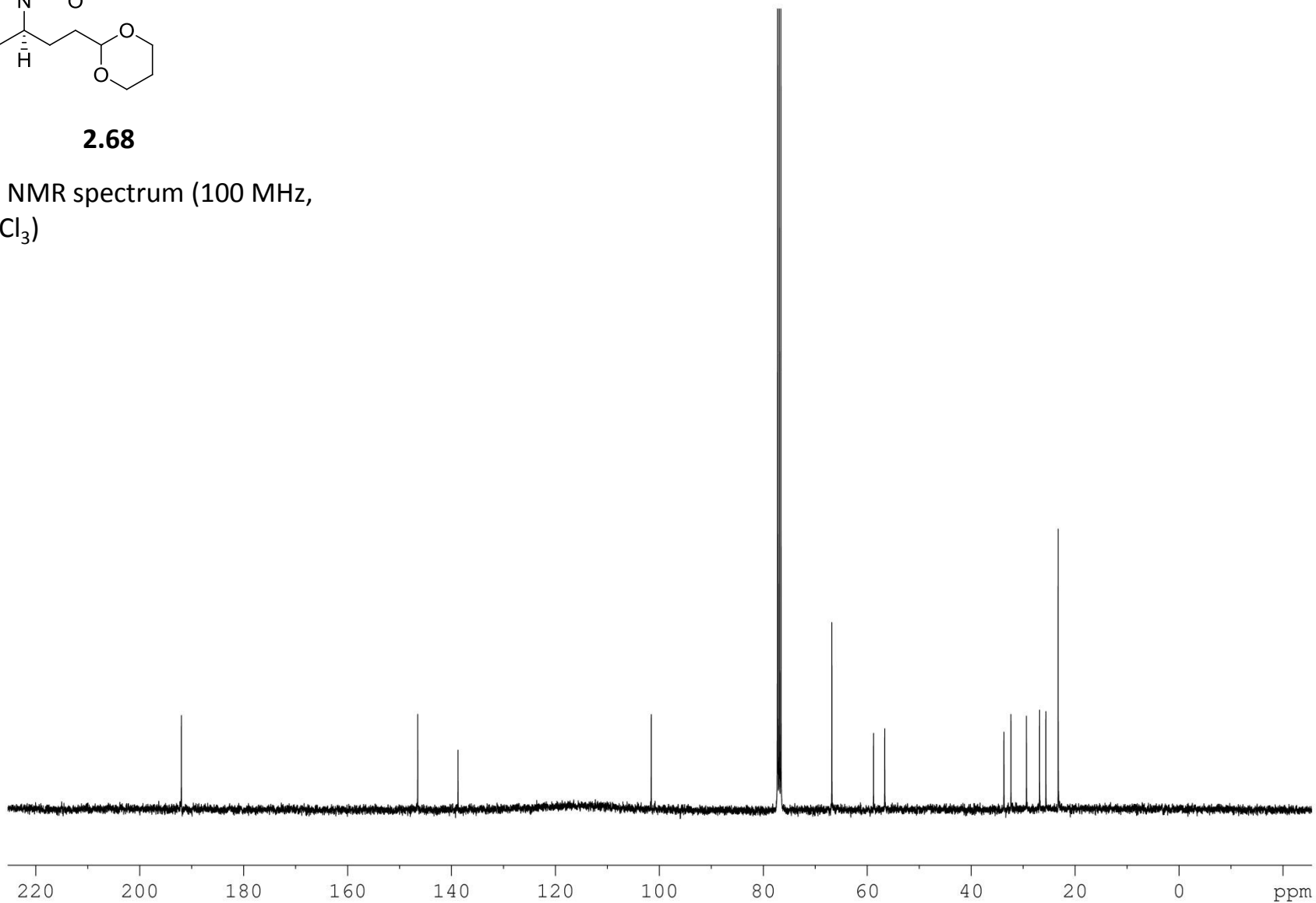
¹H NMR spectrum (400 MHz,
CDCl₃)

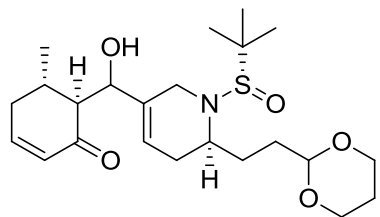




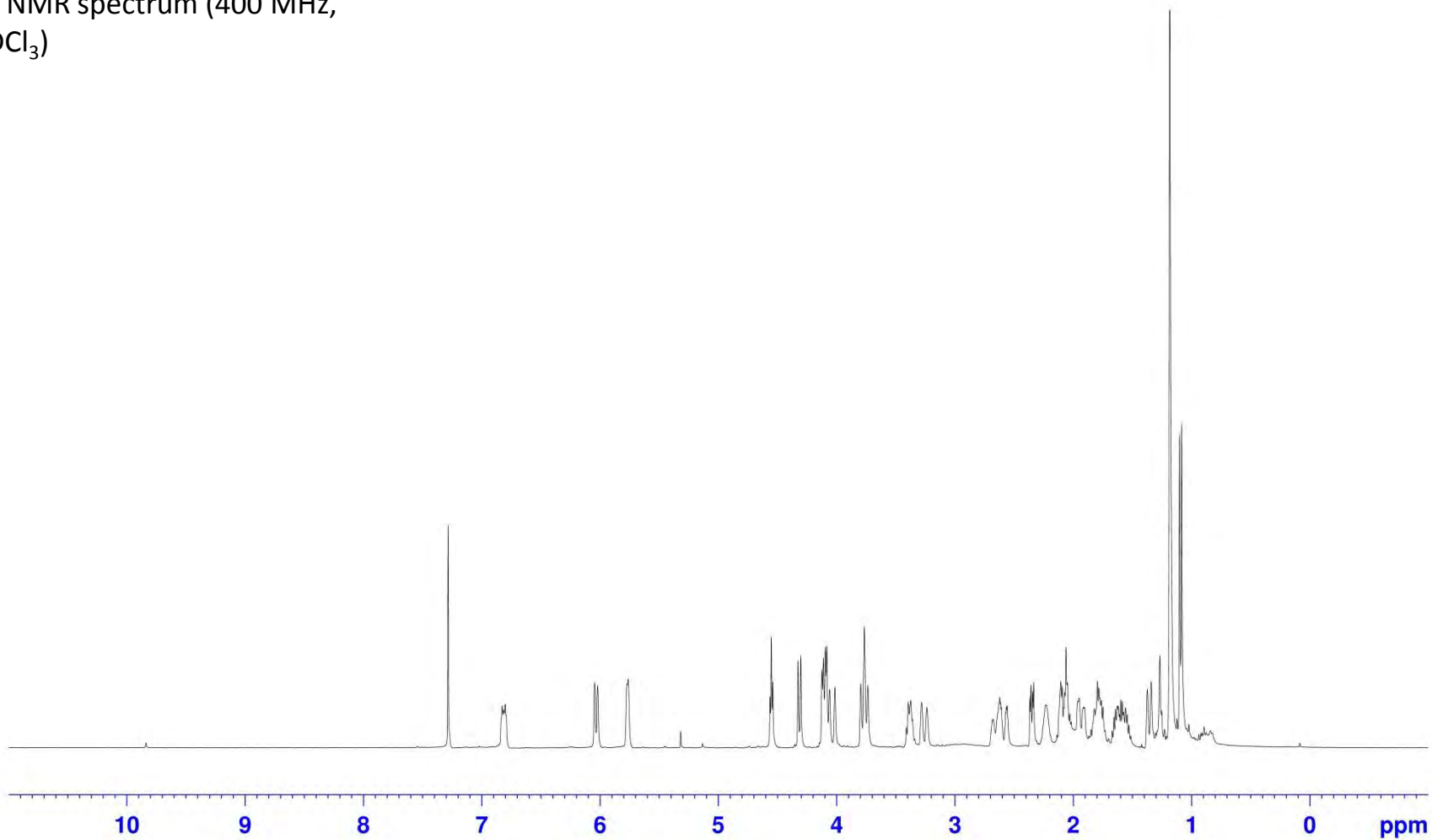
2.68

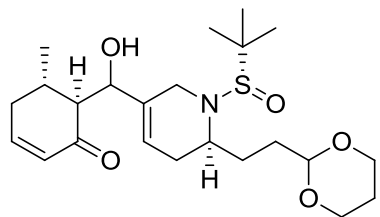
¹³C NMR spectrum (100 MHz,
CDCl₃)



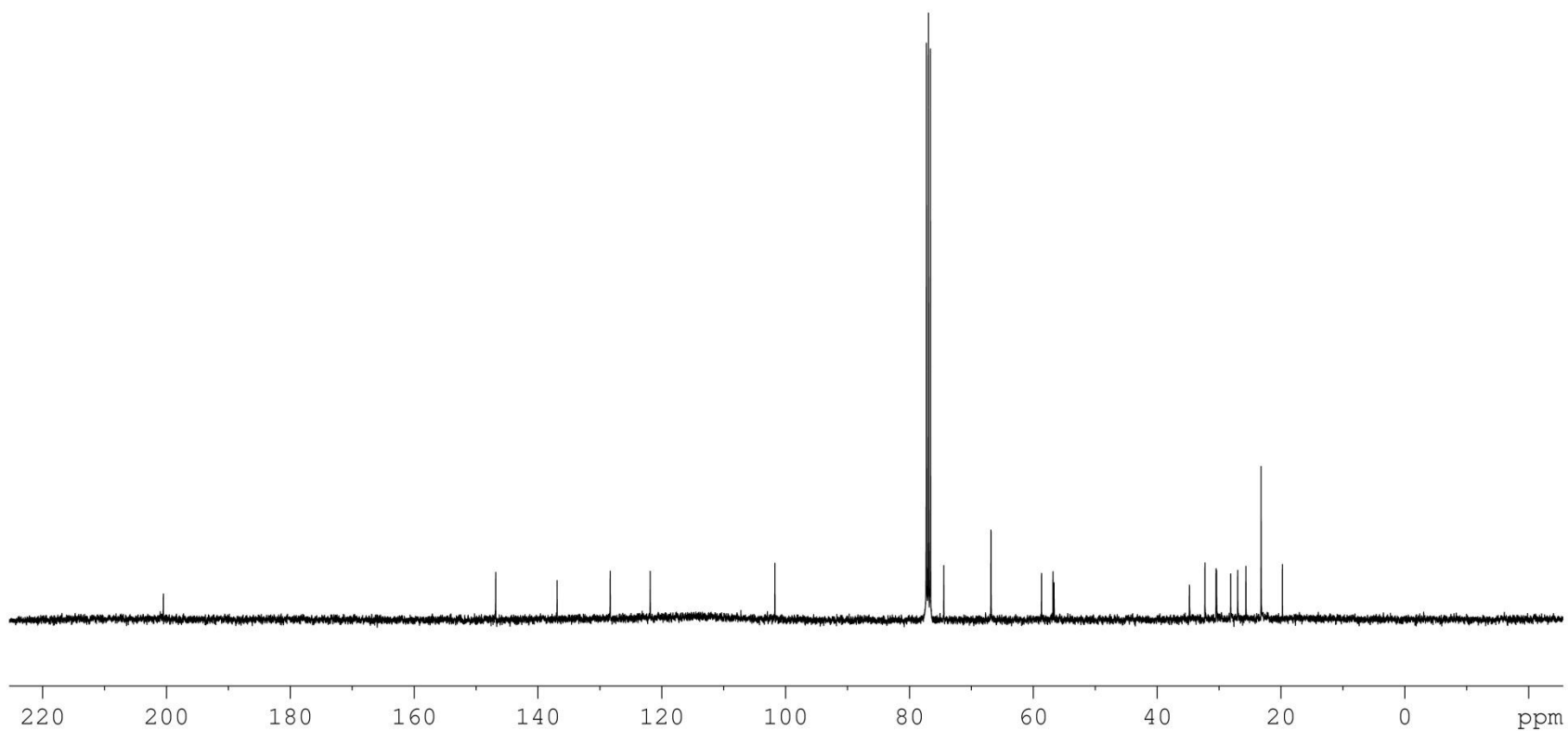


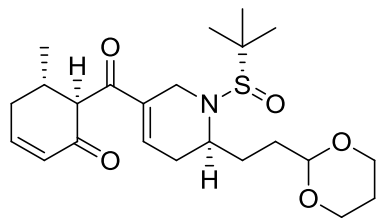
¹H NMR spectrum (400 MHz, CDCl₃)





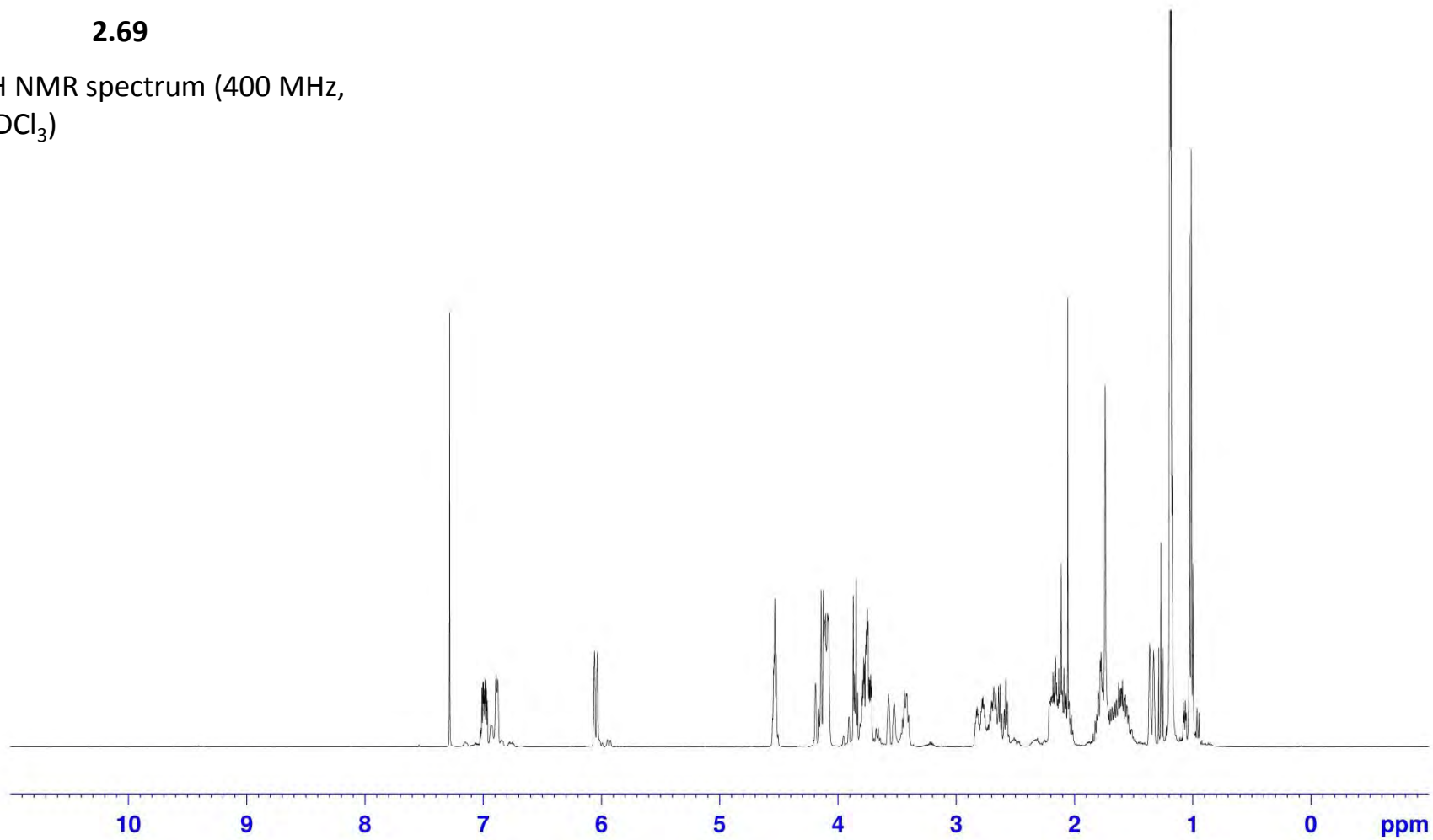
¹³C NMR spectrum (100 MHz,
CDCl₃)

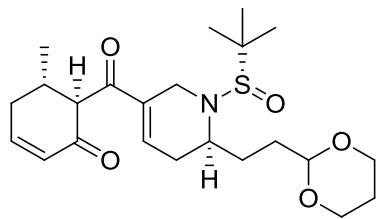




2.69

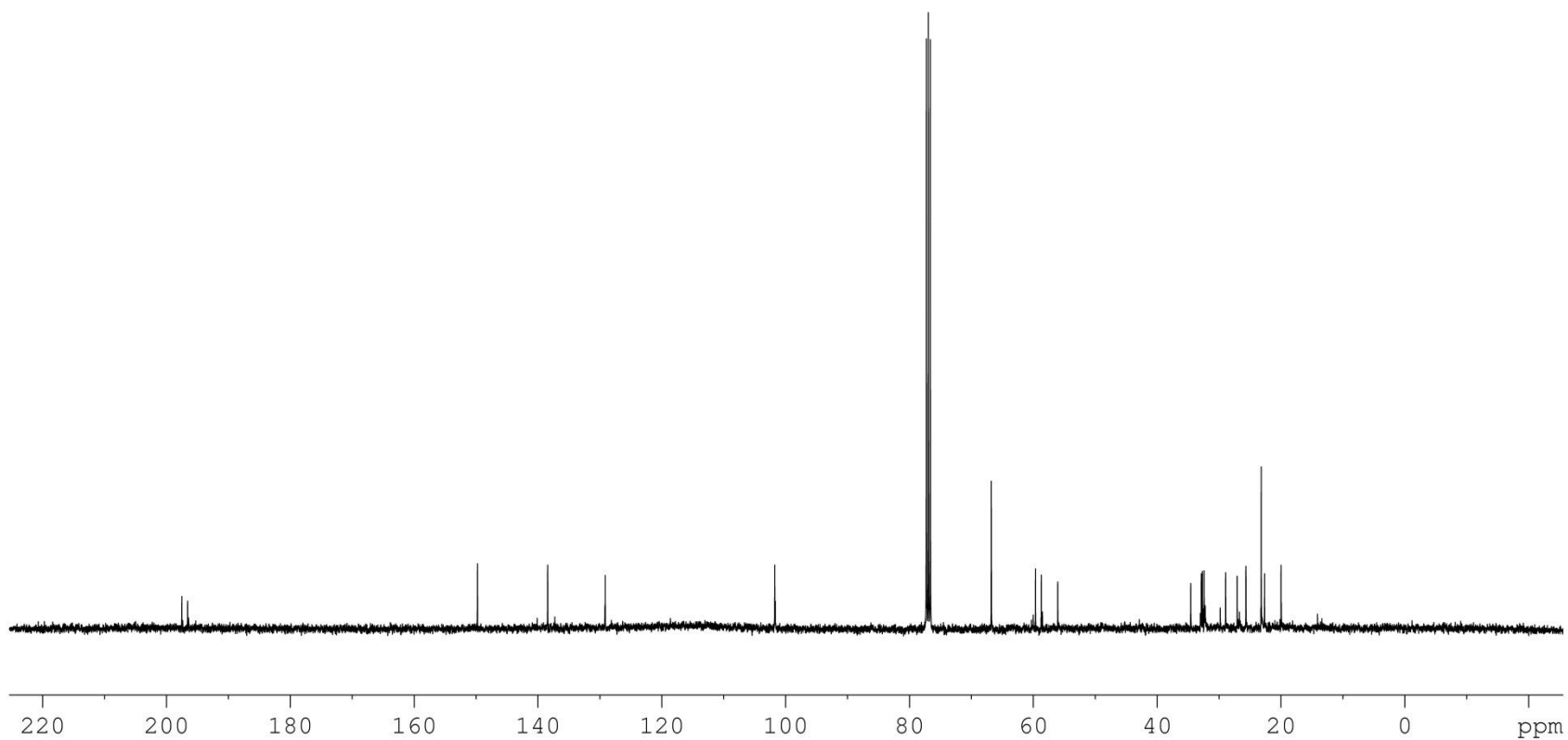
¹H NMR spectrum (400 MHz,
CDCl₃)

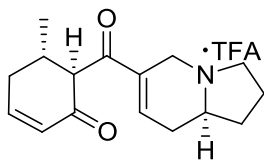




2.69

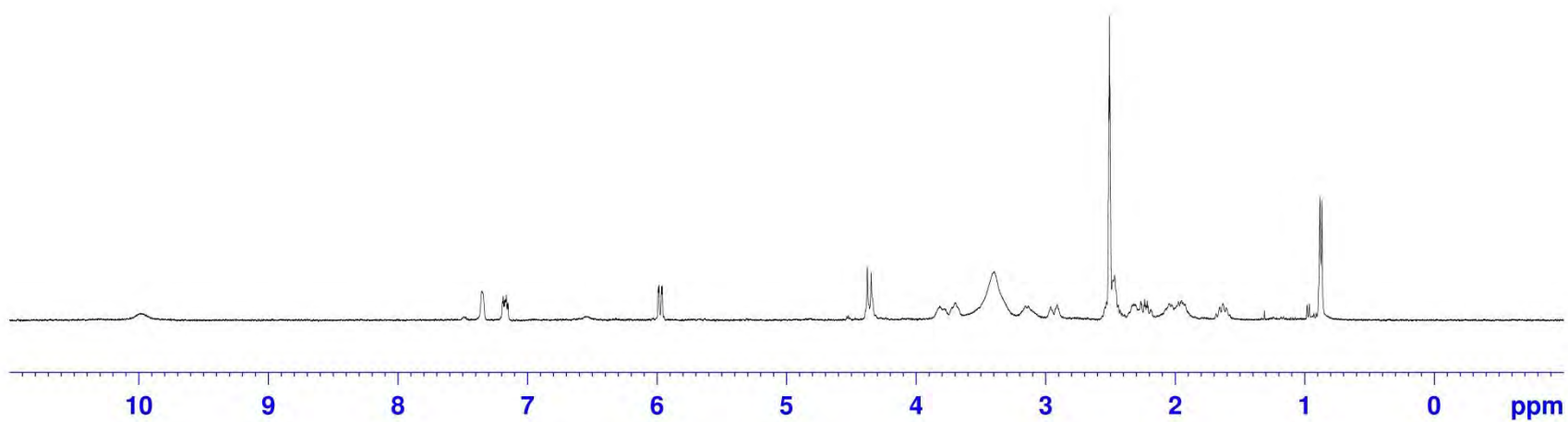
^{13}C NMR spectrum (100 MHz,
 CDCl_3)

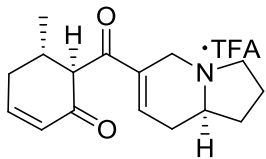




2.70

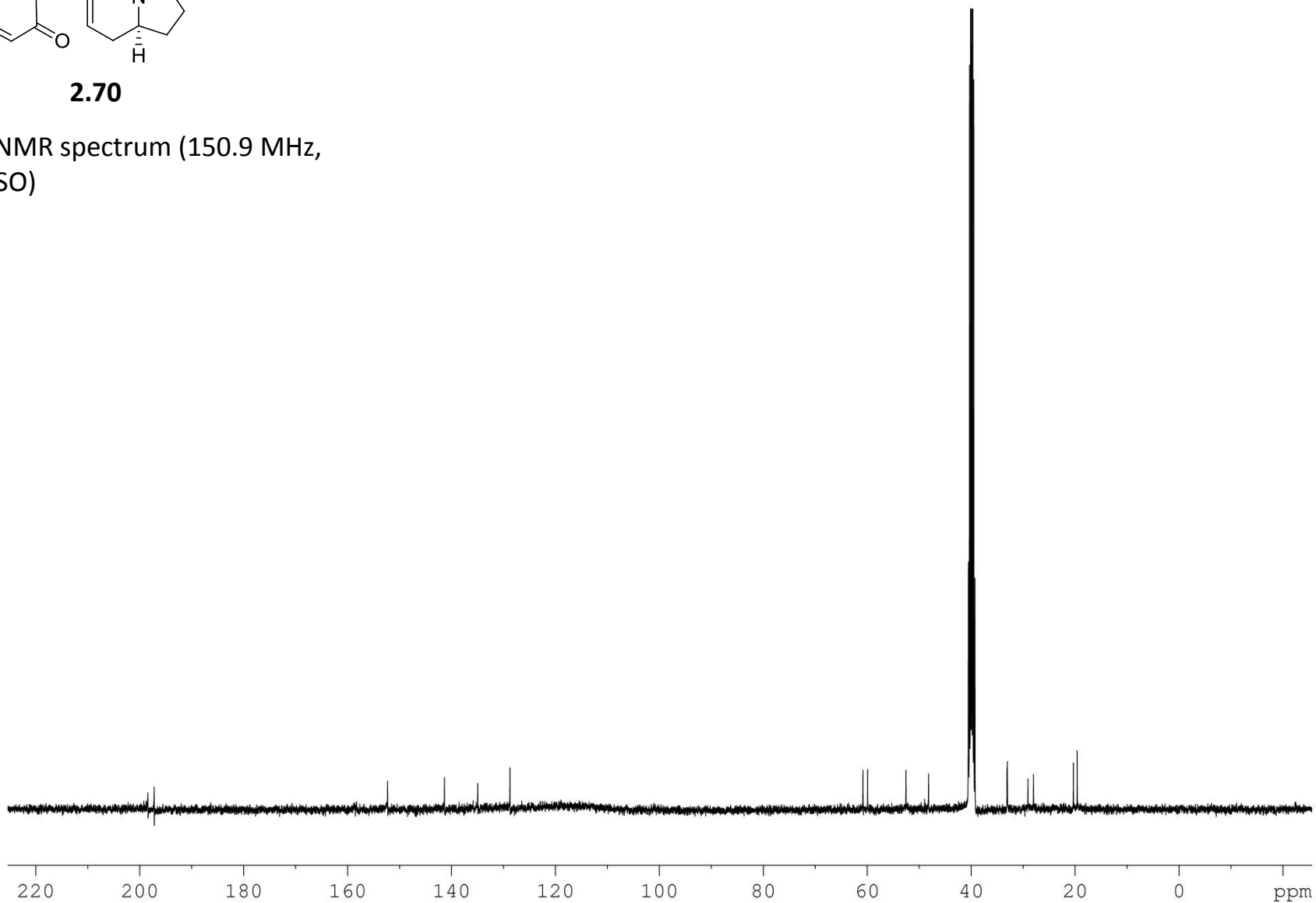
¹H NMR spectrum (600 MHz,
DMSO)

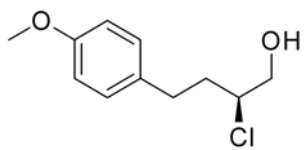




2.70

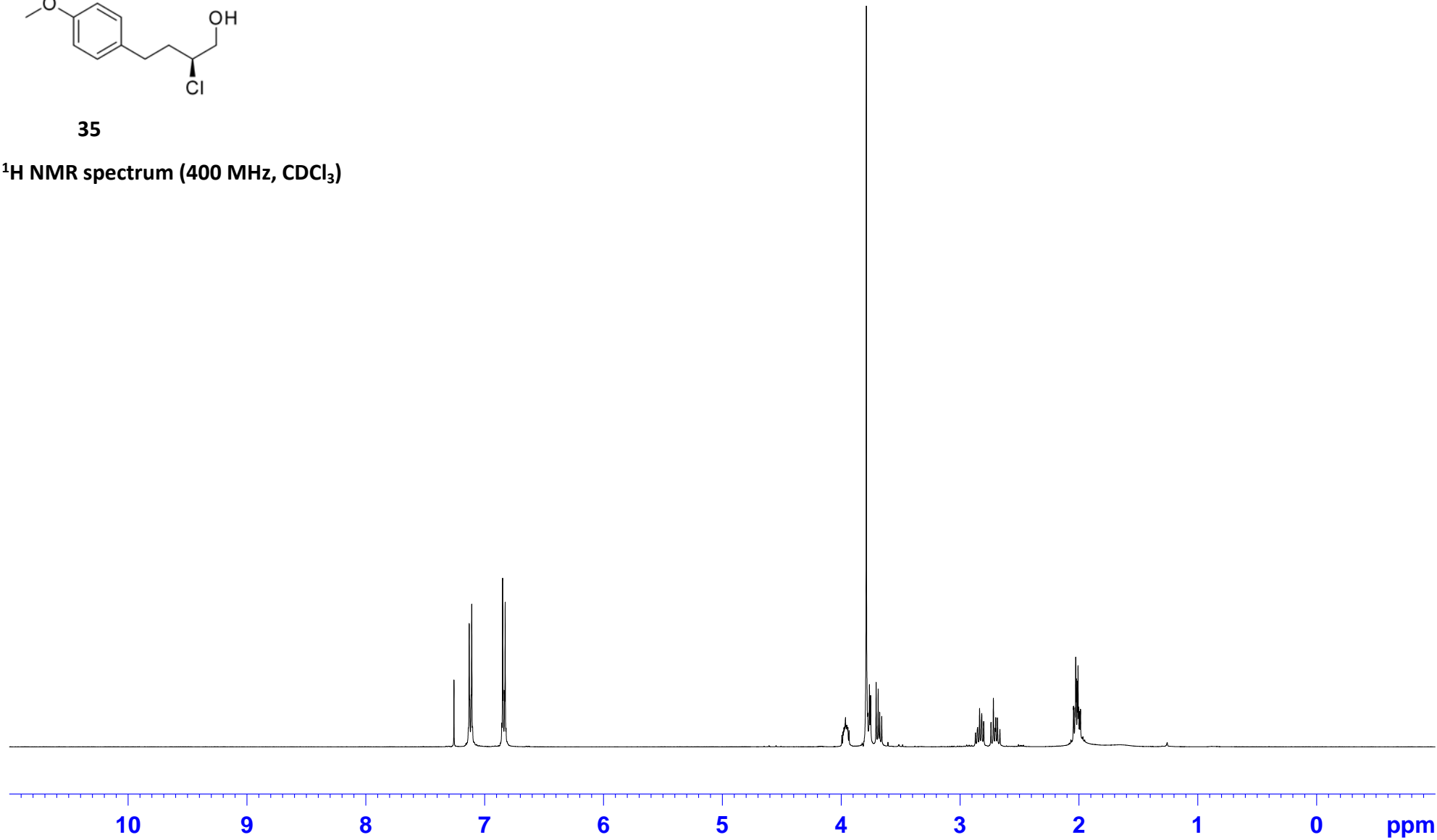
^{13}C NMR spectrum (150.9 MHz,
DMSO)

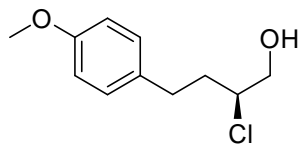




35

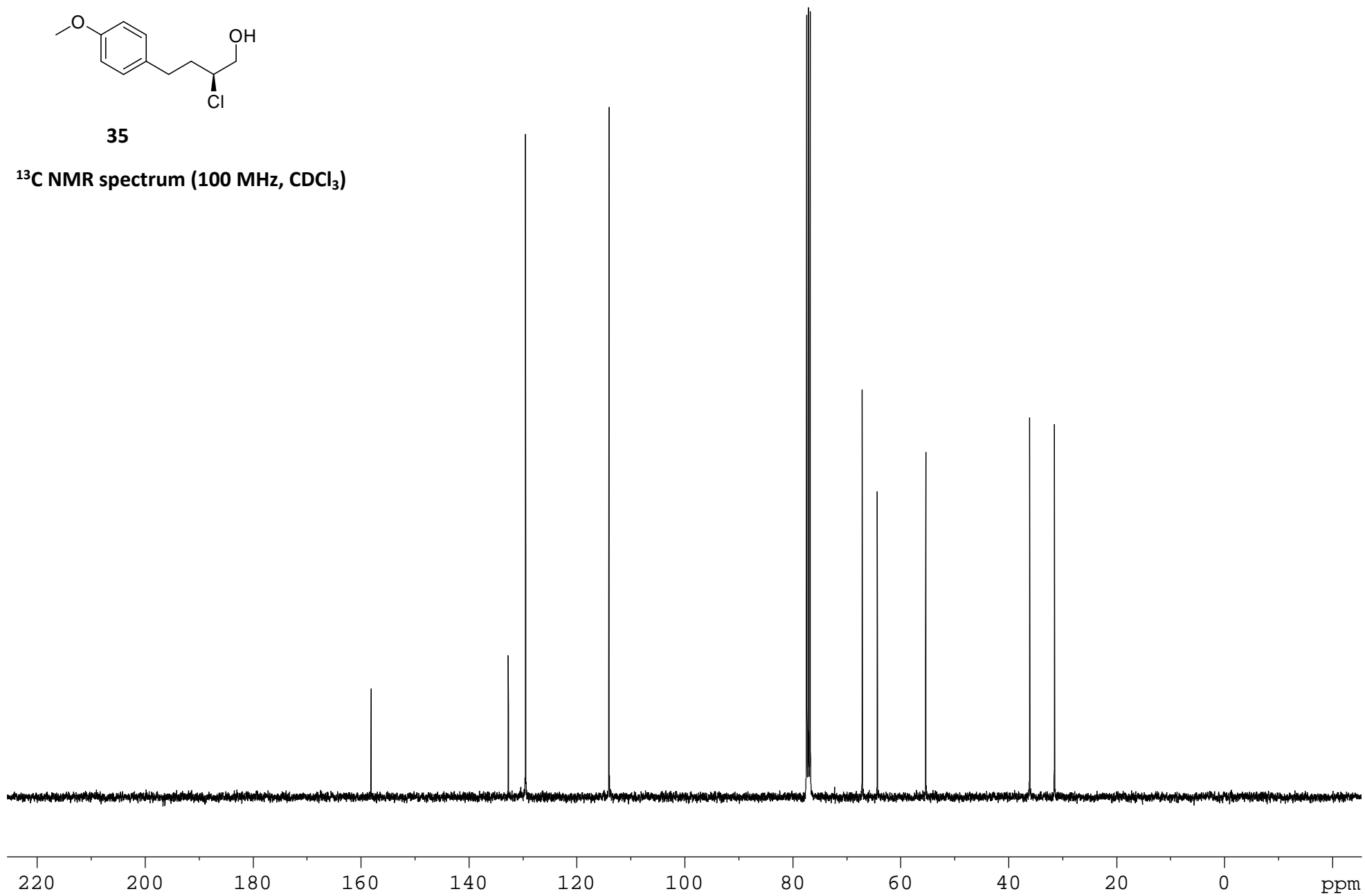
^1H NMR spectrum (400 MHz, CDCl_3)

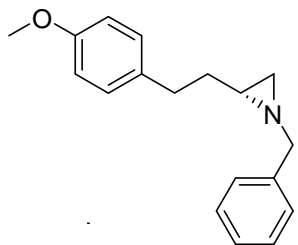




35

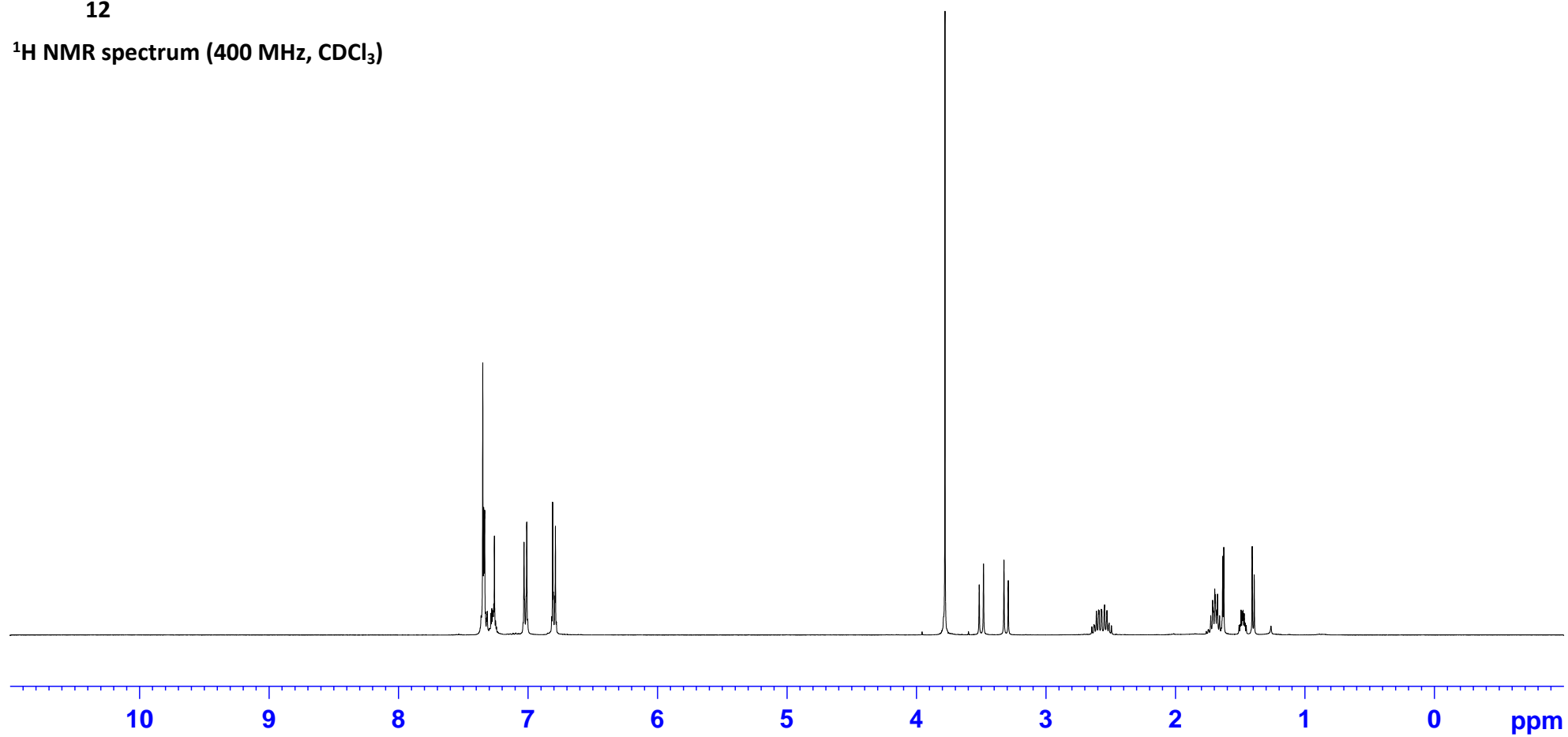
¹³C NMR spectrum (100 MHz, CDCl₃)

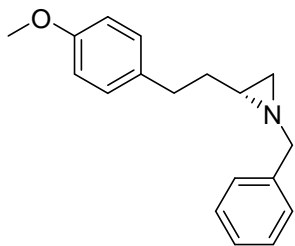




12

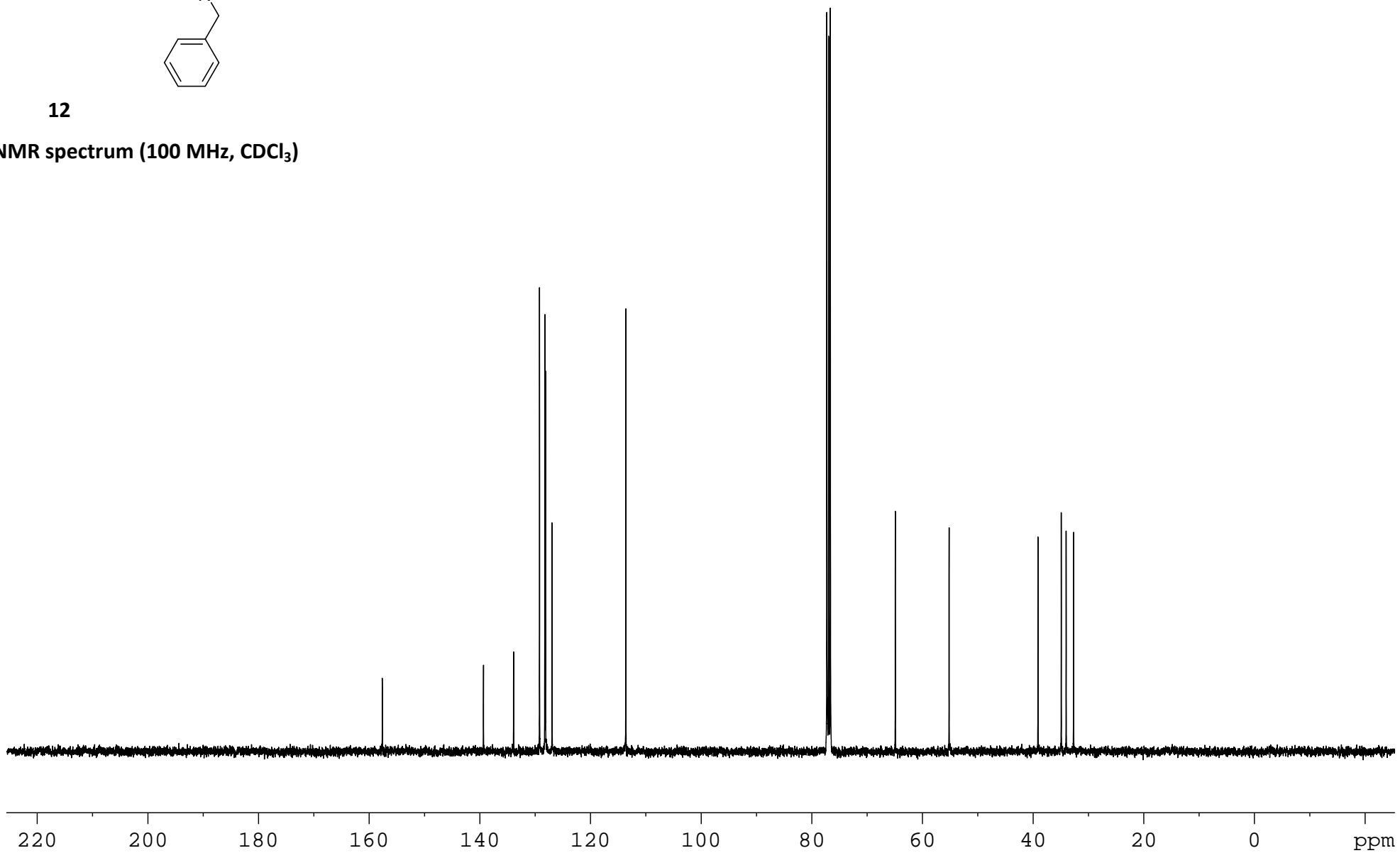
^1H NMR spectrum (400 MHz, CDCl_3)

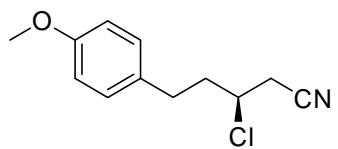




12

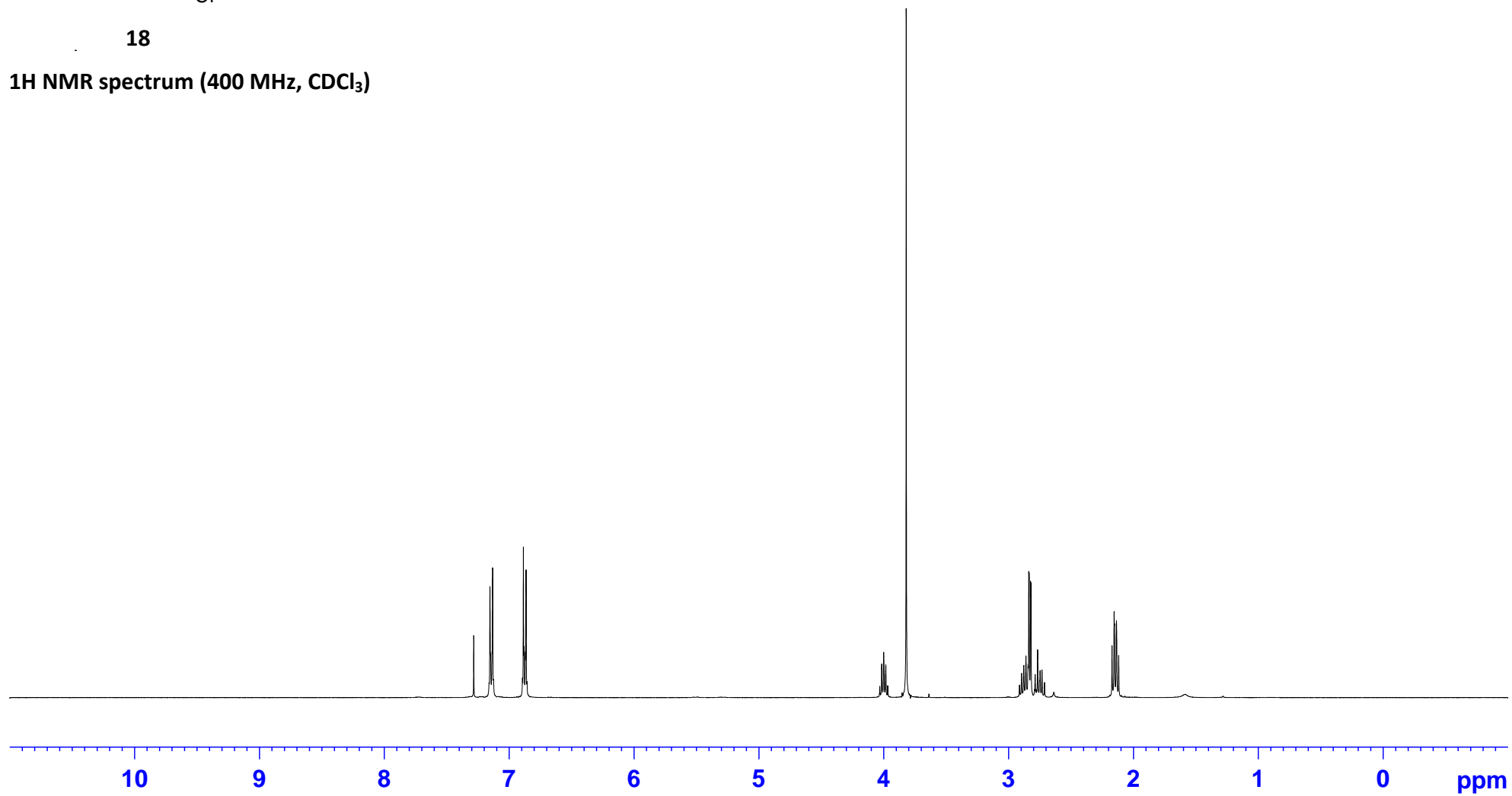
¹³C NMR spectrum (100 MHz, CDCl₃)

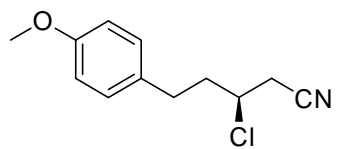




18

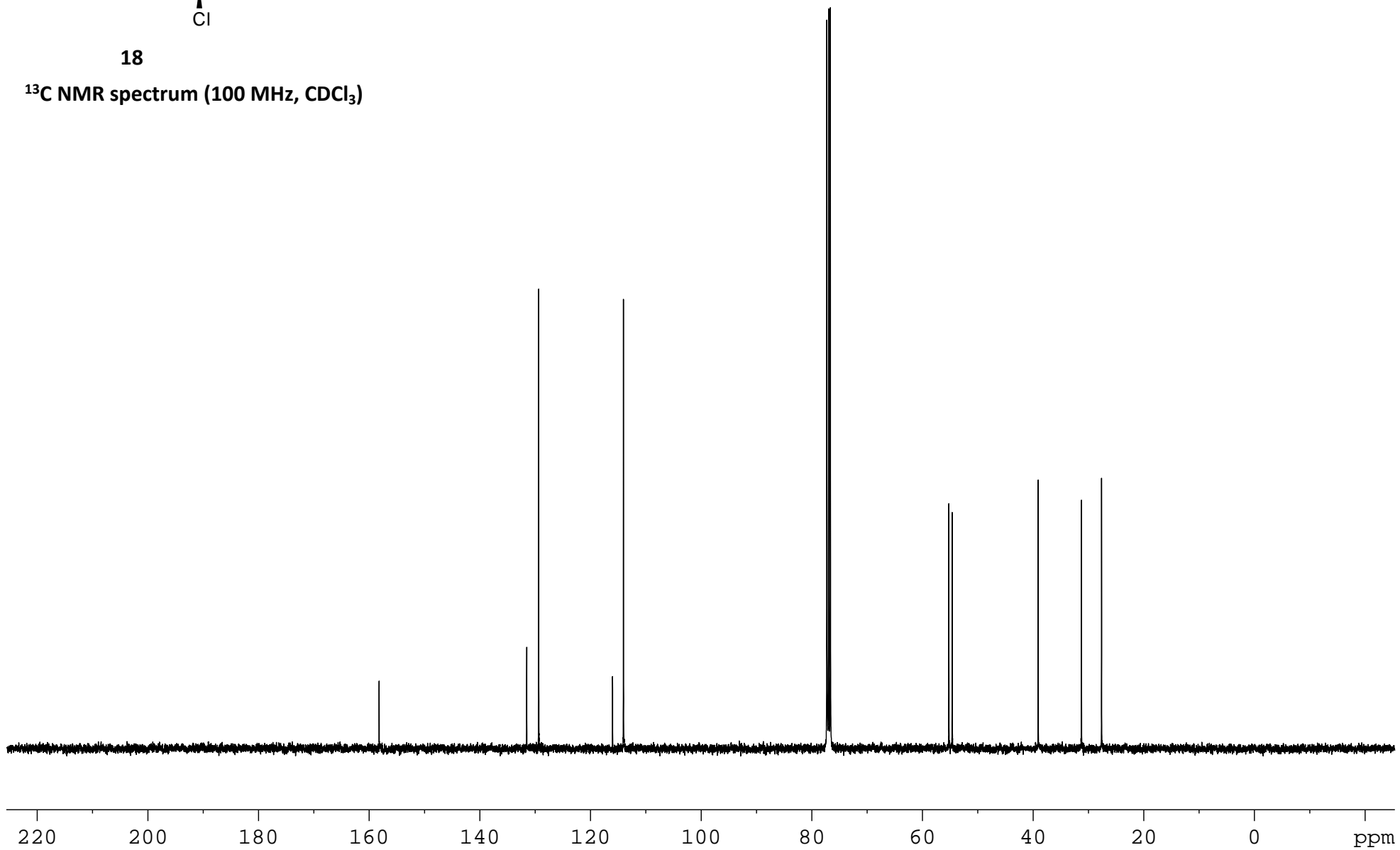
¹H NMR spectrum (400 MHz, CDCl₃)

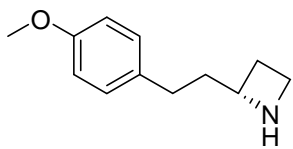




18

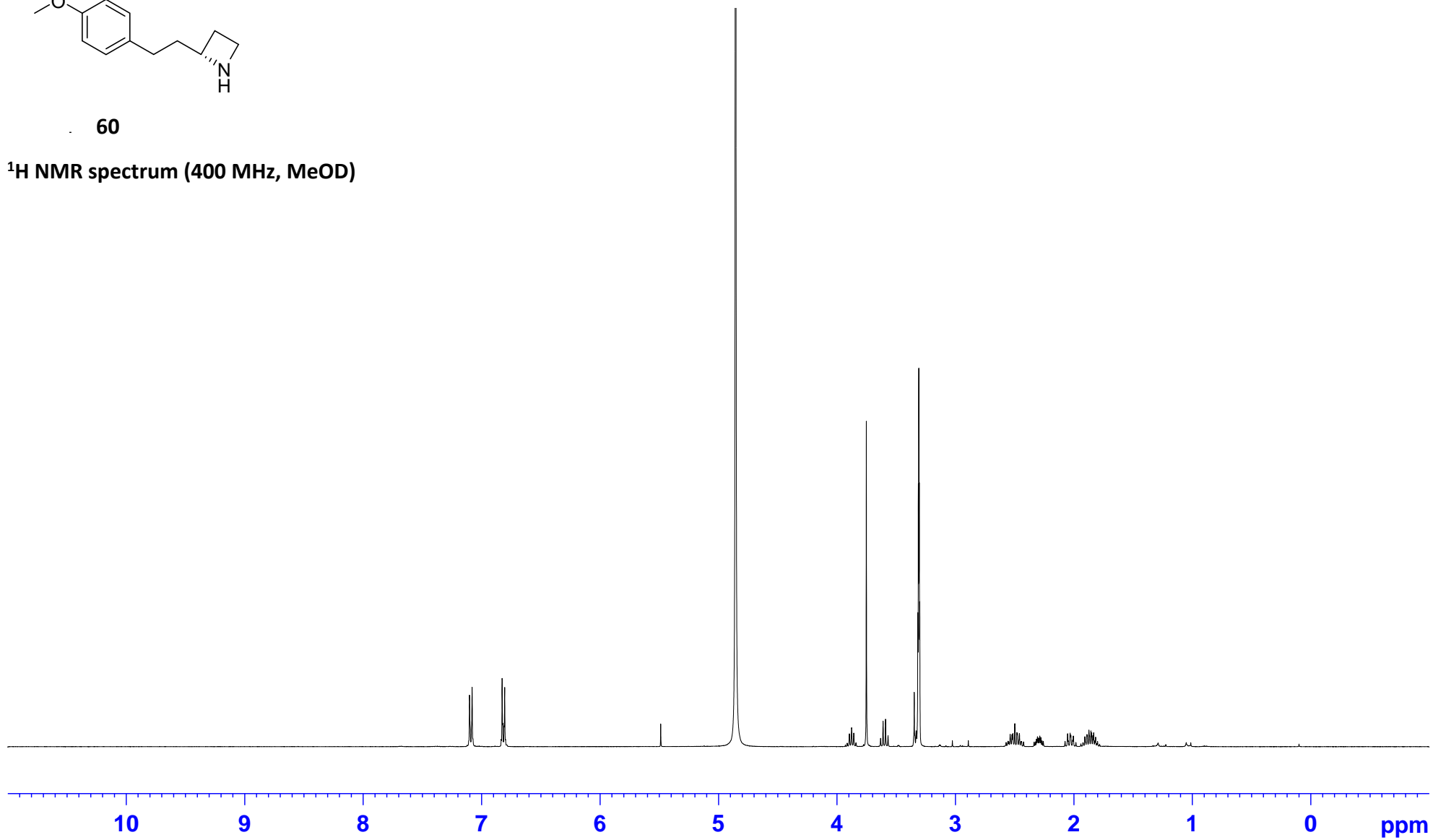
¹³C NMR spectrum (100 MHz, CDCl₃)

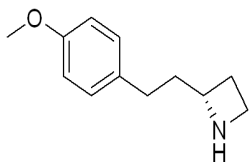




60

¹H NMR spectrum (400 MHz, MeOD)





60

¹³C NMR (100 MHz, MeOD)

159.38

135.03

130.27

114.81

59.72

55.65

49.01

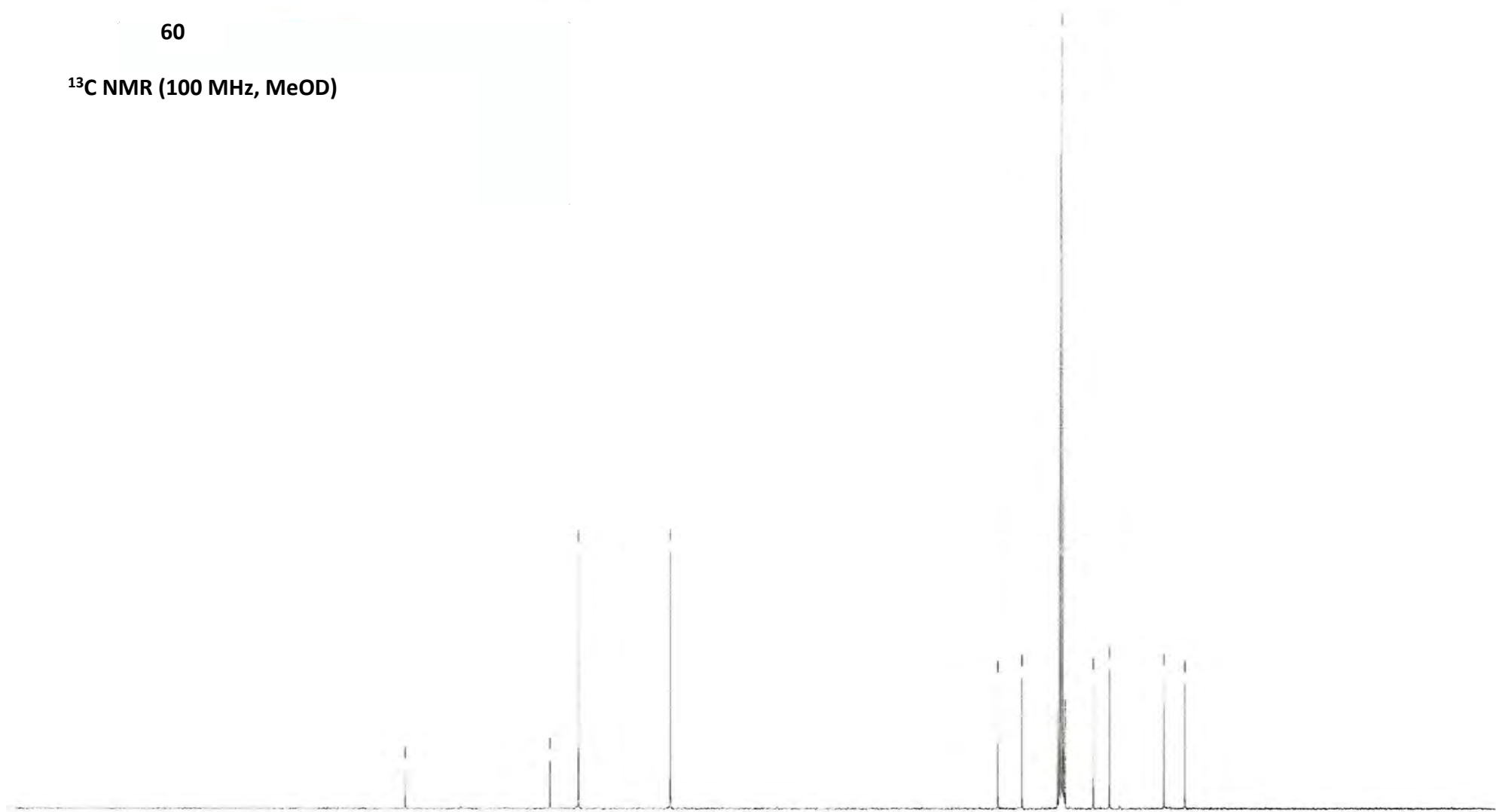
43.65

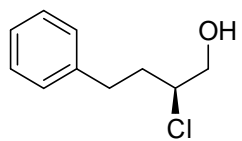
40.91

31.75

28.22

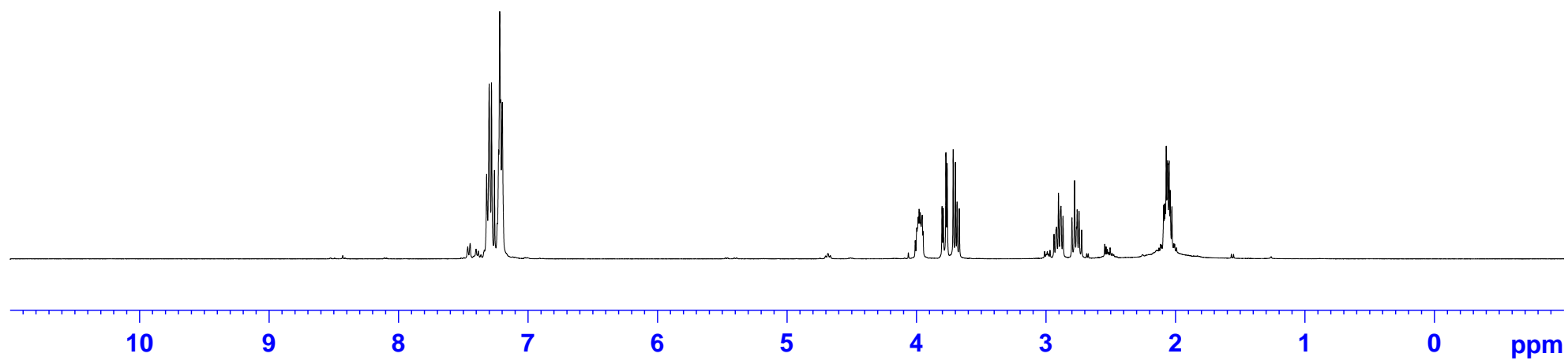
220 200 180 160 140 120 100 80 60 40 20 0 ppm

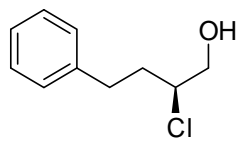




36

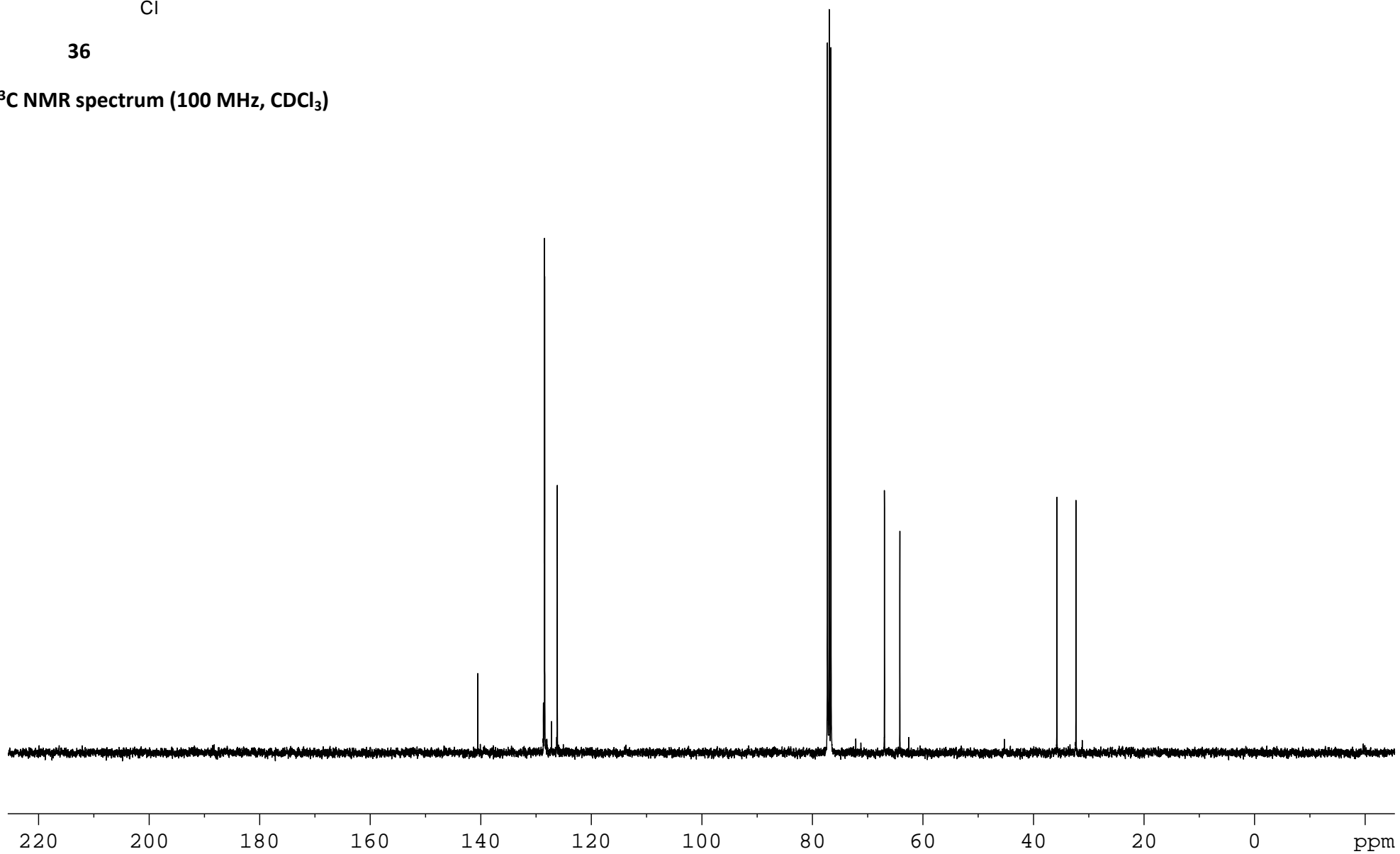
^1H NMR spectrum (400 MHz, CDCl_3)

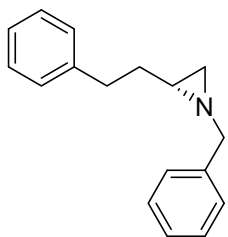




36

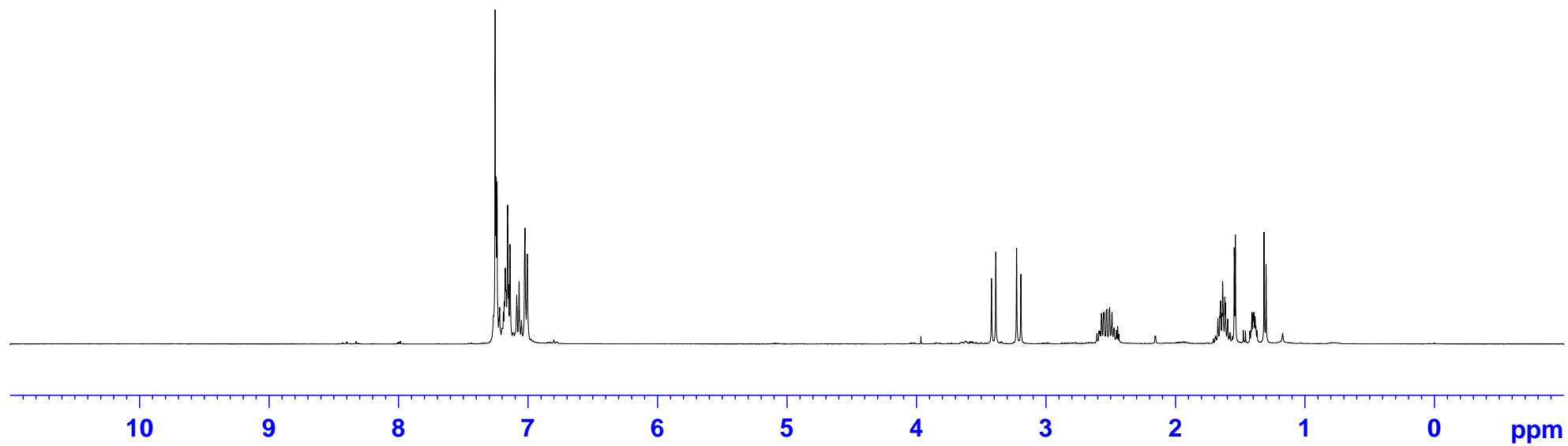
^{13}C NMR spectrum (100 MHz, CDCl_3)

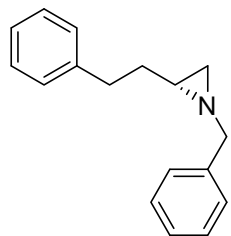




11

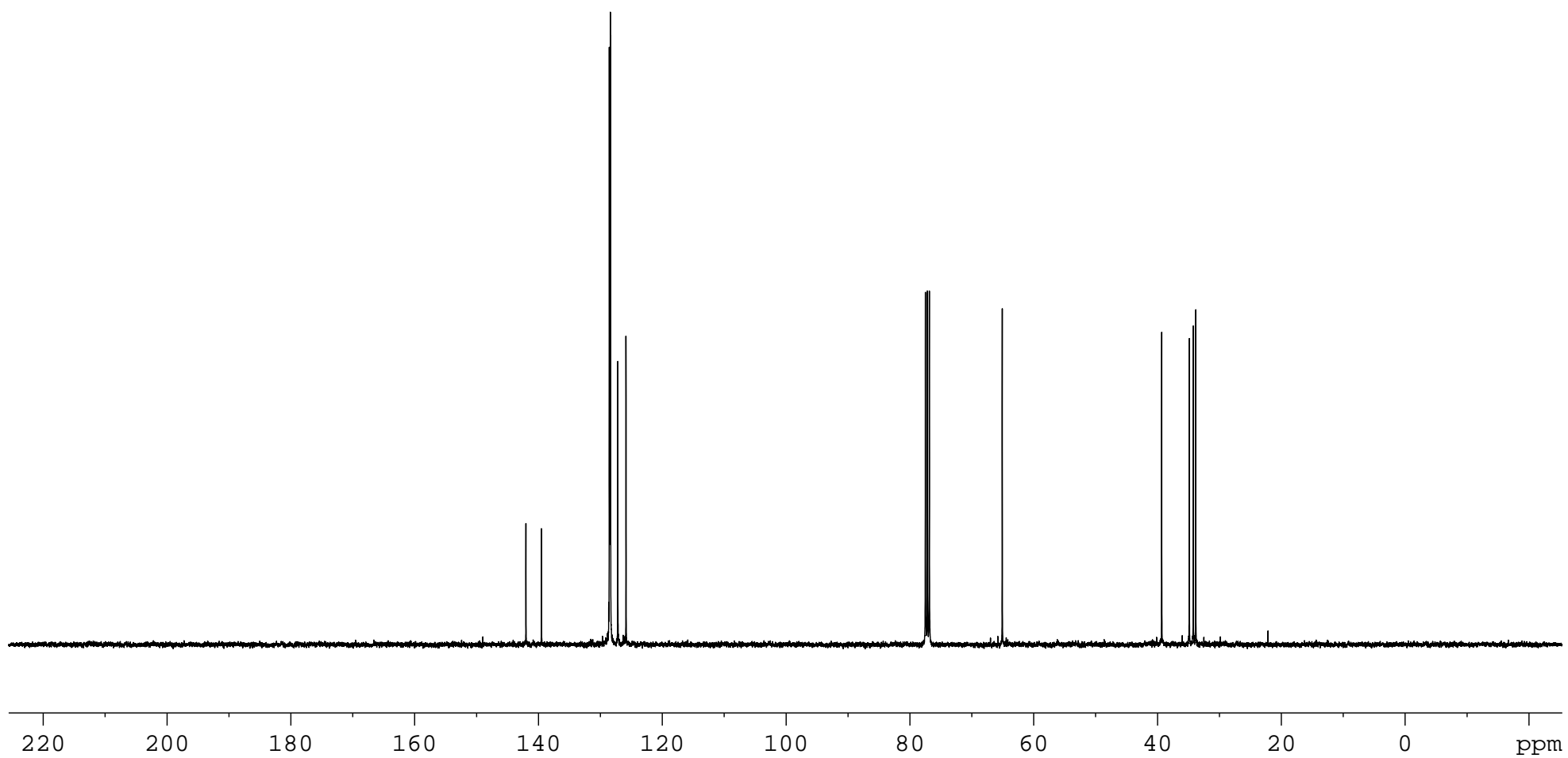
^1H NMR spectrum (400 MHz, CDCl_3)

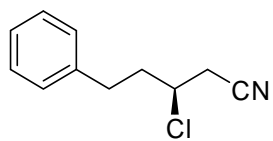




11

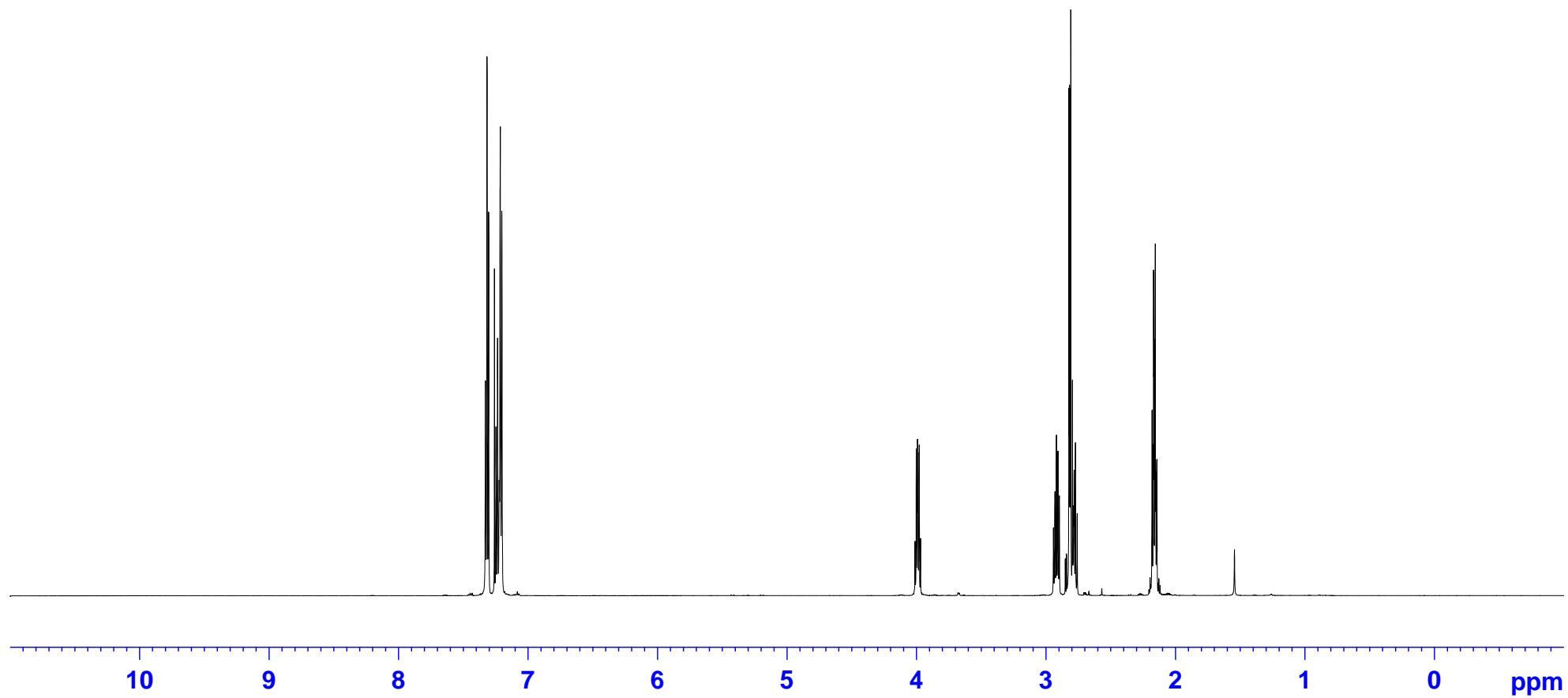
¹³C NMR spectrum (100 MHz, CDCl₃)

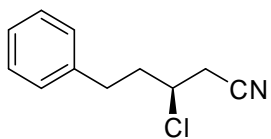




17

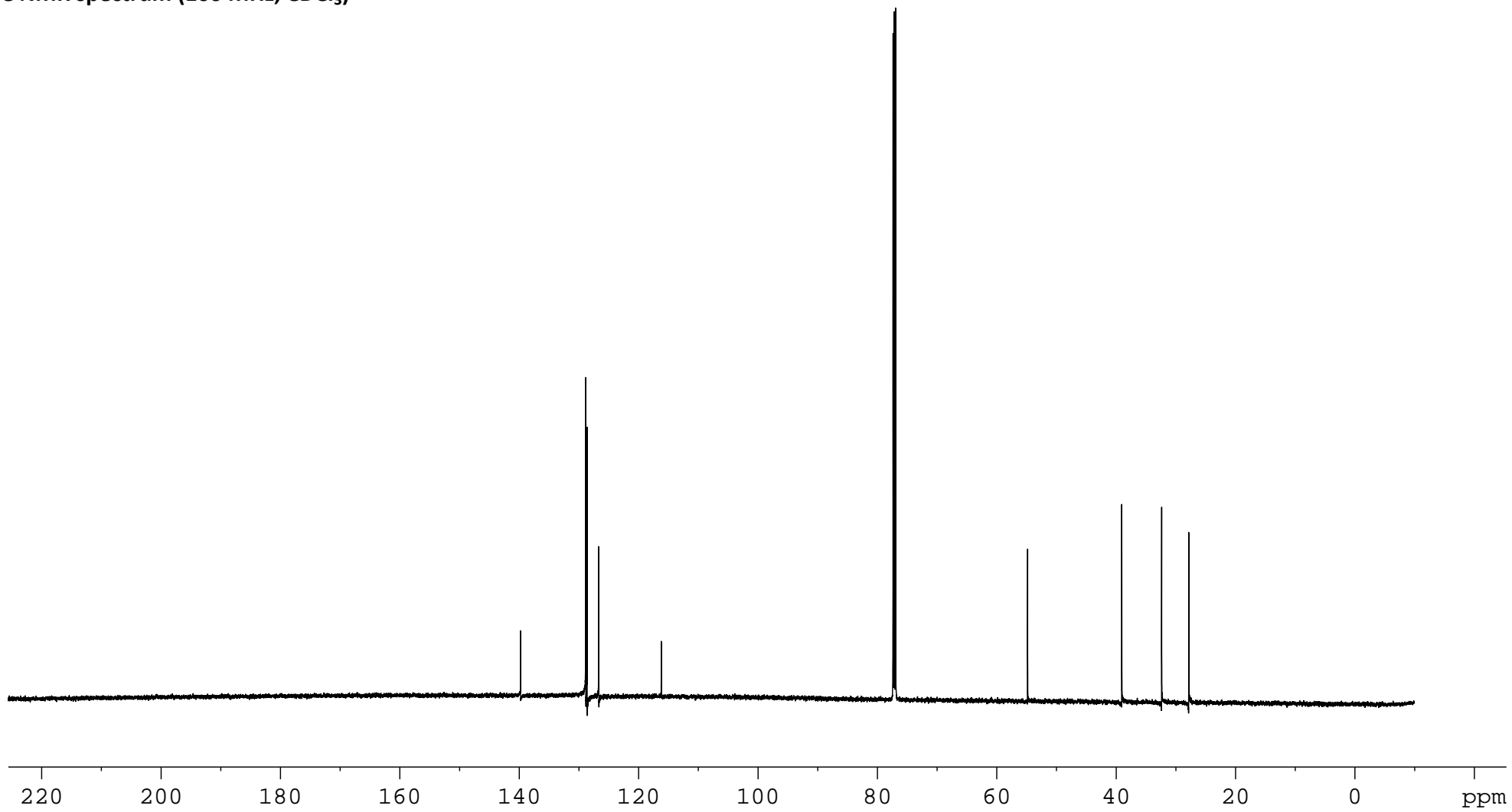
^1H NMR spectrum (400 MHz, CDCl_3)

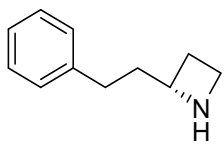




17

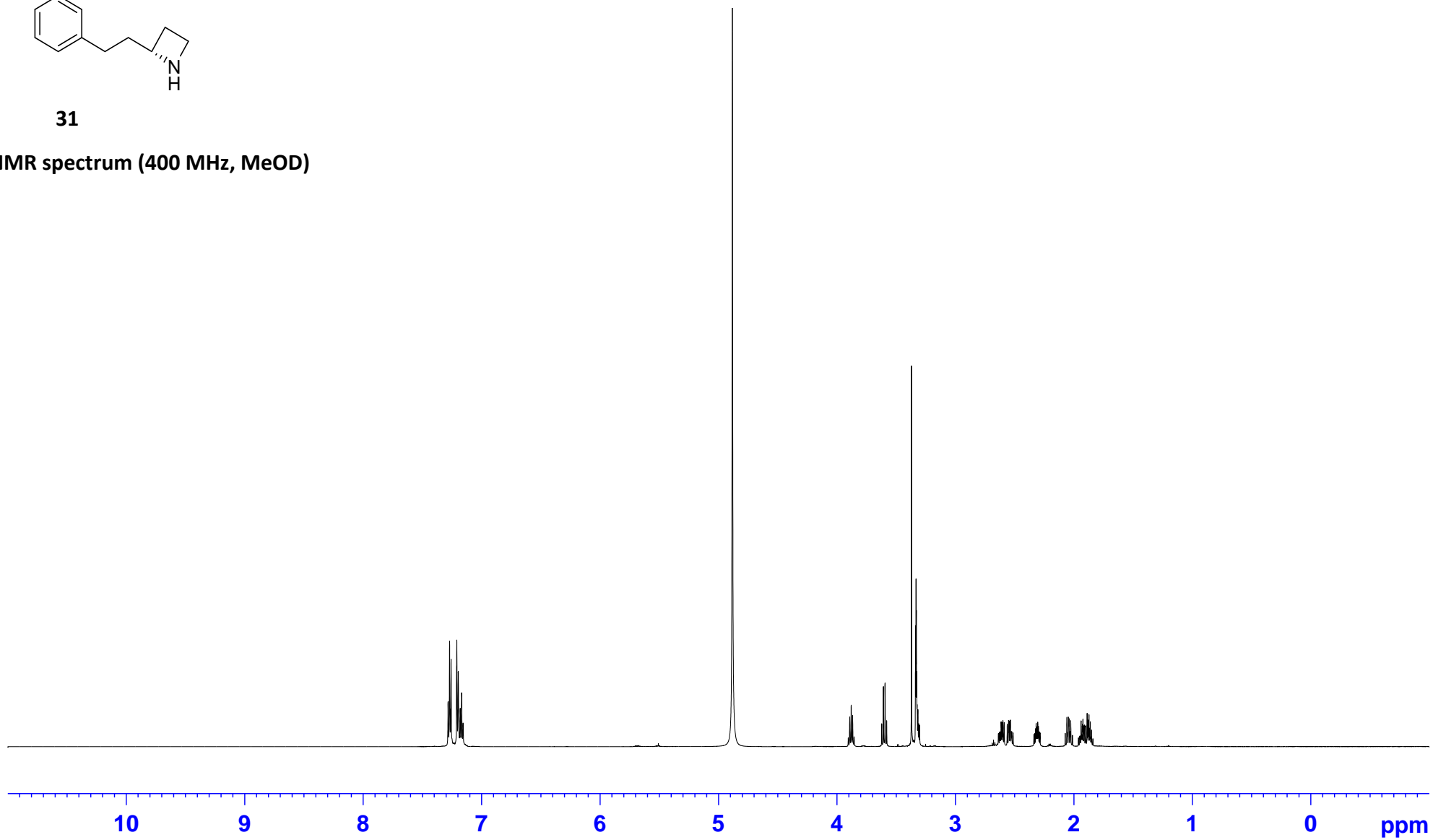
¹³C NMR spectrum (100 MHz, CDCl₃)

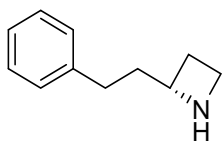




31

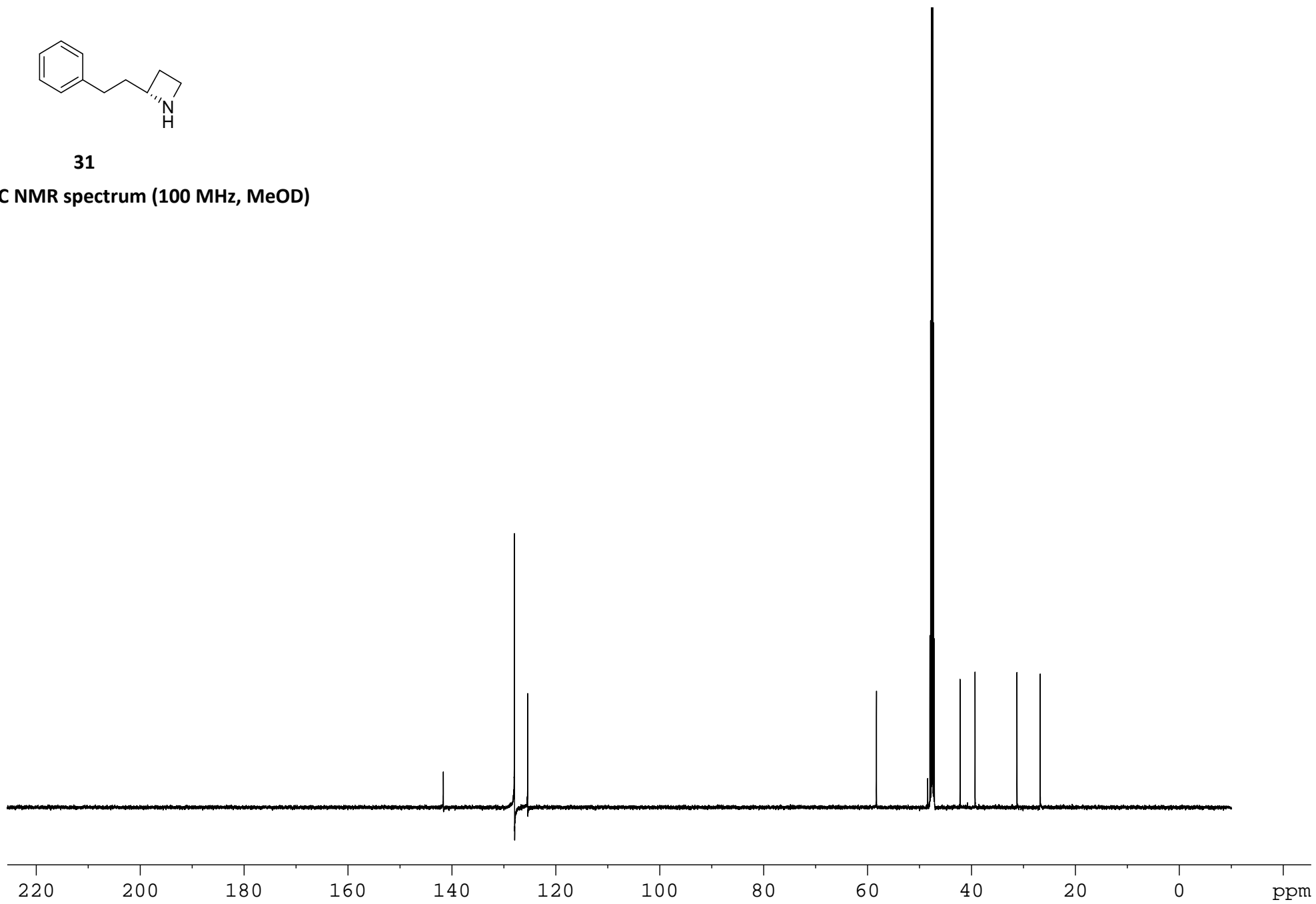
¹H NMR spectrum (400 MHz, MeOD)

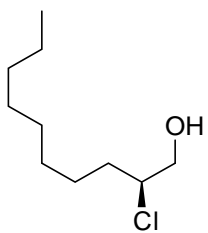




31

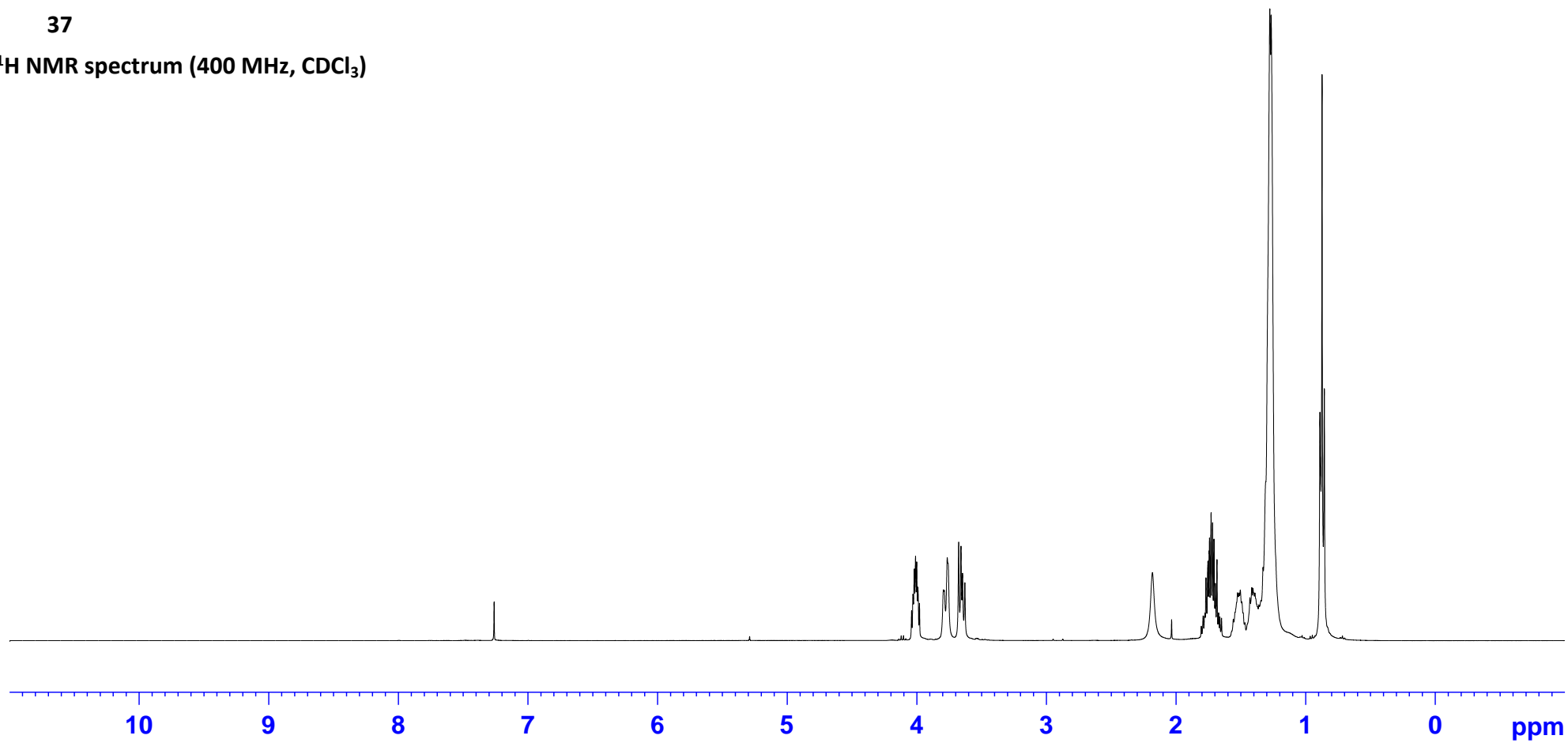
¹³C NMR spectrum (100 MHz, MeOD)

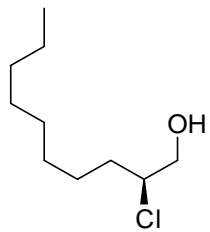




37

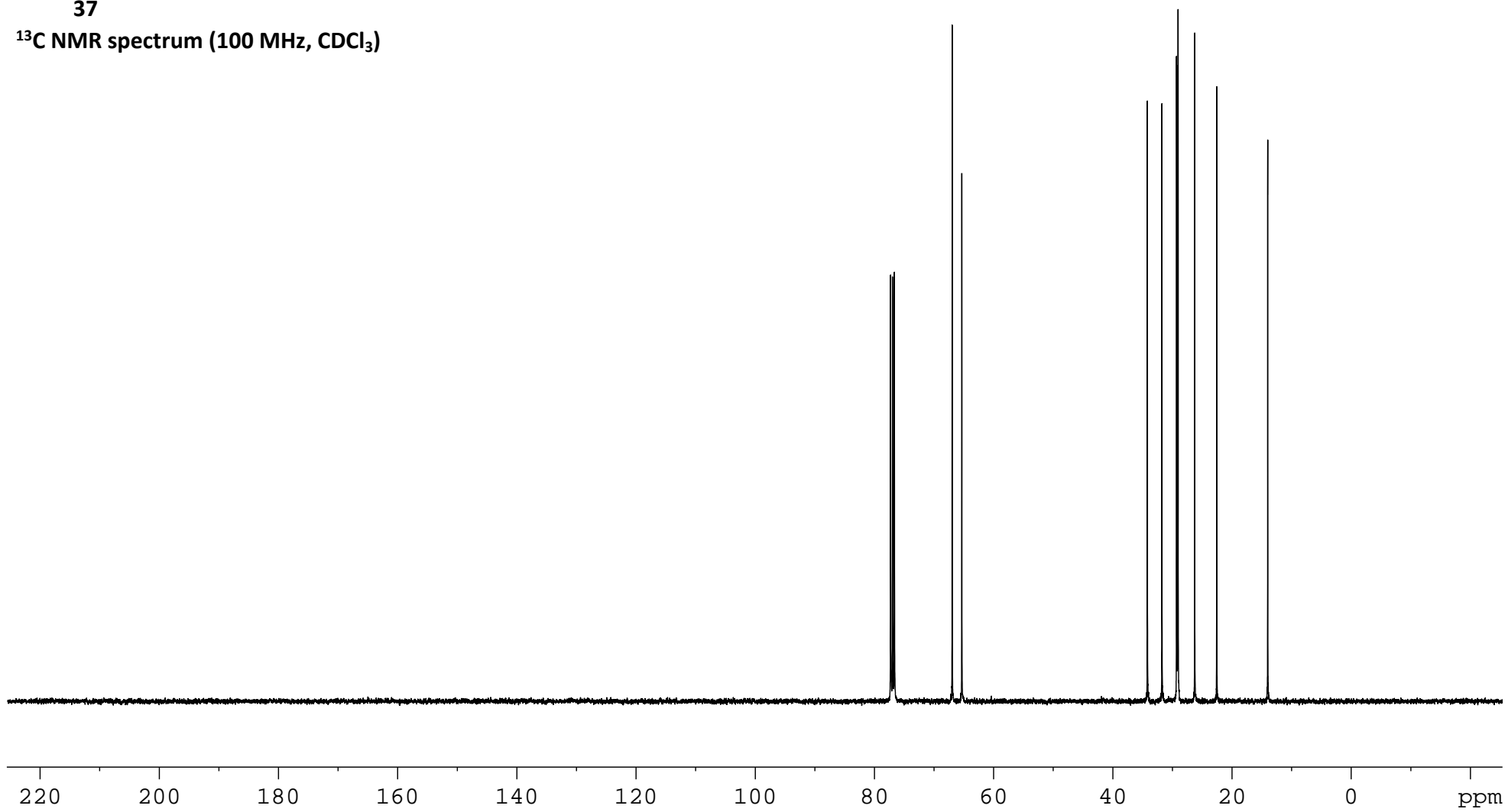
^1H NMR spectrum (400 MHz, CDCl_3)

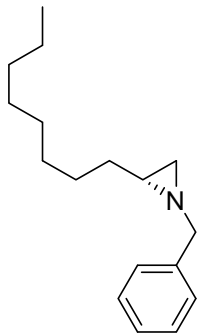




37

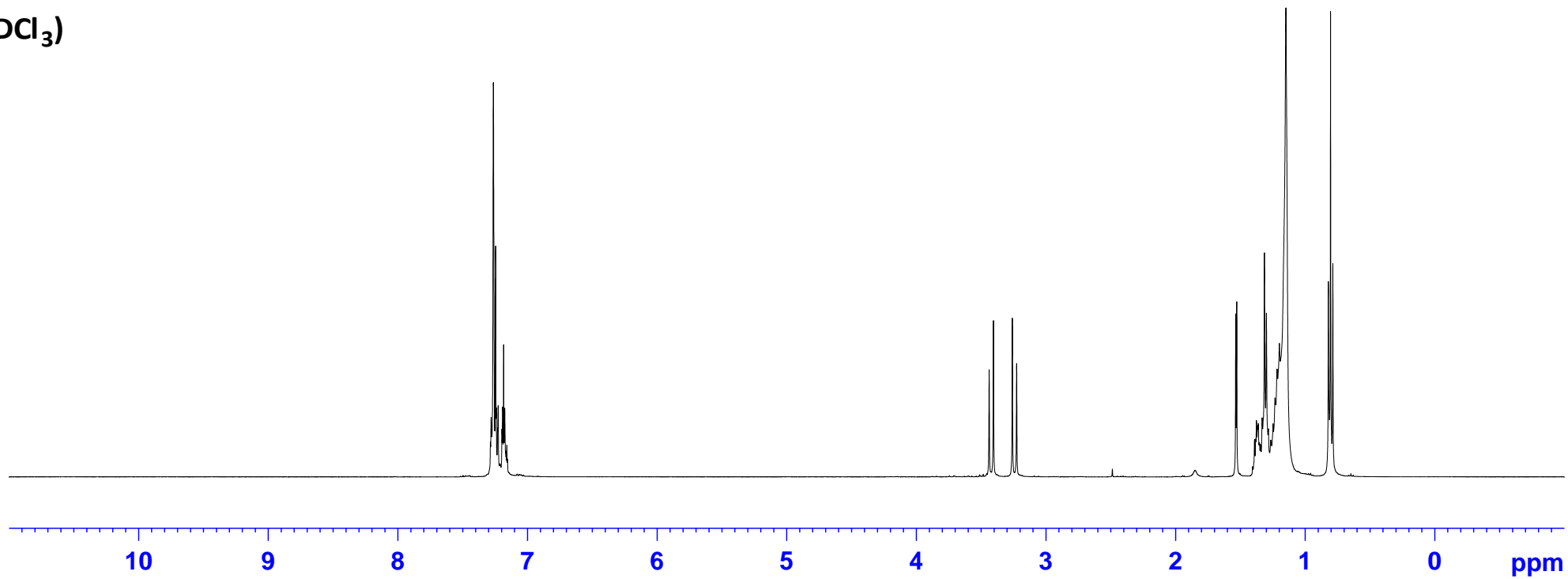
¹³C NMR spectrum (100 MHz, CDCl₃)

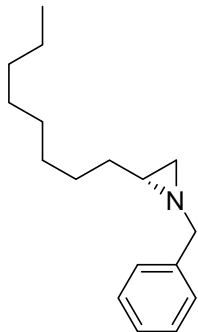




14

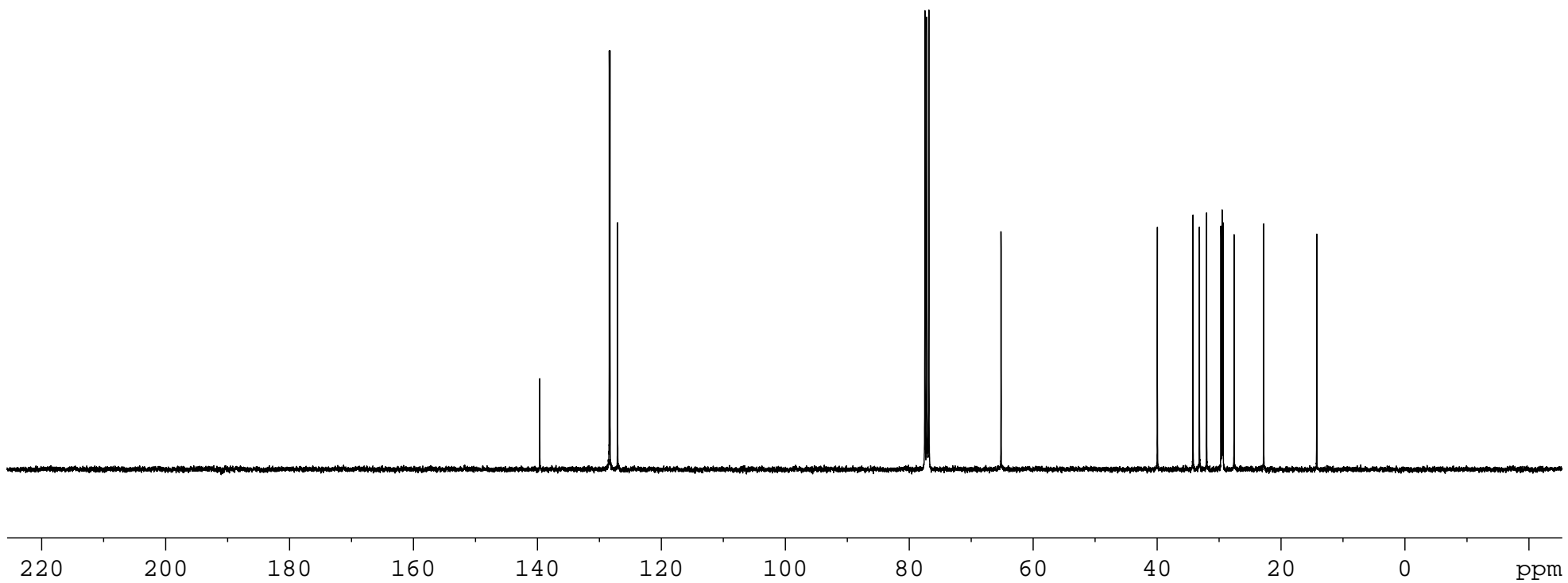
^1H NMR spectrum (400 MHz,
 CDCl_3)

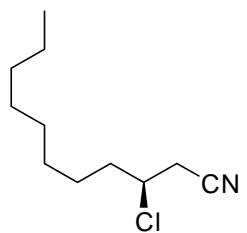




14

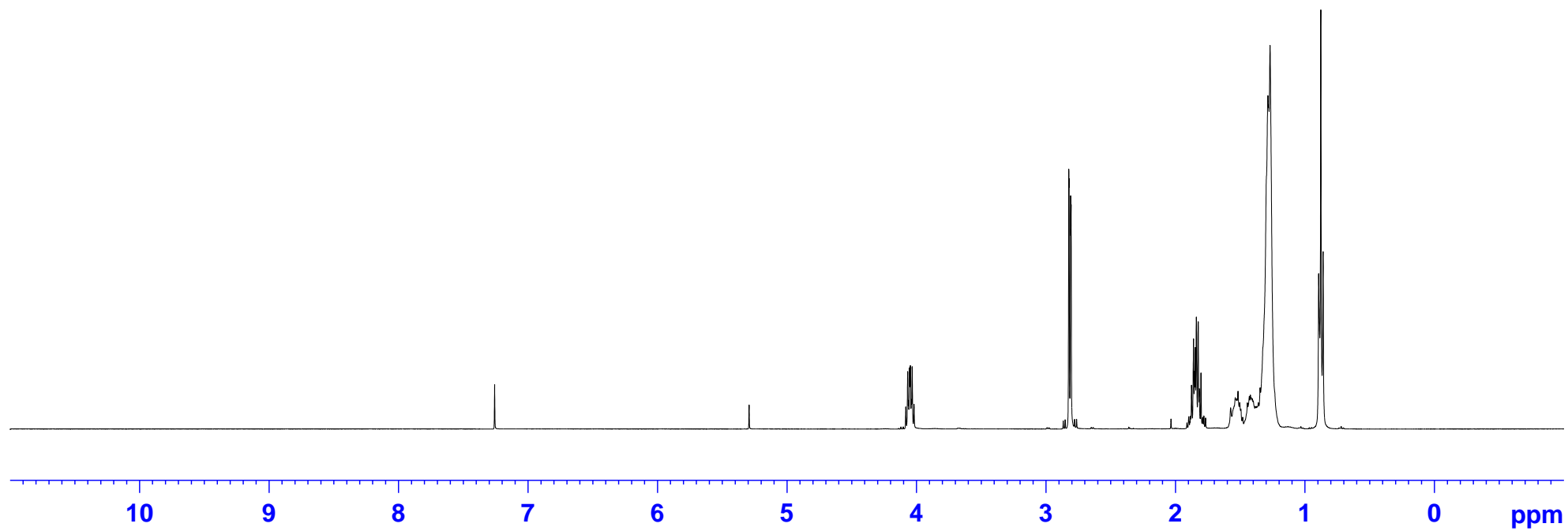
¹³C NMR spectrum (100 MHz,
CDCl₃)

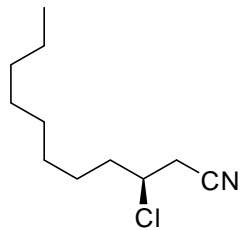




20

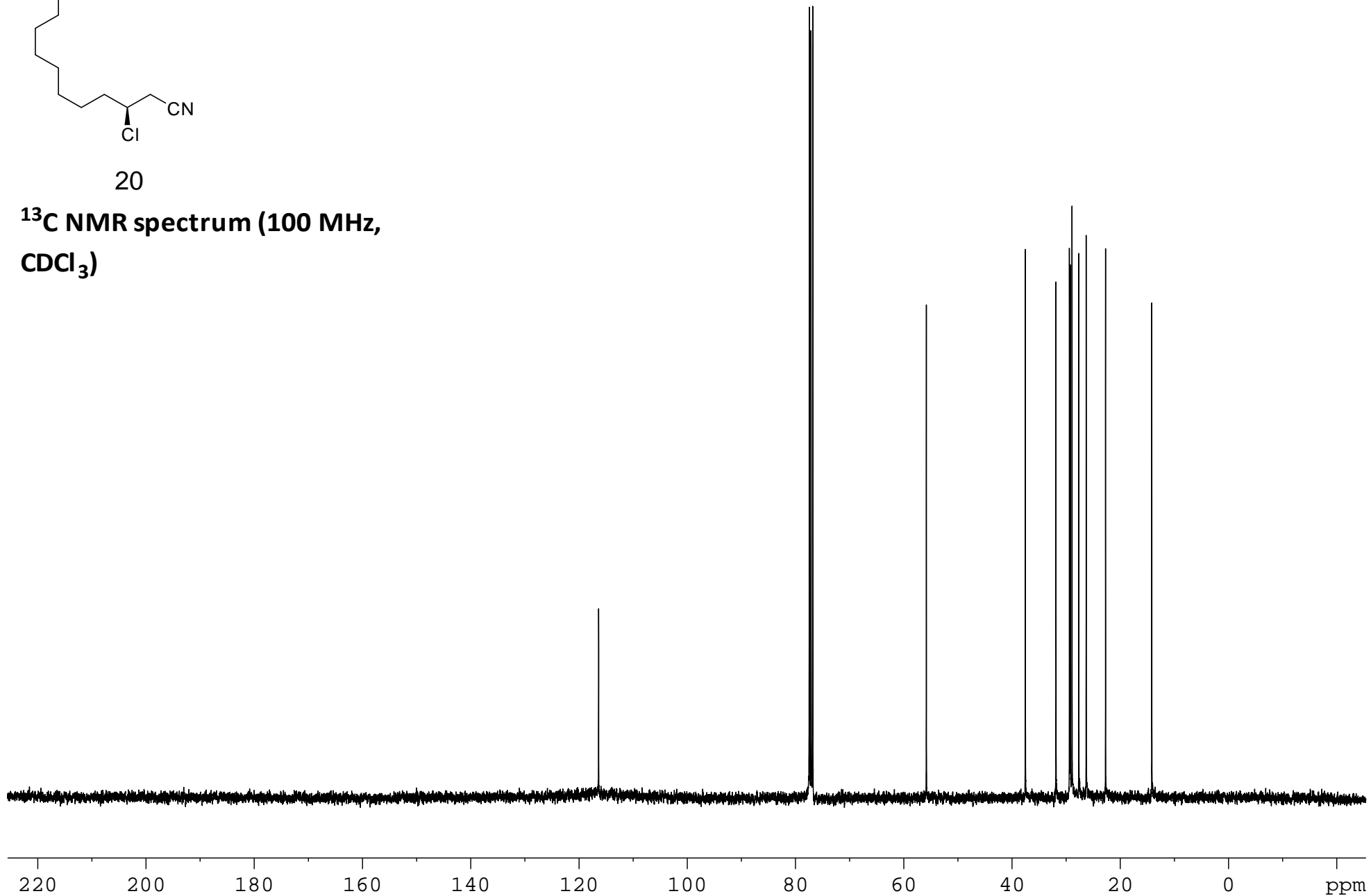
¹H NMR spectrum (400 MHz,
CDCl₃)

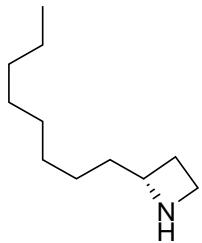




20

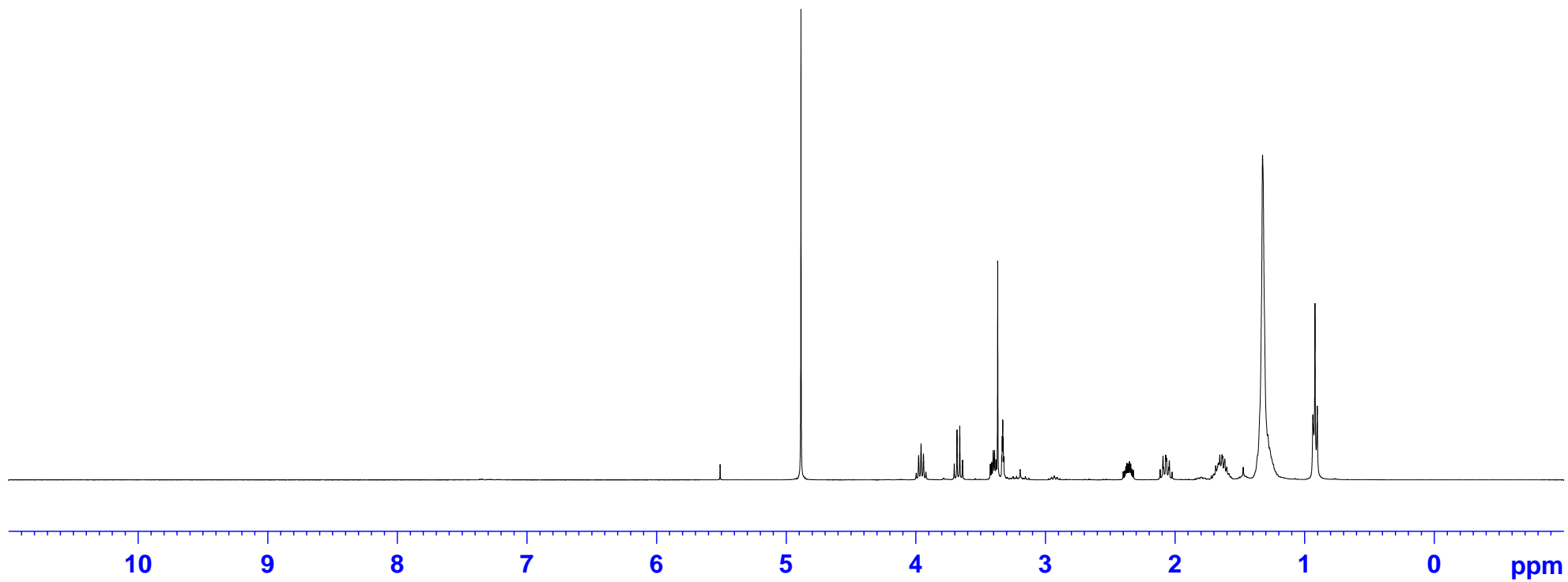
**^{13}C NMR spectrum (100 MHz,
 CDCl_3)**

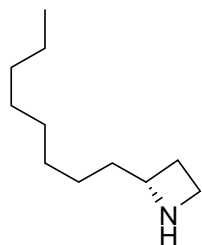




33

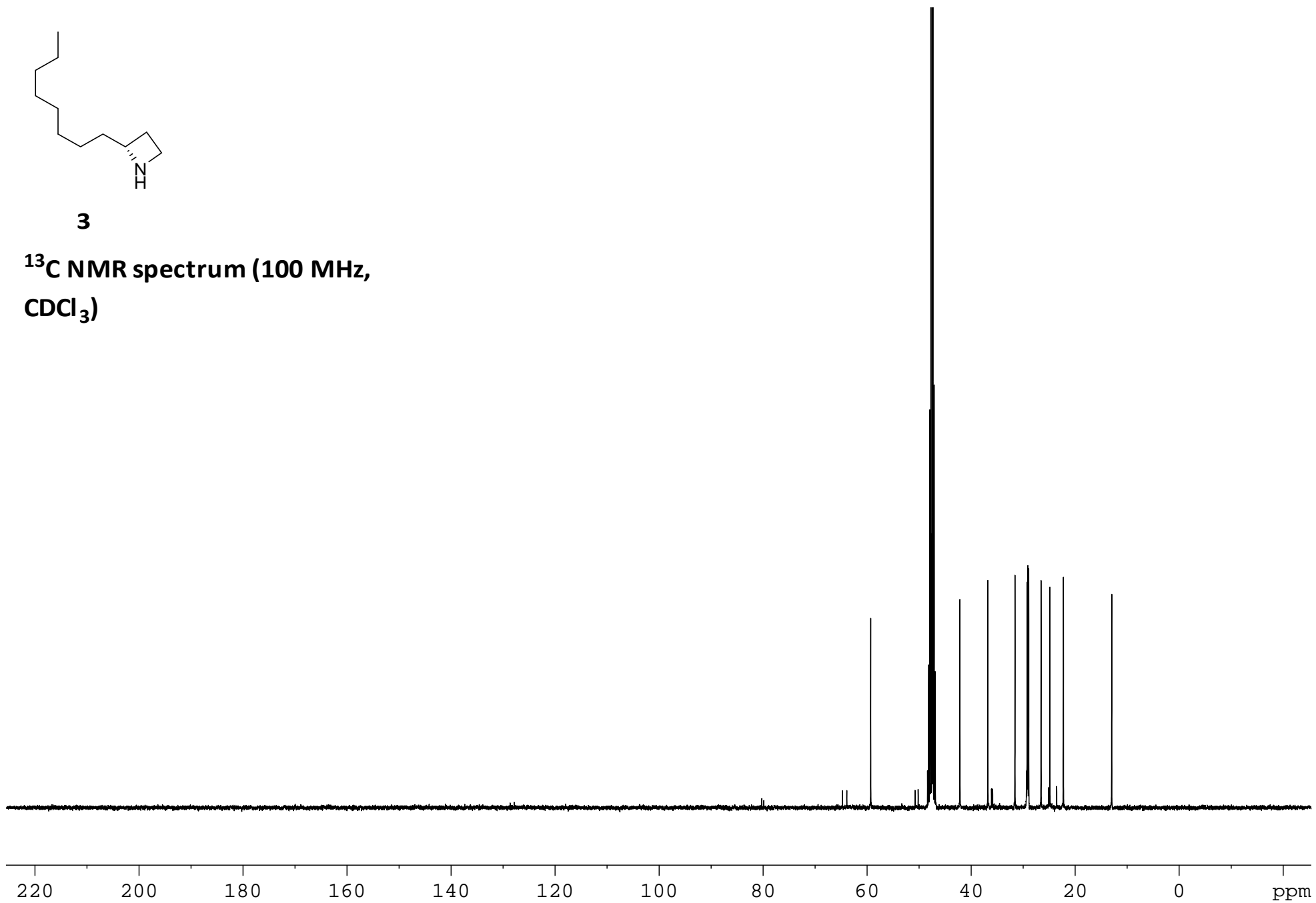
^1H NMR spectrum (400 MHz, U \)

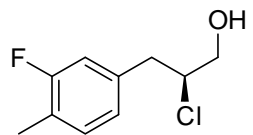




3

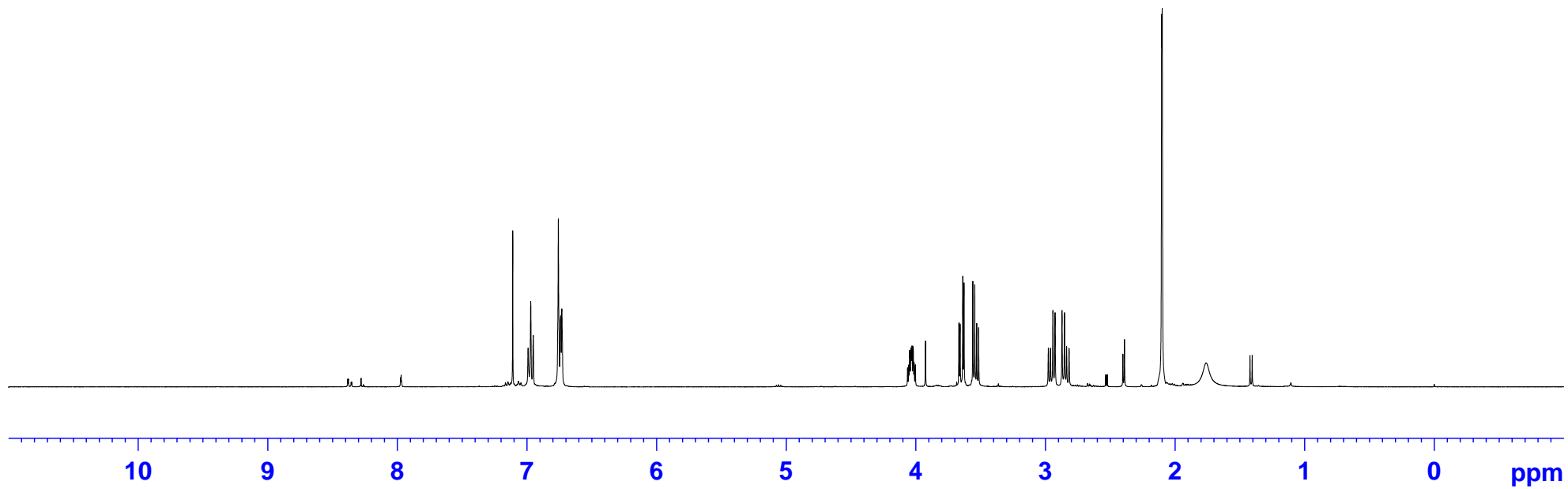
**^{13}C NMR spectrum (100 MHz,
 CDCl_3)**

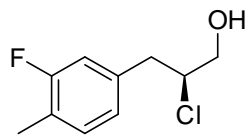




3

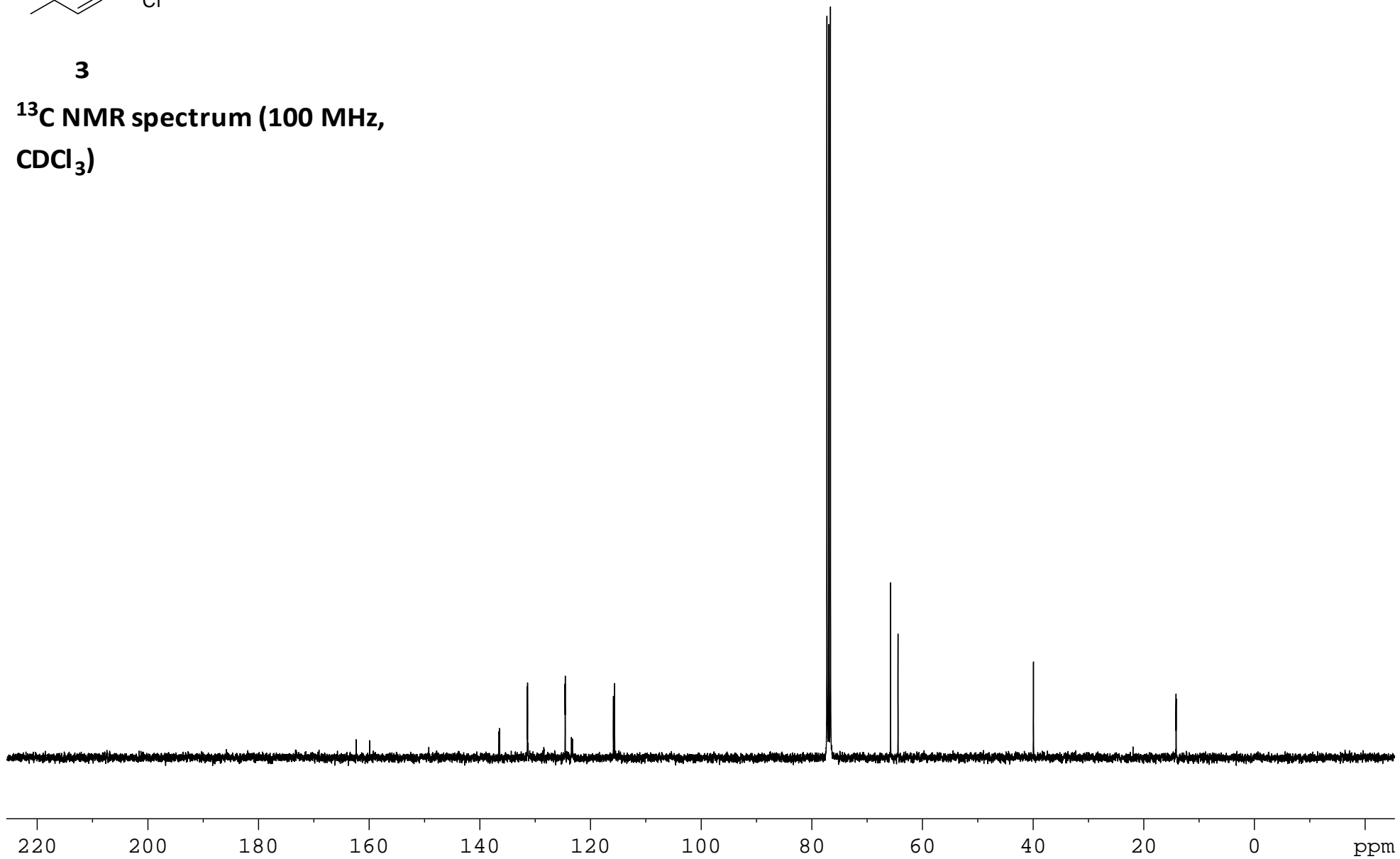
**¹H NMR spectrum (400 MHz,
CDCl₃)**

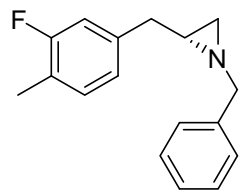




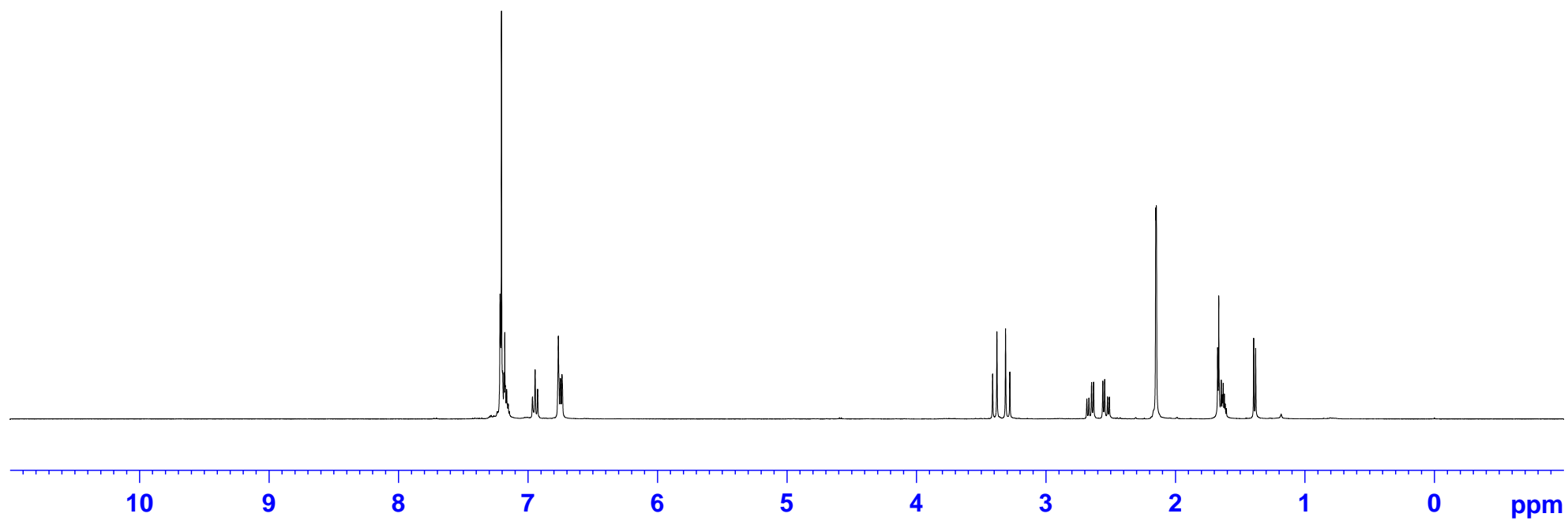
3

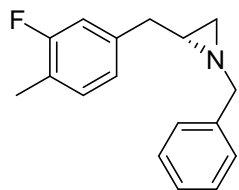
**^{13}C NMR spectrum (100 MHz,
 CDCl_3)**



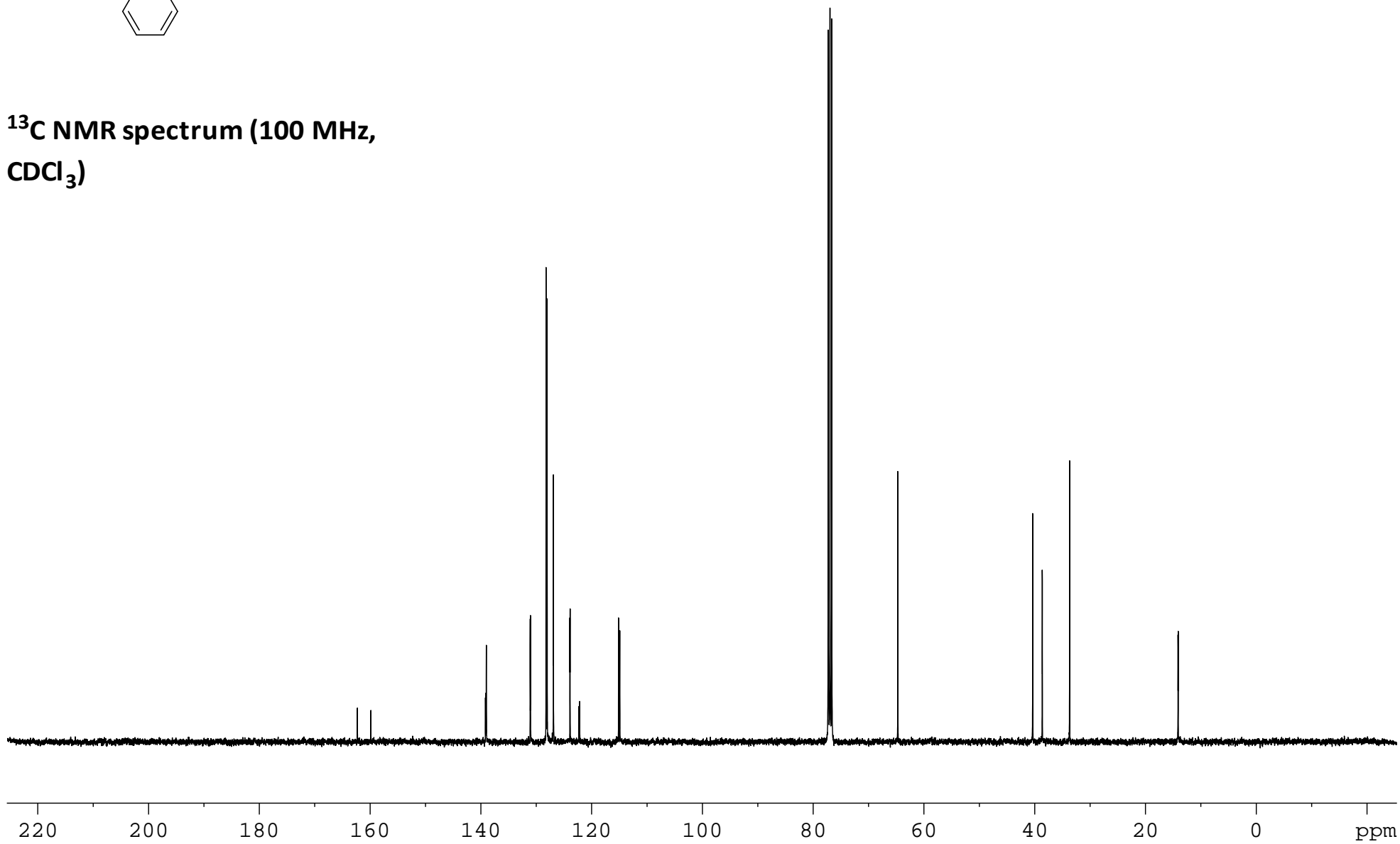


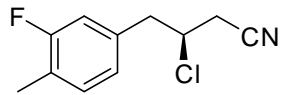
**^1H NMR spectrum (400 MHz,
 CDCl_3)**



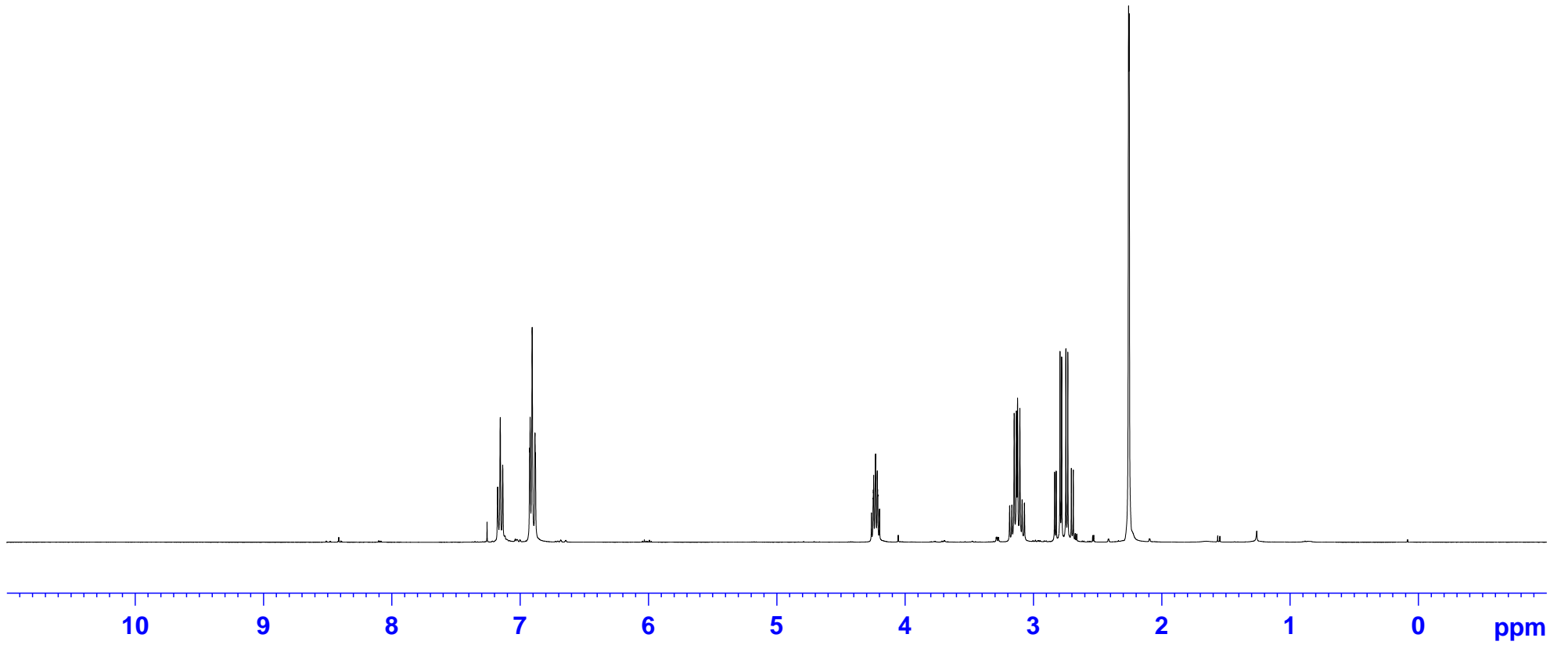


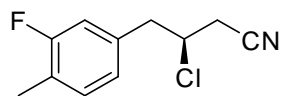
**^{13}C NMR spectrum (100 MHz,
 CDCl_3)**



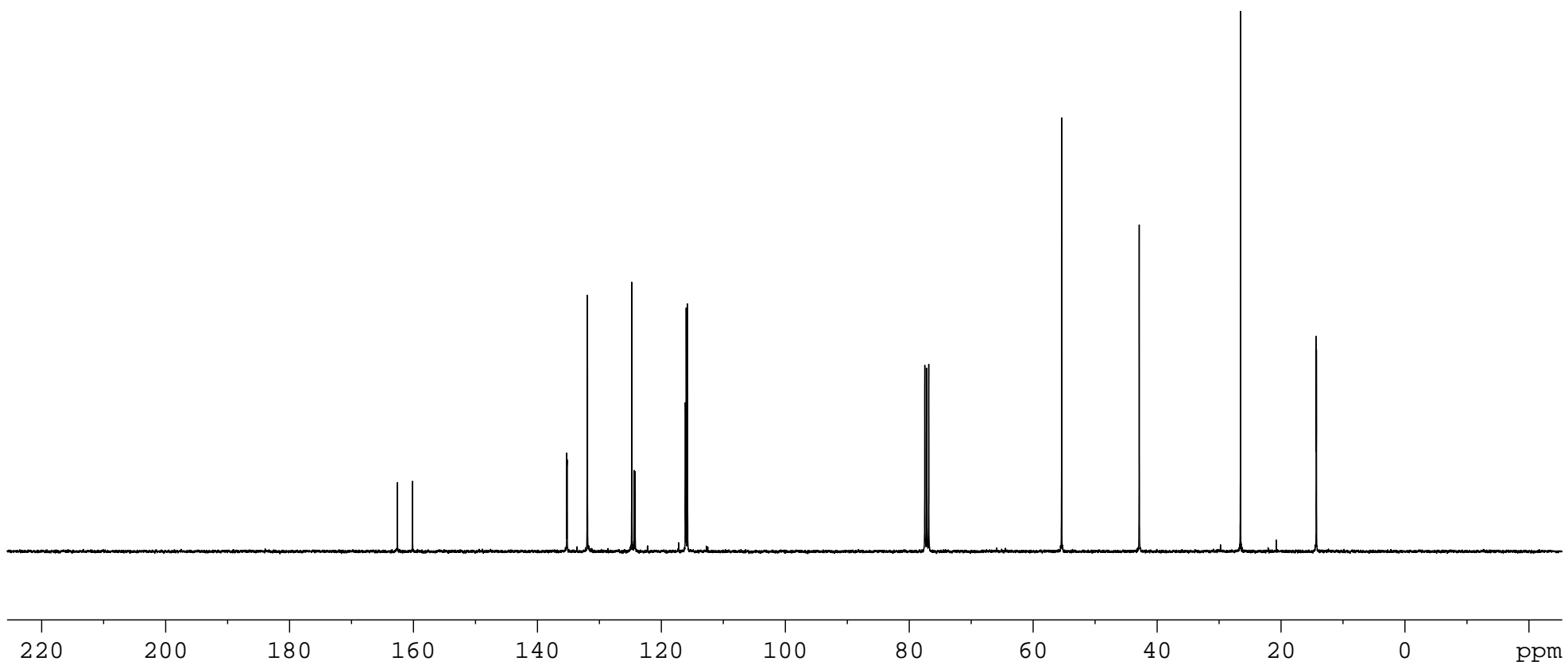


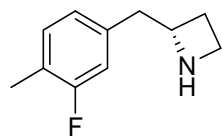
¹H NMR spectrum (400 MHz,
CDCl₃)





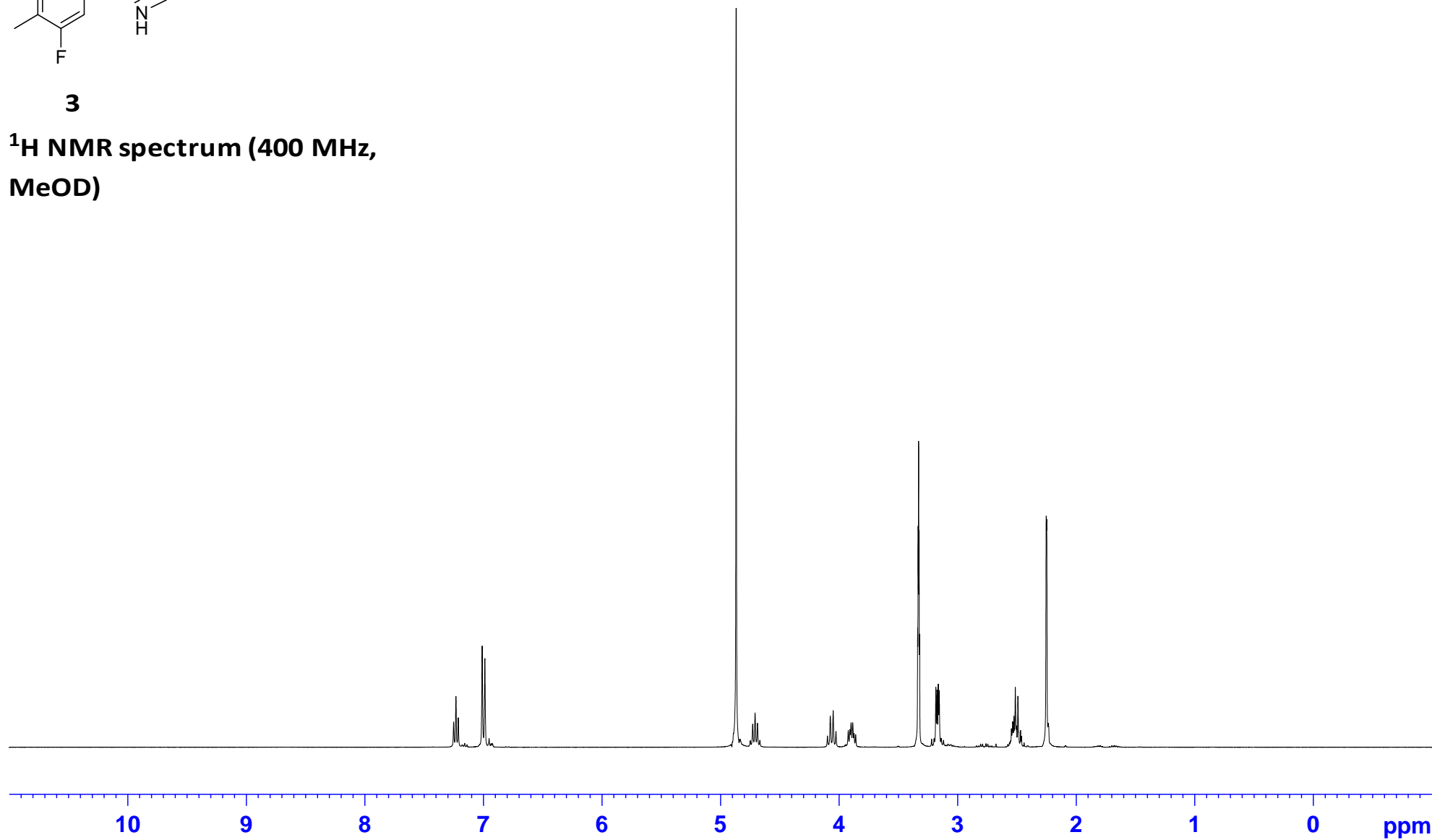
**¹³C NMR spectrum (100 MHz,
CDCl₃)**

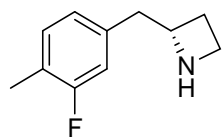




3

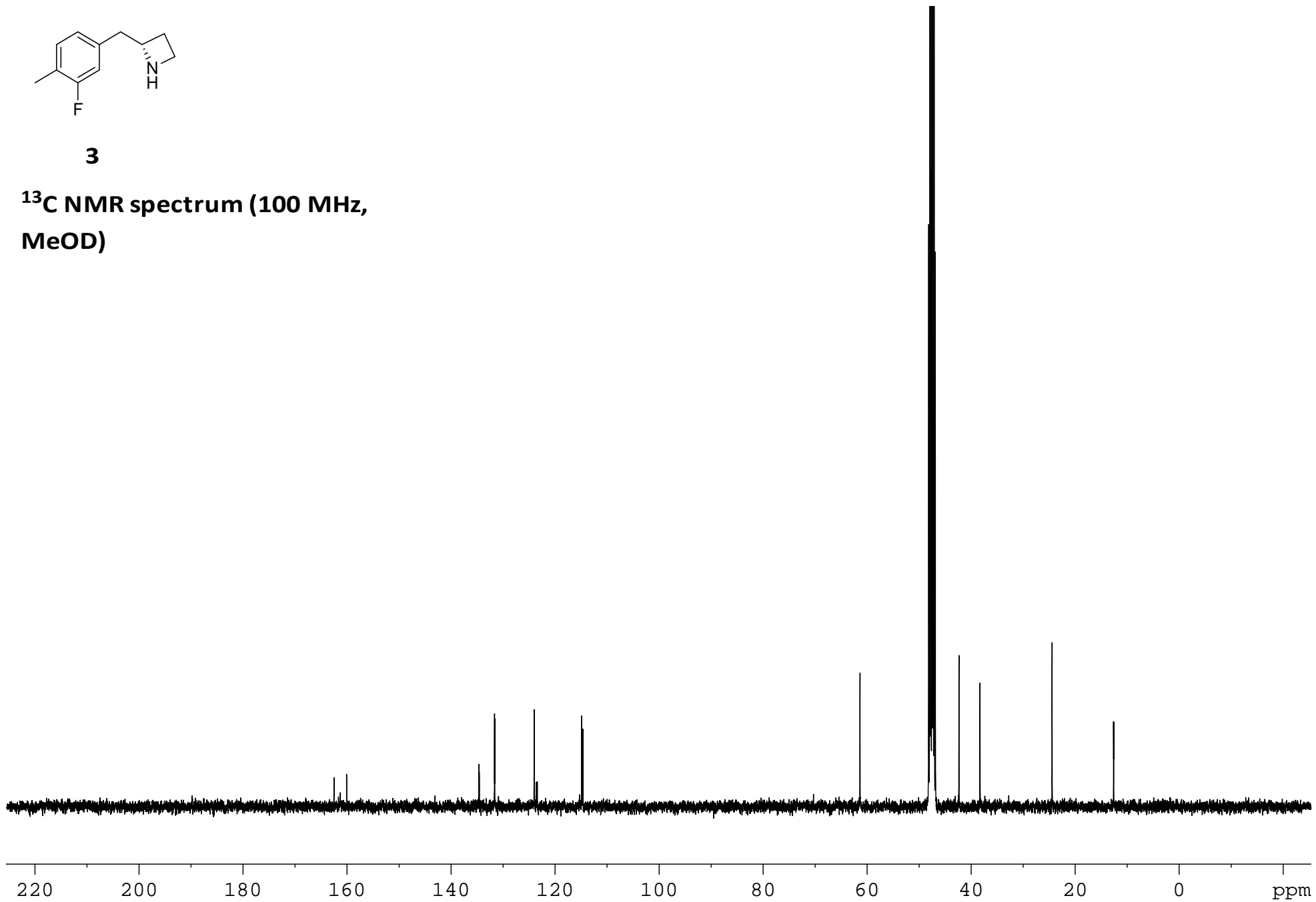
**¹H NMR spectrum (400 MHz,
MeOD)**

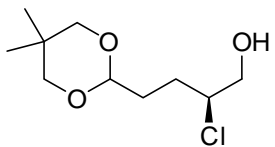




3

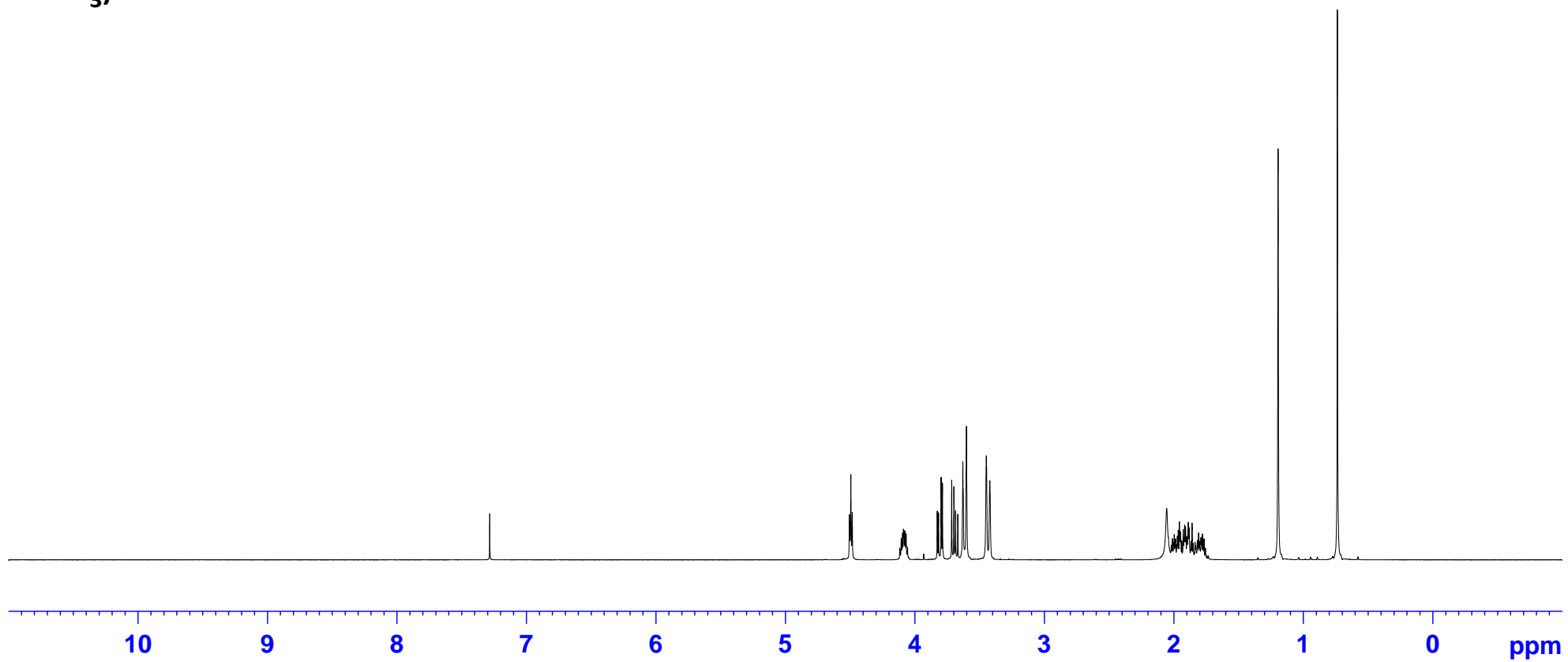
**¹³C NMR spectrum (100 MHz,
MeOD)**

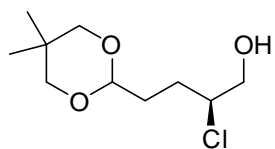




3

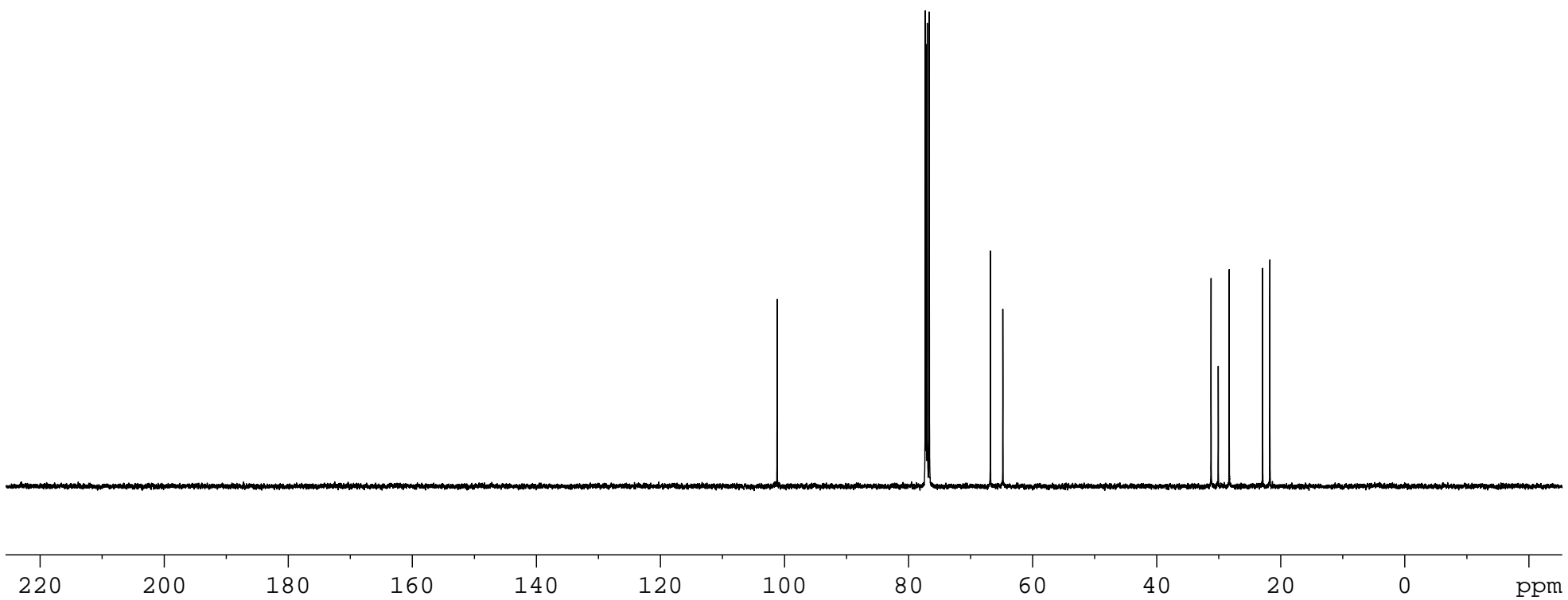
^1H NMR spectrum (400 MHz,
 CDCl_3)

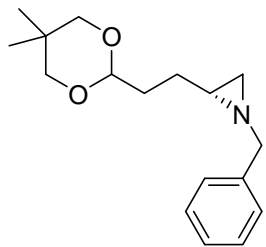




39

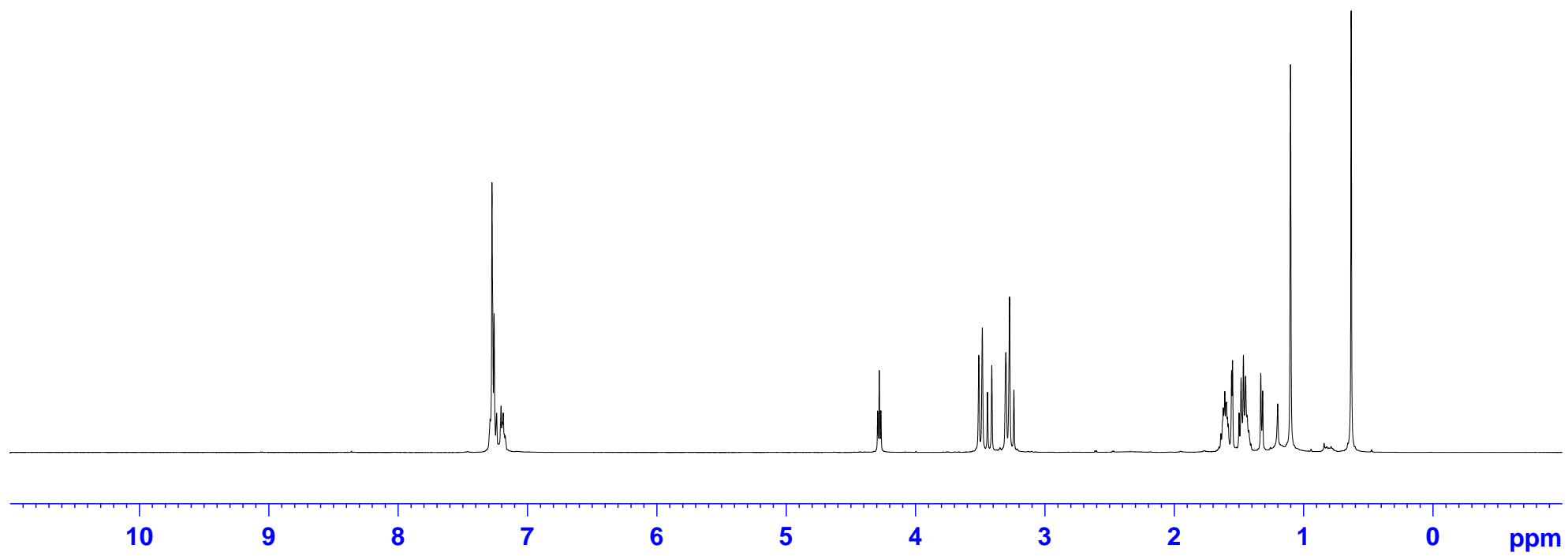
**¹³C NMR spectrum (100 MHz,
CDCl₃)**

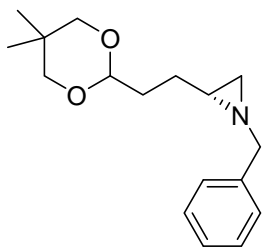




13

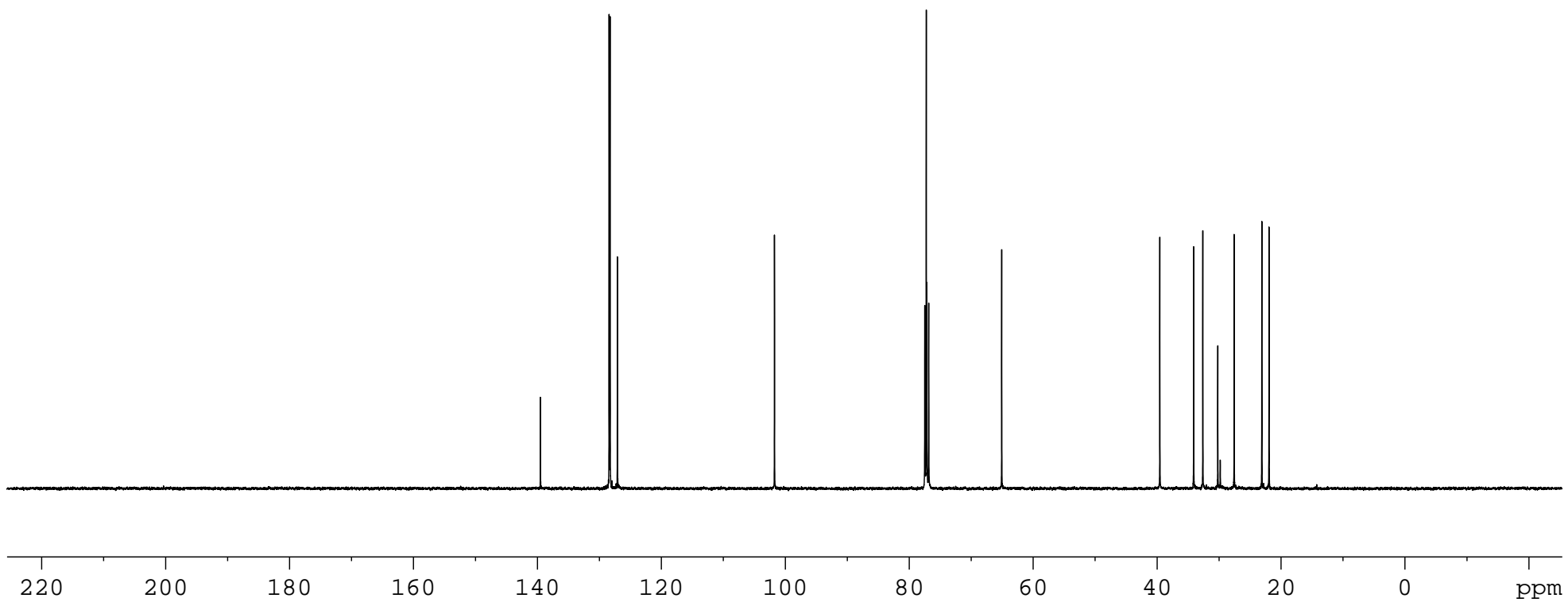
^1H NMR spectrum (400 MHz, CDCl_3)

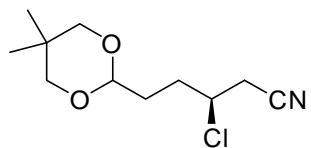




13

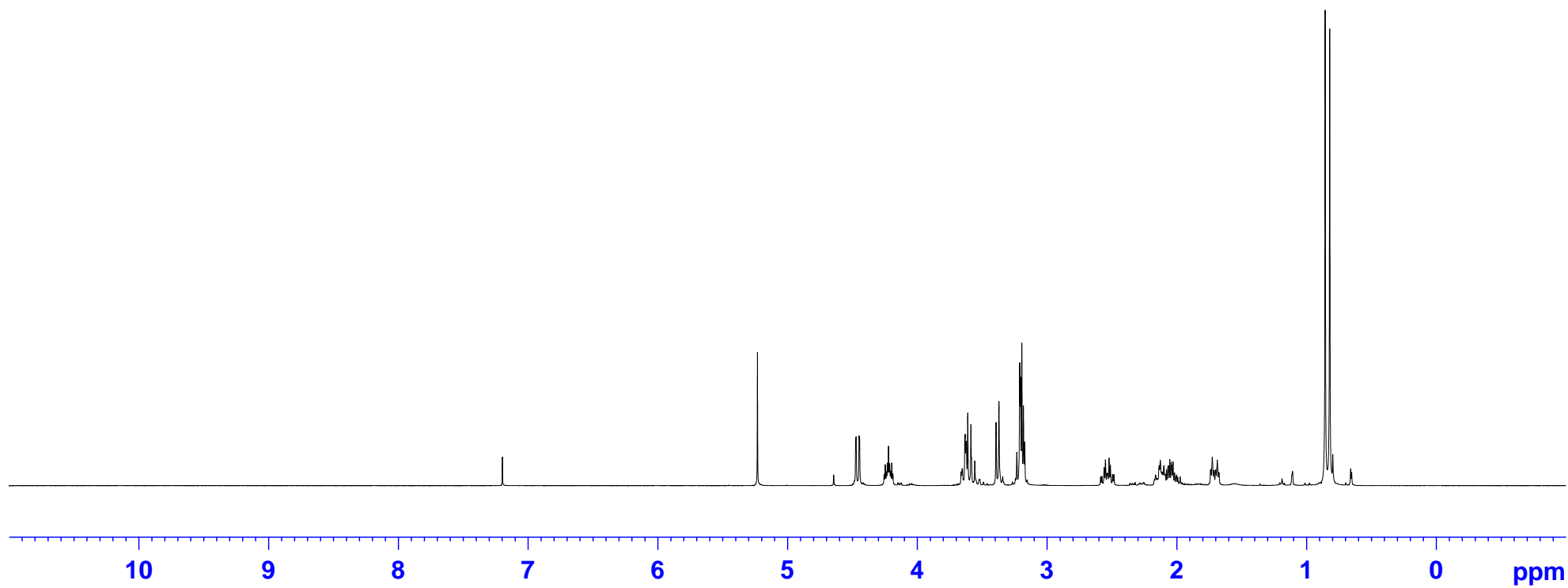
**^{13}C NMR spectrum (100 MHz,
 CDCl_3)**

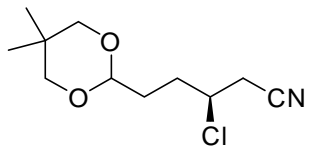




1

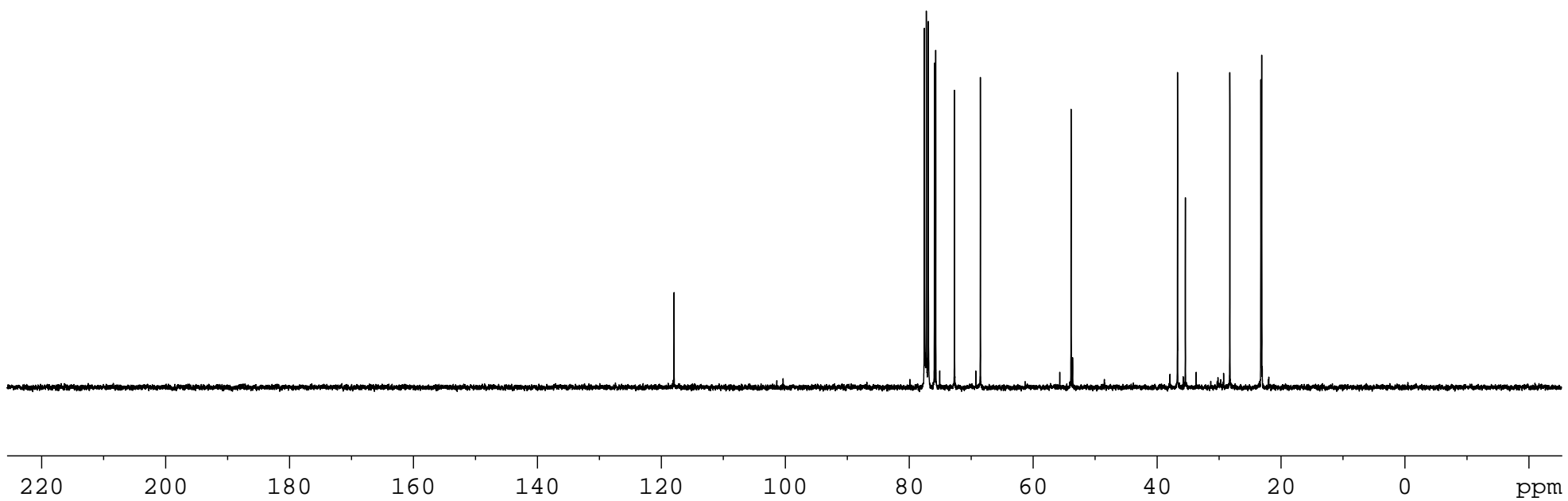
**^1H NMR spectrum (400 MHz,
 CDCl_3)**

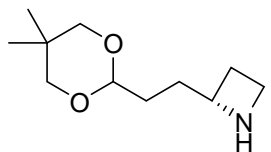




19

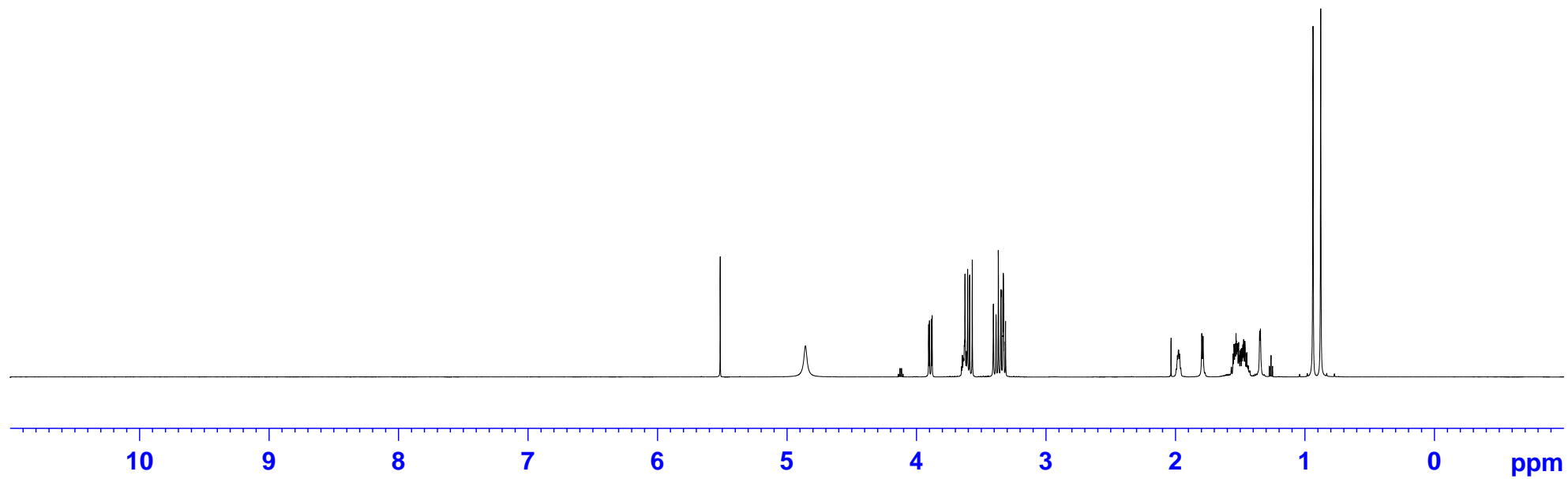
**^{13}C NMR spectrum (100 MHz,
 CDCl_3)**

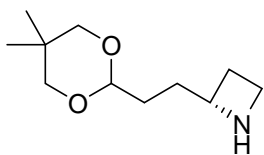




32

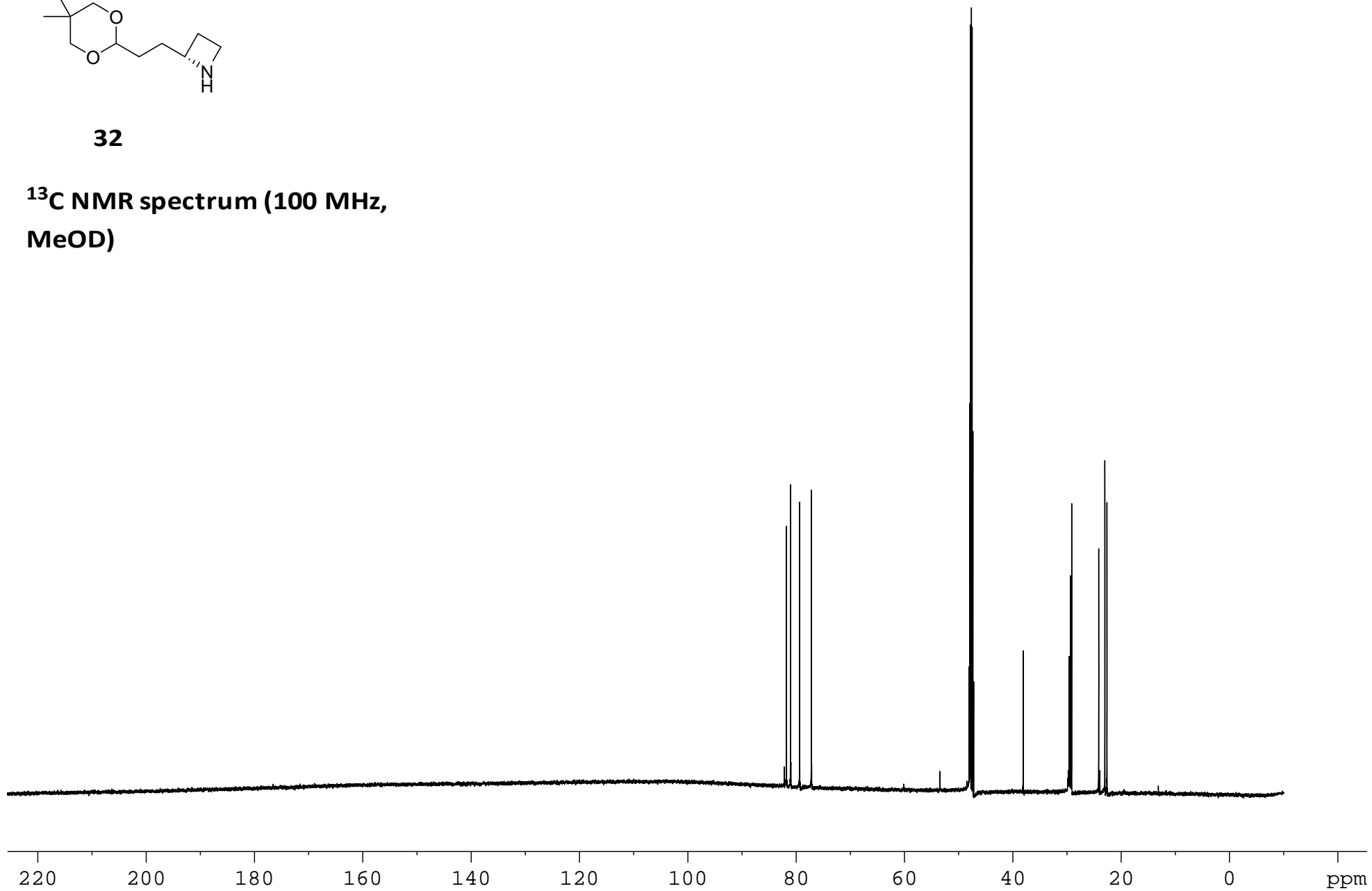
¹H NMR spectrum (400 MHz,
MeOD)

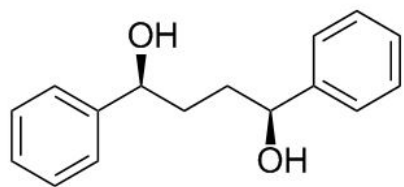




32

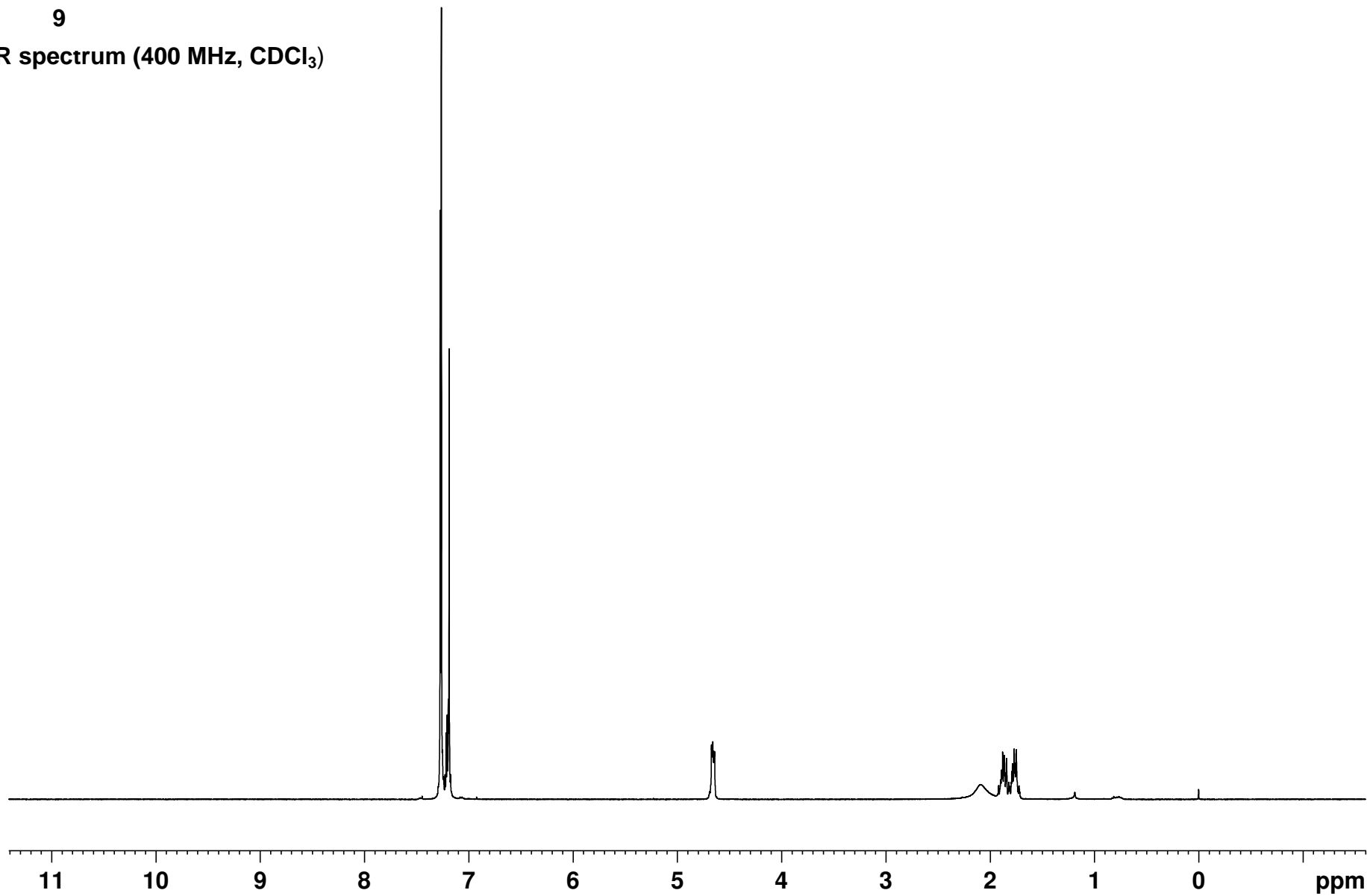
**^{13}C NMR spectrum (100 MHz,
MeOD)**

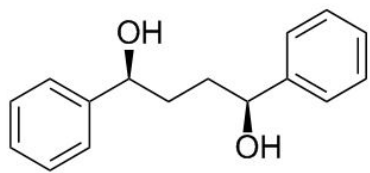




9

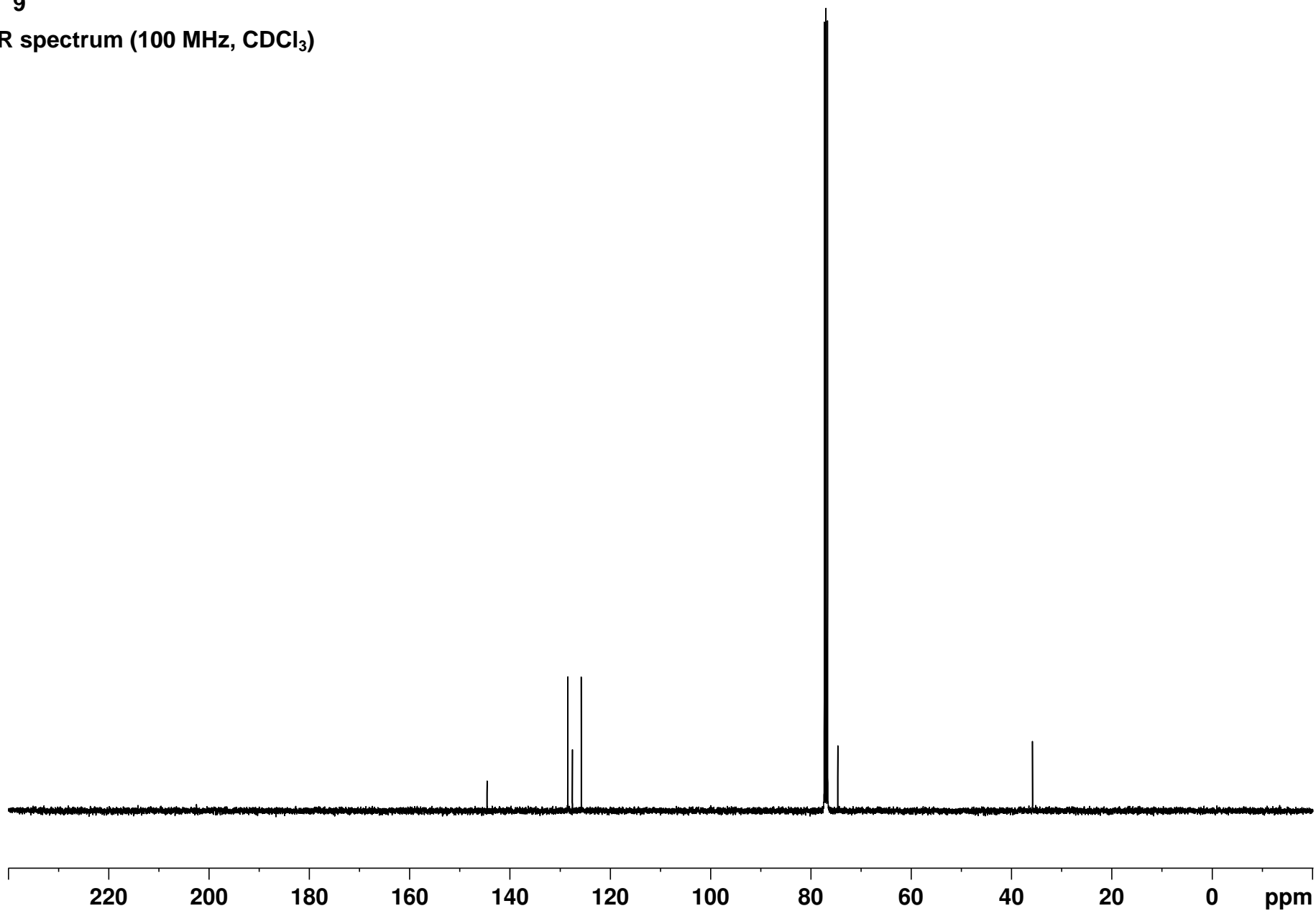
^1H NMR spectrum (400 MHz, CDCl_3)

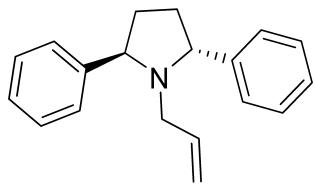




9

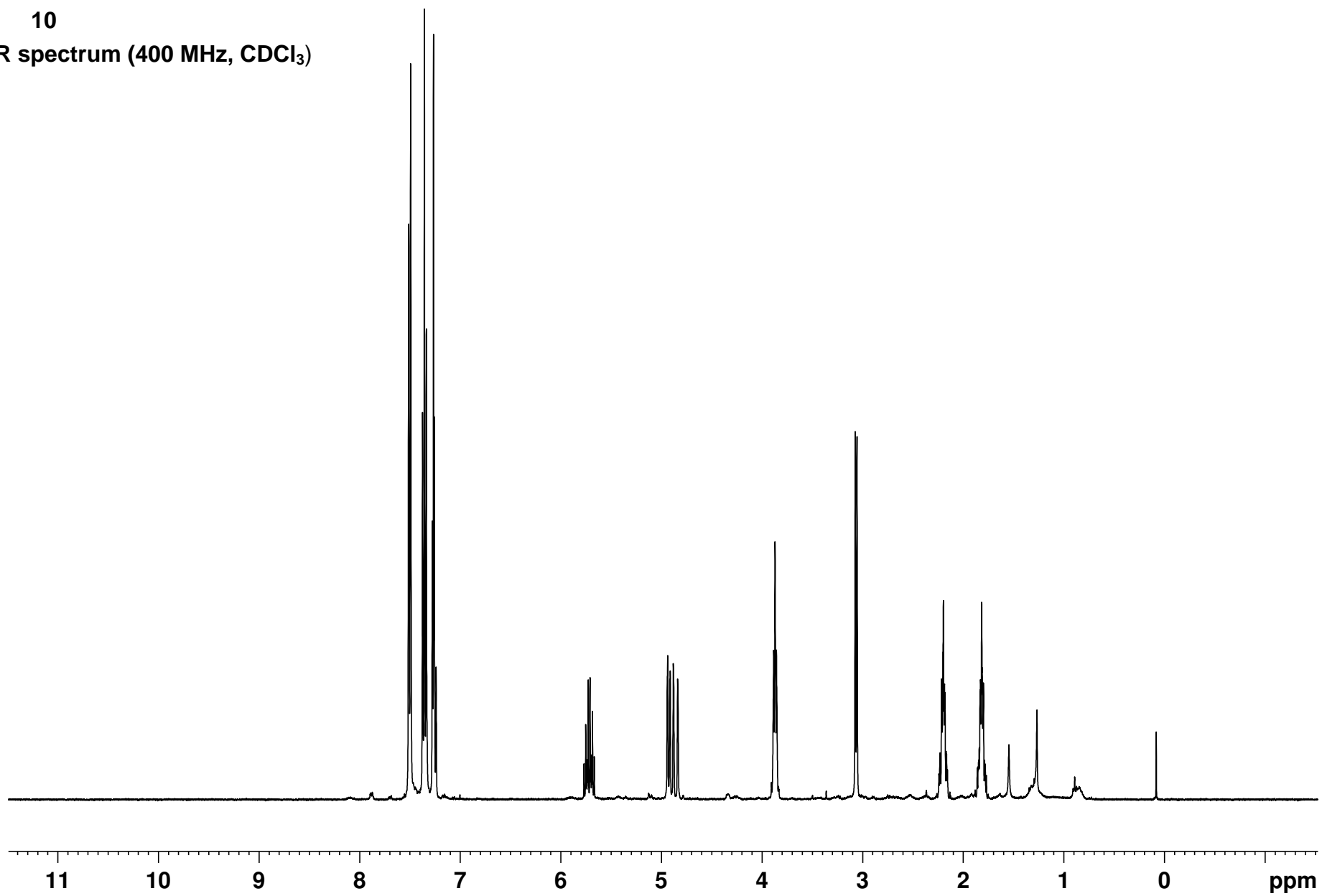
^{13}C NMR spectrum (100 MHz, CDCl_3)

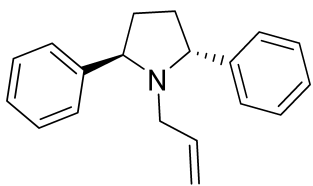




10

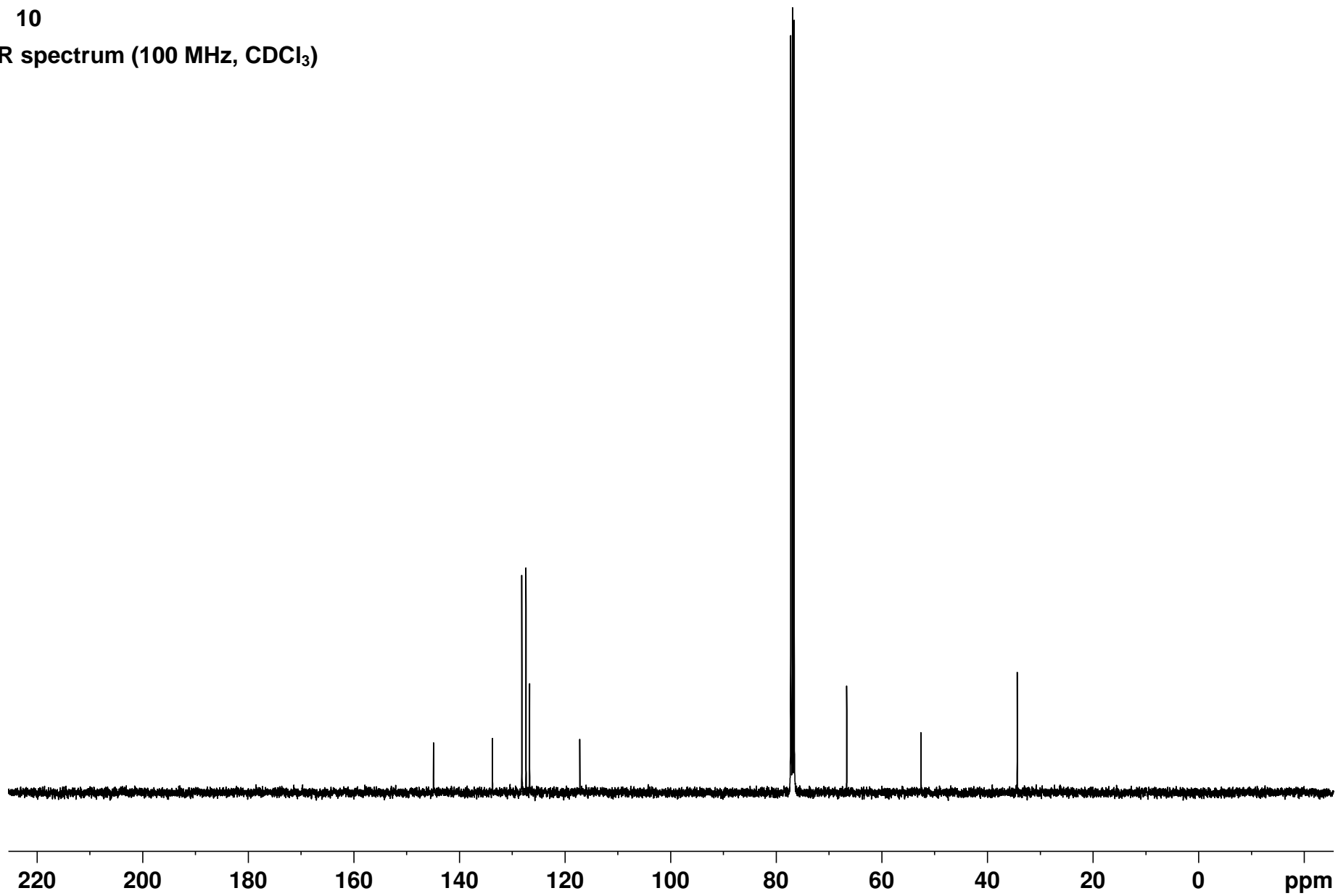
¹H NMR spectrum (400 MHz, CDCl₃)

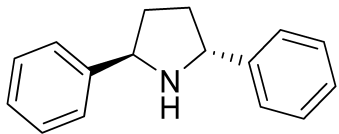




10

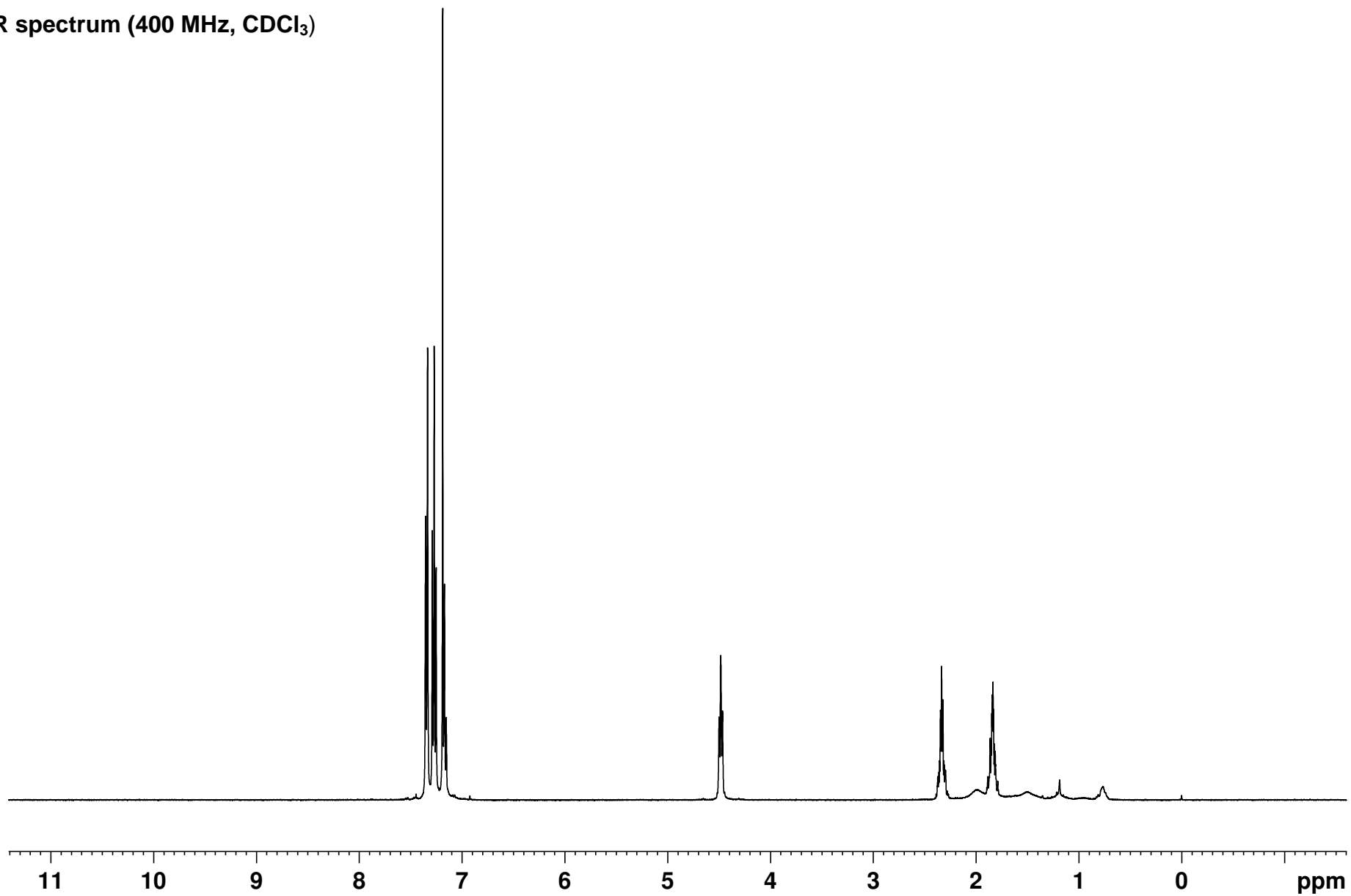
^{13}C NMR spectrum (100 MHz, CDCl_3)

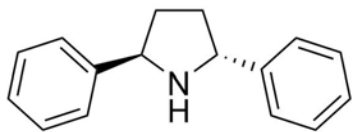




2

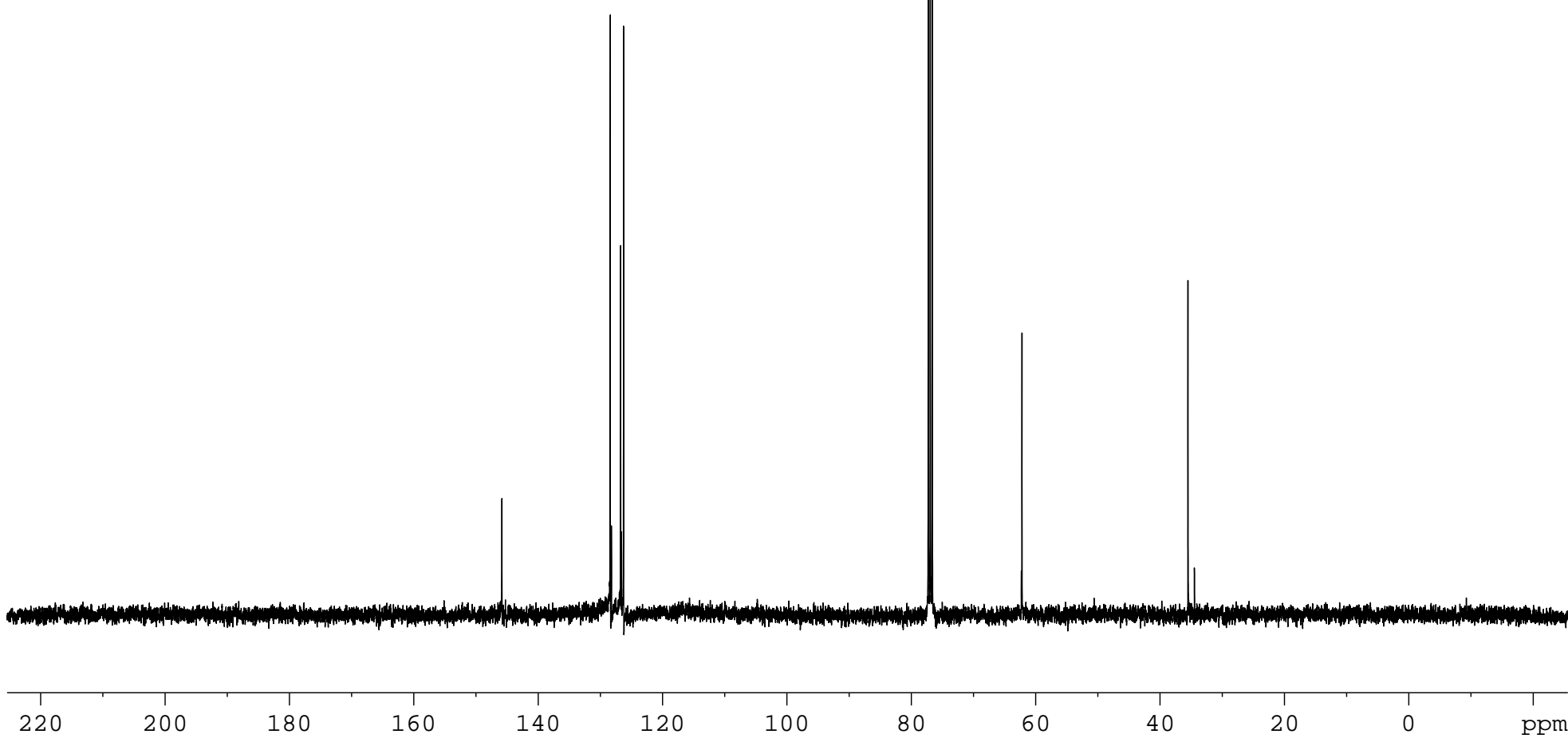
^1H NMR spectrum (400 MHz, CDCl_3)





2

^{13}C NMR spectrum (100 MHz, CDCl_3)

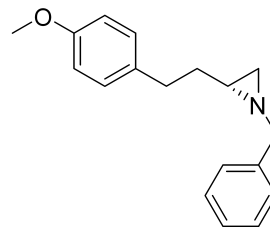


Sample Name: TJS-5-147
User:

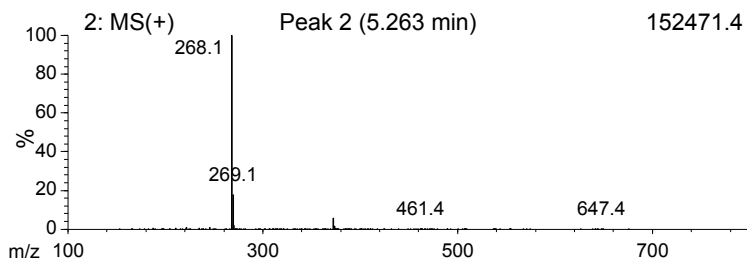
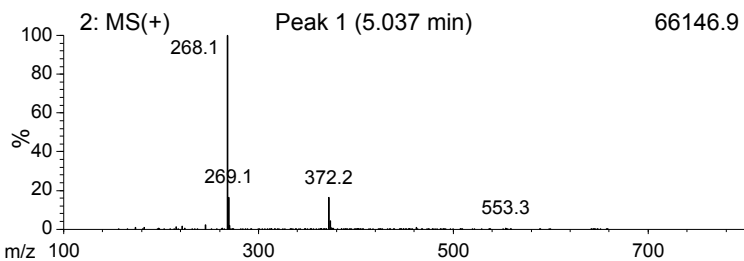
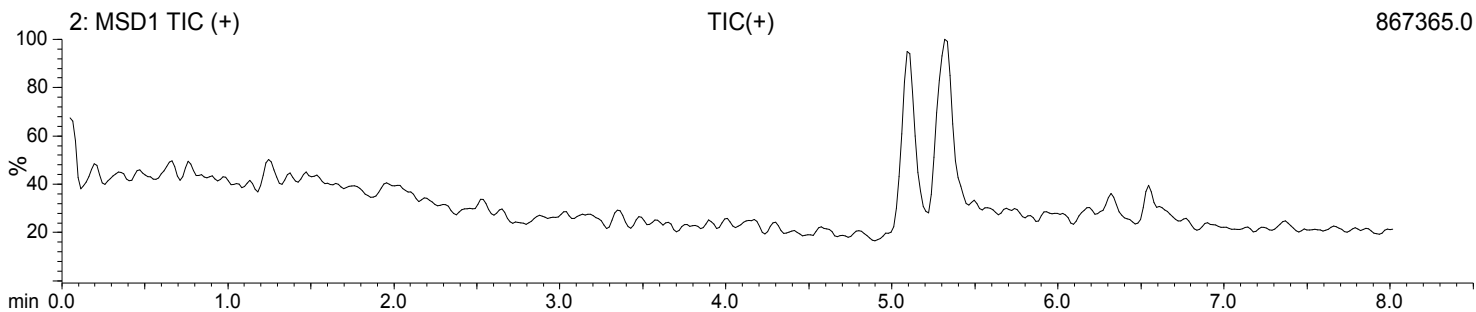
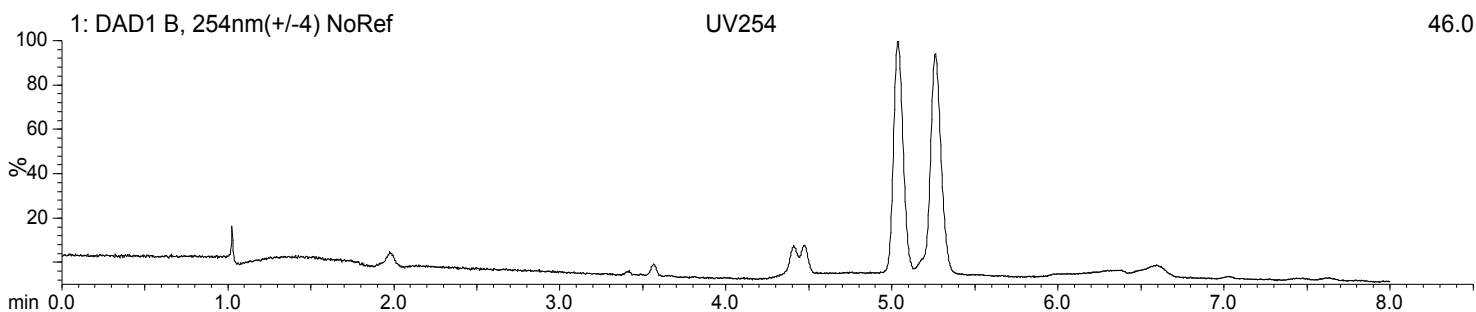
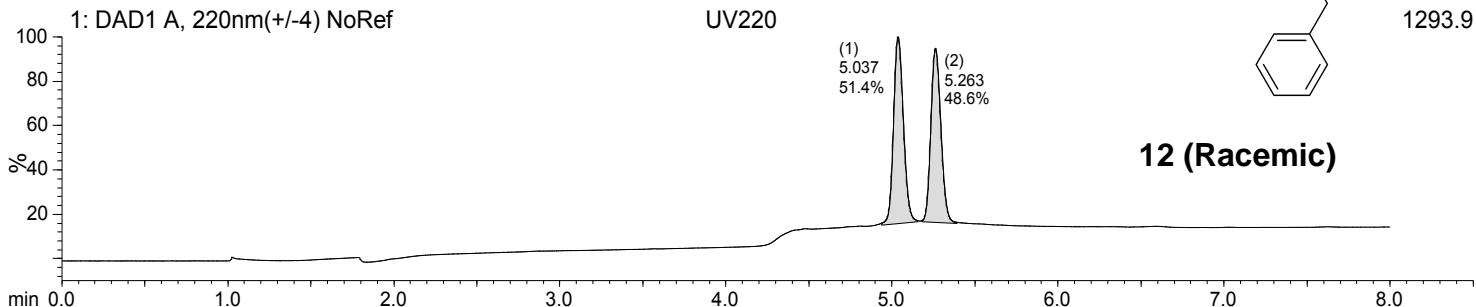
Acquired: 4/1/2014 8:26 AM
Filename:
C:\CHEM32\1\DATA\SINGLE 2014-04-01 08-24-46\2BB-0101.D

Method LUX CELLULOSE-2 2-20 IPA Description:
DEA.M
Location: 1,2:B,2

Peak #	Time	Area % UV220	Area % UV254	Area % TIC(+)	BPM
1	5.037	51.4	0.0	0.0	268.1
2	5.263	48.6	0.0	0.0	268.1



12 (Racemic)



VCNDD MRB4-12475 Agilent SFCMS

Sample Name: TJS-5-66
User:

Acquired: 2/12/2013 9:56 AM

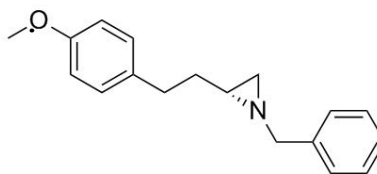
Method: LUX_CELLULOSE-

Filename:

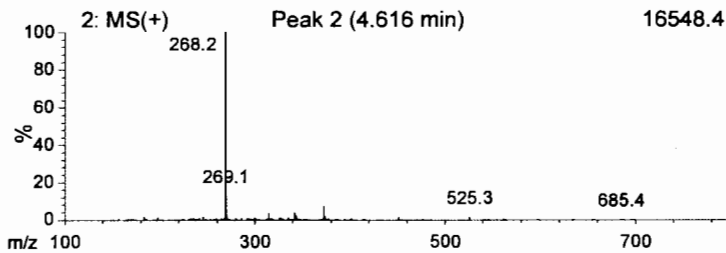
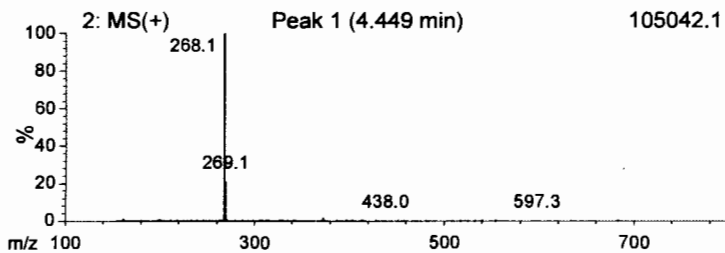
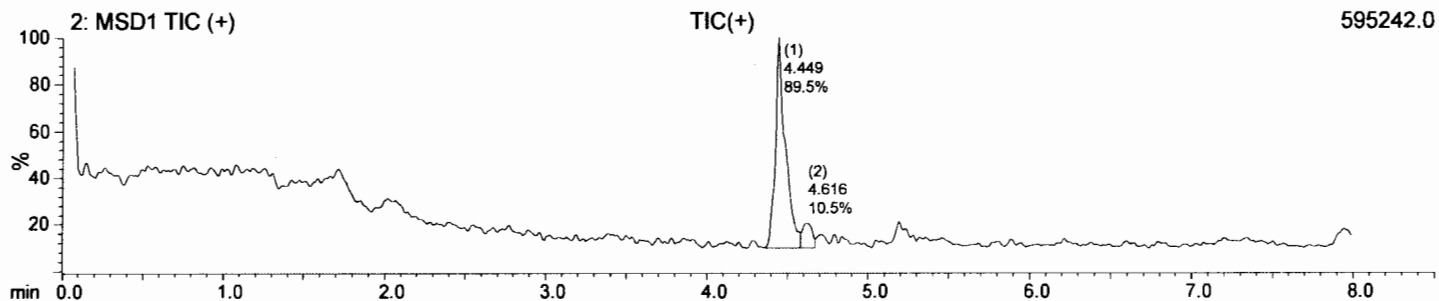
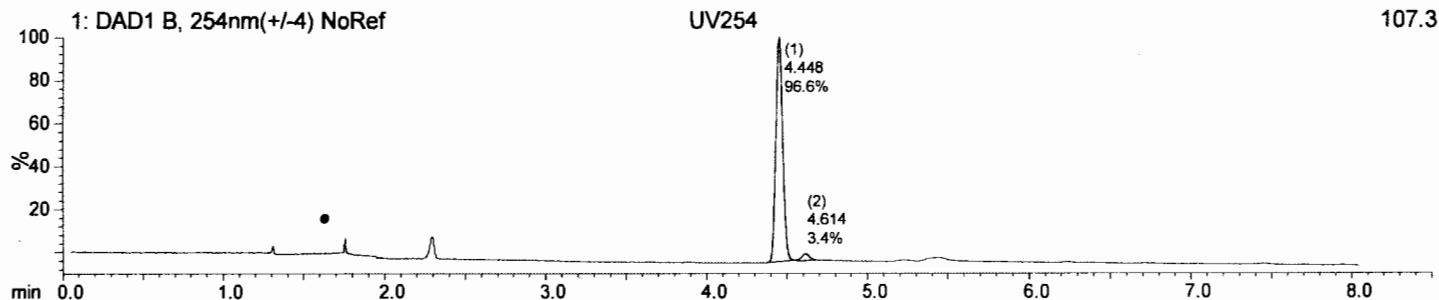
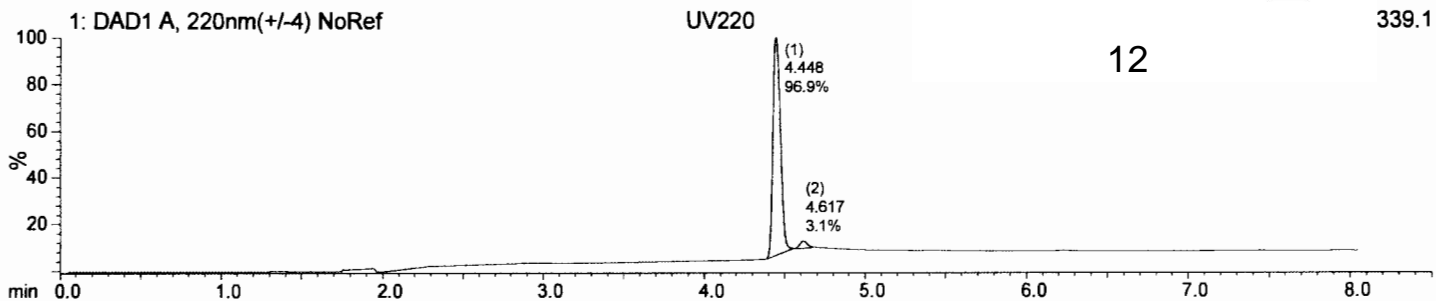
2_OZ_1_30_IPA.M

C:\CHEM32\1\DATA\SINGLE 2013-02-12 09-43-58\1AD-0201.D

Location: 1,1:A,4



Peak #	Time	Area % UV220	Area % UV254	Area % TIC(+)	BPM
1	4.448	96.9	96.6	89.5	268.1
2	4.616	3.1	3.4	10.5	268.2



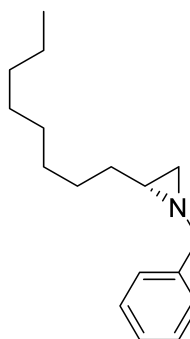
Sample Name: TJS-5-146
User:

Acquired: 4/1/2014 10:32 AM
Filename:
C:\CHEM32\1\DATA\SINGLE 2014-04-01 10-30-26\2BA-0101.D

Method IA 2-20 MEOH DEA.M
Location: 1,2:B,1

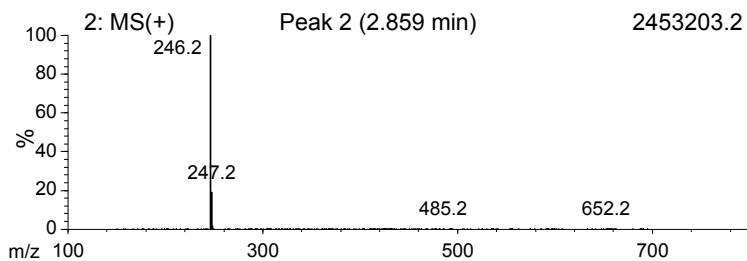
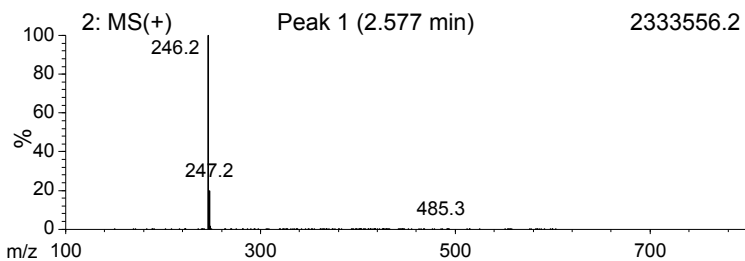
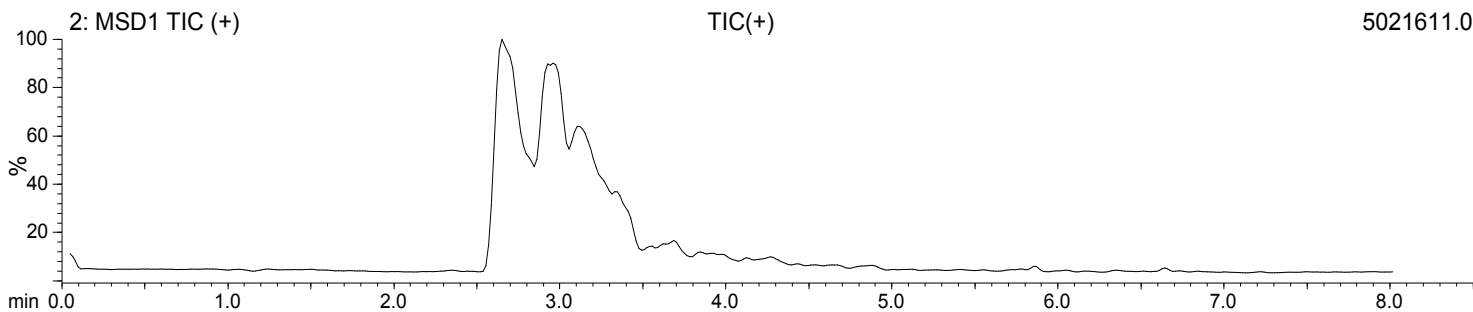
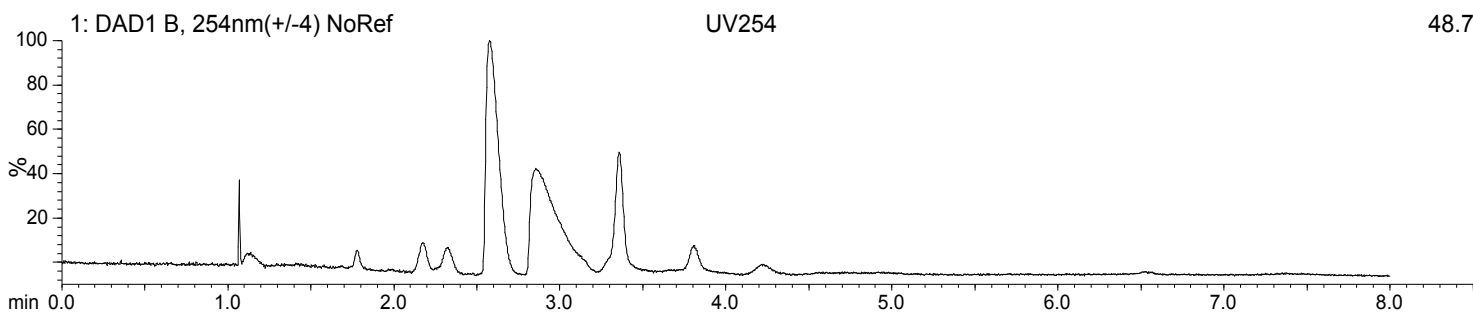
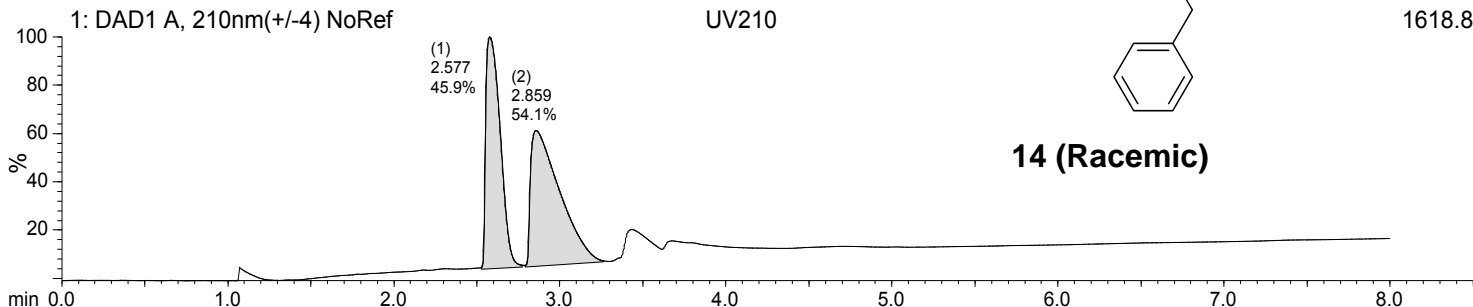
Description:

Peak #	Time	Area % UV210	Area % UV254	Area % TIC(+)	BPM
1	2.577	45.9	0.0	0.0	246.2
2	2.859	54.1	0.0	0.0	246.2



14 (Racemic)

1618.8



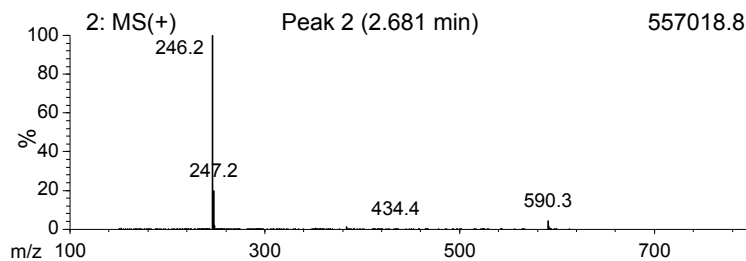
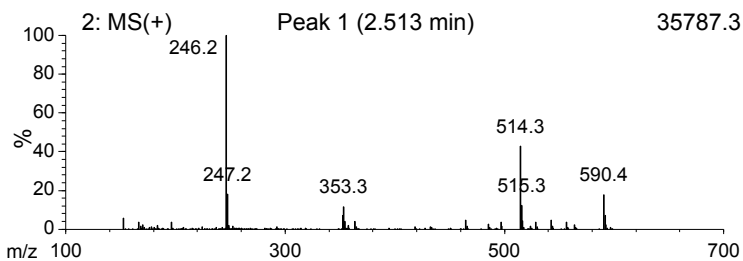
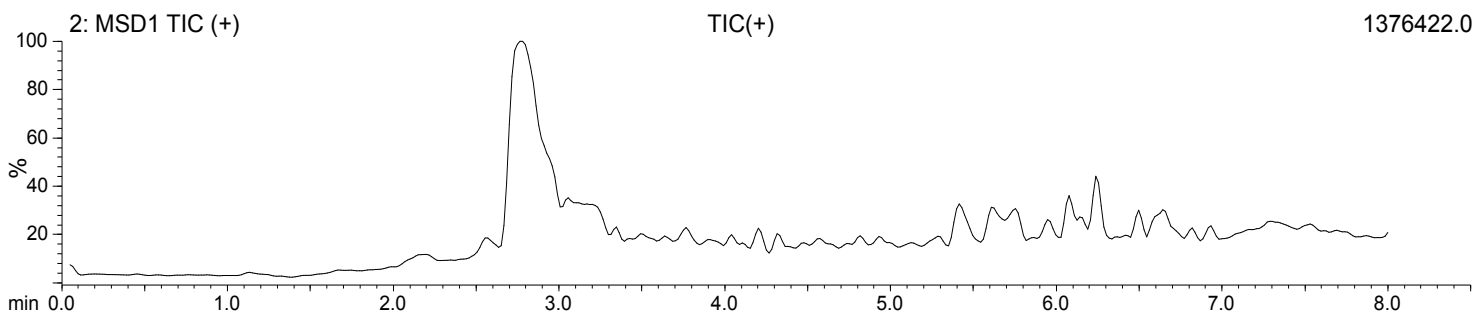
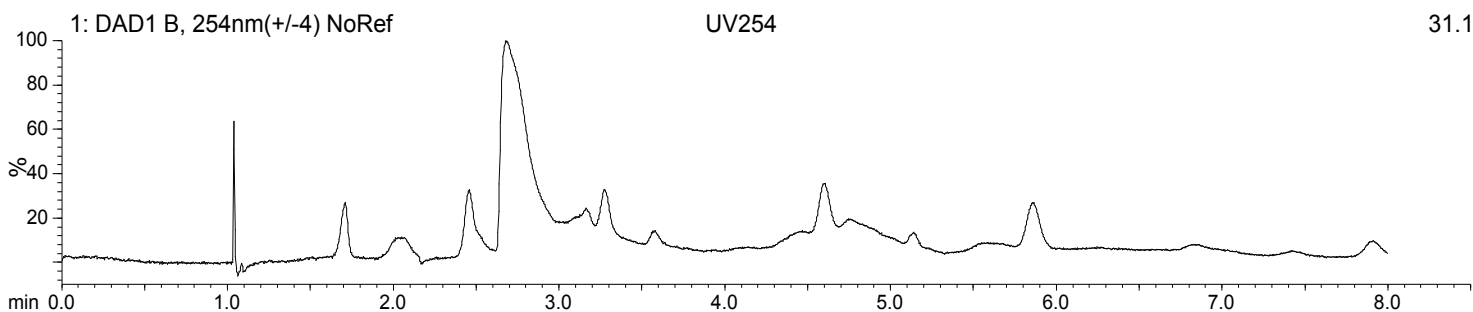
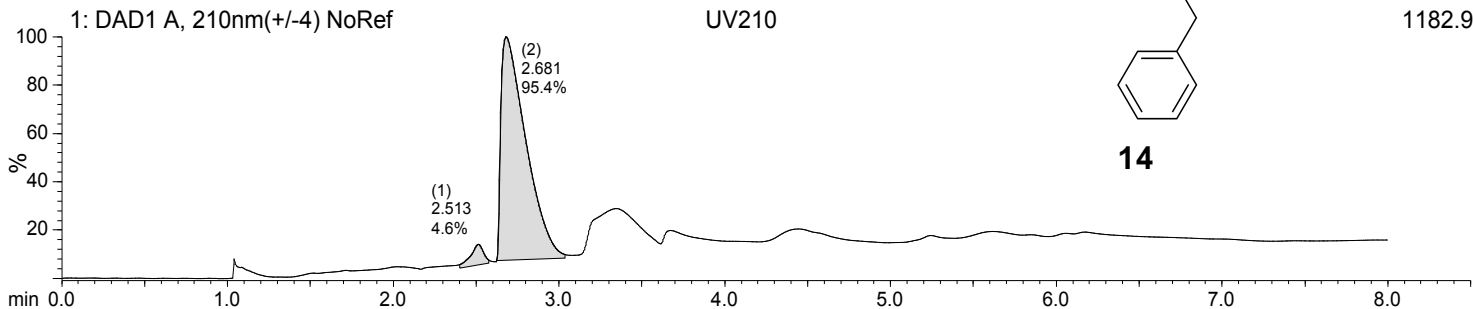
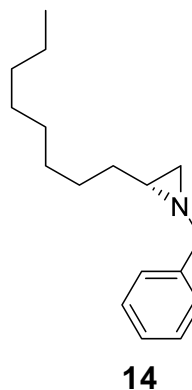
Sample Name: TJS-5-163
User:

Acquired: 11/17/2014 3:24 PM
Filename:
C:\CHEM32\1\DATA\SINGLE 2014-11-
17 15-22-49\2FB-0101.D

Method IA 2-20 MEOH DEA.M
Location: 1,2:F,2

Description:

Peak #	Time	Area % UV210	Area % UV254	Area % TIC(+)	BPM
1	2.513	4.6	0.0	0.0	246.2
2	2.681	95.4	0.0	0.0	246.2

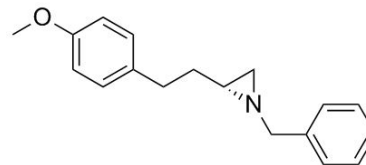


Sample Name: TJS-5-160 racemic
User:

Acquired: 12/16/2014 10:07 AM
Filename:
C:\CHEM32\1\DATA\SINGLE 2014-12-16 09-55-14\1AF-0201.D

Method IC 2-20 IPA DEA.M
Location: 1,1:A,6

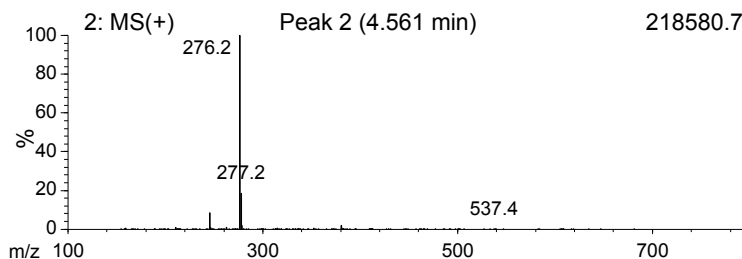
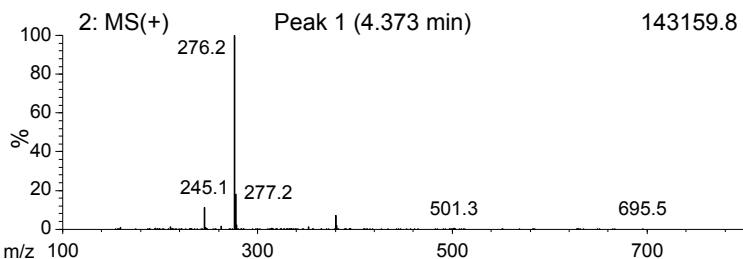
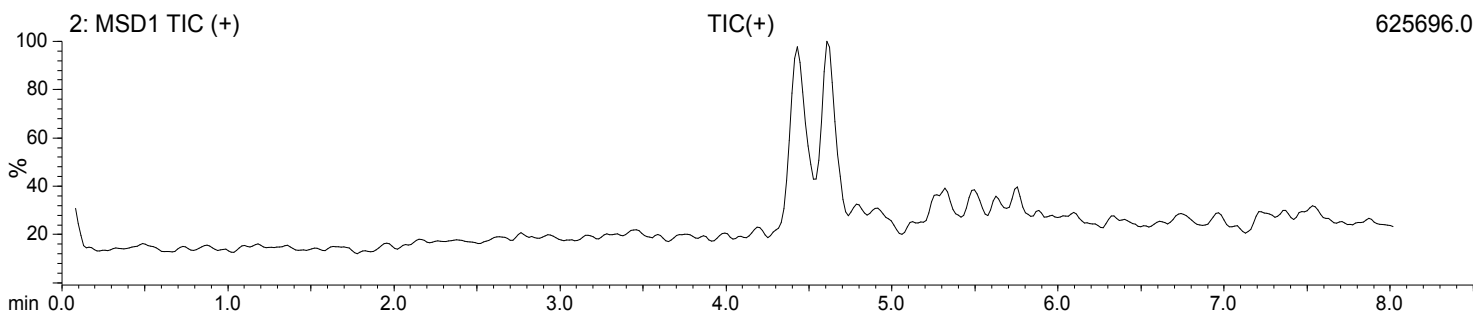
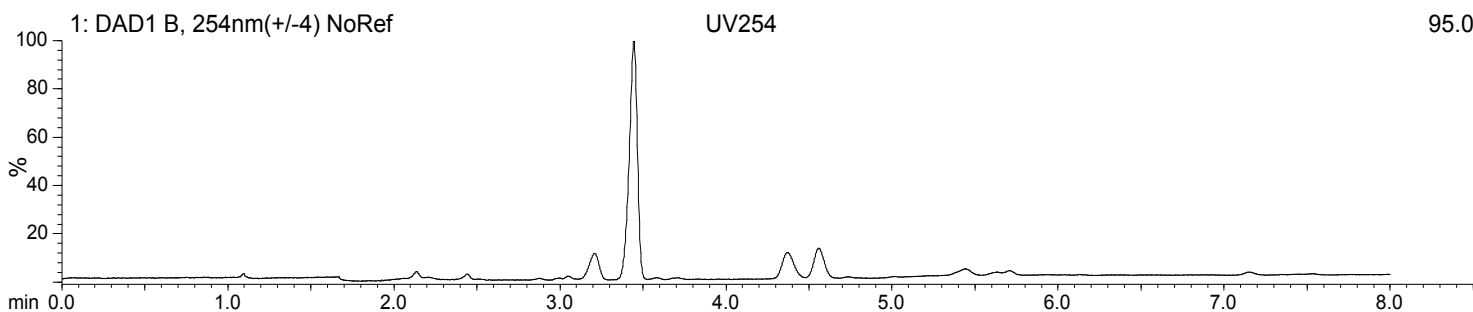
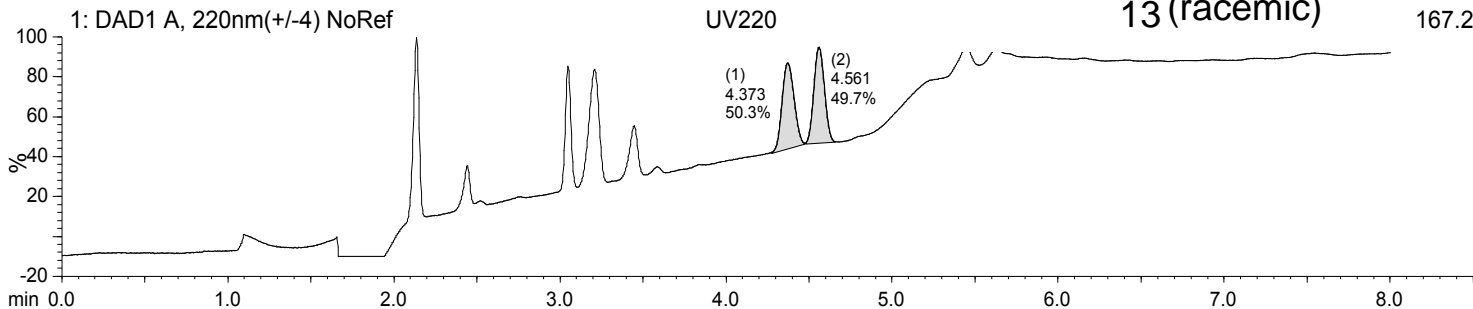
Description:



Peak #	Time	Area % UV220	Area % UV254	Area % TIC(+)	BPM
1	4.373	50.3	0.0	0.0	276.2
2	4.561	49.7	0.0	0.0	276.2

13 (racemic)

167.2



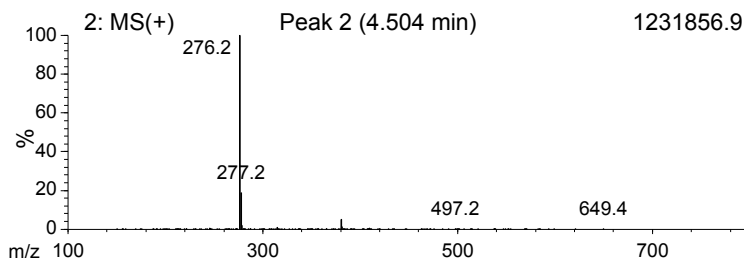
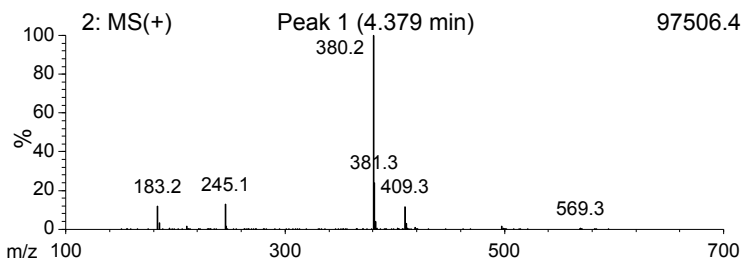
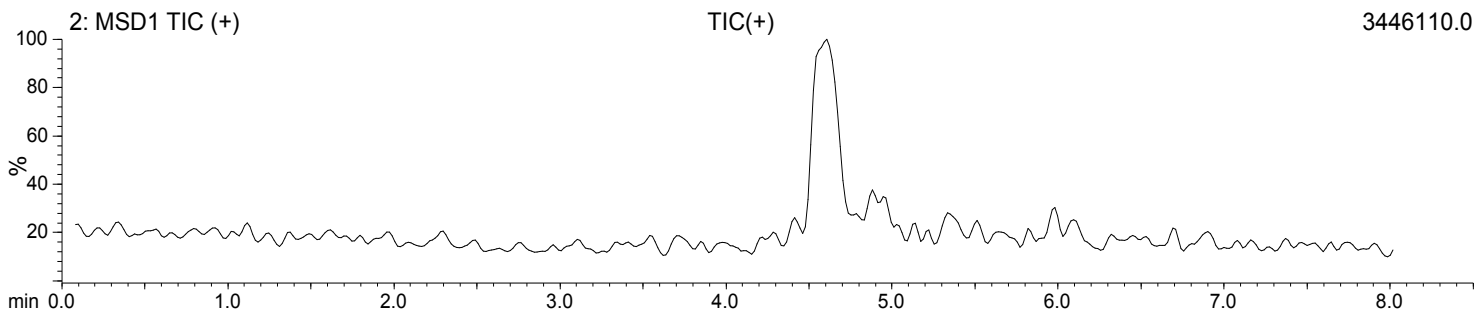
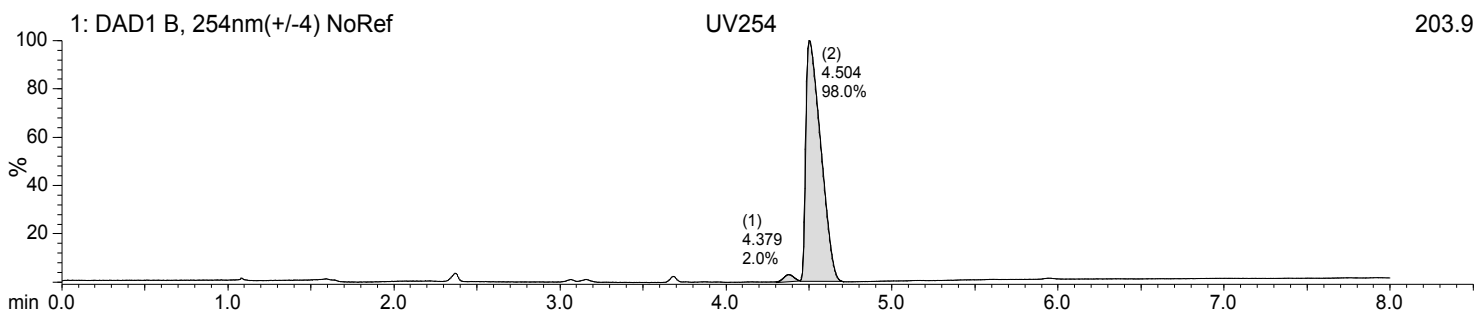
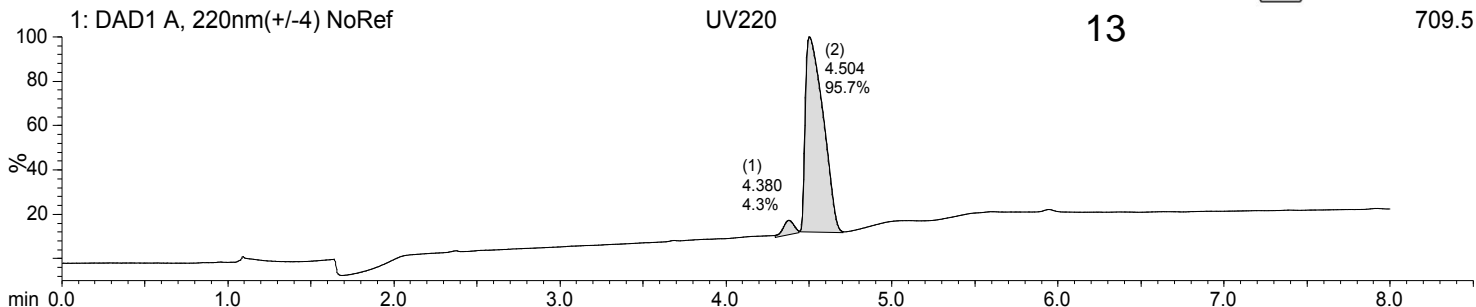
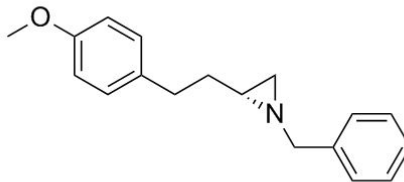
Sample Name: TJS-6-33
User:

Acquired: 12/16/2014 2:29 PM
Filename:
C:\CHEM32\1\DATA\SINGLE 2014-12-16 14-17-53\1AH-0201.D

Method IC 2-20 IPA DEA.M
Location: 1,1:A.8

Description:

Peak #	Time	Area % UV220	Area % UV254	Area % TIC(+)	BPM
1	4.380	4.3	2.0	0.0	380.2
2	4.504	95.7	98.0	0.0	276.2



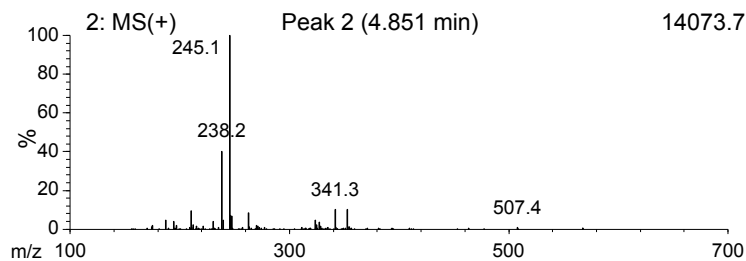
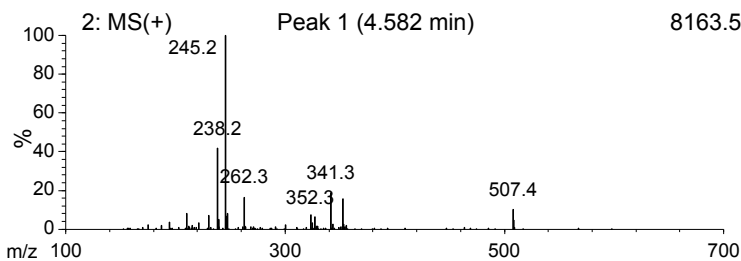
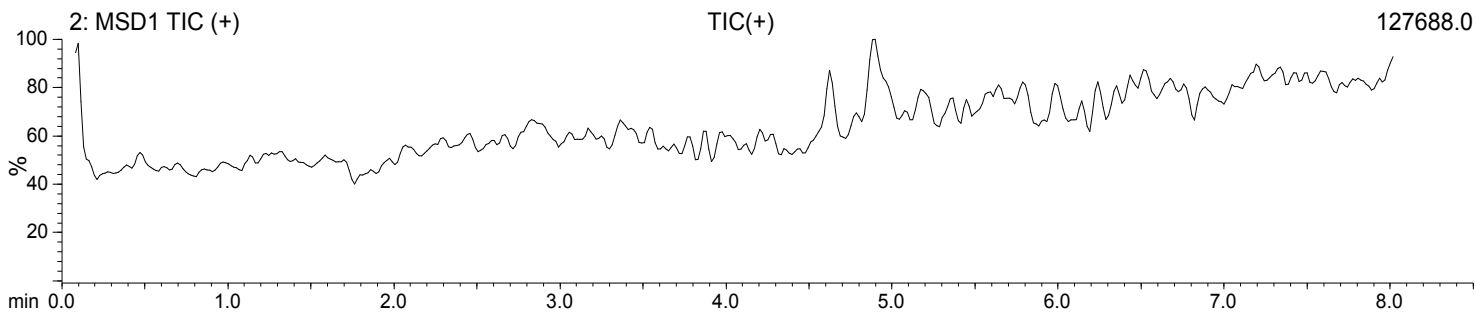
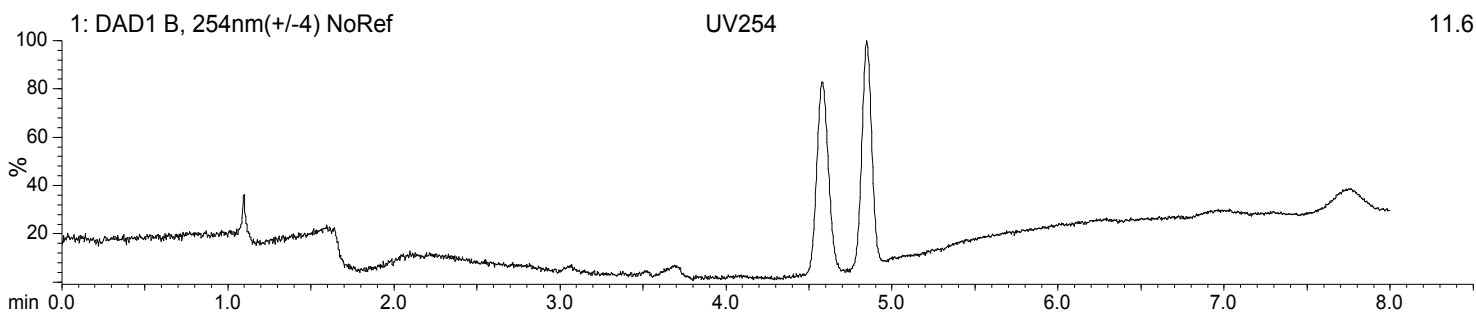
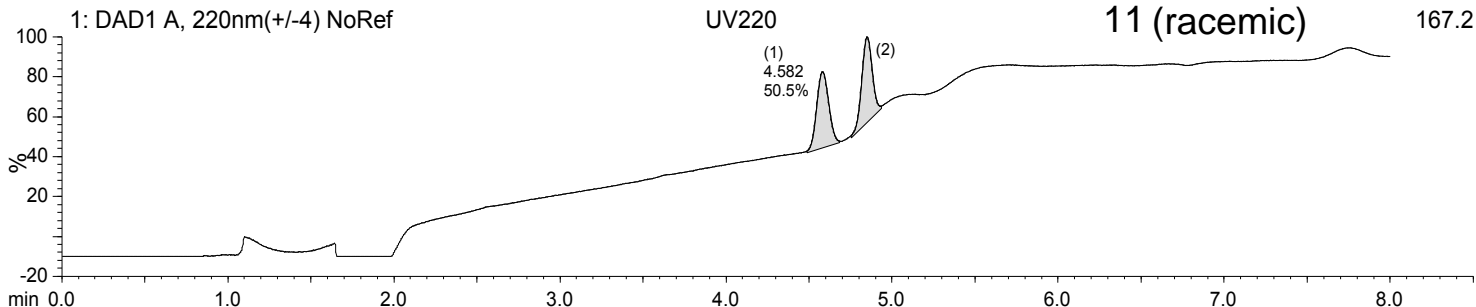
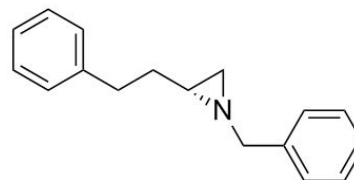
Sample Name: TJS-5-175 racemic
User:

Acquired: 12/15/2014 3:01 PM
Filename:
C:\CHEM32\1\DATA\SINGLE 2014-12-15 14-49-34\1AG-0201.D

Method IC 2-20 IPA DEA.M
Location: 1,1:A,7

Description:

Peak #	Time	Area % UV220	Area % UV254	Area % TIC(+)	BPM
1	4.582	50.5	0.0	0.0	245.2
2	4.851	49.5	0.0	0.0	245.1

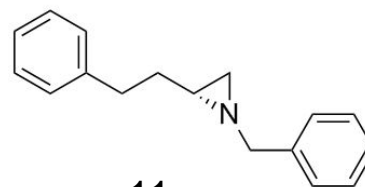


Sample Name: TJS-5-175 enantiomer
User:

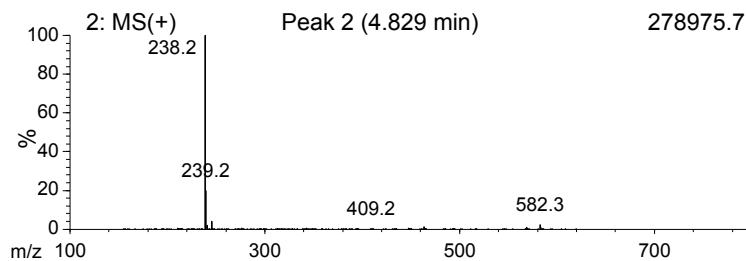
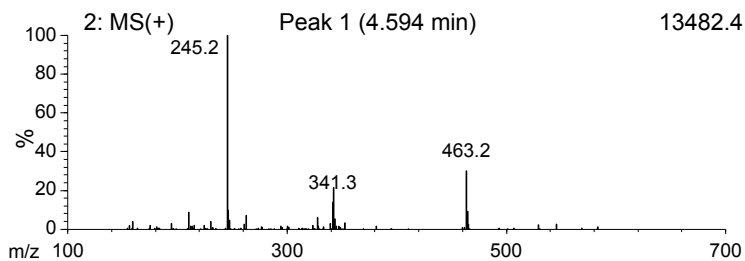
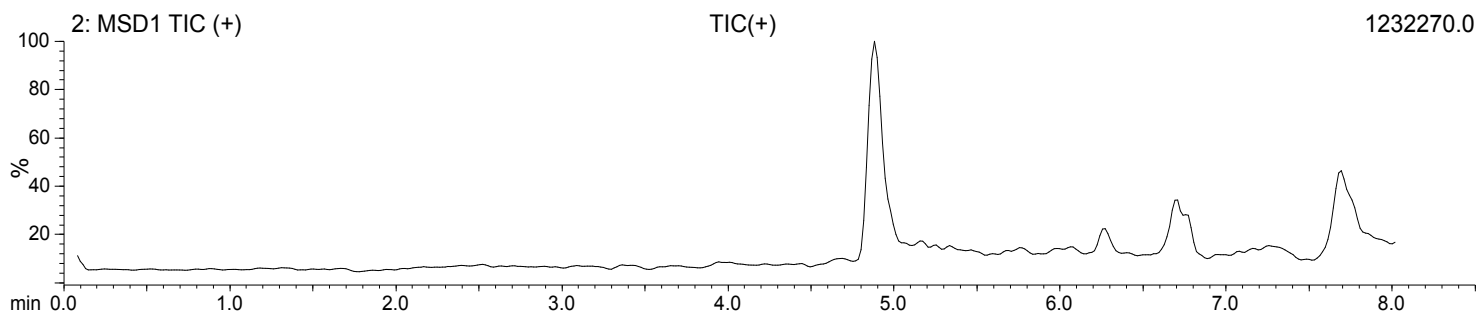
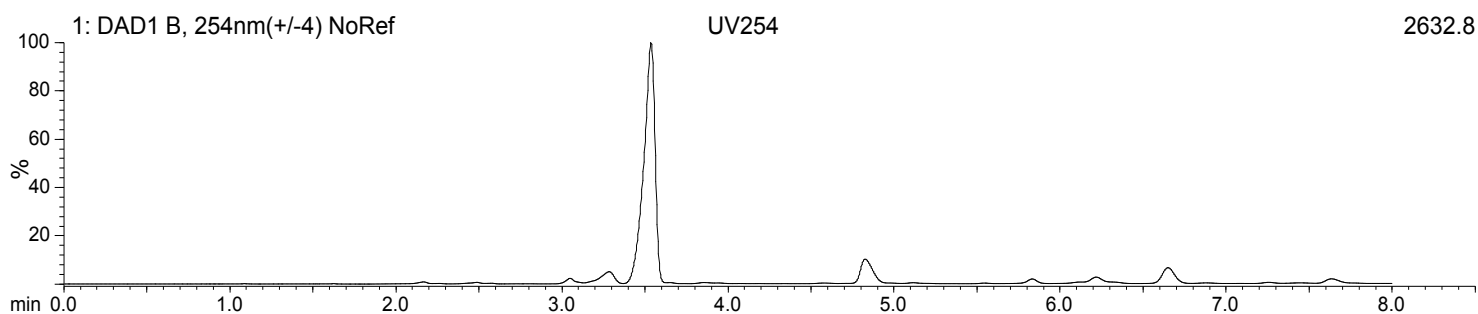
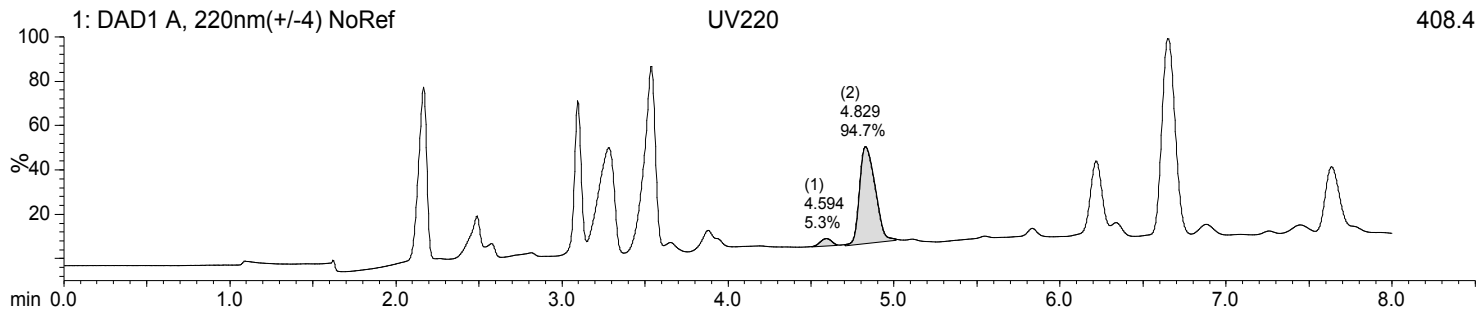
Acquired: 12/15/2014 3:21 PM
Filename:
C:\CHEM32\1\DATA\SINGLE 2014-12-15 14-49-34\1AF-0401.D

Method IC 2-20 IPA DEA.M
Location: 1,1:A,{

Description:



Peak #	Time	Area % UV220	Area % UV254	Area % TIC(+)	BPM
1	4.594	5.3	0.0	0.0	245.2
2	4.829	94.7	0.0	0.0	238.2



Sample Name: TJS-6-36
User:

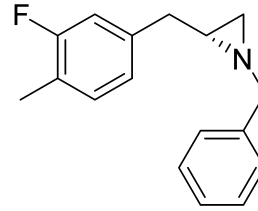
Acquired: 11/26/2014 7:34 AM

Method LUX CELLULOSE-2 2-20 IPA Description:

Filename:

DEA.M

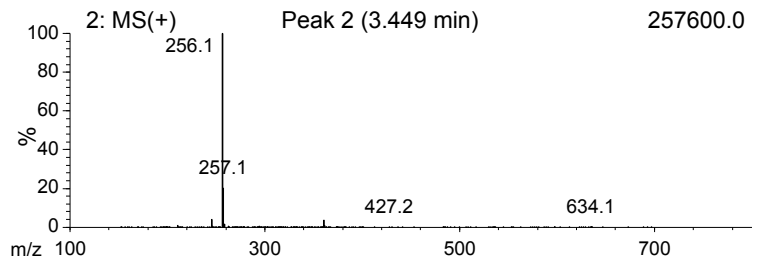
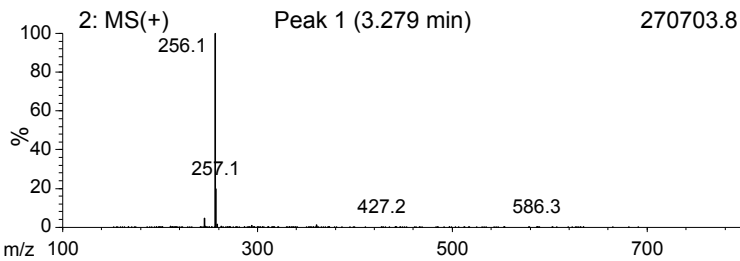
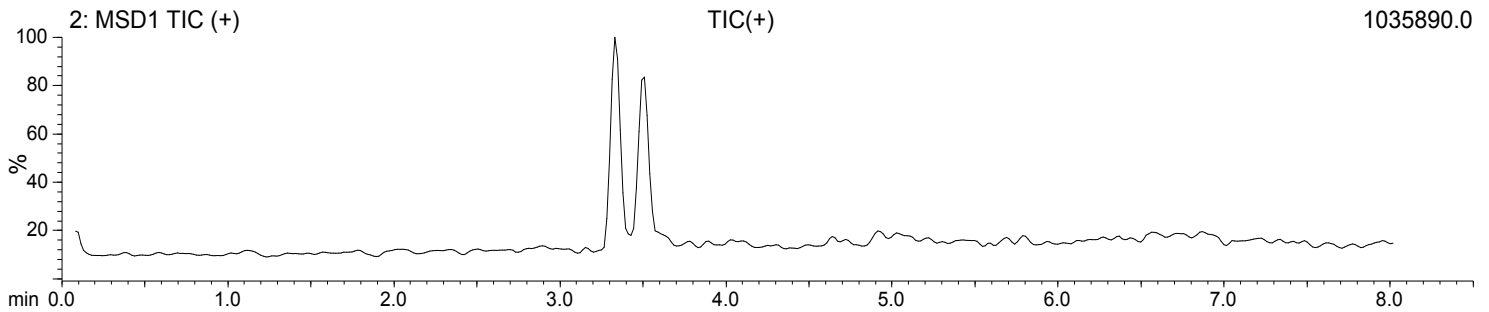
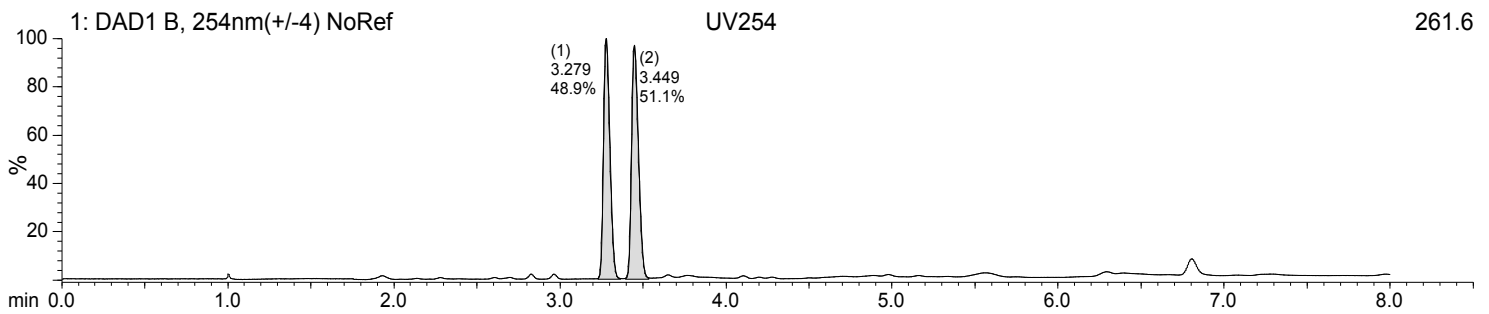
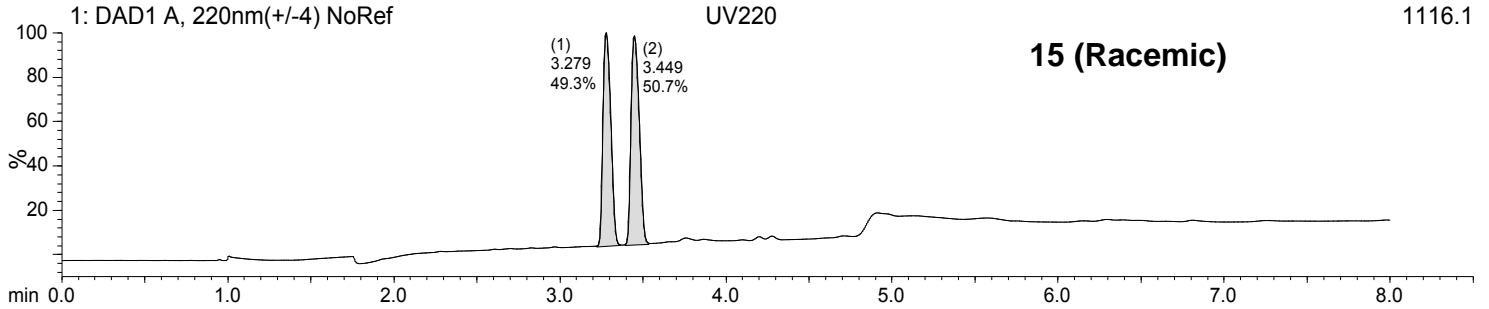
C:\CHEM32\1\DATA\SINGLE 2014-11-26 07-00-32\1AI-0401.D Location: 1,1:A,9



15 (Racemic)

1116.1

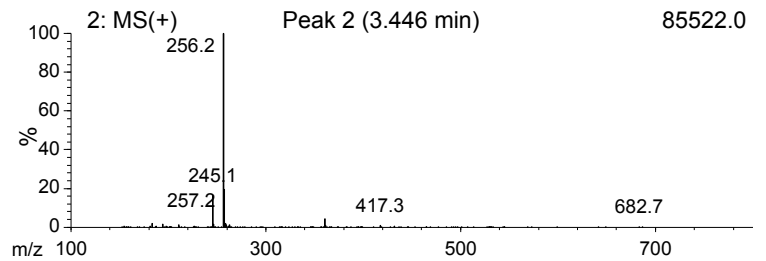
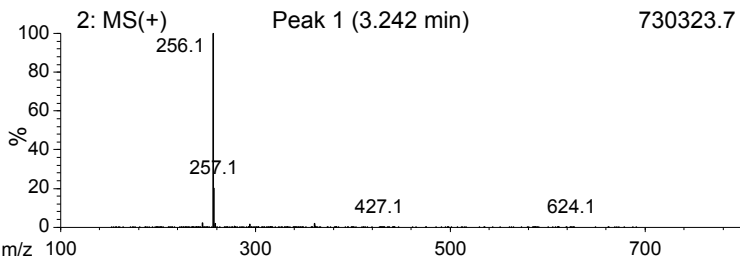
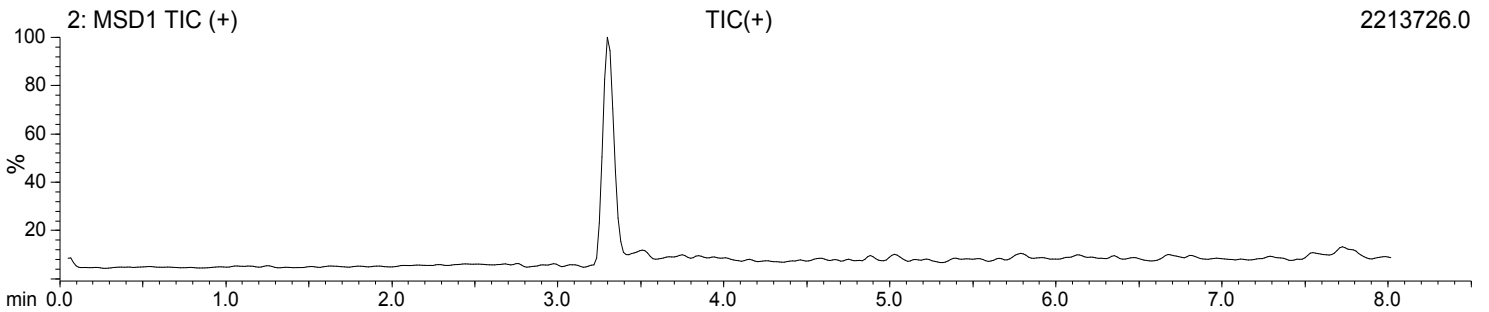
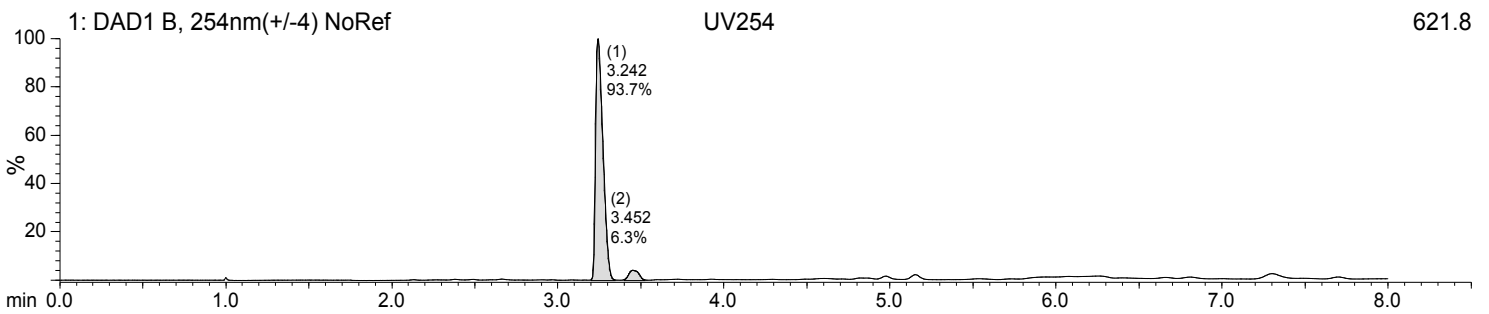
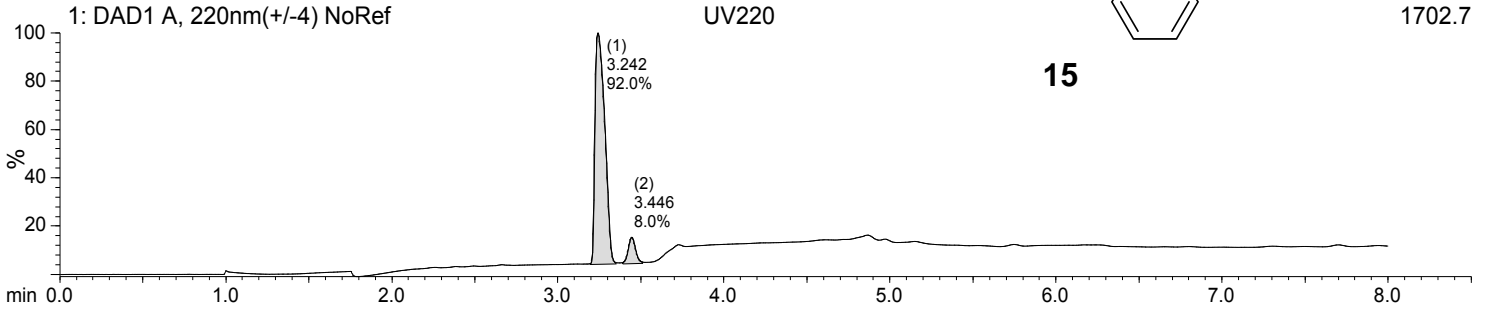
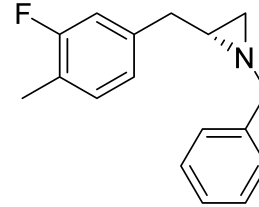
Peak #	Time	Area % UV220	Area % UV254	Area % TIC(+)	BPM
1	3.279	49.3	48.9	0.0	256.1
2	3.449	50.7	51.1	0.0	256.1



Sample Name: TJS-6-43
User:

Acquired: 11/26/2014 7:54 AM Method LUX CELLULOSE-2 2-20 IPA Description:
 Filename: DEA.M
 C:\CHEM32\1\DATA\SINGLE 2014-11-26 07-52-33\1BA-0101.D Location: 1,1:B,1

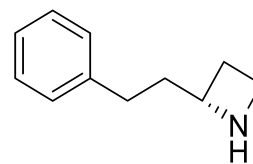
Peak #	Time	Area % UV220	Area % UV254	Area % TIC(+)	BPM
1	3.242	92.0	93.7	0.0	256.1
2	3.449	8.0	6.3	0.0	256.2



Sample Name: TJS-5-55
User:

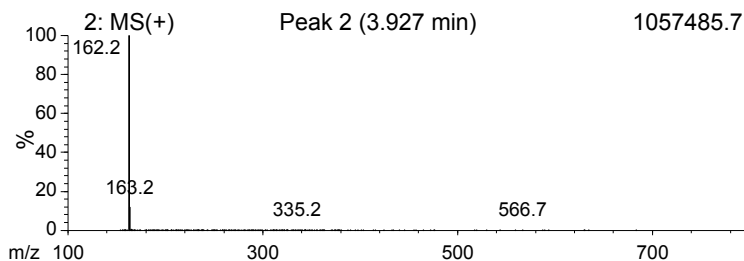
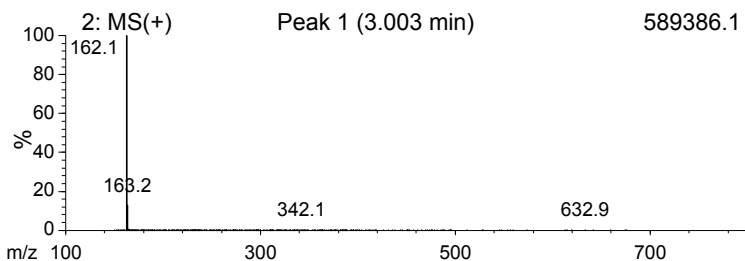
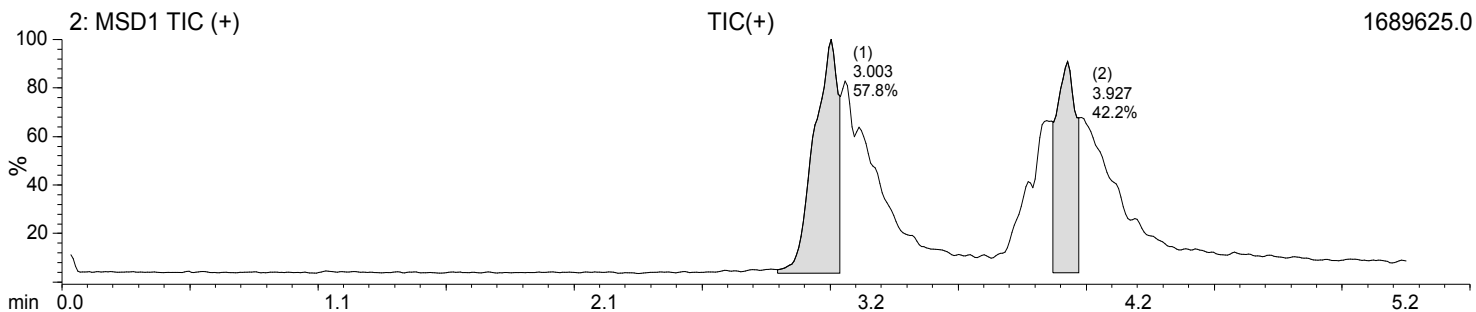
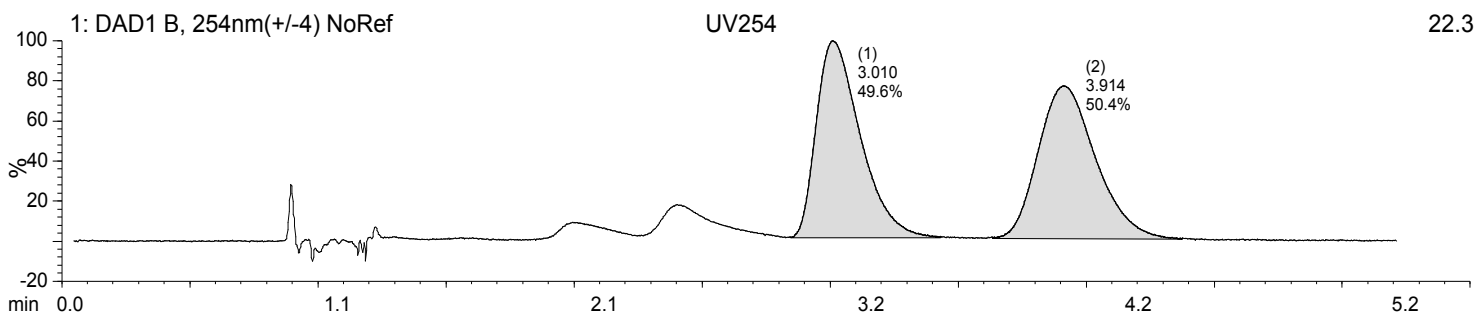
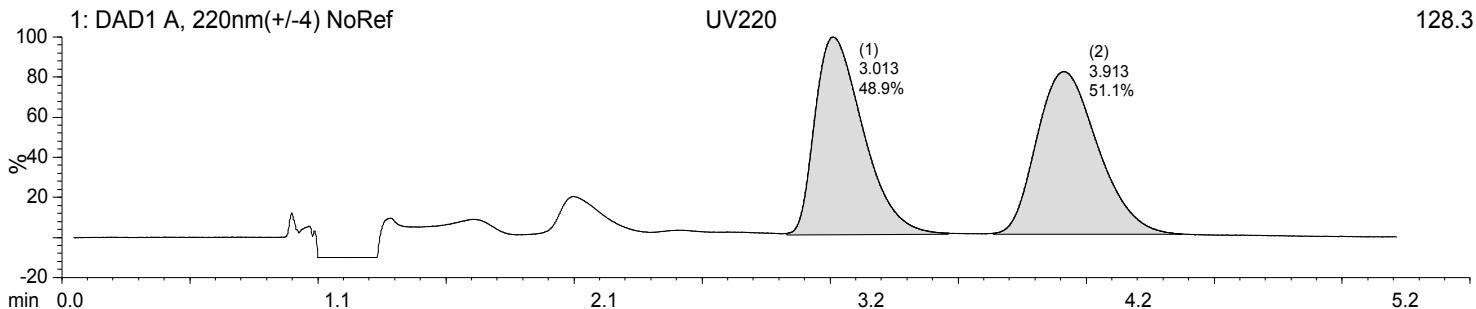
Acquired: 1/24/2013 12:14 PM
Filename:
C:\CHEM32\1\DATA\SINGLE 2013-01-24 12-12-40\2EE-0101.D

Method: CHIRALPAK_IC_30_IPA.M
Location: 1,2:E,5



31 (Racemic)

Peak #	Time	Area % UV220	Area % UV254	Area % TIC(+)	BPM
1	3.009	48.9	49.6	57.8	162.1
2	3.918	51.1	50.4	42.2	162.2

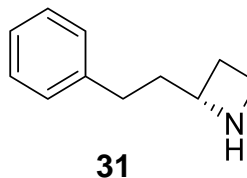


Sample Name: TJS-6-18
User:

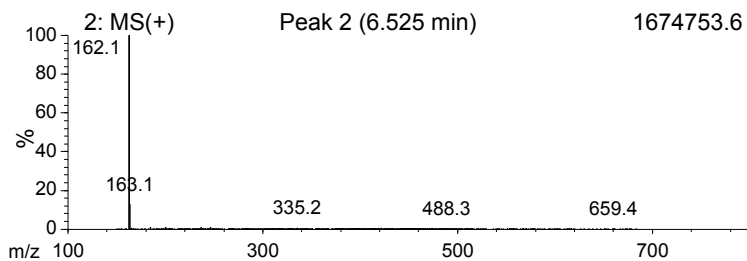
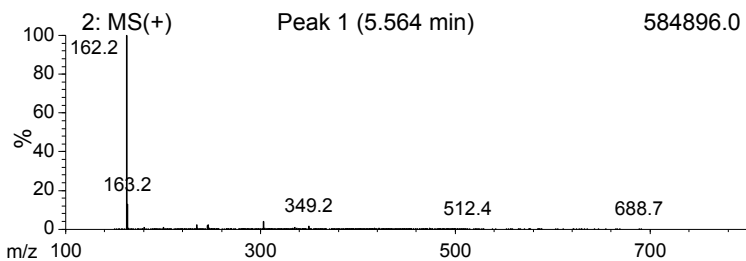
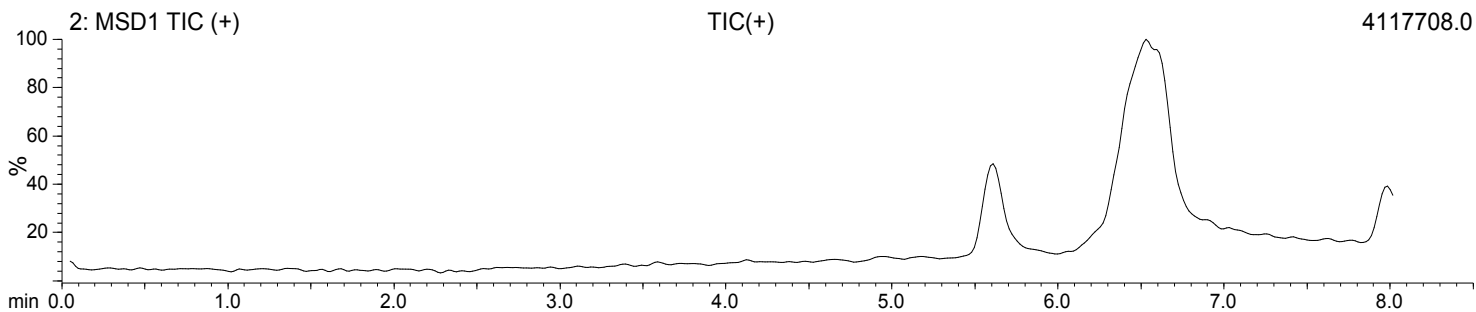
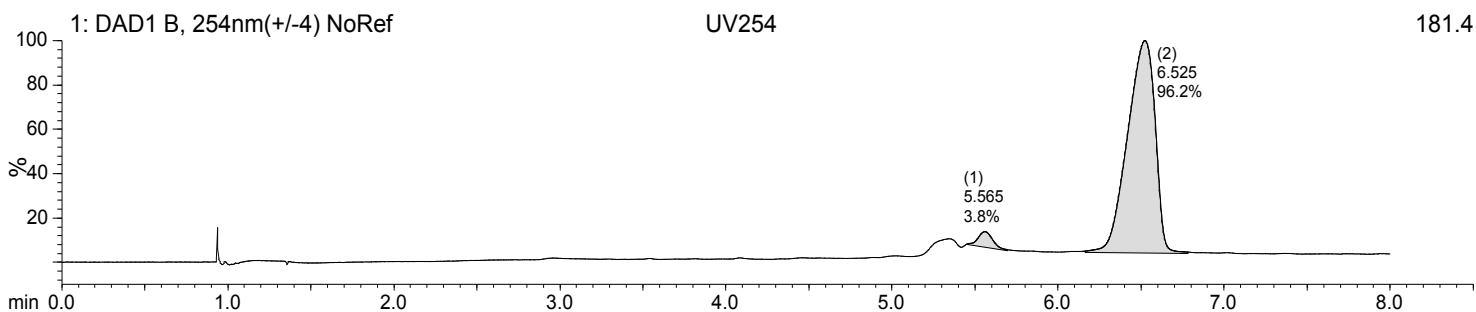
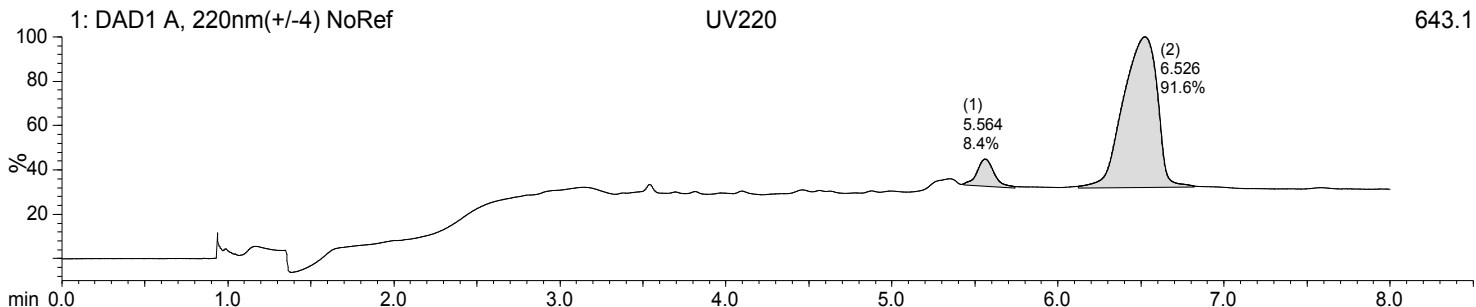
Acquired: 11/26/2014 11:07 AM
Filename:
C:\CHEM32\1\DATA\SINGLE 2014-11-26 11-06-02\1AF-0101.D

Method IC 5-50 IPA DEA.M
Location: 1,1:A,6

Description:



Peak #	Time	Area % UV220	Area % UV254	Area % TIC(+)	BPM
1	5.565	8.4	3.8	0.0	162.2
2	6.526	91.6	96.2	0.0	162.1

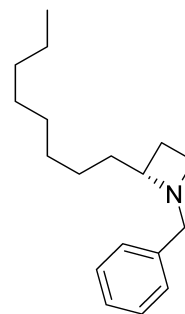


Sample Name: TJS-6-15 racemic
User:

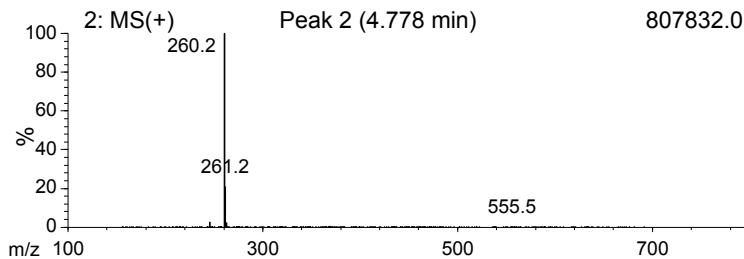
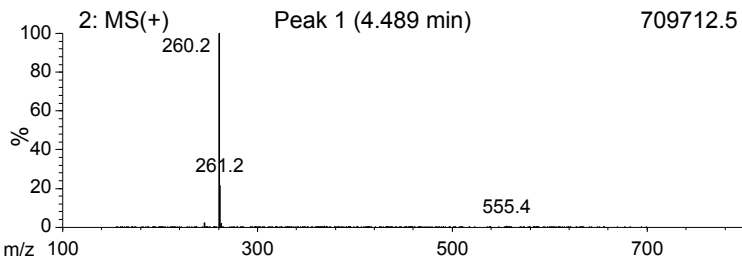
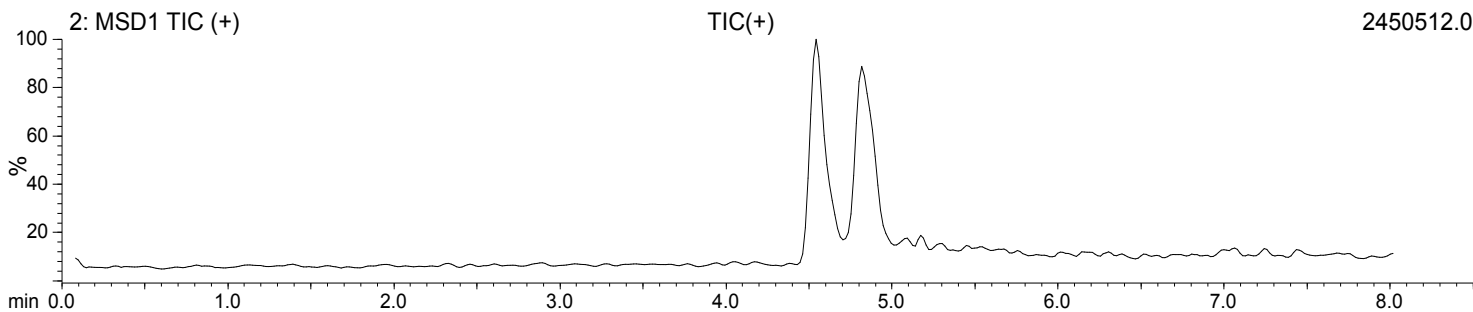
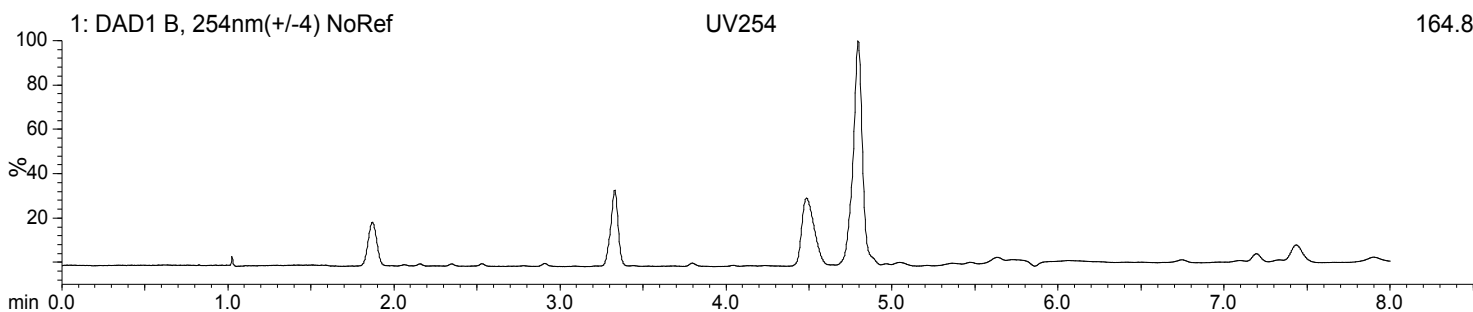
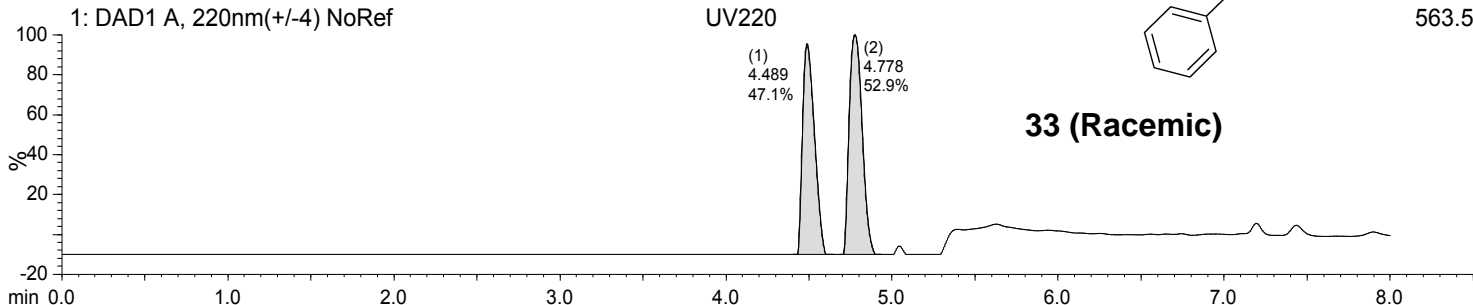
Acquired: 11/25/2014 2:49 PM
Filename:
C:\CHEM32\1\DATA\SINGLE 2014-11-25 14-38-20\1AG-0201.D

Method LUX CELLULOSE-4 2-20 IPA Description:
DEA.M
Location: 1,1:A,7

Peak #	Time	Area % UV220	Area % UV254	Area % TIC(+)	BPM
1	4.489	47.1	0.0	0.0	260.2
2	4.778	52.9	0.0	0.0	260.2



33 (Racemic)

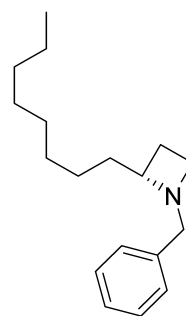


Sample Name: TJS-6-27
User:

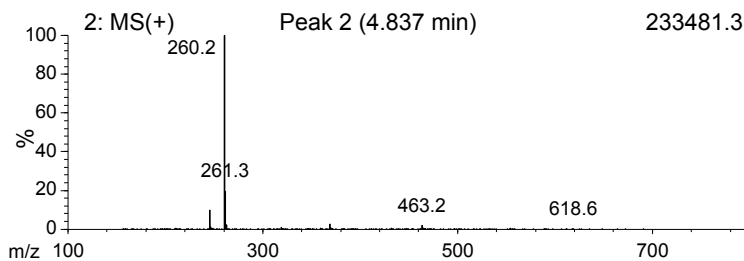
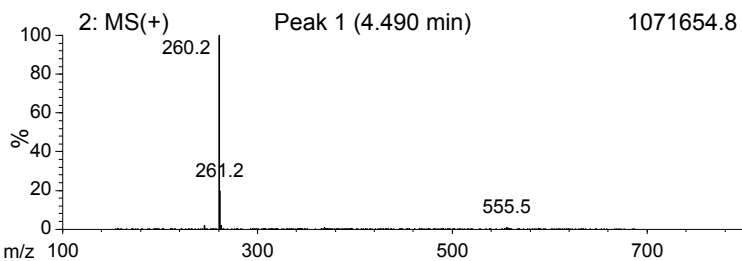
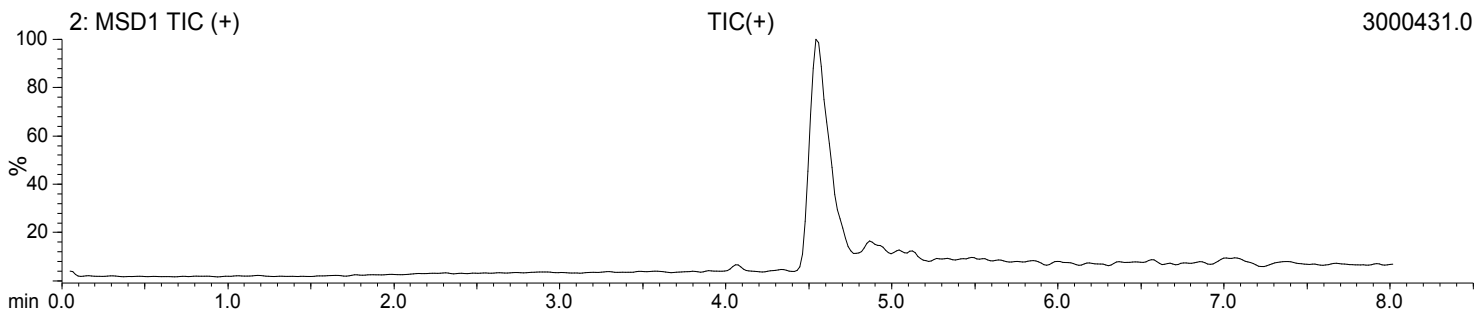
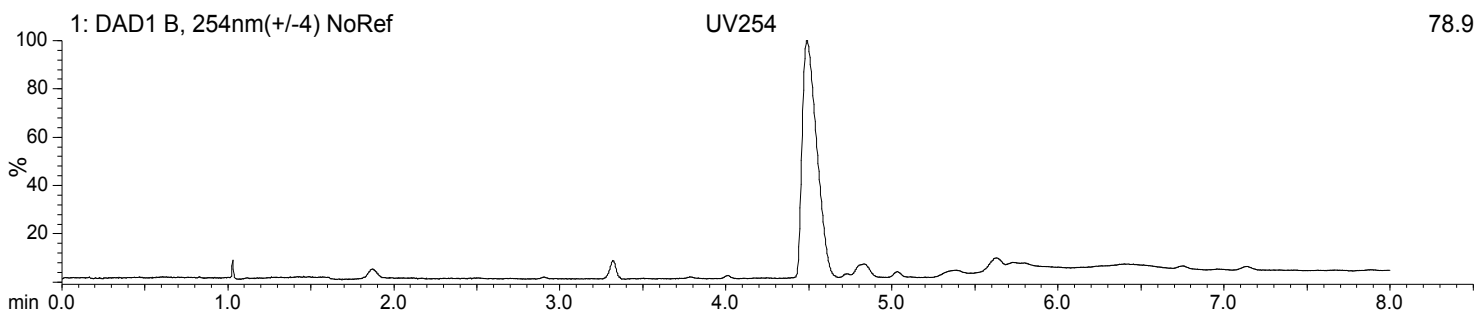
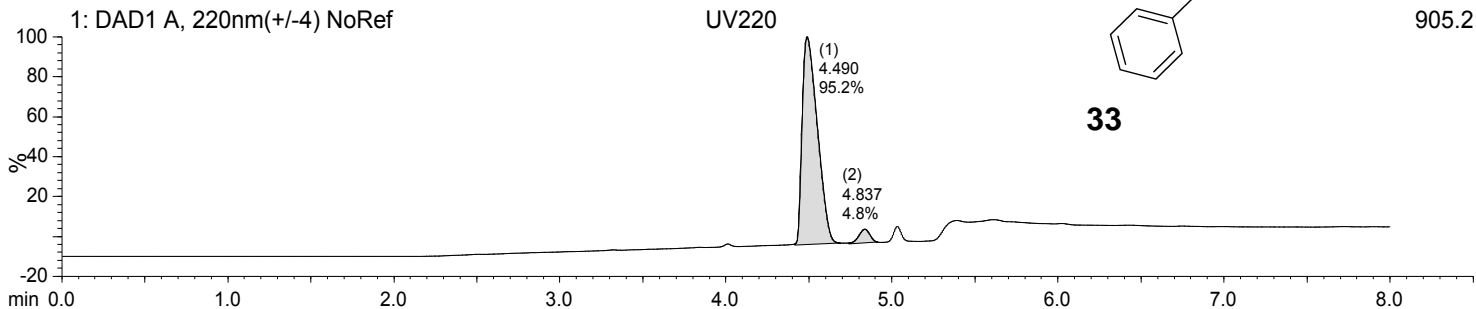
Acquired: 11/25/2014 2:40 PM
Filename:
C:\CHEM32\1\DATA\SINGLE 2014-11-25 14-38-20\1AF-0101.D

Method LUX CELLULOSE-4 2-20 IPA Description:
DEA.M
Location: 1,1:A,6

Peak #	Time	Area % UV220	Area % UV254	Area % TIC(+)	BPM
1	4.490	95.2	0.0	0.0	260.2
2	4.837	4.8	0.0	0.0	260.2



33

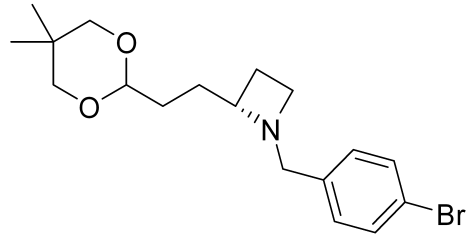


Sample Name: TJS-6-26 racemic
User:

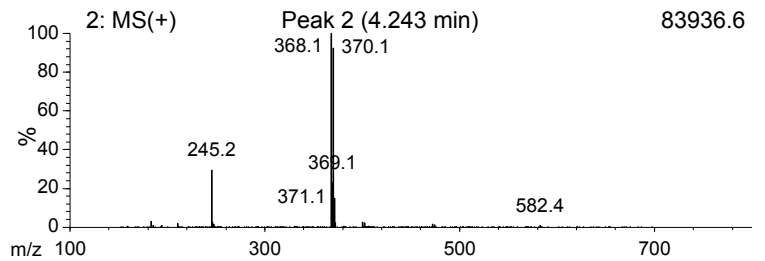
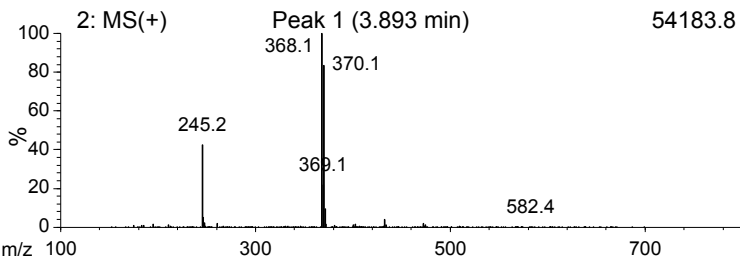
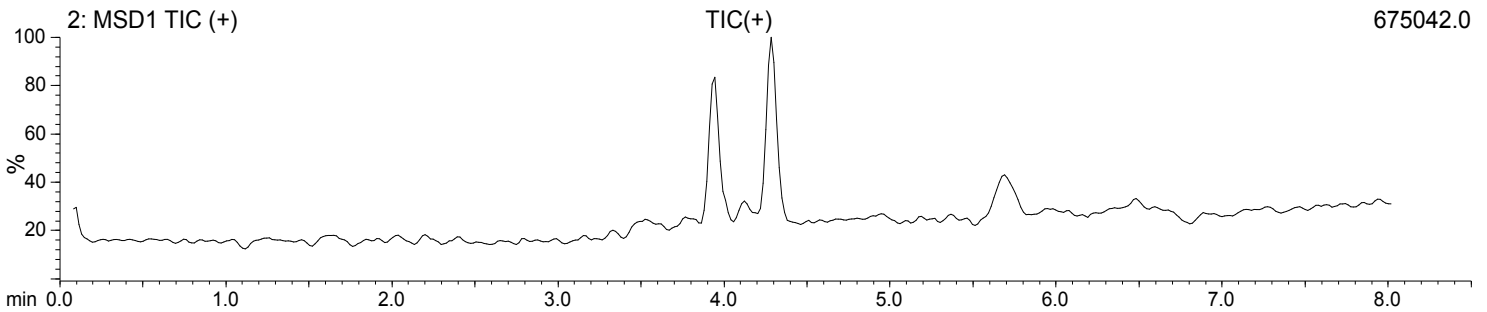
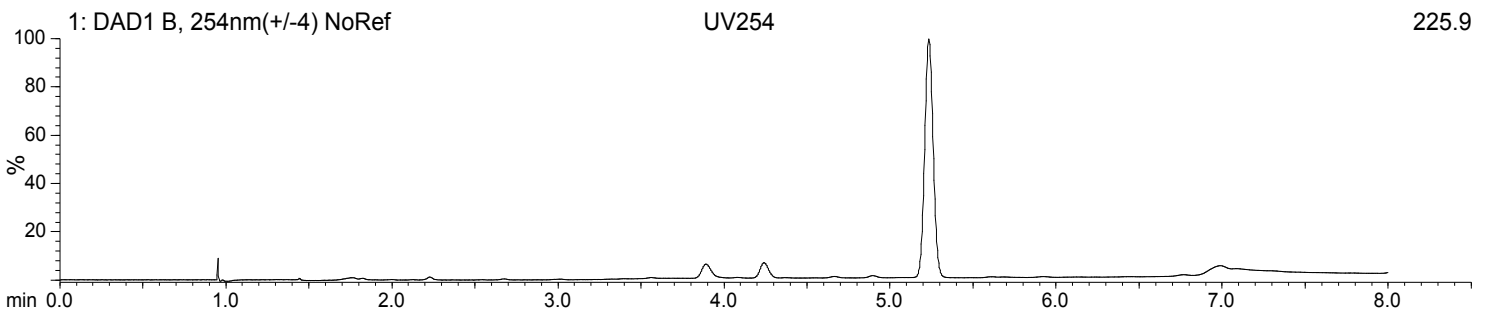
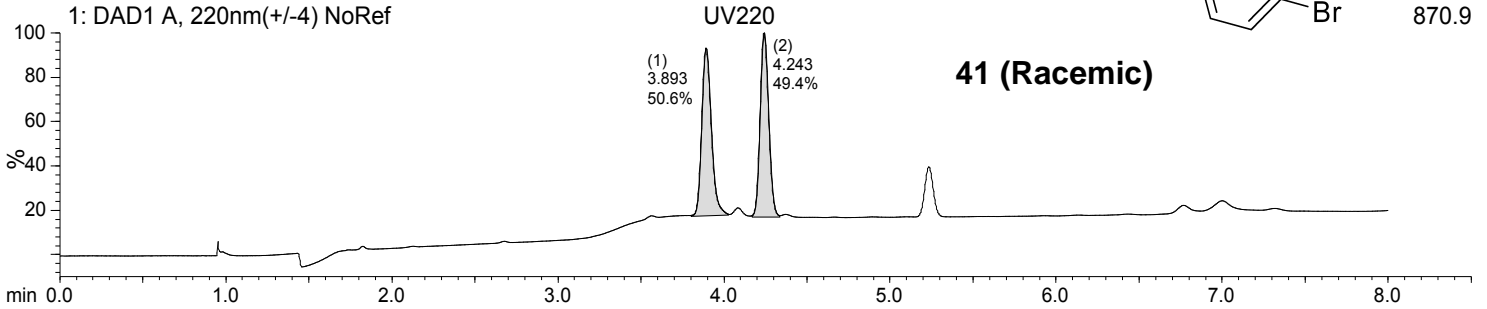
Acquired: 11/26/2014 8:24 AM
Filename:
C:\CHEM32\1\DATA\SINGLE 2014-11-26 07-52-33\1AH-0401.D

Method IC 5-30 IPA DEA.M
Location: 1,1:A,8

Description:



Peak #	Time	Area % UV220	Area % UV254	Area % TIC(+)	BPM
1	3.893	50.6	0.0	0.0	368.1
2	4.243	49.4	0.0	0.0	368.1

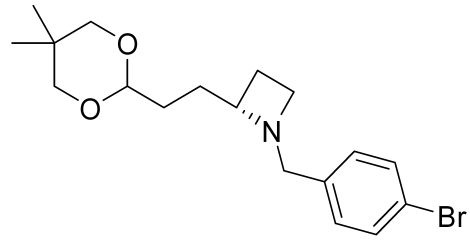


Sample Name: TJS-6-38
User:

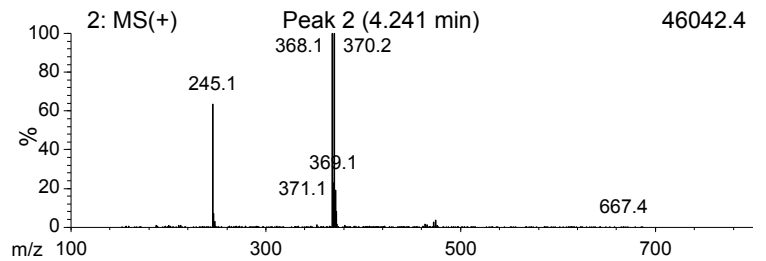
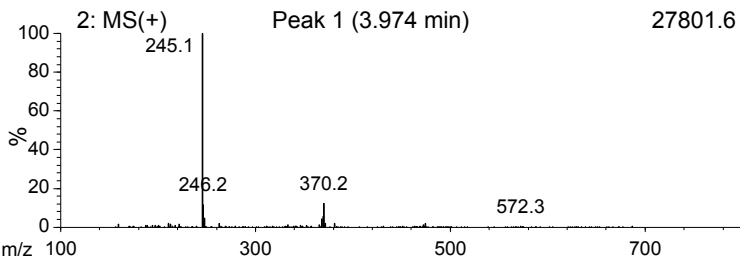
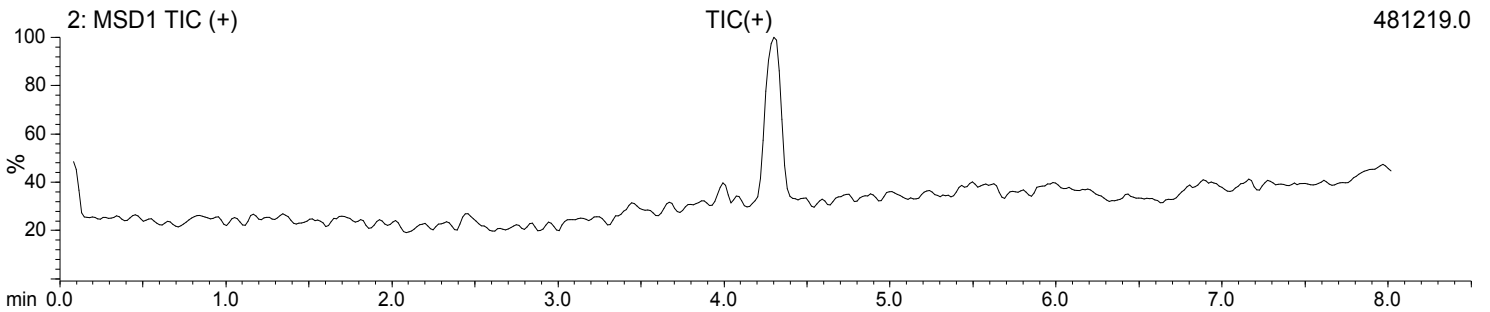
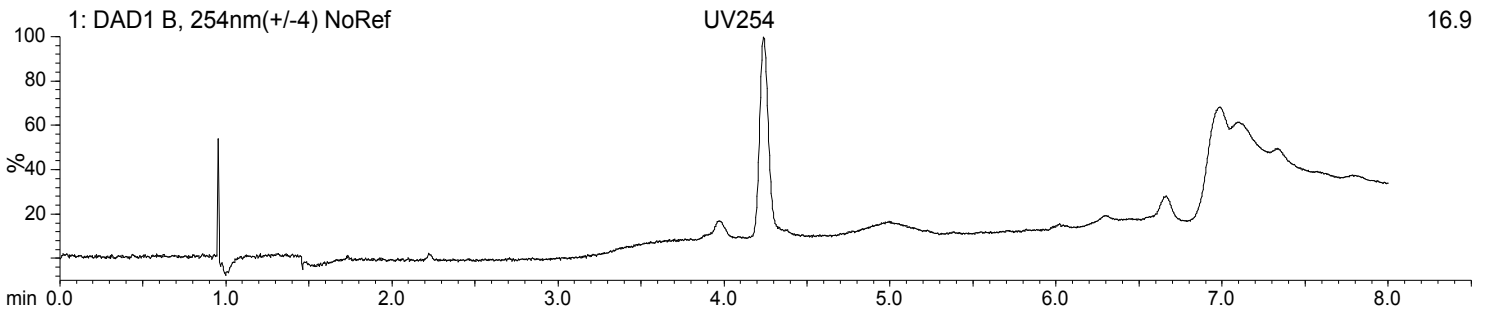
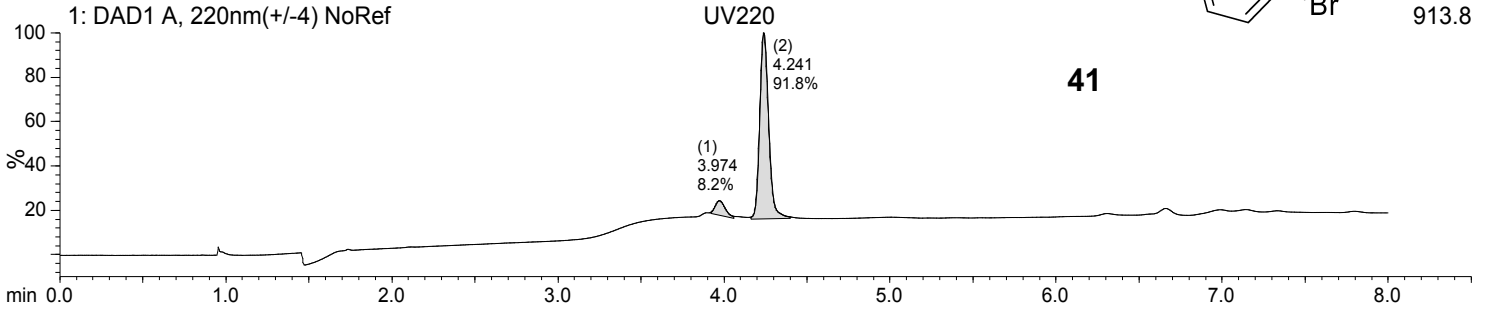
Acquired: 11/26/2014 8:14 AM
Filename:
C:\CHEM32\1\DATA\SINGLE 2014-11-26 07-52-33\1BB-0301.D

Method IC 5-30 IPA DEA.M
Location: 1,1:B,2

Description:



Peak #	Time	Area % UV220	Area % UV254	Area % TIC(+)	BPM
1	3.974	8.2	0.0	0.0	245.1
2	4.241	91.8	0.0	0.0	368.1

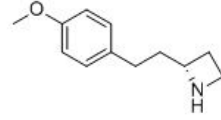


VCNDD MRB4-12475 Agilent SFCMS

Sample Name: TJS-5-59 racemic
User:

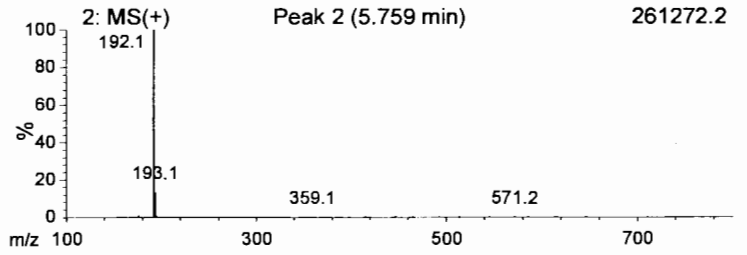
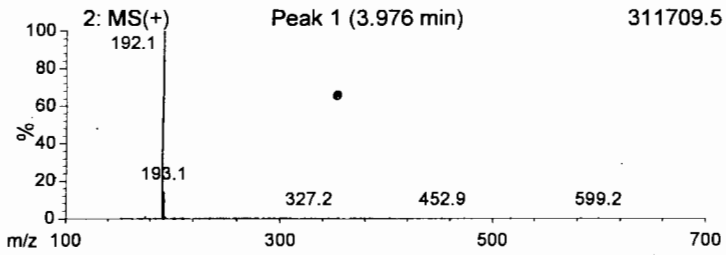
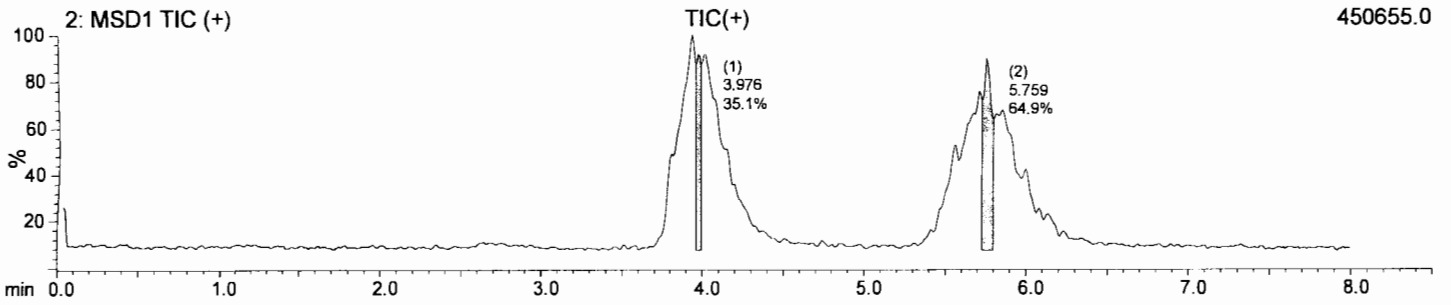
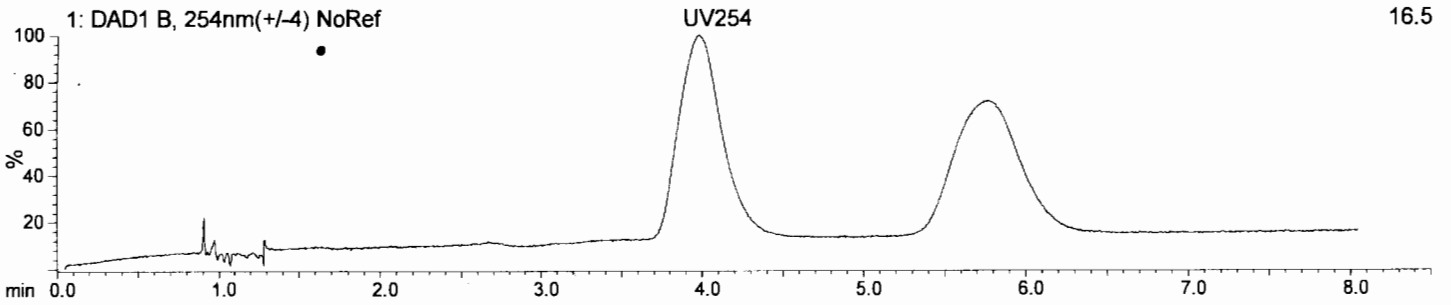
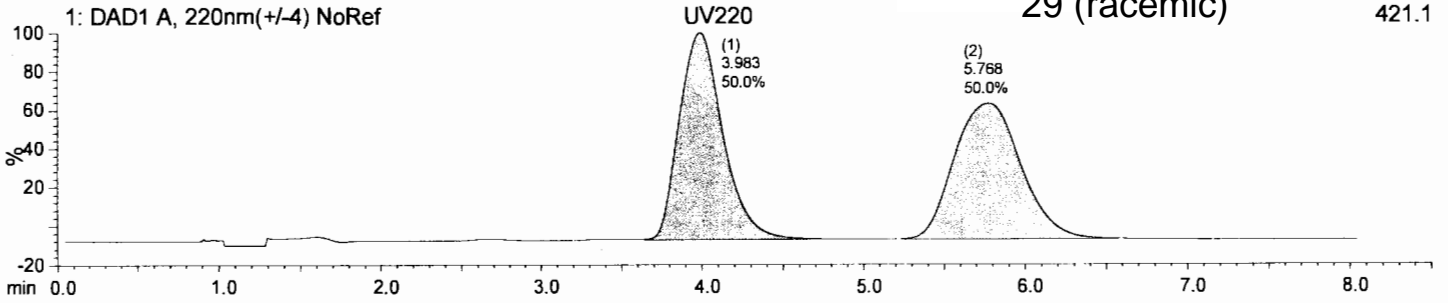
Acquired: 1/25/2013 1:21 PM
Filename:
C:\CHEM321\DATA\SINGLE 2013-01-25 13-19-34\2FA-0101.D

Method: CHIRALPAK_IC_30_IPA.M
Location: 1,2:F,1



29 (racemic)

Peak #	Time	Area %		Area %	BPM
		UV220	UV254	TIC(+)	
1	3.980	50.0	0.0	35.1	192.1
2	5.764	50.0	0.0	64.9	192.1



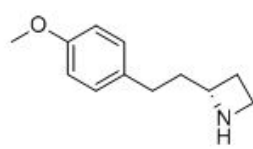
VCNDD MRB4-12475 Agilent SFCMS

Sample Name: TJS-5-53 chiral
User:

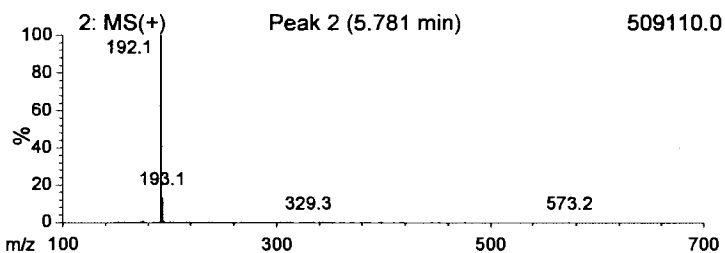
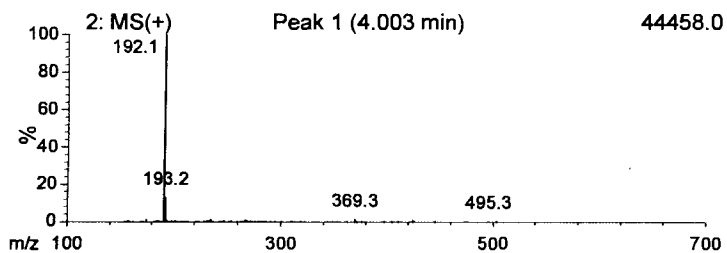
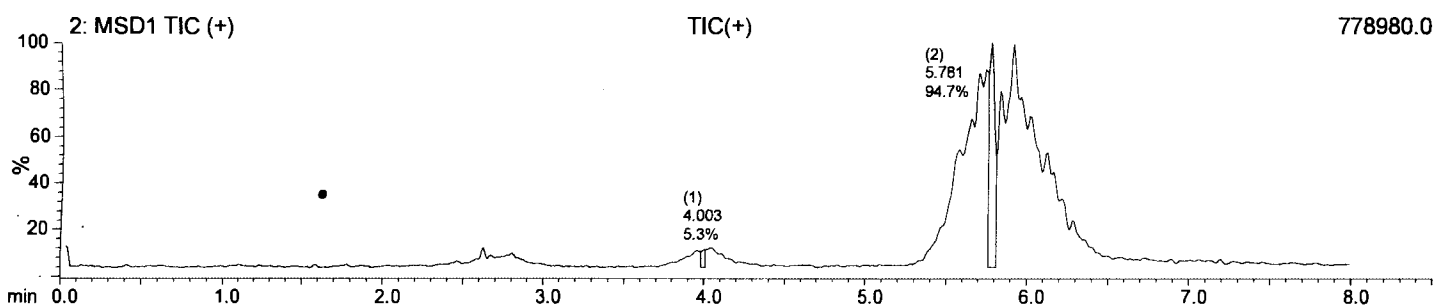
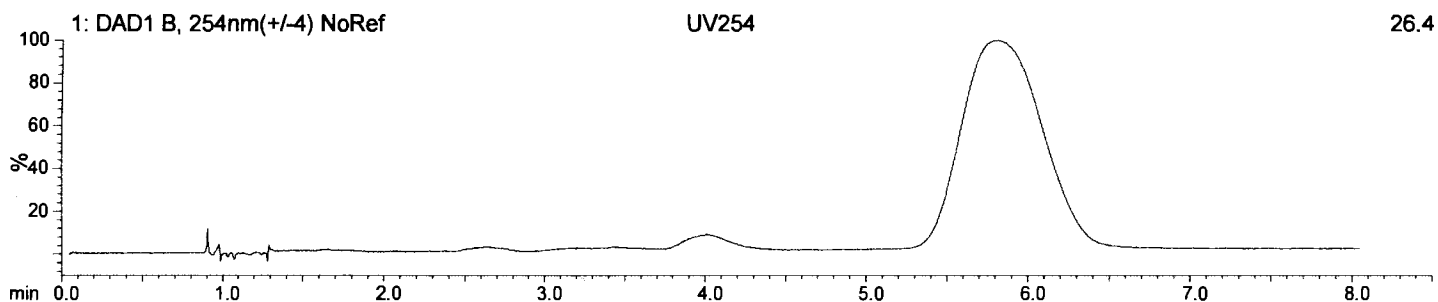
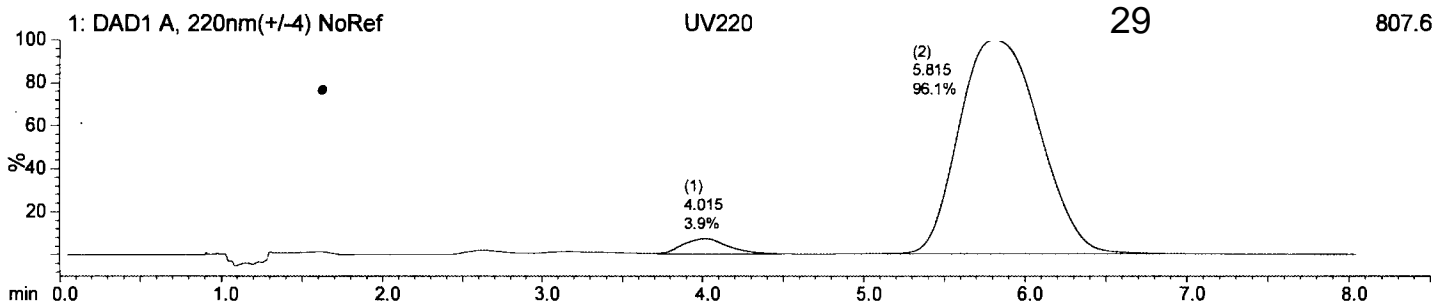
Acquired: 1/25/2013 1:32 PM
Filename:
C:\CHEM32\1\DATA\SINGLE 2013-01-25 13-31-01\2FB-0101.D

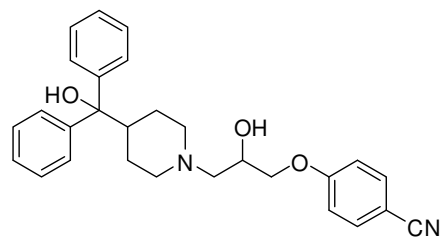
Method: CHIRALPAK_IC 30 IPA.M
Location: 1,2:F,2

17 2
2

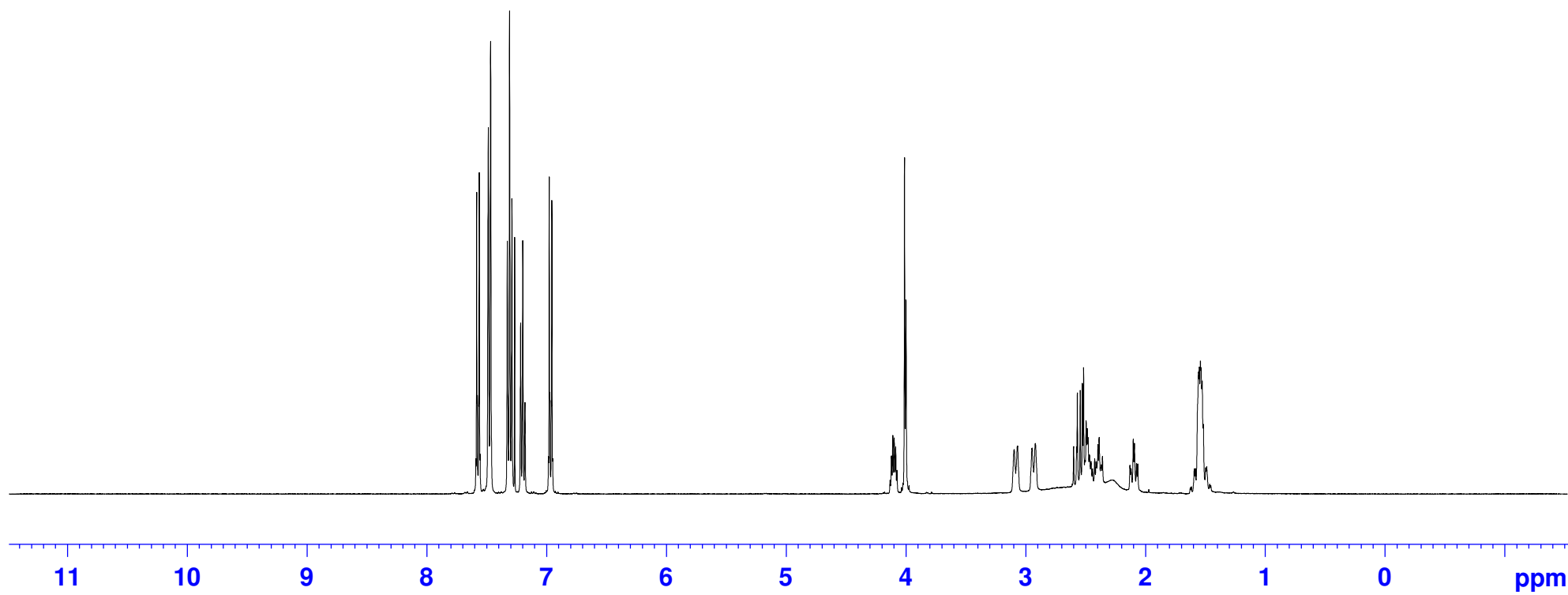


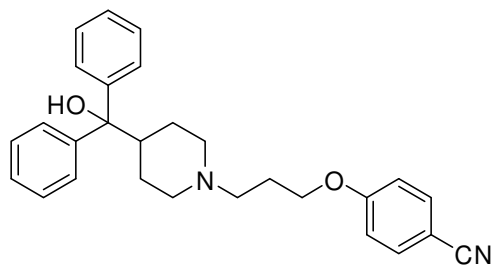
Peak #	Time	Area %			BPM
		UV220	UV254	TIC(+)	
1	4.009	3.9	0.0	5.3	192.1
2	5.798	96.1	0.0	94.7	192.1



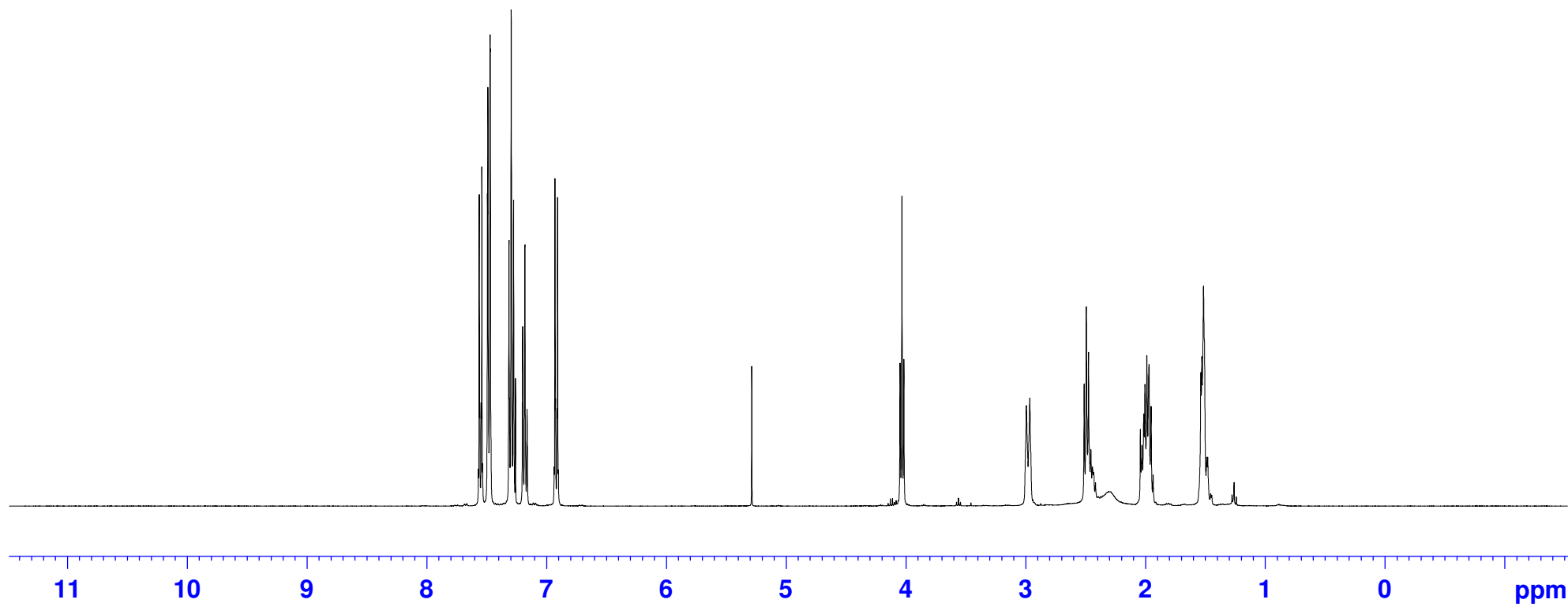


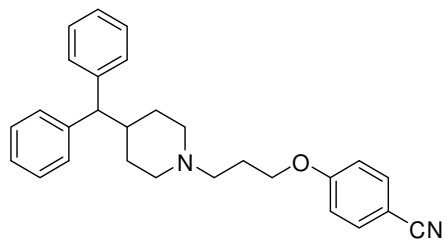
4.1
¹H NMR Spectrum
(400 MHz, CDCl₃)



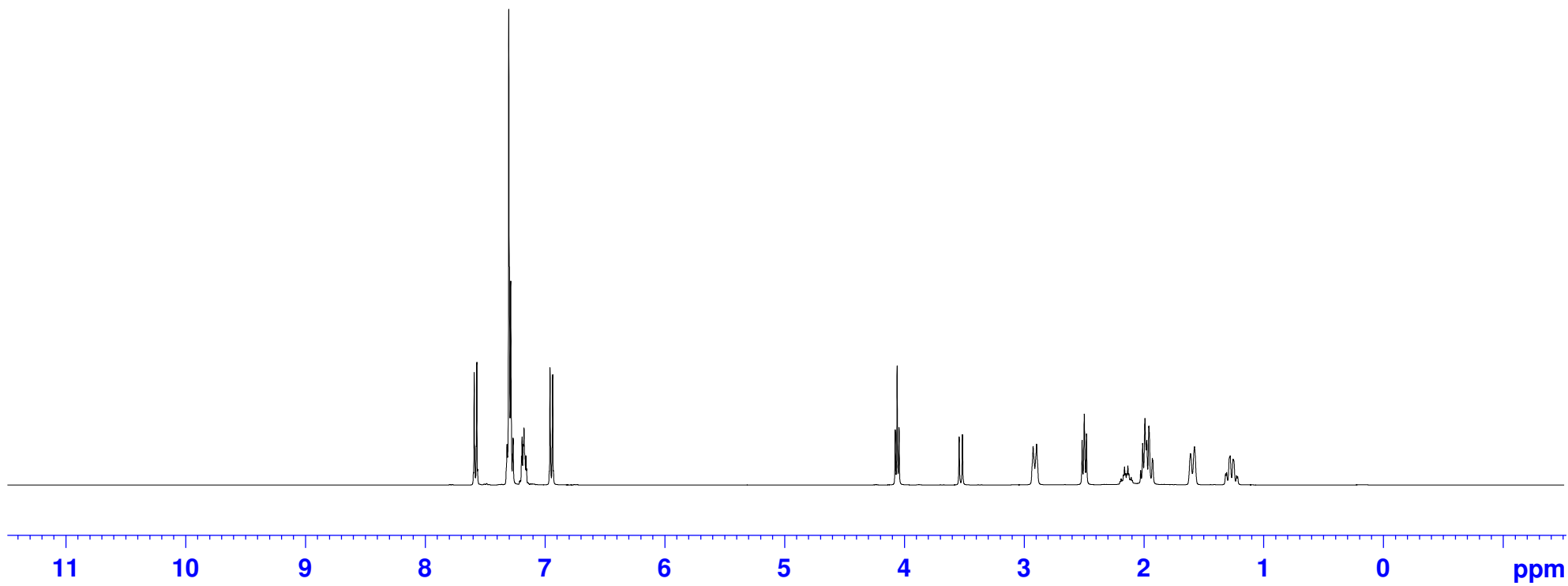


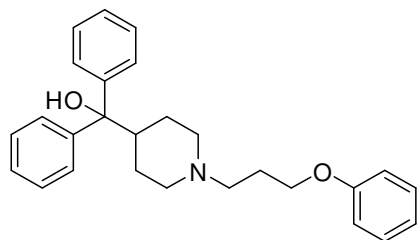
4.2
¹H NMR Spectrum
(400 MHz, CDCl₃)



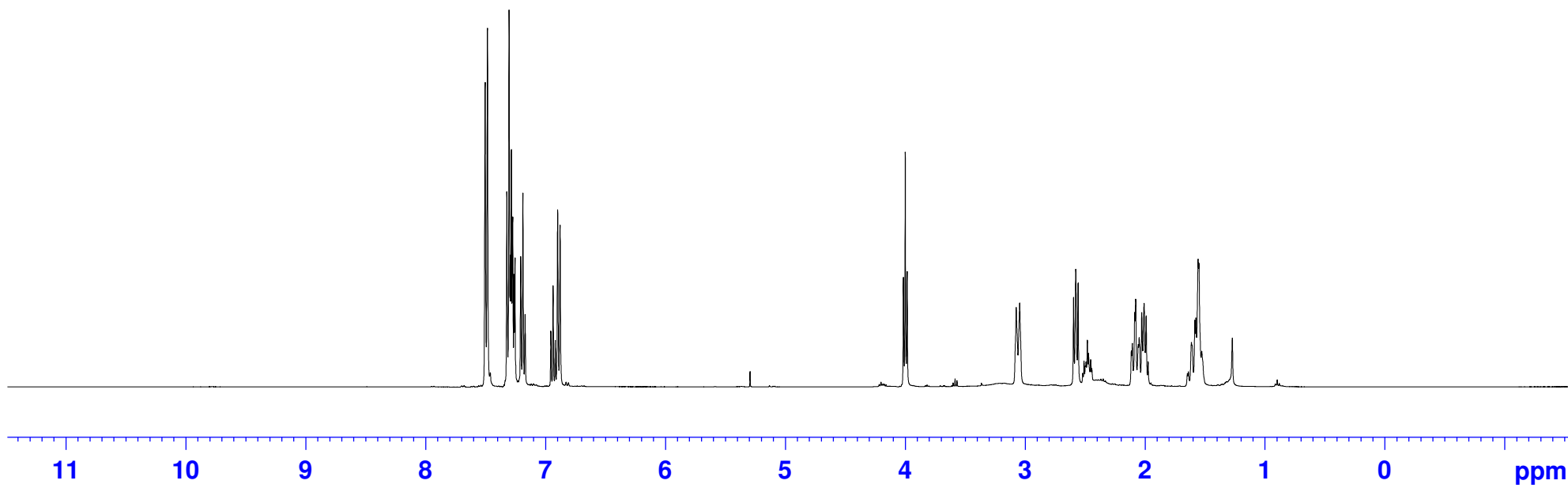


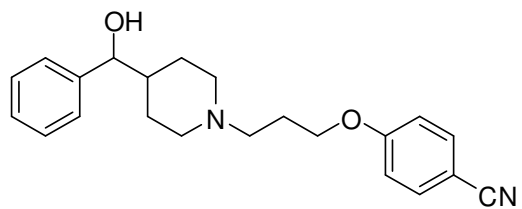
4.5
¹H NMR Spectrum
(400 MHz, CDCl₃)



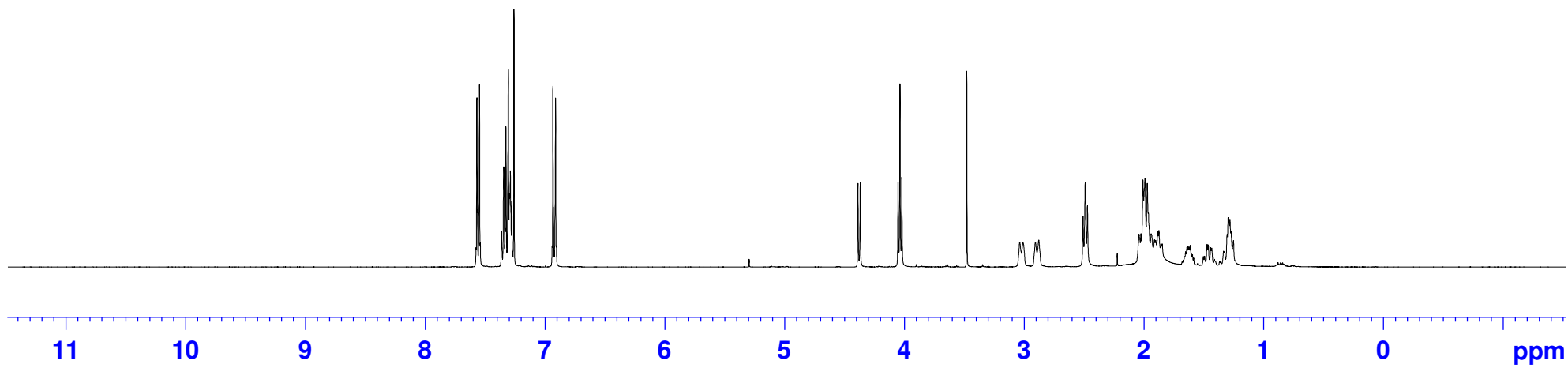


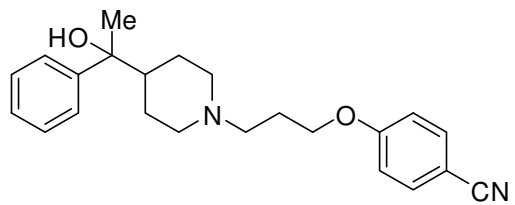
4.6
¹H NMR Spectrum
(400 MHz, CDCl₃)



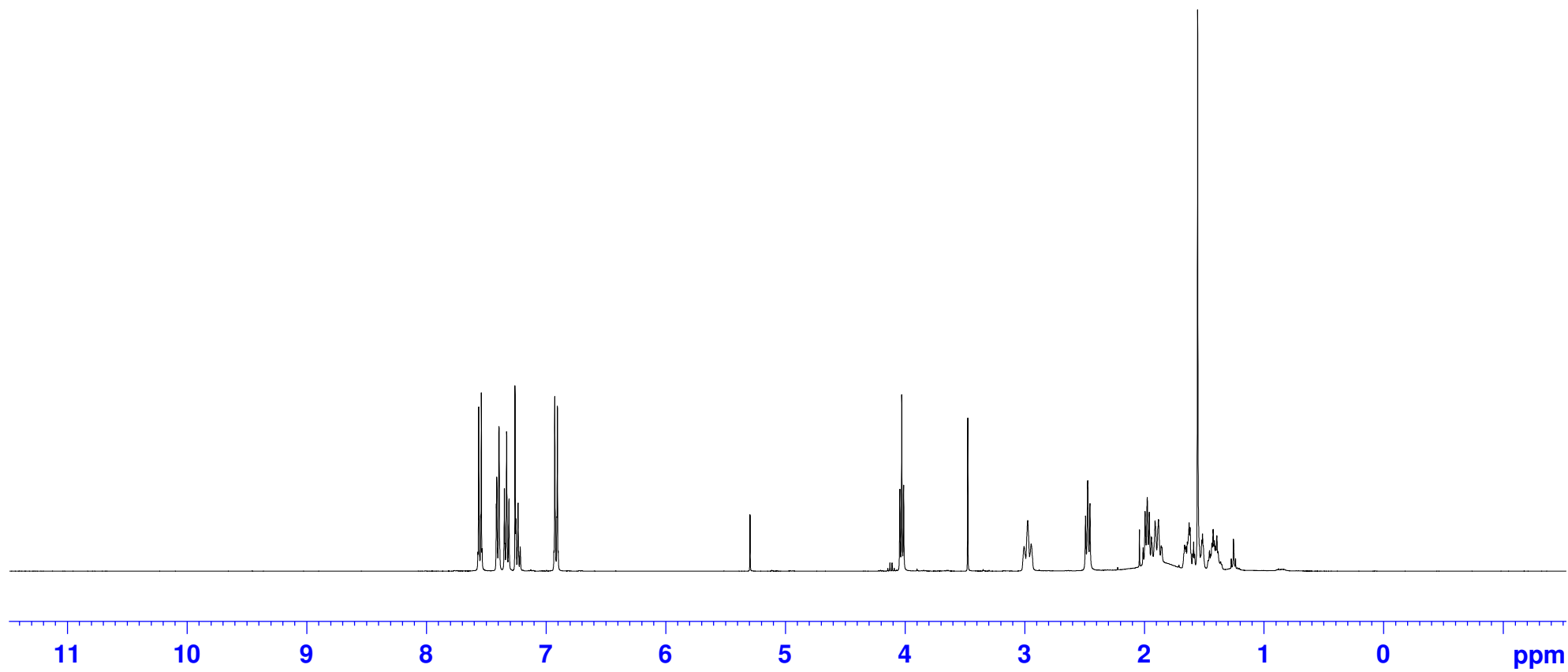


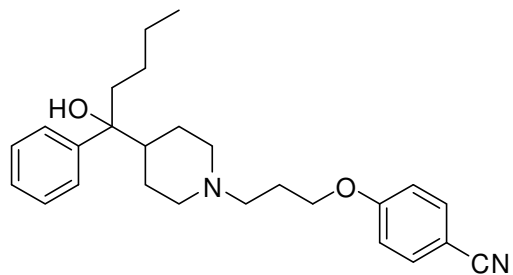
4.7
¹H NMR Spectrum
(400 MHz, CDCl₃)



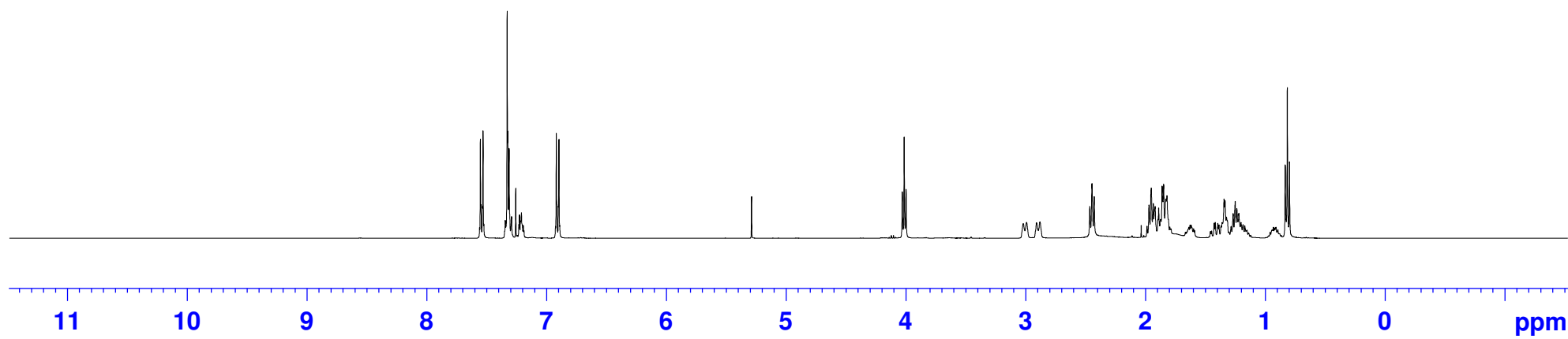


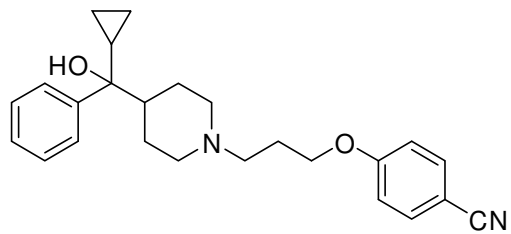
4.8
¹H NMR Spectrum
(400 MHz, CDCl₃)



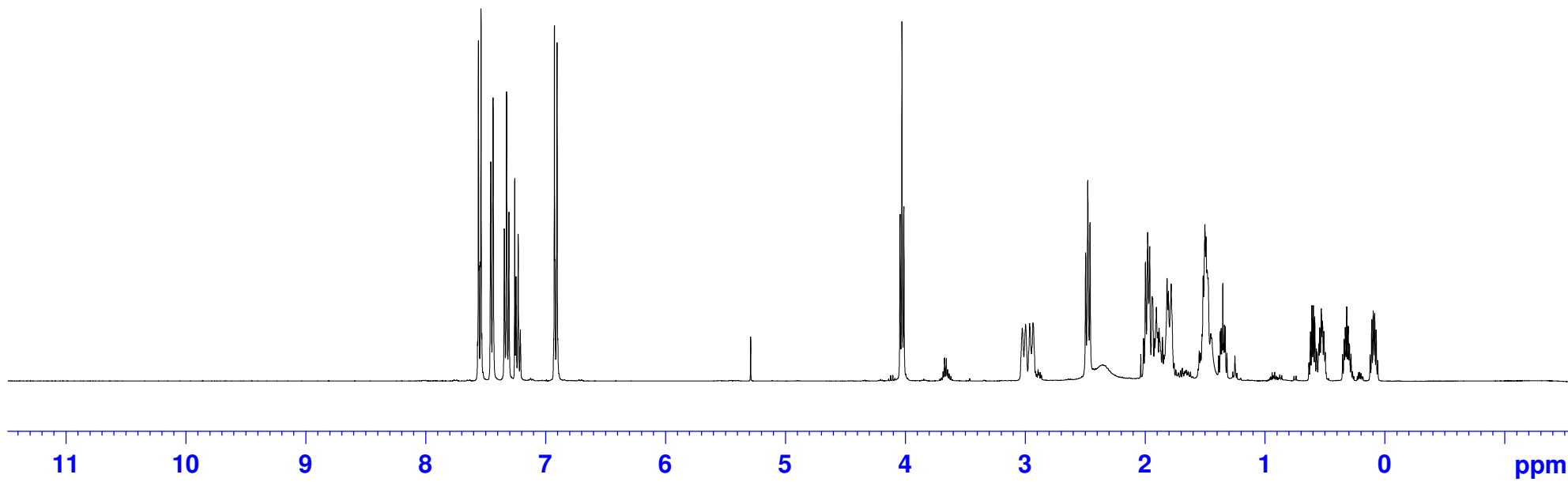


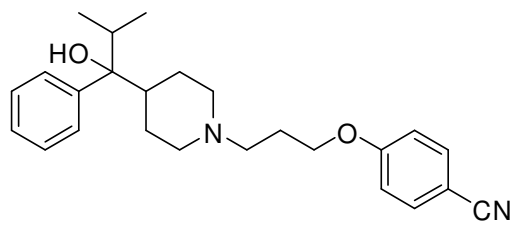
4.9
¹H NMR Spectrum
(400 MHz, CDCl₃)



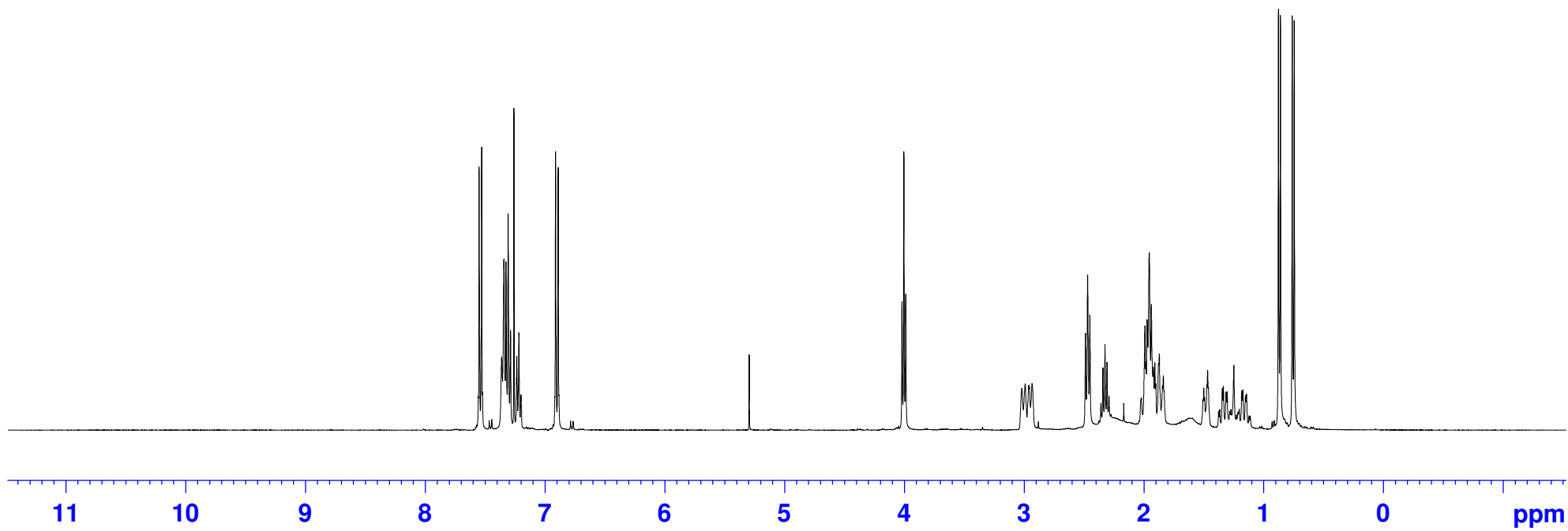


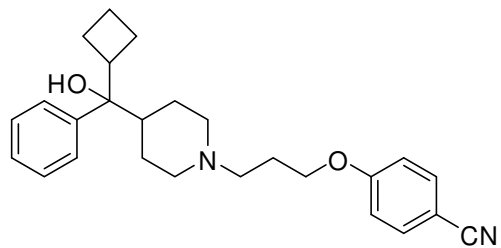
4.10
¹H NMR Spectrum
(400 MHz, CDCl₃)



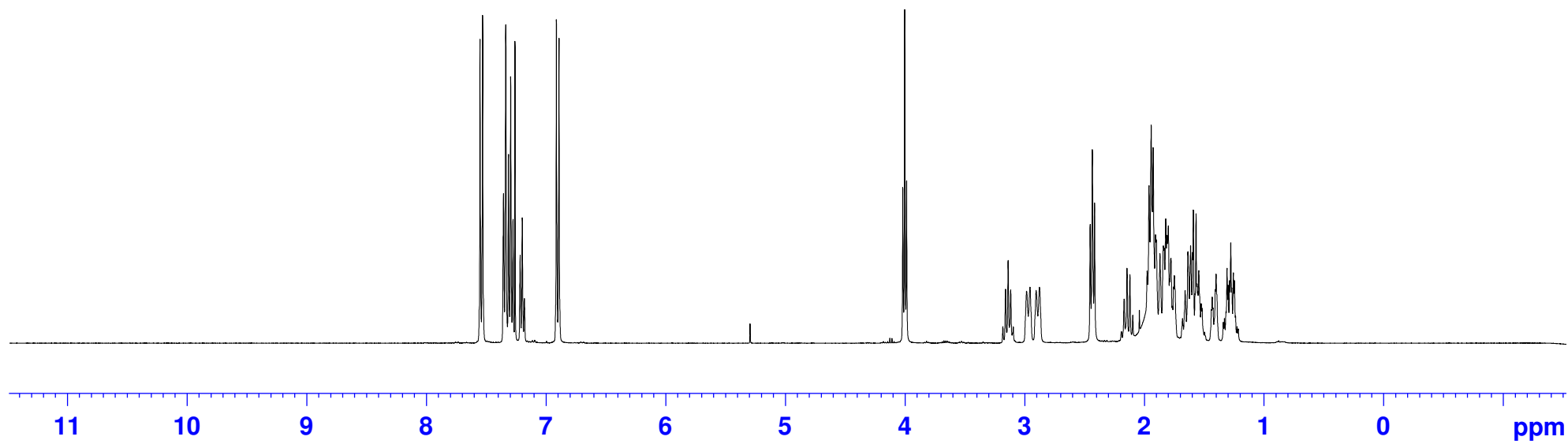


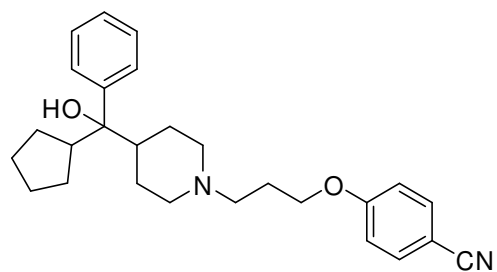
4.11
¹H NMR Spectrum
(400 MHz, CDCl₃)



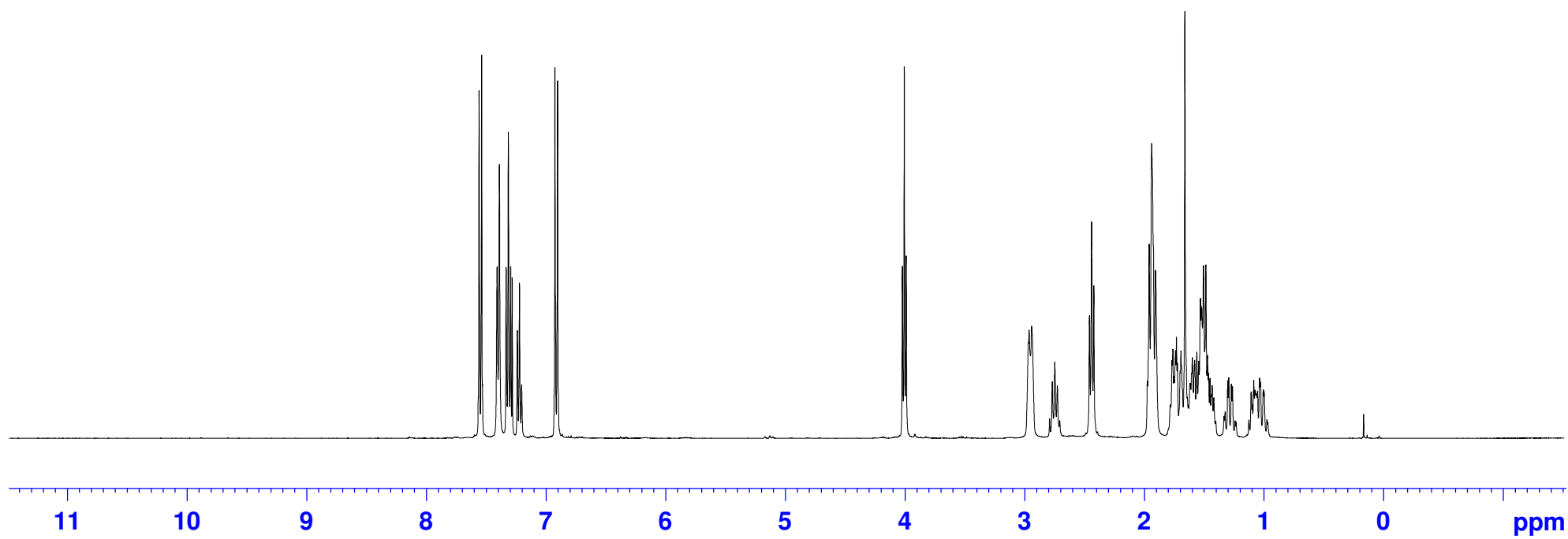


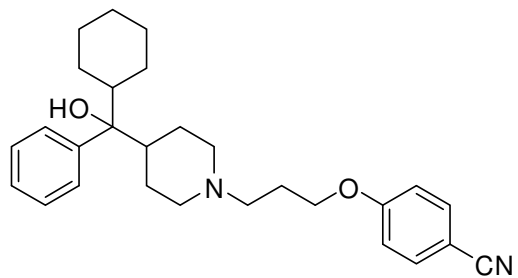
4.12
¹H NMR Spectrum
(400 MHz, CDCl₃)



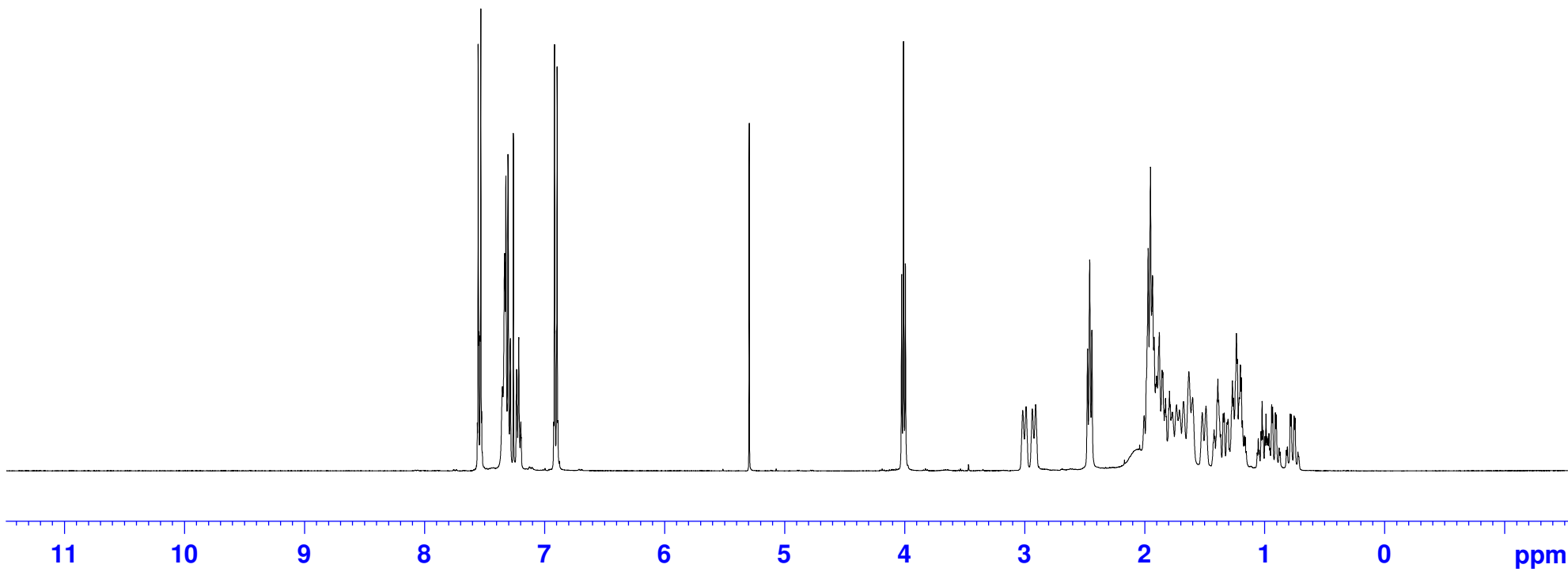


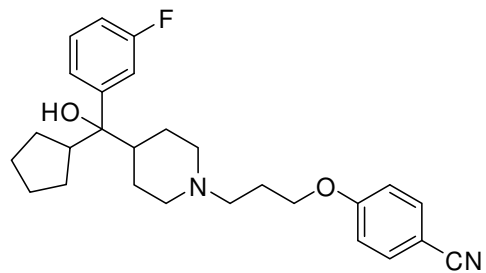
4.13
¹H NMR Spectrum
(400 MHz, CDCl₃)



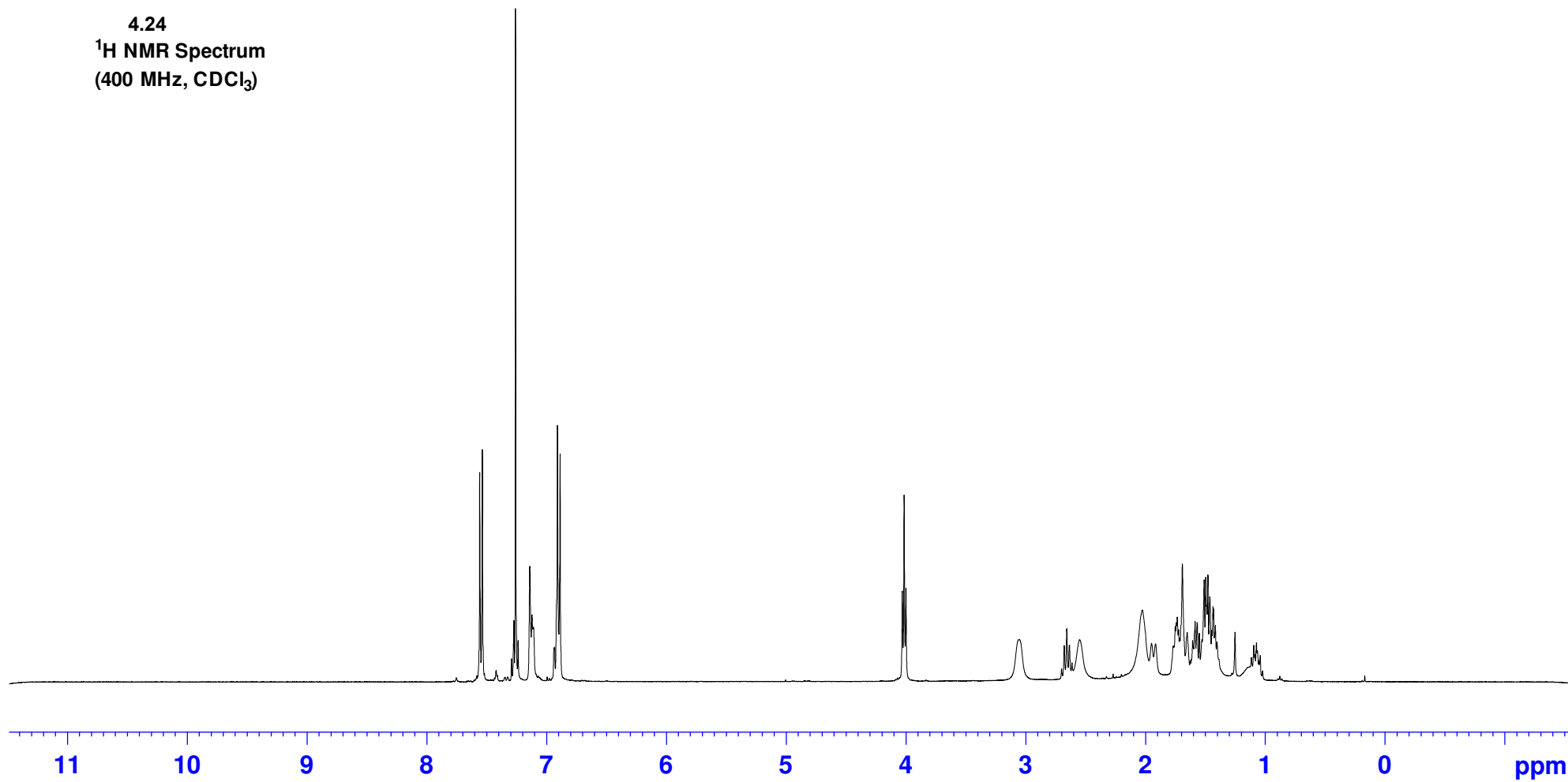


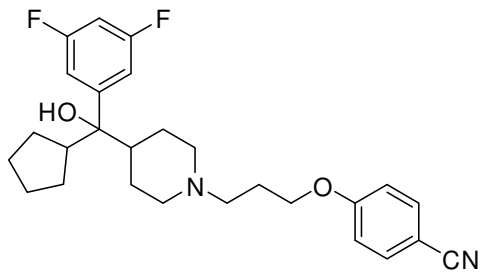
4.14
¹H NMR Spectrum
(400 MHz, CDCl₃)



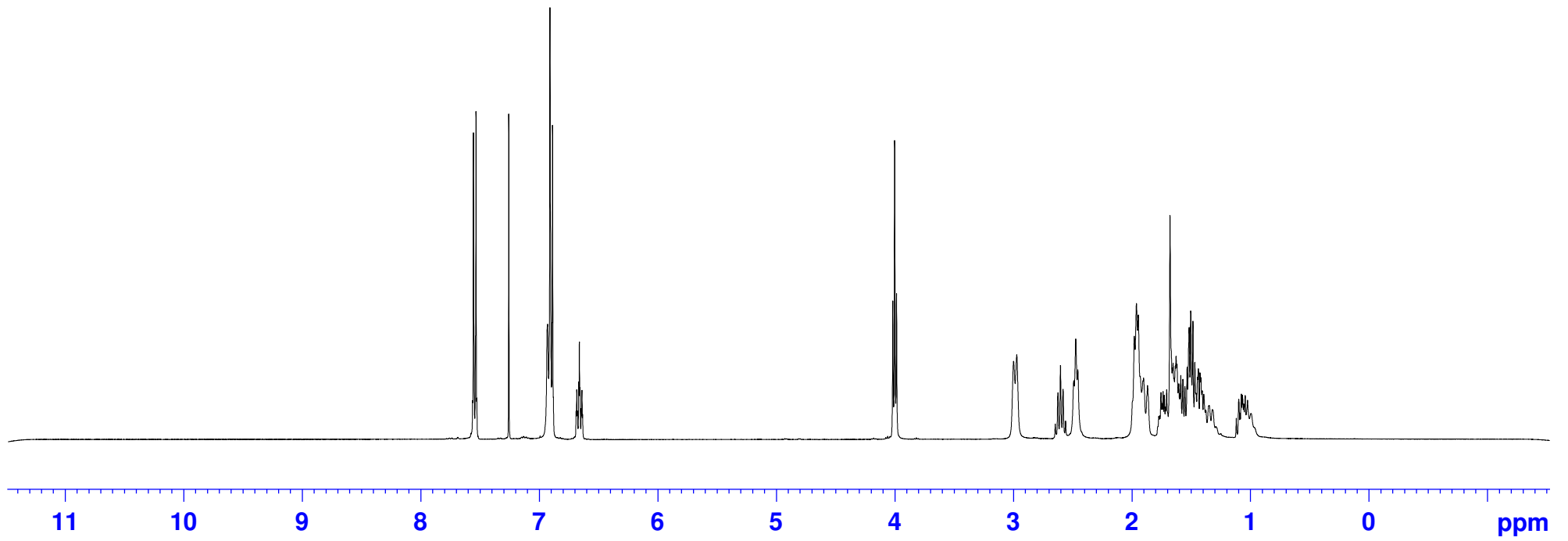


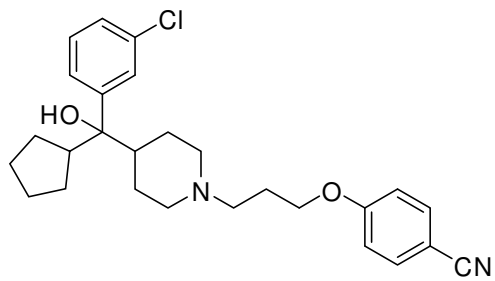
4.24
¹H NMR Spectrum
(400 MHz, CDCl₃)



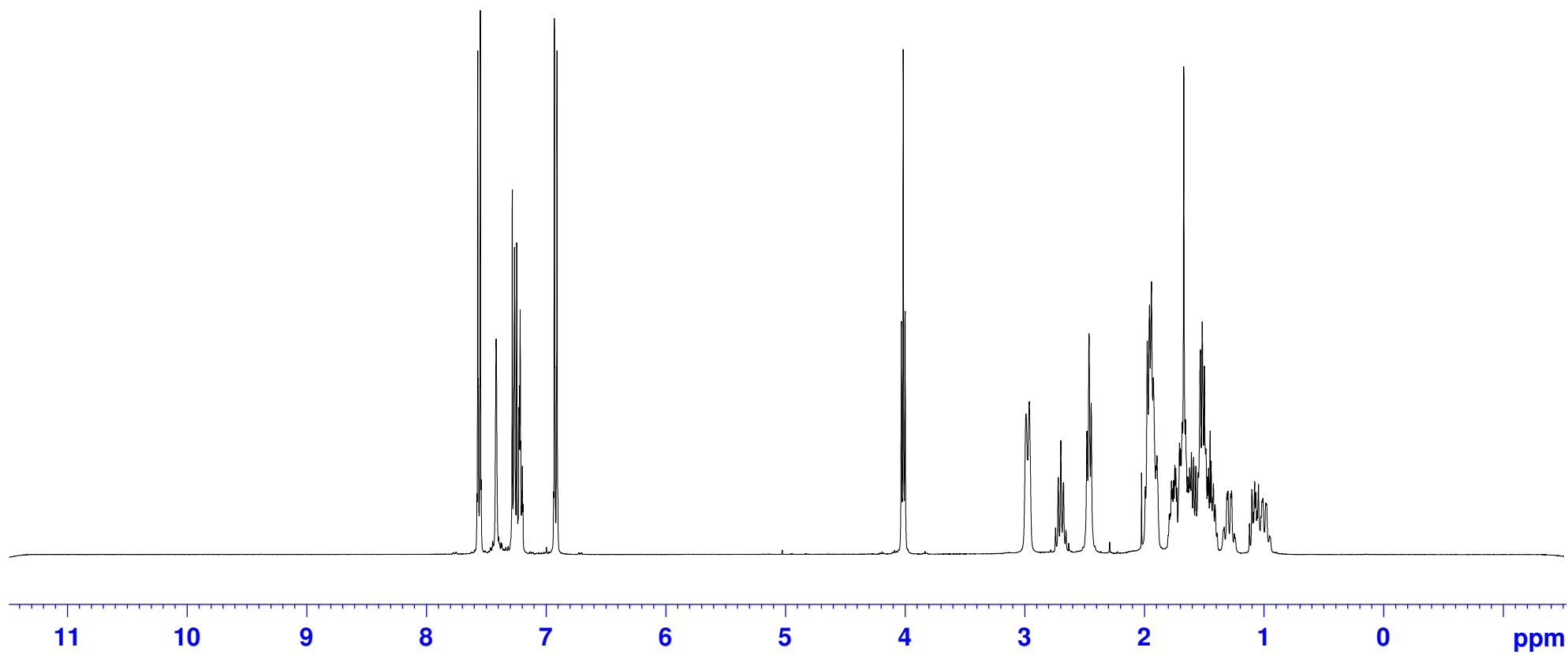


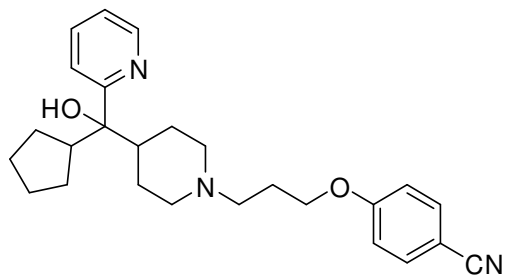
4.25
¹H NMR Spectrum
(400 MHz, CDCl₃)



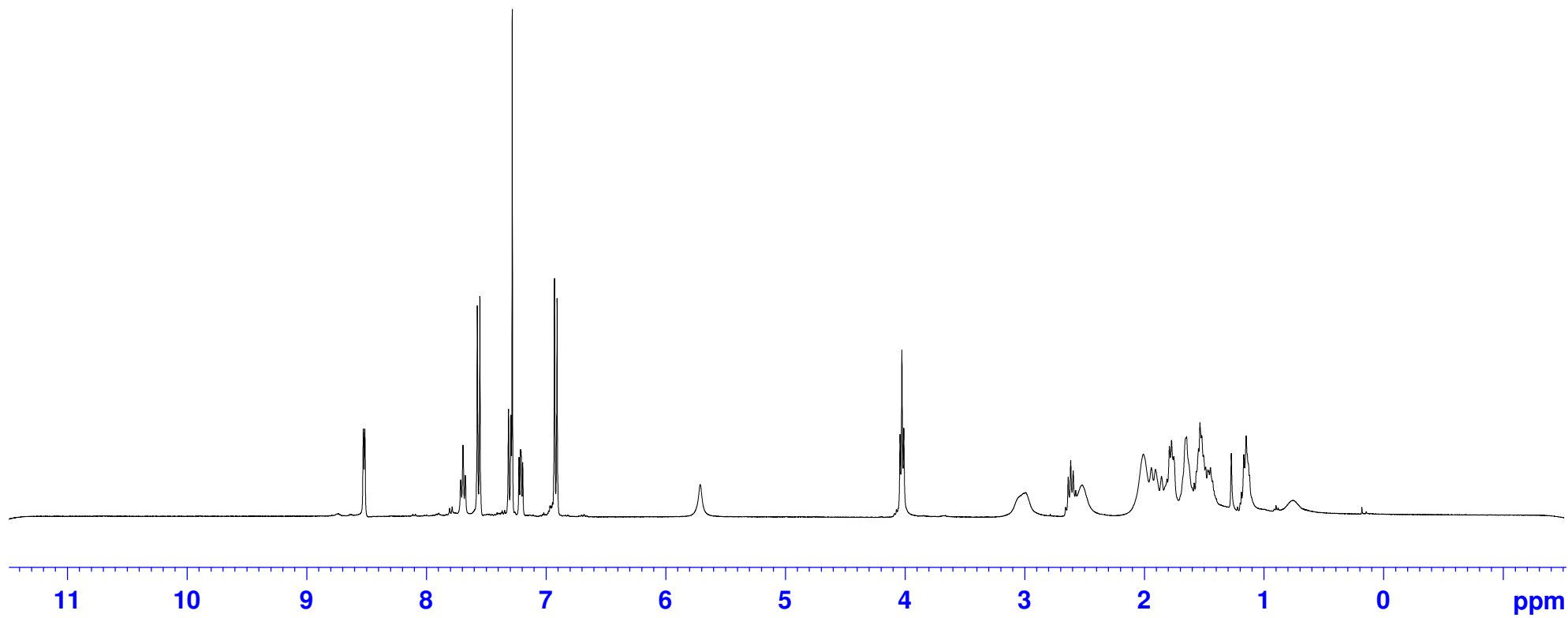


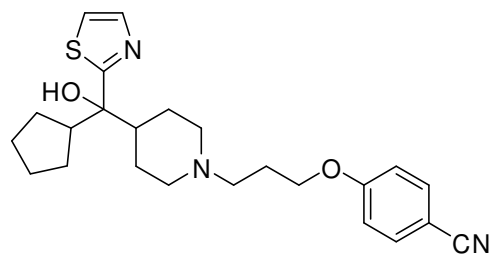
4.26
¹H NMR Spectrum
(400 MHz, CDCl₃)



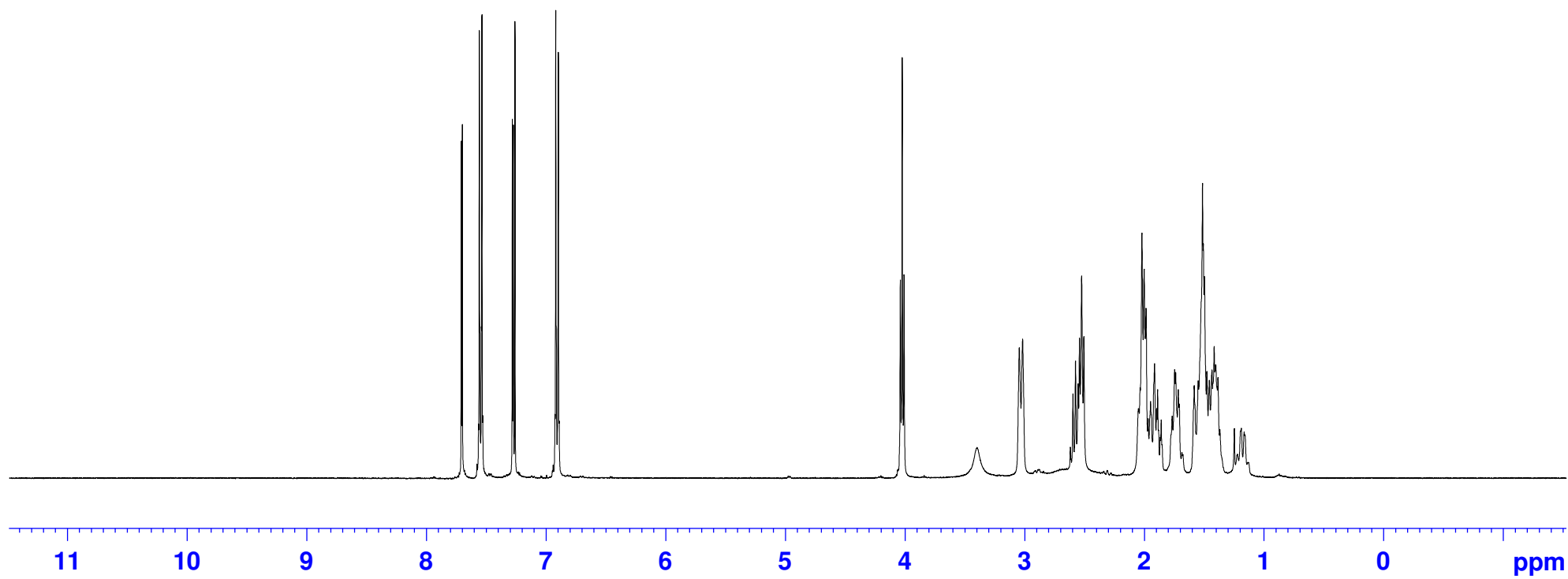


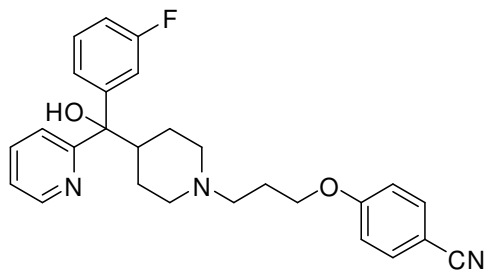
4.27
¹H NMR Spectrum
(400 MHz, CDCl₃)



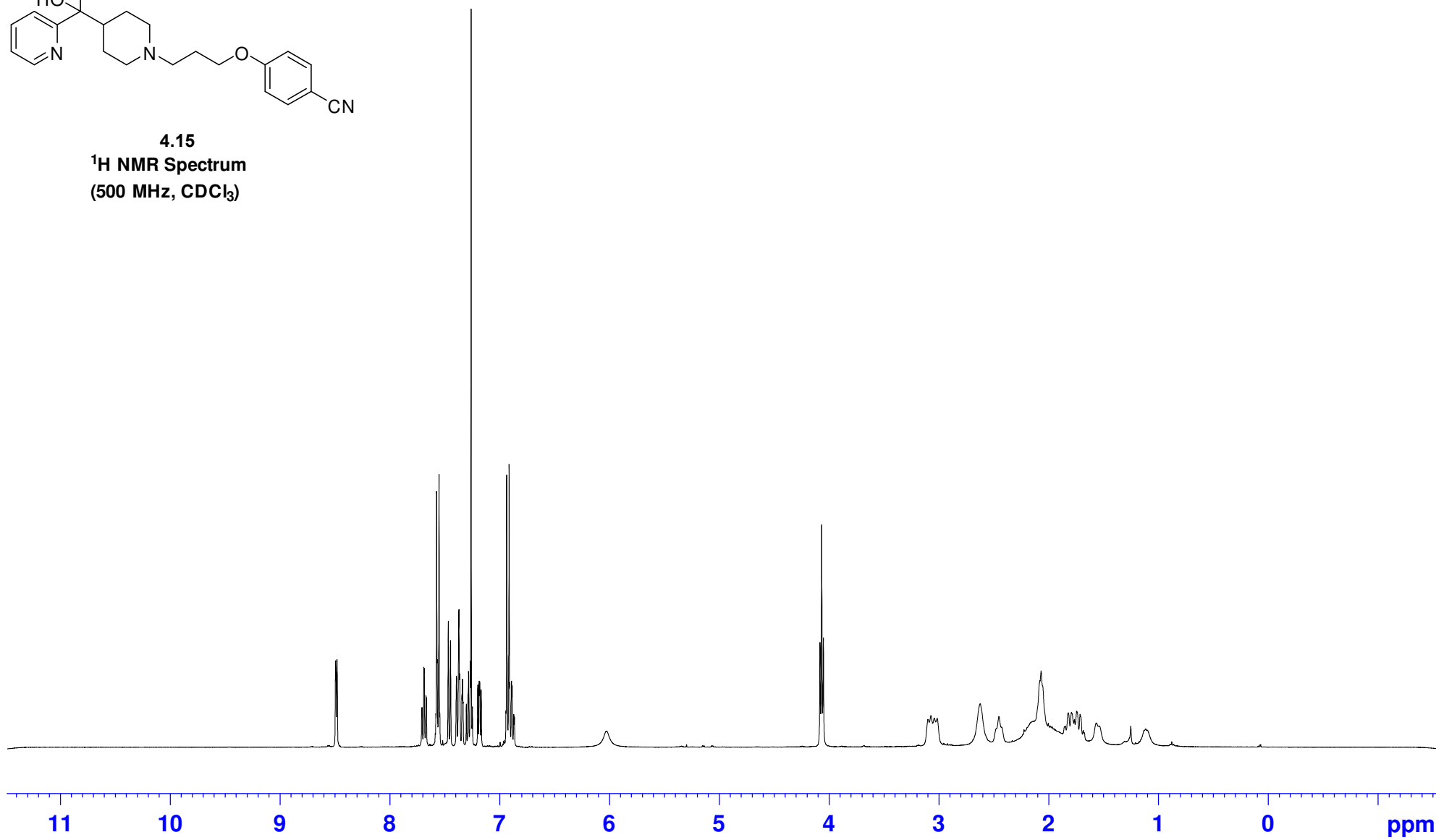


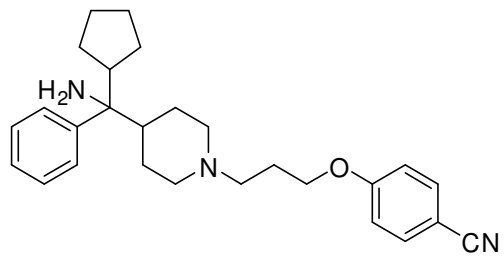
4.28
¹H NMR Spectrum
(400 MHz, CDCl₃)



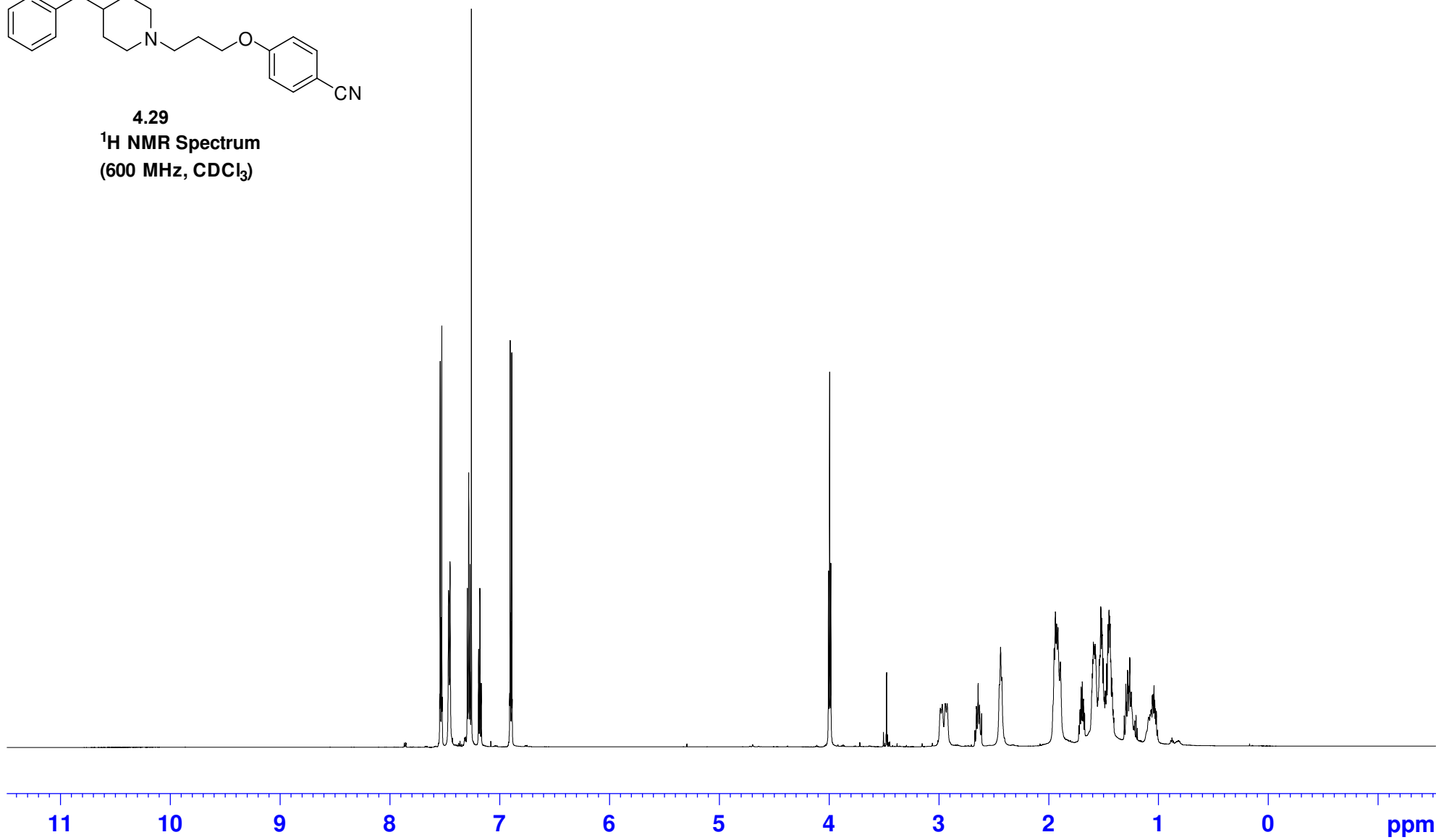


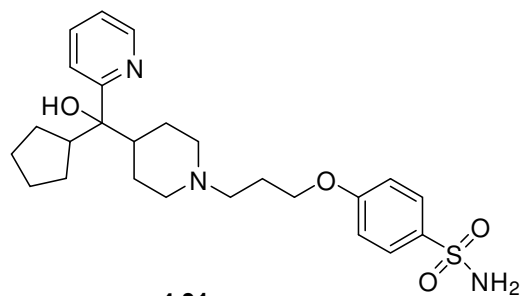
4.15
¹H NMR Spectrum
(500 MHz, CDCl₃)



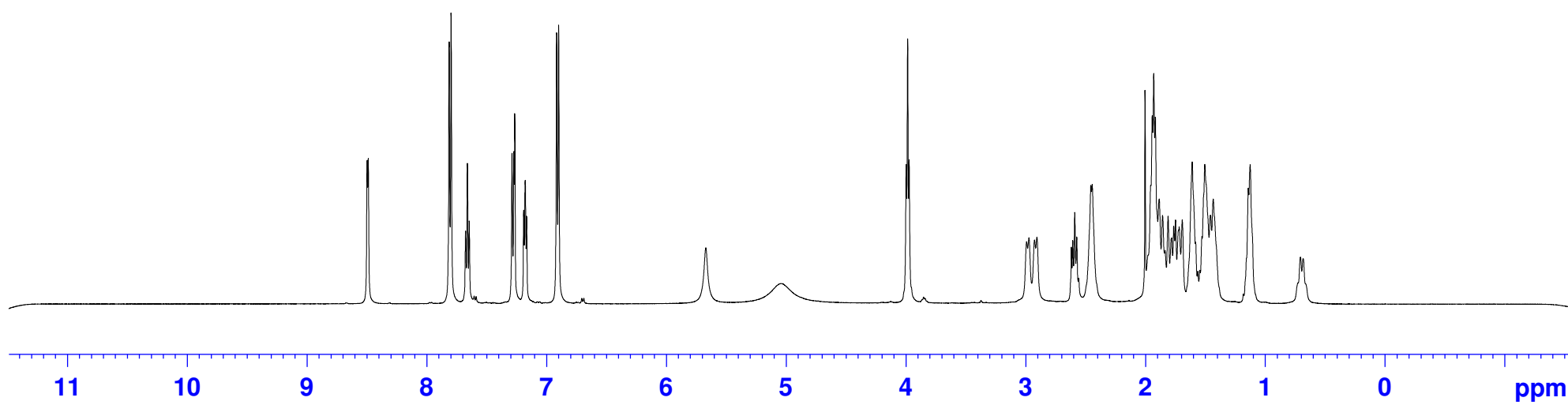


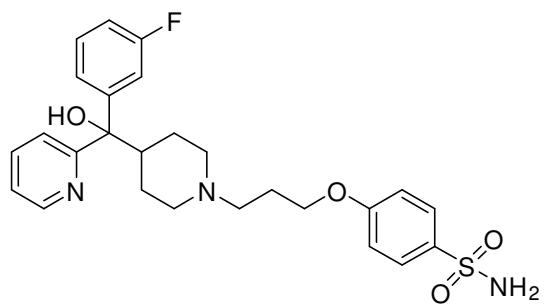
4.29
¹H NMR Spectrum
(600 MHz, CDCl₃)



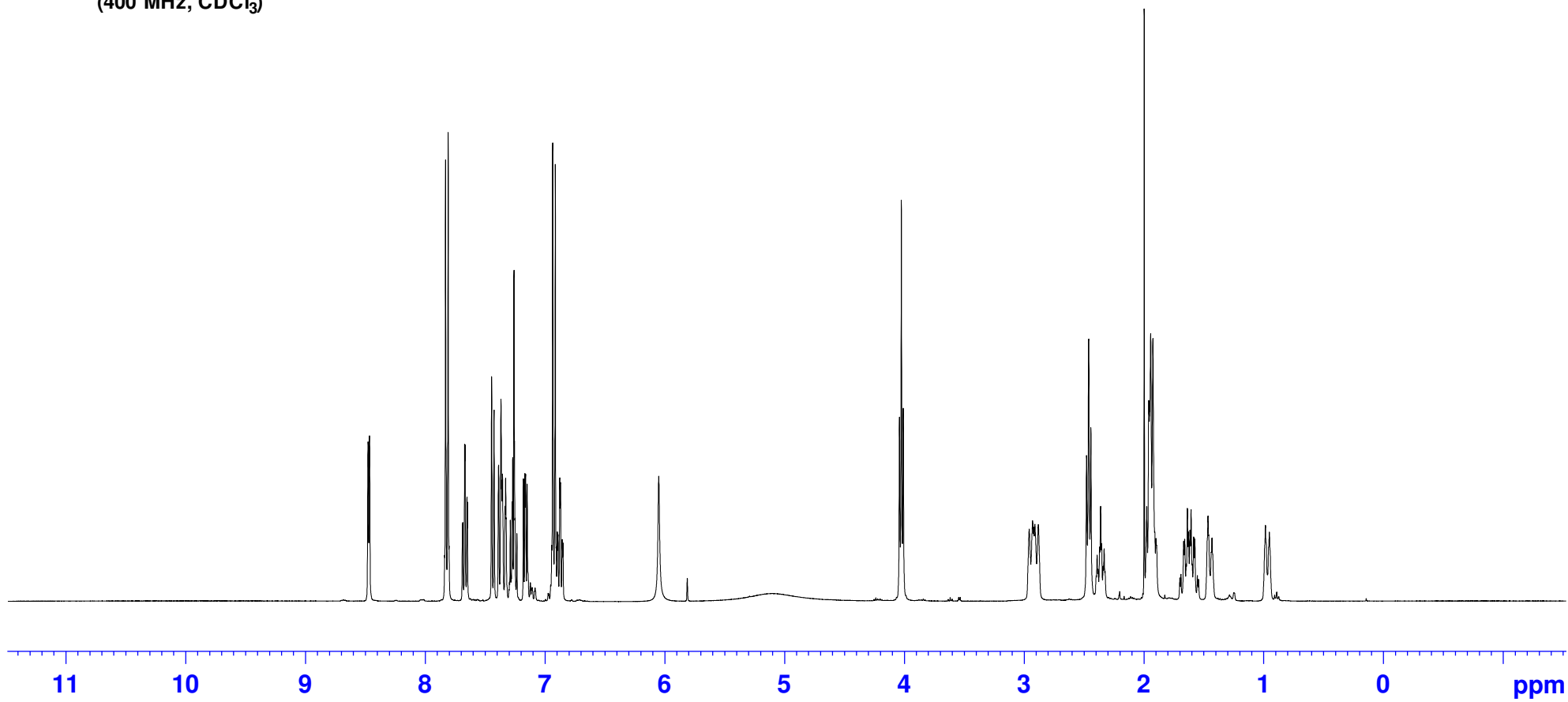


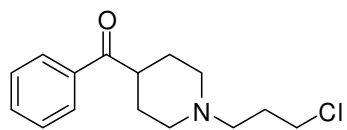
4.31
¹H NMR Spectrum
(500 MHz, CDCl₃)



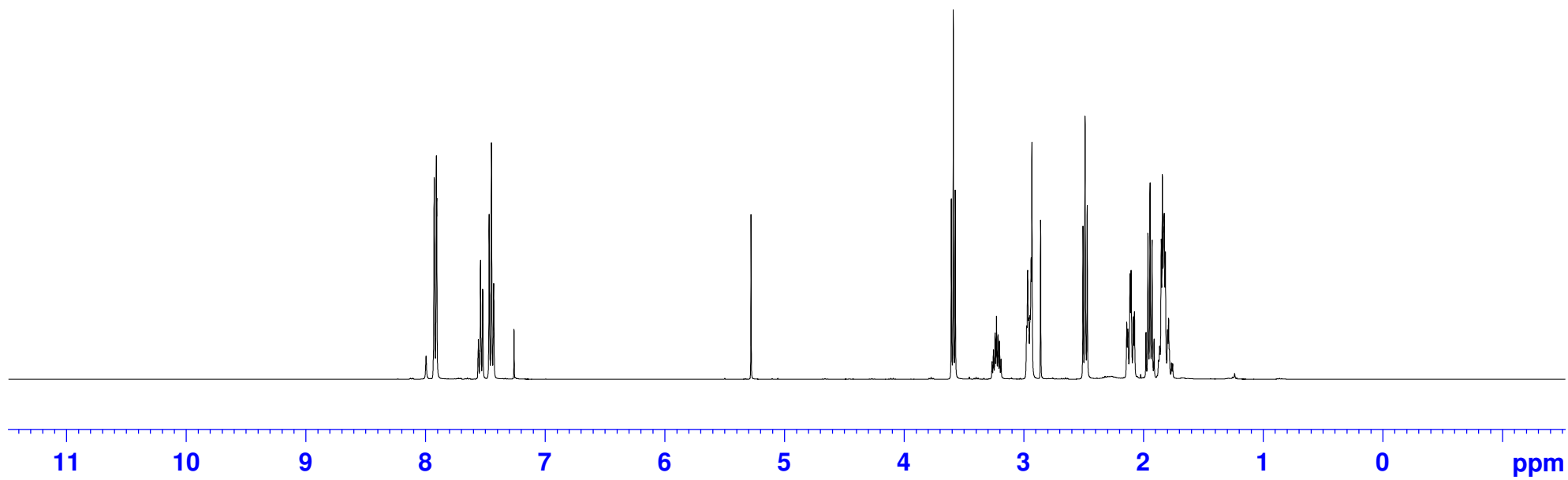


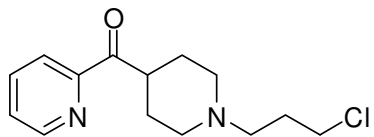
4.16
¹H NMR Spectrum
(400 MHz, CDCl₃)



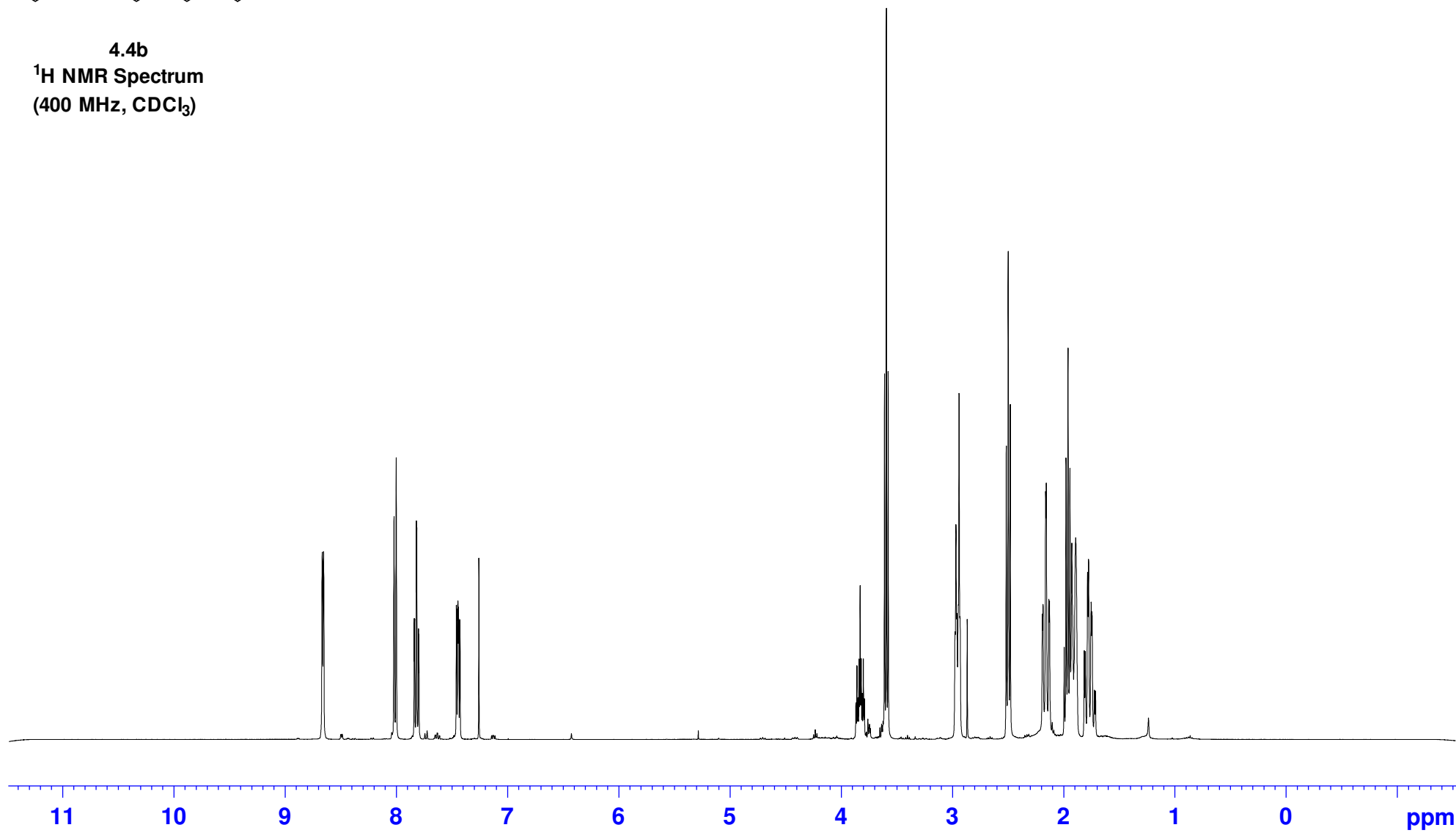


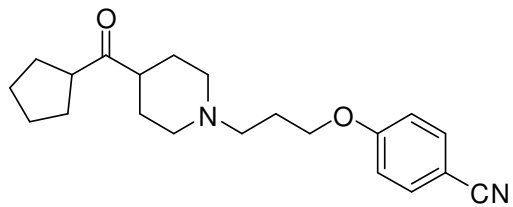
4.4a
¹H NMR Spectrum
(400 MHz, CDCl₃)



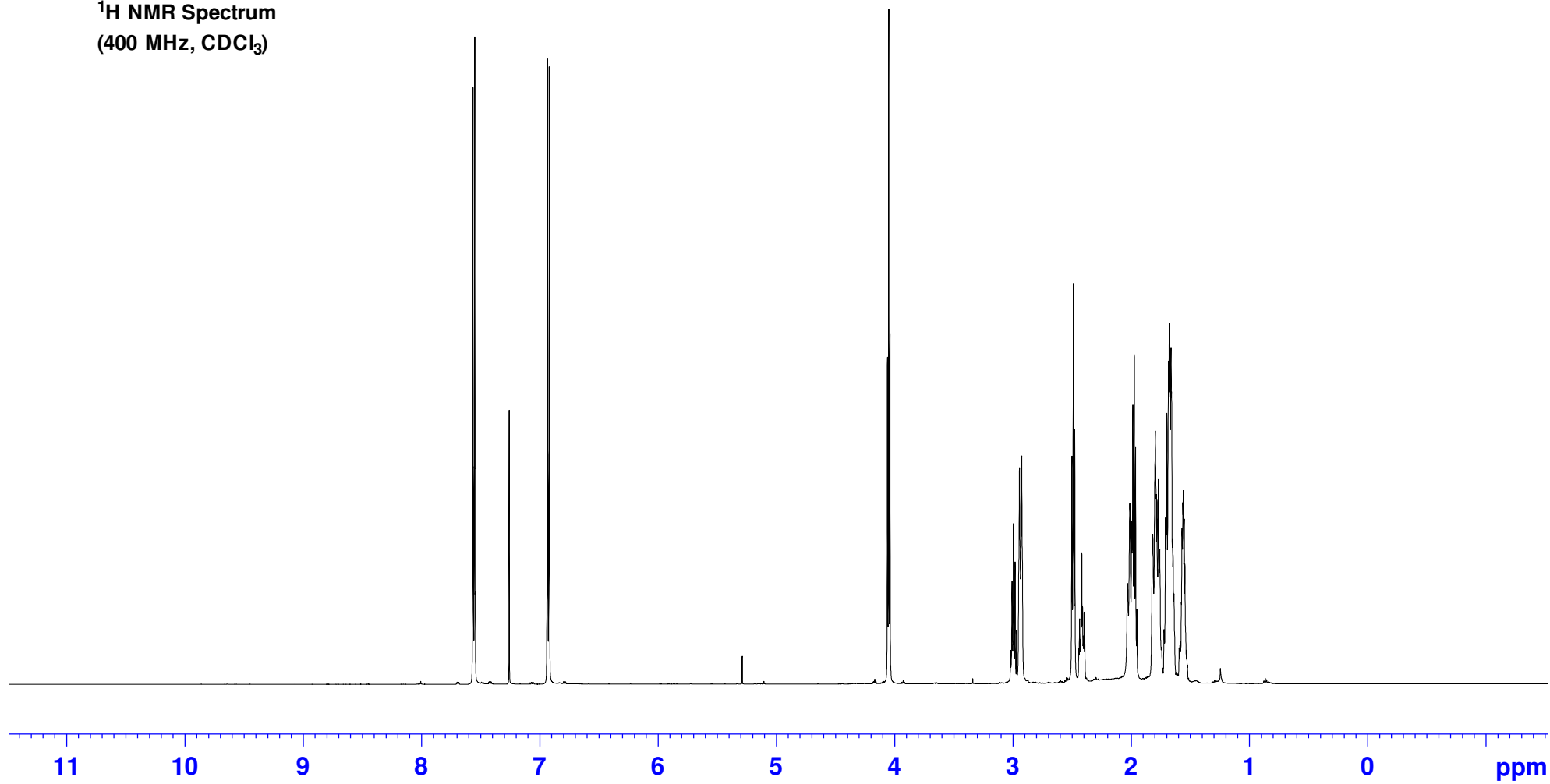


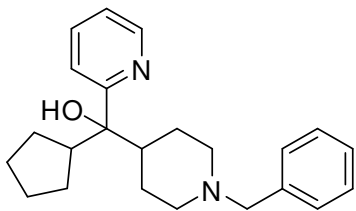
4.4b
¹H NMR Spectrum
(400 MHz, CDCl₃)



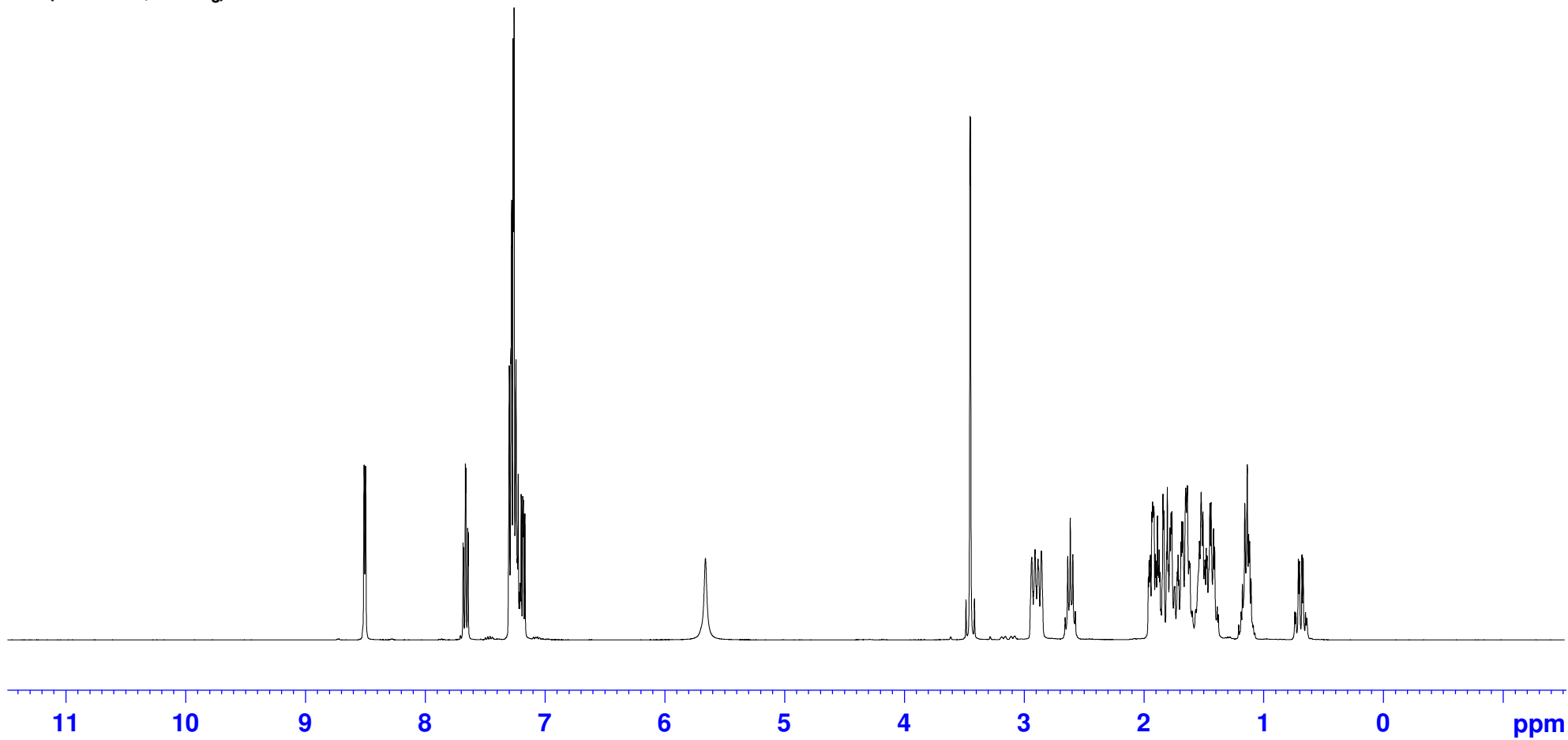


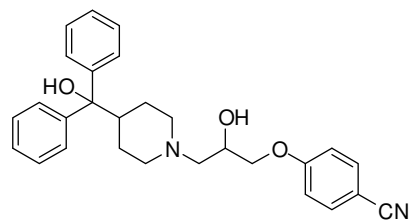
4.23
¹H NMR Spectrum
(400 MHz, CDCl₃)



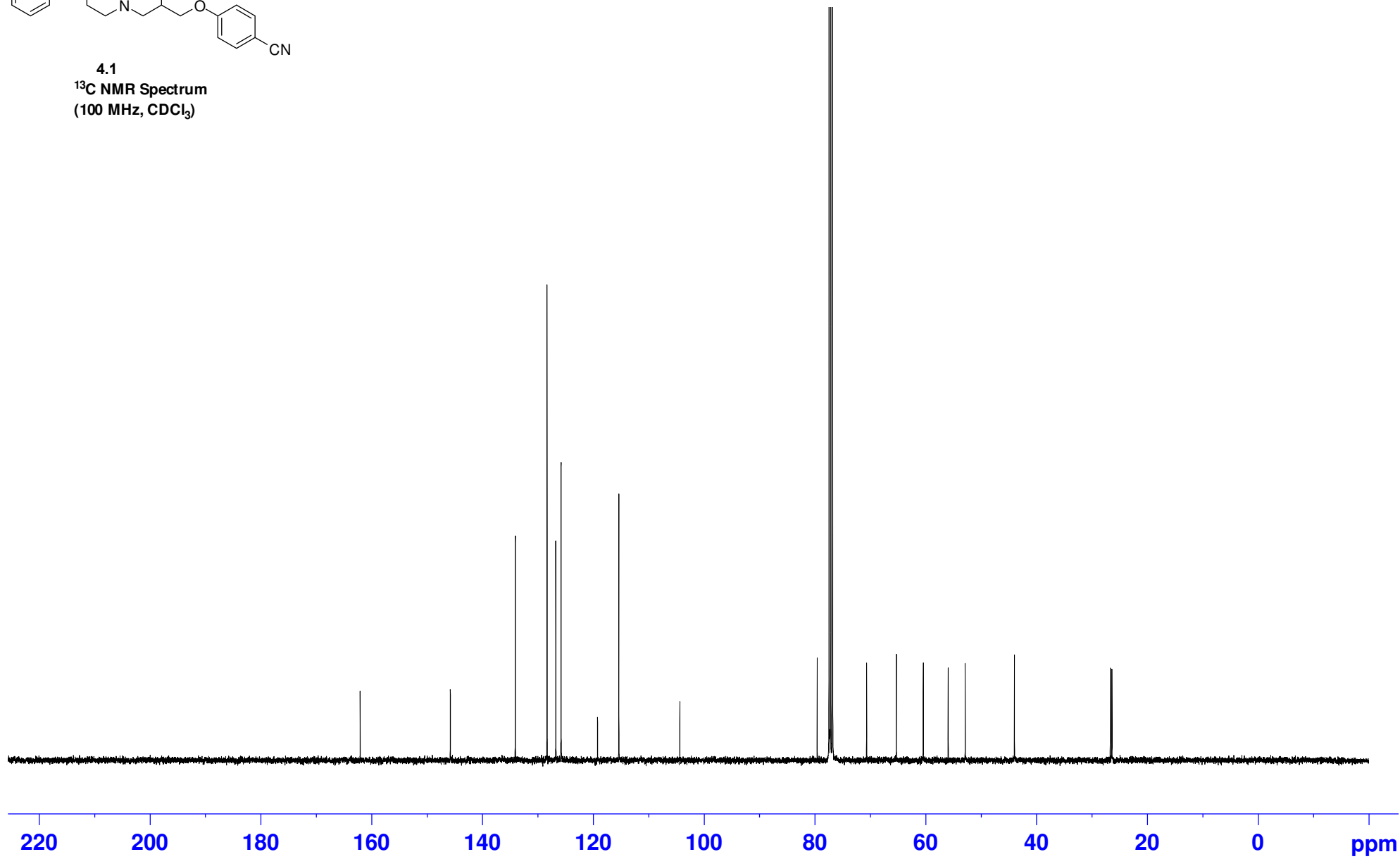


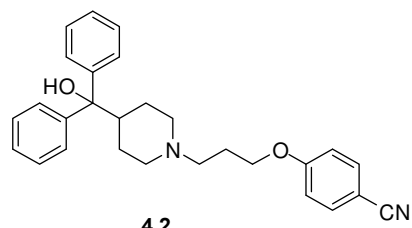
4.33
¹H NMR Spectrum
(400 MHz, CDCl₃)



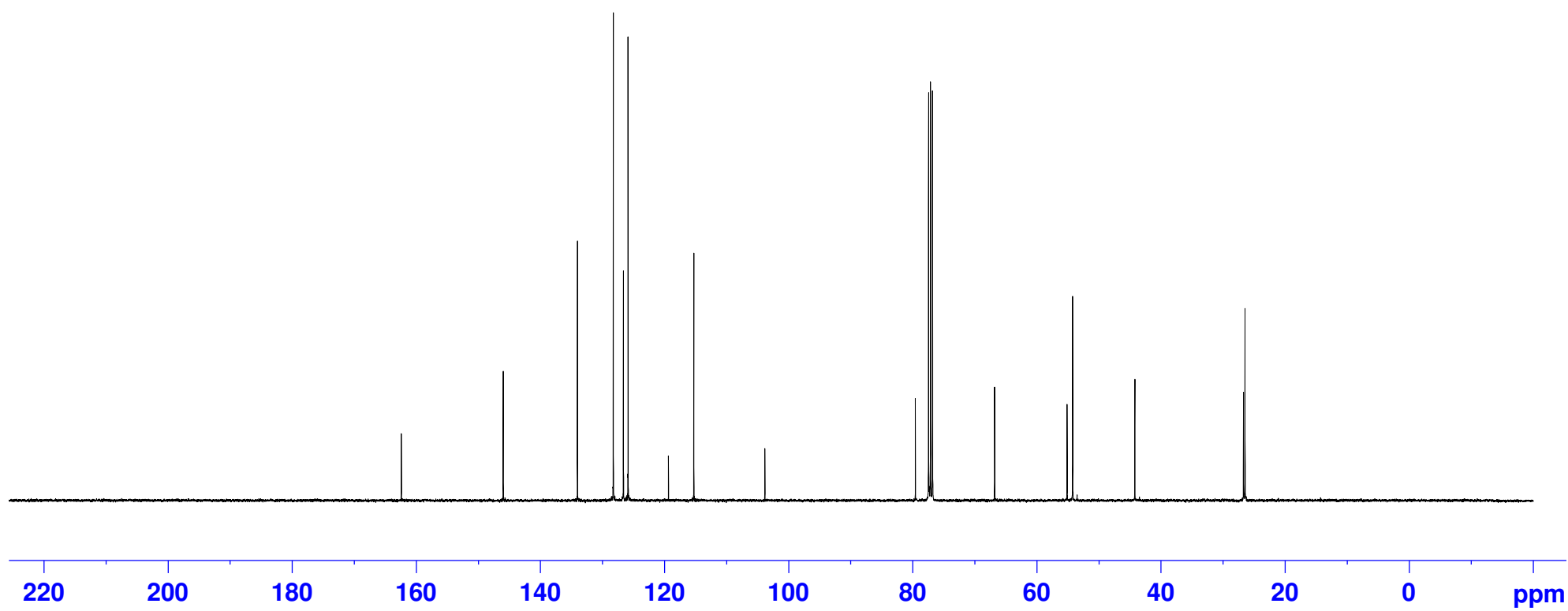


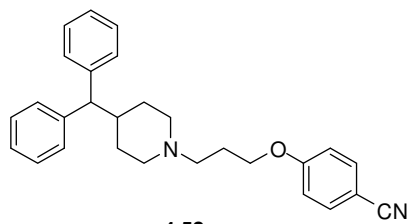
4.1
¹³C NMR Spectrum
(100 MHz, CDCl₃)





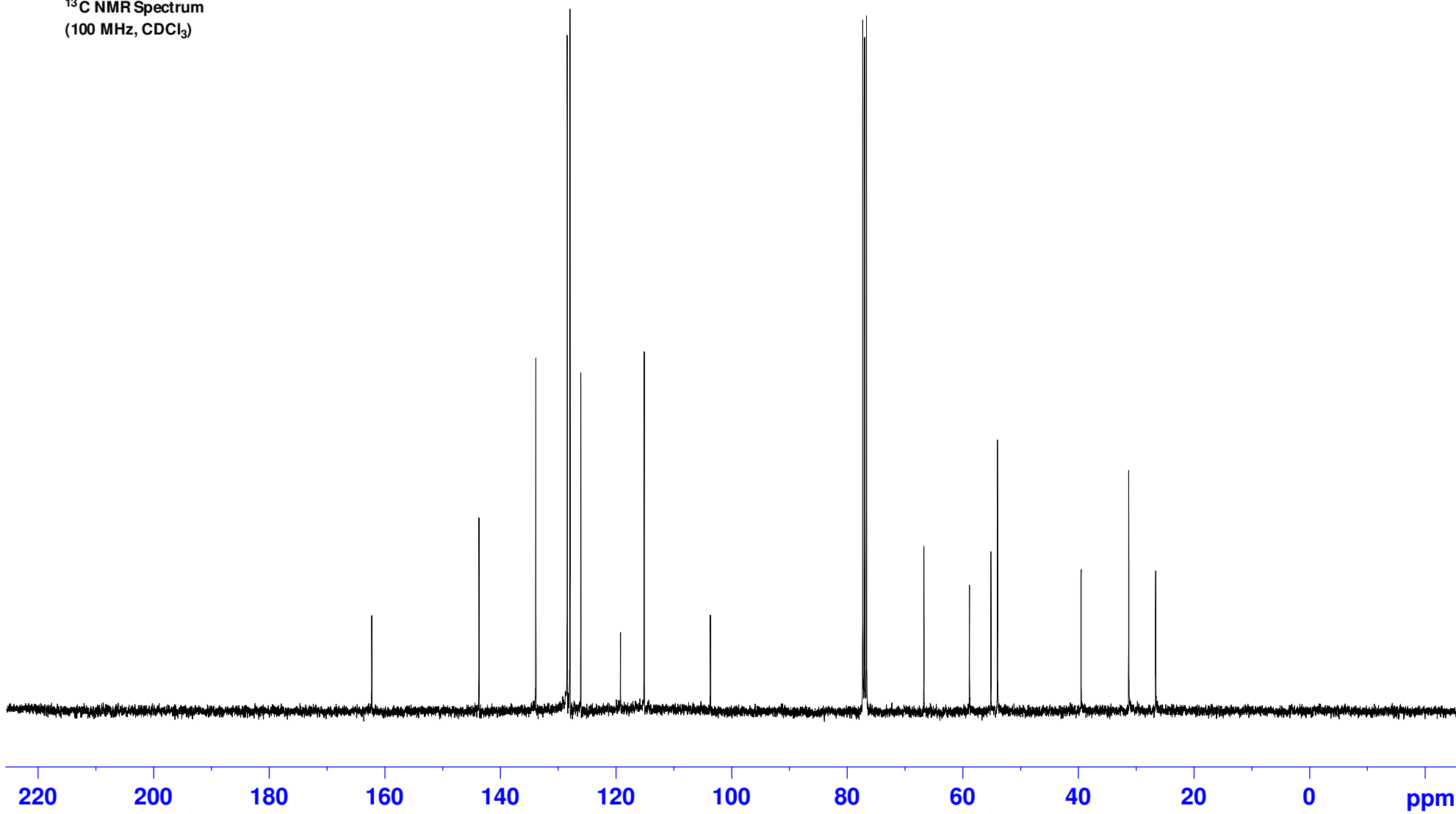
4.2
¹³C NMR Spectrum
(100 MHz, CDCl₃)

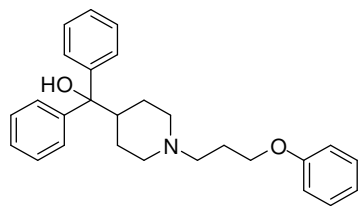




4.53

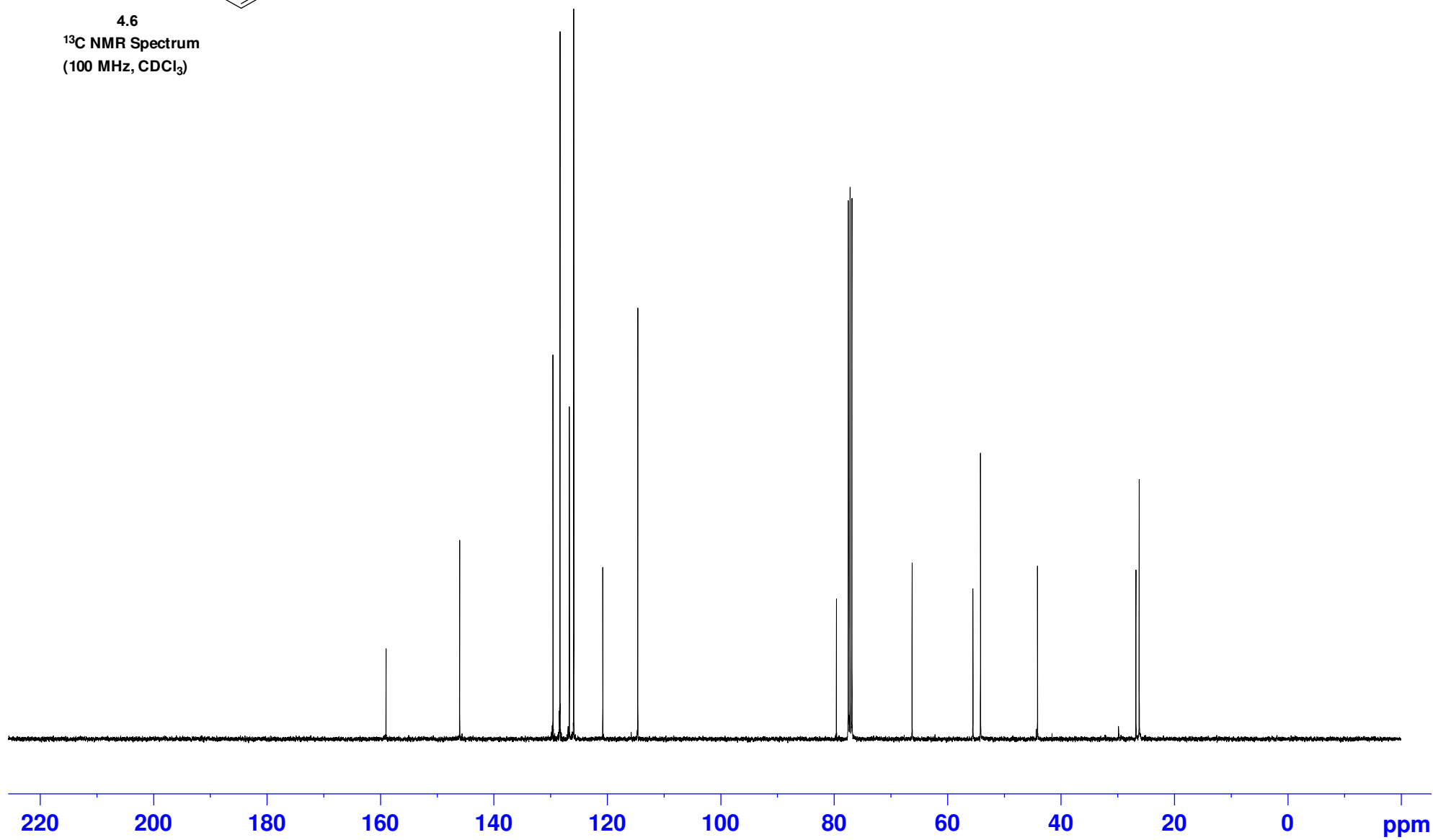
¹³C NMR Spectrum
(100 MHz, CDCl₃)

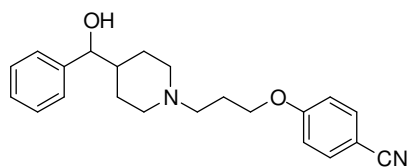




4.6

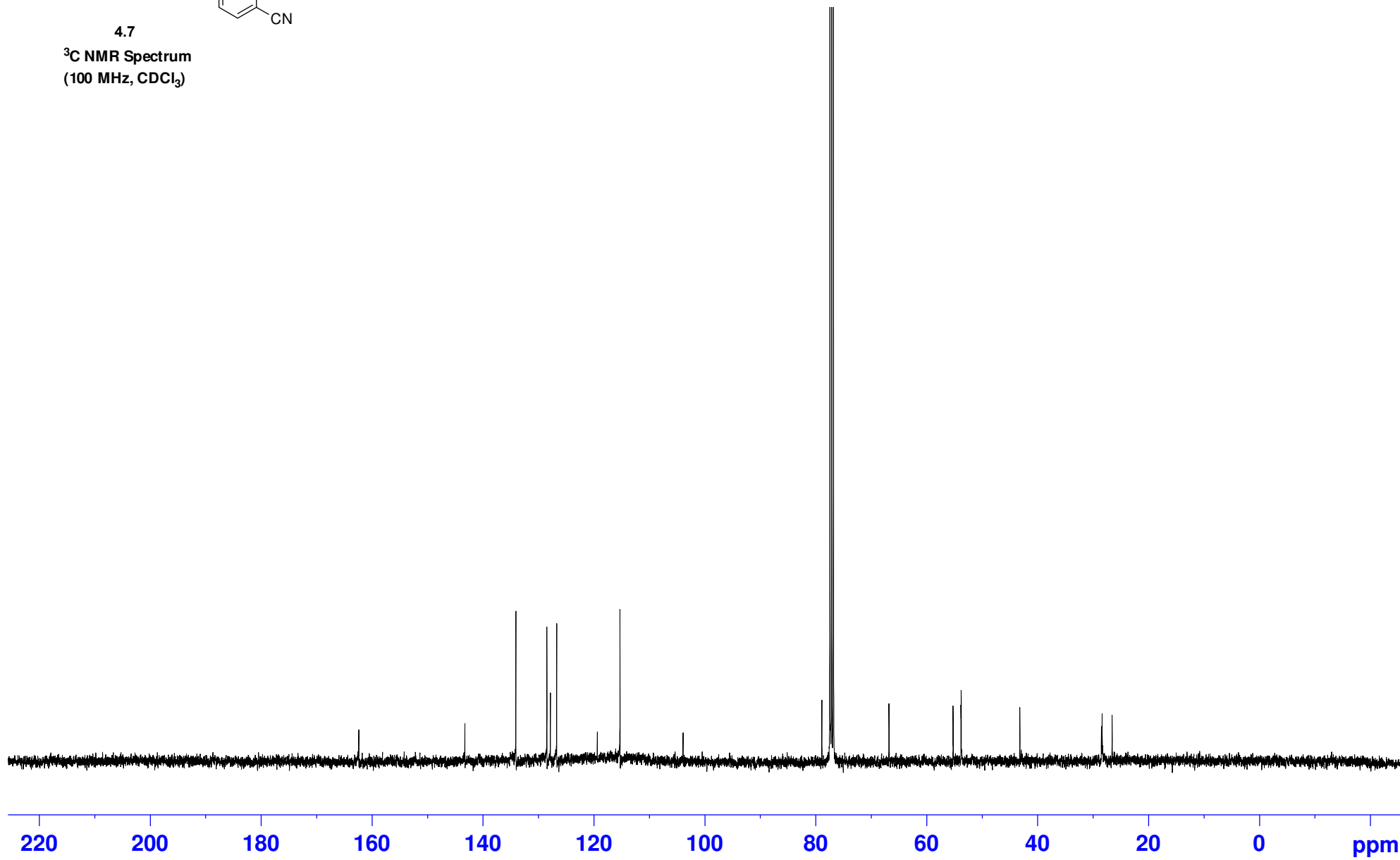
¹³C NMR Spectrum
(100 MHz, CDCl₃)

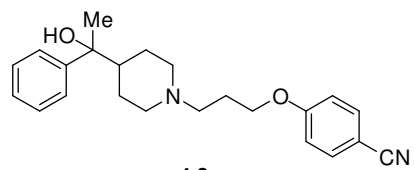




4.7

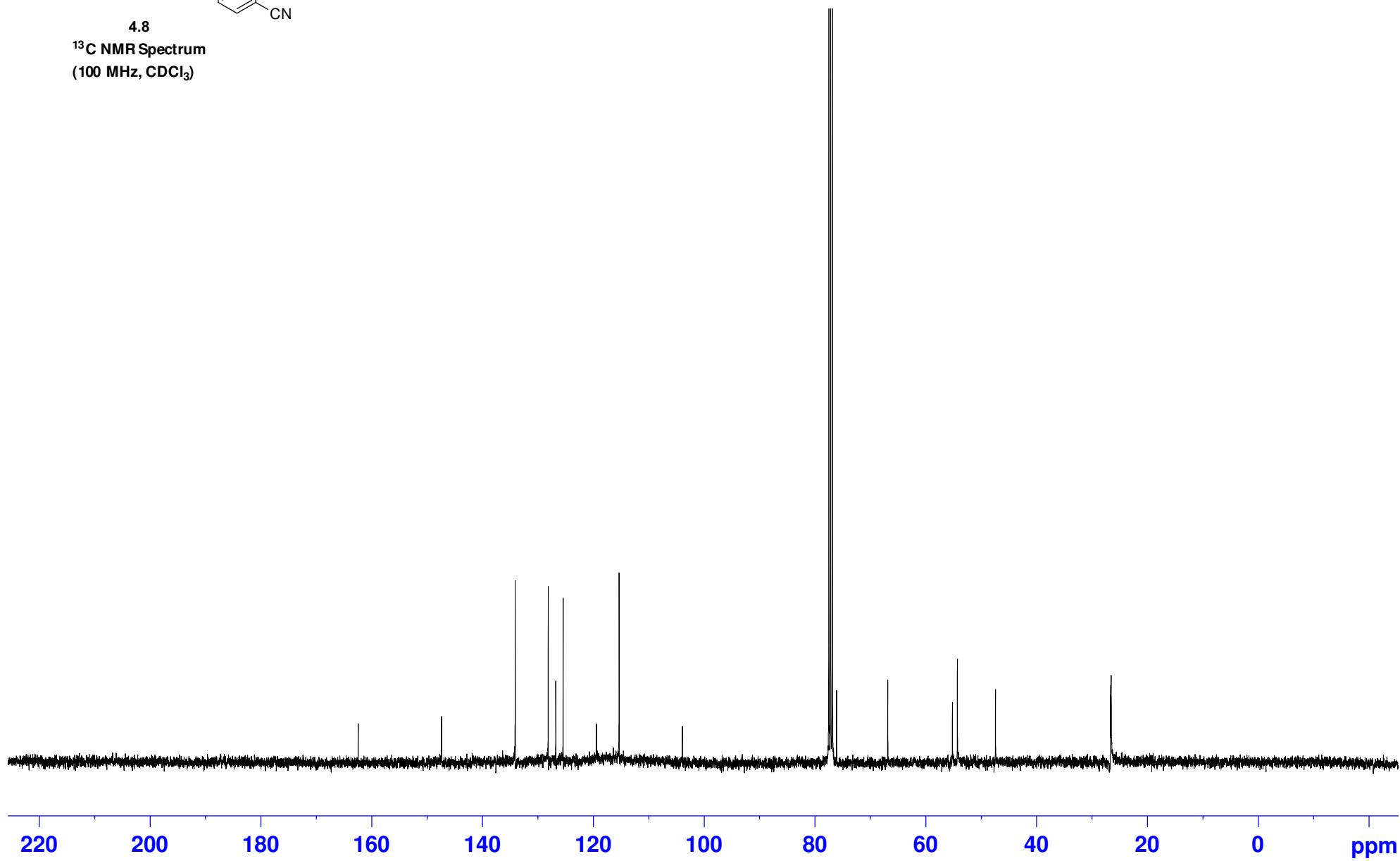
¹³C NMR Spectrum
(100 MHz, CDCl₃)

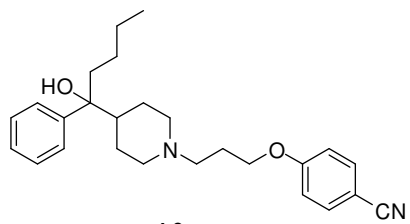




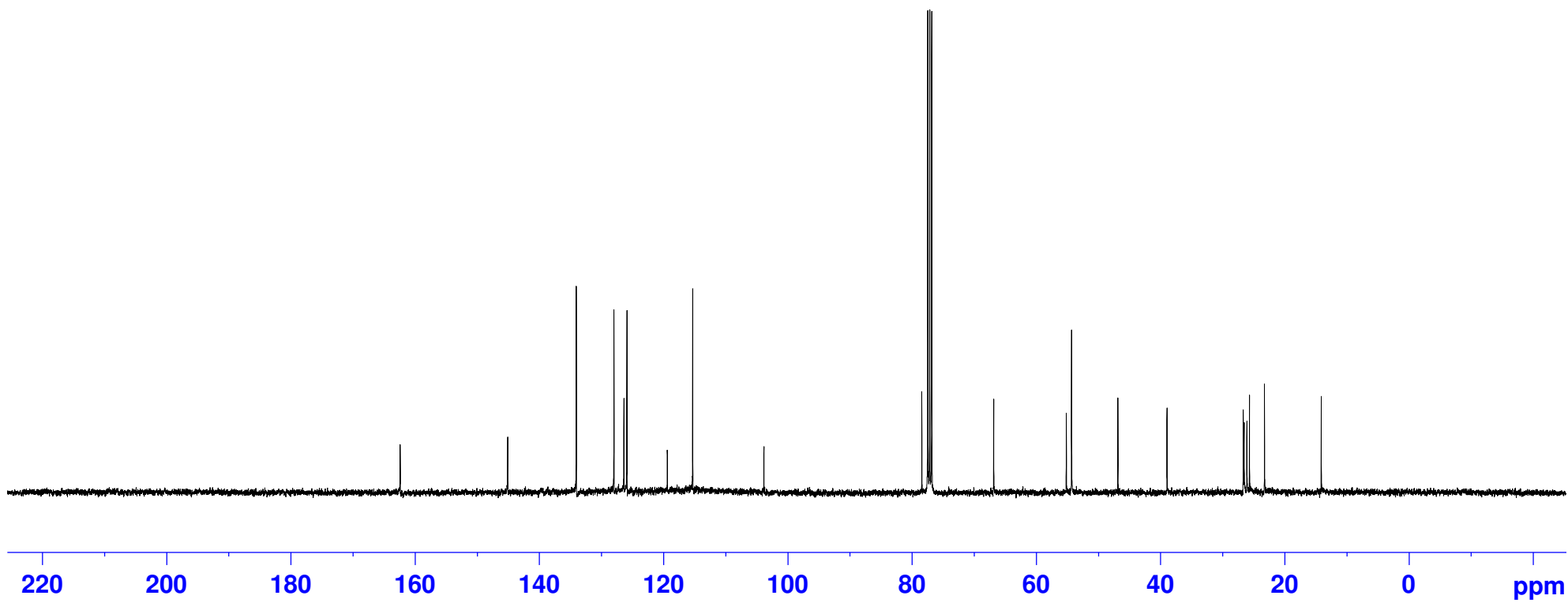
4.8

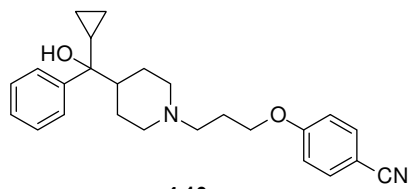
¹³C NMR Spectrum
(100 MHz, CDCl₃)





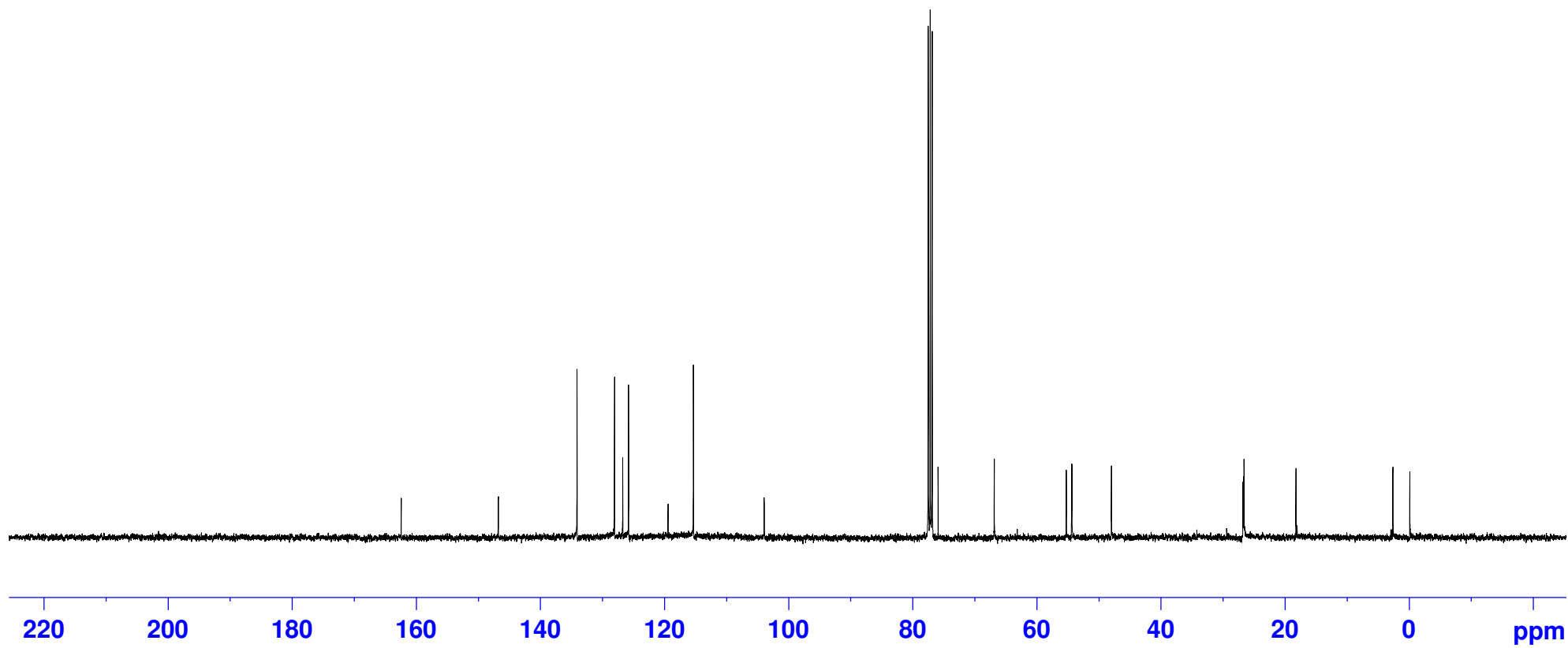
4.9
¹³C NMR Spectrum
(100 MHz, CDCl₃)

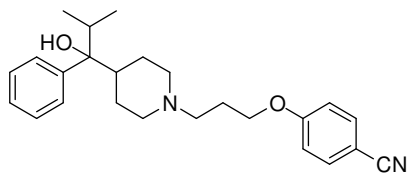




4.10

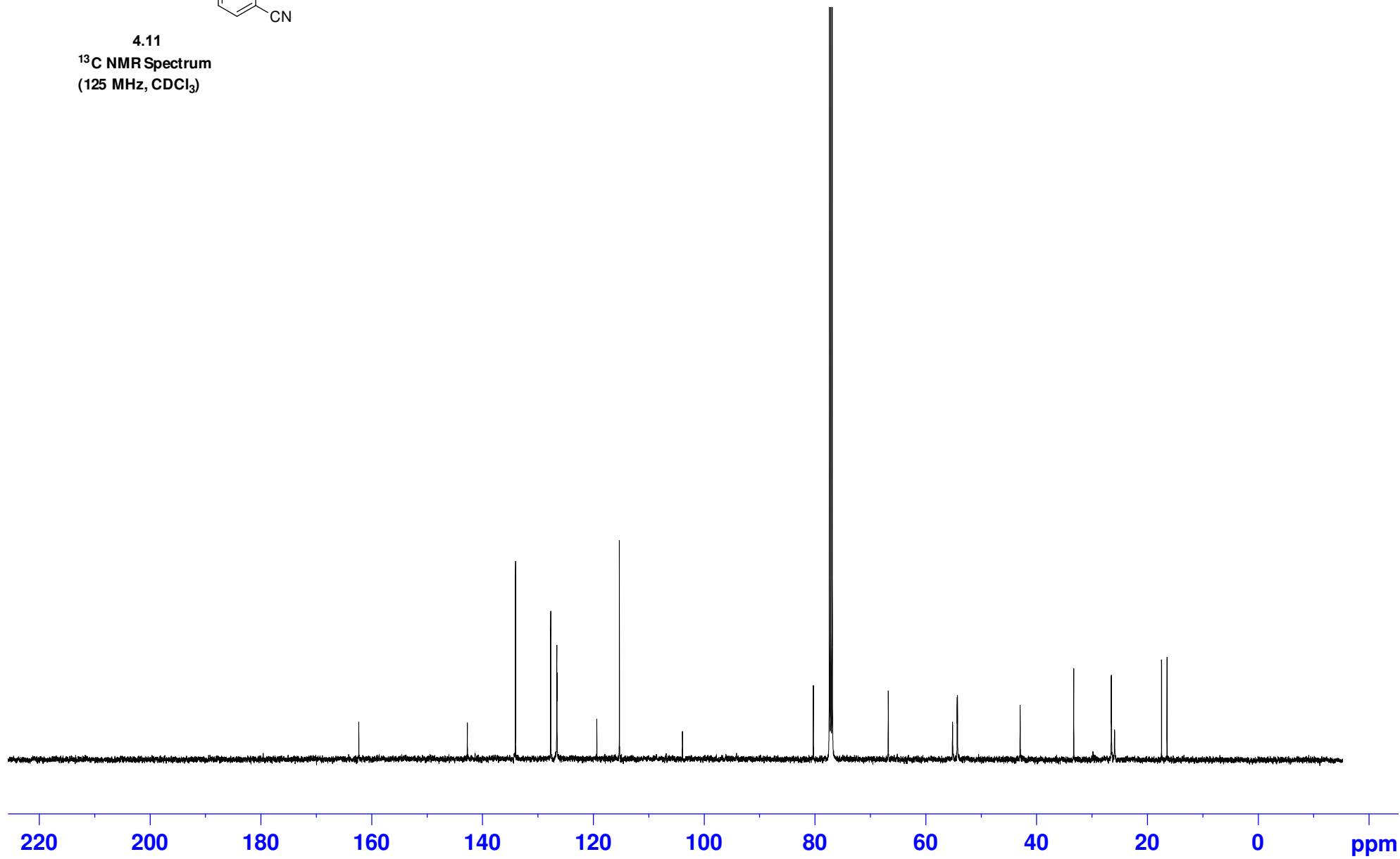
^{13}C NMR Spectrum
(100 MHz, CDCl_3)

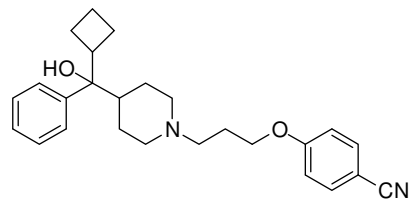




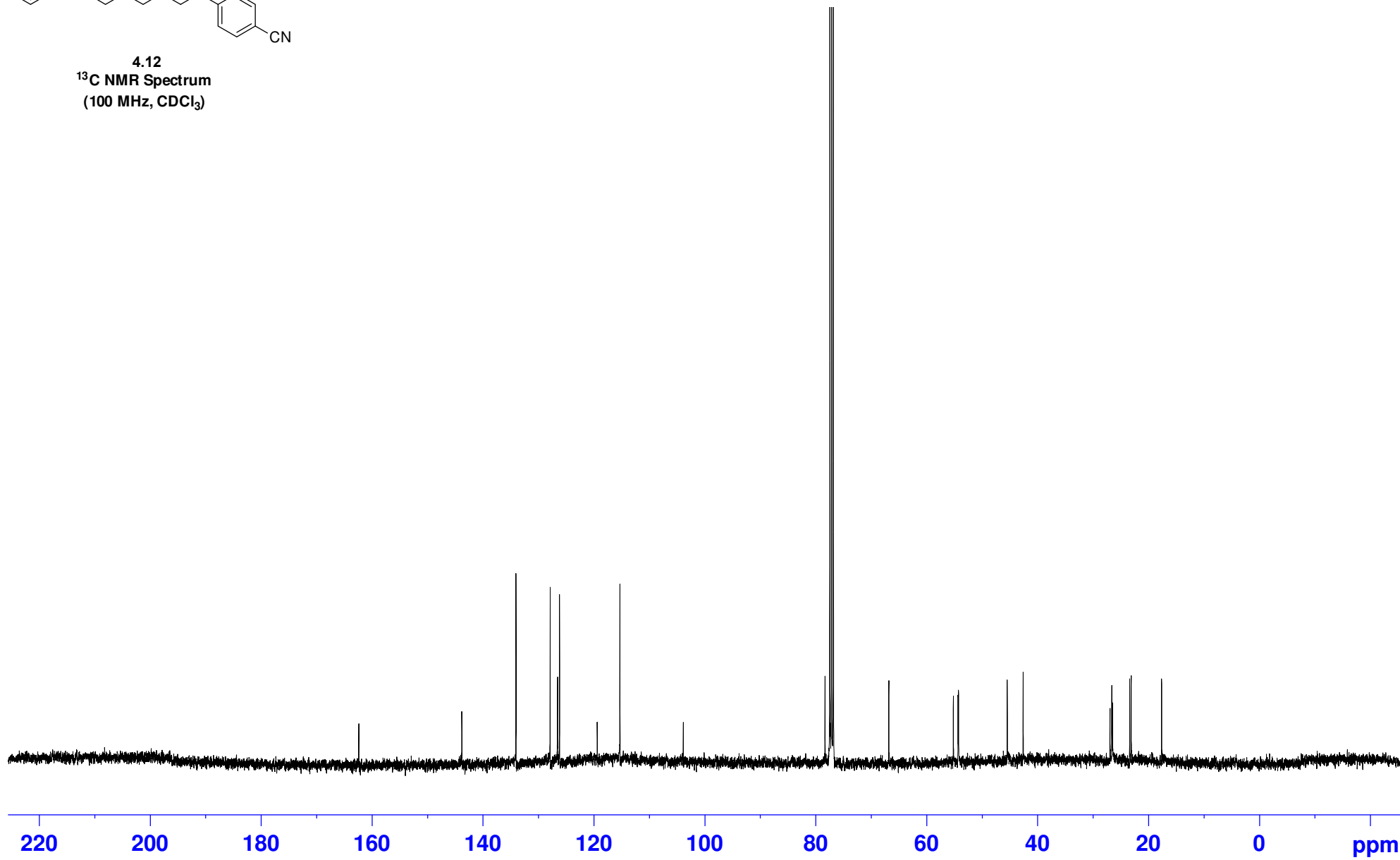
4.11

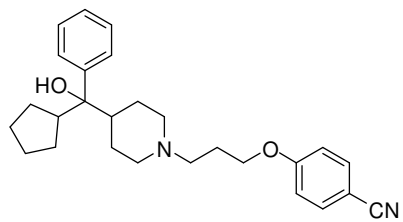
¹³C NMR Spectrum
(125 MHz, CDCl₃)





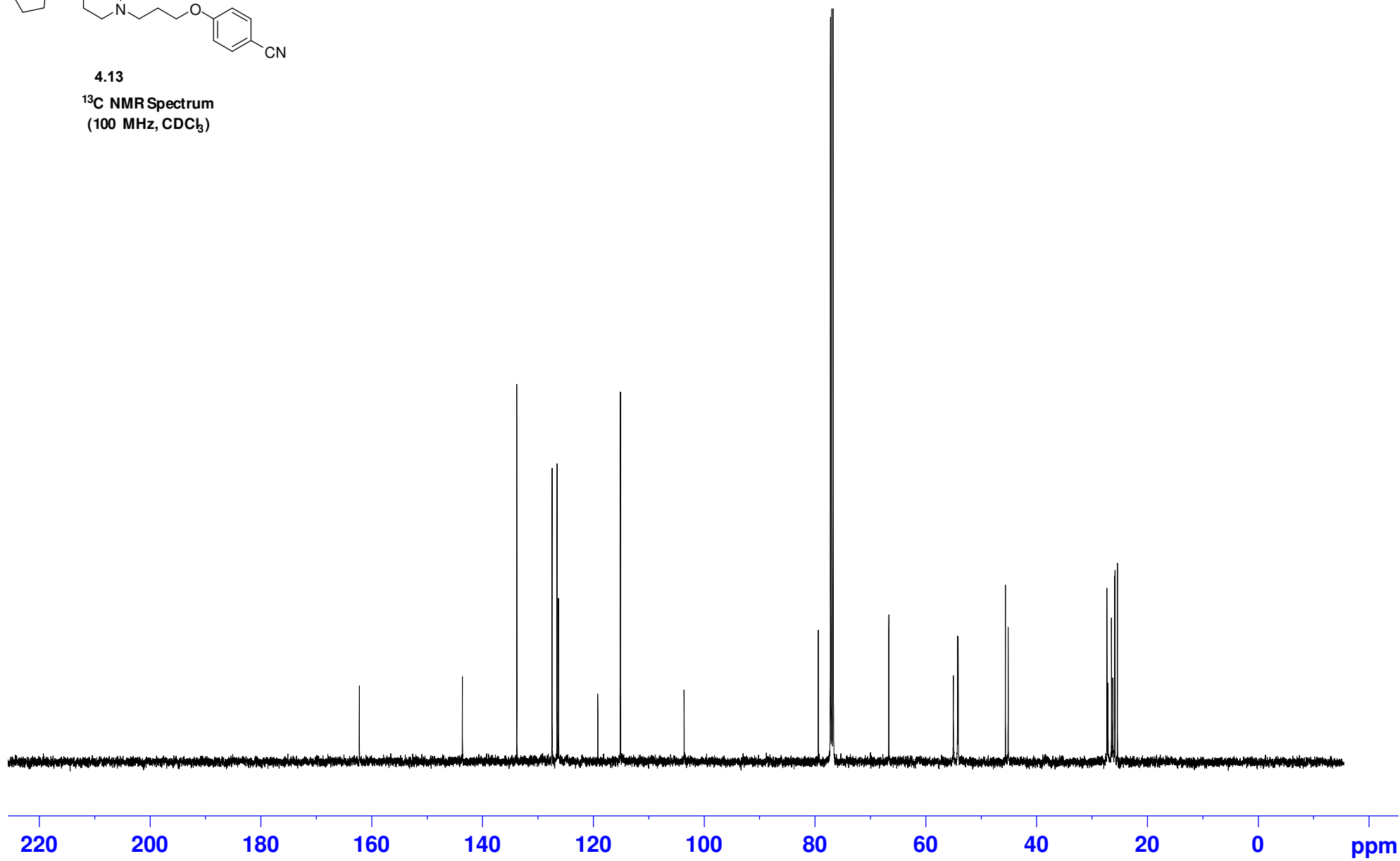
4.12
¹³C NMR Spectrum
(100 MHz, CDCl₃)

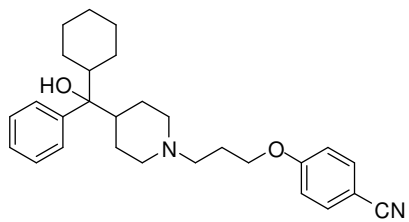




4.13

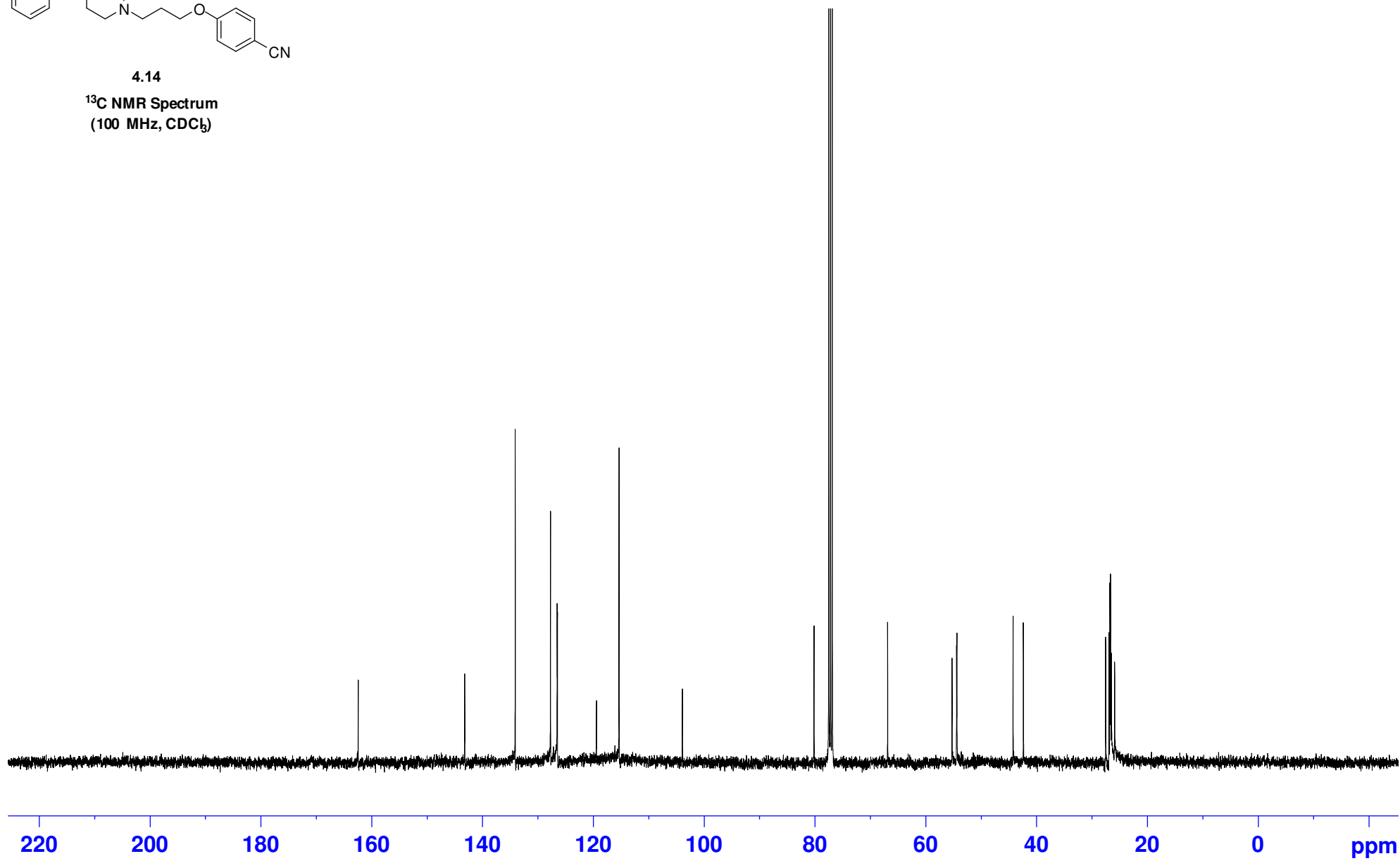
¹³C NMR Spectrum
(100 MHz, CDCl₃)

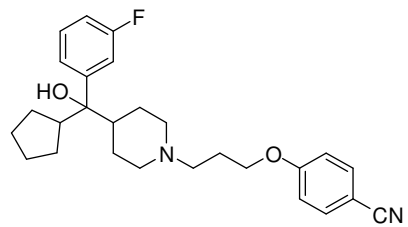




4.14

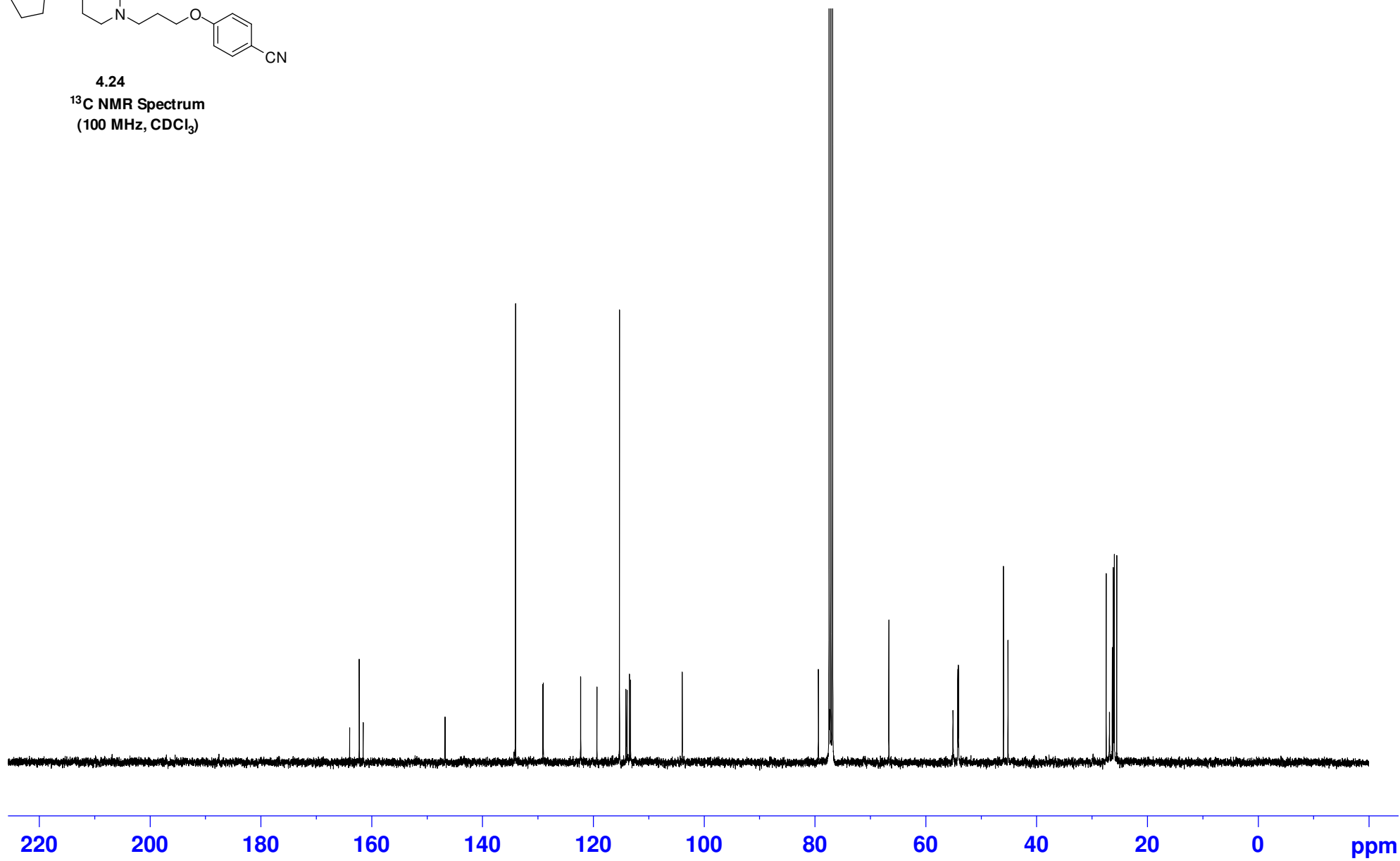
^{13}C NMR Spectrum
(100 MHz, CDCl_3)

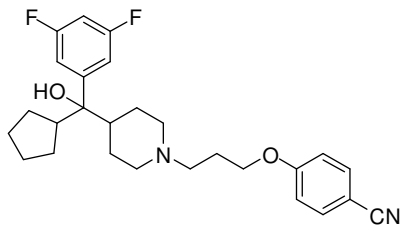




4.24

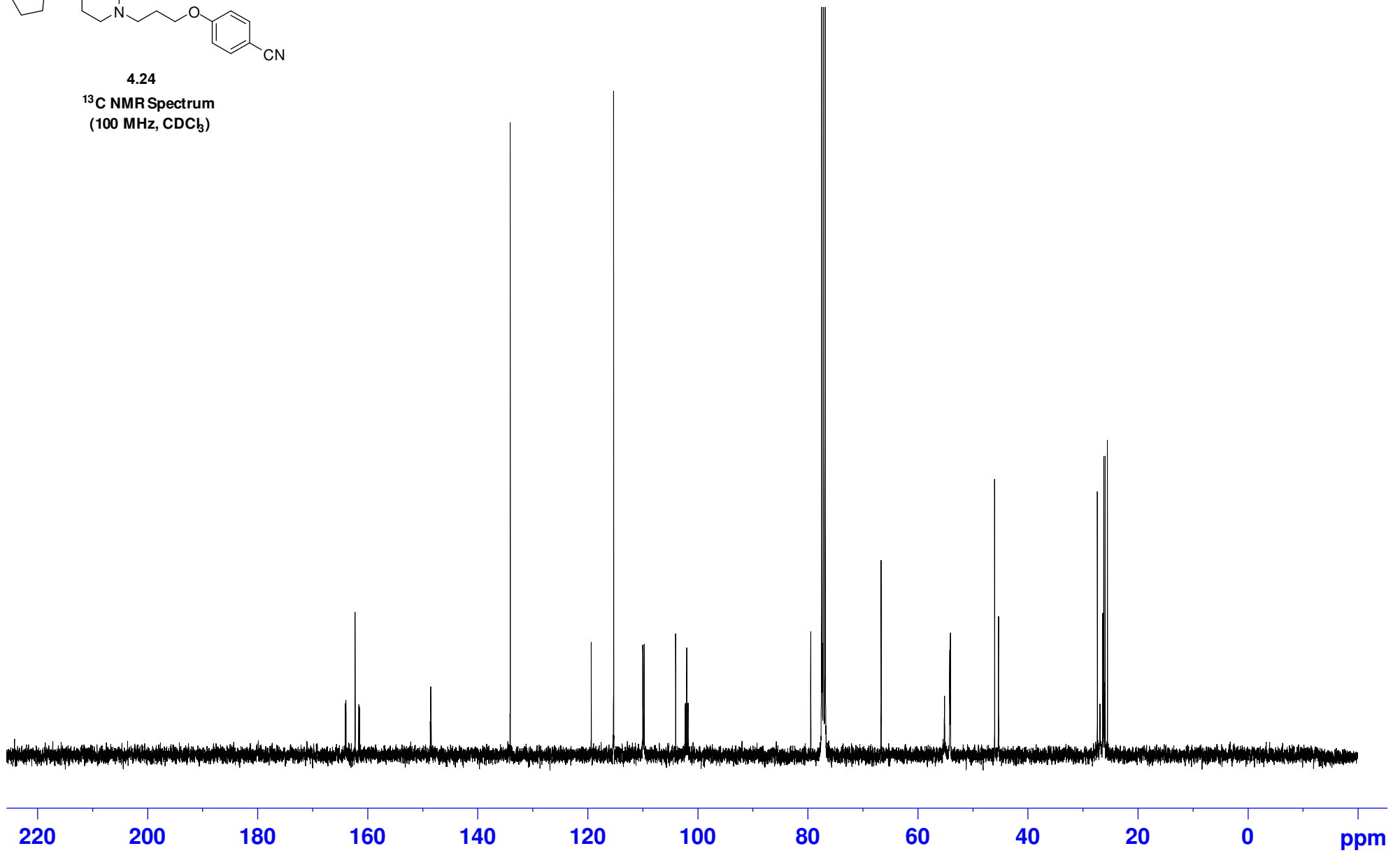
¹³C NMR Spectrum
(100 MHz, CDCl₃)

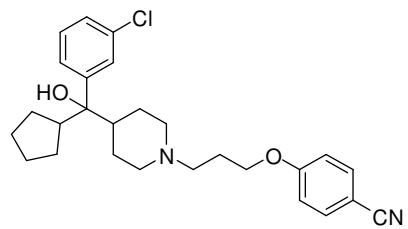




4.24

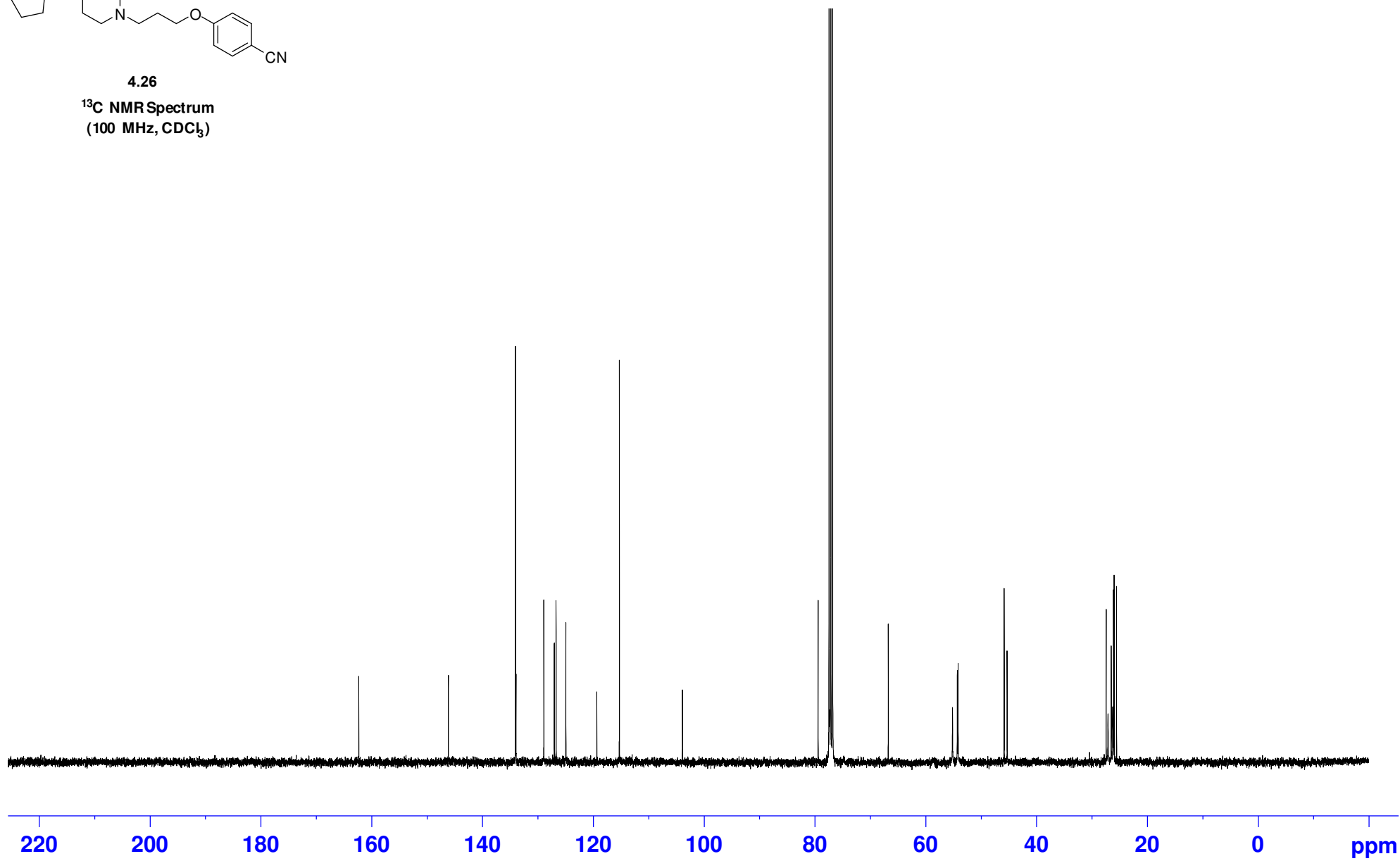
¹³C NMR Spectrum
(100 MHz, CDCl₃)

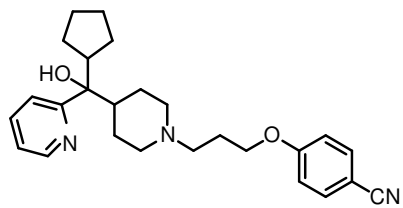




4.26

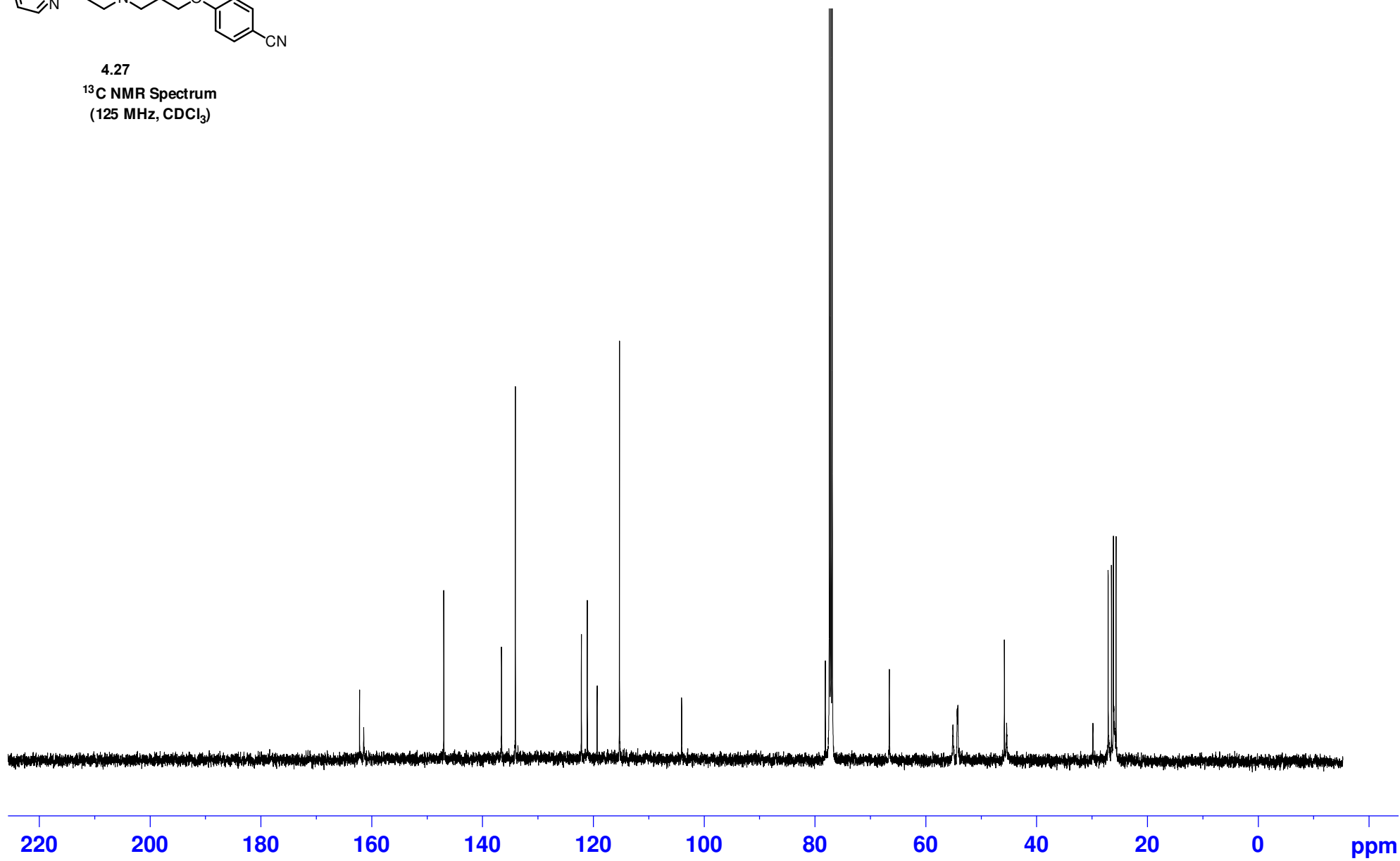
¹³C NMR Spectrum
(100 MHz, CDCl₃)

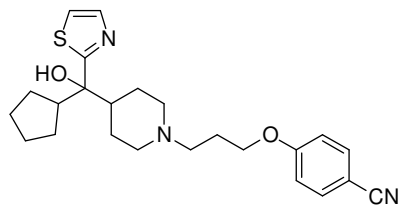




4.27

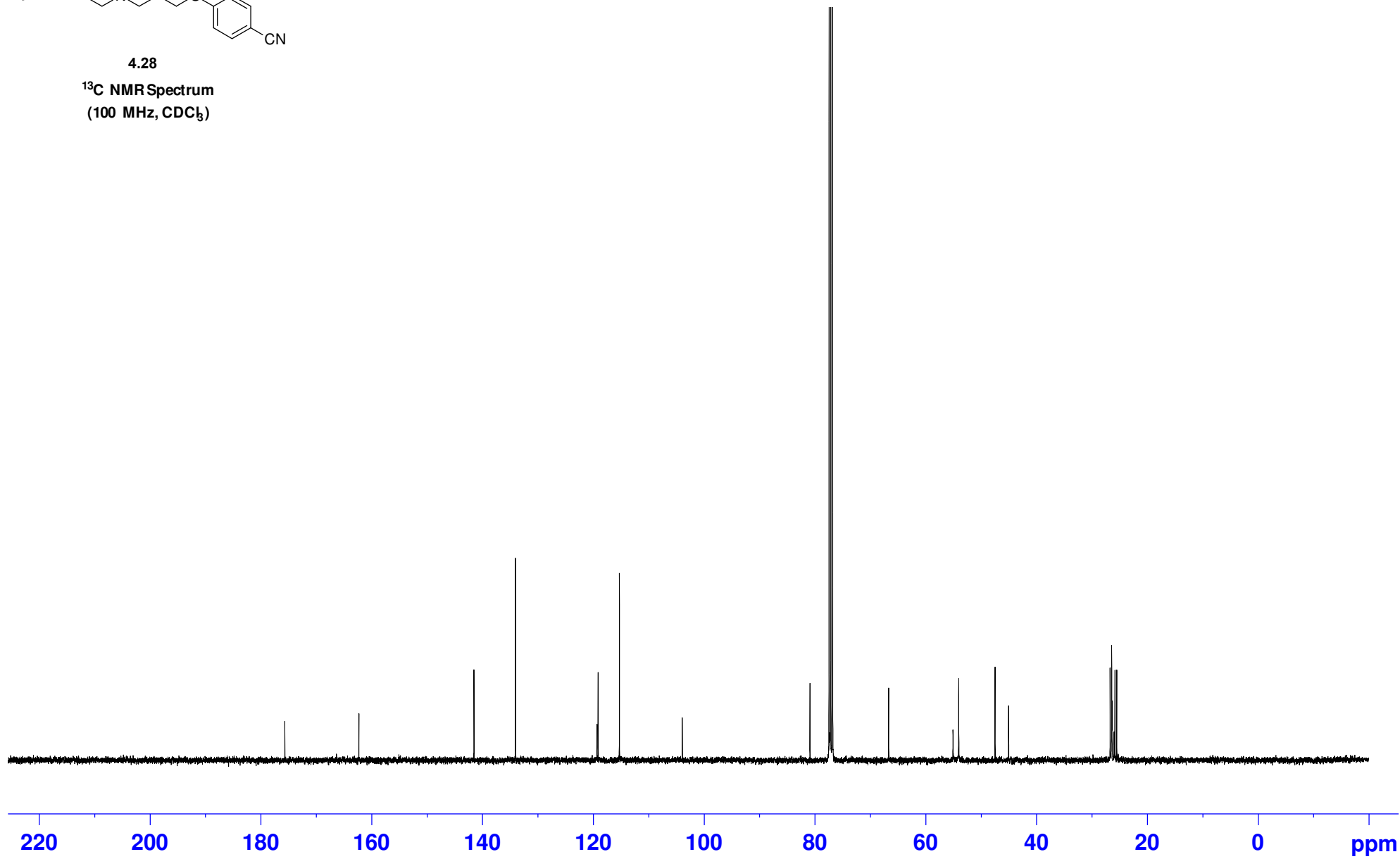
¹³C NMR Spectrum
(125 MHz, CDCl₃)

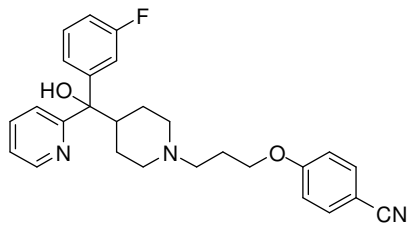




4.28

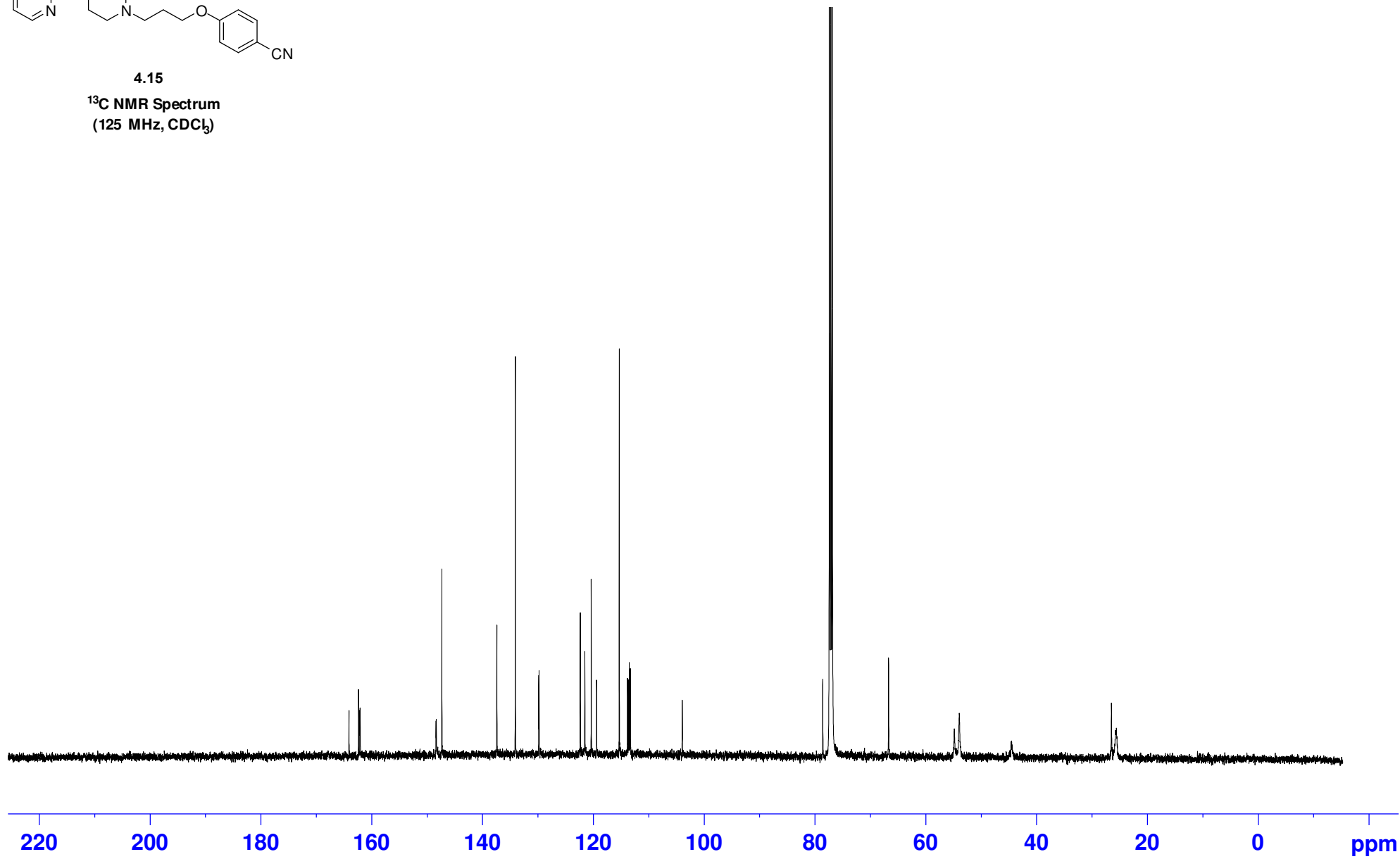
¹³C NMR Spectrum
(100 MHz, CDCl₃)

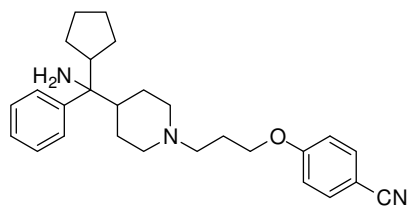




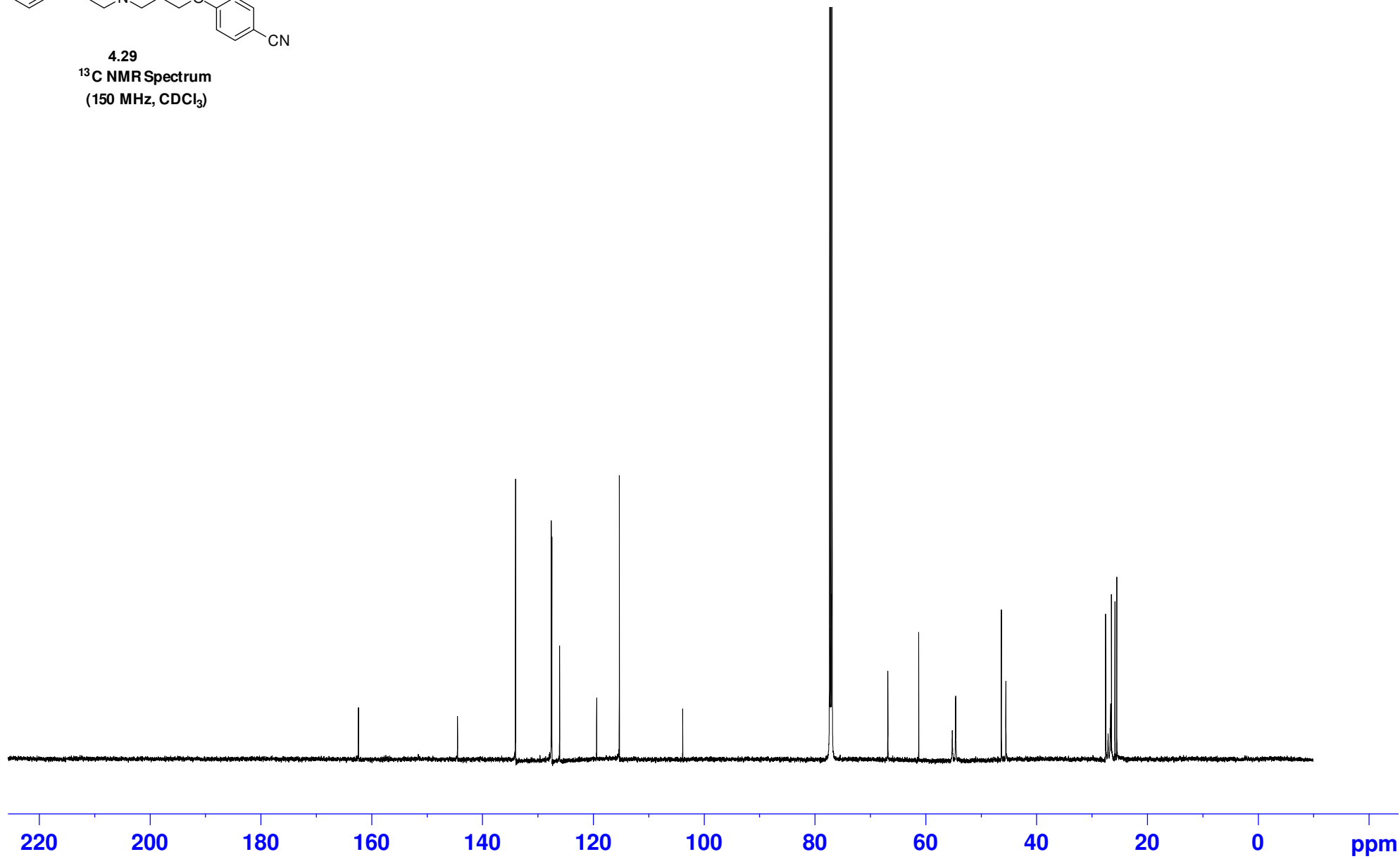
4.15

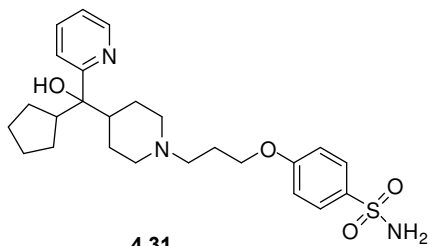
¹³C NMR Spectrum
(125 MHz, CDCl₃)





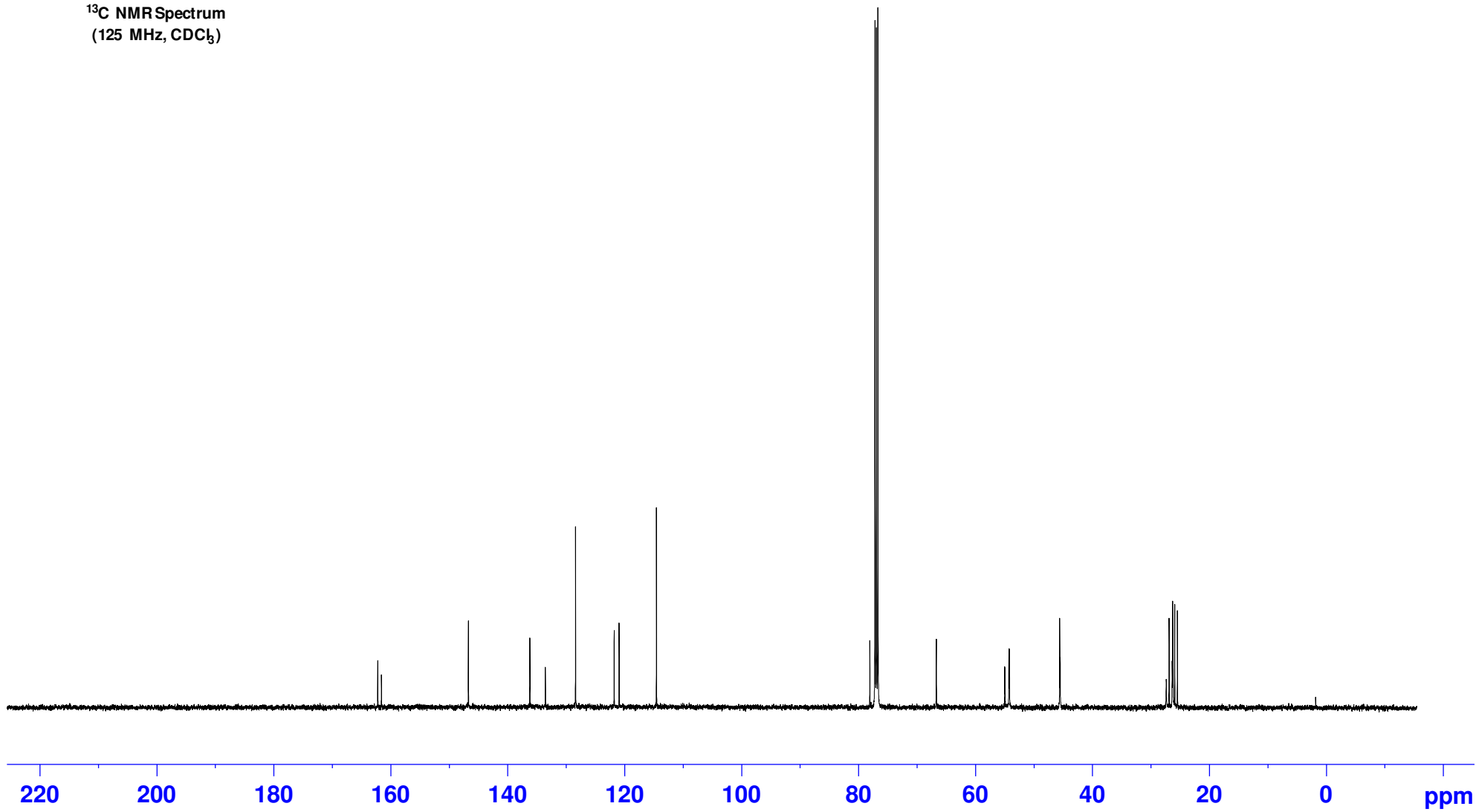
4.29
¹³C NMR Spectrum
(150 MHz, CDCl₃)

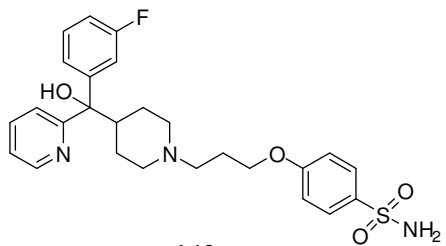




4.31

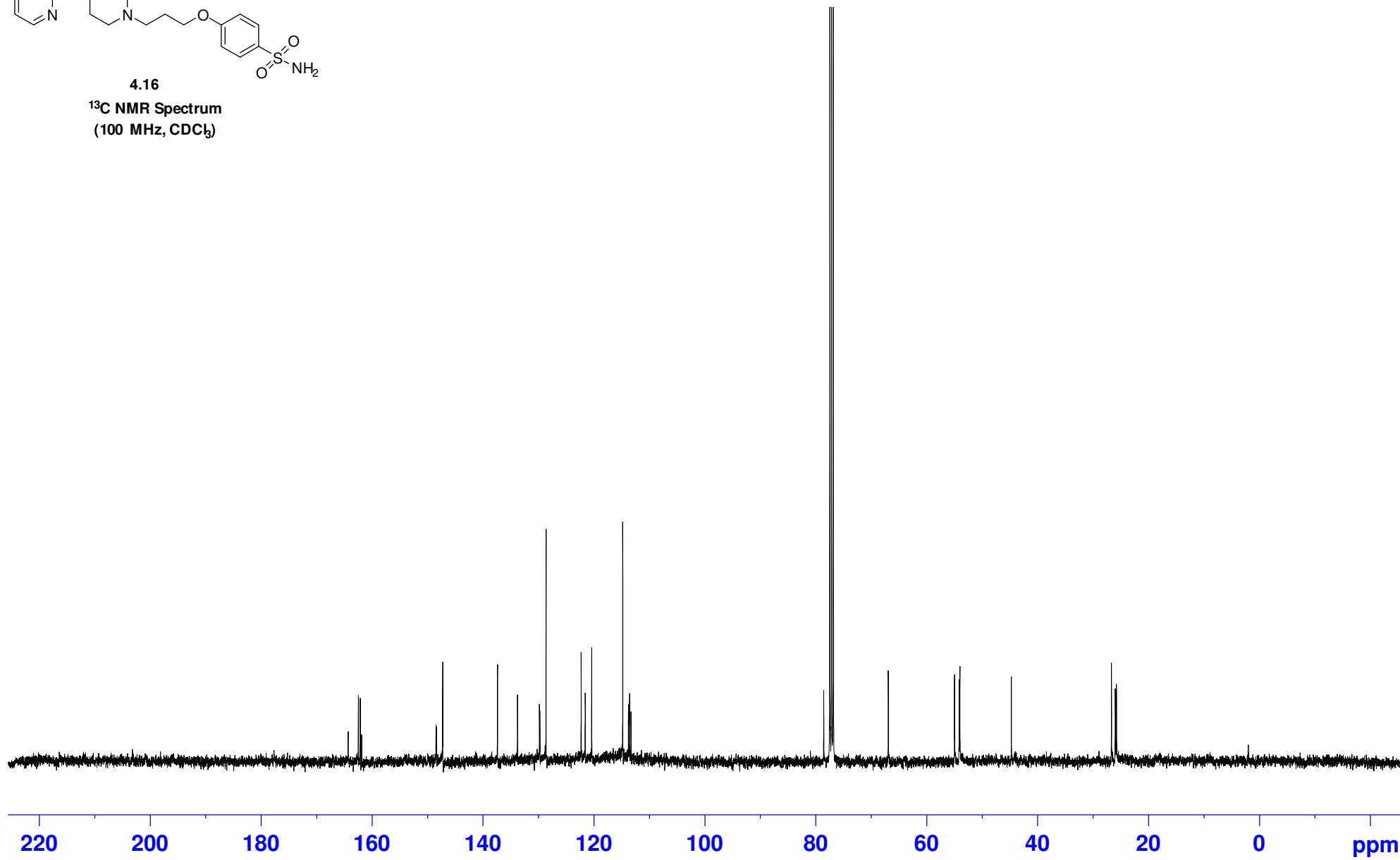
¹³C NMR Spectrum
(125 MHz, CDCl₃)

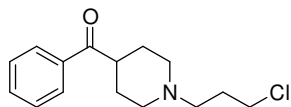




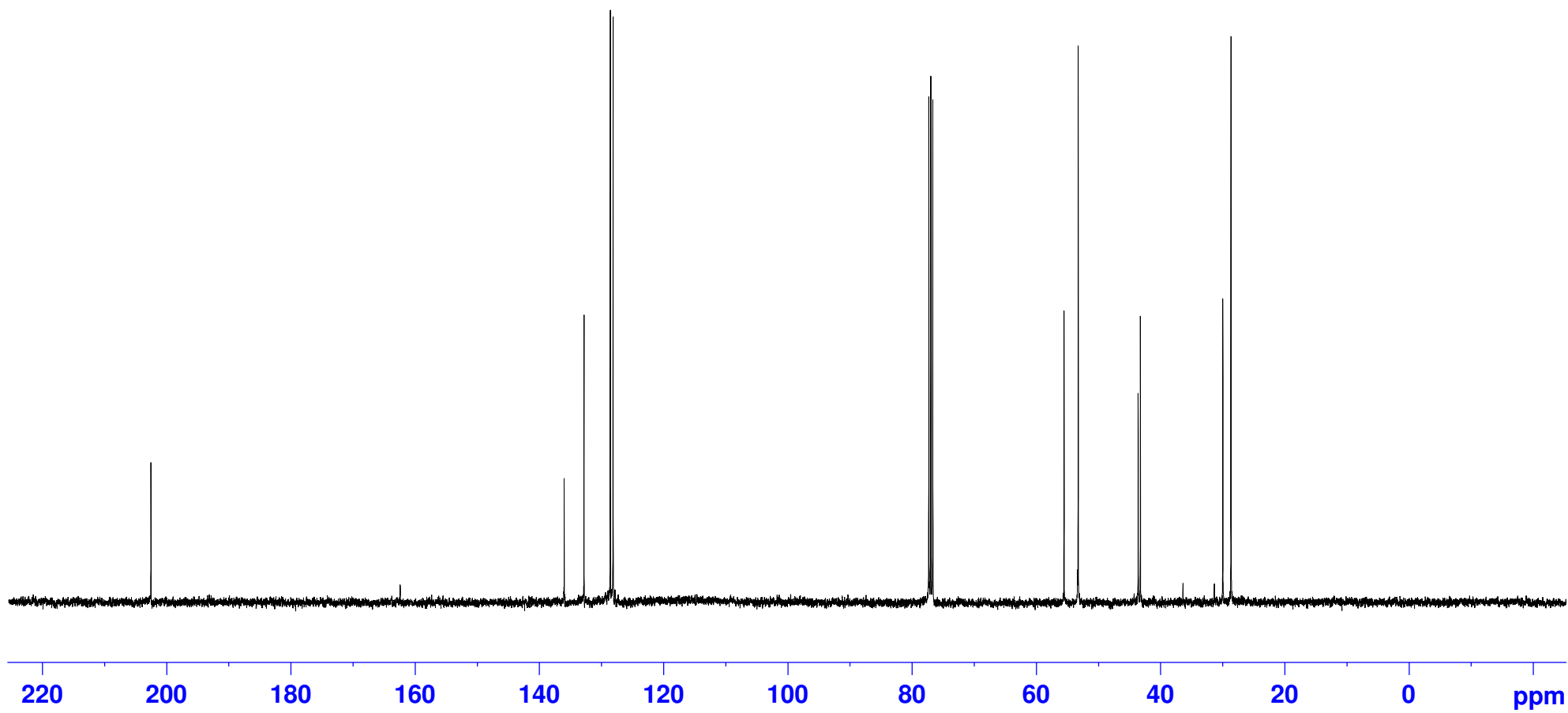
4.16

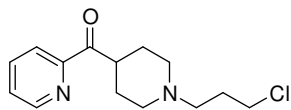
¹³C NMR Spectrum
(100 MHz, CDCl₃)





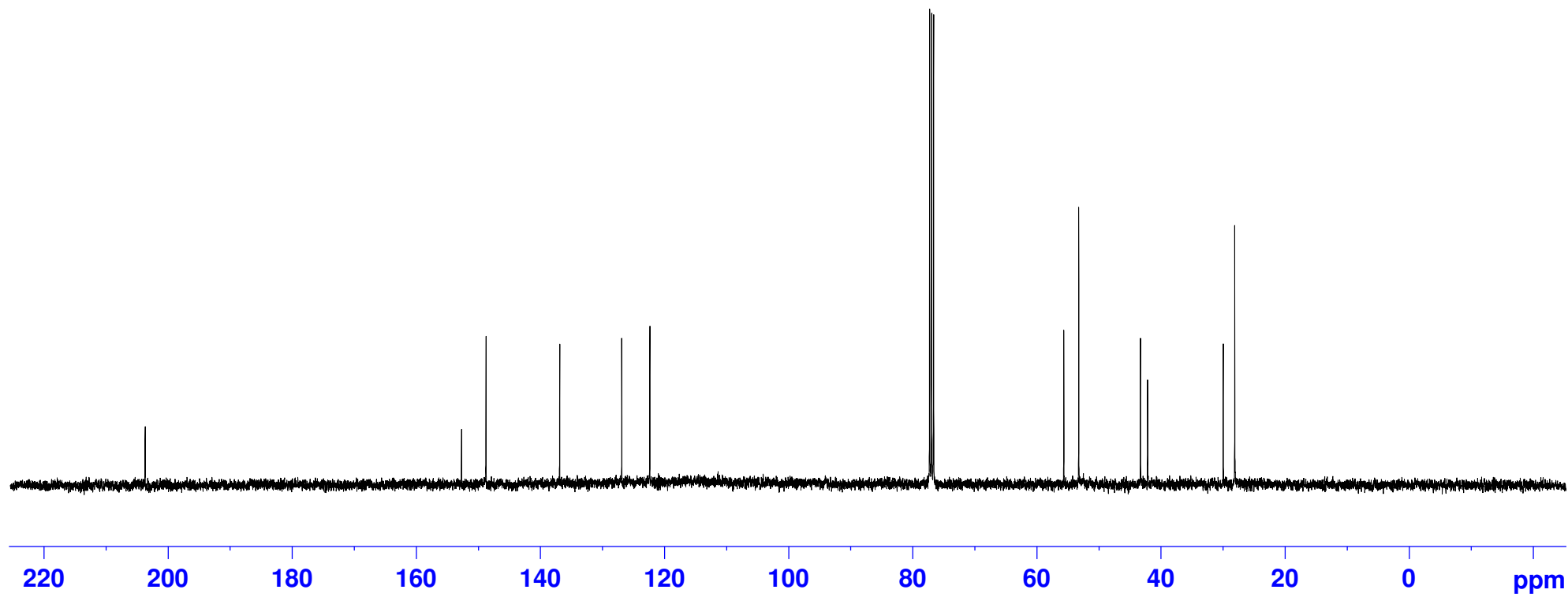
4.4a
¹³C NMR Spectrum
(100 MHz, CDCl₃)

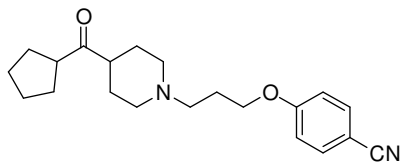




4.4b

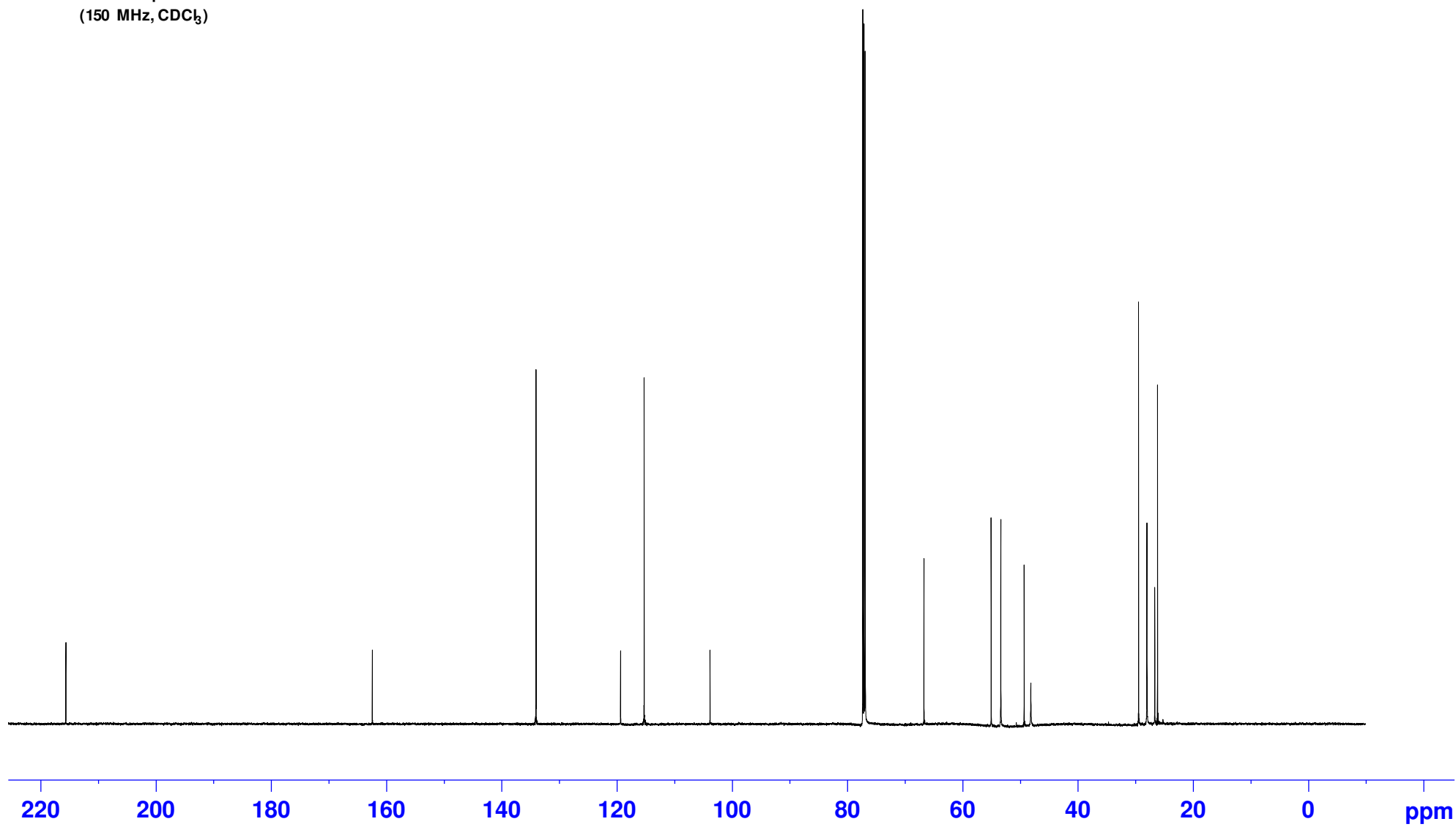
¹³C NMR Spectrum
(100 MHz, CDCl₃)

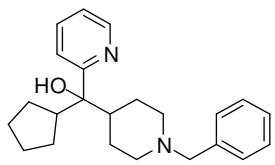




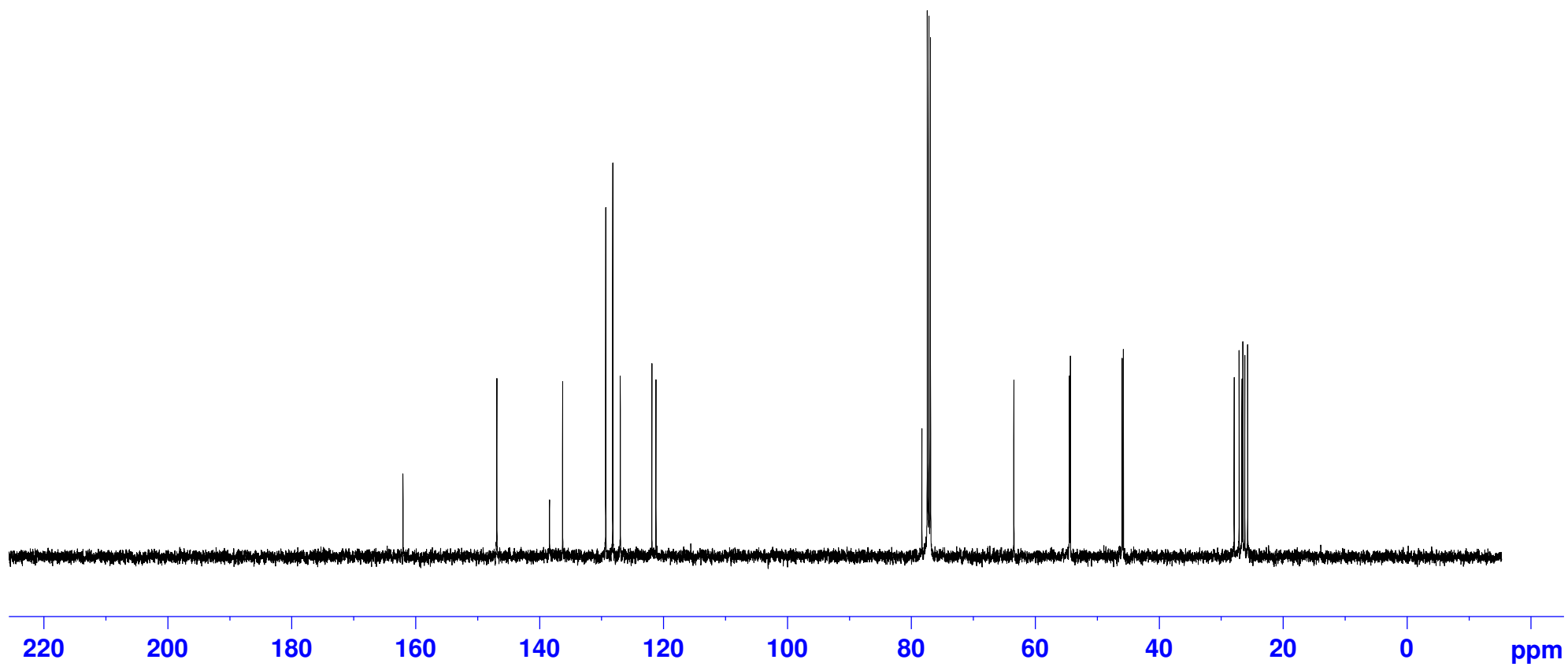
4.23

¹³C NMR Spectrum
(150 MHz, CDCl₃)

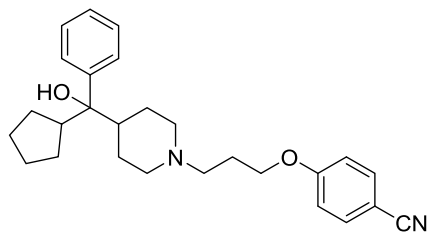




4.33
¹³C NMR Spectrum
(100 MHz, CDCl₃)



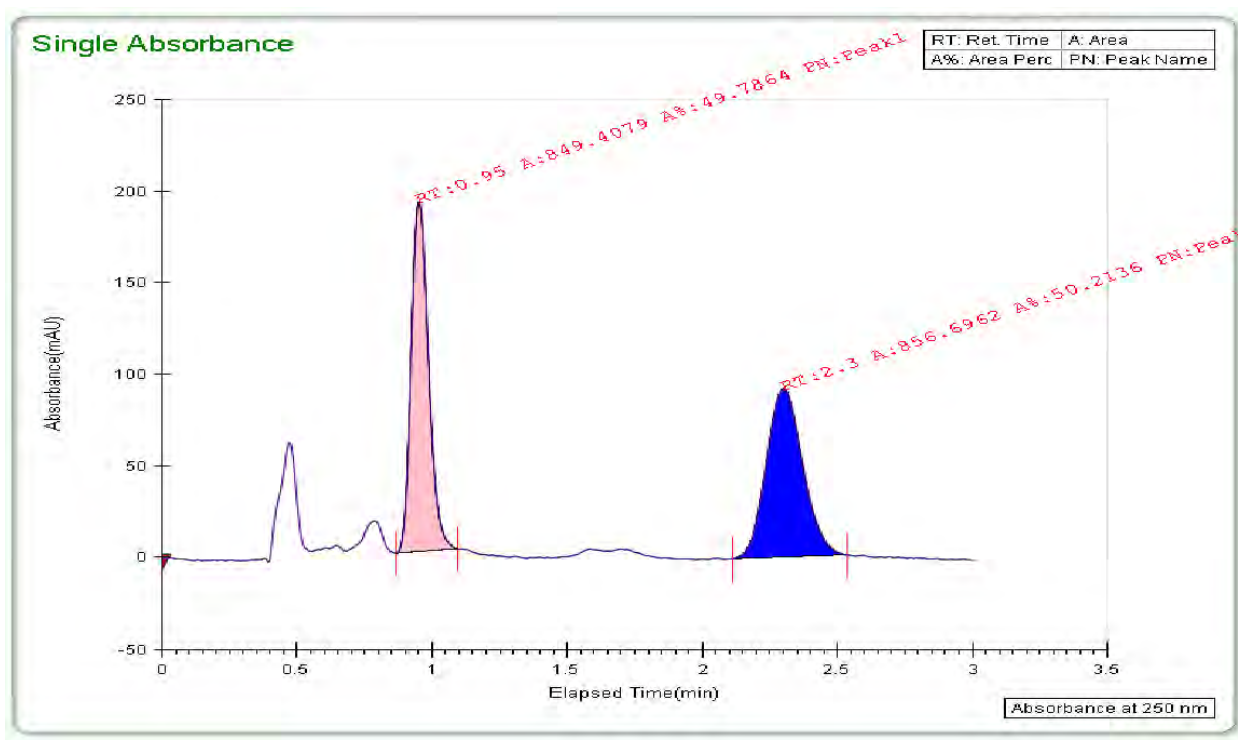
4. Chiral SFC Traces



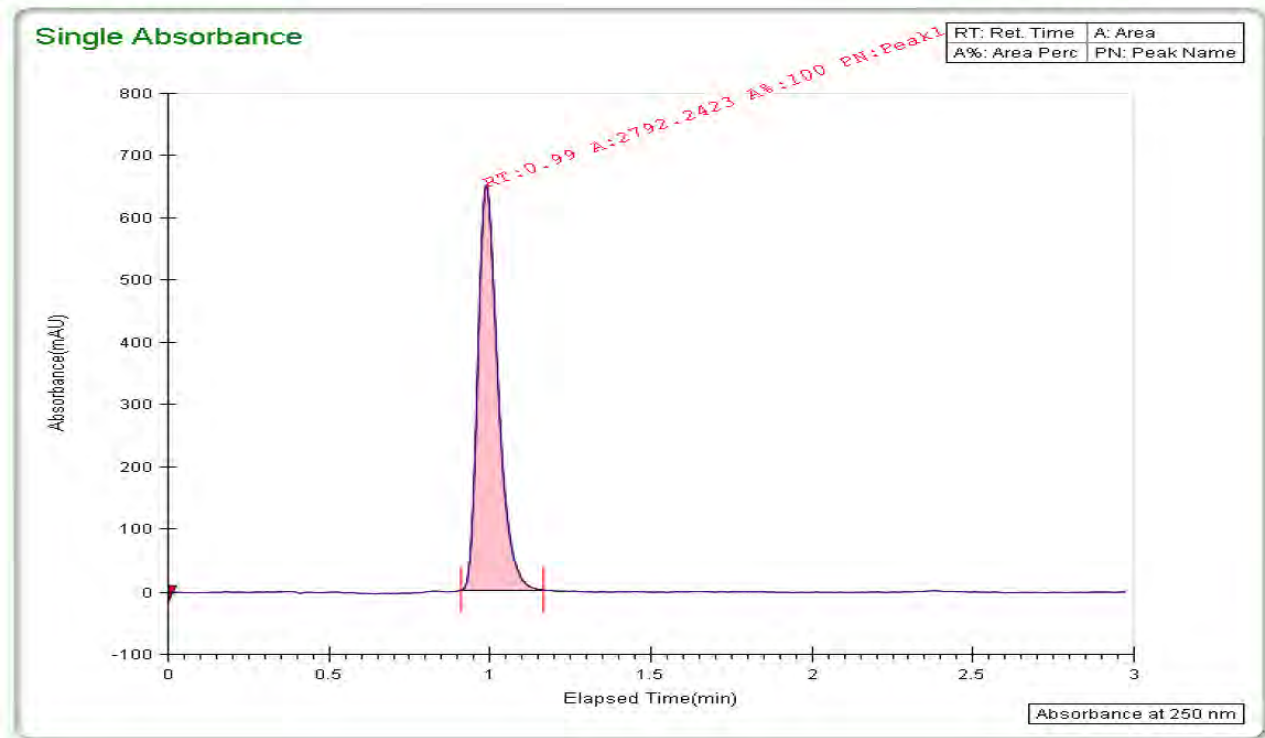
4-(3-(4-(cyclopentyl(hydroxy)(phenyl)methyl)piperidin-1-

yl)propoxy)benzonitrile, 4.13:

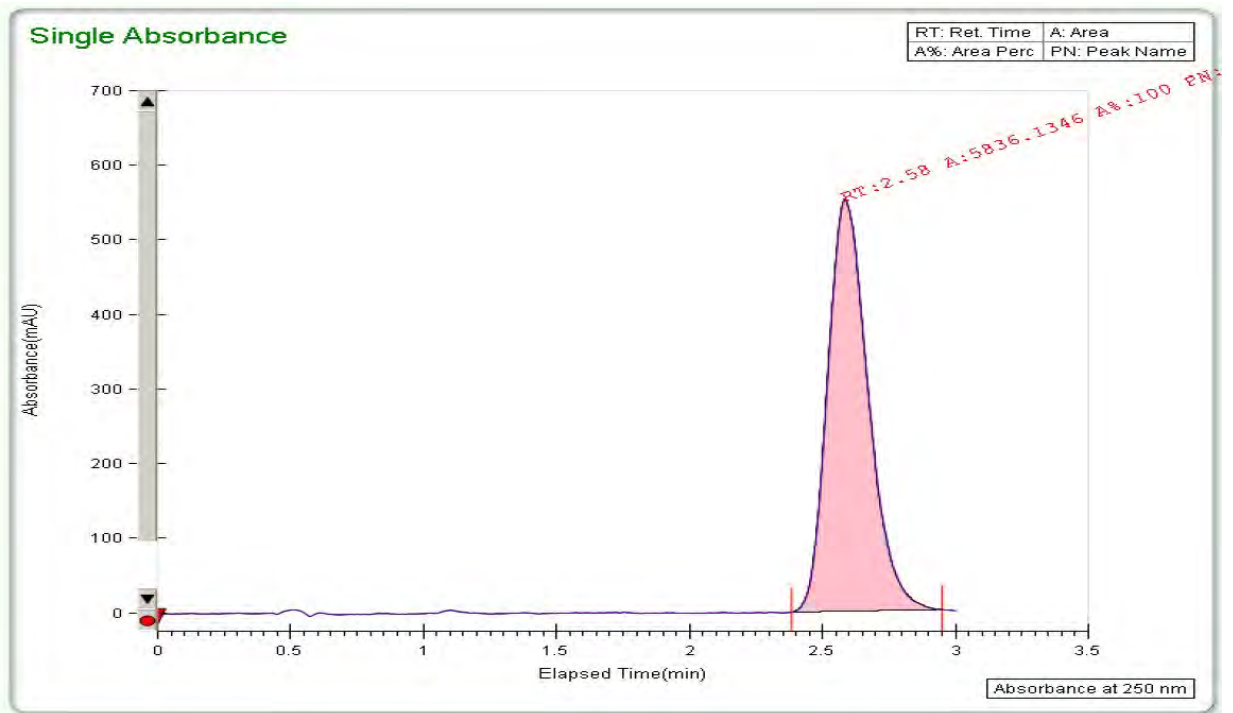
Semi-preparative purification:

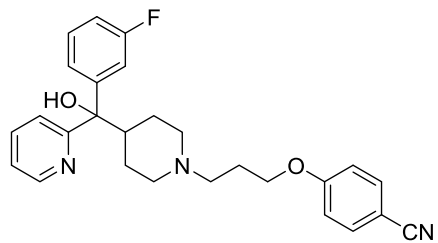


First Eluting Peak:



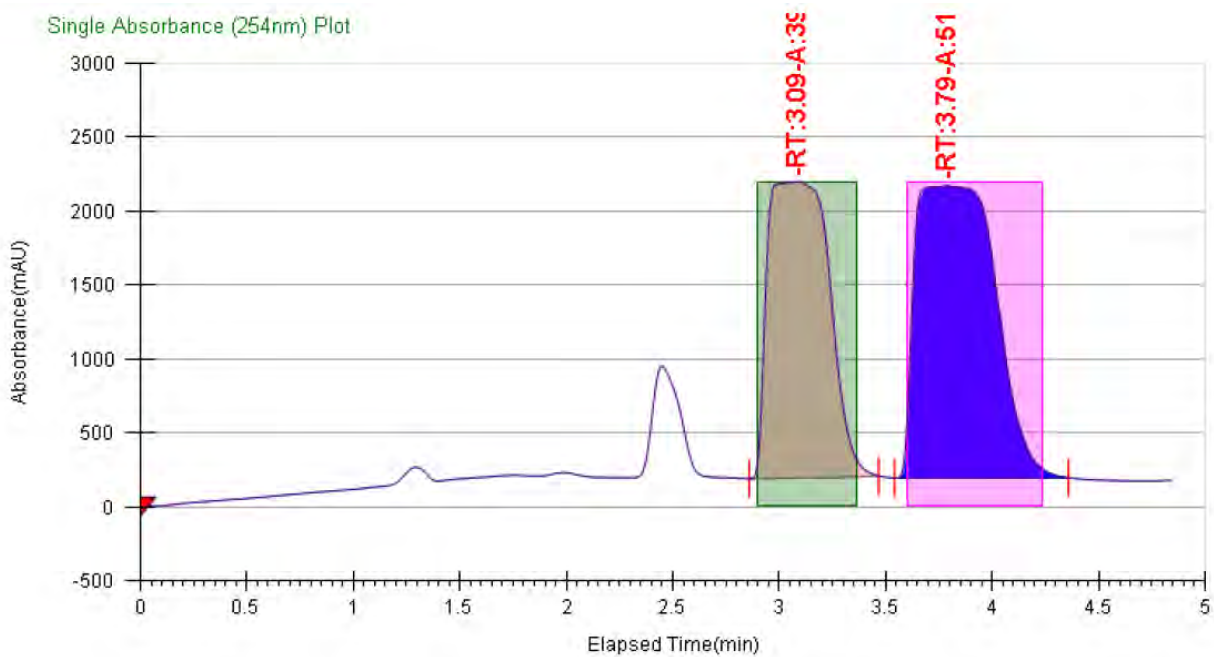
Second Eluting Peak:



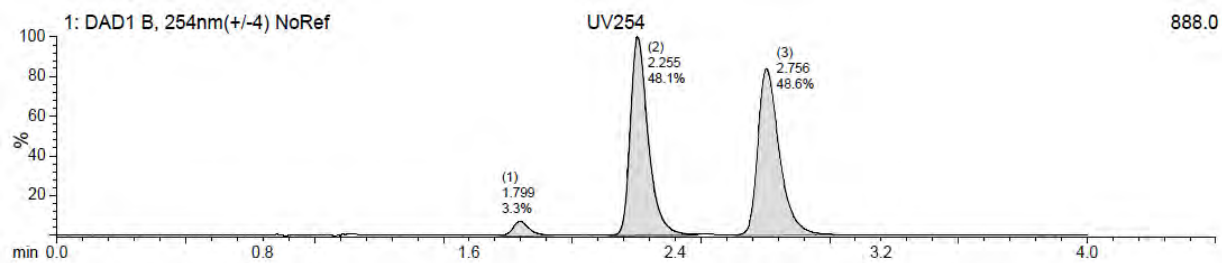


4-(3-(4-((3-fluorophenyl)(hydroxy)(pyridin-2-yl)methyl)piperidin-1-yl)propoxy)benzonitrile, 4.15:

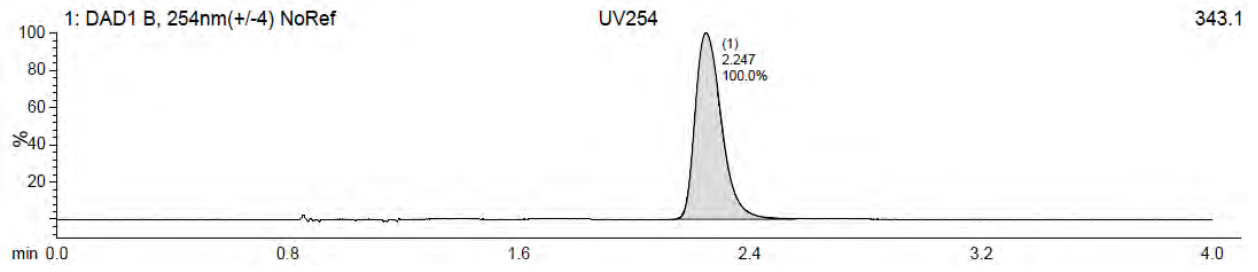
Semi-preparative purification:



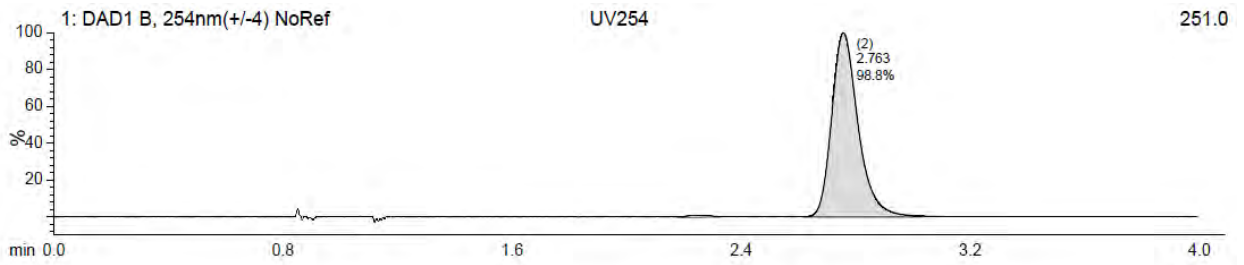
Racemic Analytical Chiral SFCMS:

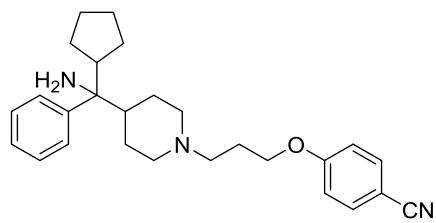


First Eluting Peak:



Second Eluting Peak:

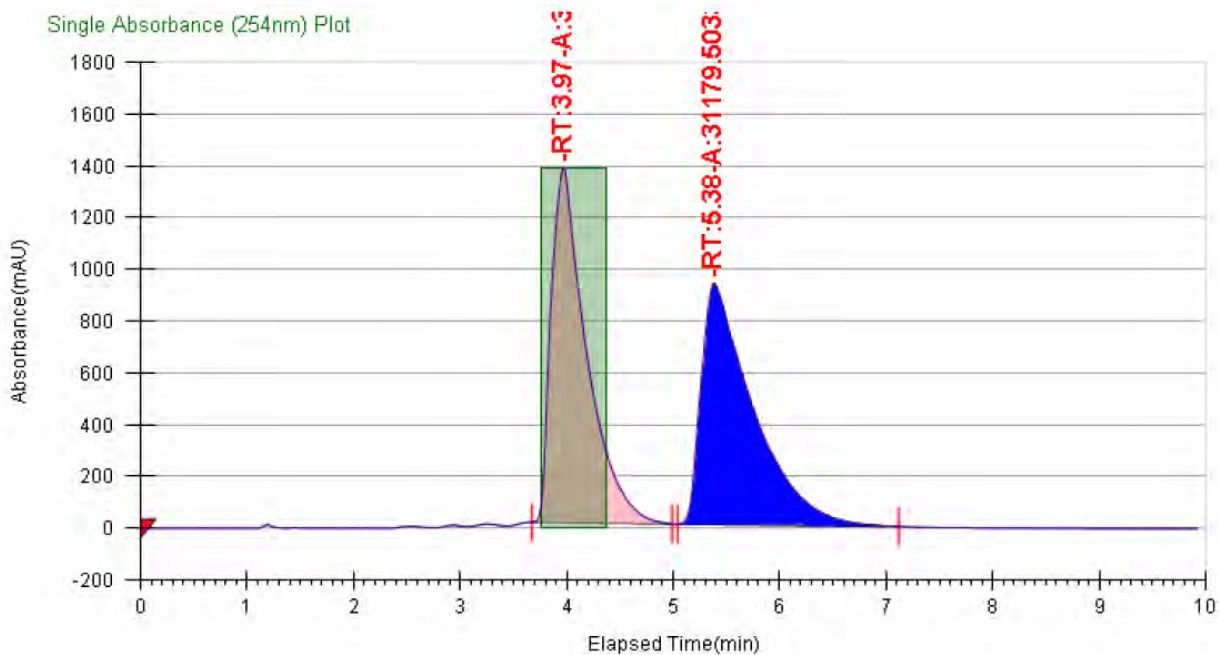




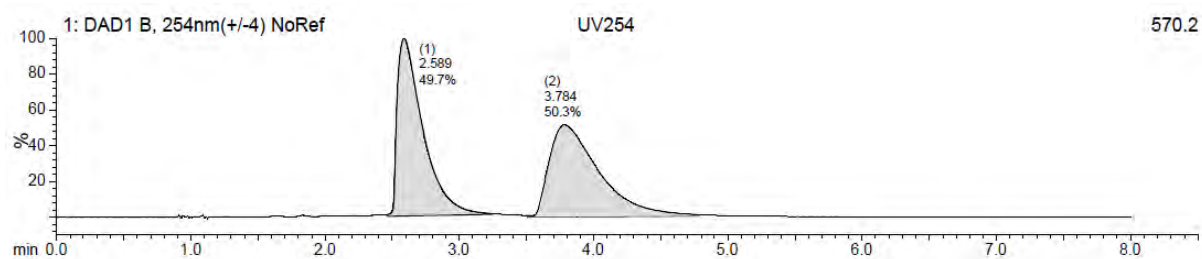
4-(3-(4-(cyclopentyl(hydroxy)(phenyl)methyl)piperidin-1-

yl)propoxy)benzonitrile, 4.29:

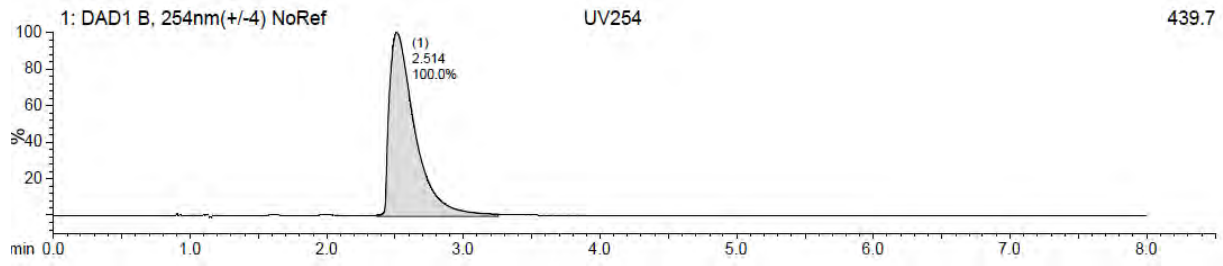
Semi-preparative purification:



Racemic Analytical Chiral SFCMS:



First Eluting Peak:



Second Eluting Peak:

